



HAL
open science

Synthesis and biological evaluation of neutral glycosyltransferase inhibitors

Shuai Wang

► **To cite this version:**

Shuai Wang. Synthesis and biological evaluation of neutral glycosyltransferase inhibitors. Organic chemistry. Université Claude Bernard - Lyon I, 2013. English. NNT : 2013LYO10175 . tel-01131147

HAL Id: tel-01131147

<https://theses.hal.science/tel-01131147>

Submitted on 27 Mar 2015

HAL is a multi-disciplinary open access archive for the deposit and dissemination of scientific research documents, whether they are published or not. The documents may come from teaching and research institutions in France or abroad, or from public or private research centers.

L'archive ouverte pluridisciplinaire **HAL**, est destinée au dépôt et à la diffusion de documents scientifiques de niveau recherche, publiés ou non, émanant des établissements d'enseignement et de recherche français ou étrangers, des laboratoires publics ou privés.



N° d'ordre

Année 2013
THESE DE L'UNIVERSITE DE LYON

Délivrée par

L'UNIVERSITE CLAUDE BERNARD LYON 1

ECOLE DOCTORALE DE CHIMIE

DIPLOME DE DOCTORAT

(arrêté du 7 août 2006)

soutenue publiquement le 24 octobre 2013 par

Shuai WANG

**Synthèse et Evaluation Biologique d'Inhibiteurs Neutres de
Glycosyltransférases**

Directeur de thèse : Dr. Sébastien VIDAL

Prof. Peter G. GOEKJIAN (Université Lyon 1)

Prof. Philippe COMPAIN (Université de Strasbourg)

Prof. Stéphane VINCENT (Université de Namur, Belgium)

Dr. Sébastien VIDAL (Université Lyon 1)

Dr. Gerd WAGNER (King's College London, United Kingdom)

Dr. Pierre-Alexandre DRIGUEZ (Sanofi)

Président

Rapporteur

Rapporteur

Directeur de thèse

Examineur

Examineur

UNIVERSITE CLAUDE BERNARD - LYON 1

Président de l'Université

M. François-Noël GILLY

Vice-président du Conseil d'Administration

M. le Professeur Hamda BEN HADID

Vice-président du Conseil des Etudes et de la Vie Universitaire

M. le Professeur Philippe LALLE

Vice-président du Conseil Scientifique

M. le Professeur Germain GILLET

Directeur Général des Services

M. Alain HELLEU

COMPOSANTES SANTE

Faculté de Médecine Lyon Est – Claude Bernard

Directeur : M. le Professeur J. ETIENNE

Faculté de Médecine et de Maïeutique Lyon Sud – Charles Mérieux

Directeur : Mme la Professeure C. BURILLON

Faculté d'Odontologie

Directeur : M. le Professeur D. BOURGEOIS

Institut des Sciences Pharmaceutiques et Biologiques

Directeur : Mme la Professeure C. VINCIGUERRA

Institut des Sciences et Techniques de la Réadaptation

Directeur : M. le Professeur Y. MATILLON

Département de formation et Centre de Recherche en Biologie Humaine

Directeur : M. le Professeur P. FARGE

COMPOSANTES ET DEPARTEMENTS DE SCIENCES ET TECHNOLOGIE

Faculté des Sciences et Technologies

Directeur : M. le Professeur F. DE MARCHI

Département Biologie

Directeur : M. le Professeur F. FLEURY

Département Chimie Biochimie

Directeur : Mme le Professeur H. PARROT

Département GEP

Directeur : M. N. SIAUVE

Département Informatique

Directeur : M. le Professeur S. AKKOUCHE

Département Mathématiques

Directeur : M. le Professeur A. GOLDMAN

Département Mécanique

Directeur : M. le Professeur H. BEN HADID

Département Physique

Directeur : Mme S. FLECK

Département Sciences de la Terre

Directeur : Mme la Professeure I. DANIEL

UFR Sciences et Techniques des Activités Physiques et Sportives

Directeur : M. C. COLLIGNON

Observatoire des Sciences de l'Univers de Lyon

Directeur : M. B. GUIDERDONI

Polytech Lyon

Directeur : M. P. FOURNIER

Ecole Supérieure de Chimie Physique Electronique

Directeur : M. G. PIGNAULT

Institut Universitaire de Technologie de Lyon 1

Directeur : M. C. VITON

Institut Universitaire de Formation des Maîtres

Directeur : M. A. MOUGNIOTTE

Institut de Science Financière et d'Assurances

Administrateur provisoire : M. N. LEBOISNE

Acknowledgement

First of all I would like to thank my supervisor, Dr. Sébastien Vidal, for giving me an opportunity to be a member of Laboratoire de Chimie Organique 2 at Institut de Chimie et Biochimie Moléculaires et Supramoléculaires, Université Claude Bernard Lyon 1, and for providing guidance and direction over the years. He always encouraged me and gave me excellent suggestions which enable me to finish my thesis successfully.

I would like to thank Prof. Jean-Marc Lancelin, the director of graduate school of Chemistry in Lyon. We met each other in China for an interview and he introduced me to Prof. Peter G. Goekjian, the director of group LCO2. Then, I could get a chance to apply a scholarship with Dr. Sébastien Vidal and work in the group.

During my PhD, I was honored to work with Prof. Monica M. Palcic at Carlsberg Laboratory for biological evaluation. I obtained a good training in enzymatic assays in her research group. I would like to express my appreciation for her professional guidance and her support.

My extraordinary thank goes to Dr. Dominique Lafont, my colleague of LCO2, who gave me many excellent suggestions on glycosylation to solve the problems encountered during my work. His profound knowledge on glycosylation was unforgettable and I benefit a lot from it.

During my project, I was able to communicate and cooperate with scientists from different scientific areas. In such an environment, it was very productive. Therefore, I would like to thank all our collaborators involved in the thesis, Prof. Reko Leino in Åbo Akademi University, Prof. David Voadlo in Simon Fraser University, Anne-sophie Vercoutter-Edouart, Marlène Mortuaire and Tony Lefebvre in Université des Sciences et Technologies de Lille but also Dr. Ofelia Maniti and Prof. Agnès Girard-Egrot in Université Lyon 1.

Moreover, I would like to show my thanks to our group members (current and former), Jean-Pierre Praly, Peter G. Goekjian, Pierre Strazewski, David Gueyrard, Karine Descroix, Julie Guiard, Joseph d'Attoma, Samuel Habib, Meriem Smadhi, Nicolas Galanos, Marc-Olivier Charlin, Huu vinh Trinh, who were always nice and helpful for my lab work and made my stay in Lyon amusing.

Furthermore, I would like to express my gratitude to many staff members in the analytical labs, the NMR spectroscopy lab and the mass spectroscopy lab. They did a lot of work to support my Ph.D. program.

I would like to thank Profs. Peter G. Goekjian, Philippe Compain, Stéphane Vincent and Drs. Gerd Wagner, Pierre-Alexandre Driguez for reading through my thesis and serving on my Ph.D. examination board.

Great thanks to Ministère de l'Enseignement Supérieur et de la Recherche France for financial support.

Last but not least, I would like to express my special thanks to my best friend, Xibo Yan, he was always there whenever I needed help. I cherished all the wonderful moments that we spent together to discover Europe.

Finally, I would like to dedicate my work to my parents, Chunjing Li and Xiaohua Wang.

List of Abbreviations

| | |
|-----------------------|---|
| Ac | acetyl |
| Ac ₂ O | acetic anhydride |
| AgOTf | silver triflate |
| Alloc | allyloxycarbonyl |
| aq. | aqueous |
| BAIB | bis(acetoxyiodo)benzene |
| Bn | benzyl |
| Boc | <i>tert</i> -butyloxycarbonyl |
| Boc-Gly-OSu | Boc-glycine- <i>N</i> -hydroxysuccinimide ester |
| BSA | Bovine serum albumin |
| BSP | 1-benzenesulfinyl piperidine |
| Bz | benzoyl |
| calcd | calculated |
| COSY | correlation spectroscopy |
| CuAAC | Cu (I)-catalyzed azide-alkyne cycloaddition |
| DCC | <i>N,N'</i> -dicyclohexylcarbodiimide |
| DDQ | 2,3-dichloro-5,6-dicyano-1,4-benzoquinone |
| DIC | <i>N, N'</i> -diisopropyl carbodiimide |
| DIPEA | <i>N,N</i> -diisopropylethylamine |
| DMAP | 4-dimethylaminopyridine |
| DMDO | dimethyldioxirane |
| DMF | <i>N,N'</i> -dimethylformamide |
| DMSO | dimethylsulfoxide |
| DNA | deoxyribonucleic acid |
| DTBMP | 2,6-di- <i>t</i> -butyl-4-methylpyridine |
| DTT | dithiothreitol |
| <i>E. coli</i> | <i>Escherichia coli</i> |
| equiv. | equivalent |
| Fmoc | fluorenylmethyloxycarbonyl |
| Fuc | fucose |
| Gal | galactose |
| GalNAc | <i>N</i> -acetyl galactosamine |
| α -1,3-GalT | α -1,3-galactosyltransferase |
| α -1,4-GalT | α -1,4-galactosyltransferase |
| β -1,4-GalT | β -1,4-galactosyltransferase |
| Glc | glucose |
| GlcNAc | <i>N</i> -acetyl-D-glucosamine |
| Glu | glutamine |
| GTA | Human blood group A <i>N</i> -acetylgalactosaminyltransferase |
| GTB | Human blood group B galactosyltransferase |
| GT | glycosyltransferases |
| h | hour |
| hEGF | human epidermal growth factor |
| HOBt | <i>N</i> -hydroxybenzotriazole |
| HTS | high-throughput screening |
| IC ₅₀ | median inhibition concentration |
| <i>J</i> | coupling constant |
| <i>K</i> _m | Michaelis-Menten constant |
| <i>K</i> _i | inhibition constant |
| <i>m</i> -CPBA | meta-chloroperoxybenzoic acid |
| MEGM | mammary epithelial cell growth medium |

| | |
|-------------------|--|
| min | minute(s) |
| MS | mass spectrometry |
| MS 4Å | molecular sieves 4Å |
| <i>m/z</i> | mass to charge ratio (mass spectrometry) |
| NBS | <i>N</i> -bromosuccinimide |
| NDPH | nucleoside diphosphate |
| NIS | <i>N</i> -iodosuccinimide |
| NMR | nuclear magnetic resonance |
| OGA | <i>O</i> -linked- <i>N</i> -acetyl-glucosaminase |
| OGT | <i>O</i> -linked <i>N</i> -acetyl-glucosaminyl transferase |
| PBS | phosphate buffer saline |
| Ph | phenyl |
| POPC | phosphatidylcholine |
| ppm | parts per million (NMR data) |
| Py | pyridine |
| quant. | quantitative |
| R_f | retention factor |
| RMSD | root-mean-square deviation |
| RNA | ribonucleic acid |
| r.t. | room temperature |
| satd | saturated |
| SDS-PAGE | sodium dodecyl sulfate polyacrylamide gel electrophoresis |
| sLe^x | Sialyl-Lewis ^x |
| S_{N2} | bimolecular nucleophilic substitution |
| S_{Ni} | internal return nucleophilic substitution |
| ssm | secondary-structure matching |
| TBAF | tetra- <i>n</i> -butylammonium fluoride |
| TBDMS | <i>tert</i> -butyldimethylsilyl |
| TEMPO | 2,2,6,6-tetramethylpiperidine-1-oxyl |
| TFA | trifluoroacetic acid |
| Tf | trifluoromethanesulfonate |
| Tf ₂ O | triflic anhydride |
| TfOH | trifluoromethanesulfonic acid |
| THF | tetrahydrofuran |
| TLC | thin layer chromatography |
| TMS | trimethylsilyl |
| TPR | tetratricopeptide repeats |
| Troc | 2,2,2-trichloroethyl-carbamate |
| TTBP | tris(tribromoneopentyl)phosphate |
| UDP | uridine diphosphate |
| [α] | specific rotation |
| λ_{max} | maximum absorption |
| °C | degree Celsius |

General Introduction

The work presented in this thesis was performed under guidance of Dr. Sébastien VIDAL conducted in Laboratoire de Chimie Organique 2 at Institut de Chimie et Biochimie Moléculaires et Supramoléculaires of Université Claude Bernard Lyon 1 and financially supported by Ministère de l'Enseignement supérieur et de la Recherche France. In 2006, a series of C-glycosyl ethylphosphonophosphate analogues of natural sugar donor were synthesized and evaluated as different glycosyltransferases inhibitors then published by our group. The present work was a continuation of this work. The aim of this project was to explore neutral sugar donor analogues of glycosyltransferase as inhibitors instead of the ionic natural substrates which are not capable of cell membrane penetration.

Compared with glycosidases, the development of inhibitors of glycosyltransferases was relatively slow due to more complex structures and catalytic mechanisms. The importance of glycosyltransferases in biology was presented and the development of glycosyltransferase inhibitors focused on galactosyltransferases (GalT) and *O*-linked *N*-acetyl-glucosaminyl transferase (OGT) was reviewed in **Chapter I**. Two types of nonionic inhibitors of GT with either pyridine moiety or amino-acid derivative as surrogate of the diphosphate unit of the natural UDP-sugar donors of GT were designed and synthesized. The synthetic part of these analogues was presented in **Chapters II** and **III**, respectively. The biological evaluation was performed on 6 glycosyltransferases. All the analogues synthesized were evaluated on 5 galactosyltransferases (β -1,4-GalT, α -1,4-GalT, α -1,3-GalT, GTB and a human blood group mutant AAGlyB). The best candidates were further studied with co-crystallization which gave information on the binding mode. Our designed “neutral” inhibitors of the pyridine surrogate type could chelate the manganese cation in the active binding site of the enzyme. The pyridine-containing analogues in the GlcNAc series as natural sugar donor analogues of UDP-GlcNAc were selected for *O*-linked *N*-acetyl-glucosaminyl transferase (OGT) assays, enzymatic assays and cell assays. The best inhibitors obtained from GalT and OGT assays were then submitted to an artificial cell membrane penetration test, lipid bilayer penetration test. The result revealed that the galactosyl pyridine containing derivative possessed a strong interaction with POPC while the glucose derivative did not. All the biological evaluation mentioned above was included in **Chapter IV**. An overall conclusion was given including possible directions for further optimization to obtain more potent glycosyltransferase inhibitors.

All the work present was finished within three years including two visits (nine weeks totally) to the Carlsberg Laboratory for biological evaluation. All the experiment details were mentioned in **Chapter V** and the literature references were listed afterwards.

Table of contents

| | |
|--|-----|
| Acknowledgement | 5 |
| List of Abbreviations | 7 |
| General Introduction | 9 |
| Table of contents | 11 |
| Résumé en français | 13 |
| Chapter I : Introduction – Glycosyltransferases and inhibitors of glycosyltransferases | 19 |
| I.1 Carbohydrates in biology | 21 |
| I.2 Glycosyltransferases | 22 |
| I.2.1 Structural features and classification | 23 |
| I.2.2 Catalytic mechanism | 24 |
| I.2.3 Glycosyltransferases in biology | 25 |
| I.3 Inhibitors of glycosyltransferases | 28 |
| I.3.1 Inhibitors of galactosyltransferases | 29 |
| I.3.2 Inhibitors of <i>O</i> -linked <i>N</i> -acetylglucosamine transferase (OGT) | 36 |
| I.4 Project aim | 38 |
| I.4.1 Synthesis of UDP-sugar analogues | 39 |
| I.4.2 Biological evaluations | 39 |
| Chapter II : Synthesis of neutral glycosyltransferase inhibitors - Pyridine as a pyrophosphate surrogate | 41 |
| II.1 Introduction | 43 |
| II.1.1 Chemical aspects | 44 |
| II.2 Investigation of glycosylation methods of a “basic” acceptor | 51 |
| II.2.1 Galactosylation | 53 |
| II.2.2 Modifications on the pyridine-based acceptor | 56 |
| II.2.3 <i>N</i> -Acetylglucosaminyl donors | 57 |
| II.2.4 Other glycosyl donors (Glc, Man, Fuc, Rha, Lac) | 59 |
| II.3 Synthesis of UDP-sugar analogues based on glycosylation and amide bond chemistries | 62 |
| II.4 Synthesis of UDP-sugar analogues based on azide-alkyne and amide bond chemistries | 65 |
| II.5 Conclusion | 69 |
| Chapter III : Design and synthesis of neutral glycosyltransferase inhibitors - Amino-acids as pyrophosphate surrogates | 71 |
| III.1 Galactosylation of serine-based acceptors | 74 |
| III.3 Synthesis of serine derivatives containing UDP-Gal mimetics | 75 |
| III.4 Conclusion | 82 |
| Chapter IV: Inhibition studies towards glycosyltransferases | 83 |
| IV.1 Introduction | 85 |
| IV.1.1 Radiochemical GalT enzymatic assays | 87 |
| IV.1.2 Cell assays | 87 |
| IV.1.3 Artificial cell membrane penetration test | 87 |
| IV.2 Results and discussion | 88 |
| IV.2.1 GalT inhibition studies | 88 |
| IV.2.2 OGT inhibition studies | 96 |
| IV.2.3 Evaluation of membrane permeation | 100 |

| | |
|---|-----|
| IV.3 Conclusion | 103 |
| General Conclusion | 105 |
| Perspectives | 107 |
| Chapter V : Experimental section | 109 |
| V.1 General methods. | 111 |
| V.2 Synthesis and characterization | 112 |
| V.3 Cloning, expression and purification of GTs | 186 |
| V.4 Enzymatic assays | 186 |
| V.5 Crystallization and structure refinement | 187 |
| V.6 Non-Linear Dixon plots and Michaelis-Menten plots | 189 |
| V.7 Cell assays | 195 |
| V.8 Permeation assays | 195 |
| V.9 Docking studies | 196 |
| Bibliography | 197 |

Résumé en français

Les saccharides sont présents à la surface de la cellule et dans le cytosol, libres ou associés à d'autres biomolécules. Ils jouent de nombreux rôles dans les organismes vivants et sont conjugués à d'autres biomolécules pour former des glycolipides ou des glycoprotéines. Ils sont notamment impliqués dans la transduction du signal, la circulation intracellulaire des protéines, l'adhésion ou la reconnaissance ou la différenciation cellulaire, le développement neuronal, l'inflammation, la réponse immunitaire, la métastase, mais aussi l'infection virale ou bactérienne (**Figure 1**). Au fur et à mesure des élucidations des rôles des saccharides, l'intérêt grandit en chimie, biochimie et biologie pour définir plus exactement le rôle d'un saccharide précis et pour examiner son potentiel thérapeutique.

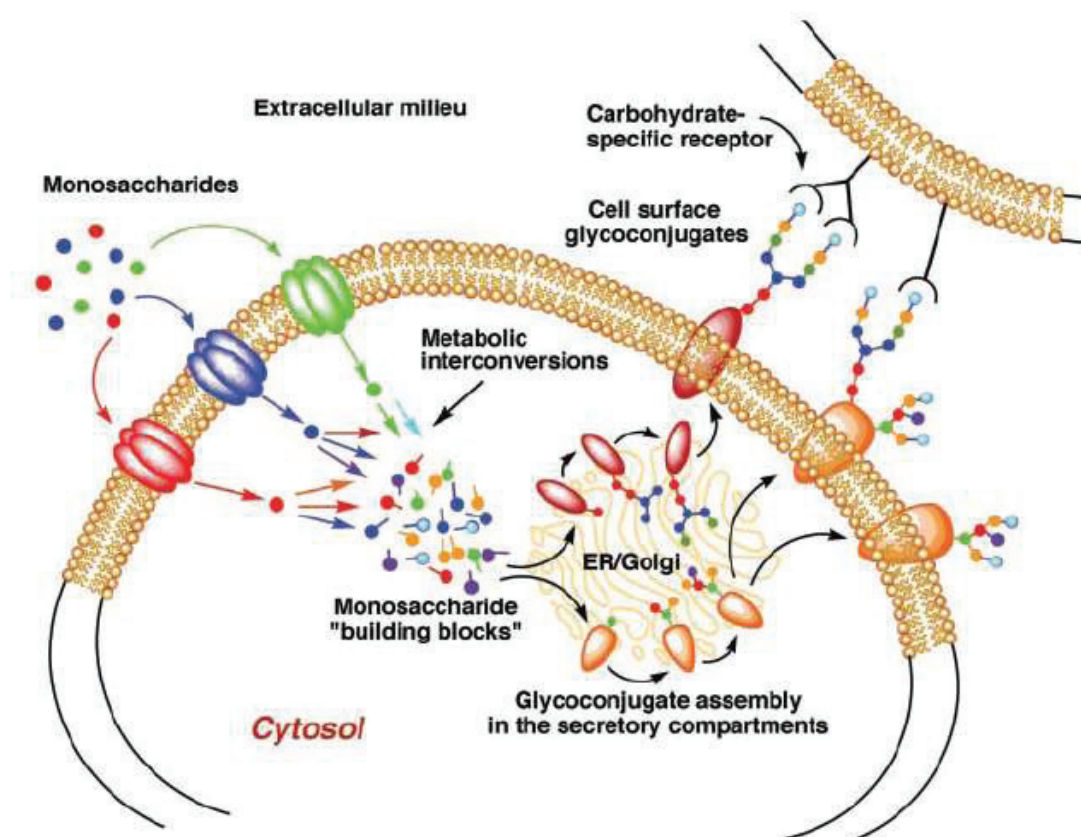


Figure 1. Implications des oligosaccharides dans divers processus biologiques.¹

La dégradation et la biosynthèse des oligosaccharides, polysaccharides et glycoconjugués est catalysée par les glycosidases et glycosyltransférases (GTs) respectivement. De nombreux travaux de recherche ont été consacrés au développement d'inhibiteurs de GTs. Ces inhibiteurs peuvent servir de sondes moléculaires pour étudier les fonctions biologiques des glycoconjugués et des GTs et envisager des applications biomédicales.

Les inhibiteurs de GTs peuvent être classés en quatre types: les analogues du donneur, analogues de l'accepteur, les analogues bi-substrat et les molécules identifiées par criblage à haut débit. Ce projet de thèse présente la conception, la synthèse, l'évaluation biologique et l'analyse structurale de deux types d'analogues du donneur. L'idée de base est de créer des analogues neutres de NDP-sucre (substrats naturels des GTs) utilisant un motif pyridine ou amino-acide en remplacement du pyrophosphate. La faible biodisponibilité des analogues

chargés (anioniques ou cationiques) de NDP-sucre suggère le développement d'analogues neutres pour fournir des inhibiteurs capables de traverser les membranes cellulaires et donc d'envisager des évaluations *in cellulo* ou *in vivo* et donc des applications fondamentales en biologie ou appliquées en médecine. Les galactosyltransférases (GalTs) et la *O*-linked *N*-acetylglucosamine transférase (OGT) récemment identifiée ont été sélectionnées comme cibles dans ce projet.

La pyridine et la sérine sont les deux motifs sélectionnés pour remplacer le groupement pyrophosphate (**Figure 2**). L'incorporation d'un motif pyridine devrait permettre de créer des interactions avec le métal (Mn^{2+}) présent dans le site catalytique de l'enzyme et aussi des liaisons hydrogène avec l'enzyme (**Figure 2A-D**). L'autre série d'analogues incorporant un amino-acide (**Figure 2E-F**) permet d'obtenir une fonction amine ou acide pour une diversification supplémentaire. L'introduction de plusieurs groupes fonctionnels devrait permettre là aussi de créer des interactions favorables avec le métal et l'enzyme. Les saccharides impliqués dans ces synthèses sont donc le galactose, la *N*-acétyl glucosamine et le glucose.

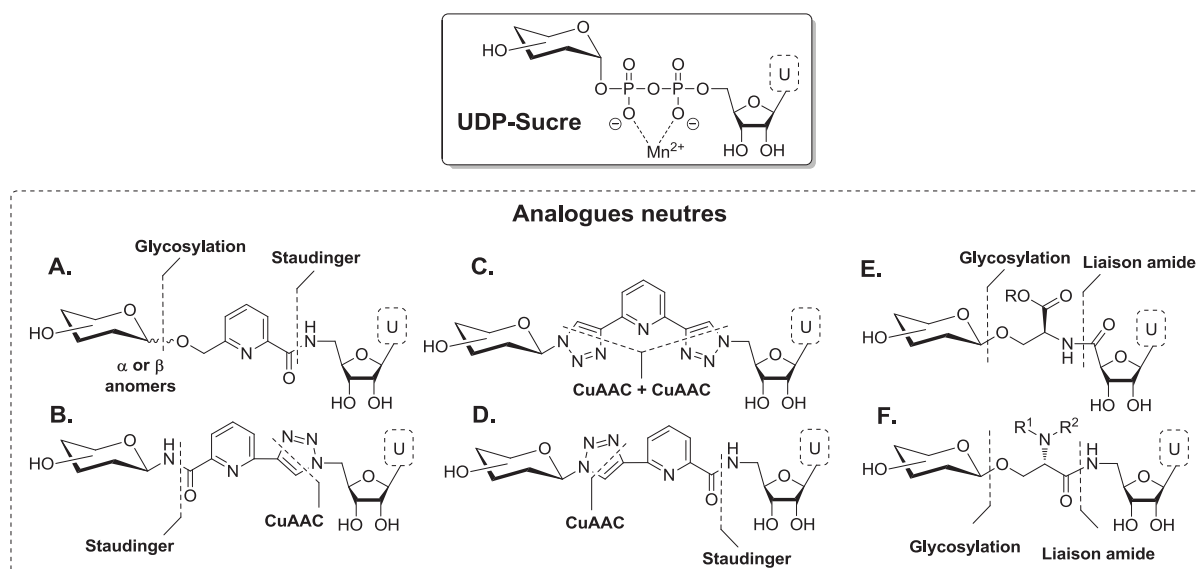


Figure 2. Structures et approches synthétique des analogues d'UDP-sucre.

La synthèse des inhibiteurs neutres de GTs s'effectue par une combinaison de liaison *O*-glycosidique, amide ou triazole. L'une des premières étapes de ces synthèses était la *O*-glycosylation d'un motif pyridine ou sérine qui a dû être étudiée en détail. Le 6-(hydroxyméthyl)picolinate de méthyle ainsi qu'un dérivé azido-sérine ont été choisis comme substrat de référence pour cette étude. Une série de 20 donneurs de glycosyle en série glucose, galactose, fucose, lactose, mannose, rhamnose and *N*-acétyl glucosamine et divers groupements activants de la position anomère (acétate, bromure, trichloracétimide, thiopyridine) ainsi qu'un nombre de conditions d'activation ont été évaluées (**Tableau 1**). Cette étude a permis d'identifier les conditions optimales de glycosylation pour divers monosaccharides et ont pu être appliquées pour la synthèse d'inhibiteurs de GTs.

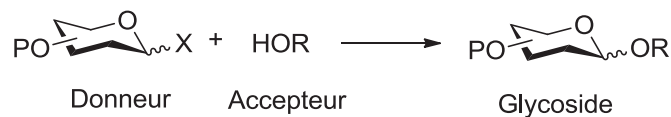
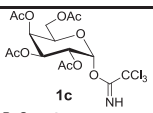
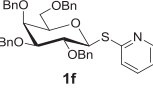
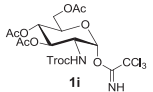
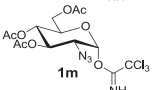
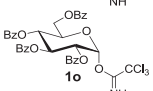
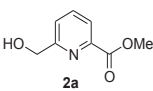
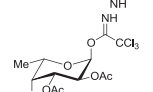
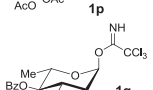
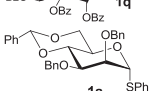
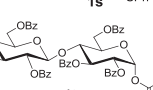
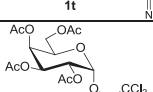
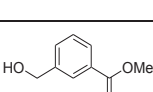
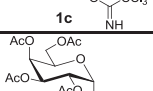
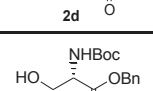
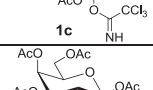
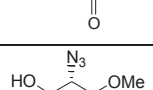


Tableau 1. Conditions optimales de glycosylation pour les motifs pyridine et sérine.

| Donneur | Accepteur | Rapport Donneur: Accepteur | Temp. Temps | Promoteur | Rendement Rapport α : β |
|---|---|----------------------------------|-----------------------------|---|--|
|  | | 1.5:1 | -20°C, 2 h | BF ₃ ·Et ₂ O (2 eq.) | 46% β |
|  | | 1:1 | 50°C, 78 h | MeI (4.5 eq.), 4Å MS | 75% α |
|  | | 1.1:1 | -20°C, 3 h | BF ₃ ·Et ₂ O (2 eq.) | 66% β |
|  | | 1.5:1 | -20°C, 2 h; rt, 16 h | BF ₃ ·Et ₂ O (4 eq.) | 82% 72:28 |
|  |  | 1.3:1 | -20°C, 22.5 h | TMSOTf (2 eq.), 4Å MS | 61% β |
|  | | 1.5:1 | -20°C, 2 h | BF ₃ ·Et ₂ O (2 eq.) | 39% β |
|  | | 1.3:1 | -20°C, 4 h | TMSOTf (0.8 eq.) | 66% α |
|  | | 1:1.15 | -60°C, 0.5 h; -78°C, 3 h | BSP (1.2 eq.), TTBP (1.5 eq.), Tf ₂ O (1.3 eq.), 1-octene (2 eq.) | 80% 19:81 |
|  | | 1:1 | -20°C, 4 h | BF ₃ ·Et ₂ O (2 eq.) | 51% β |
|  |  | 1:3 | -20°C, 1 h | BF ₃ ·Et ₂ O (0.2 eq.) | 79% β |
|  |  | 2.5:1 | -20°C, 9 h | BF ₃ ·Et ₂ O (0.5 eq.) | 15% β |
|  |  | 1.5:1 | 0°C, 17 h | SnCl ₄ (5 eq.)/ CF ₃ CO ₂ Ag (2.5 eq.) | 55% β |

La conjugaison du monosaccharide, du bras espaceur (pyridine ou sérine) et du nucléoside (uridine) utilisant des liaisons *O*-glycosidique, amide ou triazole a fourni une large famille inhibiteurs « neutres » de GTs (**Figure 3-4**).

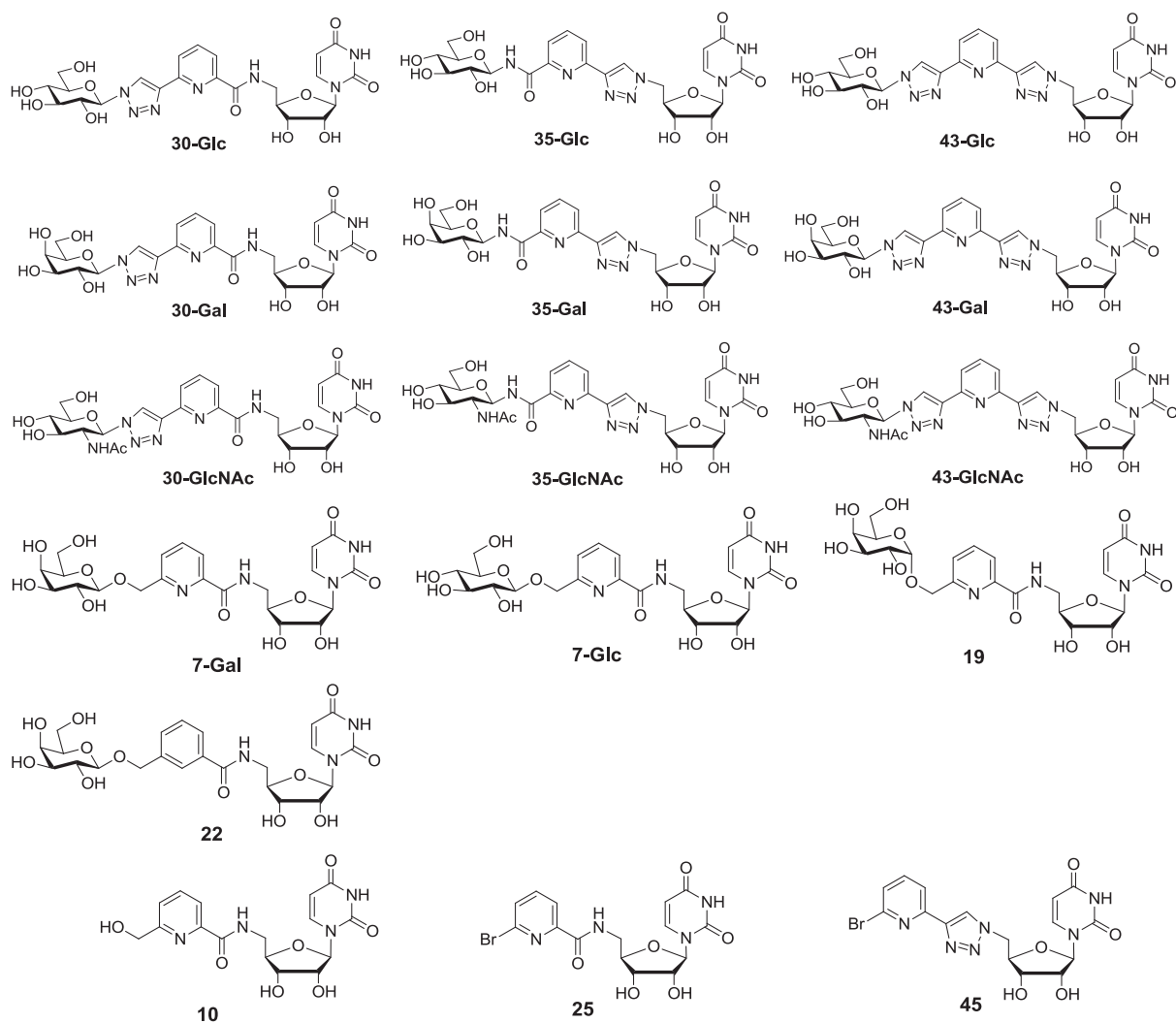


Figure 3. Structures des inhibiteurs « neutres » utilisant la pyridine pour remplacer le motif pyrophosphate et testés pour l'inhibition de GTs.

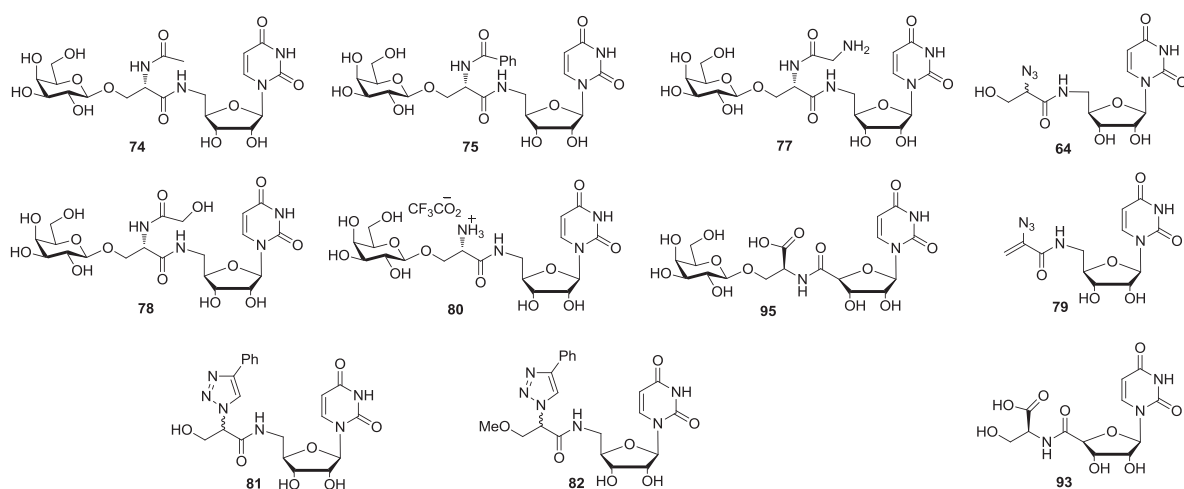


Figure 4. Structures des inhibiteurs « neutres » utilisant la sérine pour remplacer le motif pyrophosphate et testés pour l'inhibition de GTs.

L'évaluation biologique des analogues de l'UDP-Gal et de l'UDP synthétisés a été effectuée sur 5 GalTs incluant la β -1,4-galactosyltransférase (β -1,4-GalT), la α -1,4-galactosyltransférase (α -1,4-GalT), la α -1,3-galactosyltransférase (α -1,3-GalT), la human blood group B

galactosyltransférase (GTB), et une galactosyltransférase mutante (AAGlyB) mais aussi la *O*-linked *N*-acetylglucosamine transférase (OGT).

La première série d'inhibiteurs basés sur le motif pyridine a montré de meilleures inhibitions dans le cas des *O*-glycosides que pour les composés incorporant un lien triazole. Le meilleur inhibiteur **7-Gal** a une valeur d'IC₅₀ de 152 μM pour la β-1,4-GalT. Une étude cristallographique de trois inhibiteurs co-cristallisés dans le site catalytique de l'enzyme mutante AAGlyB a démontré l'intérêt du motif pyridine qui oriente le saccharide dans une direction totalement différente du substrat naturel (UDP-Gal) de l'enzyme mais qui permet aussi de chélater le cation métallique même s'il est déplacé de quelques angströms de sa position initiale (**Figure 5**).

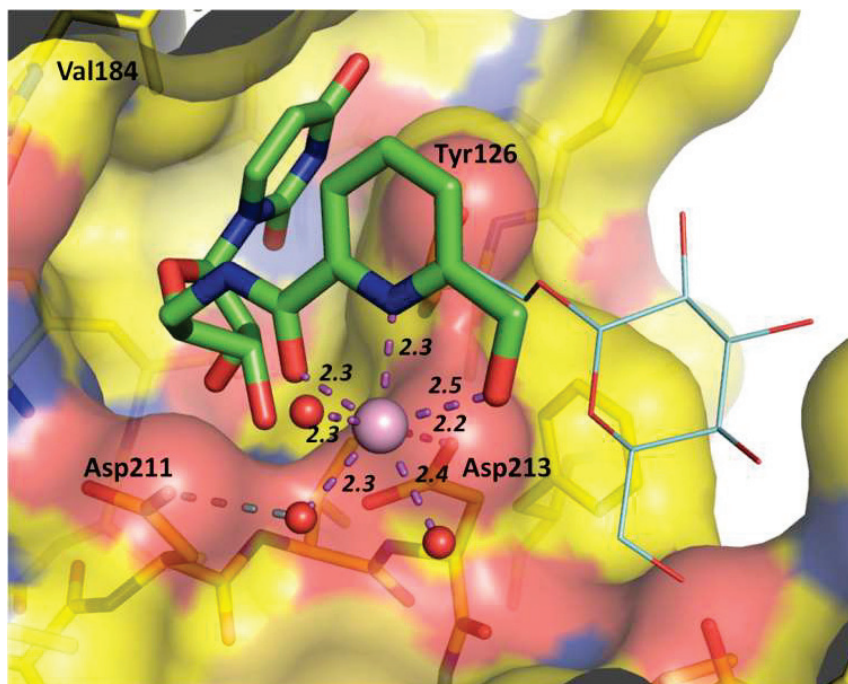


Figure 5. Coordination du manganèse (sphère rose) dans le complexe **7-Glc**/AAGlyB (PDB_ID:4KC1). **7-Glc** est représenté en vert. Une autre conformation pour le composé **19** est représentée en cyan.

Huit inhibiteurs incorporant le motif pyridine ont été évalués pour leur inhibition de l'OGT. L'inhibition de ces composés est très modeste et le meilleur composé **35-Glc** a présenté une constante d'inhibition (K_i) de 422 μM. L'inhibition de l'OGT lors de tests cellulaires n'ont pas donné de résultats positifs indiquant que les inhibiteurs n'ont pas d'effet au niveau cellulaire.

Des études complémentaires de "docking" moléculaire ont montré que des interactions étaient bien créées entre les motifs pyridine, triazole et le squelette de l'enzyme. Là encore, le monosaccharide pointe dans une direction différente de sa position naturelle et n'interagit presque pas avec l'enzyme (**Figure 6**). Ces résultats confirment les observations faites sur les études cristallographiques avec AAGlyB.

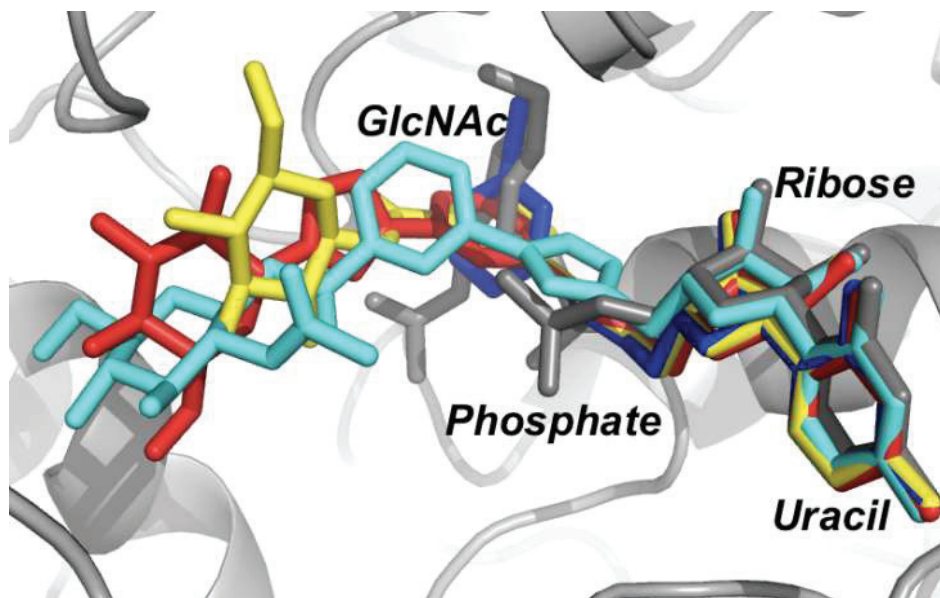


Figure 6. Superposition des composés et comparaison avec le substrat naturel UDP-GlcNAc complexés avec l’OGT humaine (gris: UDP-GlcNAc; rouge: **43-Glc**; bleu: **45**; jaune: **35-Glc**; cyan: **35-GlcNac**).

L’étude d’inhibition enzymatique de la seconde série d’inhibiteurs incorporant la sérine a révélé que la nature du lien entre le saccharide et le nucléoside est très important afin d’orienter de façon optimale l’inhibiteur dans le site catalytique. Quasiment tous les composés sont de faibles inhibiteurs (**74**, **75**, **77**, **78**, **80**, **92**) et la meilleure inhibition a été mesurée pour le composé **80** avec 38% inhibition pour AAGlyB à 1 mM.

Le concept d’inhibiteur “neutre” au lieu d’inhibiteurs chargés pour une meilleure biodisponibilité et donc de perméation cellulaire a pu être vérifié en utilisant un modèle utilisant les liposomes de POPC pour les deux meilleurs inhibiteurs de GalT (**7-Gal**) et de l’OGT (**35-Glc**). Malgré leur similarité structurale, les deux composés ont donné des résultats différents. Le composé **7-Gal** a présenté une forte affinité pour la membrane de POPC du liposome sans pour autant pouvoir la traverser alors que le composé **35-Glc** ne s’est pas associé au liposome.

Les différents résultats biologiques obtenus pour ces composés ont fourni des informations importantes de relation structure-activité pour la conception rationnelle d’une nouvelle génération d’inhibiteurs de GTs. Des améliorations sont proposées sur la base de la première famille d’analogues utilisant le motif pyridine et en tenant compte des aspects conformationnels des molécules ciblées pour obtenir des interactions optimales avec les enzymes et donc des inhibiteurs potentiellement puissants et sélectifs.

Chapter I : Introduction – Glycosyltransferases and inhibitors of glycosyltransferases

Chapter I : Introduction – Glycosyltransferases and inhibitors of glycosyltransferases

I.1 Carbohydrates in biology

Carbohydrates are present at the cell surface and within the cell, dissociated or conjugated. These carbohydrates play numerous and important roles in living organisms. Glucose (**Figure I-1.a**), a 6-carbon monosaccharide or hexose, is the major and direct energy source for organism metabolism. Ribose and the related 2-deoxyribose (**Figure I-1.b**), 5-carbon monosaccharides or pentoses, are building blocks of RNA and DNA respectively, which take and transmit hereditary information. Polysaccharides, which consist of repeated monomer units joined by glycosidic bonds, serve as energy storage (e.g. glycogen in liver and muscle cells of humans) and as structural components (e.g. cellulose in plants) in living organisms.

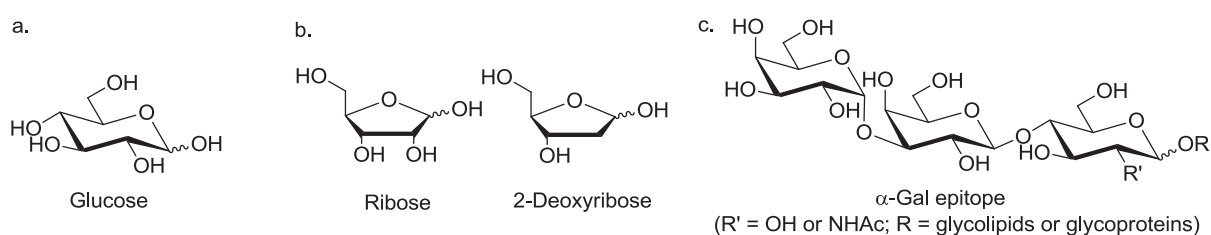


Figure I-1. Structure of glucose, ribose, deoxyribose and α -Gal epitope

It is notable that most of the carbohydrates present in living organisms are conjugated to other important biomolecules to form glycolipids or glycoproteins. These glycoconjugates are involved in numerous biological processes (**Figure I-2**), such as signal transduction, intracellular trafficking of proteins, cell adhesion, cell recognition, cell differentiation, development of the neuronal network, inflammation, immune response, metastasis and bacterial infection.¹⁻⁴ For example, to solve the worldwide shortage of organs for clinical implantation, xenotransplantation from a pig or baboon is one of the solutions, which is aimed at treating patients who have life-threatening and debilitating illnesses with cells or tissues. Whereas the α -Gal epitope (**Figure I-1.c**) sets a limit for its real clinical application, the α -gal epitope is abundantly synthesized on glycolipids and glycoproteins in non-primate mammals and New World monkeys. In contrast, in humans, apes and Old World monkeys the gene to generate the related enzyme that could catalyze the biological synthesis was inactivated, which results in the absence of this epitope and, instead, anti-Gal antibody is produced. The subsequent immune response of the antibody, in some transplantation cases, may result in the immediate death of the recipient. A study demonstrated that gene knockout pigs may avoid this immunological problem.⁵

As more and more carbohydrates related biological processes are elucidated, there is great interest in biology, biochemistry and chemistry to define the exact biological roles of a given carbohydrate and examine its potential therapeutic applications. After the development of proteomics and genomics, glycomics appear as the next broad scientific challenge to the realm of scientific research.⁶⁻⁸

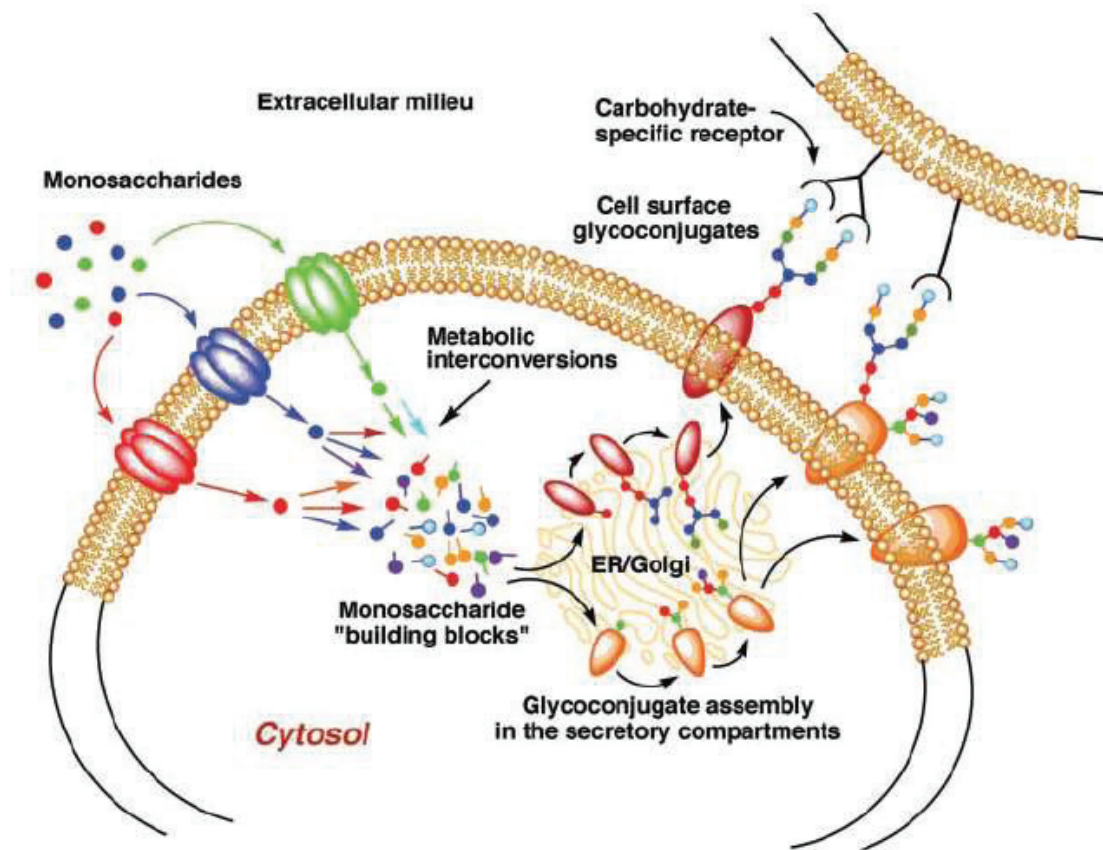


Figure I-2. Importance of glycoconjugates in biological processes.¹

I.2 Glycosyltransferases

Glycosyltransferases are ubiquitous enzymes that catalyze the transfer of sugar moieties from activated donor molecules to specific acceptor molecules, either with retention or inversion configuration of the anomeric carbon.⁹ The donor substrate of glycosyltransferases can be sugar nucleotide derivatives (e.g. UDP-Gal, CMP-NeuAc) and lipid phosphates (e.g. polyprenol phosphates, sugar-1-phosphates). Nucleotide sugar-dependent glycosyltransferases are termed as Leloir enzymes, in honor of 1970² Nobel Prize winner Luis F. Leloir, the scientist who discovered sugar nucleotides. In contrast, the non-Leloir enzymes may utilize lipid phosphates and other glycosides as donors. Leloir enzymes are in charge of most of the glycoconjugates synthesis in cells, especially in mammals.¹⁰ Among an extensive range of nucleotide sugar donors utilized by organisms, only 9 sugar nucleotide donors are used by mammals (**Figure I-3**). The acceptor substrates of glycosyltransferases have huge varieties, that can be other sugars, lipids, proteins or nucleic acids.¹¹ For metal-dependent GTs of the GT-A fold, the pyrophosphate moiety of the donor interacts with cations (e.g., Mn^{2+} or Mg^{2+}) with coordination to two aspartate residues within a DXD (aspartate-any residue-aspartate) motif. The metal such as magnesium or manganese assists binding to the (di)phosphate leaving group and is essential for the activity of the enzyme. Also, it is known that some glycosyltransferases (e.g. OGT) exhibit different catalytic modes which do not require a metal.

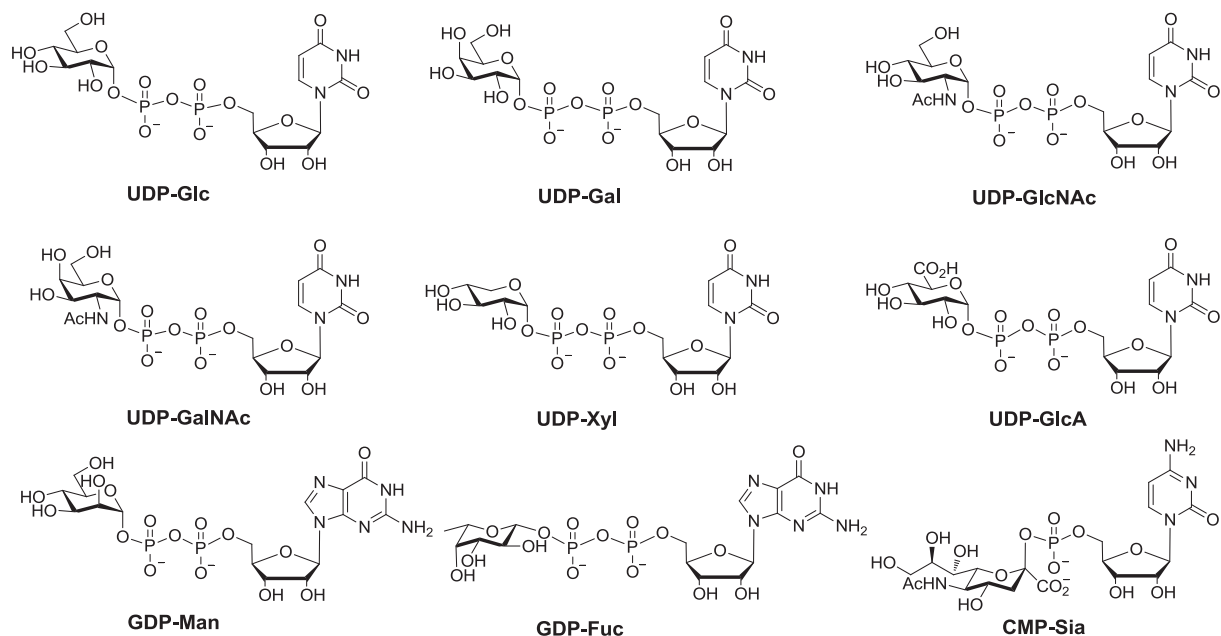


Figure I-3. 9 Sugar nucleotide donors used by mammals.

I.2.1 Structural features and classification

Although glycosyltransferases utilize considerable diversity of donors or acceptors and exhibit product specificity, the 3D structures of GT are highly conserved.¹¹ The CAZy database proposes a continuously updated classification of glycosyltransferases based on the sequence of the enzymes.^{9, 12} A hierarchical system with an increasing functional predictive power from folds, clans, families and subfamilies is presented. 94 Distinct families have been listed in CAZy database up to May 2013.¹³ The large size of the GT family also shows the potential infinite diversities of glycosylated products in Nature.

The reported glycosyltransferase structures have been classified into three folds called GT-A, GT-B and GT-C (**Figure I-4**). The first 3-D structure for GT-A fold was reported for SpsA, an inverting enzyme from *Bacillus subtilis*.¹⁴ The overall architecture of the GT-A fold is composed of two tightly associated $\beta/\alpha/\beta$ domains, the sizes of which may vary slightly leading to the formation of a continuous central β -sheet (**Figure I-4.a**). The first determined 3-D structure for GT-B fold was reported in 1994 for a DNA-modifying β -glucosyltransferase from bacteriophage T4.¹⁵ Like the GT-A fold, the architecture of GT-B enzymes consists of two $\beta/\alpha/\beta$ Rossmann-like domains. However, the two domains are less tightly associated and face each other with the active-site lying within the resulting cleft (**Figure I-4.b**). The third glycosyltransferase fold termed as GT-C was identified in 2008 as a soluble C-terminal domain of the *Pyrococcus furiosus* oligosaccharyltransferase STT3.¹⁶ It is a novel architecture with α -helical domain surrounded by three β -sheet rich domains (**Figure I-4.c**). This structure weakens the value of the GT-C classification because neither the catalytic activity of this truncated protein nor the active site of the soluble C-terminal domain were indicated. GT-A and GT-B folds are the usually adopted folding form according to X-ray structures that have been resolved. It should be noted that not all the enzymes adopting a GT-A or GT-B fold are glycosyltransferases but enzymes with other biological functions.

There is no correspondance relation between the overall fold of the enzyme and the stereochemical outcome of the enzymatic reaction.

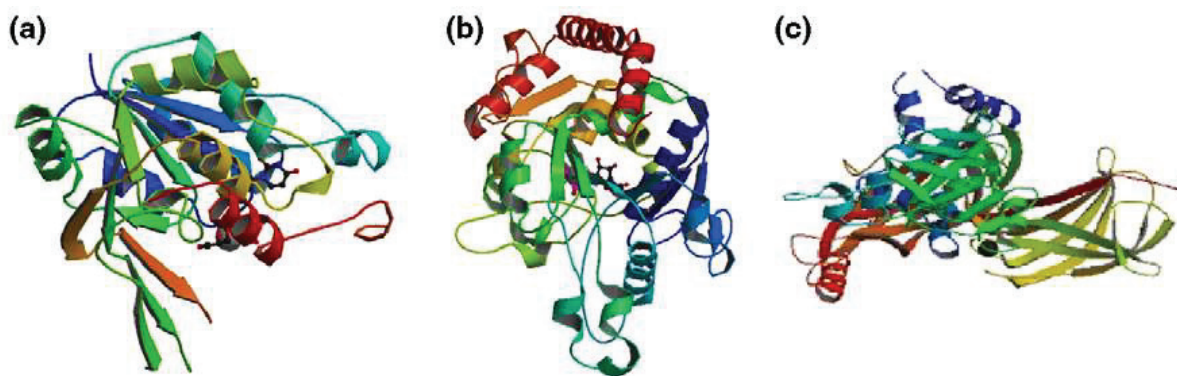


Figure I-4. General types of folds for classification of glycosyltransferases: (a) GT-A, (b) GT-B, and (c) GT-C.¹⁷

I.2.2 Catalytic mechanism

Depending on the stereochemical outcome of the enzymatic reactions with respect to the substrates (**Figure I-5**), the families of glycosyltransferases can also be classified into four different clans,⁹ either retaining or inverting configuration at the anomeric center.¹⁸

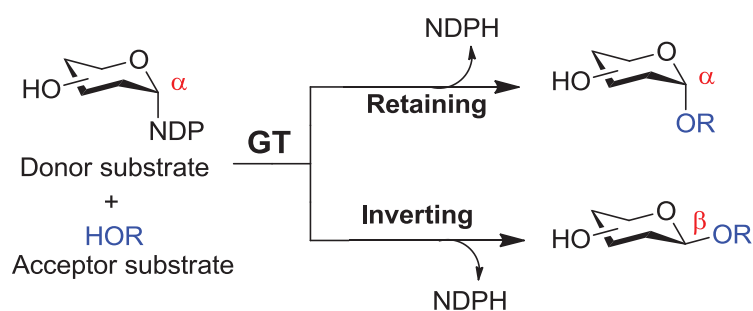


Figure I-5. Enzymatic reaction with either inverting or retaining glycosyltransferases.

The mechanism of inverting glycosyltransferases is suggested to be a direct S_{N2} -like displacement. The amino-acid chains in the catalytic site deprotonate the incoming acceptor substrate, assisting the nucleophilic attack from the opposite side of the anomeric center of the sugar donor (**Figure I-6a**).

No consensus for the mechanism of retaining glycosyltransferases has been reached but rather there are two main mechanisms proposed: double-displacement ($2 \times S_{N2}$) and internal return (S_{Ni}). Theoretically, both pathways are possible and the S_{Ni} pathway provides more experimental support.¹⁹⁻²⁰ The double-displacement mechanism involves a covalent glycosyl-enzyme intermediate and two subsequent nucleophilic displacements each occurring with inversion of configuration at the anomeric carbon and therefore leading to an overall retention of configuration (**Figure I-6b**). The other hypothesis is a S_{Ni} mechanism in which the enzyme shielding on the opposite face of the anomeric center prevents an inverting nucleophilic attack while the oxygen atom of phosphate leaving-group acts as a base to deprotonate the acceptor. Via an enzyme-mediated intermediate, the nucleophilic oxygen atom of the acceptor attaches to the anomeric carbon on the same side after phosphate oxygen leaves, resulting in a retention configuration at the anomeric carbon in the glycoside (**Figure I-6c**).

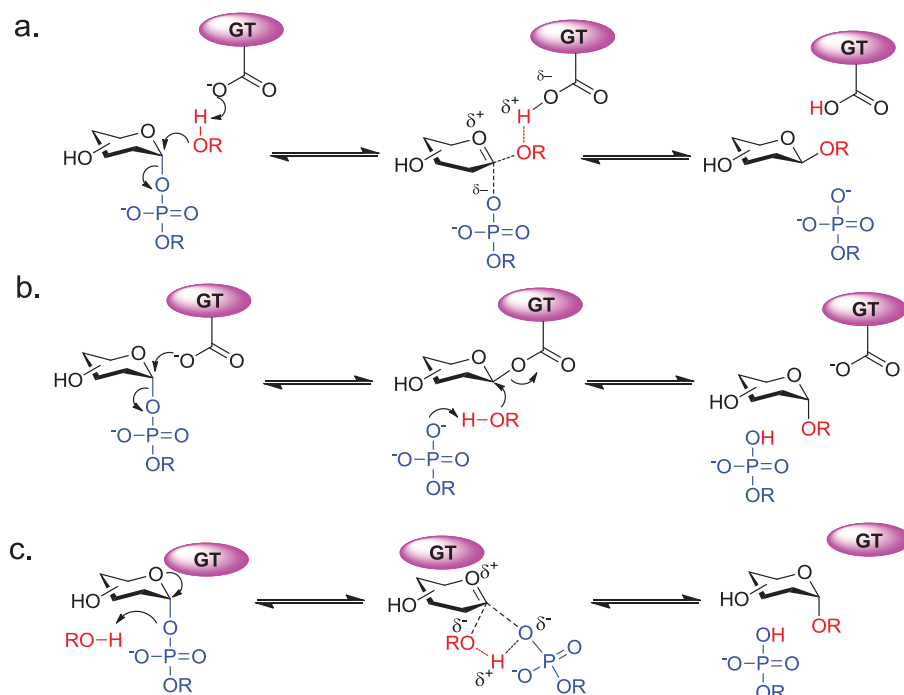


Figure I-6. Proposed mechanism for (a) inverting glycosyltransferases (b) retaining glycosyltransferases -- double-displacement mechanism and (c) retaining glycosyltransferases -- internal return mechanism.¹⁸

I.2.3 Glycosyltransferases in biology

Despite the considerable diversity of carbohydrate derivatives in living organisms, the degradation and biosynthesis of these oligosaccharides, polysaccharides and glycoconjugates are catalyzed by glycosidases (also called glycoside hydrolases or glycosyl hydrolases) and glycosyltransferases (GT). It is reported that glycosyltransferases represent approximately 1-2% of an organism's gene products.¹¹ For example, in the human genome, more than 250 glycosyltransferases are encoded while in the model plant, *Arabidopsis thaliana*, approximately 450 genes are related to glycosyltransferases.¹⁷ Although there is a myriad of GT, several of them should be particularly mentioned which are the targets of our synthesized inhibitors and have been tested in our project.

I.2.3.1 β -1,4-Galactosyltransferase

β -1,4-Galactosyltransferase (β -1,4-GalT) is an inverting enzyme catalyzing the transfer of galactose from UDP-galactose (UDP-Gal) to the 4-position of *N*-acetylglucosamine residues to form a LacNAc epitope (**Figure I-7**).²¹ β -1,4-GalT is involved in the biological synthesis of diversified glycoconjugates and it is probably the most well studied enzyme in synthesis and substrate specificity.²² Since the recombinant form of β -1,4-GalT from bovine and human origins are commercially available, it is now used as a model for the design of GT inhibitors.

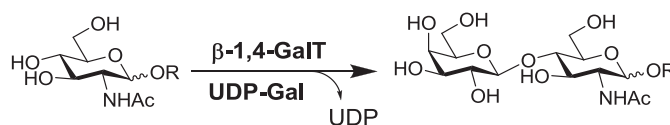


Figure I-7. Enzymatic-catalyzed glycosylation using β -1,4-galactosyltransferase (β -1,4-GalT).

I.2.3.2 α -1,4-Galactosyltransferase

α -1,4-Galactosyltransferase (α -1,4-GalT) derived from *Neisseria meningitidis* is responsible for forming a lipooligosaccharide in biosynthesis by transferring an α -galactose from active donor UDP-Gal to a lactose terminal acceptor (**Figure I-8**). One of the crucial biochemical products is glycosphingolipid globotriaosylceramide (Gb3, CD77 or P^k) which is synthesized by addition of a galactose to lactosylceramide via α -1,4-GalT (**Figure I-9**). The glycosphingolipid globotriaosylceramide plays an important role in disease spreading process, such as bacterial *Haemophilus influenza* infection.²³⁻²⁵

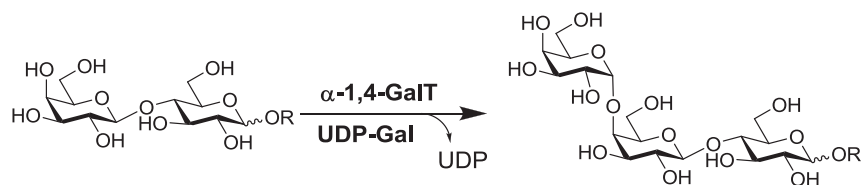


Figure I-8. Enzymatic-catalyzed glycosylation using α -1,4-galactosyltransferase (α -1,4-GalT).

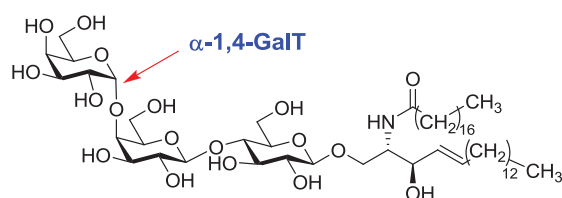


Figure I-9. Structure of glycosphingolipid globotriaosylceramide.

I.2.3.3 α -1,3-Galactosyltransferase

α -1,3-Galactosyltransferase (α -1,3-GalT) is a retaining transferase catalyzing the α -galactosylation at the 3-OH position of a terminal β -linked galactose using UDP-Gal as an activated donor (**Figure I-10**). The resulting α -Gal epitope bearing a Gal α -(1,3)-LacNAc-OR terminal (**Figure I-1. c**) is believed to be the main barrier in xenotransplantation which may cause hyperacute rejection.⁵

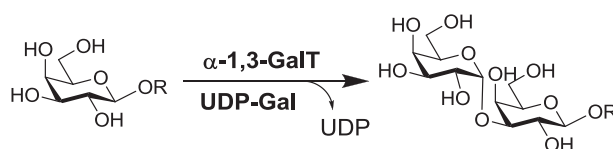


Figure I-10. Enzymatic-catalyzed glycosylation using α -1,3-galactosyltransferase (α -1,3-GalT).

I.2.3.4 Human blood group B galactosyltransferase

Human blood group B galactosyltransferase (GTB) is a retaining enzyme responsible for generating blood group B structure Gal α -(1,3)-[Fuc α -(1,2)]-Gal β -OR (where R is a glycoprotein or glycolipid) by transferring an α -galactose from active donor UDP-Gal to H-antigen disaccharide (**Figure I-11**).²⁶ In human ABO(H) blood group system, humans encoded with gene for GTB have blood group B-antigen associated with anti-A antibody, those with GTA generate blood group A-antigen associated with anti-B antibody. The coexistence of antigen and antibody blocks blood transfusion between different blood types.

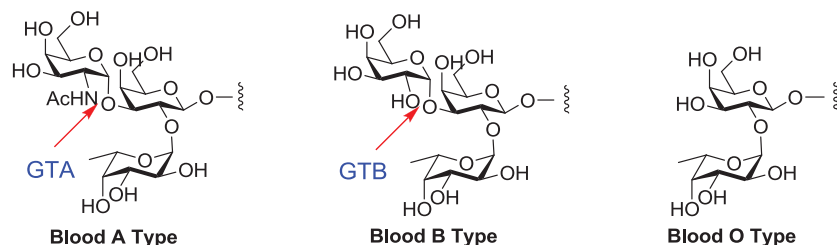


Figure I-11. Biofunction of human blood group galactosyltransferase and structure of human blood type.

I.2.3.5 Human blood group glycosyltransferase mutant (AAGlyB)

AAGlyB is a mutant of the wild type human blood group glycosyltransferase. The human blood group A and B glycosyltransferases are highly homologous differing in only four critical amino acid residues which are Arg/Gly176, Gly/Ser235, Leu/Met266, and Gly/Ala268, respectively. The name of the mutant AAGlyB gives a clue of the mutant fashion by keeping the first two amino acid residues from GTA and inherit amino acid residue 268 from GTB while mutate amino acid residue 266 to glycine which gives AAGlyB (Arg176, Gly235, Gly266, Ala268).²⁷ As for biochemical functions, GTA and GTB catalyze the final addition of a sugar moiety to H-antigen acceptors to produce blood group A and B epitopes. Different from GTB which uses UDP-Gal as a donor substrate transferring α -galactose, GTA utilizes UDP-GalNAc as the donor substrate and transfers GalNAc to the acceptors through an α -linkage. The mutant AAGlyB has dual specificity towards UDP-Gal and UDP-GalNAc and has equal efficiency to generate blood group A and B structures (**Figure I-12**).²⁸

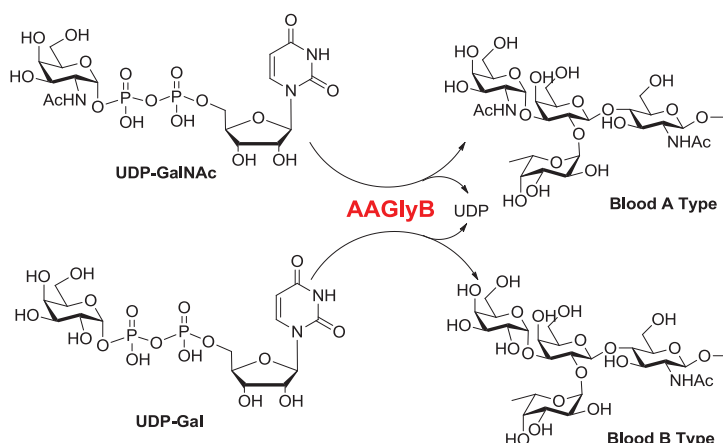


Figure I-12. Biofunction of human blood group galactosyltransferase mutant (AAGlyB).

I.2.3.6 *O*-linked *N*-acetylglucosamine transferase

A reversible *O*-GlcNAcylation of various nuclear and intracellular proteins is mediated by two enzymes, *O*-linked-*N*-acetyl-glucosaminase (OGA) and *O*-linked *N*-acetyl-glucosaminyl transferase (OGT) (**Figure I-13**). The *O*-linked *N*-acetylglucosamine transferase (OGT) is an inverting enzyme that uses UDP-GlcNAc as an active donor to transfer a GlcNAc residue to the side chain amino-acids serine or threonine of proteins.

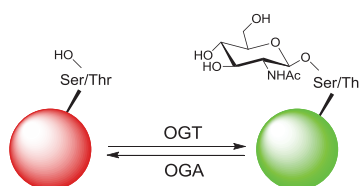


Figure I-13. Reversible *O*-GlcNAcylation mediated by OGA and OGT.

Further observation on OGT targeted proteins indicate that they are both glycosylated and phosphorylated and it exists that direct cross-talk between dynamic *O*-GlcNAc glycosylation and kinase/protein phosphatase mediated phosphorylation.²⁹⁻³⁰ The modification site may be reciprocal same-site or adjacent-site. A model taking two active sites indicates that the cross talk between glycosylation and phosphorylation may create four functional states of the target proteins (P+/G+; P+/G-; P-/G+; P-/G-) (**Figure I-14**). And it should be mentioned that observation on the *O*-GlcNAc-targeted proteins reveals that multiple sites are active towards *O*-GlcNAcylation and phosphorylation increasing the complexity in a real interaction.³¹

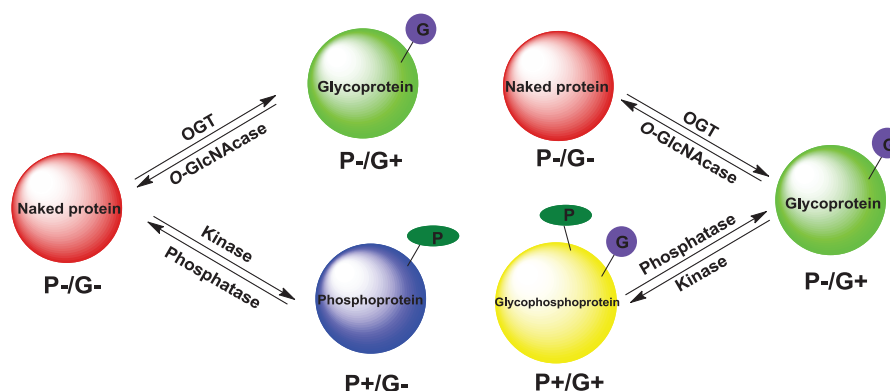


Figure I-14. Complex interaction between *O*-GlcNAc glycosylation and phosphorylation.³¹

O-GlcNAc occurs in the cytosol as other GTs, but also in the nucleus. More than 1,000 substrate proteins have been identified to date and *O*-GlcNAcylation is involved in almost all aspects of cellular metabolism.³¹⁻³² A recent work describing crystal structures of human OGT has given insight into the catalytic domain of this enzyme.³³ His498 is proposed to act as a catalytic base deprotonating the hydroxyl group of serine or threonine residue of the glycosylated protein while Lys 842 from α -side stabilizes and activates the UDP leaving group resulting the *O*-GlcNAc glycosylation occurs on the β -side (**Figure I-15**).³³ OGT has now been shown to play important roles in cancer,³⁴⁻³⁵ Alzheimer's disease³⁶⁻³⁹ and diabetes³⁹⁻⁴⁰ and being a potential therapeutic target.

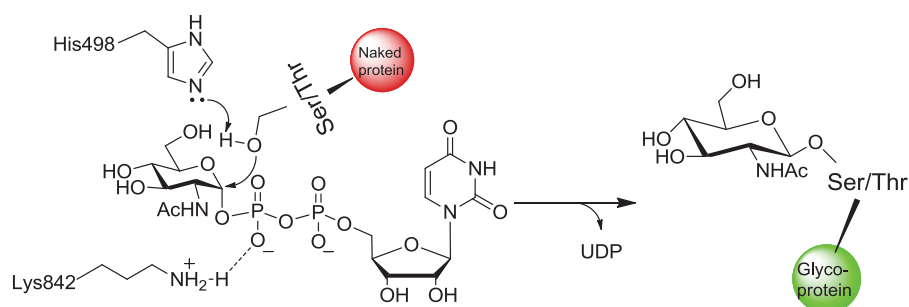


Figure I-15. Proposed catalytic mechanism for the human OGT.^{18, 33}

I.3 Inhibitors of glycosyltransferases

Based on the roles of carbohydrates in living organisms in numerous biological processes, there is great interest in determining the exact implications of a given glycoconjugate in these processes. Glycosyltransferase inhibitors may serve as molecular probes for investigations of biological functions of glycoconjugate and selective glycosyltransferase inhibitors may have biomedical applications. An analysis of the FDA Orange Book in 2005 indicates that 317

marketed drugs are enzyme inhibitors. Among the 317 marketed drugs, 71 enzymes are targeted and two GT inhibitors are found which are Ethambutol, an inhibitor of mycobacterial arabinotransferases used as an antibacterial drug, and Miglustat, a ceramide glucosyltransferase inhibitor used for treatment of Gaucher's disease (**Figure I-16**).⁴¹

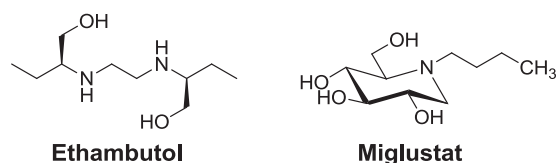


Figure I-16. Structure of Ethambutol and Miglustat.

Several reviews have been recently reported for the structure and mechanism elucidation of GT.^{11, 18, 42-43} Design of inhibitors of glycosyltransferases has been accelerated with the developments in glycobiology presenting oligosaccharides as active species (eg. blood groups, antigens) rather than "decorations" of biomolecules. Several reviews on the development of GT inhibitors have been reported recently^{17, 44} according to the biological functions of emerged inhibitors,⁴⁵⁻⁴⁷ classification of inhibitors by structural features,⁴⁸⁻⁵¹ or focusing on iminosugar-based inhibitors.⁵²⁻⁵⁴

Early research efforts on GT inhibitors could be traced back to 1987 that sugar methylenediphosphonates and nucleoside sugar phosphonic derivatives were synthesized and evaluated as GT inhibitors.⁵⁵⁻⁵⁶ It should be specially mentioned that the comparison of compounds' potency from one report to another is risky since it is demonstrated that assays conditions (pH and ionic strength) may influence the results⁵⁷⁻⁵⁸ needless to say the substrates concentrations will affect the experimental IC₅₀ values measured. With regard to the choice of individual targets, among different types of GT, a representative type of GT named galactosyltransferases (GalT) and a recently identified highly valuable *O*-linked *N*-acetylglucosamine transferase (OGT) were selected. According to structure features, inhibitors could be classified into four types, donor substrate analogues, acceptor substrate analogues, bi-substrate analogues and small molecule inhibitors identified from library screening approach or high-throughput screening. The examples presented below are not an exhaustive review of the literature but rather a focused selection of inhibitors based on the enzyme and inhibitor structural features described.

I.3.1 Inhibitors of galactosyltransferases

The UDP-Gal donor substrate of GalT is composed of three parts: a galactose moiety, a diphosphate linker and uridine. Design of donor substrate analogues could be based on modifications of either one or several simultaneous modifications.

I.3.1.1 Modification on the carbohydrate moiety

Using carbocyclic to mimic glycosyl ring is one of the examples of modification on the carbohydrate moiety (**A2**, **Figure I-17**).⁵⁹ The analogue was tested as an effective inhibitor of β -1,4-GalT and verified as a competitive inhibitor of donor substrate with a K_i value of 58 μ M. A series of mono-*O*-methylated UDP-Gal analogues were synthesized by Tsuyoshi Endo *et al.*⁶⁰ Among them, the 2-*O*-methylated UDP-Gal analogue **A3** (**Figure I-17**) showed a good inhibition of β -1,4-GalT with a calculated K_i value of 20 μ M but was also a good donor

substrate of this transferase. This showed a good compatibility of this enzyme towards modification at the 2-position.

Fluorination is another approach to obtain valuable analogues for enzymatic evaluation.⁶¹⁻⁶³ Fluorinated molecules (e.g. **A1**, **Figure I-17**) are attractive for the study of interactions between the fluorine atom and an enzyme in order to better elucidate enzymatic mechanisms.⁶⁴ A compound with fluoro-substitution at 2-position (**A4**, **Figure I-17**) was prepared by chemoenzymatic method and showed inhibitory effect on β -1,4-GalT and α -1,3-GalT with K_i values in the micromolar range.⁶⁵⁻⁶⁶ Similar fluoro-substitution at the 6-position, the compound **A5** (**Figure I-17**) showed 75% inhibition using a 10-fold molar excess relative to UDP-Gal for both β -1,4-GalT and α -1,3-GalT⁶⁷ which indicated that the presence of fluorine at C-6 does not affect the binding to enzymes.

Based on docking simulation, an analogue with a 6-substitution of a tethered naphthyl moiety (**A6**, **Figure I-17**) was designed and evaluated as human recombinant galactosyltransferase (α GalT1) inhibitor.⁶⁸ It was found that the synthesized analogue **A6** is a potent inhibitor (K_i 1.86 μ M) with respect to UDP-Gal (K_m 4.91 μ M) and mass spectrometry analysis revealed that the inhibitor could create a covalent bond with the indole ring of Trp310 located near the active site therefore blocking the binding of the respective acceptor substrate.

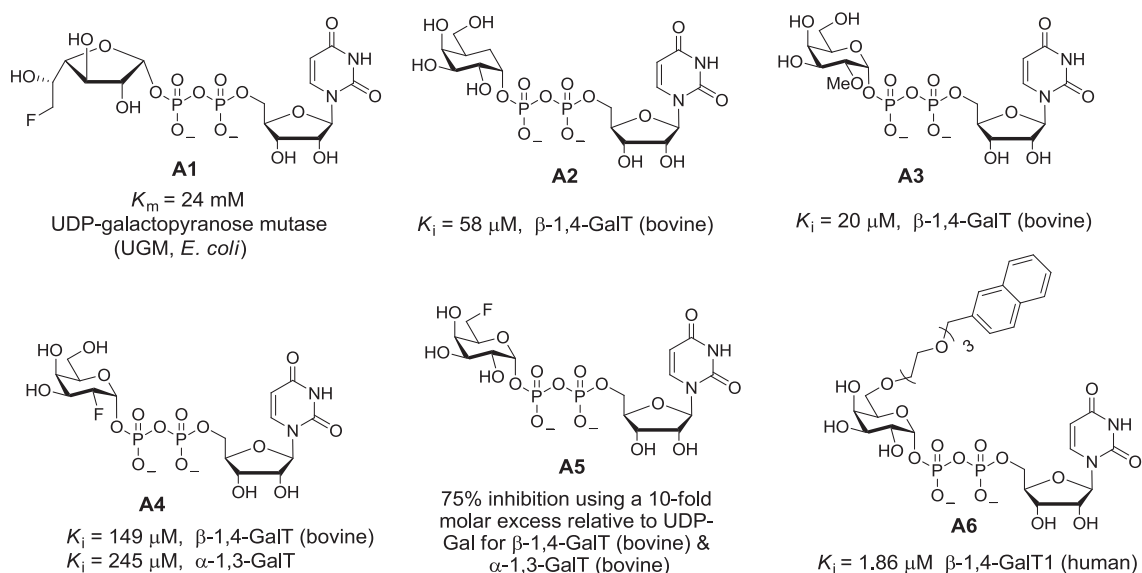


Figure I-17. Representative GalT inhibitors with modification on sugar moiety.

Iminosugar-based mimetics represent a large family in inhibitors design which has been reviewed.⁵²⁻⁵⁴ A simple five-membered galacto-iminocyclitol **B1** (**Figure I-18**) was indicated to have inhibitory activity against β -1,4-GalT.^{57, 69} Yong Jip Kim *et al.*⁷⁰ synthesized a series of UDP-galactose mimetics, using galactose-type iminosugar as a replacement of the galactose residue, a vicinal diol linker as a pyrophosphate surrogate and a thioether bond linked to the uridine part (**B2**, **Figure I-18**). The mimetics containing three segments showed strong inhibitory activity and moderate selectivity towards α -1,3-GalT among β -1,4-GalT. The inhibition studies indicated that the compound did not show a competitive mode of inhibition against UDP-Gal which means the compound could bind to the free enzyme but also to enzyme-substrate complex. Another type of UDP-Gal mimetics based on D- and L-epimers of iminosugar was synthesized by Guo-Liang Zhang *et al.*⁷¹ The uridine nucleoside was attached to an iminosugar

moiety via a variable length spacer. The best result was obtained with the L-epimer **B3** (**Figure I-18**) which displayed a moderate inhibition against α -1,3-GalT with an IC_{50} value of 320 μ M and a weak inhibitory effect towards β -1,4-GalT.

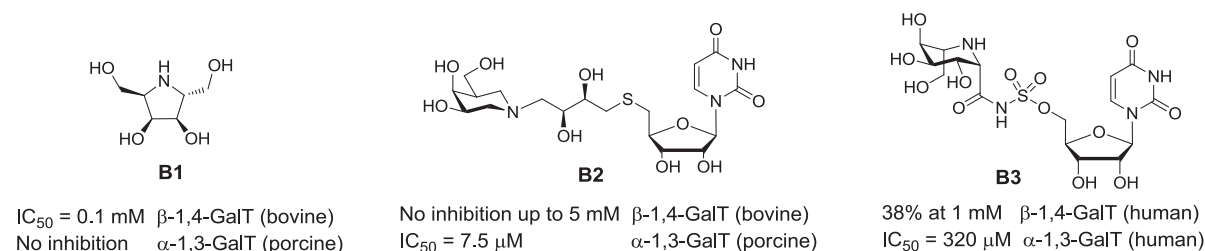


Figure I-18. Representative iminosugar based mimetics of GalT inhibitors.

I.3.1.2 Modification on the diphosphate

C-glycoside is another approach for the design of UDP-sugar analogues, which could be taken as a modification on the linker part. The derivative may keep binding affinity to the enzyme while could not be transferred to the respective acceptor, thus, serves as an inhibitor. The synthesis of C-glycosides of UDP-Gal, UDP-GlcNAc and UDP-GalNAc (**C1**, **Figure I-19**) should be mentioned here even biological evaluation data was not provided.⁷² Several years later, our group synthesized a series of C-glycosyl ethylphosphonophosphate analogues of UDP-Glc, UDP-Gal, UDP-GlcNAc and GDP-Fuc (**C2**, **Figure I-19**) and assayed the analogues *in vitro*.⁷³ The IC_{50} values of UDP-Gal, GDP-Fuc and UDP-GlcNAc analogues towards different glycosyltransferases, β -1,4-GalT, FUT3 and LgtA, were 40 μ M, 2 mM and 3.5 mM respectively. The synthesis of a pair of diastereoisomeric UDP-galactose analogues (**C3**, **Figure I-19**) were reported by V. Kolb *et al.*⁷⁴ The target of the study was the glycosylation of *Trypanosoma brucei* membranes which could cause sleeping sickness and animal African trypanosomiasis. The enzymatic results showed that both diastereoisomers were effective inhibitors towards N-glycan specific α -galactosyltransferase from trypanosomes with K_i values 21 μ M (R) and 34 μ M (S) in respect to the K_m value of UDP-Gal 20 μ M.

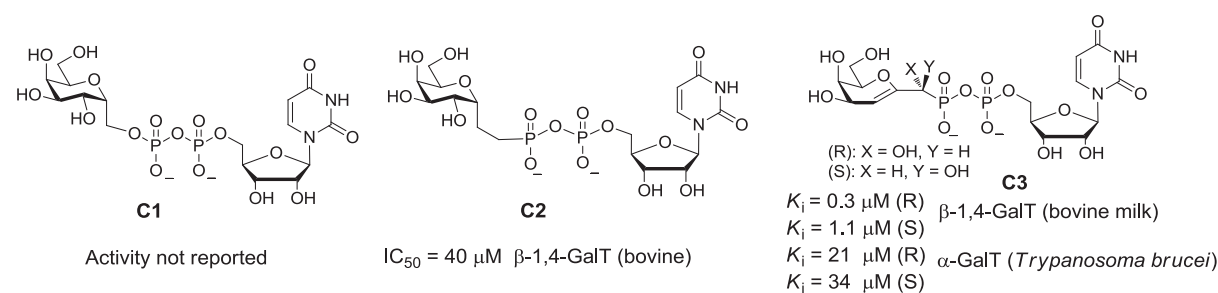


Figure I-19. Representative C-glycoside mimetics of GalT inhibitors.

Taking into consideration that donor or acceptor substrate analogues containing charged pyrophosphate moiety have limited bioavailability, scientists turned their attention to nonionic linker mimics. Malonic, tartaric, and monosaccharide moieties were employed as mimics of the pyrophosphate linker (**D1**, **Figure I-20**).⁷⁵ Among the mimics, glucose containing derivative showed inhibitory activity towards the β -1,4-GalT with a K_i value of 119.6 μ M, whereas the malonic and tartaric linkages appeared to be ineffective as replacements of the pyrophosphate moiety. Copper (I) catalysed modified Huisgen cycloaddition is widely used to rapidly and effectively construct compound libraries. A series of α -glycosides of UDP-sugar mimics were synthesized (**D2**, **Figure I-20**) taking triazole as a replacement of pyrophosphate via click

chemistry.⁷⁶ These compounds showed no inhibition against β -1,4-GalT up to 4.5 mM. The authors proposed that a bis-triazole moiety may be a more appropriate replacement for pyrophosphate. Another two types of UDP-sugar analogues using amino-acid as pyrophosphate mimics were synthesized and studied as inhibitors against GlfT2, a galactofuranosyltransferase activated in cell wall galactan biosynthesis in *Mycobacterium tuberculosis*. The first type of mimics is amino acid bridged C-glycoside analogues (**D3**, **Figure I-20**). The hypothesis by Vembaiyan *et al.*⁷⁷ was that a basic amino-acid may be beneficial for the interaction with the enzyme. Four amino-acids (lysine, glutamine, tryptophan, and histidine) were selected for the study. Among the analogues, histidine containing compound showed the best inhibitory activity with an IC_{50} value of 332 μ M. The other type of analogue which was initially designed towards MurG, a glycosyltransferase involved in bacterial peptidoglycan biosynthesis, was also evaluated as GlfT2 inhibitors.⁷⁸ In this family of compounds, a functionalized proline was linked via a variable length spacer to the uridine nucleoside. The best activity against GlfT2 among these compounds came from a phenyl modified proline derivative (**D4**, **Figure I-20**) with 80% inhibition at 1 mM while at this concentration no inhibition against MurG was observed.

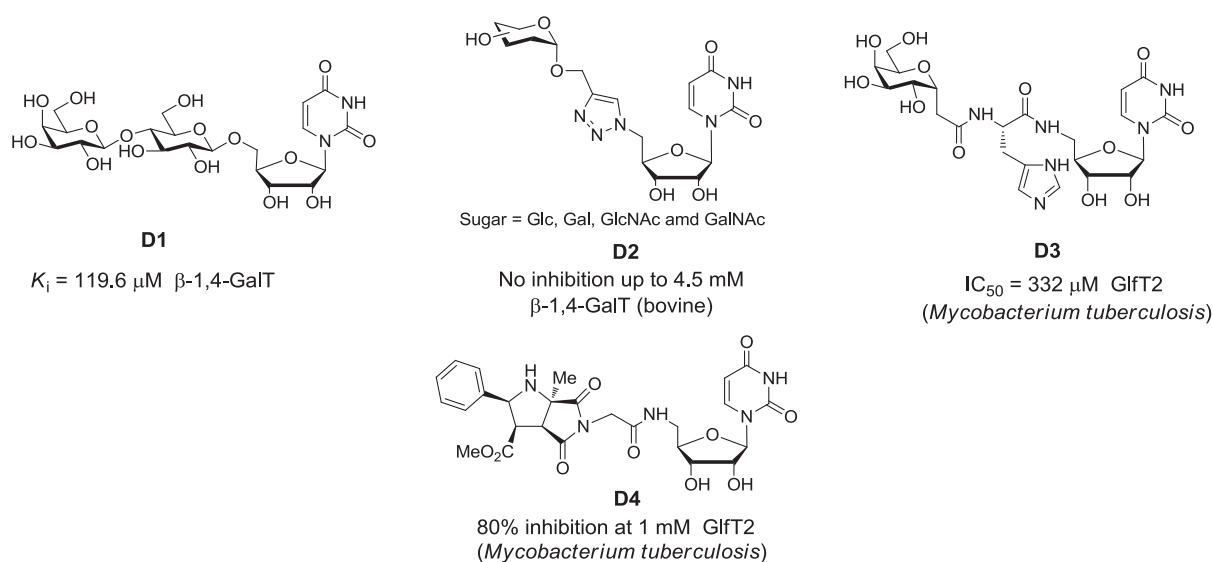


Figure I-20. Representative neutral GalT inhibitors.

I.3.1.3 Modification on the nucleoside base

Modifications on the nucleoside base are rare since the nucleoside moiety is considered as a necessary part for enzyme binding. Studies on different GalT structures disclosed that these enzymes might have compatibility towards modification at the 5-position of uridine.⁷⁹⁻⁸⁰ Different types of substituents in this position have been reported. 5-formylthien-2-yl substituted uracil UDP-Gal analogue **E1** (**Figure I-21**) was synthesized and evaluated.⁸¹ Enzymatic experiments showed this uracil-substituted analogue had broad inhibitory effect on different GalT including β -1,4-GalT, α -1,3-GalT, α -1,4-GalT, GTB, and human blood group transferase mutant AAGlyB. Crystal structure analysis of the complex with AAGlyB indicated that conformational changes of the enzyme were blocked by the substituent on the uracil ring upon binding, therefore locking the enzyme in an inactive catalytic conformation. Based on pioneering work in this area, Karine Descroix *et al.*⁸² designed and synthesized a C-glycoside derivative bearing a 5-formylthien-2-yl substituent at the 5-position of the uracil base (**E2**,

Figure I-21). UDP-Gal 4C-epimerase GalE was selected as the enzymatic target. This analogue gave a K_i value at micromolar concentration. Trifluoromethyl is another type of substituent at the 5-position of uracil base (**E3**, **Figure I-21**). The synthesis and biological evaluation was reported by Andrew Evitt *et al.*⁸³ The enzymatic evaluation showed that the decoration does not interfere with the recognition and binding with either β -1,4-GalT or α -1,4-GalT. This new type of analogue was determined as inhibitors of the tested enzymes and gave more information on structure–activity relationships for new classes of GT inhibitors design.

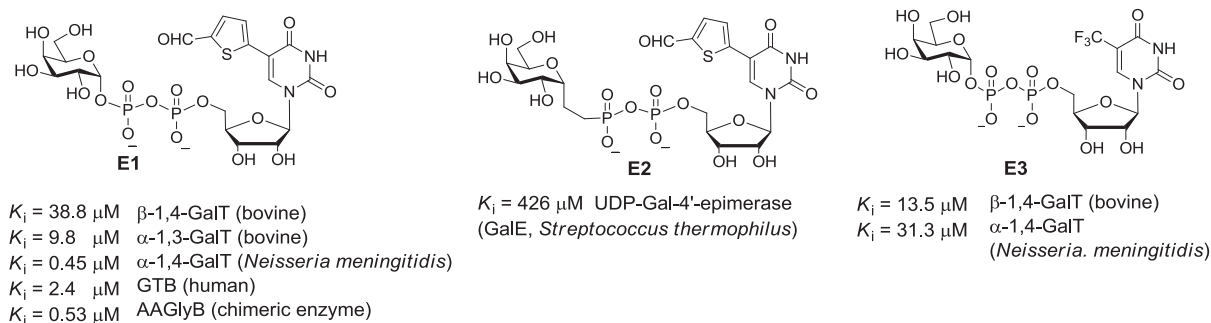


Figure I-21. Representative mimetics modification on nucleoside base.

I.3.1.4 Other aspects of UDP-sugar mimetics as GalT inhibitors

Enzymatic reactions can be equilibrated processes and the leaving moiety UDP is a natural competitive inhibitor of GT which utilize UDP-sugar as active sugar donor. Design of GT inhibitors based on structure modifications on UDP was also reported. Monosaccharide moieties were employed as mimics of the pyrophosphate linker.⁸⁴⁻⁸⁵ These mimetics gave weak inhibitors against β -1,4-GalT (**F1-F2**, **Figure I-22**). Multivalent effect, which is normally applied in design of high affinity ligands for lectins,⁸⁶ was also tested⁸⁷ on GT by synthesis of poly(uridine 5'-*p*-styrenesulfonate) (**F3**, **Figure I-22**). Enzymatic evaluation showed that this polymeric compound could inhibit the activity of β -1,4-GalT by 75% at 120 μM . The inhibition mechanism of this type of polymeric compound against GT has not been revealed to date and the application potency of synthetic polymeric compound over low-molecular-weight inhibitors still needs to be investigated.

The fact that the UDP moiety provides most of the binding affinity while the carbohydrate group adds the selectivity to the enzyme was verified by Katrin Schaefer *et al.*⁸⁸⁻⁸⁹ Based on docking experiment, two isomers were synthesized and tested by radiolabeled enzymatic assays as human blood group B galactosyltransferase (GTB) inhibitors. In their further work, the addition of an α -Gal moiety to 9-D-arabinitol-1,3,7-trihydropurine-2,6,8-trione **F4** did increase the binding affinity to GTB from a K_i value of 2.2 mM to 1.5 mM (**F5**, **Figure I-22**) and more importantly gave a selectivity to GTB over GTA which shares the same acceptor as GTB but uses UDP-GalNAc as an activated donor.

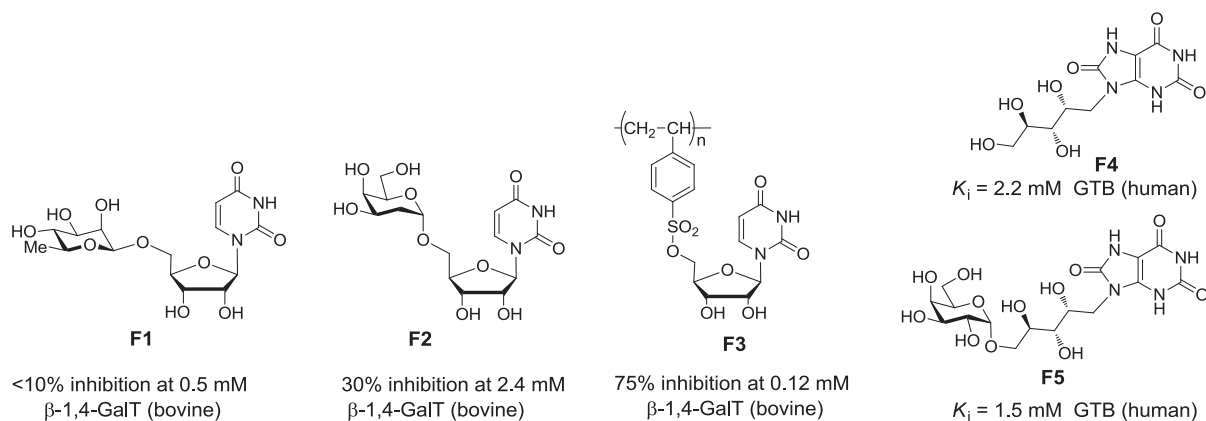


Figure I-22. Representative UDP-sugar mimetics as GalT inhibitors.

I.3.1.5 Acceptor substrate analogues as GalT inhibitors

A common strategy to design inhibitors based on acceptor substrate analogues is to synthesize the sugar deoxygenated or modified compounds at the accepting position of the relative natural acceptor (**G1-G4** and **H1-H3**, **Figure I-23, I-24**). Then, the acceptor substrate analogue may bind in the active site of the enzyme competing with the natural acceptor therefore abolishing the sugar transfer. Systematic research was performed and published by Ole Hindsgaul *et al.*⁹⁰ in 1991. Eight acceptor analogues on which the hydroxyl group undergoing glycosylation was replaced by hydrogen were synthesized and evaluated against eight different GT including FucT, GalT, GlcNAcT, GlcNAcT-V and SialylT. Half of the acceptor analogues showed no inhibitory effect towards the respective enzyme including the acceptor analogue (**G1**, **Figure I-23**) for β -1,4-GalT. This indicated that such hydroxyl groups are critical for enzymatic activity. All six possible deoxy and deoxyfluoro analogues of human boold group transferases acceptor (α -L-Fucp-(1,2)- β -D-Galp-O-(CH₂)₇CH₃) were synthesized by Todd L. Lowary *et al.*⁹¹ to study the compatibility and inhibitory effect on GTA and GTB. The study indicated that both the enzymes have no tolerance on modification at the 4-position of Gal moiety. The 6-deoxy and 6-deoxy-6-fluoro compounds are substrates for both enzymes while the 3-deoxy and 3-deoxy-3-fluoro compounds serve as competitive inhibitors, e.g. the 3-deoxy derivative (**G2**, **Figure I-23**) possess a K_i value of 14 μ M. A 4-deoxygenated acceptor analogue of α -1,4-GalT (**G3**, **Figure I-23**) was determined as an inhibitor of the enzyme with a K_i value of 16 mM similar to the K_m value (20 mM) of the natural acceptor and the analogue had been successfully co-crystallized with α -1,4-GalT.⁹² Modification of the hydroxyl group normally undergoing galactosylation could also give an inhibitor of GT. A.-C. Helland *et al.* reported that an acceptor analogue, methyl 3'-amino-3'-deoxy-*N*-acetyllactosaminide (**G4**, **Figure I-23**) in which the sugar accepting position was replaced by an amino group, is a selective inhibitor against α -1,3-GalT with a mode of inhibition which is not competitive.⁹³

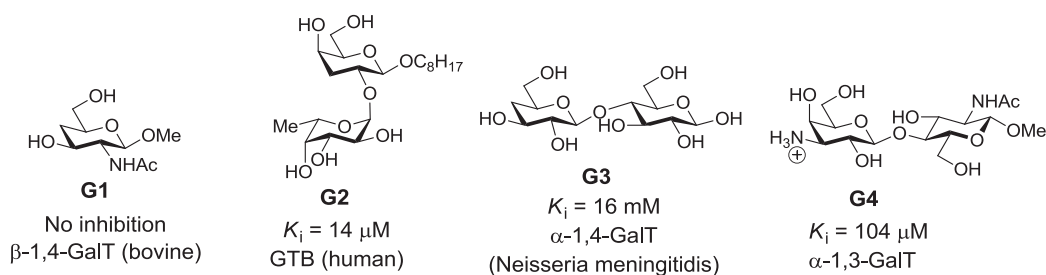


Figure I-23. Representative GT inhibitors based on acceptor substrate analogues.

A series of 3-GlcNAc or 4-GlcNAc modified peracetylated GlcNAc-1,3- β -Gal- β -*O*-naphthalenemethanol were synthesized targeting of human β -1,4-GalT 1 which is involved in the glycan biosynthesis in tumor cells.⁹⁴ The deacetylated compound indicated inhibitory effect *in vitro* and the acetylated form (**H1**, **Figure I-24**) was tested to inhibit sLe^X formation in U937 monocytic leukemia cells with an IC₅₀ value of about 30 μ M. This report is one of the rare reports that verified that the designed inhibitor does have activity *in vivo*. Analysis of acceptor substrate binding site of β -1,4-GalT gave a hint that aromatic groups may be beneficial for substrate binding in Site B.⁹⁵ A series of acceptor analogues containing either bulky aromatic group or aliphatic chain were then synthesized. Two representative analogues (**H2-H3**, **Figure I-24**) showed strong inhibition and high selectivity between β -1,4-GalT and α -1,3-GalT.

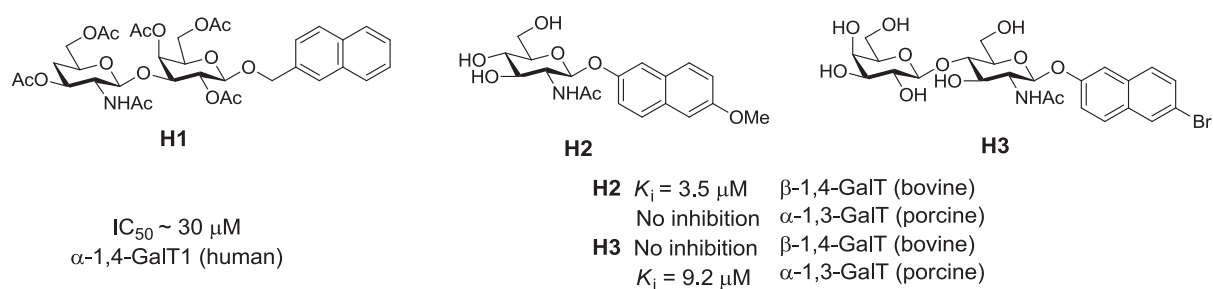


Figure I-24. Representative sugar-aromatic mimetics of the acceptor substrates.

I.3.1.6 Bisubstrate analogues

Bisubstrate analogue means that the derivative contains both features of donor and acceptor substrates. Design and synthesis of this type of inhibitor involve extensive work but a promising means to obtain the most active and selective inhibitors for a specific glycosyltransferase. To date, two examples of this type of inhibitor targeting GalT have been reported (**I1-I2**, **Figure I-25**).⁹⁶⁻⁹⁷ Both of them were designed based on a steric rearrangement of donor and acceptor components according to the transition state. As expected, they gave the best inhibition result so far towards their respective enzymatic targets.

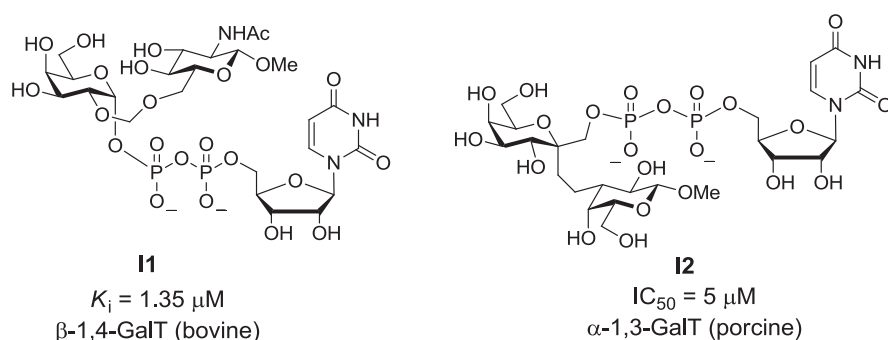


Figure I-25. Bisubstrate analogues as GalT inhibitors.

I.3.1.7 Small molecule inhibitors from library or HTS

Progress in rapid and efficient detection systems facilitates identification of small molecule inhibitors from large libraries or high-throughput screening. Simple small molecules such as organic bisphosphonates (**J1**, **Figure I-26**) and bivalent imidazolium salts (**J2**, **Figure I-26**) were found to be effective against β -1,4-GalT.^{58, 98} Another classic example is a small heterocycle (**J3**, **Figure I-26**) obtained from a Molecular Fragment Library which was

determined to exhibit weak inhibition against GT with a special mechanism simultaneously interfering with metal ion and substrate binding.²⁸

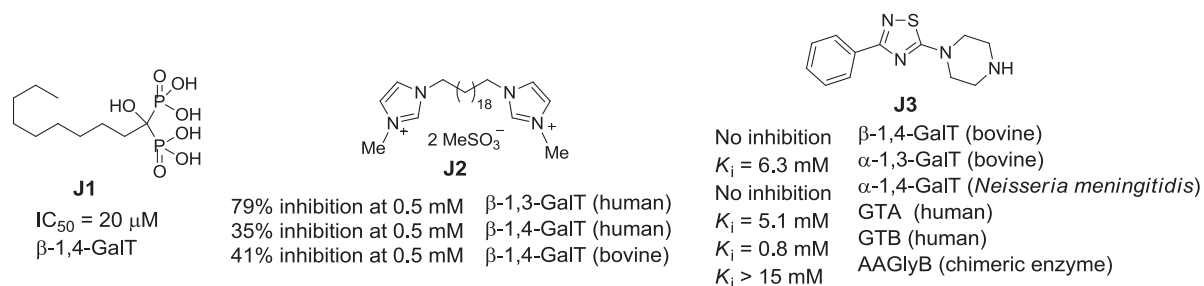


Figure I-26. Representative small molecule inhibitors from library or high-throughput screening.

I.3.2 Inhibitors of *O*-linked *N*-acetylglucosamine transferase (OGT)

O-GlcNAcylation attracts increasing interest from biologists, biochemists and chemists since more and more *O*-GlcNAcylation relevant physiological and pathological processes are elucidated, including cancer,³⁴⁻³⁵ Alzheimer's disease³⁶⁻³⁹ and diabetes.³⁹⁻⁴⁰ The *O*-GlcNAcylation is a reversible post-translational modification through catalytic formation by *O*-linked *N*-acetylglucosamine transferase (OGT) and hydrolysis by *N*-acetyl β-glucosaminidase (*O*-GlcNAcase, OGA).⁹⁹ Unlike other usual GT which are normally located in the cytosol, OGT is also present in the nucleus and mitochondria. More than 1000 substrate proteins have been identified, but no consensus sequence has been identified among them. Therefore, the study of OGT requires the design of potent inhibitors not only for fundamental research but also potential for pharmaceutical applications.

Three different isoforms of OGT have been reported (nuclear, cytoplasmic OGT (ncOGT) and mitochondrial OGT (mOGT) and a short form OGT (sOGT). The difference is the length of their tetratricopeptide repeats (TPRs), 13, 9.5, 3.5 TPRs respectively.¹⁰⁰ These three constructs of human OGT have been successfully expressed in *E. coli*. with only ΔmOGT which is 50 residues shorter than the known splice variant.¹⁰¹ There is a few research papers on OGT inhibition and the design strategy is similar to the approaches presented above for GalT.

I.3.2.1 UDP-sugar donor substrates analogues

Alloxan (**K1**, **Figure I-27**) and benzyl-2-acetamido-2-deoxy-α-D-galactopyranoside (BADGP) (**K2**, **Figure I-27**) were early determined compounds which could interfere with *O*-GlcNAcylation.¹⁰²⁻¹⁰³ Alloxan could selectively induce cell-death of insulin-producing cells in the pancreas, but the high toxicity of alloxan to different cell lines limits its further application. BADGP has been shown to be able to block the *O*-GlcNAcylation, but no evidence on its direct activity on OGT has been reported. Modification on the anomeric oxygen of UDP-GlcNAc, *C*-glycoside (**K3**, **Figure I-27**) and thioglycoside (**K4**, **Figure I-27**) were reported by Hajduch *et al.* and Dorfmueller *et al.*, separately.^{72, 104-105} While the *C*-glycoside **K3** showed weak inhibition on ncOGT, the thioglycoside **K4** gave an IC₅₀ in the micromolar range. Recently, it was shown that a synthetic carbohydrate precursor **K5** using a sulfur atom instead of oxygen in the sugar ring could be recruited by the hexosamine biosynthetic pathway (HBP) in cells and consequently inhibited OGT's function with a low micromolar EC₅₀. The counterpart of the enzymatic product of HBP (**K6**, **Figure I-27**) was synthesized and verified as

an inhibitor of OGT *in vitro* with a K_i value of 8 μM . This biosynthetic precursor **K5** gives a good example of inhibitor design capitalizing on forming the inhibitor intracellularly therefore acting on the desired enzyme.

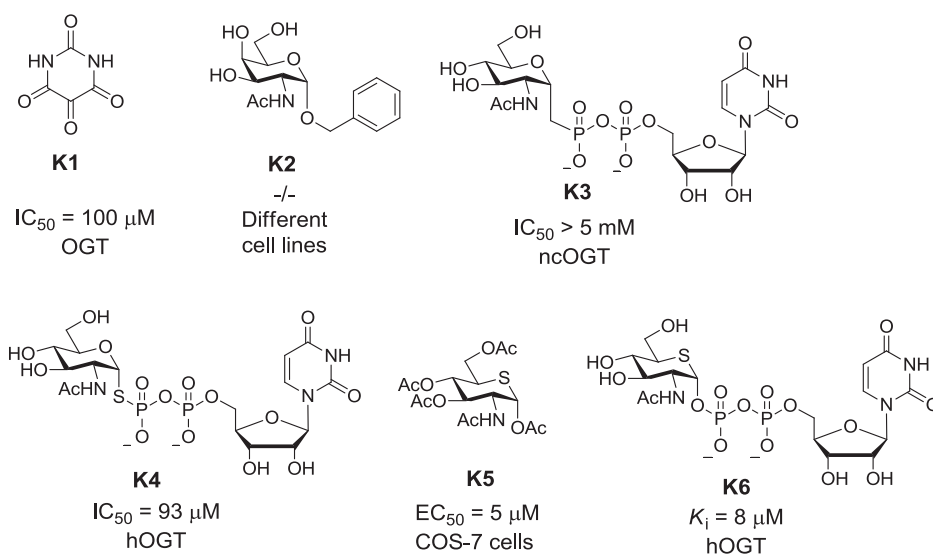


Figure I-27. Representative UDP-GlcNAc analogues as inhibitors of OGT.

I.3.2.2 Small molecule inhibitors from library or HTS

Recent developments in accurate measurement of *O*-GlcNAcylation have facilitated the discovery of small-molecule inhibitors of OGT. In late 2005, the Walker's lab used fluorescent UDP-GlcNAc analogues instead of natural sugar donor and the displacement assay was used in a HTS assay of OGT inhibitors.¹⁰¹ 102 Compounds were selected as positives among 64 416 commercial library compounds screened for a hit rate of 0.2% and 19 of these compounds were verified by a radiometric assay. The best two inhibitors selected by this screening displayed with IC_{50} values in the micromolar range (**L1-L2**, **Figure I-28**). To continue the study, chemical modifications were performed on the best inhibitor selected from the library screening.¹⁰⁶ Mechanistic studies showed that the benzoxazolinone core could functionalize as a diphosphate isostere and a double-displacement mechanism ($\text{SN}_2 \times \text{SN}_2$) was proposed based on mass spectrometry analysis of inhibitor treated enzyme (**L3**, **Figure I-28**). The concentration required for inhibition of *O*-GlcNAcylation in cells was relatively high, possibly due to decomposition or side reactions. Two years later, instead of donor modification, a peptide acceptor substrate labeled approach was utilized by the Walker's lab and the so-called "protease-protection" assay was used to screen OGT inhibitors.¹⁰⁷ Among 124 226 compounds screened, 84 compounds that inhibited OGT activity by 30% or more were identified for a hit rate of 0.065% and 9 of these compounds were verified by a radiometric assay to have IC_{50} values between 0.9 and 20 μM . The structures of 3 hits were given by the author as examples without mentioning individual activities (**L4-L6**, **Figure I-28**).

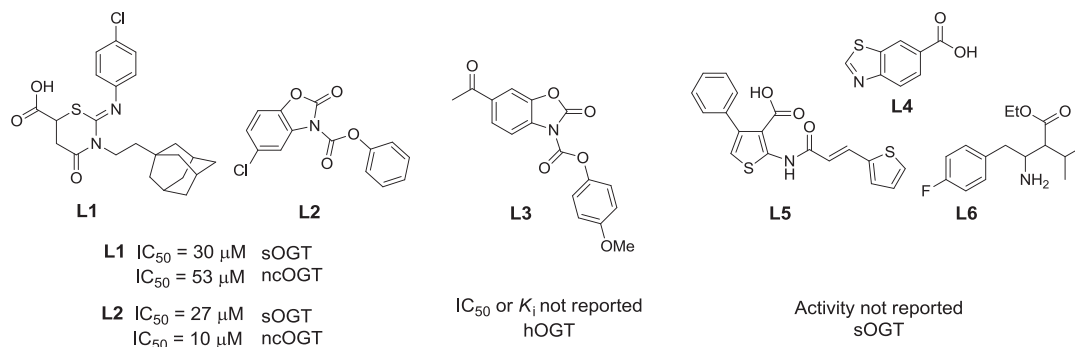


Figure I-28. Representative OGT inhibitors identified from HTS.

I.4 Project aim

Several parameters must be considered for the design of potent and selective GT inhibitors:

- (1) the inhibitor must have a sufficient affinity for the enzyme, typically in the micromolar range or at least very similar to the K_m value of the natural NDP-sugar substrate;
- (2) the inhibitor must be able to penetrate cells and therefore to cross the different cell membranes (e.g. plasmic, nuclear) to reach its target GT in the correct cellular compartment;
- (3) the inhibitor must exhibit high specificity for GT among all enzymes (e.g. kinases, phosphatases, peptidase, glycosidases) but also for only one family of GT (e.g. GalT vs FucT).

Despite the tremendous efforts for the design of GT inhibitors, reported analogues which are effective *in vivo* are still rare and studies in this aim are still challenging. The diphosphate linker is the most problematic residue due to its potential metabolic instability and poor pharmacological properties in particular with respect to cellular permeability. The current project focused on the design and synthesis of neutral inhibitors of GT. The diphosphate unit of NDP-sugars usually interacts with metallic cations. Therefore, surrogate of this moiety should be capable of retaining this property and provide chelating groups for cations. In our study, diphosphate moiety was replaced with neutral functional groups capable of binding to the active site of glycosyltransferases (**Figure I-29**) and these compounds were evaluated as GT inhibitors.

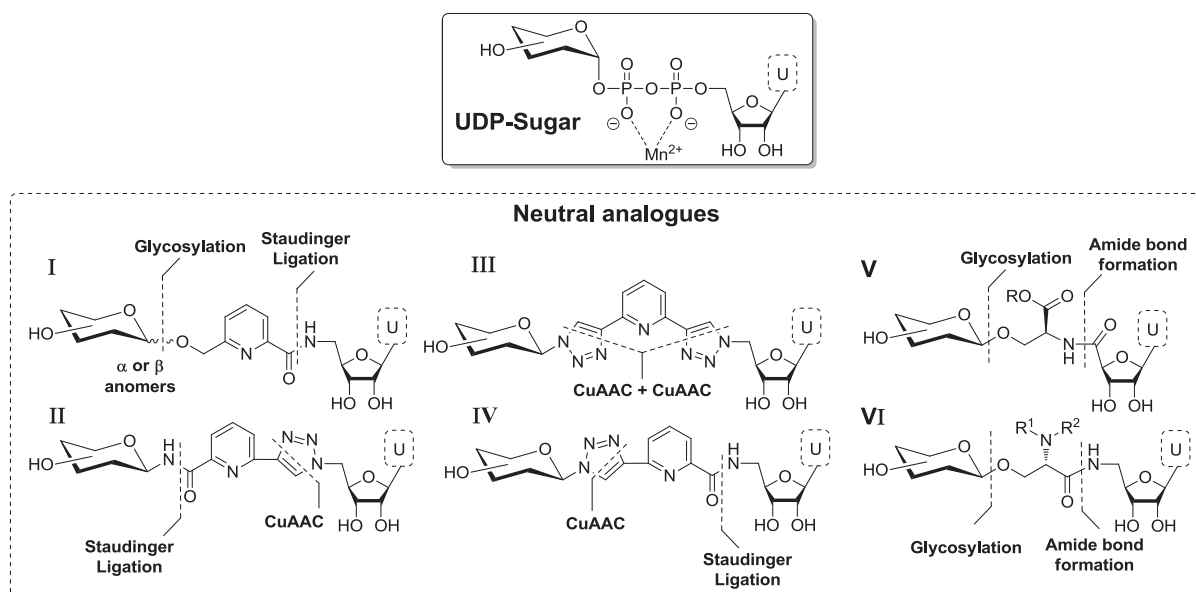


Figure I-29. Structures of the neutral UDP-sugar analogues designed and synthesized.

I.4.1 Synthesis of UDP-sugar analogues

Pyridine containing scaffold and amino acid containing linker were chosen as two types of surrogates for the diphosphate moiety. The carbohydrates used are galactose and *N*-acetyl glucosamine as the selective natural moieties for the enzymes but also glucose as a negative control. The stereochemistry at the anomeric center of the carbohydrate does not necessarily need to be identical to the natural NDP-sugar since β -anomers could also be identified as GT inhibitors.¹⁰⁸

First, we designed UDP-sugar analogues containing the pyridine moiety (**I-IV**, **Figure I-29**). It was reported that heterocyclic moieties containing a pyridine ring conjugated with two symmetric triazoles were capable for chelating metal cation.¹⁰⁹ The incorporation of a pyridine moiety to the diphosphate mimics will enhance the metal-binding and hydrogen bonding capability of this series of analogues. The conjugation of the carbohydrate, pyridine and nucleoside building blocks could be achieved through a combination of glycosylation, Staudinger- Vilarrasa ligation and Cu (I)-catalyzed azide-alkyne cycloaddition (CuAAC).

Afterwards, another series of UDP-Gal analogues functionalized with an amino-acid derived linker were synthesized (series **V-VI**, **Figure I-29**). The incorporation of an amino-acid residue between the carbohydrate and nucleoside moieties provided a functional amine or acid group which could be substituted with other functional moieties. The introduction of functional groups could favor binding to GT or interact with specific amino-acids in the active sites of GT. Glycosylation reaction conditions with serine derivatives were also investigated in this section. The construction of this library of analogues was conducted through a combination of glycosylation and amide bond chemistries.

I.4.2 Biological evaluations

The neutral inhibitors designed and synthesized were then evaluated for their inhibition activities towards five galactosyltransferases (GalT). The best inhibitors of human blood group transferase mutant AAGlyB were then selected for crystallographic studies in order to obtain the structural features of their interactions with the enzyme at the active site in a co-crystal. Eight UDP-sugar or UDP analogues which were functionalized with a pyridine ring conjugated with two symmetric triazoles were selected for OGT inhibition, enzymatic assays, cell assays and docking studies. The concept of “neutral” inhibitor instead of ionic analogues was finally tested by an artificial cell membrane penetration test on the two best inhibitor candidates against GalT or OGT.

Chapter II : Synthesis of neutral glycosyltransferase inhibitors - Pyridine as a pyrophosphate surrogate

Chapter II : Synthesis of neutral glycosyltransferase inhibitors - Pyridine as a pyrophosphate surrogate

II.1 Introduction

This chapter describes the synthesis of neutral glycosyltransferase inhibitors taking pyridine as a pyrophosphate surrogate. The syntheses of UDP-sugar analogues (**7-Gal**, **7-Glc**, **20**, **23**) and one UDP analogue (**10**) (**Figure II-1**) are based on glycosylation and amide bond chemistries. One key step in this synthetic route is the generation of the glycosidic bond with basic pyridine-containing acceptors which are quenching the Lewis Acid used as a promoter. A careful literature search provided only a handful of reports, hence a systematic study on glycosylation methods involving methyl 6-(hydroxymethyl)picolinate as a model acceptor and 20 glycosyl donors is implemented in this section.

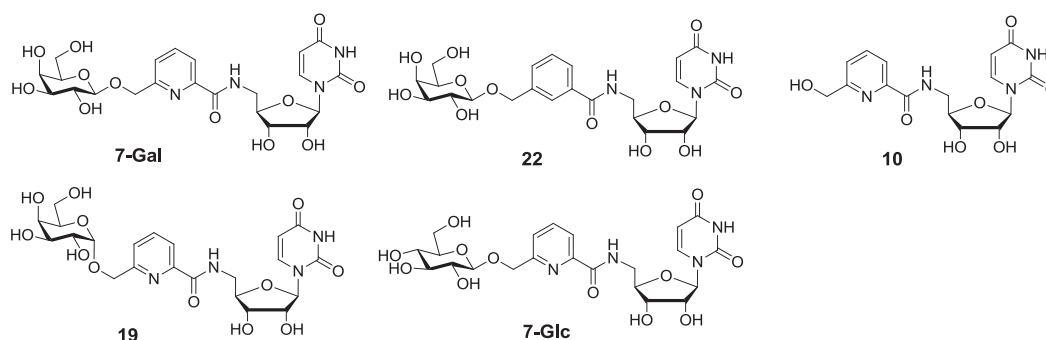


Figure II-1. Target UDP-sugar analogues using pyridine as a pyrophosphate surrogate.

A combination of amide bond chemistry and CuAAC are used for the conjugation of the carbohydrate and nucleoside moieties to the central pyridine scaffold (**Figure II-2**) for the synthesis of the second series of UDP-sugar analogues (**30-Glc**, **30-Gal**, **30-GlcNAc**, **35-Glc**, **35-Gal**, **35-GlcNAc**, **43-Glc**, **43-Gal**, **43-GlcNAc**) and two UDP analogues (**25**, **45**) using pyridine as a pyrophosphate surrogate. The syntheses are performed in galactose, glucose and *N*-acetyl glucosamine series. Two synthetic routes, namely pathway **A** from Sugar-to-Nucleoside and pathway **B** from Nucleoside-to-Sugar, are applied in the glucose series in order to compare their efficiency. The introduction of a desymmetrized bis-alkyne pyridine intermediate provided access to the “one-pot” synthesis of bis-triazole analogues **43** rapidly through CuAAC conjugations with sequential deprotection of the alkyne groups.

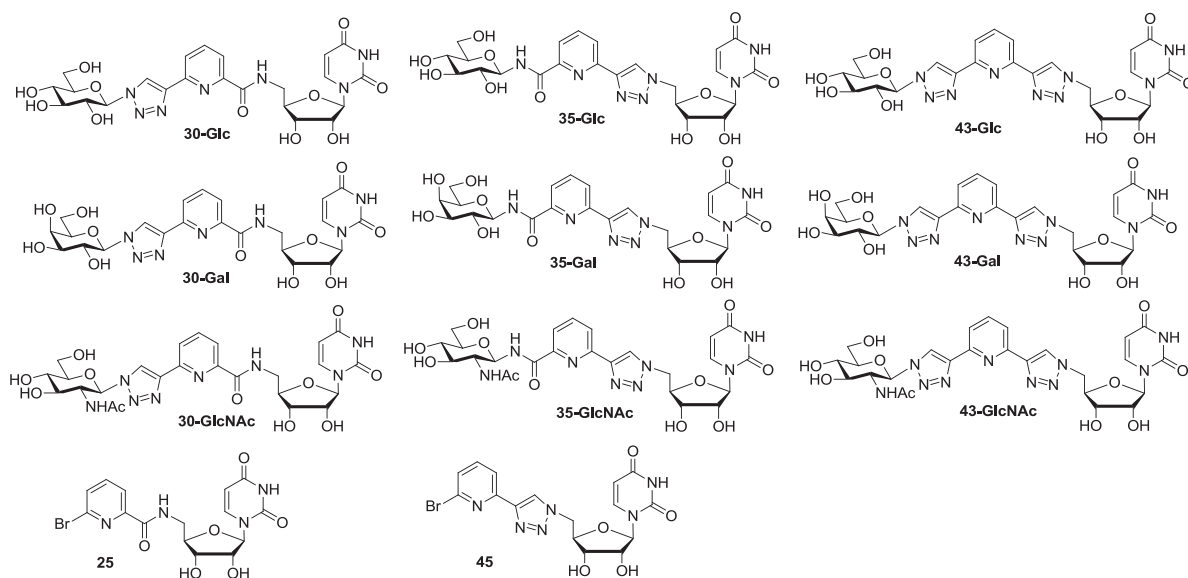


Figure II-2. Target UDP-sugar analogues using pyridine as a pyrophosphate surrogate.

II.1.1 Chemical aspects

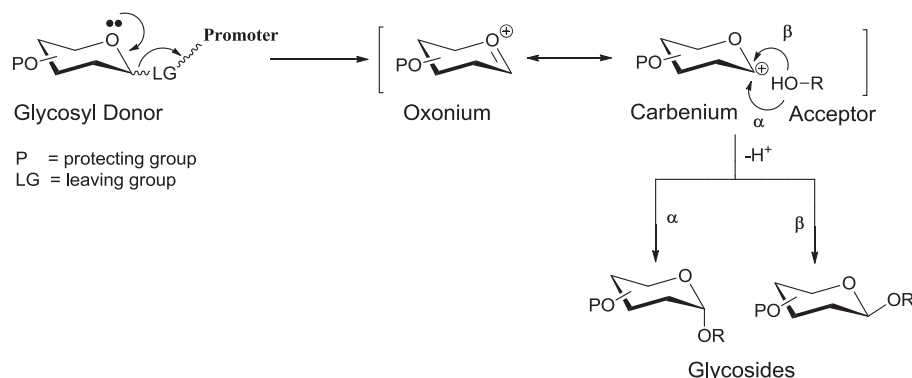
Apart from rare synthetic benefits obtained from enzymatic engineering, a large series of compounds were constructed towards glycosyltransferase inhibition based on chemical synthesis. The chemistries involved are mainly phosphonate chemistry, sulphur chemistry, carbohydrate chemistry, “Click” chemistry, amide or ester bond formation chemistry. The main chemical methods, glycosylation, amide bond chemistry and “Click” chemistry, were also used in the present study and briefly reviewed in this section with highlight of mechanism and the influence of key parameters.

II.1.1.1 Glycosylation

Despite the considerable diversity of carbohydrate derivatives in living organisms, the biosynthesis of these oligosaccharides, polysaccharides and glycoconjugates are catalyzed by different GT. Different types of glycosidic bonds, such as *O*-glycoside, *S*-glycoside and *N*-glycoside, are present in Nature. Among them, *O*-glycosides are the most abundant and important species. The enzymatic syntheses of *O*-glycosides in living organisms implemented by GT are highly specific and selective. Despite the merit of enzymatic synthesis, the availability of genetically engineered enzyme and complexity of glycoconjugates limit the real application of enzymatic synthesis in most of cases. Besides, UDP-sugars, sugar donors for enzymatic synthesis, are either expensive or difficult to produce in a large scale.¹¹⁰⁻¹¹¹ Thus, chemical synthesis is a major tool to access diversified glycoconjugates to study their biological roles therefore plays a crucial role in carbohydrate chemistry.¹¹²⁻¹¹⁴

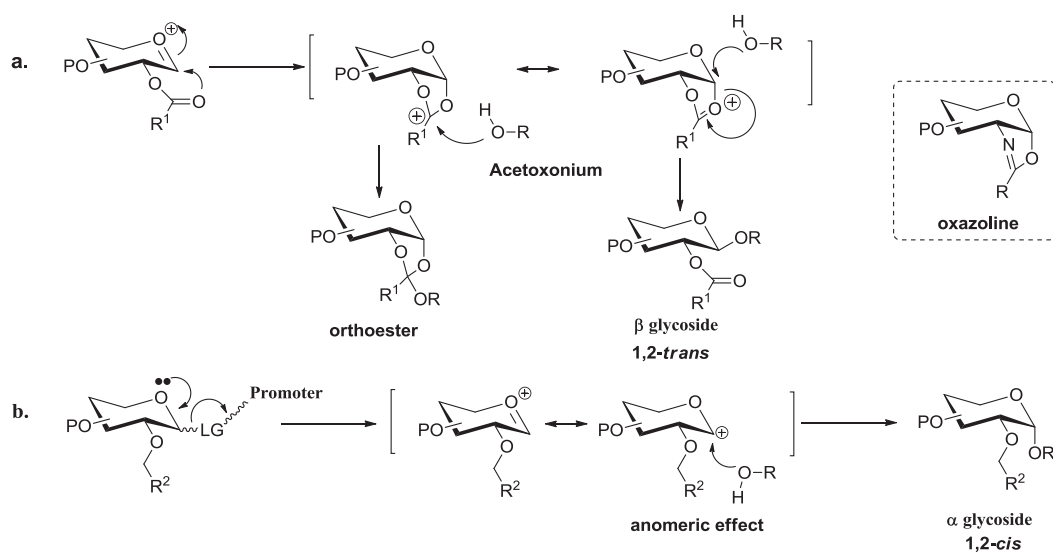
The formation of a covalent bond between the anomeric position of a glycosyl donor and a glycosyl acceptor yields a new stereogenic carbon atom (**Scheme II-1**). The linkage formed may either be axial or equatorial. Efficient, regioselective and stereoselective creation of glycosidic linkages is challenging and sensitive to a large number of factors, such as leaving group at the anomeric center, protecting groups applied for donors and acceptors, promoters or even solvents. The leaving group (**LG**, **Scheme II-1**) present at the anomeric position of glycosyl donors requires activation of a promoter (i.e., Lewis or Brønsted acid) in order to

generate the reactive oxonium/carbenium ion intermediate which will then undergo a nucleophilic attack by the glycosyl acceptor. In order to control the stereochemical outcome of a glycosylation, the protecting group at the 2-position of the glycosyl donor is a major parameter.

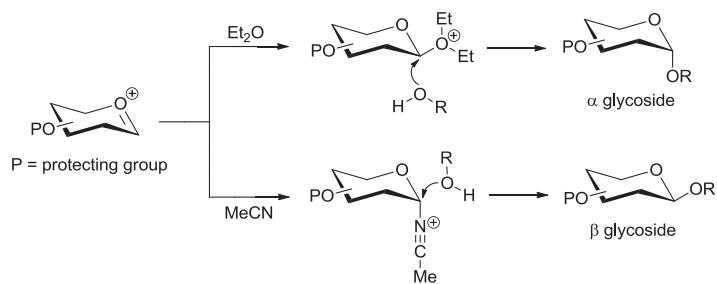


Scheme II-1. Schematic representation of a glycosylation reaction.

Normally, a participating group, typically an acetate or benzoate ester, will form an acetoxonium ion intermediate which would block the attack from the α -face thus forming mainly β -glycoside, also described as 1,2-*trans* glycoside (**a**, **Scheme II-2**). Meanwhile, the formation of the acetoxonium ion intermediate potentially increased the possibility of a byproduct forming, namely orthoester. *N*-acetyl glucosamine derivatives are the optative examples which favor the formation of oxazoline intermediate which are stable enough to be separated (**a**, **Scheme II-2**). A non-participating group, such as a benzyl ether, will predominantly give α -glycoside or 1,2-*cis* glycoside favoured by the anomeric effect¹¹⁵ (**b**, **Scheme II-2**). Meanwhile, other reaction conditions, promoter, solvent, temperature and even the sequence of addition of reactants, may also influence the outcome of a glycosylation reaction. The solvent has a preference for interaction in axial (MeCN) or equatorial (Et₂O) position thus favoring the nucleophilic attack of the acceptor on the opposite face (**Scheme II-3**).²⁵⁷



Scheme II-2. Schematic representation of a glycosylation reaction with a participating or a non-participating group at the 2-position of glycosyl donor.



Scheme II-3. Schematic representation of the influence of solvent in glycosylations.²⁵⁷

II.1.1.1.1 Sugar donors

A wide variety of sugar derivatives containing leaving groups at the anomeric carbon are used as sugar donors in glycosylation (**Table II-1**).

One of the first glycosylation methods published in the 19th century was Fischer glycosylation which used directly native sugars as glycosyl donors. This reaction with alcohols in the presence of protic acid is an equilibrated process which results a mixture of kinetic furanosides and thermodynamic pyranosides. Modifications have been made on the original conditions which permit a better control of the ratio.¹¹⁶ Peracetylated sugars are readily available and have also been used as glycosyl donors. However, the acetyl group is not a good leaving group, so specific conditions are required. Lewis acids, such as SnCl_4 ¹¹⁷ and $\text{BF}_3 \cdot \text{Et}_2\text{O}$,¹¹⁸ were well applied to activate the glycosyl esters. While two or three component catalytic systems, eg. $\text{SnCl}_4\text{-AgClO}_4$ or $\text{SnCl}_4\text{-CF}_3\text{CO}_2\text{Ag}$,¹¹⁹⁻¹²¹ were also applicable in this case which could reduce the amount of Lewis acids required.

Glycosylations with glycosyl bromides and chlorides catalyzed by heavy metal salts were known as the Koenigs-Knorr reaction.¹²² Ag_2O and Ag_2CO_3 were the frequently used promoters¹²³ and $\text{Hg}(\text{CN})_2/\text{HgBr}_2$ were the Helferich variant.¹²⁴ Later, AgOTf was employed for a better solubility and was examined as one of the most efficient heavy metal promoters.¹²⁵ A different type of promoter for this kind of donor was *in situ* anomerization. Et_4NBr or Bu_4NBr was used in combination with base to convert the less active α -glycosyl bromides into their highly reactive β -anomers which underwent rapid $\text{S}_{\text{N}}2$ substitution resulting in α -glycosides.¹²⁶ The drawback of this method is its limitation to only glycosyl halides whereas the advantage is the high α -stereoselectivity.

Glycosyl trichloroacetimidates were developed in Richard R. Schmidt's group and known as Schmidt donors. They are relatively stable under basic or neutral conditions but readily reactive under acidic activation. $\text{BF}_3 \cdot \text{Et}_2\text{O}$ and TMSOTf were frequently used promoters.¹²⁷⁻¹²⁸ Glycosyl trifluoroacetimidates were also effective sugar donors and had been introduced into glycosylation.¹²⁹

The merit of thioglycosides is their stability. They are relatively shelf stable, tolerant to diverse reaction conditions, readily converted into other types of donors and more interestingly relative activity between different substituents can be used to program multistep glycosylations. The activation process (**Scheme II-4**) is initiated by an electrophile which forms a sulfonium ion with the thioglycoside making a better leaving group. Loss of the sulfonium ion part leads to the common oxonium/carbenium ion intermediate which will then reacts with a glycosyl acceptor resulting in the desired glycoside. One of the activating

methods uses sulfenyl derivatives under Lewis acid catalysis, such as 1-benzenesulfinyl piperidine (BSP)/triflic anhydride (Tf₂O).¹³⁰ The alkylating agent MeI¹³¹ is also applicable for activating thioglycosides which are normally 2-pyridyl thioglycosides and afford 1,2-*cis*-glycosides with good stereoselectivities.

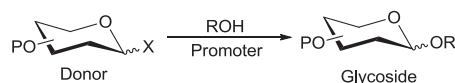
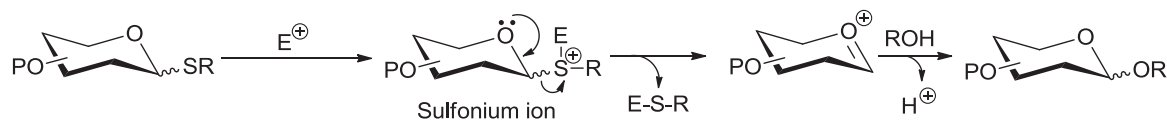


Table II-1. Frequently used sugar donors and activating systems.

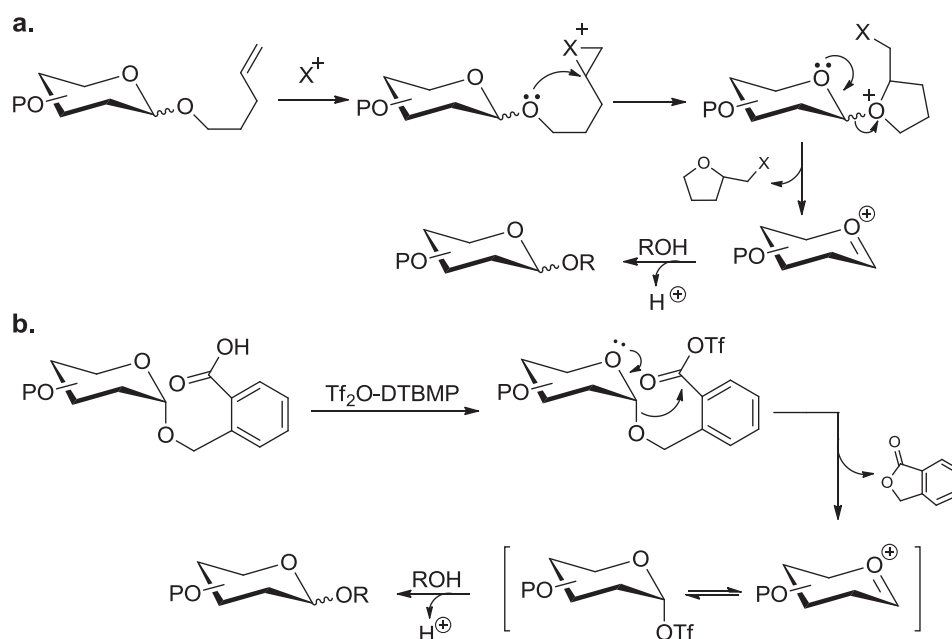
| Entry | Donor | Promoter | Ref. |
|-------------------|-------|---|---------|
| Hemiacetal | | BF ₃ ·Et ₂ O, FeCl ₃ | 116 |
| | | SnCl ₄ | 117 |
| Glycosyl ester | | BF ₃ ·Et ₂ O | 118 |
| | | SnCl ₄ -AgClO ₄ | 119 |
| | | SnCl ₄ -CF ₃ CO ₂ Ag | 120-121 |
| | | Ag ₂ O, Ag ₂ CO ₃ | 123 |
| Glycosyl bromides | | Hg(CN) ₂ , HgBr ₂ | 124 |
| | | AgOTf | 125 |
| | | Et ₄ NBr, Bu ₄ NBr | 126 |
| | | | |
| Imidates | | BF ₃ ·Et ₂ O | 127 |
| | | TMSOTf | 128 |
| | | | |
| Imidates | | TMSOTf | 129 |
| | | | |
| Thioglycosides | | BSP, Tf ₂ O | 130 |
| | | MeI | 131 |
| O-Glycosides | | NIS, TfOH | 132 |
| | | DTBMP, Tf ₂ O | 133 |
| Glycals | | DMDO, ZnCl ₂ | 134 |
| Oxazolines | | TMSOTf | 135 |



Scheme II-4. Activation of thioglycosides by electrophilic reagents.

O-Glycosides containing specific leaving group precursors could also serve as sugar donors. *n*-Pentenyl glycosides introduced by Fraser-Reid¹³⁶ are good examples of this type of donors. *n*-Pentenyl glycosides could be remotely activated by halogen derivatives, especially iodinated species, eg. NIS-TfOH¹³², by forming an iodonium intermediate followed by intramolecular cyclization (**a**, **Scheme II-5**). Another example of this kind of *O*-glycosides activated by remoted activation is 2'-carboxybenzyl glycoside (**b**, **Scheme II-5**).¹³³ The 2'-carboxybenzyl glycoside reacts with Tf₂O in the presence of DTBMP forming a lactone,

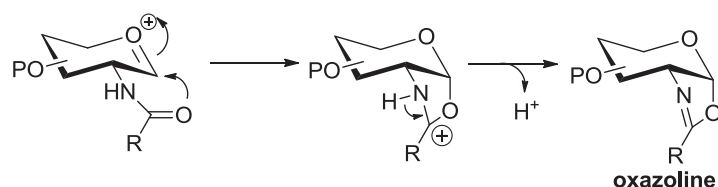
thus providing the active glycosylating intermediate. This method is highly recommended for the synthesis of β -mannopyranosides.



Scheme II-5. Remote activation of *n*-pentenyl glycosides **a** and 2'-carboxybenzyl glycosides **b**.

Another versatile sugar donor is the 1,2-anhydro glycal derivative. The efficient activation method via oxidation with dimethyldioxirane (DMDO) affords epoxides which are active glycosylating species under regioselective ring opening usually catalyzed by $ZnCl_2$.¹³⁴ The deactivating-activating methodology could also be used in multisteps programmed synthesis and another potential property of using this method is to provide an unprotected hydroxyl group at the 2-position which could be further converted or functionalized.

The last type of donors which will be discussed in this section is oxazolines. The 2-acetamido-2-deoxy group in *N*-acetyl-D-glucosamine and *N*-acetyl-D-galactosamine reacts differently in glycosylation reactions in comparison to their counterparts. The reason related is that the *N*-acyl group is an excellent participating group. As the leaving group activated, the neighboring group *N*-acyl participates the formation of an intermediate resulting the stable oxazoline formed (**Scheme II-6**). The oxazoline can be further activated with $TMSOTf$ ¹³⁵ to afford the 1,2-*trans*-glycoside.



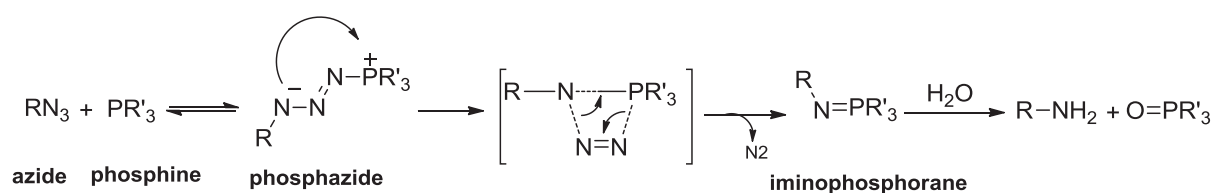
Scheme II-6. Formation of oxazoline.

II.1.1.2 Staudinger-Vilarrasa reaction

Amide bond, named also peptide bond, is a chemical covalent bond formed between a carboxylic acid and an amine by condensation reaction. Amide bond is widespread in Nature as found in proteins which are composed by amino-acids oligomerized through amide bonds. The peptide bond is neutral, possessing both hydrogen-bond accepting and donating capabilities and

metabolically stable compared to ester bond. An analysis of the Comprehensive Medicinal Chemistry database shows that over 25% of the known drugs bearing the amide bonds.¹³⁷⁻¹³⁸

Simply mixing an amine and an acid will give a stable organic salt. Direct condensation of the salt could occur under high temperature (160-180°C),¹³⁹ but these reaction conditions are not compatible with heat-sensitive functional groups. Thus, activation and appropriate protecting groups are needed. Common activated carboxyl derivative have been used, such as acyl halides, acyl azides, acylimidazoles, anhydrides or esters.¹³⁸ Different protecting groups could be applied to the corresponding strategies according to respective synthetic requirement. An amine group could also be obtained from its precursor azido group by combination of the azide with a phosphine (or phosphate) followed by hydrolysis (**Scheme II-7**) which is named Staudinger reaction or Staudinger reduction.¹⁴⁰



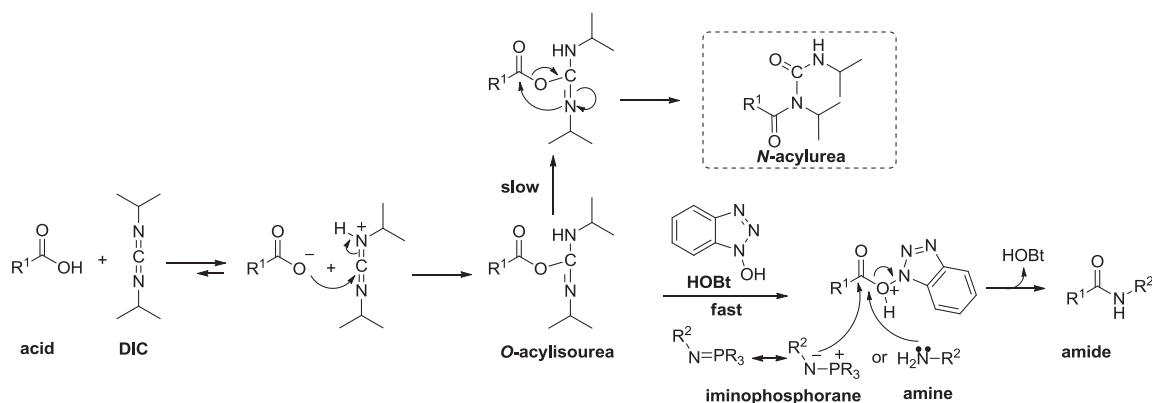
Scheme II-7. Phosphine mediated reaction of converting azide into amine.¹⁴⁰

Later, effort was made to form an amide bond directly between Staudinger iminophosphorane and activated carboxylic acids (**Scheme II-8**) such as anhydrides,¹⁴¹⁻¹⁴² acyl halides¹⁴³⁻¹⁴⁴ and other activated esters.¹⁴⁵⁻¹⁴⁸ This general process was named Staudinger-Vilarrasa reaction¹⁴⁹⁻¹⁵¹ in view of the seminal work in this area performed in professor Jaume Vilarrasa's group (University of Barcelona, Spain).



Scheme II-8. Direct formation of amide bond from carboxyl derivatives, organic azides and phosphines.

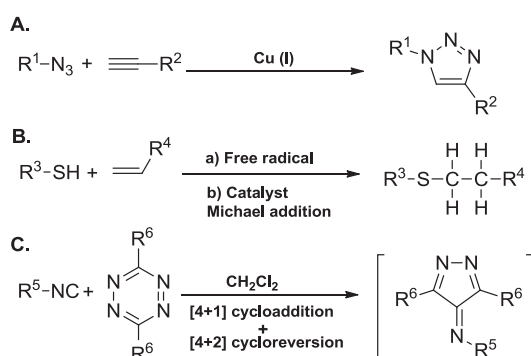
Based on the previous results obtained in our department,¹⁴⁹⁻¹⁵¹ the activation method of carboxylic acids used in the present work is a combination of diisopropyl carbodiimide (DIC) and hydroxybenzotriazole HOBt (**Scheme II-9**). DIC reacts with the carboxylic acid to form an *O*-acylisourea. *N*-acylurea could be formed by acetyl transfer, but this side reaction could be avoided by adding HOBt. The intermediate ester generated is relatively stable but still reactive. Then, nucleophilic attack by iminophosphorane or amine affords the amide derivative. DIC was chosen rather than DCC for mainly one reason that DIC is a liquid having a better dispersion in the reaction than the crystalline DCC. HOBt was added in order to avoid side reactions and also suppress the possible racemization. Commercially available HOBt is stabilized by water as monohydrate crystal due to the explosive property of anhydrous HOBt. This hydrated HOBt requires careful treatment (coevaporation with toluene) before use for reactions to obtain anhydrous conditions.



Scheme II-9. Amide bond formation between activated esters and iminophosphoranes or amines.

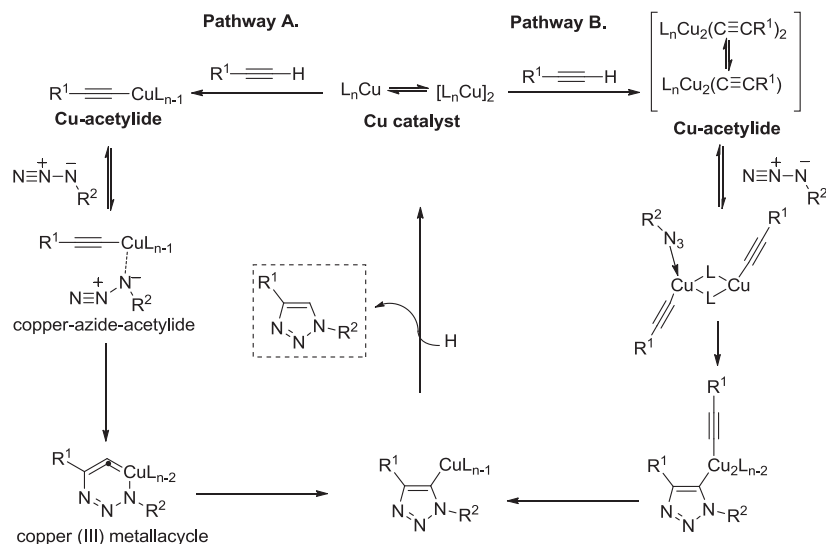
I.1.1.3 “Click” chemistry – Copper(I)-catalyzed Azide-Alkyne Cycloaddition (CuAAC)

“Click” chemistry is a chemical concept first proposed by K. B. Sharpless in 2001.¹⁵² It involves reactions that are high efficient, easy to be performed, wide in scope, with high atom economy and lead to byproducts that are inoffensive and can easily be removed. The application of “Click” chemistry to construct diversified chemical libraries is highly valuable mainly in pharmaceutical and material sciences. Among the numerous chemical reactions developed, several reaction types are better meeting the criteria and are now popularly known as one of the members of “Click” chemistry. These reactions are [3+2] cycloaddition such as Copper (I)-catalyzed Azide-Alkyne Cycloaddition (CuAAC),¹⁵³ thiol-ene click reactions,¹⁵⁴ but also [4+1] cycloaddition between isocyanides and tetrazines (**Scheme II-10**).¹⁵⁵



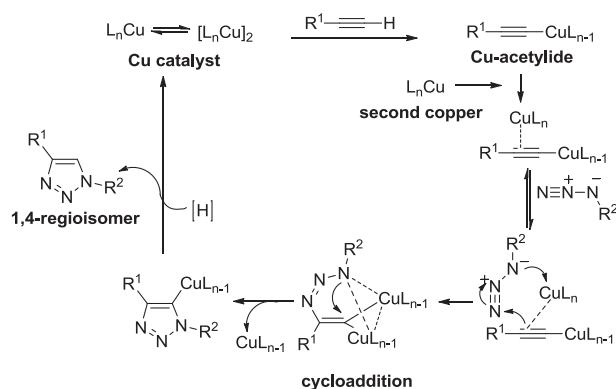
Scheme II-10. Examples of reaction types known as “Click” chemistry.

Among these efficient chemical methods, CuAAC was selected for the construction of glycosyltransferase inhibitors in the present study. The mechanism of CuAAC reaction was studied and proposed mainly by two different research groups at the Scripps Research institute, K. B. Sharpless’ group and Valery V. Fokin’s group. Firstly, a stepwise mechanism involving a six-membered copper(III) metallacycle intermediate was proposed based on computational studies (Pathway A, **Scheme II-11**) in 2005.¹⁵⁶ The process involves generation of a Cu-acetylide complex followed by coordination with an azide to form a copper-azide-acetylide complex. Cycloaddition takes place at this point to form an unusual metallacycle intermediate followed by protonation to afford regioselectively the 1,4-regioisomer.



Scheme II-11. Proposed mechanism for CuAAC by K. B. Sharpless *et al.*¹⁵⁶ (Pathway A) and Valery V. Fokin *et al.*¹⁵⁷ (Pathway B).

Later that year, a dinuclear copper intermediate involved in the mechanism was proposed by Valery V. Fokin (Pathway B, **Scheme II-11**).¹⁵⁷ Followed by further research, this group provided more experimental evidence supported their mechanistic interpretation in 2013 (**Scheme II-11**).¹⁵⁸ Real-time monitoring of the cycloaddition process indicated that two atoms of copper are required to promote the process while without adding exogenous copper catalyst the Cu-acetylide is not reactive. Further crossover experiments employing isotopically enriched copper revealed that the two coppers involved contribute equally to the process indicating a rapid exchange during the cycloaddition step (**Scheme II-12**). Therefore, a dinuclear copper intermediate mechanism is now clearly demonstrated for the CuAAC.



Scheme II-12. Dinuclear copper intermediated identified in the mechanism for CuAAC proposed by Valery V. Fokin *et al.*¹⁵⁸

II.2 Investigation of glycosylation methods of a “basic” acceptor

An initial step for the synthesis of neutral analogues of UDP-sugar incorporating a pyridine glycoside is the glycosylation of hydroxymethylpyridine derivatives. Surprisingly, a careful survey of the literature for the glycosylation of such glycosyl acceptors did not afford many results and most of these were poor in terms of isolated yields of glycosides (**Figure II-3**).

Pyridoxine can be glycosylated on the hydroxymethyl groups at positions 4' or 5', or both, and is better known as vitamin B₆. In these initial reports, the glycosidic bond formation of pyridoxine had been studied by different glycosidases (**1-3**, **Figure II-3**).¹⁵⁹⁻¹⁶¹ In another

series of experiments, the influence of borate was evaluated in order to obtain a regioselective glucosylation of pyridoxine at the 4'- or 5'-position by microorganisms.¹⁶²⁻¹⁶³ The glycosyl donors used in these reports were natural (oligo)saccharides, sucrose or dextrans but also chemically modified carbohydrates such as *p*-nitrophenyl (PNP) or α -bromo activated glycosides. Nevertheless, under the aforementioned conditions using enzymatic or microbial glycosylations, a maximum yield of 40% was achieved. Despite these bio-catalyzed synthetic strategies inspired by natural enzymes or microorganisms did not require extensive protecting group chemistry and could provide the desired glycosides in high anomeric stereoselectivity, the yields obtained remained quite low and did not call for further applications.

In an organic chemistry approach, only a few reports have been identified. The glucuronylation of ciamexon (an immunomodulating agent with application in diabetes) was achieved from the corresponding α -glucuronopyranosyl bromide donor using silver(I) salt as a promoter leading to the desired glucuronide in 45% yield (**4**, **Figure II-3**).¹⁶⁴ The reaction conditions were quite sensitive and the use of basic medium (*sym*-collidine) influenced the reaction affording a large portion of undesired orthoester. This problem could be overcome by using excess of silver triflate (3 equivalents) most probably in order to balance the basicity of the pyridine acceptor. The formation of the orthoester intermediate could not be prevented in the glycosylation between acetobromoglucose and 2-vinyl-5-hydroxymethylpyridine derivative using AgOTf as the promoter¹⁶⁵ in a study for the design of peptide functionalizing agents (**5**, **Figure II-3**). Again, an excess of promoter (1.5 equivalents) was used but led to exclusive formation of the orthoester intermediate in 73% yield since the same amount of acceptor was used and its basicity could therefore not be totally balanced. A subsequent rearrangement in the presence of trimethylsilyl triflate (TMSOTf) afforded the desired glycoside in 32% yield corresponding to an overall yield of only 24% over two steps. In another case, isomaltulose was used as a precursor for α -glucosylated hydroxymethylpyridine derivatives (**6**, **Figure II-3**).¹⁶⁶ Acid dehydration of isomaltulose afforded a glucosylated furfural which could be transformed into a pyridine moiety through two additional synthetic steps. The overall process did not afford the desired compounds in good yields (< 5%) but represents yet another possibility for the construction of the pyridine scaffold from natural source.

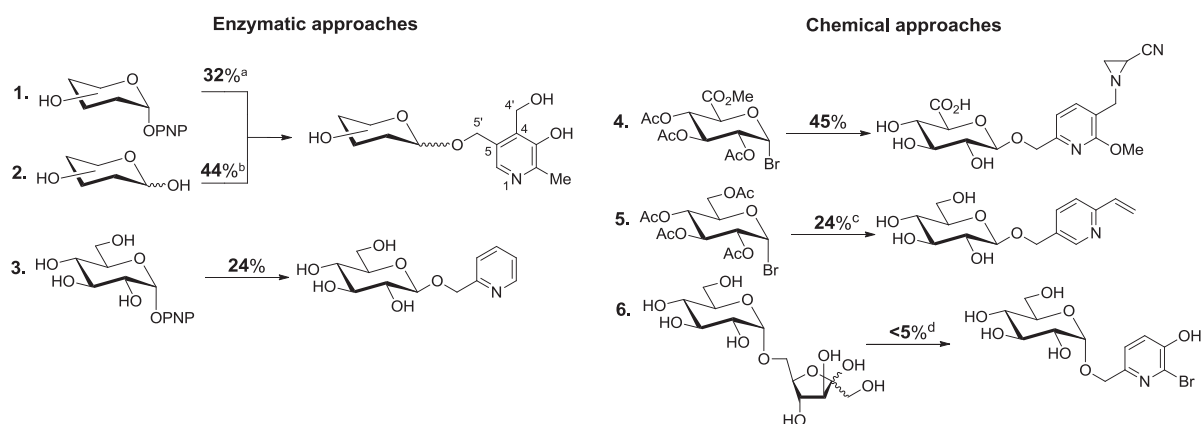
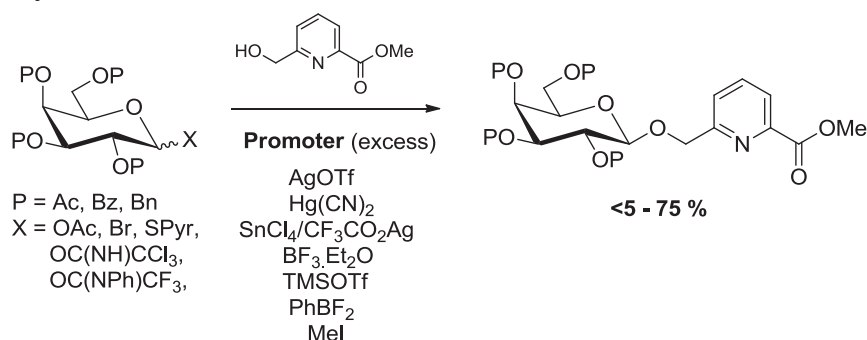


Figure II-3. Enzymatic and chemical approaches to the synthesis of glycosylated hydroxymethylpyridine derivatives. a. Yield reported for galactose derivatives; b. The 4'-regioisomer was also isolated in a 28:72 mixture with the desired 5'-derivative desired; c. Yield calculated over two steps from the data reported; d. Yield calculated from the reported data for the multi-step process.

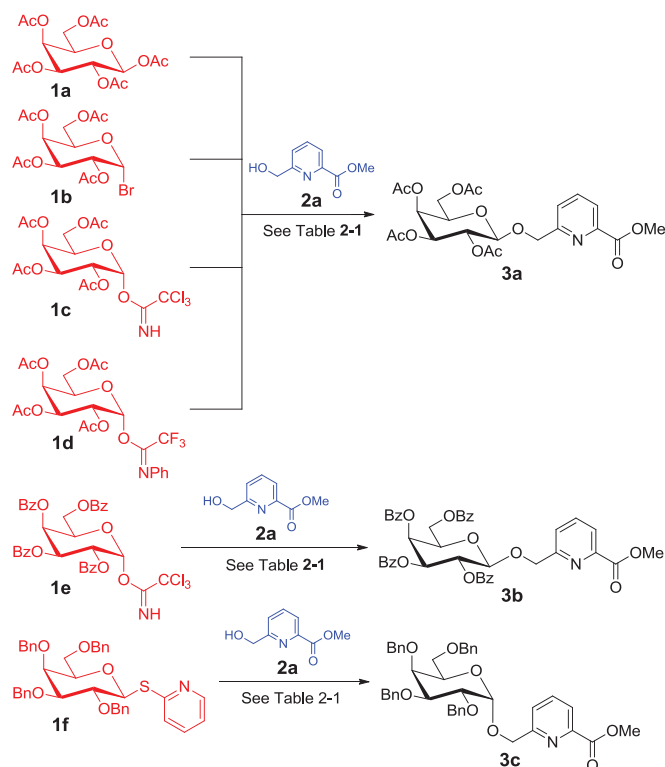
Based on the literature search, a systematic investigation of the glycosylation was performed taking methyl 6-(hydroxymethyl)picolinate as a model acceptor substrate.¹⁶⁷ A detailed study including 20 glycosyl donors was performed to determine the influence of protecting group and leaving group on the glycosyl donor as well as the nature of the promoter. 41 Different reaction conditions were tested and the optimized glycosylation methods¹⁶⁷ were applied to the synthesis of neutral inhibitors of glycosyltransferases.

II.2.1 Galactosylation



Scheme II-13. Presentation of galactosylation investigated.

The first type of glycosylation investigated employed different galactosyl donors in order to address both the influence of protecting groups on the carbohydrate moiety as well as the different leaving groups at the anomeric position (**Scheme II-13**). When a Lewis acid was used as promoter, it was added in excess in order to balance the basicity of the pyridine-based acceptor and in almost all cases, an excess of glycosyl donor was used to ensure maximal functionalization of the acceptor.



Scheme II-14. Galactosylation of methyl 6-(hydroxymethyl)picolinate **2a** with galactosyl donors **1a-f**.

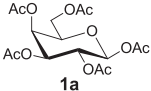
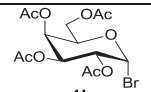
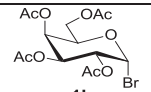
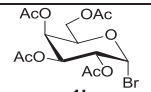
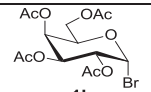
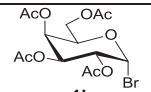
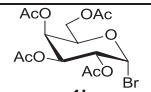
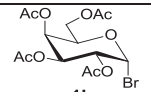
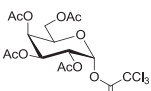
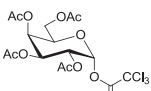
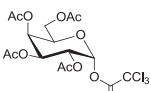
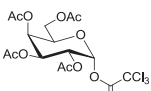
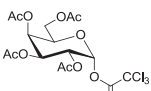
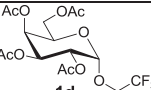
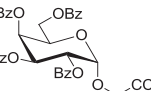
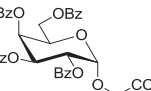
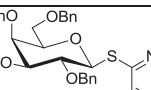
A series of 6 different galactosyl donors **1a-f** were synthesized and used in the present study (**Scheme II-14**). Peracetylated galactose **1a** was firstly chosen because of less synthetic steps required for its preparation. An efficient synthetic methodology for glycosylation from peracetylated sugar donors and catalyzed by silver and tin salts was re-investigated by our group.¹⁶⁸ In this case, only a slight spot corresponding to the glycoside could be detected by TLC which was not isolated (Entry **1**, **Table II-2**). Then, we turned to the Koenigs-Knorr glycosylation system using galactopyranosyl bromide **1b** as sugar donor (Entries **2-4**, **Table II-2**). In the first two experiments using the common silver triflate as promoter (Entries **2-3**, **Table II-2**), poor yields were obtained regardless of which donor or acceptor was used in excess. Applying the Helferich modification method¹⁶⁹ using mercury(II) cyanide (Entry **4**, **Table II-2**) as the promoter, the expected β -glycoside was formed in 11% yield. In this reaction, a mixture of acetonitrile and dichloromethane was used for optimal solubility of the reactants. These poor results prompted us to turn to more activated donors such as the galactose trichloroacetimidate **1c** which was known as a powerful glycosylating agent.¹⁷⁰⁻¹⁷¹

Boron trifluoride etherate and trimethylsilyl trifluoromethanesulfonate are the two common catalysts used when applying sugar trichloroacetimidate as the active sugar donor. When boron trifluoride etherate was used (Entries **5-10**, **Table II-2**), the best result in this respect was obtained under standard conditions with 46% yield (Entry **5**, **Table II-2**). Modifications on the reaction conditions were made, but addition of molecular sieves (Entry **6**, **Table II-2**), prolongation of reaction time (Entry **7**, **Table II-2**), changing the solvent to acetonitrile (Entry **8**, **Table II-2**), excess of acceptor (Entry **9**, **Table II-2**) or larger proportions of donor (Entry **10**, **Table II-2**) did not improve the yields. Trimethylsilyl trifluoromethanesulfonate was also investigated as a promoter for this glycosylation, but the main product isolated was the silylated acceptor **2b** (Entry **11**, **Table II-2**). A relatively neutral glycosylation condition compared to boron trifluoride etherate, was reported by the Schmidt group recently using difluoro(phenyl)borane (PhBF_2) as the glycosylation promoter.¹⁷²⁻¹⁷³ This new methodology was also evaluated (Entry **12-13**, **Table II-2**) but proved rather unsuccessful providing poor yields even at higher temperatures than initially required. We also synthesized *N*-phenyl-trifluoroacetimidate donor **1d** which was recently shown to provide better yields than the standard trichloroacetimidates¹⁷⁴ but the yield of galactoside **3a** was not improved (Entry **14**, **Table II-2**).

Benzoate protecting groups were used in some cases because they were more stable than acetates. Therefore, the benzoylated trichloroacetimidate donor **1e**¹⁷⁵⁻¹⁷⁶ was used under the best conditions obtained previously (Entry **5**, **Table II-2**). With 1.3 equivalent of donor and prolonged reaction time (Entry **15** and **16**, **Table II-2**), the yield obtained was acceptable (42%), but not improved in comparison to the acetylated donors.

Considering the “arm-disarm” concept in glycosylation,¹⁷⁷⁻¹⁸⁰ the ester protected glycosyl donors (e.g., acetates or benzoates) would be considered as disarmed and lead to poorer reactivity (i.e., longer reaction time and need for stronger promoters) while the ether protected donors (e.g., benzyl) are armed and would provide higher reactivities and better yields for the glycosylation.

Table II-2. Galactosylation of methyl 6-(hydroxymethyl)picolinate **2a** with galactosyl donors **1a-f**.

| Entry | Donor | Ratio Donor:Acceptor | Temp. Time | Promoter | Yield ^a | Product Ratio $\alpha : \beta$ |
|-------|---|----------------------|-------------------|--|--------------------|--------------------------------|
| 1 |  | 1.5:1 | 0°C to r.t., 16 h | SnCl ₄ (5 eq.) / CF ₃ CO ₂ Ag (2.5 eq.) | <5% ^b | -/- |
| 2 |  | 1:1.5 | r.t., 18 h | AgOTf (1.5 eq.) | 8% | 3a , β only |
| 3 |  | 2.5:1 | r.t., 26 h | AgOTf (1.5 eq.) | 18% | 3a , β only |
| 4 |  | 1.5:1 | r.t., 16 h | Hg(CN) ₂ (4 eq.) | 11% ^c | 3a , β only |
| 5 |  | 1.5:1 | -20°C, 2 h | BF ₃ ·Et ₂ O (2 eq.) | 46% | 3a , β only |
| 6 |  | 1.25:1 | -20°C, 4 h | BF ₃ ·Et ₂ O (2 eq.), 4Å MS | 34% | 3a , β only |
| 7 |  | 1.5:1 | -20°C, 16 h | BF ₃ ·Et ₂ O (2 eq.), 4Å MS | 32% | 3a , β only |
| 8 |  | 1.5:1 | -20°C, 2 h | BF ₃ ·Et ₂ O (2 eq.) | 36% ^d | 3a , β only |
| 9 |  | 1:3 | -20°C, 2.5 h | BF ₃ ·Et ₂ O (2 eq.) | <5% ^b | -/- |
| 10 |  | 3:1 | -20°C, 16 h | BF ₃ ·Et ₂ O (3 eq.) | 42% | 3a , β only |
| 11 |  | 1.5:1 | -20°C, 1 h | TMSOTf (0.5 eq.), 4Å MS | 5% ^e | 3a , β only |
| 12 |  | 2:1 | -78°C, 3 h | PhBF ₂ (2 eq.) | 16% | 3a , β only |
| 13 |  | 1.5:1 | -20°C, 2 h | PhBF ₂ (2 eq.) | 14% | 3a , β only |
| 14 |  | 1.5:1 | -20°C, 2 h | BF ₃ ·Et ₂ O (2 eq.) | 32% | 3a , β only |
| 15 |  | 1.3:1 | -20°C, 22 h | TMSOTf (2 eq.), 4Å MS | 33% | 3b , β only |
| 16 |  | 1.3:1 | -20°C, 20 h | BF ₃ ·Et ₂ O (3 eq.) | 42% | 3b , β only |
| 17 |  | 1:1 | 50°C, 78 h | MeI (4.5 eq.), 4Å MS | 75% | 3c , α only |

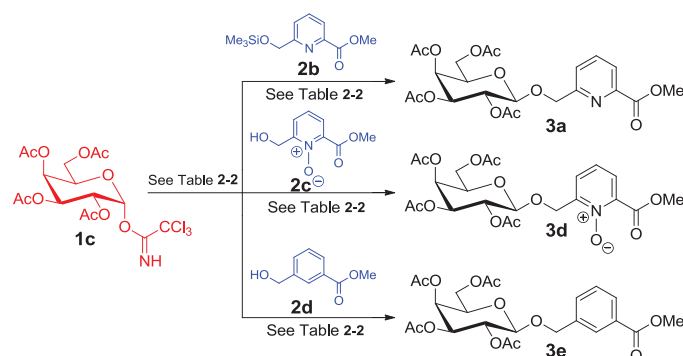
a. Values are isolated yields. b. Product could not be isolated but was detected by TLC. c. The glycosylation was performed in CH₃CN/CH₂Cl₂ (1/1, v/v). d. The glycosylation was performed in CH₃CN. e. The main product isolated was methyl 6-(trimethylsilyloxymethyl)picolinate **2b**.

The 2-thiopyridyl perbenzylated donor **1f**¹⁸¹ was therefore evaluated as a glycosyl donor for this pyridine-based acceptor. Activation by methyl iodide provided a good yield (75%) of the desired galactoside **3c** with an α configuration at the anomeric center. The α -anomer was favoured in this case due to the benzyl ether as a non-participating group at the 2-position.

As a conclusion for the galactosylation of 6-(hydroxymethyl)picolinate **2a**, the best conditions obtained to afford the desired β -anomer are using the trichloroacetimidate donor **1c** catalyzed by boron trifluoride etherate as a promoter in excess (1.5 equivalent) and with only 2 h reaction time at low temperature (-20°C). Better yields, albeit with the opposite configuration at the anomeric center, can be obtained with benzylated armed donors such as **1f**.

II.2.2 Modifications on the pyridine-based acceptor

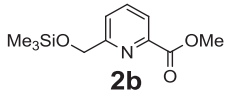
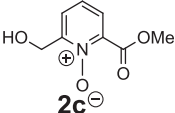
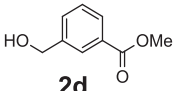
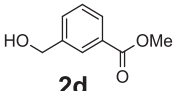
The intrinsic basicity of the pyridine-based acceptor under acid-promoted glycosylation conditions was then investigated (**Scheme II-15**) through variations on the pyridine moiety with *N*-oxide derivative **2c** and also the corresponding phenyl-based donor **2d**.



Scheme II-15. Influence of the pyridine-based acceptor on the galactosylation reaction.

The silylated acceptor **2b** was isolated from Entry **11**, **Table II-2** and reintroduced for galactosylation with the best donor **1c** identified in the previous experiments. It is known that the acidity of the promoter can trigger the cleavage of the trimethylsilyl group therefore allowing the glycosylation to proceed.¹⁸²⁻¹⁸⁴ Only a very small amount of the desired galactoside **3a** (< 5%) could be observed by TLC (not isolated) although the donor **1c** was totally consumed while the silylated acceptor **2b** was still largely unreacted (Entry **18**, **Table II-3**). Afterwards, a common method for masking the basicity of a pyridine ring was applied through oxidation to the *N*-oxide derivative **2c**.¹⁸⁵ In this case, excess of promoter was avoided but only very limited amounts of the desired galactoside **3d** could be isolated as an inseparable mixture of α and β anomers along with the hydrolyzed hemiacetal donor and unreacted acceptor (Entry **19**, **Table II-3**).

Table II-3. Influence of the pyridine-based acceptors **2b-d** with the galactosyl donor **1c**.

| Entry | Donor | Ratio Donor:Acceptor | Temp. Time | Promoter | Yield ^a | Product Ratio α : β |
|-------|---|----------------------|------------|--|--------------------|----------------------------------|
| 18 |  | 1.5:1 | -20°C, 3 h | TMSOTf (1 eq.), 4Å MS | <5% ^b | 3a |
| 19 |  | 2.25:1 | -20°C, 3 h | BF ₃ ·Et ₂ O (0.6 eq.) | 7% | 3d ^c , 32:68 |
| 20 |  | 1.5:1 | -20°C, 2 h | BF ₃ ·Et ₂ O (0.2 eq.) | 37% ^d | 3e , β only |
| 21 |  | 1:3 | -20°C, 1 h | BF ₃ ·Et ₂ O (0.2 eq.) | 79% | 3e , β only |

a. Values are isolated yields. b. Product was not isolated but identified by TLC in a very small proportion. c. Product was isolated as an inseparable mixture of hydroxylated donor, unreacted acceptor, α - and β -anomers. d. Acetylated acceptor (methyl 6-acetoxymethylbenzoate) was also isolated in 37% yield.

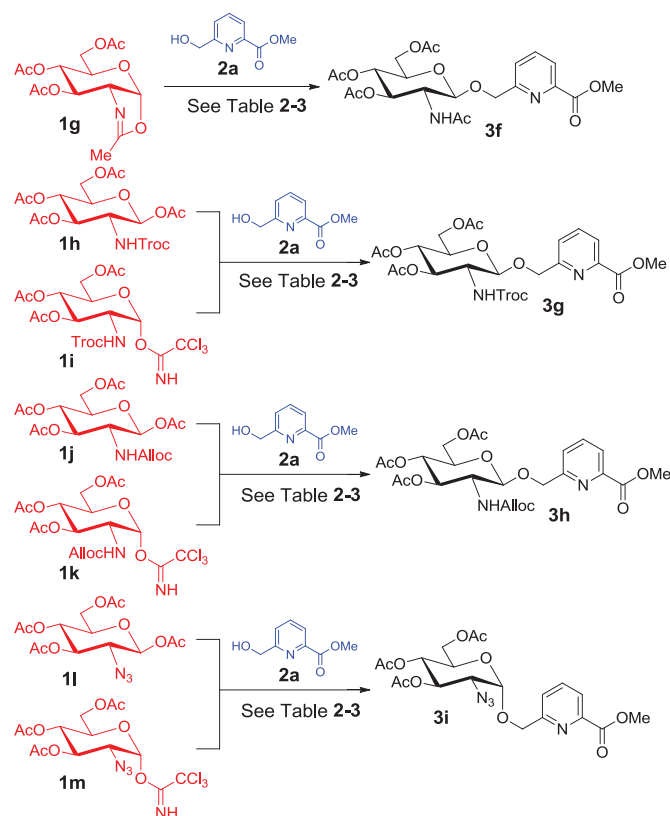
Finally, the influence of basicity of the pyridine ring could be clearly demonstrated by studying the galactosylation of methyl 6-hydroxymethylbenzoate acceptor **2d**.¹⁸⁶ When the reaction was performed under the best conditions determined previously, transfer of an acetate from the donor to the acceptor was observed with methyl 6-acetoxymethylbenzoate obtained in 37%

isolated yield (Entry **20**, **Table II-3**). Therefore, using a three-fold excess of acceptor provided a very good yield of 79% (Entry **21**, **Table II-3**). While this last result appeared promising, similar conditions, using an excess of donor did not improve the yield when the pyridine-based acceptor **2a** was used (Entry **9**, **Table II-2**).

II.2.3 *N*-Acetylglucosaminyl donors

Design and synthesis of glycosyltransferase inhibitors targeting *N*-acetylglucosaminyl transferases is part of the present research program. After assessing the parameters influencing the glycosylation reaction in the galactose series, glycosylation methodology towards *N*-acetylglucosamine (GlcNAc) series was then studied applying sugar donors **1g-m** (**Scheme II-16**).

The isoxazoline donor **1g**¹⁸⁷ is commonly employed for glycosylation in the GlcNAc series (also referred as GlcNAcylation). Two different promoters were used, but unsatisfying yields were obtained (Entries **22-23**, **Table II-4**). Then, we turned to 2-deoxy-2-amino-protected GlcNAc donors **1h-m** which could be taken as precursors of *N*-acetyl moieties (**Scheme II-16**). Carbamates, such as donors **1h-k**, are usually invoked for their good stereocontrol in favour of β -anomers through anchimeric participation while 2-azido-2-deoxy-derivatives **1l-m** would lead to α -anomers.

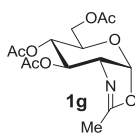
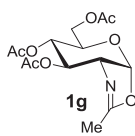
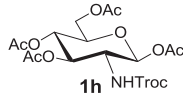
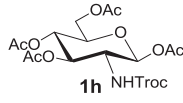
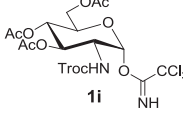
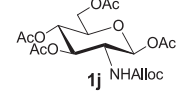
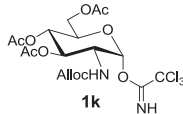
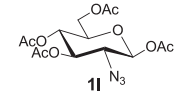
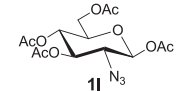
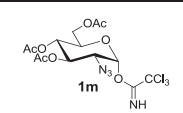
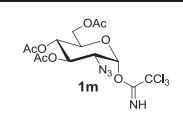


Scheme II-16. Glycosylation of methyl 6-(hydroxymethyl)picolinate **2a** with donors **1g-m**.

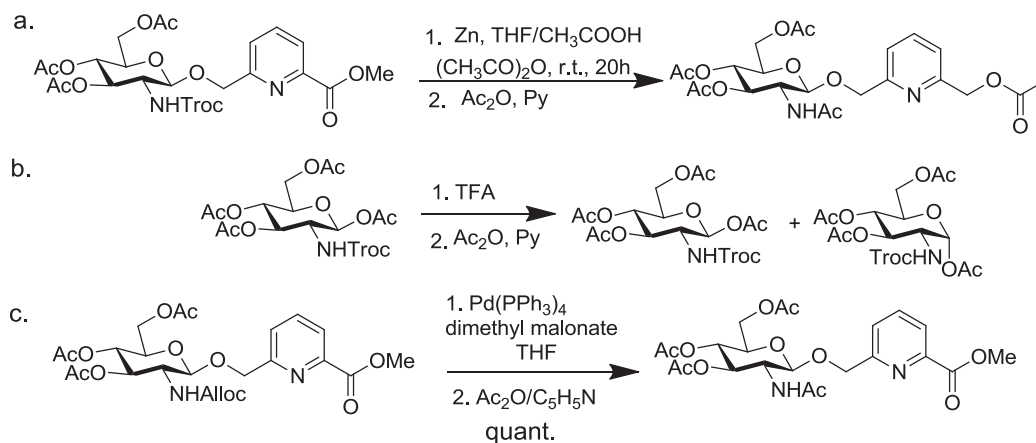
The 2,2,2-trichloroethyl-carbamate (Troc) protecting group associated with an anomeric acetate leaving group in donor **1h**¹⁸⁸⁻¹⁸⁹ improved slightly the yield of GlcNAcylation (Entry **24**, **Table II-4**) to 25%. Much better results were then obtained with the more activated donor **1i**¹⁹⁰ bearing a trichloroacetimidate as leaving group and more specifically under activation with boron trifluoride etherate as a promoter (Entries **25-26**, **Table II-4**) leading to an isolated yield of 66%.

The protecting group transformation from 2,2,2-trichloroethyl-carbamate (Troc) to NH-Ac was then performed. To our surprise, under the common reaction condition Zn/Ac₂O/AcOH in THF¹⁹¹, the Troc protecting group was replaced by acetate, but the methyl ester was also reduced to alcohol followed by acetylation as evidenced by mass spectrometry (*m/z*, [M+H]⁺ = 511.1) (**a**, **Scheme II-17**). TFA was also tried as a deprotection reagent, but a mixture of anomers was obtained without altering the Troc protecting group (**b**, **Scheme II-17**). Then, an allyl-carbamate (Alloc) protecting group was introduced in donors **1j-k**¹⁹²⁻¹⁹³ which provided moderate yields (Entries **27-28**, **Table II-4**). The protecting group transformation from NHAlloc to NHAc was carried out under reported reaction condition Pd(PPh₃)₄/dimethyl malonate in THF¹⁹⁴ followed by acetylation (**c**, **Scheme II-17**). Finally, in this case, a quantitative yield was obtained.

Table II-4. Glycosylation in the GlcNAc series with methyl 6-(hydroxymethyl)picolinate **2a**.

| Entry | Donor | Ratio Donor:Acceptor | Temp. Time | Promoter | Yield ^a | Product Ratio $\alpha : \beta$ |
|-------|---|----------------------|----------------------------|---|--------------------|---------------------------------------|
| 22 |  | 1.1:1 | 60°C, 5.5 h | CSA (1.2 eq.), 4Å MS | 17% | 3f , β only |
| 23 |  | 1.5:1 | 20°C, 22 h | BF ₃ ·Et ₂ O (3 eq.), 4Å MS | 20% | 3f , β only |
| 24 |  | 1.1:1 | -20°C, 22 h | TMSOTf (3 eq.) | 25% | 3g , β only |
| 25 |  | 1.6:1 | -20°C, 4.5 h | TMSOTf (2 eq.) | 48% | 3g , β only |
| 26 |  | 1.1:1 | -20°C, 3 h | BF ₃ ·Et ₂ O (2 eq.) | 66% | 3g , β only |
| 27 |  | 1.5:1 | -20°C, 3.5 h; r.t., 15.5 h | TMSOTf (3 eq.) | 27% | 3h , β only |
| 28 |  | 1.1:1 | -20°C, 17 h | BF ₃ ·Et ₂ O (3 eq.) | 48% | 3h ^b , β only |
| 29 |  | 1.5:1 | -20°C, 2.5 h; r.t., 16 h | TMSOTf (4 eq.) | <5% | 3i ^c |
| 30 |  | 1.5:1 | -20°C, 2.5 h; r.t., 16 h | BF ₃ ·Et ₂ O (4 eq.) | 35% | 3i , α only |
| 31 |  | 1.5:1 | -20°C, 2 h | TMSOTf (2 eq.) | 17% | 3i , α only |
| 32 |  | 1.5:1 | -20°C, 2 h; r.t., 16 h | BF ₃ ·Et ₂ O (4 eq.) | 82% | 3i , 72:28 |

a. Values are isolated yields. b. Product was isolated as a mixture of β -anomer **3h** and 0.3 eq. unreacted acceptor **2a** and could not be separated due to similar polarity. Yield was calculated excluding the unreacted acceptor **2a** based on ¹H NMR data. c. Product could not be isolated but detected by TLC. A byproduct identified as methyl 6-(acetoxymethyl)picolinate was isolated in 53% yield.



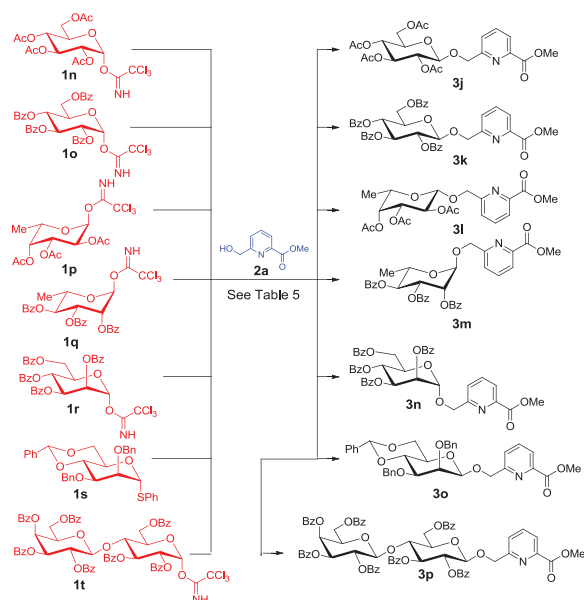
Scheme II-17. Functional group conversion of glucosamine derivatives.

The azido functionality is a general precursor of NHAc groups and its use in GlcNAcylation has two consequences. The azido group is non-participating and therefore the glycoside obtained is usually the α -anomer. The need for the 2-acetamido substituent requires a subsequent reduction/acetylation process which must be included in the synthetic strategy in terms of steps but also stability for the further elaboration of the target molecule. Nevertheless, these types of 2-azido-2-deoxy donors are quite useful and the peracetylated donor **11**¹⁹⁵⁻¹⁹⁶ (prepared from commercially available 2-azido-2-deoxy-D-glucose) was used but provided only moderate yields (Entries **29-30**, **Table II-4**). A transfer of acetyl group was observed from the glycosyl donor **11** to the acceptor **2a** affording the methyl 6-(acetoxymethyl)picolinate in 53% isolated yield (Entry **29**, **Table II-4**) when using trimethylsilyl trifluoromethanesulfonate (TMSOTf) as the promoter. The 2-azido-2-deoxy trichloroacetimidate donor **1m**¹⁹⁷ was then applied. Treated with TMSOTf, only small amounts of the desired product could be separated as the α -glycoside **3i** (Entry **31**, **Table II-4**). A very good yield of 82% could then be obtained but as a mixture of both isomers using boron trifluoride etherate as the promoter (Entry **32**, **Table II-4**).

As a short conclusion for the GlcNAcylation section, 7 different donors with various protecting groups at the 2-position under a total of 11 synthetic methodologies were performed. The best conditions found in this series were the use 2-azido-2-deoxy derivatives to obtain the α -anomer while the Alloc carbamate was favored for the preparation of β -glycosides.

II.2.4 Other glycosyl donors (Glc, Man, Fuc, Rha, Lac)

In order to broaden the scope of this glycosylation methodology of pyridine-based acceptors, the reaction was studied with several other glycosyl donors of monosaccharides (glucose, mannose, rhamnose, fucose) and one disaccharide (lactose) (**Scheme II-18**).



Scheme II-18. Glycosylation of methyl 6-(hydroxymethyl)picolinate **2a** with mono- and disaccharidic glycosyl donors **1n-t**.

II.2.4.1 Glucose. Two glucosyl donors, acetylated trichloroacetimidate **1n**¹⁹⁸ and benzoylated trichloroacetimidates **1o**,¹⁹⁹ were evaluated. The yields obtained were better (Entry **33-34**, **Table II-5**) than the results previously observed in the galactose series (Entries **2-13** and **21-22**, **Table II-2**).

II.2.4.2 Fucose and Rhamnose. Glycosylation using 6-deoxyhexoses such as L-fucose is also important due to the relevant biological implications of such carbohydrates in cancer and bacterial infections.²⁰⁰ The acetylated trichloroacetimidate fucosyl donor **1p**²⁰¹ was therefore reacted under the best conditions elaborated in the galactose series leading to a moderate isolated yield of 39% of fucoside **3l** (Entry **35**, **Table II-5**). The rhamnosyl donor **1q**²⁰² was studied in a collaboration with Reko Leino's research group in Åbo University (Finland). Catalyzing by TMSOTf, the benzoylated rhamnosyl trichloroacetimidate **1q** afforded a better yield of 66% in comparison with the acetylated fucosyl trichloroacetimidate donor **1p** (Entry **36**, **Table II-5**).

II.2.4.3 Mannose. Two mannosyl donors, benzoylated trichloroacetimidate mannosyl donor **1r**²⁰³ and bicyclic containing armed donor **1s**,²⁰⁴ were evaluated with Prof. Leino's team. Under activation of $\text{BF}_3 \cdot \text{Et}_2\text{O}$ and TMSOTf, the trichloroacetimidate donor **1r** afforded the desired α -mannoside **3n** in moderate yields (Entries **37-38**, **Table II-5**). When a 4,6-benzylidene protecting group was introduced to the phenyl thioglycoside **1s**, better yields were obtained (Entries **39-40**, **Table II-5**). More interestingly, when this bicyclic system was used, the unusual β -mannoside **3o** was favoured. β -Mannoside **3o** was isolated as the only glycoside with a yield of 68% using TMSOTf-NIS as promoters. Changing the catalytical system to BSP- Tf_2O improved slightly the yield although stereoselectivity was poorer. The confirmation of configurations at the anomeric carbon of mannosides **3n** and **3o** was based on 1J coupling constants. The 1J coupling constants measured between the anomeric carbon (C-1) and the anomeric proton (H-1) with values above 170 Hz was assigned for α -mannosides versus values below 160 Hz were measured for β -mannosides.²⁰⁵

II.2.4.4 Lactose. Another disaccharide, the benzoylated trichloroacetimidate lactosyl donor **1t**²⁰⁶ was reacted with the acceptor **2a** using boron trifluoride etherate as a promoter and afforded the desired lactoside **3p** in 51% isolated yield (Entry 41, Table II-5).

Table II-5. Glycosylation of methyl 6-(hydroxymethyl)picolinate **2a** with mono- and disaccharidic glycosyl donors **1n-t**.

| Entry | Donor | Ratio Donor:Acceptor | Temp. Time | Promoter | Yield ^a | Product Ratio $\alpha : \beta$ |
|-------|-------|----------------------|-----------------------------|---|--------------------|---------------------------------------|
| 33 | | 1.5:1 | -20°C, 22 h | BF ₃ ·Et ₂ O (3 eq.) | 55% | 3j , β only |
| 34 | | 1.3:1 | -20°C, 22.5 h | TMSOTf (2 eq.), 4Å MS | 61% | 3k^b , β only |
| 35 | | 1.5:1 | -20°C, 2 h | BF ₃ ·Et ₂ O (2 eq.) | 39% | 3l , β only |
| 36 | | 1.3:1 | -20°C, 4 h | TMSOTf (0.8 eq.) | 66% | 3m , α only |
| 37 | | 1.3:1 | -20°C, 22.5 h | BF ₃ ·Et ₂ O (2 eq.) | 48% | 3n^c , α only |
| 38 | | 1.3:1 | -20°C, 22.5 h | TMSOTf, (2 eq.) | 22% | 3n^c , α only |
| 39 | | 1.3:1 | -40°C, 5.5 h | TMSOTf, (2 eq.), NIS (1.56 eq.) | 68% | 3o^d , β only |
| 40 | | 1:1.15 | -60°C, 0.5 h; -78°C, 3 h | BSP (1.2 eq.), TTBP (1.5 eq.), Tf ₂ O (1.3 eq.), 1-octene (2 eq.) | 80% | 3o^e , 19:81 |
| 41 | | 1:1 | -20°C, 4 h | BF ₃ ·Et ₂ O (2 eq.) | 51% | 3p , β only |

a. Values are isolated yields. b. Product was isolated as a mixture of β -anomer **3k** and 0.2 eq. unreacted acceptor **2a** and could not be separated due to similar polarity. Yield was calculated excluding the unreacted acceptor **2a** based on ¹H NMR data. c. Configuration at the α -anomeric center was confirmed by the ¹J_{C-1,H-1} = 172.4 Hz value. d. Configuration at the β -anomeric center was confirmed by the ¹J_{C-1,H-1} = 155.5 Hz value. e. Configuration at the α -anomeric center was confirmed by the ¹J_{C-1,H-1} = 171.5 Hz value.

As a conclusion for the investigation of glycosylation methods on pyridine-based acceptors, a series of 20 glycosyl donors derived from glucose, galactose, mannose, fucose, rhamnose and lactose and a large number of activating groups at the anomeric center (e.g., acetate, bromide, trichloroacetimidate, thiopyridine) and a complete set of activating conditions were evaluated. The pyridine moiety was identified to have a negative influence on the reaction in comparison to the “phenyl-based” donor **2d**. Therefore, the basicity of the pyridine ring could be verified as a limitation to the outcome of the glycosylation reaction. The best conditions for the glycosylation of the model donor methyl 6-(hydroxymethyl)picolinate **2a** could provide isolated yields of glycosides from 46% to 82% with different type of glycosyl donors. And the

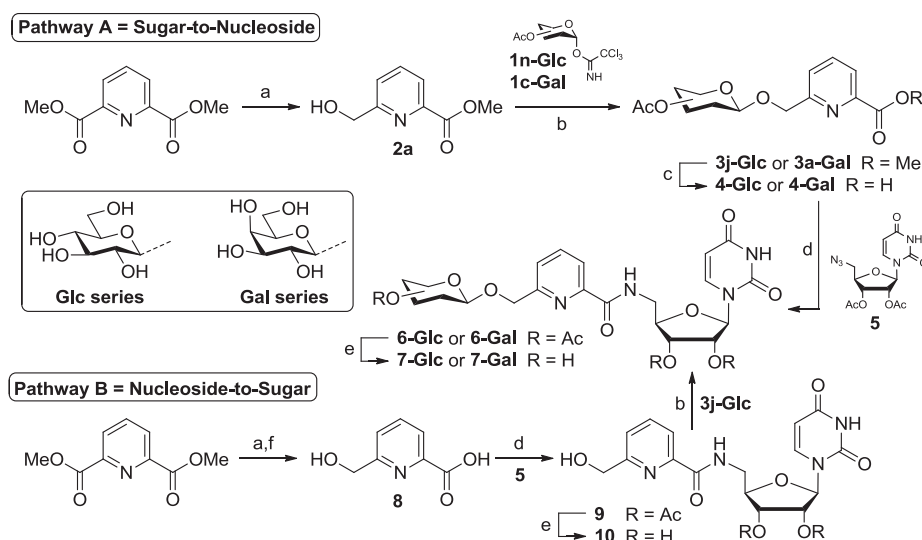
optimized glycosylation methods could then be applied to the synthesis of the target neutral inhibitors of glycosyltransferases.

II.3 Synthesis of UDP-sugar analogues based on glycosylation and amide bond chemistries

For synthesis of UDP-sugar analogues containing pyridine as a pyrophosphate surrogate, a combination of glycosylation and Staudinger-Vilarrasa reactions was used and two synthetic routes, namely pathway A from “sugar-to-nucleoside” and pathway B from “nucleoside-to-sugar”, were investigated (Schemes II-19 and II-20).

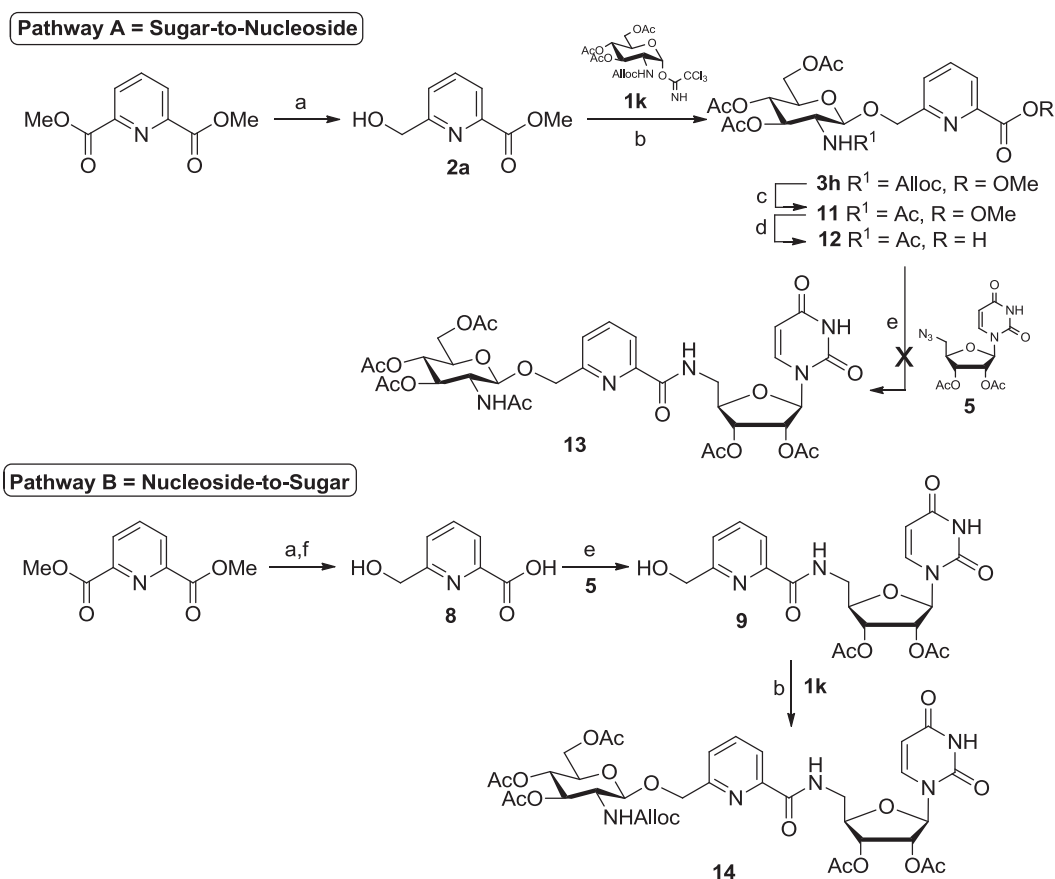
The synthetic route from “sugar-to-nucleoside” (Pathway A, Scheme II-19), synthesis of Gal derivative and Glc derivative as a negative control, started from dimethyl pyridine-2,6-dicarboxylate, after monoreduction to alcohol **2a**,⁸⁵ glycosylation of the 6-hydroxymethylpyridine derivative **2a** provided the β -glycosides **3j-Glc** and **3a-Gal** in good yields.¹⁶⁷ The methyl ester attached to the pyridine ring was then selectively unmasked in the presence of acetates to afford the carboxylic acids **4-Glc** and **4-Gal**. These compounds could then be engaged in a Staudinger-Vilarrasa reaction with 5'-azido-uridine **5** to afford the acetylated amides **6-Glc** and **6-Gal**. Removal of the acetates gave access to the desired GT inhibitor candidates **7-Glc** and **7-Gal**.

With similar synthetic methodology, the route from “nucleoside-to-sugar” gives a more flexible approach to introduce the sugar moiety at the end of the synthesis (Pathway B, Scheme II-19). The mono-ester **2** was converted to the acid **8** which was conjugated with 5'-azido-uridine **5** to afford the amide **9** which underwent glycosylation to provide the glycosides **7-Glc** and **7-Gal**. The key intermediate compound **9** was also deprotected and evaluated as a uridine-diphosphate (UDP) analogue **10** in the later enzymatic assays since UDP is known as a natural inhibitor of GT and testing UDP analogues will provide information on the influence of the carbohydrate moiety.



Scheme II-19. Synthesis of neutral GT inhibitors containing a galactose or glucose moiety using a combination of glycosylation and Staudinger-Vilarrasa ligation through two different pathways. *Reagents and conditions:* (a) NaBH₄, MeOH/CH₂Cl₂, r.t., 3h, 56%; (b) BF₃·Et₂O, CH₂Cl₂, -20°C, 2h, 55% for **3j-Glc**, 46% for **3a-Gal**, 33% for **6-Glc**; (c) NaI, C₅H₅N, 120°C, 5h, 52% for **4-Glc**, 76% for **4-Gal**; (d) PMe₃, DIC, HOBT, THF, r.t., 16h, 61% for **6-Glc**, 31% for **6-Gal**, 17% for **9**; (e) NaOMe, MeOH, 63% for **7-Glc**, quant. for **7-Gal**, quant. for **10**; (f) NaOH, MeOH/H₂O, 100°C (μW), 10 min, quant.

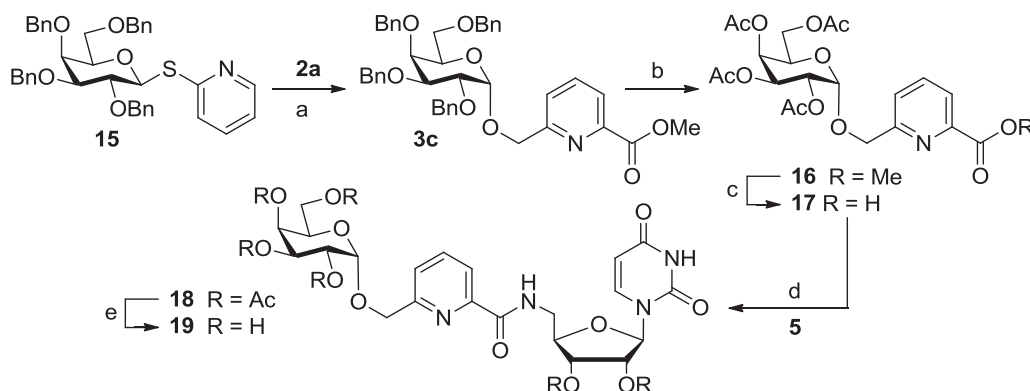
Similar synthetic routes were then applied to obtain UDP-GlcNAc analogue (**Scheme II-20**). Surprisingly, after glycosylation of mono-ester **2** with NH-Alloc trichloroacetimidate **1k**, followed by protecting group transformation to glycoside **11** and ester deprotection, the acid derivative **12** did not react with 5'-azido-uridine derivative **5** to afford the desired amide **13**. As a consequence, the unreacted acid **12** and 5'-amino-uridine derivative **5** were recovered. The other synthetic route was also investigated (**Pathway B, Scheme II-20**). Although the best glycosylation conditions determined previously were applied to acceptor **9** with NH-Alloc trichloroacetimidate **1k**, only traces of the desired glycoside **14** were observed after purification and further confirmed by mass spectrometry (m/z , $[M+H]^+ = 834.2$). Thus, the reaction condition to synthesize this type of UDP-GlcNAc analogue must be further optimized.



Scheme II-20. Synthesis of neutral GT inhibitors containing a glucosamine moiety using a combination of glycosylation and Staudinger-Vilarrasa ligation through two different pathways. *Reagents and conditions:* (a) NaBH_4 , $\text{MeOH}/\text{CH}_2\text{Cl}_2$, r.t., 3h, 56%; (b) $\text{BF}_3 \cdot \text{Et}_2\text{O}$, CH_2Cl_2 , -20°C , 17 h, 48% for **3h**, <5% for **14**; (c) $\text{Pd}(\text{PPh}_3)_4$, dimethyl malonate, THF, r.t., 24h, quant.; (d) NaI , $\text{C}_5\text{H}_5\text{N}$, 120°C , 5h; (e) PMe_3 , DIC, HOBT, THF, r.t., 16h, 17% for **9**; (f) NaOH , $\text{MeOH}/\text{H}_2\text{O}$, 100°C (μW), 10 min, quant.

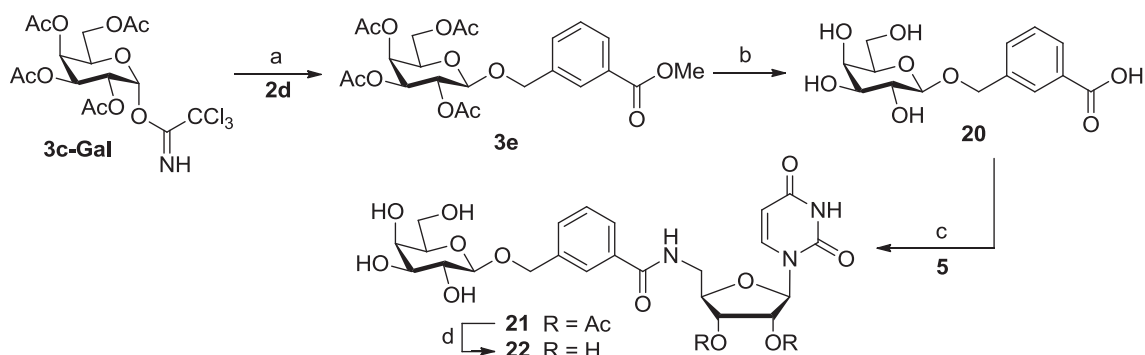
The “sugar-to-nucleoside” approach was then performed to obtain the α -isomer analogue of UDP-Gal (**Scheme II-21**). For this purpose, the benzylated galactosyl donor **15** was glycosylated with the 6-hydroxymethylpyridine derivative **2a** to provide the α -galactoside **3c**. At this point, attempted debenzoylation under hydrogenation conditions (Pd/C , H_2 1 to 8 atm.) did not affect the benzyl ethers but rather reduced the pyridine ring to a piperidine as a mixture of diastereoisomers as observed by ^1H NMR and mass spectrometry (m/z , $[M+H]^+ = 696.2$). Similar phenomenon was reported by Hironao Sajiki *et al.*²⁰⁷⁻²⁰⁸ that hydrogenolysis of benzyl ether with Pd/C could be selectively inhibited at the presence of pyridine. Other reaction

conditions such as DDQ,²⁰⁹⁻²¹⁰ $\text{Ph}_3\text{C}^+\text{BF}_4^{-211}$, NBS²¹² and $(n\text{-Bu}_4\text{N})_2\text{S}_2\text{O}_8$ ²¹³ were also tested but with either no reaction or decomposition of the starting material. Finally, the benzyl ethers were successfully removed by bromination/oxidative cleavage conditions²¹⁴⁻²¹⁵ and the crude mixture was then reacylated to provide the acetyl-protected compound **16** in 42% yield. After hydrolysis to the acid derivative **17** and formation of an amide bond to compound **18**, another pyridine containing UDP-Gal analogue **19** was obtained after deacetylation. This analogue could provide information about the importance of the configuration at the anomeric center towards GalT inhibition.



Scheme II-21. Synthesis of the α -galactoside inhibitor candidate through glycosylation and Staudinger-Vilarrasa ligation. *Reagents and conditions:* (a) MeI, CH_2Cl_2 , 50°C , 78h, 75%; (b) i) NaBrO_3 , Na_2SO_4 , $\text{EtOAc}/\text{H}_2\text{O}$, r.t., 2h then ii) Ac_2O , $\text{C}_5\text{H}_5\text{N}$, r.t., 3h, 42% for two steps; (c) NaI, $\text{C}_5\text{H}_5\text{N}$, 120°C , 5h, quant.; (d) PMe_3 , DIC, HOBt, THF, r.t., 16h, 27%; (e) NaOMe, MeOH, 63%.

The influence of the pyridine ring upon binding to the enzyme's catalytic site can also be addressed by the synthesis of a phenyl-based inhibitor candidate **22** in which the pyridine ring was replaced by a benzene moiety (**Scheme II-22**). Taking hydroxymethylbenzoate **2d** as acceptor, the galactoside **3e** was obtained with 79% yield.¹⁶⁷ In the case of phenyl derivative **3e**, selective deprotection of methyl ester versus acetate applying sodium iodide did not work and left the starting material unchanged. Whereas, after hydrolysis of all ester functions, the acid glycoside **20** reacted with 5'-azido-uridine **5** to afford the partially acetylated amide **21** under Staudinger-Vilarrasa conditions with moderate yield (43%) which was then converted to the hydroxylated GT inhibitor candidate **22**.



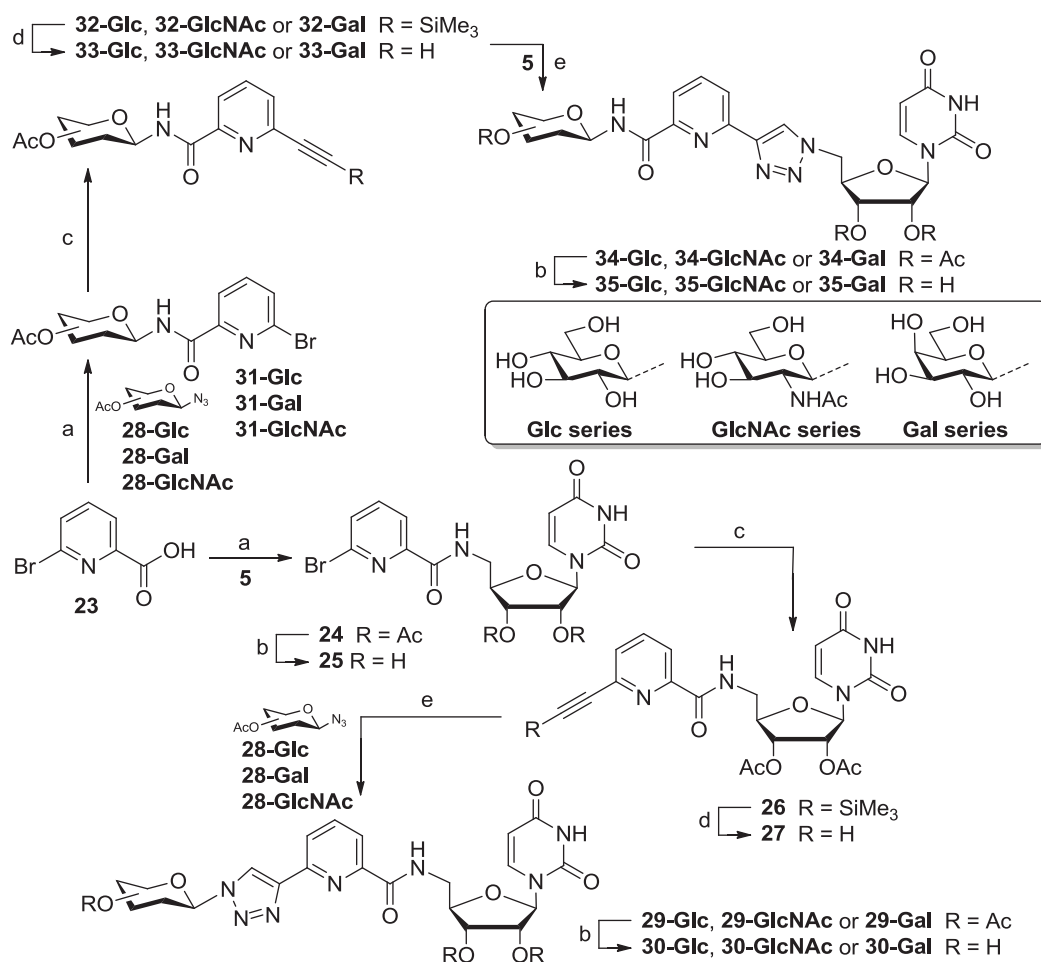
Scheme II-22. Synthesis of a phenyl-based pyrophosphate analogue through β -galactosylation and Staudinger-Vilarrasa ligation. *Reagents and conditions:* (a) methyl 5-hydroxymethylbenzoate, $\text{BF}_3 \cdot \text{Et}_2\text{O}$, CH_2Cl_2 , -20°C , 1h, 79%; (b) LiOH, THF/ H_2O , r.t., 48h, 93%; (c) PMe_3 , DIC, HOBt, THF, r.t., 16h, 43%; (d) NaOMe, MeOH, 73%.

II.4 Synthesis of UDP-sugar analogues based on azide-alkyne and amide bond chemistries

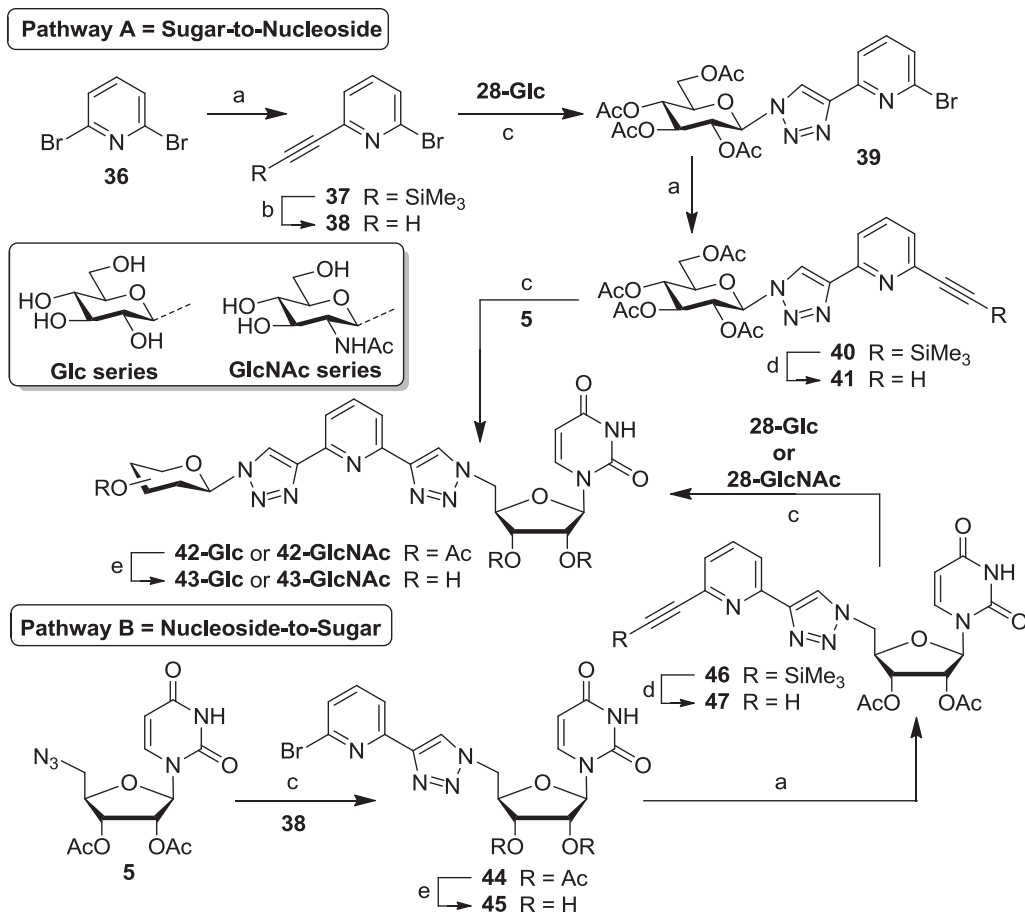
In order to use a combination of amide bond and triazole for the design of UDP-sugar analogues, the syntheses were started from commercially available 6-bromopicolinic acid **23** (**scheme II-23**). Conjugation of acid **23** with 5'-azido-uridine **5** under Staudinger-Vilarrasa reaction conditions afforded the amide intermediate **24** which could also be deprotected to compound **25** and evaluated as an UDP analogue. After functionalization with an alkynyl group through Sonogashira reaction, the alkynylated pyridine derivative **26** was readily converted to the terminal alkyne derivative **27**. Conjugation with different glycosyl azides involving glucose **28-Glc**, galactose **28-Gal** and *N*-acetyl glucosamine **28-GlcNAc** under CuAAC conditions afforded the protected UDP-sugar analogues **29** which were deprotected to the GT inhibitor candidates **30**.

In the other synthetic route, with similar strategy but reverse positions of the amide and triazole moieties, another series of GT inhibitor candidates **35** was synthesized. 6-Bromopicolinic acid **23** was reacted with different glycosyl azides **28** to form an amide bond between sugar moiety and the pyridine scaffold. Then, Sonogashira reaction between the bromo-pyridine derivative **31** and trimethylsilylacetylene afforded the alkynylated pyridine derivative **32**. Subsequent deprotection of the silyl group, CuAAC conjugation with 5'-azido-uridine **5** and hydrolysis of the acetate protecting groups afforded the desired GT inhibitor candidates **35** (**Scheme II-23**).

In the syntheses of the last family of GT inhibitors with two triazoles building blocks, two synthetic routes were again investigated in the glucose series in order to compare their efficiency (**Scheme II-24**). In **pathway A**, from "Sugar-to-Nucleoside", the commercially available 2,6-dibromopyridine was mono-functionalized with an alkynyl group **37**.²¹⁶ After deprotection of the silyl group, CuAAC conjugation with glucosyl azide **28-Glc** afforded the bromo-intermediate **39**. Subsequent Sonogashira reaction to obtain **40** and desilylation provided the desired terminal alkyne **41**. Final CuAAC with 5'-azido-uridine **5** followed by removal of the ester protecting groups gave the desired GT inhibitor candidate **43-Glc**. With similar chemistry but reverse sequence, first forming a triazole between 5'-azido-nucleoside **5** and mono-terminal alkyne derivative **38**, then transforming the functional group from bromo to alkynyl under Sonogashira reaction, then desilylating and CuAAC coupling and final hydrolysis of the protecting groups afforded the GT inhibitor candidate **43-Glc** through **pathway B**. In terms of the total yield, we obtained 43% yield in **pathway A** over 7 steps while **pathway B** gave the desired compound **43-Glc** in 21% over 5 steps. Even if the yield with the **pathway B** is slightly lower, the merit of this synthetic route lies in the introduction of different carbohydrate moieties conveniently at the end of the synthetic sequence providing a convenient divergent approach to a family of GT inhibitors. Therefore, **pathway B** was employed to the synthesis of the *N*-acetyl glucosamine derivative **43-GlcNAc** (**Scheme II-24**).

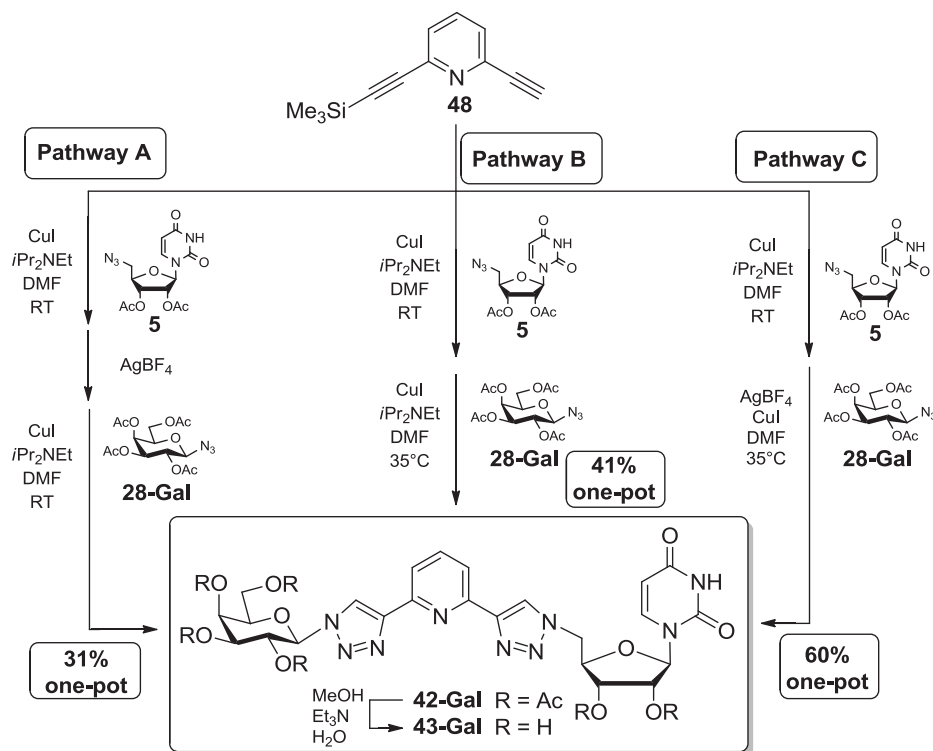


Scheme II-23. Synthesis of three different series of neutral GT inhibitors using a combination of Staudinger-Vilarrasa ligation and CuAAC. *Reagents and conditions:* (a) PMe₃, DIC, HOBt, THF, r.t., 16h, 37% for **24**, 78% for **31-Glc**, quant. for **31-Gal**, 95% for **31-GlcNAc**; (b) NaOMe, MeOH, 28°, 28% for **25**, 78% for **30-Glc**, quant. for **30-GlcNAc**, 80% for **30-Gal**, 85% for **35-Glc**, 85% for **35-GlcNAc**, 78% for **35-Gal**; (c) Me₃SiC≡CH, Pd(PPh₃)₄, CuI, *i*Pr₂NH, PhMe, r.t., 48, 90% for **32-Glc**, 98% for **32-GlcNAc**, 93% for **32-Gal**; (d) *n*Bu₄NF, THF/MeOH, r.t., 4h, 50% for two steps **27**, 77% for **33-Glc**, 66% for **33-GlcNAc**, 79% for **33-Gal**; (e) CuSO₄, sodium ascorbate, *t*BuOH/H₂O, 35°C, 48h, 83% for **34-Glc**, 68% for **34-GlcNAc**, 64% for **34-Gal**, 80% for **29-Glc**, 50% for **29-GlcNAc**, 44% for **29-Gal**.



Scheme II-24. Synthesis of two 2,6-*bis*-triazolyl-pyridyl-based neutral GT inhibitors using two subsequent CuAAC conjugations. *Reagents and conditions:* (a) $\text{Me}_3\text{SiC}\equiv\text{CH}$, $\text{Pd}(\text{PPh}_3)_4$, CuI , $i\text{Pr}_2\text{NH}$, PhMe , r.t., 48h, 95% for **40**, 71% for **46**; (b) K_2CO_3 , THF/MeOH , r.t., 2h, 79% for two steps; (c) CuI , $i\text{Pr}_2\text{NEt}$, DMF , 100°C (μW), 15 min, 93% for **39**, 74% for **42-Glc** pathway **A**, 86% for **42-Glc** pathway **B**, 40% for **42-GlcNAc**, 95% for **44**; (d) $n\text{Bu}_4\text{NF}$, MeOH , r.t., 4h, 96% for **41**, 52% for **47**; (e) Et_3N , MeOH , H_2O , r.t., 82% for **43-Glc** or NaOMe , MeOH , r.t., 2h, 39% for **43-Glc**, 91% for **43-GlcNAc**, 83% for **45**.

The idea of “One-pot” synthesis of 2,6-*bis*-triazolyl-pyridyl-based neutral GT inhibitor by two sequential CuAAC was then tested in the galactose series (**Scheme II-25**). The introduction of two orthogonally protected alkyne moieties on a multivalent scaffold was reported as a rapid approach to obtain hetero-functionalized compounds through CuAAC conjugations through sequential deprotection of the alkyne groups.²¹⁷ In our study, we used the desymmetrized 2,6-*bis*-acetylene pyridine derivative **48**²¹⁸ as the key intermediate for the synthesis of our target GalT inhibitor candidate **43-Gal** (**Scheme II-25**).



Scheme II-25. “One-pot” synthesis of a 2,6-bis-triazolyl-pyridyl-based neutral GalT inhibitor using two sequential CuAAC cycloadditions.

Our initial attempt was performed under the conditions described by Aucagne and Leigh.²¹⁷ The intermediate **48** was first coupled with 5'-azido-uridine **5** followed by removal of the silyl protecting group by adding silver tetrafluoroborate. Another portion of catalysts and the azido galactose **28-Gal** were added to allow the second CuAAC coupling to be proceed (**Pathway A, Scheme II-25**). We isolated the desired acetylated derivative **42-Gal** in 31% yield, although the synthesis reported²¹⁷ was almost quantitative (>95%). In this preliminary experiment, we noticed that the silyl orthogonally protecting group was not stable under the reaction condition since a small amount of desilylated intermediate was observed by TLC after the first CuAAC coupling. It is known that the silyl protecting group could be removed by weak base, such as K_2CO_3 ²¹⁶ and the basic conditions are probably responsible for this partial deprotection. To further improve the reaction condition, we added the azido galactose **28-Gal** and more base (DIPEA) after the first CuAAC coupling (**Pathway B, Scheme II-25**). A slight increase of the temperature from 20°C to 35°C allowed a clean deprotection of the silyl protecting group and the global yield was then increased to 41%. Finally, we obtained an optimal yield of 60% when silver salts were reintroduced for the deprotection concomitantly with the second CuAAC reagents (**Pathway C, Scheme II-25**). This sequential double-CuAAC synthetic strategy involved three synthetic steps performed with two subsequent additions of reagents in a “one-pot” procedure leading to a global yield of 60% which corresponds to 84% yield for each step. The acetates protecting groups were then removed to afford the target GalT inhibitor candidate **43-Gal**.

II.5 Conclusion

Glycosylation is promoted by acid promoters rendering the reactions with basic acceptors challenging. A systematic investigation of glycosylation methods on pyridine-based acceptors was performed, involving (1) a series of 20 glycosyl donors derived from glucose, galactose, mannose, fucose, rhamnose and lactose) (2) a large number of activating groups at the anomeric center (e.g., acetate, bromide, trichloroacetimidate, thiopyridine) and (3) a complete set of activating conditions. The pyridine moiety was identified to have a negative influence on the reaction compared with the glycosylation result with a “phenyl-based” donor **2d**. Therefore, the basicity of the pyridine ring could be verified as a limitation to the outcome of the glycosylation reaction. The best conditions for the glycosylation of the model donor methyl 6-(hydroxymethyl)picolinate **2a** could provide isolated yields of glycosides from 46% to 82% with different types of glycosyl donors. The optimized glycosylation methods were then applied to the synthesis of neutral inhibitors of glycosyltransferases. Four UDP-sugar analogues (**7-Gal**, **7-Glc**, **20** and **23**) and one UDP analogue (**10**) were synthesized (**Figure II-1**), including α - and β -galactoside (**7-Gal**, **7-Glc**), one β -glucoside (**20**) containing a pyridine moiety and one phenyl-based inhibitor candidate **23**. These candidates prepared were then evaluated as GalT inhibitors.

The synthesis of another type of GT inhibitors containing eleven candidates was achieved in a minimum number of steps from readily available starting materials using two conjugation techniques: Staudinger-Vilarrasa reaction and azide-alkyne cycloaddition (CuAAC). The syntheses were performed in galactose, glucose and *N*-acetyl glucosamine series. The galactose-containing derivatives **30-Gal**, **35-Gal**, **43-Gal** were selected as GalT inhibitor candidates while the *N*-acetyl glucosamine-based compounds **30-GlcNAc**, **35-GlcNAc**, **43-GlcNAc** were evaluated as OGT inhibitors. As negative controls, the glucose derivatives were also synthesized to assess the influence of the carbohydrate moiety on the selectivity and inhibitory properties towards different enzymes. Two synthetic routes, from “Sugar-to-Nucleoside” and from “Nucleoside-to- Sugar”, were applied in the synthesis of glucose series in order to compare the efficiency (**Table II-6**). In both cases, the latter synthetic route afforded a slightly lower yield. However, the advantage of this synthetic route lies in the introduction of different carbohydrate moieties conveniently at the end of the synthetic sequence providing a convenient approach to obtain a family of GT inhibitors. An orthogonally protected *bis*-alkynyl pyridine was introduced to obtain inhibitor candidates in a minimum number of steps. Two UDP analogues **25** and **45** were also prepared in order to obtain more information about the influence of the carbohydrate on enzymatic binding.

Table II-6. Comparison of two different synthetic strategies.

| Entry | Sugar-to-Nucleoside | | Nucleoside-to-Sugar | |
|------------------------------|---------------------|-----------|---------------------|-----------|
| | Number of steps | yield (%) | Number of steps | yield (%) |
| 7-Glc (Scheme II-19) | 5 | 6 | 5 | 2 |
| 43-Glc (Scheme II-24) | 7 | 43 | 5 | 21 |

Chapter III : Design and synthesis of neutral glycosyltransferase inhibitors - Amino-acids as pyrophosphate surrogates

Chapter III : Design and synthesis of neutral glycosyltransferase inhibitors - Amino-acids as pyrophosphate surrogates

This chapter describes the synthesis of neutral glycosyltransferase inhibitor candidates using amino-acid derivatives as pyrophosphate surrogates. Two types of analogues were designed (**Figure III-1**), conjugating the uridine moiety through either the amine or carboxylic acid group of the amino-acid linker. The incorporation of an amine, azido or carboxylic acid groups allowed further substitution with other functional moieties favoring binding to GT or interaction with specific amino-acids in the active sites of GT.

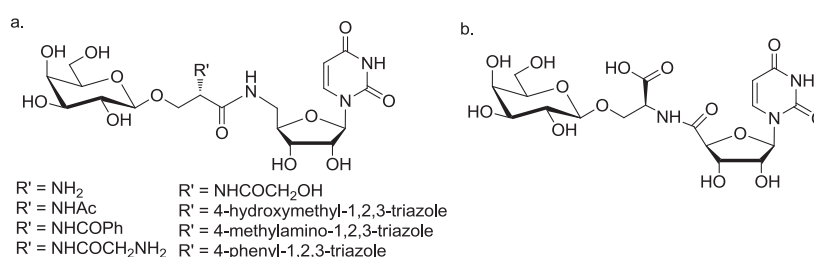


Figure III-1. Designed glycosyltransferase inhibitors using amino-acid derivatives as pyrophosphate surrogates.

Eight UDP-sugar analogues (**74**, **75**, **77**, **78**, **80**, **81**, **82** and **95**) and three UDP analogues (**64**, **79** and **93**) (**Figure III-2**) were synthesized based on our design. The key steps in this synthesis were the generation of the glycosidic bond with serine-based derivatives and an amide bond formation afterwards with uridine. Glycosylation of amino-acid residue is a biological phenomenon which has been commonly found in protein post-translational modification²¹⁹ and widespread studied in protein chemistry²²⁰⁻²²². Nevertheless, the reaction condition needs to be optimized for each specific case. Therefore, glycosylation conditions with serine derivatives were also investigated in this section.

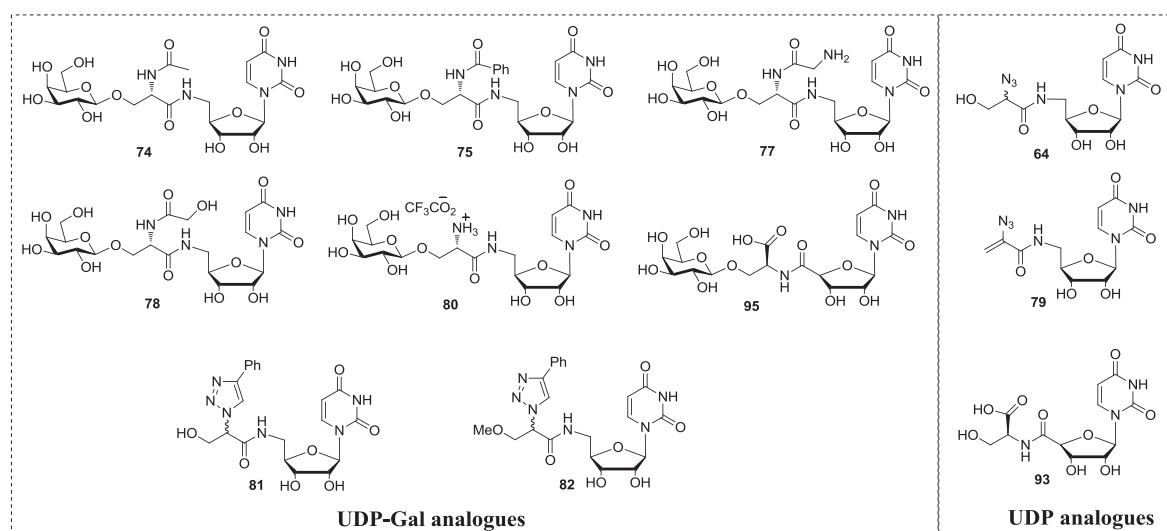
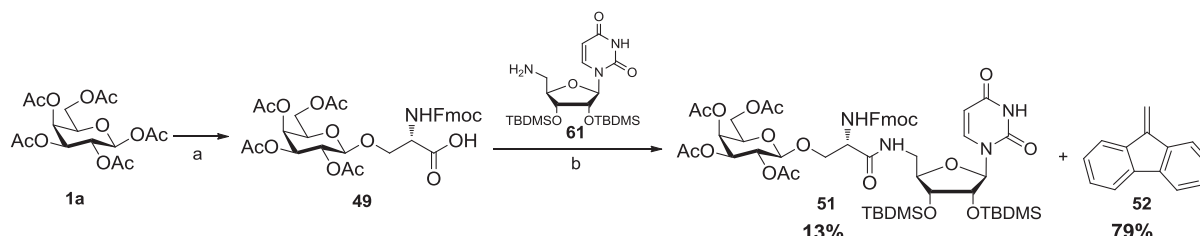


Figure III-2. Synthesized UDP-Gal and UDP analogues using serine derivatives as pyrophosphate surrogates.

III.1 Galactosylation of serine-based acceptors

In an initial attempt, galactosylation was performed under reported method²²³ with fluorenylmethyloxycarbonyl (Fmoc) protected serine. The galactoside **49** was obtained in 45%. Nevertheless, the Fmoc protecting group was not stable under the amide bond coupling reaction with the 5'-amino-uridine **61**. Only 13% yield of the desired amide was obtained and 9-methylene-9H-fluorene **52** was isolated as a byproduct of the reaction while 79% percent of the reactant **49** was decomposed (**Scheme III-1**).



Scheme III-1. Synthesis of amino-acid containing mimetics through glycosylation and amide bond formation. *Reagents and conditions:* (a) FmocSerOH, $\text{BF}_3 \cdot \text{Et}_2\text{O}$, CH_3CN , r.t., 16h, 45%; (b) EDCI.HCl, DIEA, TBTU, DMF, r.t., 16h, 13%.

The *tert*-butyloxycarbonyl (Boc) protecting group was then employed in the synthesis. To our disappointment, the galactosylation with free or benzyl protected carboxyl group of *N*-Boc serine derivatives **53** and **54** and three common galactosyl donors (peracetylated galactose **1a**, galactopyranosyl bromide **1b**, galactose trichloroacetimidate **1c**) (**Table III-1**), the best yield obtained was 15% by reaction between donor **1c** and *N*-Boc serine benzyl ester **54** under boron trifluoride etherate activation (**Entry 6, Table III-1**).

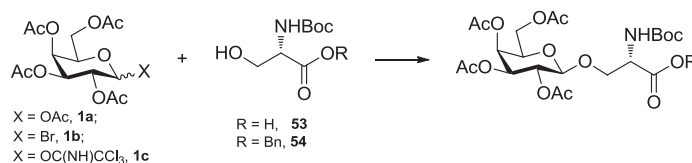


Table III-1. Glycosylation of *N*-Boc serine derivatives with different galactosyl donors **1a-c**.

| Entry | Donor | Acceptor | Ratio Donor: Acceptor | Temp. Time | Promoter |
|-------|-------|----------|-----------------------|-------------------|--|
| 1 | | R = H | 1:1.2 | 0°C to r.t., 24 h | $\text{BF}_3 \cdot \text{Et}_2\text{O}$ (3 eq.), CH_3CN |
| 2 | | R = Bn | 2.5:1 | 0°C to r.t., 48 h | SnCl_4 (5 eq.)/ $\text{CF}_3\text{CO}_2\text{Ag}$ (2.5 eq.) CH_2Cl_2 |
| 3 | | R = H | 1:2.8 | 0°C to r.t., 22 h | I_2 (1.5 eq.), CH_3CN |
| 4 | | R = Bn | 1:1.7 | 0°C to r.t., 24 h | I_2 (1.5 eq.), CH_3CN |
| 5 | | R = Bn | 2:1 | 0°C to r.t., 53 h | AgOTf (1 eq.), CH_2Cl_2 |
| 6 | | R = Bn | 2.5:1 | -20°C, 9 h | $\text{BF}_3 \cdot \text{Et}_2\text{O}$ (0.5 eq.), CH_2Cl_2 |

Then, we turned our attention to an amino-acid precursor such as azido-functionalized serine derivative **57**. An efficient synthetic methodology for glycosylation taking peracetylate sugar **1a** as donor and silver and tin salts¹²⁰⁻¹²¹ was first tried in this case (**Entry 7, Table III-2**). A

moderate yield of 55% for the desired β -glycoside was obtained. The more reactive sugar donor galactose trichloroacetimidate **1c** was further examined with no better yield (45%) obtained (**Entry 8, Table III-2**). Then, the benzoylated sugar donor galactose trichloroacetimidate **1e** was evaluated for the glycosylation which could give a better yield of 67% but with difficulty in purification. At this point, the glycosylation method applying the simplest sugar donor **1a** affording moderate yield was selected for our synthetic route (**Scheme III-2**).

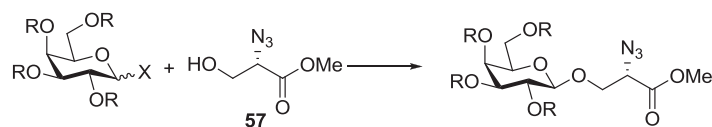


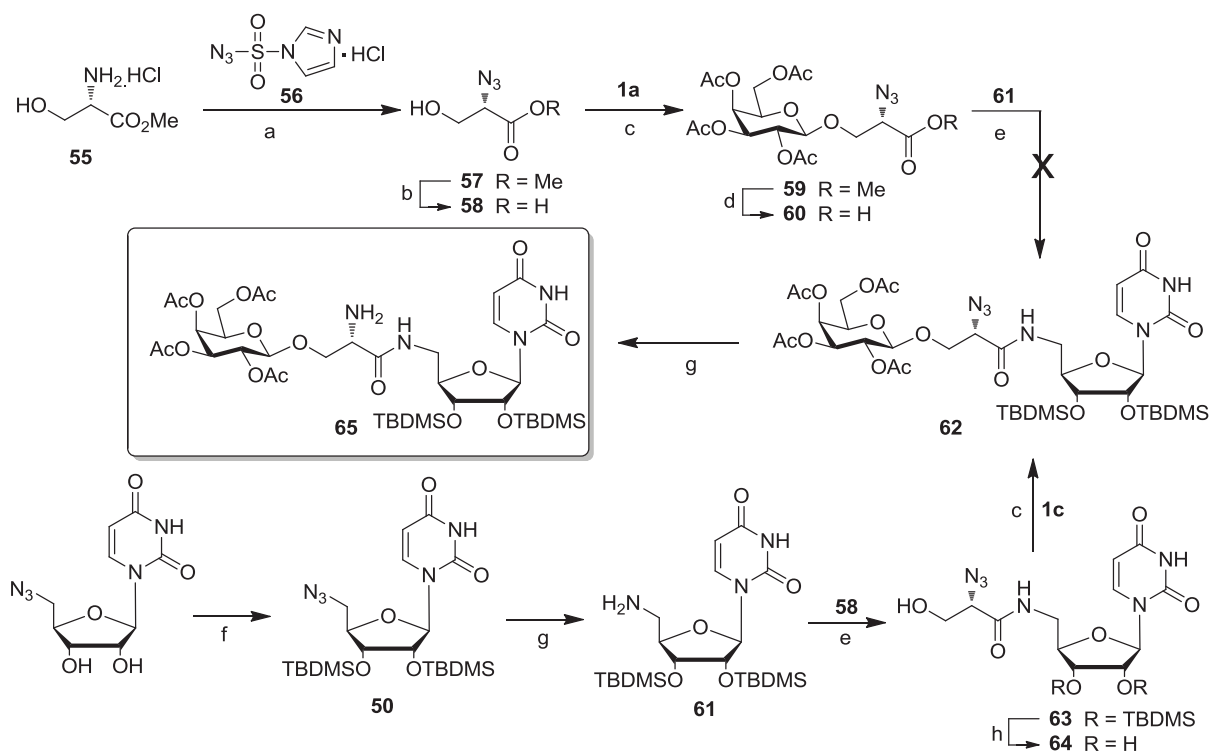
Table III-2. Glycosylation study of serine precursor derivative **57** with different galactosyl donors **1a**, **1c** and **1e**.

| Entry | Donor | Ratio Donor: Acceptor | Temp. Time | Promoter | Yield ^a (%) | Product |
|-------|-------|-----------------------------|---------------|--|---------------------------|--------------------------|
| 7 | | 1.5:1 | 0°C, 17 h | SnCl ₄ (5 eq.)/AgCO ₂ CF ₃ (2.5 eq.) CH ₂ Cl ₂ | 55 | 59 , β only |
| 8 | | 1.5:1 | -20°C, 2 h | BF ₃ ·Et ₂ O (0.2 eq.), CH ₂ Cl ₂ | 45 | 59 , β only |
| 9 | | 1.5:1 | -20°C, 2.5 h | BF ₃ ·Et ₂ O (0.2 eq.), CH ₂ Cl ₂ | 66 | 66 , β only |

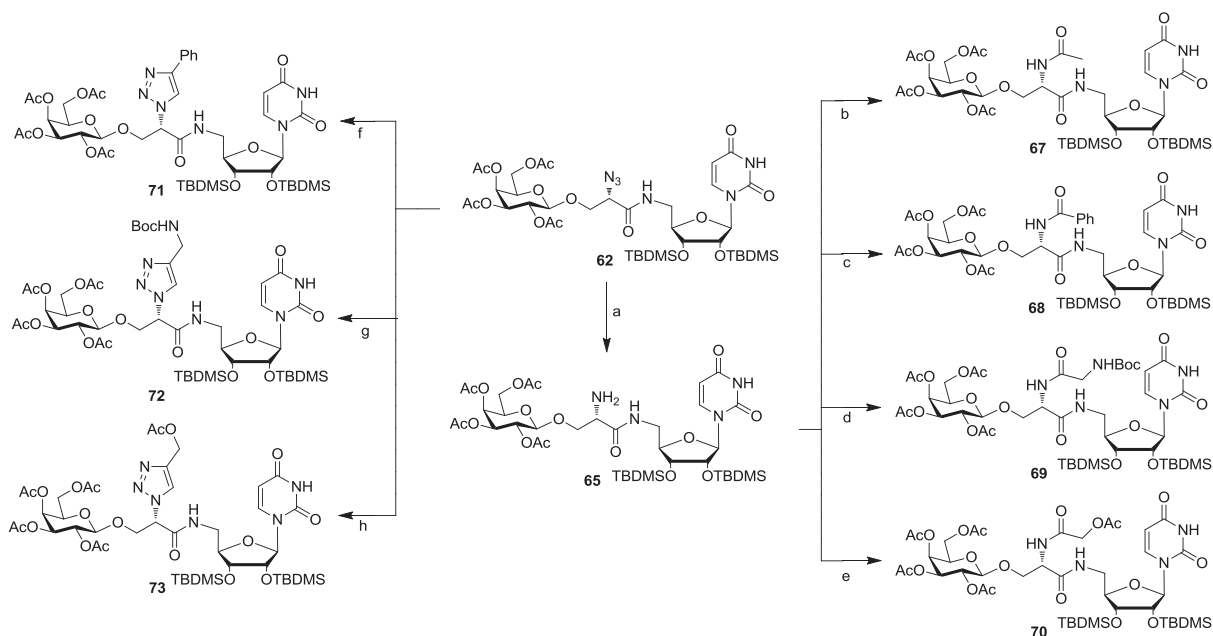
a. Isolated yield. b. Product was obtained as a mixture of the glycoside and the decomposed sugar donor. Yield was calculated based on the glycoside in the mixture.

III.3 Synthesis of serine derivatives containing UDP-Gal mimetics

Azido-functionalized serine methyl ester **57** was synthesized according to literature method²²⁴⁻²²⁵ starting from methyl serine hydrochloride **55** via a diazo transfer reaction with retention of configuration.²⁵⁹ Glycosylation under optimized conditions (**Table III-2**) afforded the glycoside **59** in 55% yield. The amide-bond coupling between acid **60** and silyl ether protected 5'-amino-uridine **61** did not give the desired amide under DCC/HOBt activation. Then, the synthetic strategy was changed to start from 5'-azido-uridine. After protection of the hydroxyl group of 5'-azido-uridine followed by hydrogenation of the azido group, the uridine residue **61** was first condensed with serine derivative **58** before glycosylation. The reaction with amide **63** taking peracetylated sugar **1a** as donor and activation by silver and tin salts did not afford the desired glycoside. In contrast, the reaction using the trichloroacetimidate **1c** afforded a good yield (61%) of the amide **62** (**Scheme III-2**). Then, the two key intermediates azido **62** and amine **65** were prepared for further functionalization.



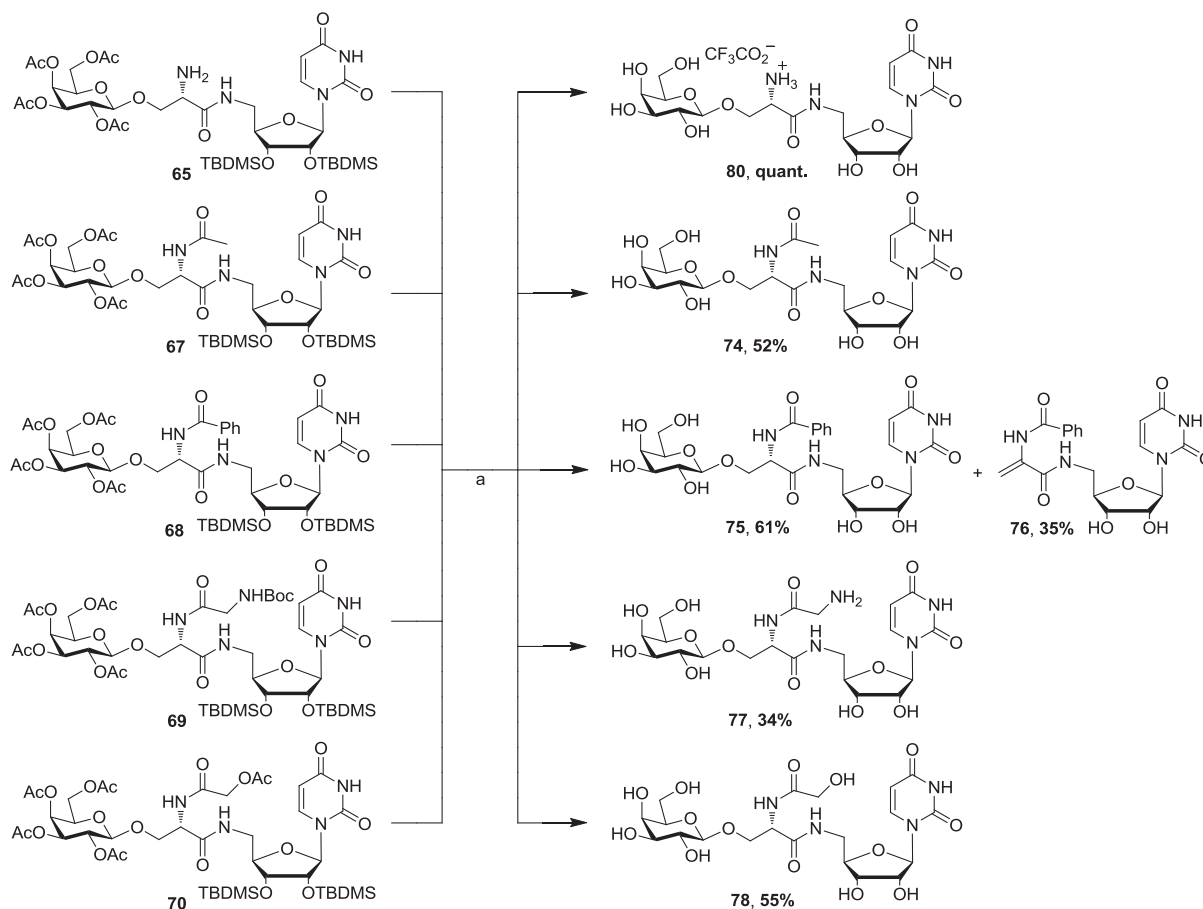
Scheme III-2. Synthesis of amino acid containing mimetics through glycosylation and Staudinger-Villarsa ligation. *Reagents and conditions:* (a) K_2CO_3 , $\text{CuSO}_4 \cdot 5\text{H}_2\text{O}$, MeOH, r.t., 5 h, 61%; (b) LiOH, THF/ H_2O , r.t., 2h, quant.; (c) SnCl_4 (5 eq.)/ $\text{CF}_3\text{CO}_2\text{Ag}$ (2.5eq.), CH_2Cl_2 , 0°C , 17h, 55% for **59**; $\text{BF}_3 \cdot \text{Et}_2\text{O}$, CH_2Cl_2 , -20°C , 2h, 61% for **62**; (d) NaI, Pyridine, 120°C , 5h; (e) DCC, HOBT, DMAP, THF, r.t., 16h, 30% for **63**; (f) TBDMSCl, imidazole, pyridine, r.t., 40 h, 93%; (g) H_2 , Pd/C, MeOH, r.t., 4h, 85% for **61** or PPh_3 , THF/ H_2O , r.t., 16h for access of **67** in **Scheme III-3**; (h) 90% TFA, $\text{CH}_2\text{Cl}_2/\text{H}_2\text{O}$, quant.



Scheme III-3. Functionalization of amino-acid containing mimetics through amide bond chemistry and CuAAC. *Reagents and conditions:* (a) equals to (g) of **Scheme III-2**; (b) Ac_2O , Pyridine, r.t., 16 h, 21% for two steps; (c) benzoyl chloride, DIPEA, CH_2Cl_2 , r.t., 16 h, 82% for two steps; (d) Boc-Gly-OSu, DCC, CH_2Cl_2 , r.t., 16 h, 58% for two steps; (e) acetoxyacetyl chloride, DIPEA, CH_2Cl_2 , r.t., 16 h, 43% for two steps; (f) phenylacetylene, DIPEA, DMF, microwave, 100°C , 15 min, quant.; (g) *N*-Boc-propargylamine, DIPEA, DMF, microwave, 100°C , 15 min, 58%; (h) propargyl acetate, CuI, DIPEA, DMF, microwave, 100°C , 15 min, 56%.

The azido **62** was functionalized by CuAAC with terminal phenyl, acetoxymethyl or Boc protected amine, compounds **71-73** (Scheme III-3). For comparison with the triazole linkage, amide-bond chemistry was applied to the intermediate amine **65** for the coupling to afford terminal methyl, phenyl, acetoxymethyl or Boc protected amine, compounds **67-70** (Scheme III-3).

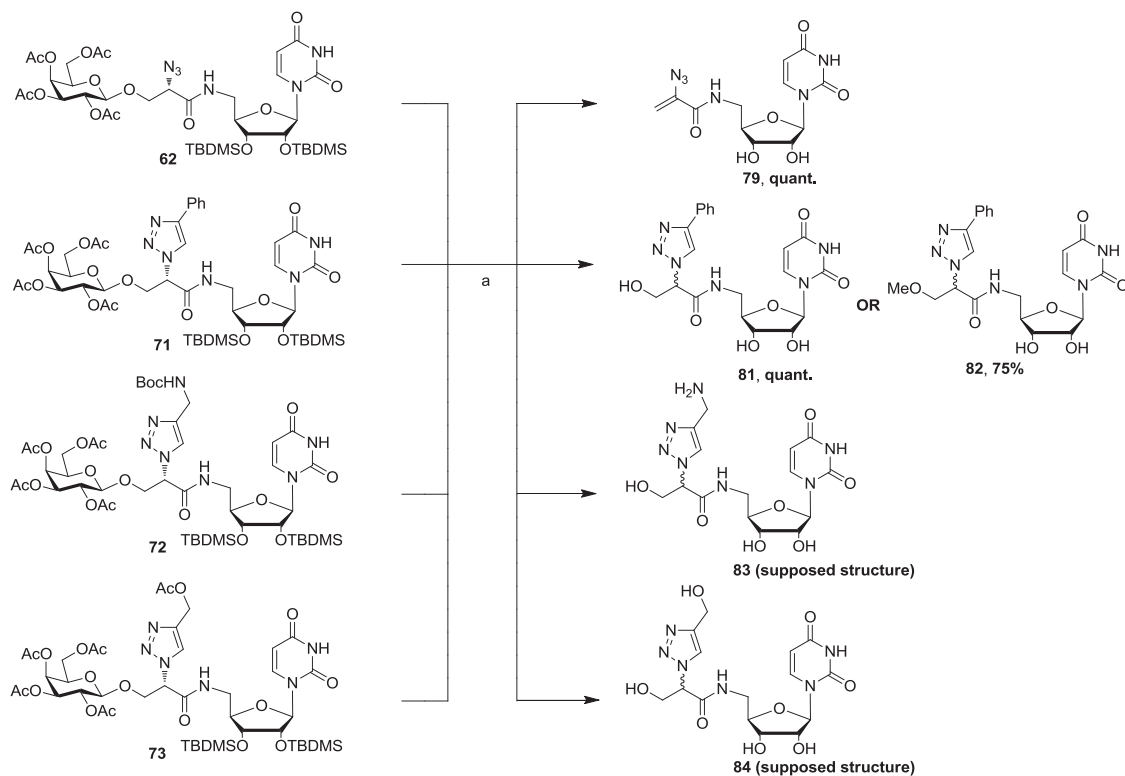
Deprotection of the derivatives sequentially by 90% TFA in CH₂Cl₂/H₂O for silyl ethers and Boc followed by hydrolysis with base were performed. The derivatives with free amino group (compound **65**) or amide derivatives **67-70** provided the desired products with yields ranging from 52% to quantitative with exception of derivative **68** which gave 61% yield of the desired compound with 35% of a conjugated alkene byproduct **76** (Scheme III-4).



Scheme III-4. Deprotection of amino-acid containing UDP-Gal mimetics. *Reagents and conditions:* a. 1. 90% TFA, CH₂Cl₂/H₂O, r.t., 16 h; 2. LiOH, THF/H₂O, r.t., 2 h, 34% - quantitative for two steps.

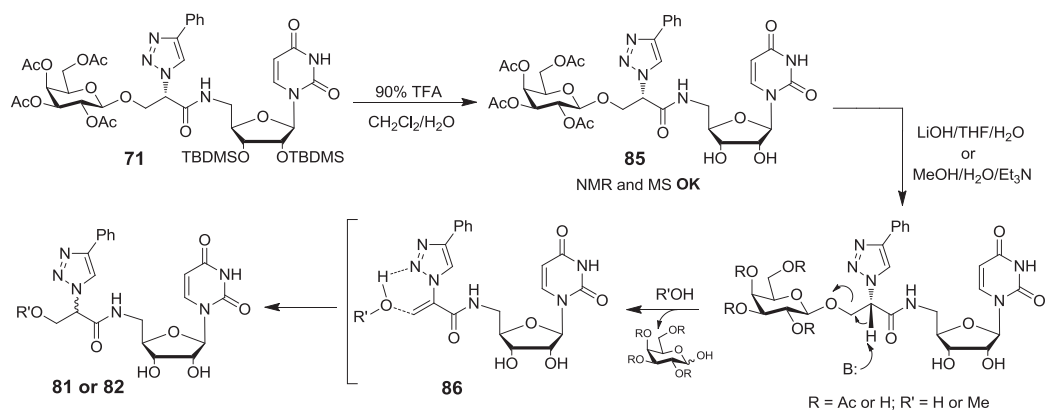
In comparison (Scheme III-5), the alkene byproduct **79** was obtained quantitatively from azido derivative **62**. Furthermore, for derivatives containing a triazole moiety (compounds **71-73**), nucleophilic Michael-addition byproducts on alkene intermediates were found as only products for these cases. Two different deprotection systems were applied for derivative **71**. After deprotection of silyl ether by 90% TFA, the expected desilylated intermediate was isolated which was confirmed by ¹H proton spectra and HR-MS (*m/z*, [M+H]⁺ = 789.2523, [M+Na]⁺ = 811.2355). Then, the product was divided into two fractions. In the first one, LiOH/H₂O/THF was employed for deacetylation. The amount of LiOH was fixed at 1.2 eq. for each acetate group and the pH of the reaction medium was adjusted to 9~10. A pair of diastereoisomers **81** was obtained resulting from an addition of H₂O at the alkene byproduct.

In the parallel reaction in which smoother conditions for the deacetylation were used ($\text{Et}_3\text{N}/\text{H}_2\text{O}/\text{MeOH}$), a pair of diastereoisomers **82** was obtained resulting from the addition of methanol to the alkene byproduct. In cases of derivatives **72-73** containing nucleophilic amino group of **72** and hydroxyl group of **73**, the products were more complex. Possible intermolecular additions might occur resulting in oligomeric species or even intramolecular additions. Due to the small quantity of **72** and **73** and the uncertainty of the composition, these two products **83** and **84** were not tested in enzymatic assays.



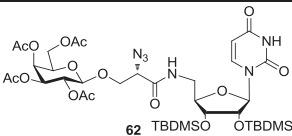
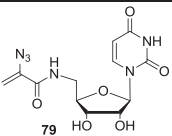
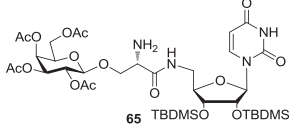
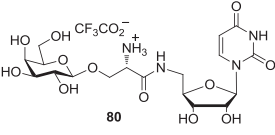
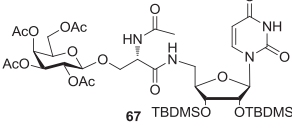
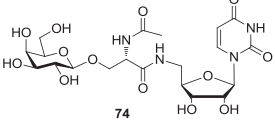
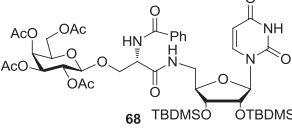
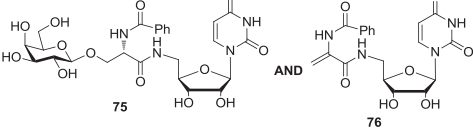
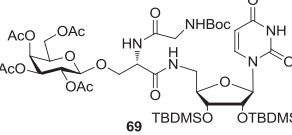
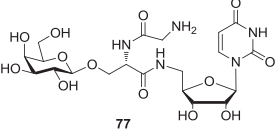
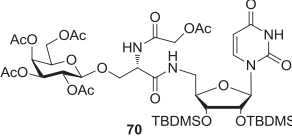
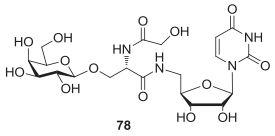
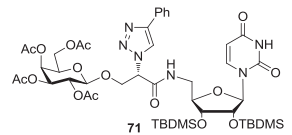
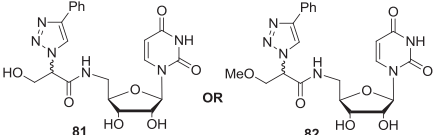
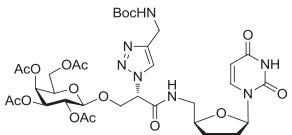
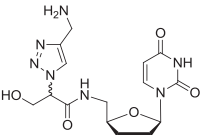
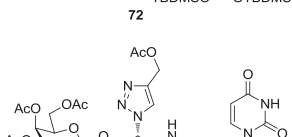
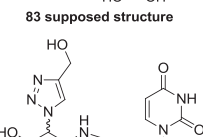
Scheme III-5. Deprotection of amino-acid containing mimetics. *Reagents and conditions:* (a) 1. 90% TFA, $\text{CH}_2\text{Cl}_2/\text{H}_2\text{O}$, r.t., 16 h; 2. LiOH, $\text{THF}/\text{H}_2\text{O}$, r.t., 2 h or Et_3N , $\text{MeOH}/\text{H}_2\text{O}$, r.t., 24 h for **82**, 75%-quant. for two or three steps.

A possible mechanism of this process was proposed as shown in **Scheme III-6**. After desilylation by 90% TFA, the proton at the stereocenter bearing the triazole was attacked by a base leading to the elimination intermediate **86** which was followed by nucleophilic Michael-addition resulting in the formation of product **81** or **82** depending on the reaction medium (H_2O or MeOH). The results of deprotection are summarized in **Table III-3** and **Table III-4**.



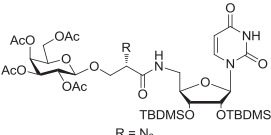
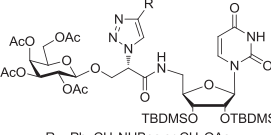
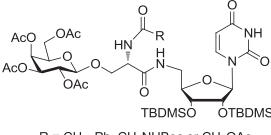
Scheme III-6. Proposed mechanism for base-induced elimination followed by Michael-addition.

Table III-3. Deprotection of serine-based derivatives.

| Entry | Reactant | Product ^b | Yield ^a (%) |
|-------|---|--|--|
| 10 |  |  | quant. |
| 11 |  |  | quant. |
| 12 |  |  | 56% |
| 13 |  |  | 61% for 75 , 35% for 76 |
| 14 |  |  | 34% |
| 15 |  |  | 56% |
| 16 |  |  | quant. for 81 , 75% for 82 ^c |
| 17 |  |  | -/- |
| 18 |  |  | -/- |

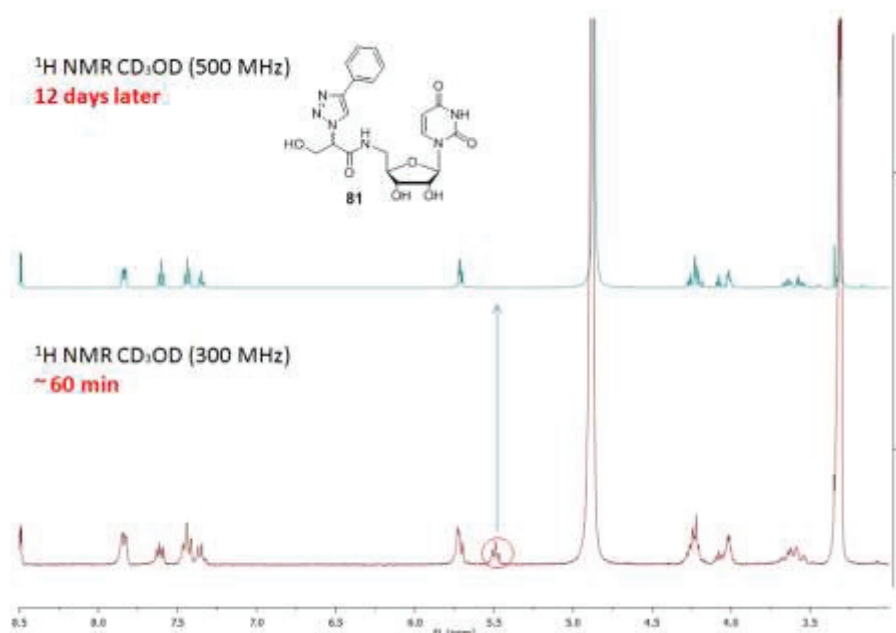
a. Isolated yields. b. Without further indication, the reaction conditions for deprotection are as follows: 1. 90% TFA, CH₂Cl₂/H₂O, r.t., 16 h; 2. LiOH, THF/H₂O, r.t., 2 h; c. The reaction conditions for deprotection are as follows: 1. 90% TFA, CH₂Cl₂/H₂O, r.t., 16 h; 2. LiOH, THF/H₂O, r.t., 2 h for **81** or Et₃N, MeOH/H₂O, r.t., 24 h for **82**.

Table III-4. Summary of deprotection of serine-based derivatives.

| Compound |  |  |  |
|------------------|---|--|---|
| | R = N ₃ | R = Ph, CH ₂ NHBoc or CH ₂ OAc | R = CH ₃ , Ph, CH ₂ NHBoc or CH ₂ OAc |
| Elimination | √ | √ | < 36% |
| Michael addition | × | √ | × |

Another interesting phenomenon was observed on NMR spectra of products **81** and **82**. Over 10 days of spectrum analysis, the proton attached to the asymmetric carbon linked with the triazole moiety was completely or partially deuterated for products **81** and **82**, respectively. The proton and the corresponding tertiary carbon atom did not show up in the respective ^1H NMR and ^{13}C NMR of products **81** (a, **Figure III-3**) while the proton and carbon at the same position of product **82** (b, **Figure III-3**) behaved slightly different since the exchange was slower (>10 days). Deuteration was previously described to cause “losing” signals in the ^1H and ^{13}C NMR.²²⁶ The integration of the proton resonating at 5.63 ppm was 0.36 which correlated with a weak carbon peak centered at 64.6 ppm of the ^{13}C NMR (**Figure III-4**). The integration inferior to 1 and clear correlation with its carbon atom by HSQC indicated that the protons on the serine backbone of products **81** and **82** are acidic enough to be exchangeable.

a.



b.

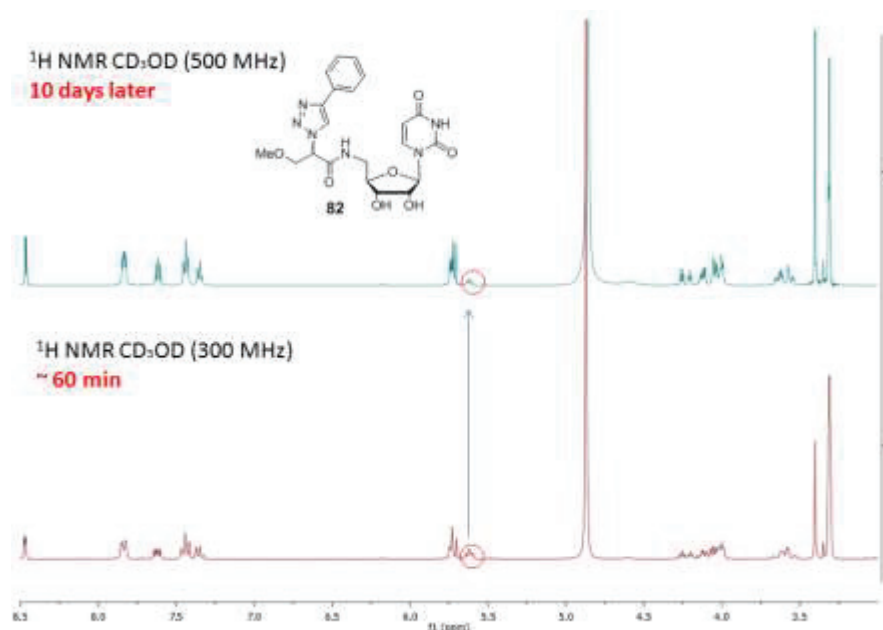


Figure III-3. Comparison of ^1H NMR spectra (500 MHz, CD_3OD) of **81** and **82** measured immediately (~ 60 min) and several days later.

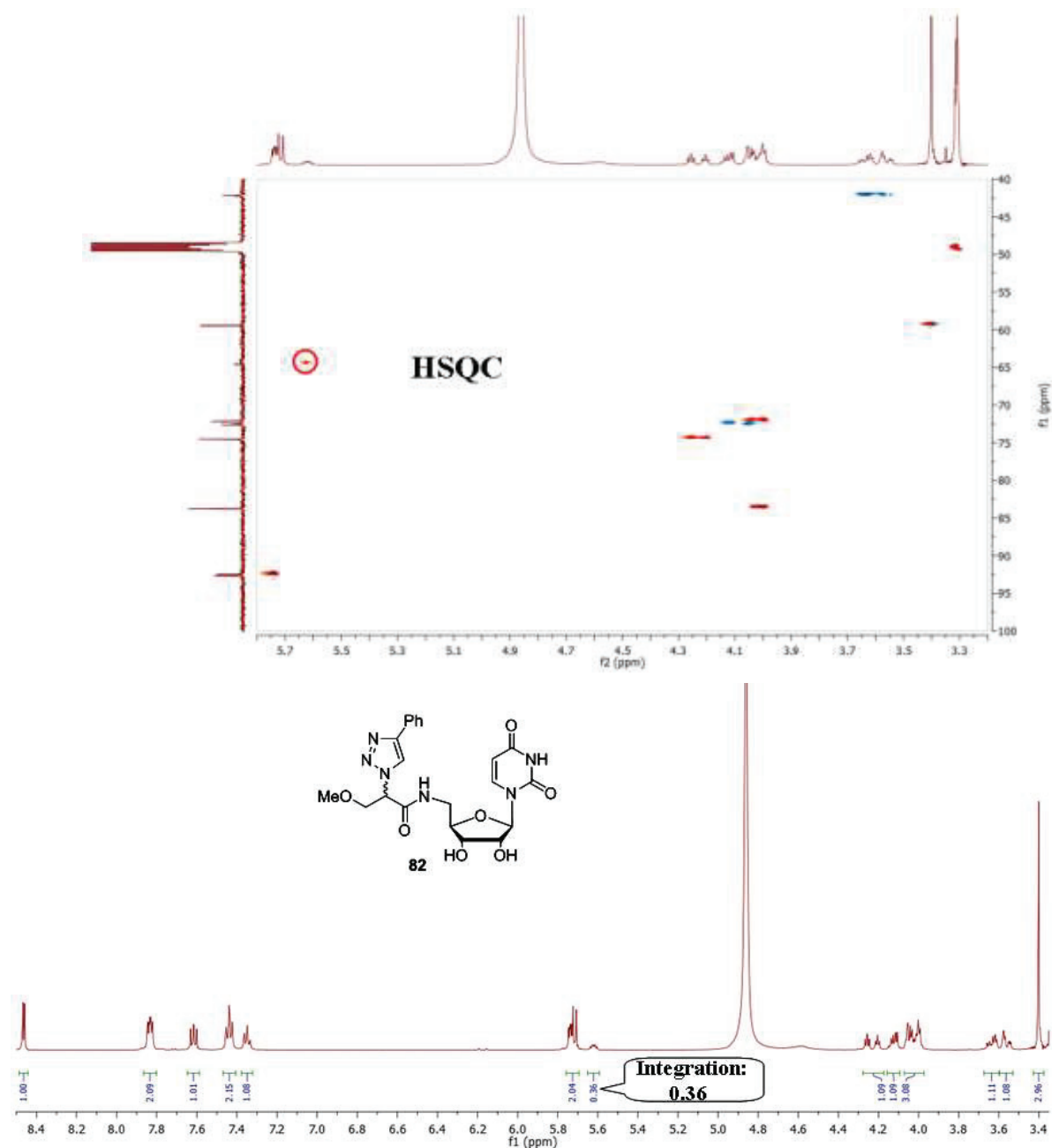
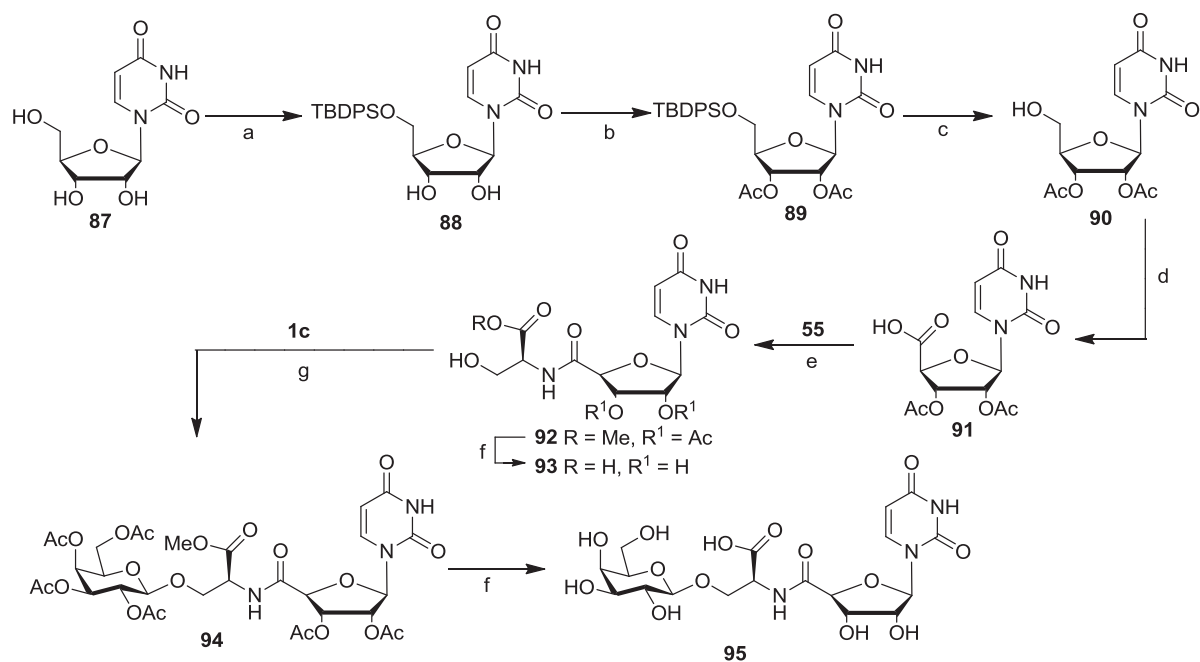


Figure III-4. NMR data (500 MHz, CD₃OD) of the deprotected product **82**.

Another type of serine-based UDP-Gal analogues was synthesized through amide-bond formation between the amino group of the serine backbone and a carboxyl group of a uridine derivative (**Scheme III-7**). Starting from uridine **87**, selective protection of the primary alcohol followed by acetylation afforded the protected uridine **89** in 88% yield for two steps. After desilylation, the primary alcohol **90** was oxidized to carboxyl derivative **91** under reported method.²²⁷ The sequence of the addition of reactants is crucial for the synthesis of the amide bond (Chapter VI, method **I** and **II** of compound **92**). Adding a base to the mixed pre-dried reaction mixture (method **I**) gave 36% yield of the desired amide **92** and 24% of methyl ester resulting from the transesterification from **55** to **91**. Adding a mixture of **91**/HOBt in acetonitrile into the pre-base treated methyl serine ester **55**/DCC in acetonitrile avoided the formation of transesterified methyl ester thus afforded amide the **93** in 90% yield. Galactosylation of the amide **93** using the galactose trichloroacetimidate **1c** catalyzed by boron trifluoride etherate afforded the protected analogue **94** in 40% yield. Hydrolysis of the analogue **94** gave a UDP-Gal analogue **95**.



Scheme III-7. Synthesis of amino acid containing mimetics through glycosylation and amide bond chemistry. *Reagents and conditions:* (a) TBDPSCl, imidazole, pyridine, r.t., 27 h; (b) Ac₂O, Pyridine, r.t., 16 h, 88% for two steps; (c) TBAF, THF, r.t., 2 h, 70%; (d) TEMPO, BAIB, CH₃CN/H₂O, -5°C, 20 h, 81%; (e) DCC, HOBT, MeCN, r.t., 24 h, 36% for method I, 90% for method II; (f) LiOH, THF/H₂O, r.t., 2 h, 71% for **93**, 50% for **95**; (g) BF₃·Et₂O, CH₂Cl₂, -20°C, 2h, 40%.

III.4 Conclusion

The syntheses of glycosyltransferase inhibitors using amino-acid derivatives as pyrophosphate surrogates were studied in this chapter. Eight UDP-sugar analogues (**74**, **75**, **77**, **78**, **80**, **81**, **82** and **95**), three UDP analogues (**64**, **79**, **93**) (Figure III-2) have been synthesized. The glycosylation conditions of serine derivatives including Boc protected derivatives and the azido precursors were carefully studied. The optimized conditions were further utilized for analogues syntheses. The incorporation of an amino-acid residue between the carbohydrate and uridine moieties provided a functional amine, azido or acid group to be further substituted with other functional moieties. The introduction of functional groups which could favor binding to GT or interact with specific amino-acids in the active sites of GT was studied including phenyl, hydroxyl or amino group. Unusual byproducts were observed in the final deprotection steps and a possible mechanism of this process was proposed. The inhibitory properties of analogues prepared in this chapter will be further studied in **Chapter IV** against 5 galactosyltransferases.

Chapter IV: Inhibition studies towards glycosyltransferases

Chapter IV: Inhibition studies towards glycosyltransferases

IV.1 Introduction

This chapter describes the evaluation of the synthetic analogues against different glycosyltransferases. A collaboration with Prof. Monica M. Palcic (Carlsberg Laboratory, Copenhagen, Denmark) provided access to five GalTs (β -1,4-galactosyltransferase (β -1,4-GalT), α -1,4-galactosyltransferase (α -1,4-GalT), α -1,3-galactosyltransferase (α -1,3-GalT), human blood group B galactosyltransferase (GTB), a mutant of the wild type human blood group glycosyltransferase (AAGlyB)). IC_{50} and K_i measurements, mechanistic studies and crystallographic data could therefore be obtained. *O*-linked *N*-acetylglucosamine transferase (OGT) was the second main enzyme studied in this project through collaboration with Prof. David Vocadlo (Simon Fraser University, Vancouver, Canada). IC_{50} and K_i measurements were performed as well as docking studies in collaboration with Prof. Mario Pinto (Simon Fraser University, Vancouver, Canada). OGT inhibition studies were also performed in a cell-based assay in collaboration with the group of Prof. Tony Lefebvre (Unité de Glycobiologie Structurale et Fonctionnelle, Université de Lille). As outlined in **Chapter I**, these enzymes are crucial for the biosynthesis in living organisms and the study on these enzymes has potential applications in carbohydrate related disease therapies.

According to structural features and biological targets, the prepared analogues could be divided into three groups, candidates using (1) pyridine moiety or (2) amino-acid derivatives as pyrophosphate surrogates tested against GalT and candidates using (3) pyridine as pyrophosphate surrogate evaluated as OGT inhibitors, listed in **Figure IV-1**, **Figure IV-2** and **Figure IV-3**, respectively. The carbohydrates used are galactose and *N*-acetyl glucosamine as the selective natural substrates for the enzymes. Glucose was also selected as a negative control. The best inhibitors (**7-Glc**, **7-Gal** and **19**) of human blood group transferase mutant AAGlyB were then selected for crystallographic studies in order to obtain the structural features of their interactions with the enzyme at the active site. An artificial cell membrane penetration test was also studied in collaboration with Dr. Ofelia Maniti and Prof. Agnes Girard-Egrot in our institute.

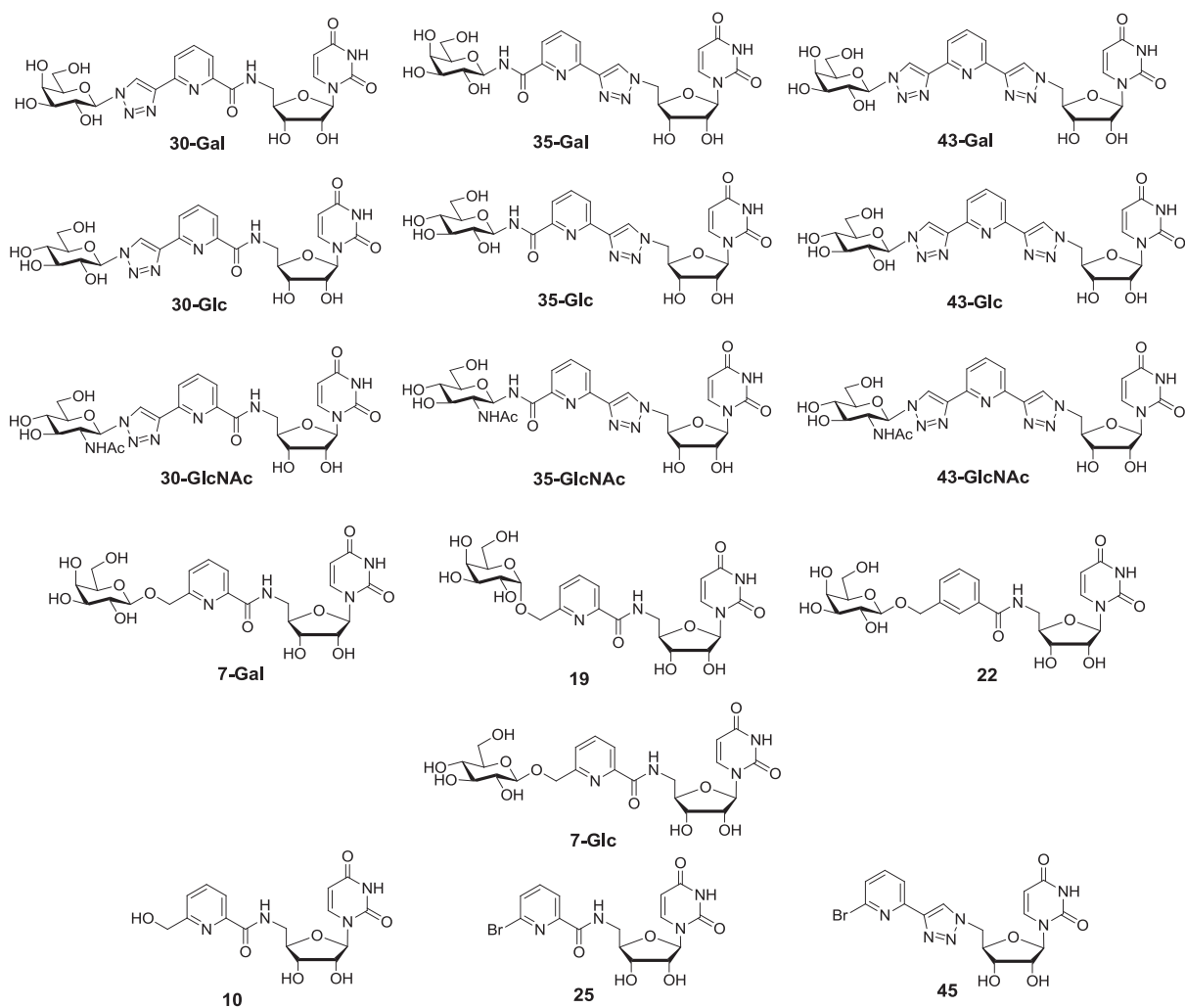


Figure IV-1. Structures of neutral UDP-Gal and UDP analogues as GalT inhibitor candidates using pyridine as a pyrophosphate surrogate.

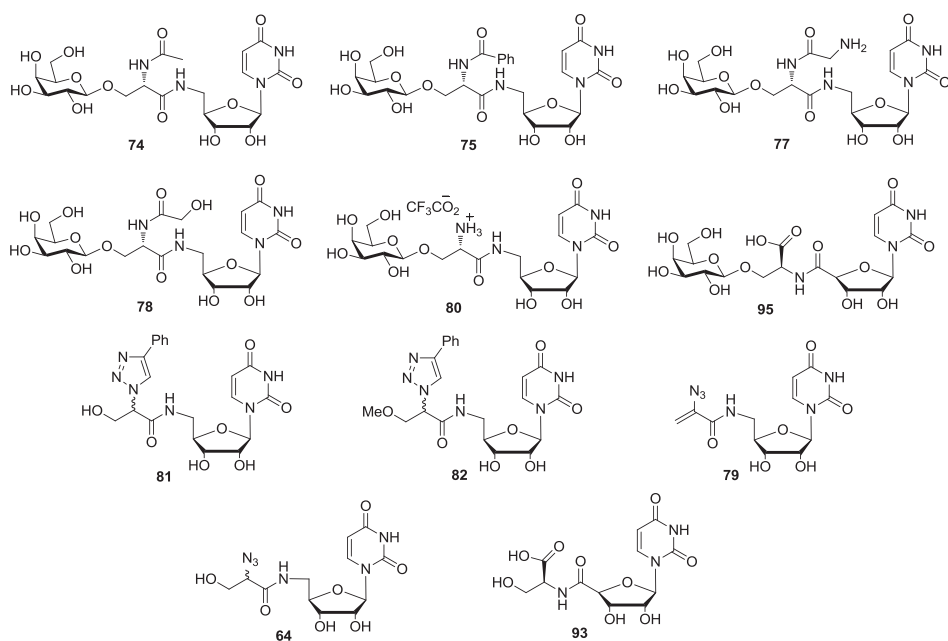


Figure IV-2. Structures of neutral UDP-Gal and UDP analogues as GalT inhibitor candidates using amino-acid derivatives as a pyrophosphate.

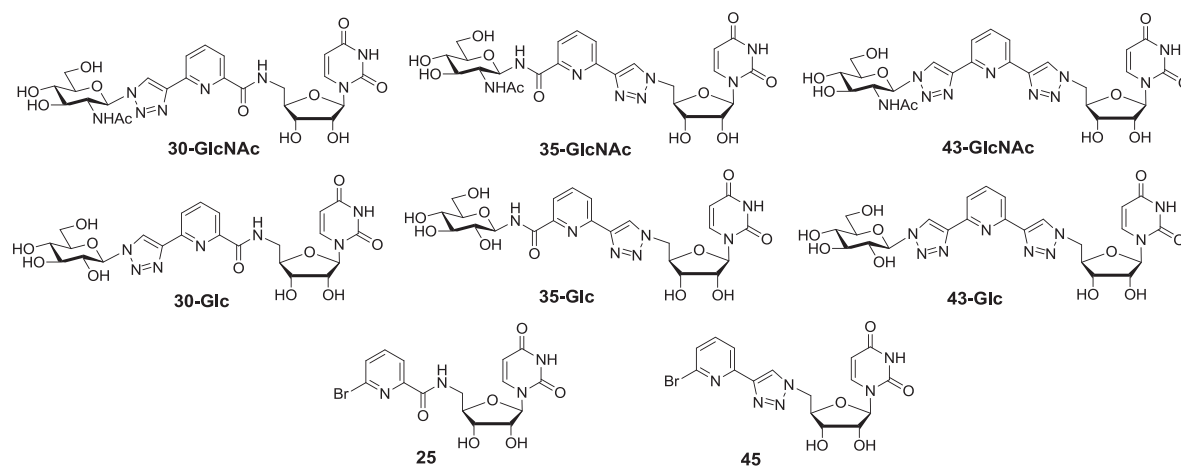


Figure IV-3. Structures of neutral UDP-GlcNAc and UDP analogues as OGT inhibitor candidates using pyridine as a pyrophosphate surrogate.

IV.1.1 Radiochemical GalT enzymatic assays

Progress in GT enzymatic assays development has been recently reviewed⁴², including radiochemical and chromatographic methods, label-free and fluorescence-based GT assays. The choice of assay depends on individual requirements. The most popular and commonly used radiochemical method was employed in our project for its high sensitivity and well established protocol. The assay is based on modification of the sugar donor by a radioactive element, subsequently quantification of the radioactive-labelled sugar transfer by scintillation counter, as outlined below (**Figure IV-4**). Tritiated uridine-5'-diphosphogalactose (UDP-[³H]Gal) was used as the radioactive substrate and GalT was used to construct the target oligosaccharide of each GalT. IC₅₀ and K_i could be determined based on the residual radioactivity measurement of the product after workup.

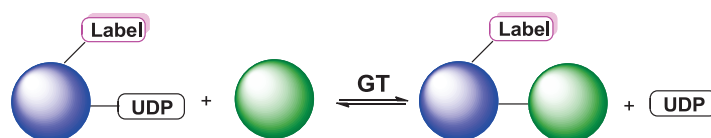


Figure IV-4. Radiochemical GT assay.⁴²

IV.1.2 Cell assays

To evaluate the possible permeation of our designed inhibitor through cell membranes, 3 different cell lines were chosen, MCF7, MCF10A and HeLa cells, with increasing concentrations of inhibitors. The influence on the *O*-GlcNAc cell cycling was determined after 24h or 48h treatment by Western blot using the anti-*O*-GlcNAc antibody RL2. In parallel, a known OGT inhibitor Ac-5SGlcNAc (2-acetamido-1,3,4,6-tetra-*O*-acetyl-2-deoxy-5-thio- α -D-glycopyranose) was chosen as a positive control of the *in cellulo* OGT inhibition.²²⁸

IV.1.3 Artificial cell membrane penetration test

Membrane permeation capability of the best inhibitor candidates were evaluated by an artificial cell membrane penetration test. Liposomes, made of phosphatidylcholine (POPC), was taken as a model for the test since POPC represents about 50 % of membrane content. Two methods were used for reciprocal confirmation of the evaluation. In the “out-in” method, prepared liposomes were incubated with inhibitor solutions to evaluate the amount of compound that

could penetrate the lipid bilayer to get inside of the liposomes. In the “in-out” approach, liposomes were prepared with the presence of the inhibitor to obtain inhibitor loaded liposomes.

IV.2 Results and discussion

IV.2.1 GalT inhibition studies

IV.2.1.1 Enzymatic evaluations (IC_{50} / K_i)

The first generation of candidates using pyridine moiety as pyrophosphate surrogate was tested against GalT applying radioactive assays, structures as listed in **Figure IV-1**. As a preliminary assessment, compounds were evaluated as inhibitors of five galactosyltransferases at a concentration of 1 mM of inhibitor, using K_m concentrations of donor and high concentrations of acceptor substrates (**Table IV-1**). Among the compounds, the derivatives synthesized through glycosylation (**7-Glc**, **7-Gal**, **19**, **22**) exhibited better inhibition than those obtained through CuAAC (**30-Glc**, **30-Gal**, **30-GlcNAc**, **35-Glc**, **35-Gal**, **35-GlcNAc**, **43-Glc**, **43-Gal**, **43-GlcNAc**).

Table IV-1. Enzymatic evaluation of neutral analogues containing pyridine as pyrophosphate surrogate.

| Inhibitor | β -1,4-GaIT | | GTB | | α -1,4-GaIT | | α -1,3-GaIT | | AAGlyB | |
|-----------|-------------------------|---|-------------------------|---|-------------------------|---|-------------------------|---|-------------------------|---|
| | % Inhibition at 1 mM | IC ₅₀ ^a (μ M) | % Inhibition at 1 mM | IC ₅₀ ^a (μ M) | % Inhibition at 1 mM | IC ₅₀ ^a (μ M) | % Inhibition at 1 mM | IC ₅₀ ^a (μ M) | % Inhibition at 1 mM | IC ₅₀ ^a (μ M) |
| 7-Glc | 13 | | 11 | | 23 | | 19 | | 47 | 1220 |
| 7-Gal | 100 | 152 | 84 | 262 | 80 | 546 | 99 | 320 | 93 | 493 |
| 19 | 97 | 334 | 53 | 725 | 37 | 1597 | 79 | 602 | 80 | 584 |
| 22 | 78 | 573 | 23 | | 27 | | 39 | 1020 | 19 | |
| 10 | 19 | | 33 | | 22 | | 16 | | 35 | |
| 25 | 9 | | 28 | | 1 | | 0 | | 20 | |
| 45 | 9 | | 38 | 1231 | 21 | | 32 | | 40 | 1035 |
| 30-Gal | 34 | | 10 | | 2 | | 11 | | 22 | |
| 30-Glc | 12 | | 1 | | 0 | | 11 | | 14 | |
| 30-GlcNAc | 22 | | 20 | | 0 | | 8 | | 16 | |
| 35-Gal | 0 | | 38 | 2304 | 8 | | 26 | | 31 | |
| 35-Glc | 15 | | 18 | | 17 | | 6 | | 14 | |
| 35-GlcNAc | 31 | | 8 | | 22 | | 21 | | 7 | |
| 43-Gal | 15 | | 34 | | 11 | | 22 | | 19 | |
| 43-Glc | 100 | 634 | 36 | 1767 | 33 | 1962 | 30 | 1061 | 36 | 1417 |
| 43-GlcNAc | 0 | | 29 | | 16 | | 26 | | 32 | |
| Uridine | | >1000 | | 1587 | | >3000 | | >1000 | | >1000 |
| UMP | | 313 | | 10 | | >1000 | | 130 | | 2 |
| UDP | | 25 | | 5 | | 62 | | 53 | | 1 |

a. Analogues which have an inhibition >35% at 1 mM (concentration of donor at K_m value and concentration of acceptor at K_m value or higher) were selected for IC₅₀ measurements. The IC₅₀ values were determined by constructing a dose-response curve and examining the effect of 10 different concentrations of each inhibitor ranging from 0 to 3000 μ M at concentration of donor of $1/5^{\text{th}}$ K_m value and concentration of acceptor at K_m value or higher.

The most potent compounds are glycosides containing a galactose moiety, **7-Gal** and **19**, the β and α -anomers, respectively. Interestingly, the α -anomer **19** which has the same α -anomeric configuration as the natural UDP-Gal donor was always a weaker inhibitor with 37-97% inhibition in comparison with the β -anomer **7-Gal** which inhibited the five enzymes between 80-100%. Compound **7-Glc**, the same β -glycoside but bearing a glucose moiety, was a very weak inhibitor of all of the enzymes except for AAGlyB where 47% inhibition was observed.

The bromo-pyridine analogues of UDP, namely compounds **25** and **45**, lacking saccharide moieties, were weaker inhibitors, as well as the alcohol derivative **10**. This observation illustrates that the introduction of a carbohydrate moiety is important for inhibition of the enzymes.

Compound **22** containing a phenyl moiety rather than pyridine was less effective for the retaining enzymes (GTB, AAGlyB, α -1,4-GalT and α -1,3-GalT) with 19-39% inhibition, while the inverting β -1,4-GalT was inhibited at 78%. Therefore, the influence of the nitrogen atom in the pyridine-containing inhibitors is crucial as rationalized later in the crystallographic studies.

Compound **43-Glc** with *bis*-triazolyl pyridine moieties was a potent inhibitor of β -1,4-GalT (100% inhibition) and a weak inhibitor of the retaining enzymes (30-36%). Surprisingly, the compound **43-Gal** bearing a natural galactosyl moiety was a weaker inhibitor than **43-Glc**. Compounds **30** and **35** with triazolyl pyridine were also weak inhibitors. The GlcNAc derivatives **30-GlcNAc**, **35-GlcNAc** and **43-GlcNAc** tested generally exhibited weak inhibition against these galactosyltransferases. In these series, the influence of the carbohydrate moiety was less detrimental than for glycosylated compounds, **7**, **19** and **22**.

The mode of inhibition of the most active compounds **7-Gal** was next determined as a competitive inhibitor of UDP-Gal using high concentrations of acceptor and varying the concentration of inhibitor at low and high concentrations of donor. Non-linear plots were observed in Dixon plots for AAGlyB and β -1,4-GalT, suggesting a complex mode of inhibition (**Figures V.9.1** and **V.6.5A**, **Chapter V**). This complex behaviour was confirmed in Michaelis-Menten plots which showed mixed inhibition with effects on both V_{\max} and K_m at high concentrations of **7-Gal** (**Figures V.6.2** and **V.6.6**, **Chapter V**). Compound **7-Gal** was also a mixed inhibitor of α -1,4-GalT (**Figure V.6.8**, **Chapter V**), α -1,3-GalT (**Figure V.6.10**, **Chapter V**) and GTB (**Figure V.6.12**, mixed at high inhibitor concentrations, competitive at low inhibitor concentrations, **Chapter V**). Non-linear Dixon plots were also obtained from evaluation of compound **19** with β -1,4-GalT (**Figure V.6.3**, **Chapter V**) and AAGlyB (**Figure V.6.5B**, **Chapter V**). Michaelis-Menten plots confirmed compound **19** was a mixed inhibitor of β -1,4-GalT at high concentrations (**Figure V.6.4**, **Chapter V**), competitive with UDP-Gal for AAGlyB (**Figure V.6.7**, **Chapter V**), α -1,4-GalT (**Figure V.6.9**, **Chapter V**), mixed inhibitor of α -1,3-GalT and GTB at high concentrations (**Figures V.6.11** and **V.6.13**, **Chapter V**). The determination of the inhibition mechanism for the two best inhibitors towards five GalTs was summarised in **Table IV-3**.

Table IV-3. Determination of the inhibition mechanism for the two best inhibitors towards five GalTs.

| Entry | Inhibitor | 7-Gal | | 19 | | |
|-------|-------------------------------------|---------------|---------------------------------------|------------|---------------------------------------|------------|
| | | Concentration | Low conc. | High conc. | Low conc. | High conc. |
| 1 | β-1,4-GalT | | noncompetitive dominated ^a | mixed | noncompetitive dominated ^b | mixed |
| 2 | GTB | | competitive dominated ^e | mixed | competitive dominated ^c | mixed |
| 3 | α-1,4-GalT | | mixed | mixed | mixed | mixed |
| 4 | α-1,3-GalT | | mixed | mixed | competitive dominated ^d | mixed |
| 5 | AAGlyB | | competitive dominated ^a | mixed | competitive dominated ^c | mixed |

a. conc. threshold = 300 μ M; b. conc. threshold = 400 μ M; c. conc. threshold = 600 μ M; d. conc. threshold = 500 μ M; e. conc. threshold = 200 μ M.

Due to the complex inhibition patterns, applying K_i to evaluate the inhibition capability was not feasible. To obtain a relative ranking of the compounds, IC_{50} measurements were carried out with selected inhibitors which could exhibit at least 35% inhibition at 1 mM concentration. For a better comparison, IC_{50} values of uridine, UMP and UDP were also measured. For all enzymes, compound **7-Gal** (Table IV-1) was a more potent inhibitor than uridine suggesting there are additional binding interactions of the enzyme with the pyridine scaffold. It was a better inhibitor of β -1,4-GalT and α -1,4-GalT than UMP while somewhat less effective than UMP for α -1,3-GalT and much weaker than UMP for GTB and AAGlyB. The corresponding α -anomer **19** (Table IV-1) was also more effective than uridine, though weaker than UMP. Removal of the nitrogen atom from the pyridine ring or changing the nature of the sugar moiety provided weaker inhibitors **22** and **7-Glc** in this glycosylated series (Table IV-1). The introduction of triazole moieties through CuAAC was also detrimental. The neutral UDP analogues **25** and **45** in the control group did not display inhibition towards almost all enzymes tested (Table IV-1).

The second generation candidates incorporating amino-acid derivatives as pyrophosphate surrogates (Figure IV-2) was tested against the same five GalT applying radioactive assays. As a preliminary assessment, compounds were evaluated as inhibitors of galactosyltransferases at a concentration of 1 mM of inhibitor, using K_m concentrations of donor and high concentrations of acceptor substrates (Table IV-2).

Surprisingly, almost all of the glycosides (compounds **74**, **75**, **77**, **78**, **80** and **95**) were very weak inhibitors of all of the enzymes except for AAGlyB where 38% inhibition was observed for compound **80**. The vinyl azide UDP analogue **79** gave inhibitions from 15% to 66% against the five GalT tested while the corresponding diastereomers **64** with addition of water displayed less inhibition. Substitution of the azido group of compound **64** by a carboxylic acid group in the UDP analogue **93** exhibited better inhibition. Heterocyclic modification on the linker of derivatives **81** and **82** provided more potent inhibitors than the parent compound **64**. The methoxy compound **82** was relatively weaker with 0-24% inhibition in comparison with the hydroxyl compound **81** which inhibited the five enzymes between 21-47%.

Table IV-2. Enzymatic evaluation of neutral analogues containing amino-acid derivatives as pyrophosphate surrogate.

| Inhibitor | β -1,4-GaIT | | GTB | | α -1,4-GaIT | | α -1,3-GaIT | | AAGK _v B | |
|-----------------|----------------------|--------------------|----------------------|--------------------|----------------------|--------------------|----------------------|--------------------|----------------------|--------------------|
| | % Inhibition at 1 mM | K_i^a (μ M) | % Inhibition at 1 mM | K_i^a (μ M) | % Inhibition at 1 mM | K_i^a (μ M) | % Inhibition at 1 mM | K_i^a (μ M) | % Inhibition at 1 mM | K_i^a (μ M) |
| 74 | 13 | | 21 | | 0 | | 0 | | 4 | |
| 75 | 23 | | 33 | | 2 | | 9 | | 19 | |
| 77 | 29 | | 25 | | 0 | | 12 | | 9 | |
| 78 | 5 | | 25 | | 5 | | 11 | | 6 | |
| 80 | 22 | | 20 | | 1 | | 20 | | 38 | 790 |
| 95 | 20 | | 24 | | 18 | | 2 | | 13 | |
| 64 [†] | 2 | | 15 | | 2 | | 8 | | 0 | |
| 93 | 40 | 1160 | 27 | | 60 | 319 | 50 | 1204 ^b | 0 | |
| 79 | 30 | | 63 | | 15 | | 23 | | 66 | 261 |
| 81 [†] | 21 | | 45 | | 28 | | 39 | 984 | 47 | 1133 ^b |
| 82 [†] | 16 | | 24 | | 0 | | 23 | | 20 | |

a. Analogues which have an inhibition >35% at 1 mM were selected for K_i measurements at concentration of donor at K_m value and concentration of acceptor at K_m value or higher.

b. For compounds with which mixed inhibition modes were observed, IC_{50} values were determined by constructing a dose-response curve and examining the effect of 10 different concentrations of each inhibitor ranging from 0 to 3000 μ M at concentration of donor at $1/5^{th}$ K_m value and concentration of acceptor at K_m value or higher.

*. Mixture of two diastereoisomer.

Most of these compounds were identified as competitive inhibitors. K_i measurements were applied to selected inhibitors which could exhibit at least 35% inhibition at 1 mM concentration (**Table IV-2**). For compounds with which mixed inhibition modes were observed by Michaelis-Menten plots (**Figure V.6.14 - Figure V.6.16, Chapter V**), IC_{50} values were determined by constructing a dose-response curve.

It should be noted that among the second generation candidates, four inhibitors (**77**, **80**, **93** and **95**) are either anionic or cationic compounds at physiological pH. Compound **77** possesses an amino group on the glycine residue while compound **80** directly on the serine backbone. Without bearing a galactose residue, compound **93** is an UDP analogue but could also serve as a GT inhibitor. As for enzymatic activity, the ionic groups on these four compounds displayed no beneficial or detrimental effect towards inhibition of GTs.

IV.2.1.2 Crystallographic studies with AAGlyB

To better understand the basis for the complex inhibition patterns of the first generation of candidates using pyridine moiety as pyrophosphate surrogate, the well characterized AAGlyB enzyme which readily crystallizes was used to investigate the mode of binding of **7-Gal**, **19** and **7-Glc**. Crystals of the apo-protein were soaked with the compounds and their structures were solved and refined on the ESRF synchrotron facilities in Grenoble (France).

The protein structures in all three crystals are essentially identical and closely resemble that in PDB_ID:2RJ7 for the AAGlyB mutant,²²⁹ which includes an UDP-Gal molecule in the binding site. All three inhibitors (**7-Gal**, **7-Glc** and **19**) are bound to the protein in a nearly identical manner. The uridine groups overlap very closely with those in 2RJ7, with the linker to the pyridine ring also in a conformation resembling that of the first phosphate group in UDP-Gal (**Figure IV-5**). The conformation of the pyridine ring deviates strongly from that of the phosphates in UDP-Gal, with the ring extending roughly perpendicularly to and away from uridine. In any case, the pyridine ring projects the hexopyranoses to a different position compared to the conformation observed for 2RJ7 (**Figure IV-5**). The pyridine ring in the inhibitors is roughly occupying the space of side chains of Lys346, Arg352 and, to a lesser extent, His348 in which the basic side chains of Lys346 and Arg352 are originally coordinated the pyrophosphate and stabilize it as a leaving group. The amide and anomeric oxygens, together with the pyridine nitrogen, chelate the Mn^{2+} ion which is displaced from its position in GTA/GTB by more than 2Å. As a result, the Mn^{2+} ion is not bound to both side chains of Asp211 and Asp213 but rather only Asp213 through the carboxylic oxygen.

Only one conformation of the glucose anomeric oxygen was observed for **7-Glc** while two alternative positions were observed for **7-Gal** of which only one can chelate the manganese. The sugar moieties are not visible in the electron density map, most likely disordered between several conformations, and hence could not be modeled. In the case of the α -galactoside **19**, two alternative conformations of the anomeric oxygen were also observed. In the conformation not chelating the manganese, the galactose group is visible with weak electron density and is modeled with reduced occupancy (**Figure IV-6**). The identification of the galactose moiety suggests that hexoses are present in the crystals but in disordered conformations preventing their modeling and crystallographic description.

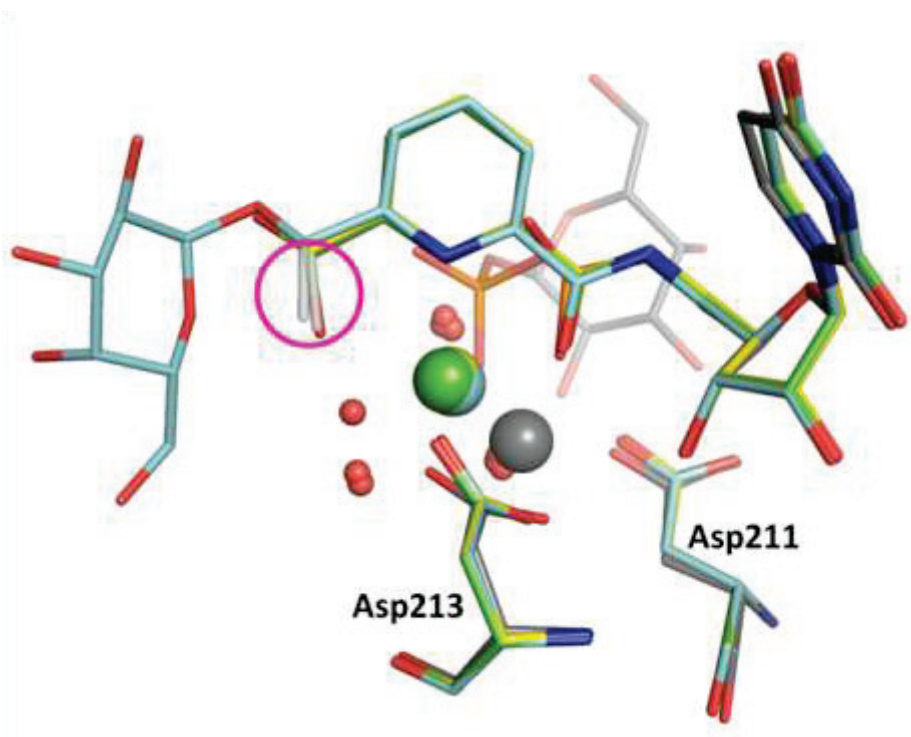


Figure IV-5. Superposition of all three inhibitors and UDP-Gal from PDB_ID:2RJ7. 2RJ7 is shown with gray carbons, 7-Gal with yellow carbons, 19 with cyan carbons, 7-Glc with green carbons. 7-Gal and 19 adopted a second conformation for the anomeric oxygen colored transparent white and shown inside the pink circle; the sugars, likely disordered, are not visible in the electron density for those conformations. For UDP-Gal, the phosphates and the galactose can be seen in the back in orange and gray. Also sticks of Asp211 and Asp213 are included with the same color code. The large spheres are the manganese cations, colored as the corresponding carbons. Also the waters in the coordination spheres are shown as smaller spheres for all three inhibitors.

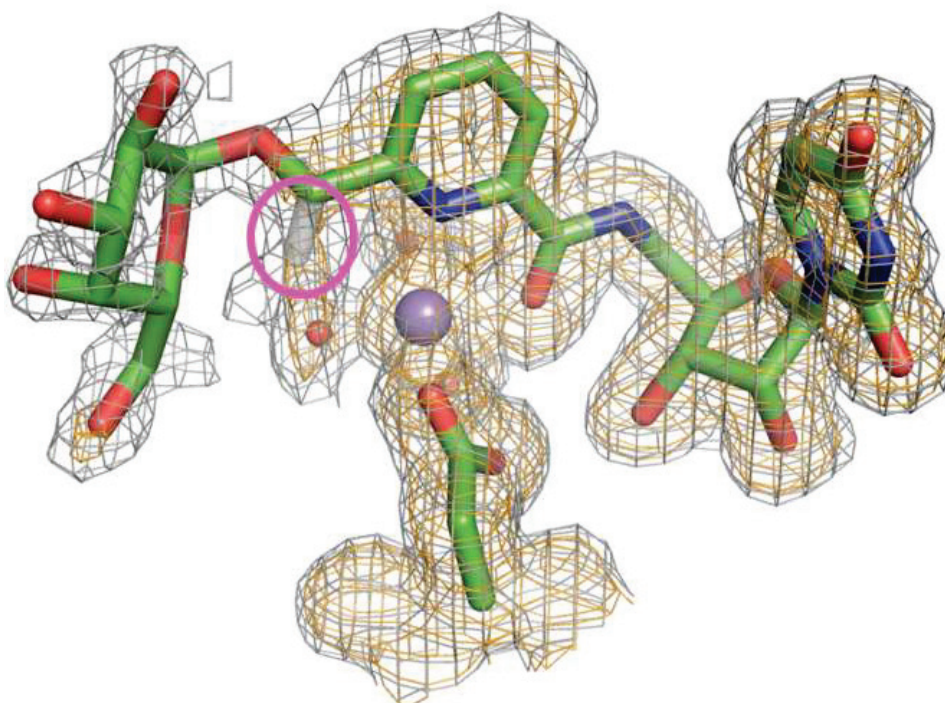


Figure IV-6. Electron density for compound 19, manganese in the AAGlyB structure (PDB_ID:4KC4). The anomeric oxygen is observed in two alternative conformations, but the galactose could only be modeled for one of them. The second conformation, with only the oxygen visible as a transparent rod, is marked with the pink circle. The orange mesh is electron density from the $2F_o - F_c$ map contoured at 1.0σ , while the gray mesh is the same map contoured at 0.4σ . The side chain in the lower part is from Asp213 chelating the Mn^{2+} cation.

The manganese cation is affected by the chelating inhibitors and displaced from its normal position by a 4 Å. In crystal structures of GTA and GTB, the Mn²⁺ is bound to the carboxylic groups of Asp211 and Asp213, as well as to the pyrophosphate of UDP or UDP-Gal in a tetra-coordinated structure. In 7-Glc/AAGlyB complex, the original position is occupied by a water molecule which is then involved in the coordination sphere of the displaced manganese and hydrogen bonded to the amide carbonyl of the inhibitors, Asp211 and Asp213 (**Figure IV-7**). The Mn²⁺ cation itself has a longer ligand distances and is heptacoordinated with the amide and anomeric oxygens, the pyridine nitrogen and three water molecules. The coordination sphere can be described as a pentagonal bipyramid with three of the equatorial positions occupied by the pyridine nitrogen and its adjacent carboxylic oxygens at 2.3 Å, 2.5 Å and 2.3 Å respectively (**Figure IV-7**). These three atoms, the pyridine ring and the manganese are coplanar. The last two equatorial positions in the manganese's coordination sphere are occupied by water molecules at 2.3 Å and 2.4 Å, respectively. The two axial positions are filled by a water molecule at 2.3 Å and a carboxylic oxygen from Asp213 at 2.2 Å. The pyridine ring is in Van der Waals contact with the hydroxyl oxygen of Tyr126 which has a stacking interaction with uracil. The hydroxyl group is roughly in the center of the π electronic cloud of the pyridine.

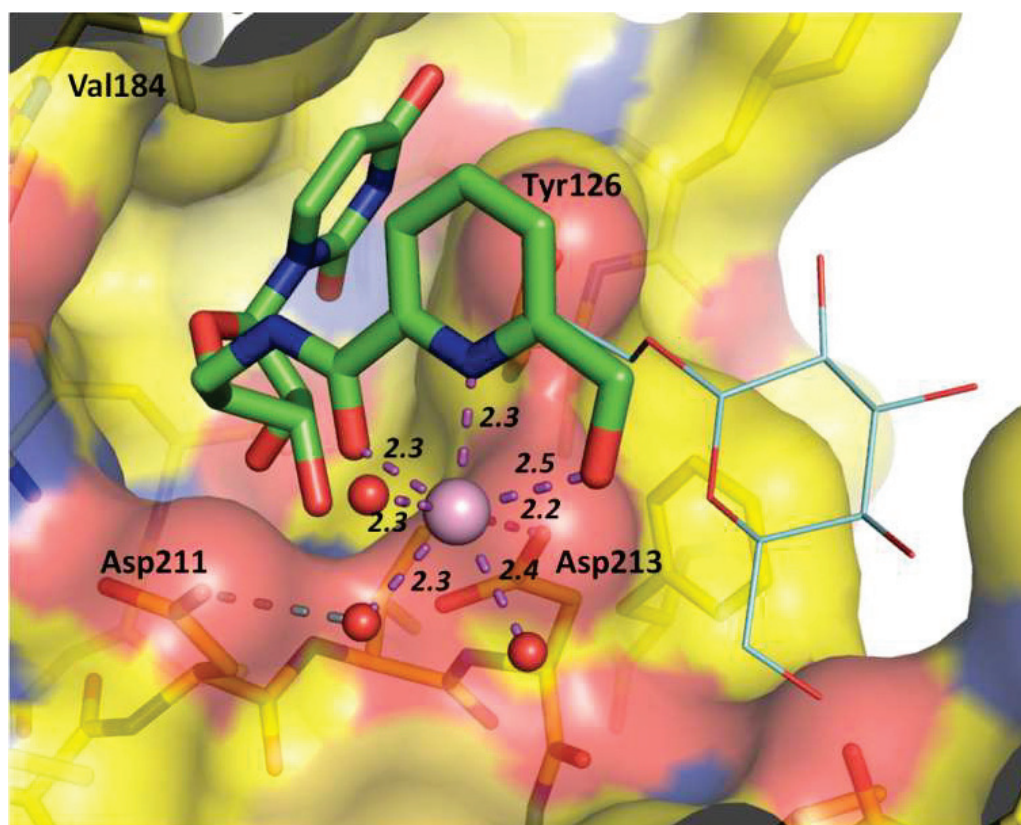


Figure IV-7. Coordination sphere of Mn²⁺ in the 7-Glc complex (PDB_ID:4KC1). 7-Glc is shown in thick sticks with green carbons. The alternative conformation of α -galactoside **19** is also presented in thin sticks with blue carbons, showing the galactose. The manganese is shown in pink. AAGlyB is shown as a semitransparent surface representation colored according to the closest atom and containing a stick model of the protein with yellow carbons.

Compounds **79**, **80** and **81** of the second generation of candidates using amino acid as pyrophosphate surrogate have been soaked with apo form of AAGlyB to gain more Structure Activity Relationship (SAR) information on inhibitors design. The results obtained still need

some refinements and discussions with our collaborators and will be reported in due course in our coming publications.

IV.2.2 OGT inhibition studies

IV.2.2.1 Enzymatic evaluation

Eight UDP-GlcNAc or UDP analogues functionalized with a pyridine ring conjugated with one or two triazoles (**Figure IV-8**) were selected for OGT inhibition evaluation.

A preliminary radioactive OGT assay was performed at 50 μM concentration, typical concentration used for the best OGT inhibitors. The compounds exhibit only a limited inhibitory effect on human OGT at 50 μM with the best inhibition of 19% observed for **35-Glc** (**Figure IV-8**). Analogues displaying more than 10% inhibition at 50 μM were then subjected to IC_{50} measurements (**Table IV-3**) which gave IC_{50} values of 336 μM , 708 μM and 1608 μM for **35-Glc**, **45** and **43-Glc**, respectively. The best compound among this series is **35-Glc**, a glucose derivative linked to the pyridine moiety by an amide bond and connected to the nucleoside part through a triazole moiety. Further kinetic study showed that this analogue was a competitive inhibitor with a K_i value of 422 μM (**Figure VI.9.17**, chapter VI).

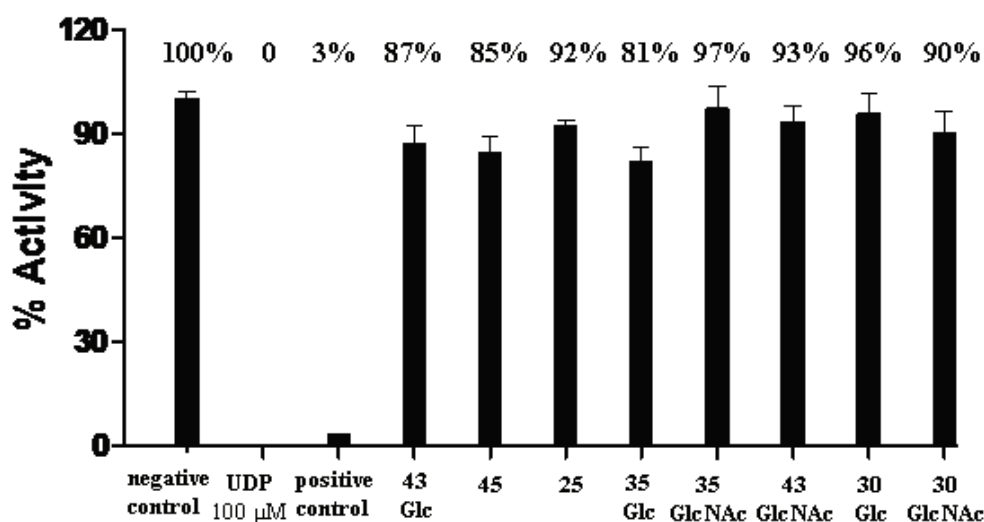


Figure IV-8. Inhibition activity of the UDP-Sugar and UDP analogues against OGT at 50 μM .

Table IV-3. IC_{50} measurements of neutral analogues containing pyridine derivatives as pyrophosphate surrogates.

| Inhibitor | IC_{50} (μM) |
|---------------|------------------------------------|
| 35-Glc | 336 |
| 45 | 708 |
| 43-Glc | 1608 |

IV.2.2.2 Docking studies

To gain insight into the binding mode of these compounds to OGT, 4 compounds **43-Glc**, **45**, **35-Glc**, and **35-GlcNAc** were selected for docking experiments using the known structure of OGT in complex with UDP-GlcNAc (PDB : 4GZ5). The best ranking pose of each OGT inhibitor was selected for docking (**Figure IV-9**). The uridine moieties of the four inhibitors showed nearly perfect overlap, almost identical to the binding mode of UDP-GlcNAc.

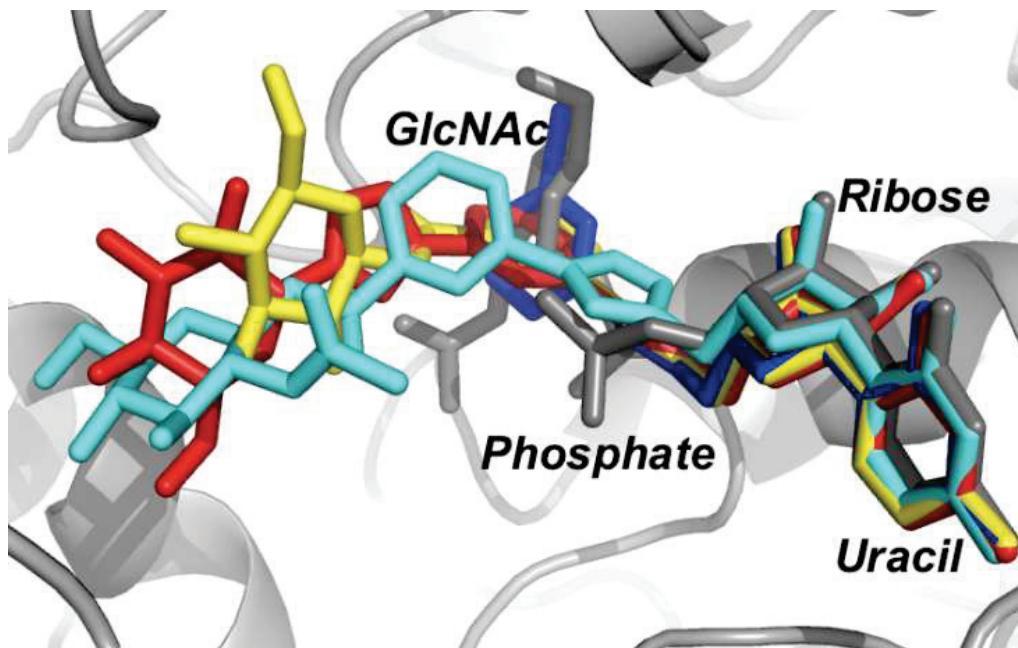


Figure IV-9. Overview of the best docking poses in comparison with the natural substrate UDP-GlcNAc (grey: OGT, grey sticks: UDP-GlcNAc; red sticks: **43-Glc**; blue sticks: **45**; yellow sticks: **35-Glc**; cyan sticks: **35-GlcNAc**). Different regions of UDP-GlcNAc are labeled in black text.

The triazole linkers of **43-Glc**, **45**, and **35-Glc** shared the same orientation and location, with N2 forming a hydrogen bond with the hydroxyl group of Thr922 and N3 interacting with the nitrogen on the backbone of Thr921 (**Figure IV-10**). These polar interactions between triazoles and amino-acid residues of OGT resembled the polar interactions between β -phosphate of UDP-GlcNAc and OGT (shown with grey dashed line in **Figure IV-10**). This interaction was absent in the model of **35-GlcNAc** which may explain why this derivative showed weaker inhibitory activity.

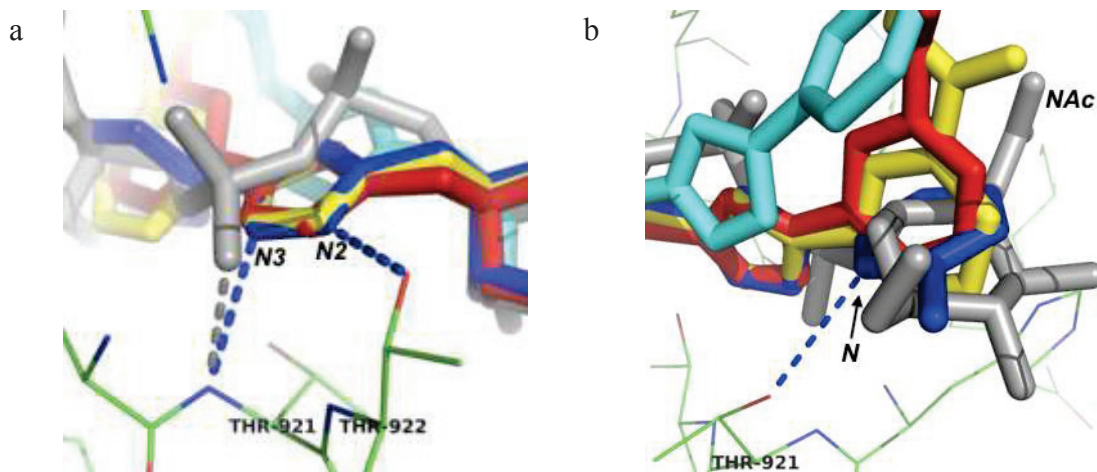


Figure IV-10. Comparison of substrate and inhibitor binding modes in the catalytic site of hOGT (Grey sticks: UDP-GlcNAc; red sticks: **43-Glc**; blue sticks: **45**; yellow sticks: **35-Glc**; cyan sticks: **35-GlcNAc**). (a) Hydrogen bonds (blue dashed lines) were formed with N2 and N3 of the triazole; the polar interaction between the β -phosphate of UDP-GlcNAc and Thr921 is also shown (grey dashed line) for comparison. (b) The pyridine nitrogen of compound **45** forms a hydrogen bond with the hydroxyl group of Thr921.

As for the hexose sugar head parts of compounds **43-Glc**, **35-Glc** and **35-GlcNAc**, the orientation did not mimick that of the natural substrate UDP-GlcNAc (**Figure IV-11**). The carbohydrate moiety did not display a lot of interactions with OGT. This poor interaction with

the enzyme could explain the poor selectivity observed between Glc- and GlcNAc-based inhibitors.

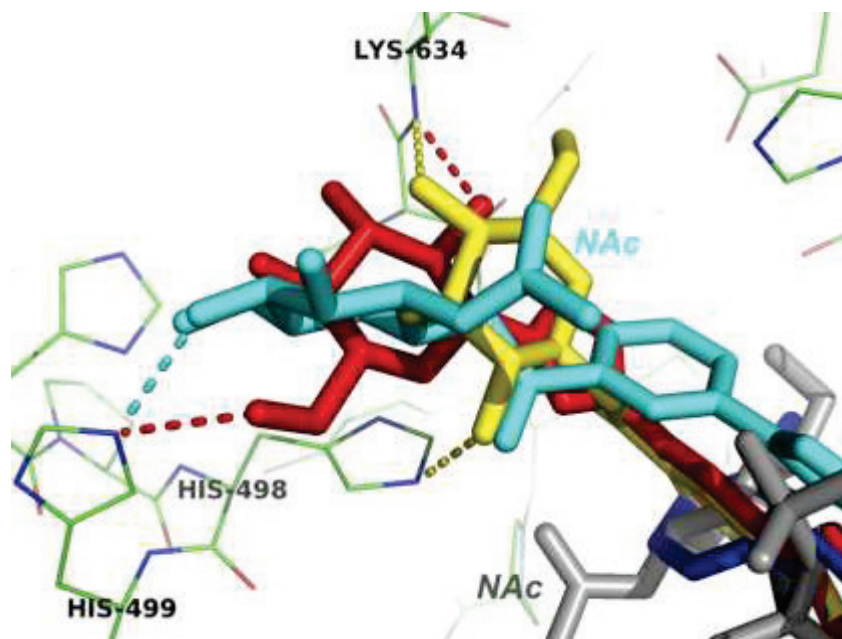


Figure IV-11. Inhibitor binding within the Glc/GlcNAc portion (Grey sticks: UDP-GlcNAc; red sticks: **43-Glc**; blue sticks: **45**; yellow sticks: **35-Glc**; cyan sticks: **35-GlcNAc**). Dashed lines indicate hydrogen bonds from different inhibitors. The acetamido group of UDP-GlcNAc and **35-GlcNAc** are labeled in cyan text.

The bromopyridine moiety of compound **45** partially overlapped with the GlcNAc ring of UDP-GlcNAc. In comparison, the three derivatives **43-Glc**, **35-Glc** and **35-GlcNAc** adopted an orientation perpendicular to that of the natural substrate UDP-GlcNAc. In the Glc series, both **43-Glc** and **35-Glc** could form hydrogen bonds with His498, His499 and Lys634, whereas the GlcNAc derivative **35-GlcNAc** was involved in a single hydrogen bond interaction with His499 (**Figure IV-11**). The acetamido group of **35-GlcNAc** showed no direct interaction with the enzyme backbone.

As a short conclusion, the uridine moieties of these four inhibitors showed identical binding mode to the natural substrate of UDP-GlcNAc. The polar interactions formed between triazole linkers and OGT could mimic the binding function of β -phosphate of UDP-GlcNAc whereas the carbohydrate moieties of **43-Glc**, **35-Glc** and **35-GlcNAc** were oriented to a different direction far from the original pyranose pocket. The bromo-pyridine UDP analogue **45**, among the four compounds applied for docking experiment, exhibited the best mimicry of the natural substrate GlcNAc in terms of binding geometry. These modeling studies therefore reveal why the glucose derivatives (**35-Glc**, **43-Glc**) exhibited relatively better inhibitory effect compared to the glucosamine counterpart **35-GlcNAc**.

IV.2.2.2 Inhibition of O-GlcNAcylation in a cell-based assay

No significant decrease in O-GlcNAc protein level was observed with 50 μ M and 100 μ M of any of the selected compounds, whereas O-GlcNAcylation of proteins was strongly decreased when cells were treated with 50 μ M of the positive control Ac-5SGlcNAc (**Figure IV-12**). The best inhibitor **35-Glc** was tested with higher concentrations (100 μ M, 200 μ M and 500 μ M) on three different cell lines (MCF7, MCF10A and HeLa cells). No obvious decrease could be

observed by Western-blot analysis (**Figure IV-13**). These results suggested that these compounds may not inhibit OGT in cells.

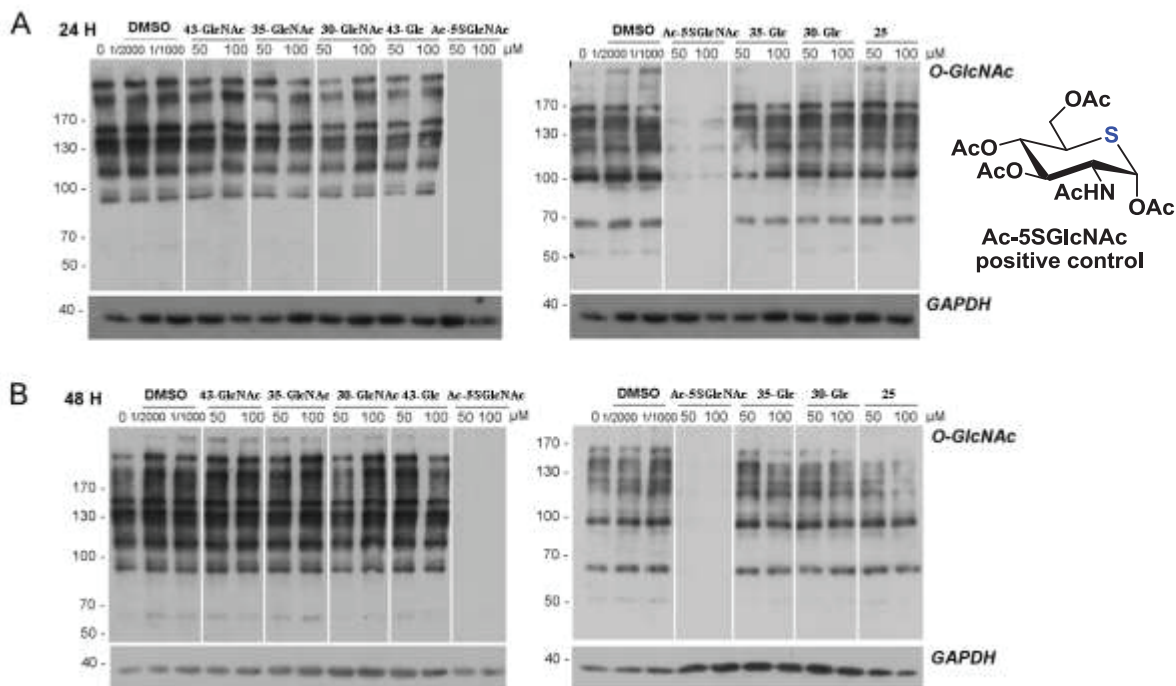


Figure IV-12. MCF7 cells were treated for 24 hours (A) or 48 hours (B) with DMSO (vehicle), inhibitors 43-GlcNAc, 35-GlcNAc, 30-GlcNAc, 43-Glc, 35-Glc, 30-Glc, 25 or Ac-5SGlcNAc at indicated concentrations. O-GlcNAc level was examined by immunoblotting using RL2 antibody. GAPDH was used as loading control. Representative results of 3 independent experiments.

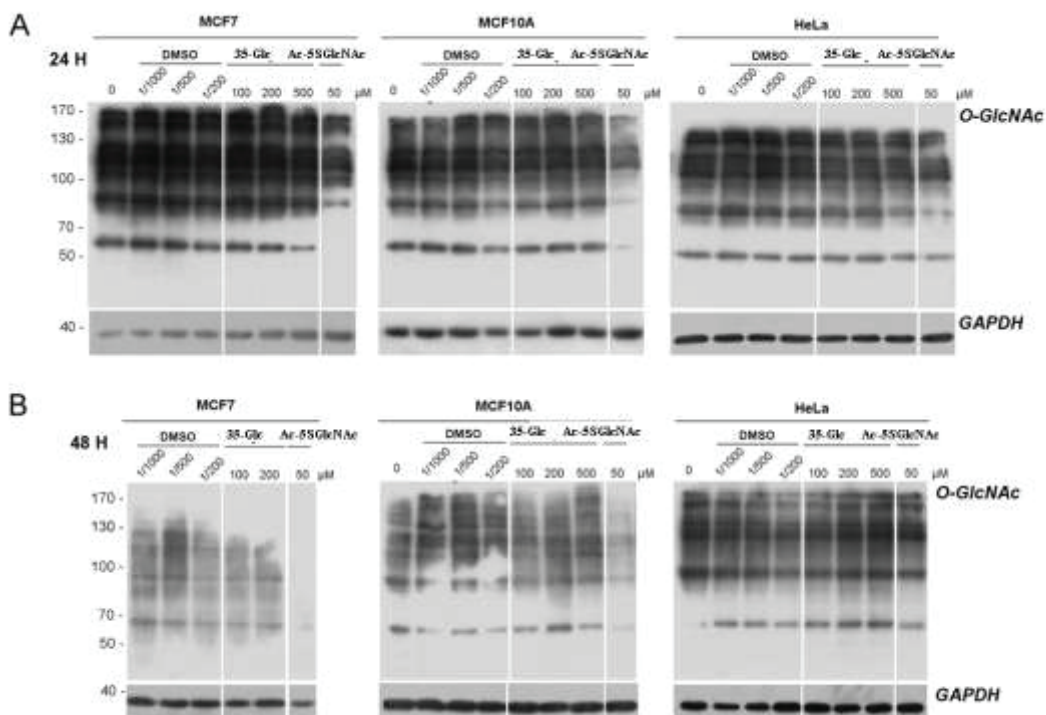


Figure IV-13. MCF7, MCF10A and HeLa cells were treated for 24 hours (A) or 48 hours (B) with DMSO (vehicle), 35-Glc or Ac-5SGlcNAc at indicated concentrations. O-GlcNAc level was examined by immunoblotting using RL2 antibody. GAPDH was used as loading control. Representative results of 2 independent experiments.

Enzymatic studies revealed that this series of compounds could exhibit inhibitory effect on human OGT with the best inhibition of 19% observed for **35-Glc** at 50 μM . Docking study confirmed that the uridine moieties of these inhibitors could bind to OGT identical to the natural substrate of UDP-GlcNAc and polar interactions were created between triazole linkers and OGT. But cell assay suggested that these compounds may not inhibit OGT *in vivo*. So an artificial cell membrane penetration test was performed for the most potent compound **35-Glc** to evaluate its permeation capability.

IV.2.3 Evaluation of membrane permeation

Membrane penetration capability of the best inhibitor candidates against GalT or OGT (**7-Gal** and **35-Glc**, respectively) were evaluated by an artificial cell membrane penetration test. Liposomes made of phosphatidylcholine (POPC, **Figure IV-14**) were used as a model and UV-vis absorption was used to quantify the amount of inhibitors present in solution. Two methods were used in the evaluation, named method **I** and **II** as shown in **Scheme IV-1**. In method **I**, prepared liposomes were incubated with synthesized inhibitor candidate in a shaking incubator. Then, liposome-complex fraction was separated from free inhibitors by G-25 column (size exclusion chromatography, large molecules, liposome fraction in our case, leave the column first). UV absorption at λ_{max} was measured for each fraction to evaluate the amount of inhibitor incorporated into the liposomes. Incubation was performed for liposome-inhibitor complex fractions. Further separation was performed to evaluate the amount of inhibitor released by gradient of concentration. The opposite approach was performed to confirm the previous results. In method “in-out” **II**, liposomes were prepared with inhibitor solution to incorporate the inhibitor in the liposomes. Liposomes were separated from excess inhibitors by G-25 column. The liposome complex fraction was further incubated. After 24 hours, the mixture was purified by G-25 to evaluate the amount of inhibitor released from the liposomes.

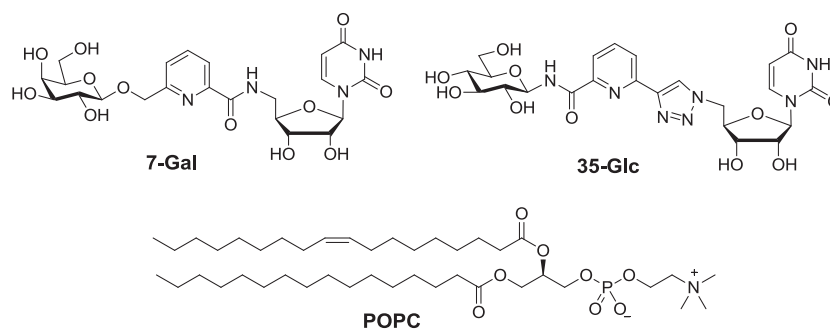
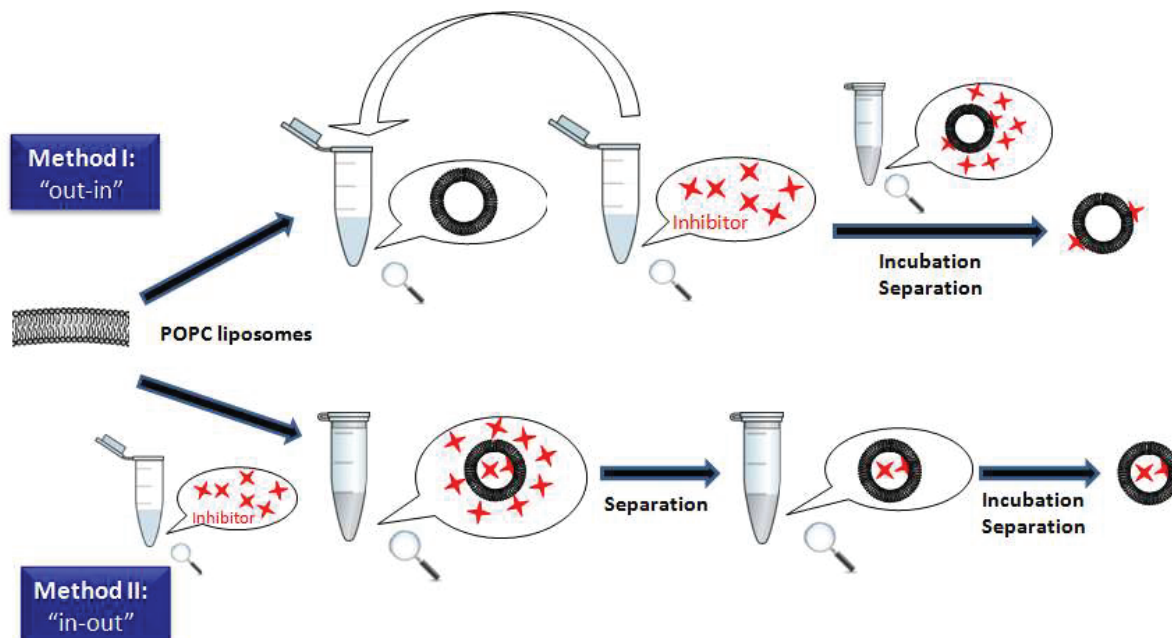


Figure IV-14. Structure of POPC and analogues evaluated in membrane permeation experiments.



Scheme IV-1. Lipid bilayer penetration test taken POPC as a model.

UV titrations of the two compounds were performed to define calibration curves between absorption and concentrations of inhibitors (**Figures IV-15** and **Figure IV-16**).

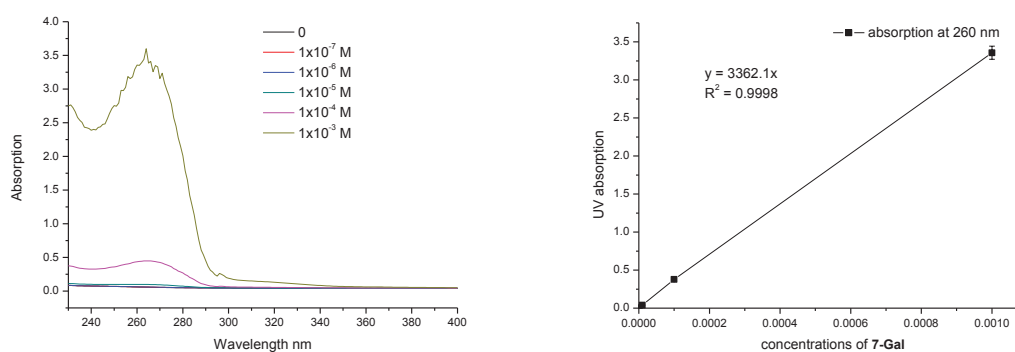


Figure IV-15. UV-titration of **7-Gal**. For UV-titration, UV absorption of **7-Gal** at concentrations of 1×10^{-7} M, 1×10^{-6} M, 1×10^{-5} M, 1×10^{-4} M, 1×10^{-3} M in $1 \times$ PBS buffer were measured in duplicates. Linear regression fit of **7-Gal** was taken at 260 nm ($\lambda_{\max} = 263$ nm).

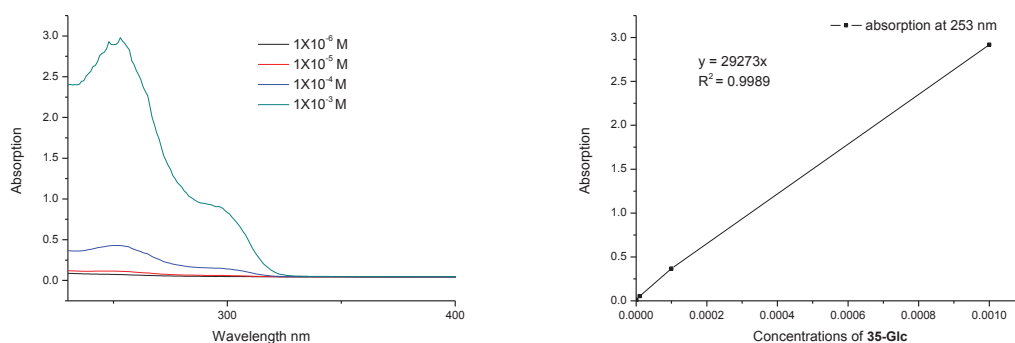


Figure IV-16. UV-titration of **35-Glc**. For UV-titration, UV absorption of **35-Glc** at concentrations of 1×10^{-6} M, 1×10^{-5} M, 1×10^{-4} M, 1×10^{-3} M in $1 \times$ PBS buffer were measured in duplicates. Linear regression fit of **35-Glc** was taken at 253 nm ($\lambda_{\max} = 253$ nm and a shoulder peak at 300 nm).

For compound **7-Gal**, in **Method I**, after incubation with the inhibitor solution (1×10^{-2} M), the liposome fraction was readily separated from the free inhibitors (**Figure IV-17a**, fraction 4 for liposomes complex and fractions 7-11 for free inhibitors). Analysis of the UV absorption spectra of the complex fraction indicated that about 2.3% of the compound was complexed with liposomes (**Figure IV-17b**, black line: spectrum of liposome only; red line: spectrum of fraction 4). Further incubation of the fraction 4 at 37°C for 24 hours was performed but no free inhibitor could be separated from this fraction (**Figure IV-17c**) indicating that inhibitors could interact with liposomes but cannot be released, probably sequestered at the surface of the liposomes.

In comparison, **Method II** was performed. After the preparation of liposomes with inhibitors solution (1×10^{-2} M), free inhibitors were separated from the liposome complex fraction (**Figure IV-18a**, fraction 4 for liposomes complex and fractions 7-11 for free inhibitor). UV spectra analysis of this fraction indicated that a fraction of the compound was indeed captured inside of the liposomes (**Figure IV-18b**). Further incubation and separation was carried out but no apparent free inhibitor fraction could be isolated from the complex fraction 4 (**Figure IV-18c**). Together with the results obtained from **Method I**, this phenomenon revealed that the inhibitor **7-Gal** could interact and be associated with liposomes. The complex formed is relatively stable therefore the affinity of **7-Gal** towards liposomes was demonstrated.

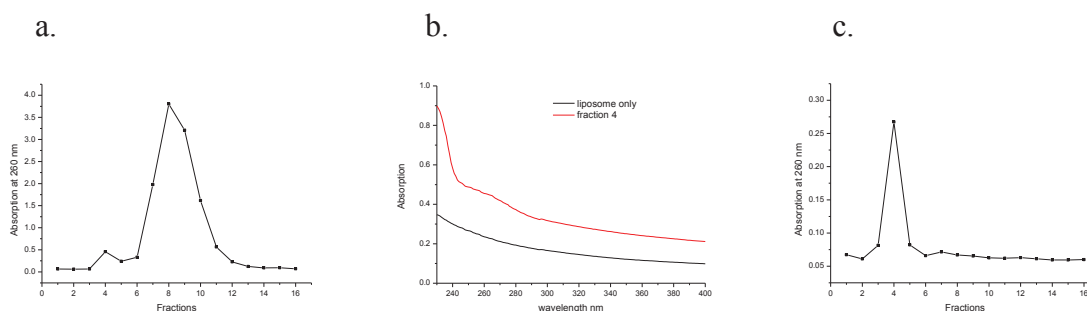


Figure IV-17. a. UV absorption at 260 nm; b. UV spectra of liposome complex fraction (fraction 4, in red), compared with liposome only (in black). c. UV absorption at 260 nm (second separation).

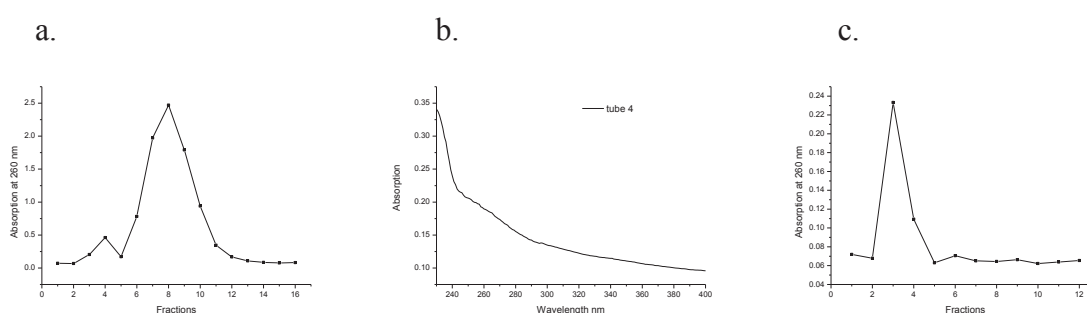


Figure IV-18. a. UV absorption at 260 nm (first separation); b. UV spectra of fraction 4; c. UV absorption at 260 nm (second separation).

The same methodology was performed for compound **35-Glc**. Despite the very similar structures of **7-Gal** and **35-Glc**, the results obtained for **35-Glc** varied in this model study. In **Method I** a small fraction of liposomes was separated from the free inhibitor after incubation of the liposomes with **35-Glc** solution (1×10^{-2} M) (**Figure IV-19a**). The comparison of UV spectra of fraction 3 and buffer fraction 1 did not show apparent presence of inhibitors with the liposomes (**Figure IV-19b**). In **Method II**, the inhibitor-liposome complexes were well

separated from free inhibitors (**Figure IV-20a**). The smooth peak and shoulder peak at 253 nm and 300 nm indicated that a small portion of **35-Glc** was incorporated inside of the liposomes (**Figure IV-20b**). Further incubation of this fraction at 37°C for 24 hours did not release any inhibitor (**Figure IV-20c**). These observations showed that compound **35-Glc** could not pass through the lipid bilayer neither associate with it.

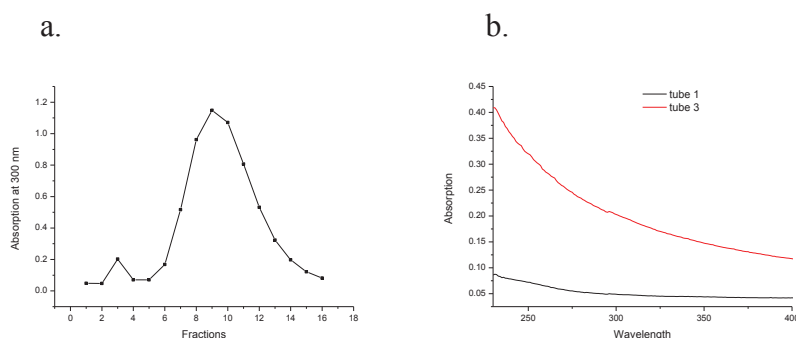


Figure IV-19. a. UV absorption at 300 nm; b. UV absorption spectra of fraction 1 and 3.

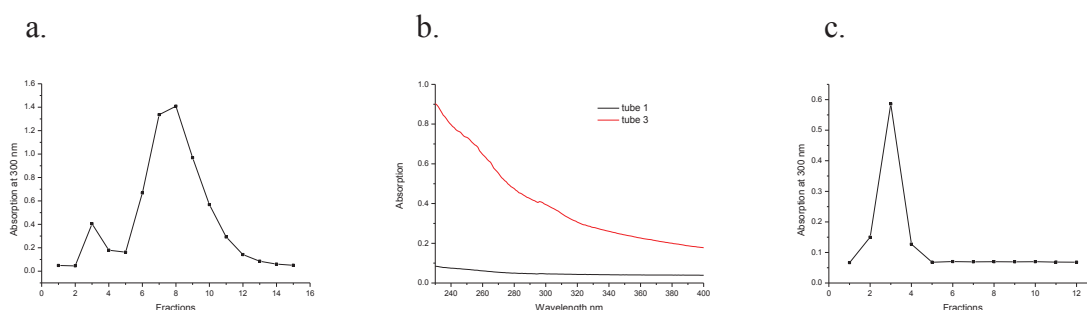


Figure IV-20. a. UV absorption at 300 nm; b. UV absorption spectra of fraction 1 and 3. c. UV absorption at 300 nm (second separation).

A sulfonylurea anti-hyperglycaemic drug (Glibenclamide[®]) with a molecular weight of 494 g.mol⁻¹ similar to our analogues, was reported to cross phospholipid bilayers.²⁵⁸ It was taken as a positive control for this study. Nevertheless, separation from the liposome fractions was unsuccessful and this molecule could therefore not be used as a positive control for this study.

IV.3 Conclusion

A total of 26 analogues with either pyridine moiety or amino-acid derivatives as pyrophosphate surrogate were evaluated as GalT inhibitors. In the first series of pyridine containing compounds, the derivatives synthesized through glycosylation exhibited better inhibition than those obtained through CuAAC. The enzymatic assays combined with the crystallographic study of the best three inhibitors revealed that:

- (1) the uracil and ribose moieties are crucial for binding;
- (2) the introduction of a carbohydrate moiety is important for selectivity and inhibition of the enzymes;
- (3) the pyridine based linker between the ribose and hexoses has multiple effects, including orienting the hexoses away from the galactose position in UDP-Gal, displacing the manganese from its original position by chelating and preventing the folding of the C-terminal tail of AAGlyB keeping it in a closed form;
- (4) the inhibitors displayed mixed binding modes, neither competitive nor noncompetitive

inhibitors.

The enzymatic study of the second series of amino-acid derivatives indicated that:

- (1) an appropriate design of neutral linker between the ribose and hexoses is important to orient the molecule to the proper binding site;
- (2) the introduction of a hydrophobic moiety on the backbone of linker could increase the binding affinity with GalT;
- (3) the decoration of a hydrogen donating group could contribute to the formation of hydrogen bond therefore increasing the binding affinity.

Among the derivatives synthesized, 8 UDP-sugar or UDP analogues were selected for OGT inhibition, including enzymatic assays and cell assays. The enzymatic evaluation indicated that this series of compounds has minimal inhibition effect at 50 μM and the best inhibitor has a K_i value of 422 μM . Further study showed that these compounds did not inhibit OGT function in cells. Docking studies showed that the polar interactions formed between triazole linkers and amino-acid backbone of OGT could mimic the binding function of β -phosphate of UDP-GlcNAc whereas the sugar heads of this series of compounds were pointing into a direction different from the original galactopyranose pocket.

The concept of “neutral” inhibitor instead of ionic analogues was finally verified by an artificial cell membrane penetration test on the two best inhibitor candidates against GalT or OGT (**7-Gal** and **35-Glc**). Despite minor structural modifications, the two compounds behaved differently in this model. Compound **7-Gal** showed binding affinity towards liposome while **35-Glc** showed no apparent binding or penetrating capability.

General Conclusion

The study in this thesis presented the design, synthesis, biological evaluation and structural analysis of glycosyltransferase inhibitors. The design rationale was to make analogues of NDP-sugar natural substrates incorporating a “neutral” pyridine or amino-acid derivative as the pyrophosphate surrogate. Due to the poor bioavailability of the charged native substrates, neutral inhibitors were investigated in order to provide cell permeable substrates for potential *in cellulo* or *in vivo* applications as fundamental tools for biology or even as potential drugs.

The design and synthesis of 26 GT inhibitors were performed using a combination of conjugations through *O*-glycoside, amide bond or triazole functionalities.

- (1) A systematic investigation of glycosylation methods on pyridine- or serine-based acceptors was performed. The optimized conditions were used to synthesize neutral analogues of enzyme natural substrates.
- (2) Two conjugation techniques, Staudinger-Vilarrasa reaction and azide-alkyne cycloaddition (CuAAC), were applied to obtain inhibitors candidates in a minimum number of steps. Two synthetic routes, from “Sugar-to-Nucleoside” and from “Nucleoside-to- Sugar”, were applied in the glucose series in order to compare their efficiency. An orthogonally protected *bis*-alkynyl pyridine was introduced in “one-pot” synthetic strategy to increase the efficiency.
- (3) Unusual byproducts were observed in the final deprotection steps of the serine-based analogues and a possible mechanism for this process was proposed.

The inhibition evaluation towards five galactosyltransferases and one GlcNAc transferase (OGT) revealed moderate inhibition. Nevertheless, structural analysis of the most potent compounds in complex with a glycosyltransferase revealed that the designed “neutral” pyridine linker could indeed chelate with manganese although displacing it just a few Å from its original position. The sugar head-group was oriented away from the position found in the related complex with UDP-Gal indicating a new binding mode. Eight UDP-GlcNAc or UDP analogues functionalized with a pyridine ring conjugated with one or two triazoles were selected for OGT inhibition evaluation. Enzymatic studies revealed that this series of compounds could exhibit inhibitory effect on human OGT. Docking study confirmed that the uridine moieties of these inhibitors could bind to OGT identical to the natural substrate of UDP-GlcNAc and polar interactions were created between triazole linkers and OGT. Nevertheless, cell assay suggested that these compounds may not inhibit OGT *in vivo*.

The concept of “neutral” inhibitor instead of ionic analogues was finally examined by an artificial cell membrane penetration test on the two best inhibitor candidates against GalT or OGT (**7-Gal** and **35-Glc**). Despite minor structural modifications, the two compounds behaved differently in this model. Compound **7-Gal** showed apparent binding affinity towards liposome while **35-Glc** showed no apparent binding or penetrating capability.

Perspectives

Crystal data analysis on the binding mode of these inhibitors provided useful structure-activity relationship information for future rational design (**Figure P-1**).

The 4-position of pyridine is 4 Å away from the side chain of Trp181. This position would be ideally substituted by an aliphatic or heterocyclic hydrophobic group to create Van der Waals contacts or stacking interactions with the nearby amino-acid side chain.

The glucose or galactose moiety of the inhibitor is most likely disordered. Since the function of the exo-anomeric oxygen is involved in chelation with manganese, an ester or amide bond instead of a glycosidic bond may perform better.

In the co-crystal, the glycosidic oxygen is in the proximity of the fucose residue of the acceptor and the carbon atom adjacent to the pyridine is only 3.6 Å away from O2 of the acceptor's fucose residue. This position would be ideally substituted with a linker of about three atoms attached to the acceptor to generate a bisubstrate inhibitor. This should result in an increase in both affinity and specificity of the inhibitors.

Considering the different orientation of the inhibitor synthesized in comparison to the natural substrate, more consideration should be given to the conformational plasticity of the designed compounds but not only the conformation of the targeted protein. Yet, a fine balance should be considered. If the structure of the compound is too rigid (e.g. the pyridine group), the conformational space may not orientate the carbohydrate moiety towards the proper position. Whereas, if there is too much flexibility, the molecule could in principle adopt the desired conformation but then large penalty may be required.

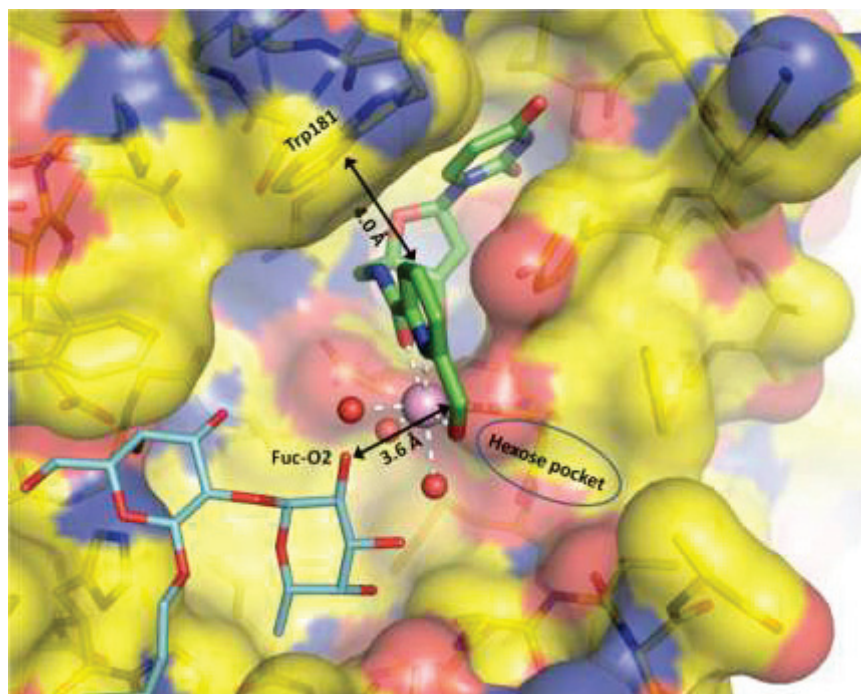


Figure P-1. Binding mode of 7-Glc. The protein is represented as a semitransparent surface with a stick model and yellow carbons, 7-Glc is represented as a thick stick model with green carbons. Acceptor α -L-Fucp-(1 \rightarrow 2)- β -D-Galp-O-(CH₂)₇-CH₃ is represented with thin sticks and cyan carbons. The manganese is the purple sphere and the white dashed lines indicate its coordination ligands, which include three water molecules (small red spheres). Black arrows indicate the distances mentioned in the text.

Chapter V : Experimental section

Chapter V : Experimental section

V.1 General methods.

All chemicals were obtained from commercial sources and used without further purification. Dichloromethane, acetonitrile and methanol were distilled over CaH_2 , CaH_2 and Mg/I_2 , respectively. All reactions were performed under an argon atmosphere. Thin-layer chromatography (TLC) was carried out on aluminum sheets coated with silica gel 60 F₂₅₄ (Merck). TLC plates were inspected by UV light ($\lambda = 254 \text{ nm}$) and developed by treatment with a mixture of 10% H_2SO_4 in $\text{EtOH}/\text{H}_2\text{O}$ (1:1 v/v) followed by heating. Silica gel column chromatography was performed with silica gel Si 60 (40–63 μm). NMR spectra were recorded at 293 K, unless otherwise stated, using a Bruker 400 or 500 MHz spectrometer. Chemical shifts are referenced relative to deuterated solvent residual peaks. The following abbreviations are used to explain the observed multiplicities: s, singlet; d, doublet; t, triplet; q, quadruplet; m, multiplet; bs, broad singlet and bd, broad doublet. Complete signal assignments were based on 1D and 2D NMR (COSY, HSQC and HMBC correlations). High resolution (HR-ESI-QToF) mass spectra were recorded using a Bruker MicroToF-Q II XL spectrometer. Optical rotations were measured using a Perkin Elmer polarimeter and values are given in $10^{-1} \text{ deg.cm}^2.\text{g}^{-1}$.

General protocol A for Staudinger-Vilarrasa conjugation. The acid (0.466 mmol, 1 eq.) and HOBt (0.839 mmol, 1.8 eq.) were co-evaporated with toluene (3×5 mL) and THF (3×5 mL). The mixture was dried under vacuum for 1 h. The mixture was dissolved in dry THF (4 mL) under argon and cooled to 0°C. DIC (0.839 mmol, 1.8 eq.) was added dropwise at 0°C. After addition, the ice-bath was removed and the reaction stirred at r.t. for 30 min. Meanwhile, the azide (0.699 mmol, 1.5 eq.) was dissolved in dry THF (4 mL) under argon and cooled to 0°C. PMe_3 (0.932 mmol, 2 eq.) was added and the reaction was stirred at 0°C. After 30 min, the solution was transferred into the flask containing the acid/HOBt solution at 0°C. The flask was washed with THF (4 mL) and the solution was transferred. The resulting reaction mixture was stirred at 0°C for 1 h then allowed to reach r.t. and stirred for an additional 16 h. The reaction mixture was diluted with water (60 mL), extracted with EtOAc (4×60 mL). The combined organic layers were washed with satd Na_2CO_3 (60 mL), H_2O (60 mL) and brine (60 mL), dried (Na_2SO_4) and concentrated. The residue was purified by silica gel column chromatography (PE to EtOAc) to afford the desired amide.

General protocol B for Sharpless CuAAC conjugation. To a solution of the alkyne (0.19 mmol, 1 eq.) and the azide (0.19 mmol, 1 eq.) in $t\text{BuOH}/\text{H}_2\text{O}$ (1/1, 5.6 mL / 280 μL) were added CuSO_4 (0.11 mmol, 0.6 eq.) and sodium ascorbate (0.228 mmol, 1.2 eq.). The reaction was stirred at 35°C for 24 h then diluted with water (20 mL) and extracted with CH_2Cl_2 (3×30 mL). The combined organic layers were dried (Na_2SO_4) and concentrated. The residue was purified by silica gel column chromatography to afford the desired triazole.

General protocol C for Meldal CuAAC conjugation. $i\text{Pr}_2\text{NEt}$ (0.036 mmol, 0.25 eq.) was added into a flask containing the azide (0.14 mmol, 1 eq.), the alkyne (0.14 mmol, 1 eq.) and CuI (0.01 mmol, 0.1 eq.) in DMF (2 mL). The reaction was stirred at r.t. overnight. After 24 h, the solution was diluted with EtOAc (50 mL), washed with satd Na_2CO_3 (2×25 mL) and H_2O (30 mL). The combined aqueous layers were extracted with EtOAc (3×30 mL). The combined organic layers were dried (Na_2SO_4) and concentrated. The residue was purified by silica gel column chromatography to afford the desired triazole.

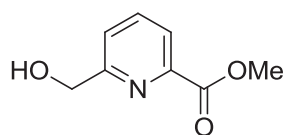
General protocol D for Sonogashira reaction. The bromo-arene (1.0 mmol, 1 eq.), Pd(PPh₃)₄ (0.1 mmol, 0.1 eq.) and CuI (0.1 mmol, 0.1 eq.) were dissolved in toluene (25 mL) and the solution was degassed with argon. Then, trimethylsilylacetylene (3.0 mmol, 3 eq.) and diisopropylamine (2.2 mmol, 2.2 eq.) were added. The reaction was stirred for 48 h at r.t. protected from light then poured into satd NH₄Cl (100 mL). The aqueous layer was extracted with CH₂Cl₂ (3×100 mL). The combined organic layers were washed with H₂O (100 mL) and brine (100 mL), dried (Na₂SO₄) and concentrated. The residue was then purified by silica gel column chromatography to afford the desired product.

General protocol E for the Zemplén deacetylation. In a flask containing the acetylated compound (1.0 eq.) in MeOH (3 mL) was slowly added solid NaOMe until pH ≥ 9. The reaction was stirred at r.t. for 3 h. DOWEX 50W×2 Resin (Fluka, 50-100 mesh, H⁺ Form) was added to neutralize the reaction until pH~6. Then, the reaction mixture was filtrated and concentrated in vacuum to afford the corresponding deprotected compound.

General protocol F for desilylation. TBAF (1.4 eq.) was added dropwise into a flask containing the trimethylsilylethynyl derivative (1.0 eq.) in MeOH (4 mL). The reaction was stirred at r.t. for 4 h. Then, the reaction was poured into water (50 mL), extracted with CH₂Cl₂ (4 ×50 mL). The combined organic layers were dried over Na₂SO₄. The solvent was evaporated and the residue was purified to afford the corresponding deprotected compound.

General protocol G for the synthesis of compounds 74-75 and 77-81. The protected compound (1.0 eq.) was solubilized with CH₂Cl₂ (0.5 mL). Then, 90% TFA (2.2 mL) was added dropwise. After addition, the reaction was stirred at r.t. overnight. MeOH (3 mL) and H₂O (5 mL) were then added into the reaction. The solvent was removed by evaporation and the residue was used directly for the reaction of next step. Aq. LiOH solution (1.2 eq. for each acetate group, in 1 mL of H₂O) was added dropwise into a solution of the residue solubilized in THF (2 mL) at r.t. After addition, the reaction mixture was stirred at r.t. for 2 h. Then, the reaction mixture was concentrated and the residue was purified by C18 reverse phase column chromatography (100% H₂O to 100% MeOH) to afford the corresponding deprotected compound.

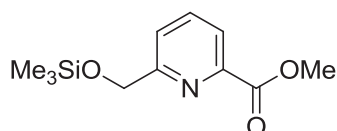
V.2 Synthesis and characterization



Methyl 6-(hydroxymethyl)picolinate (**2a**)²³⁰

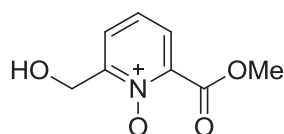
Sodium borohydride (390 mg, 10.3 mmol, 1.0 eq.) was slowly added at 0°C to a stirred solution of dimethyl pyridine-2,6-dicarboxylate (2.00 g, 10.3 mmol, 1.0 eq.) in MeOH/CH₂Cl₂ (100 mL, 7:3). The reaction mixture was stirred at room temperature for 3 h. Then, the reaction was neutralized by adding satd aq. NH₄Cl solution (40 mL). After extraction with CH₂Cl₂ (3×50 mL), the combined organic layers were dried (Na₂SO₄) and the solvent was evaporated. The resulting crude residue was purified by silica gel column chromatography (PE:EtOAc, 6:4 to 1:1) to afford compound **2a** as white solid (970 mg, 5.8 mmol, 56%). R_f= 0.16 (EtOAc:PE = 1:1); ¹H NMR (300 MHz, CDCl₃), δ (ppm): 8.04 (d, J = 7.8 Hz, 1H, H_{Pyr}), 7.85 (t, J = 7.8 Hz,

1H, H_{Pyr}), 7.53 (d, *J* = 7.8 Hz, 1H, H_{Pyr}), 4.86 (d, *J* = 5.3 Hz, 2H, OCH_{2a}), 4.00 (s, 3H, OMe), 3.41 (t, *J* = 5.3 Hz, 1H, OH).



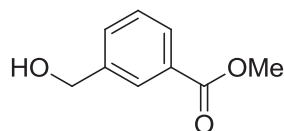
Methyl 6-(trimethylsilyloxymethyl)picolinate (2b)

Product isolated from glycosylation (**Entry 11**, see page 108). ¹H NMR (400 MHz, CDCl₃), δ (ppm): 7.99 (d, *J* = 7.7 Hz, 1H, H_{Pyr}), 7.84 (t, *J* = 7.7 Hz, 1H, H_{Pyr}), 7.72 (d, *J* = 7.7 Hz, 1H, H_{Pyr}), 4.89 (s, 2H, OCH₂), 3.98 (s, 3H, OMe), 0.17 (s, 9H, SiMe₃); ¹³C NMR (100 MHz, CDCl₃), δ (ppm): 166.0 (C=O), 162.0 (C_{Pyr}), 147.1 (C_{Pyr}), 137.7 (C_{PyrH}), 123.61 (C_{PyrH}), 123.55 (C_{PyrH}), 65.5 (OCH₂), 53.1 (OMe), -0.5 (s, 3C, SiMe₃); HRMS *m/z*: calcd. for C₁₁H₁₈NO₃Si, [M+H]⁺ 240.1050, found 240.1048; for C₁₁H₁₇NNaO₃Si, [M+Na]⁺ 262.0870, found 262.0864.



Methyl 6-(hydroxymethyl)picolinate N-oxide (2c)

Methyl 6-(hydroxymethyl)picolinate (**2a**) (200 mg, 1.2 mmol, 1.0 eq.) was dissolved in chloroform (4 mL) at 0°C. Then, *meta*-chloroperoxybenzoic acid (340 mg, 1.4 mmol, 1.2 eq.) was added. The reaction mixture was allowed to warm to r.t. and stirred overnight. The reaction was quenched with satd aq. Na₂S₂O₃ solution (10 mL) and the mixture was stirred for 2 h. Then, the mixture was extracted with CHCl₃ (11×20 mL). The organic phases were combined, dried (MgSO₄), filtered and concentrated to dryness. The resulting crude residue was purified by silica gel column chromatography (MeOH:CH₂Cl₂:CH₃COOH, 4:95.5:0.5) to afford compound **2c** as white needles (196 mg, 1.07 mmol, 89%). R_f = 0.29 (MeOH:CH₂Cl₂:CH₃COOH = 4:95.5:0.5); ¹H NMR (400 MHz, CDCl₃), δ (ppm): 7.58 (dd, *J* = 7.8, 2.0 Hz, 1H, H_{Py}), 7.48 (dd, *J* = 7.8, 2.0 Hz, 1H, H_{Py}), 7.35 (t, *J* = 7.8 Hz, 1H, H_{Py}), 4.82 (s, 2H, OCH₂), 4.01 (s, 3H, OMe); ¹³C NMR (100 MHz, CDCl₃), δ (ppm): 162.1 (C=O), 151.3 (C_{Pyr}), 141.8 (C_{Pyr}), 126.3 (C_{PyrH}), 126.0 (C_{PyrH}), 125.6 (C_{PyrH}), 61.4 (CH₂OH), 53.6 (OMe); HRMS *m/z*: calcd. for C₈H₉NNaO₄, [M+Na]⁺ 206.0424, found 206.0424.

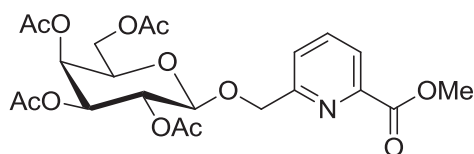


Methyl 3-hydroxymethylbenzoate (2d)²³¹

In a 3-necked 500 mL round-bottomed flask equipped with a mechanical stirrer was placed dimethyl isophthalate (20.00 g, 0.103 mol, 1.0 eq.) dissolved in acetone (200 mL). To this mixture was added dropwise over 20 min a solution of NaOH (4.33 g, 0.108 mol, 1.05 eq.) in MeOH (40 mL). The resulting milky suspension was stirred at r.t. overnight. Then, another portion of NaOH (0.433 g, 0.011 mol, 0.1 eq.) was added into the reaction and the suspension was stirred for another 5 h. The solvent was removed under vacuum and the white precipitate thus obtained was dissolved in water (400 mL). Concentrated HCl (15 mL) was added dropwise

until pH~1. Then, the suspension was filtered; the collected precipitate was washed with water (4×100 mL) and dried under vacuum at 65°C for 24 h to give white solid 18.25 g. The obtained monomethyl isophthalate was used directly without further purification.

In a 3-necked 500 mL round-bottomed flask equipped with a magnetic stirrer and a low temperature thermometer under a nitrogen atmosphere was placed monomethyl isophthalate (5.00 g, 0.027 mol, 1.0 eq.) dissolved in dry THF (125 mL). Then, this solution was placed in an ice-water bath and a solution of BH₃•SMe₂ (2M in THF, 70 mL, 0.14 mol, 5.0 eq.) was added dropwise over 90 min to maintain the temperature in the solution below 7°C. After another 15 min, the cooling bath was removed and the solution was allowed to reach ambient temperature. After 5 h, the reaction was carefully quenched (strong gas evolution) with small pieces of ice while cooling in an ice-water bath. When the gas evolution ceased, brine (50 mL) was added and the resulting mixture was extracted with diethyl ether (3×100 mL). The combined organic extracts were washed with diluted bleach (50 mL, original solution 9.6% bleach diluted 10 times), brine (50 mL) and dried (MgSO₄). The solvent was removed under vacuum to give an oil which contained a small amount of white precipitate. Diethyl ether (20 mL) was added and the solid was removed by filtration and washed with Et₂O (2×10 mL). The filtrate was concentrated to yield pale yellow oil (4.48 g). The crude oil was then purified by silica gel column chromatography (PE:EA, 4:1 to 7:3) to afford compound **2d** as colorless oil (3.77 g, 0.023 mmol, 85%). R_f= 0.17 (EtOAc:PE = 1:4); ¹H NMR (300 MHz, CDCl₃), δ (ppm): 8.00 (s, 1H, H_{Ar}), 7.93 (dd, *J* = 7.7, 1.4 Hz, 1H, H_{Ar}), 7.61 – 7.51 (m, 1H, H_{Ar}), 7.40 (t, *J* = 7.7 Hz, 1H, H_{Ar}), 4.71 (s, 2H, OCH₂), 3.89 (s, 3H, OMe).



(6-Methoxycarbonylpyrid-2-yl)methyl 2,3,4,6-tetra-*O*-acetyl-β-*D*-galactopyranoside (**3a**)

Entry 1, Table 2-2

Pure SnCl₄ (0.15 mL, 1.22 mmol, 5.0 eq.) was added dropwise (within 60 min – syringe pump) at 0°C (an ice/water bath) to a stirred solution of donor **1a** (143 mg, 0.366 mmol, 1.5 eq.), silver trifluoroacetate (135 mg, 0.61 mmol, 2.5 eq.) and methyl 6-(hydroxymethyl)picolinate (**2a**) (41 mg, 0.244 mmol, 1.0 eq.) in freshly distilled CH₂Cl₂ (4 mL). The reaction mixture was stirred at 0°C with protection of light for 48 h. Satd NaHCO₃ aq. solution (10 mL) was added into the reaction and the solution was vigorously stirred for 15 min. The suspension was filtered and the filtrate was extracted with CH₂Cl₂ (3×20 mL). The organic layers were combined, concentrated. No glycosylated product was observed.

Entry 2, Table 2-2

Distilled CH₂Cl₂ (5 mL) was added to a 10 mL Ar-flushed flask containing methyl 6-(hydroxymethyl)picolinate (**2a**) (61 mg, 0.366 mmol, 1.5 eq.), donor **1b** (100 mg, 0.244 mmol, 1.0 eq.) and AgOTf (94 mg, 0.366 mmol, 1.5 eq.) with protection of light. The reaction was stirred overnight at r.t.. The reaction mixture was diluted with CH₂Cl₂ (100 mL), filtered through celite. The organic phase was washed with satd aq. NaHCO₃ solution (50 mL) and brine (50 mL). The organic phase was dried (MgSO₄), filtered and concentrated. The residue

was purified by silica gel column chromatography (PE:EtOAc, 4:1 to 2:3) to afford compound **3a** as white foam (10 mg, 0.020 mmol, 8%).

Entry 3, Table 2-2

Distilled CH₂Cl₂ (5 mL) was added into a 10 mL Ar-flushed flask containing methyl 6-(hydroxymethyl)picolinate (**2a**) (41 mg, 0.244 mmol, 1.0 eq.), donor **1b** (250 mg, 0.61 mmol, 2.5 eq.) and AgOTf (94 mg, 0.366 mmol, 1.5 eq.). The reaction was stirred overnight at r.t. with protection of light. The reaction mixture was diluted with CH₂Cl₂ (100 mL), filtered through celite. The organic phase was washed with satd aq. NaHCO₃ solution (50 mL), brine (50 mL) and dried (MgSO₄), filtered and evaporated. The residue was purified by silica gel column chromatography (PE:EtOAc, 9:1 to 1:2) to afford compound **3a** as white foam (22 mg, 0.044 mmol, 18%).

Entry 4, Table 2-2

A solution of donor **1b** (150 mg, 0.366 mmol, 1.5 eq.) in anhydrous CH₂Cl₂ (1 mL) was added dropwise under argon with protection of light to a solution of methyl 6-(hydroxymethyl)picolinate (**2a**) (41 mg, 0.244 mmol, 1.0 eq.) and Hg(CN)₂ (246 mg, 0.978 mmol, 4.0 eq.) in dry CH₃CN (1 mL). The resulting mixture was vigorously stirred overnight. The reaction mixture was diluted with CH₂Cl₂ (5 mL) and filtered through celite. The solid was washed with CH₂Cl₂. The organic phase was washed with satd aq. NaHCO₃ solution (50 mL) and brine (50 mL). Then, the organic phase was dried (MgSO₄), filtered and concentrated. The residue was purified by silica gel column chromatography (PE:EtOAc, 9:1 to 3:2) to afford compound **3a** as white foam (13.5 mg, 0.027 mmol, 11%).

Entry 5, Table 2-2

Boron trifluoride etherate (62 μL, 0.488 mmol, 2.0 eq.) was added dropwise at -20°C to a stirred solution of methyl 6-(hydroxymethyl)picolinate (**2a**) (41 mg, 0.244 mmol, 1.0 eq.) and donor **1c** (180 mg, 0.366 mmol, 1.5 eq.) in freshly distilled CH₂Cl₂ (3 mL). The reaction mixture was stirred at -20°C for 2 h. Triethylamine (0.2 mL, 1.4 mmol, 5.7 eq.) was injected to quench the reaction. The reaction mixture was concentrated and the residue was purified by silica gel column chromatography (PE:EtOAc, 9:1 to 3:2) to afford compound **3a** as white foam (56 mg, 0.113 mmol, 46%).

Entry 6, Table 2-2

Distilled CH₂Cl₂ (3 mL) was added into a Ar-flushed flask containing methyl 6-(hydroxymethyl)picolinate (**2a**) (41 mg, 0.244 mmol, 1.0 eq.), donor **1c** (148 mg, 0.30 mmol, 1.25 eq.) and 4Å MS (200 mg – 300 mg). The reaction mixture was cooled down to -20°C. After 30 min, BF₃·Et₂O (62 μL, 0.488 mmol, 2.0 eq.) was introduced via a syringe. After 4 h, Et₃N (0.2 mL, 1.4 mmol, 5.7 eq.) was injected to quench the reaction. The reaction mixture was filtrated, the solid was washed with CH₂Cl₂, and the combined organic phases were concentrated. The residue was purified by silica gel column chromatography (PE:EtOAc, 9:1 to 3:2) to afford compound **3a** as white foam (42 mg, 0.085 mmol, 34%).

Entry 7, Table 2-2

A solution of donor **1c** (180 mg, 0.366 mmol, 1.5 eq.) in freshly distilled CH₂Cl₂ (1 mL) was added dropwise (within 60 min–syringe pump) at -20°C to a stirred solution of methyl

6-(hydroxymethyl)picolinate (**2a**) (41 mg, 0.244 mmol, 1.0 eq.) and $\text{BF}_3 \cdot \text{Et}_2\text{O}$ (62 μL , 0.488 mmol, 2.0 eq.) in freshly distilled CH_2Cl_2 (2 mL) at the presence of 4Å MS (200 mg – 300 mg). The reaction mixture was stirred overnight at -20°C . Triethylamine (0.2 mL, 1.4 mmol, 5.7 eq.) was injected to quench the reaction. The reaction mixture was filtered, the solid was washed with CH_2Cl_2 and the organic phase was concentrated. The residue was purified by silica gel column chromatography (PE:EtOAc, 9:1 to 3:2) to afford compound **3a** as white foam (40 mg, 0.080 mmol, 32%).

Entry 8, Table 2-2

Boron trifluoride etherate (62 μL , 0.488 mmol, 2.0 eq.) was added dropwise at -20°C to a stirred solution of methyl 6-(hydroxymethyl)picolinate (**2a**) (41 mg, 0.244 mmol, 1.0 eq.) and donor **1c** (180 mg, 0.366 mmol, 1.5 eq.) in freshly distilled CH_3CN (3 mL). The reaction mixture was stirred at -20°C for 2 h. Triethylamine (0.2 mL, 1.4 mmol, 5.7 eq.) was injected to quench the reaction. The reaction mixture was concentrated and the residue was purified by silica gel column chromatography (PE:EtOAc, 9:1 to 3:2) to afford compound **3a** as white foam (43 mg, 0.086 mmol, 36%).

Entry 9, Table 2-2

Boron trifluoride etherate (31 μL , 0.244 mmol, 2.0 eq.) was added dropwise at -20°C to a stirred solution of methyl 6-(hydroxymethyl)picolinate (**2a**) (61 mg, 0.366 mmol, 3.0 eq.) and donor **1c** (60 mg, 0.122 mmol, 1.0 eq.) in freshly distilled CH_2Cl_2 (3 mL). The reaction mixture was stirred at -20°C for 1.5 h. Another portion of $\text{BF}_3 \cdot \text{Et}_2\text{O}$ (31 μL , 0.244 mmol, 2.0 eq.) was added to the reaction at -20°C . After 1 h, Et_3N (0.2 mL, 1.4 mmol, 5.7 eq.) was injected to quench the reaction. The reaction mixture was filtered and the solid was washed with CH_2Cl_2 . The organic phase was concentrated. The desired glycosylated product was about 5%, estimated by TLC.

Entry 10, Table 2-2

Boron trifluoride etherate (62 μL , 0.488 mmol, 2.0 eq.) was added dropwise at -20°C to a stirred solution of methyl 6-(hydroxymethyl)picolinate (**2a**) (41 mg, 0.244 mmol, 1.0 eq.) and donor **1c** (362 mg, 0.732 mmol, 3.0 eq.) in freshly distilled CH_2Cl_2 (3 mL). The reaction mixture was stirred at -20°C for 2 h. Another portion of $\text{BF}_3 \cdot \text{Et}_2\text{O}$ (31 μL , 0.244 mmol, 1.0 eq.) was added to the reaction mixture, and stirring was maintained at -20°C for another 14 h. Triethylamine (0.2 mL, 1.4 mmol, 5.7 eq.) was injected to quench the reaction. The reaction mixture was concentrated and the residue was purified by silica gel column chromatography (PE:EtOAc, 9:1 to 1:1) to afford compound **3a** as white foam (51 mg, 0.103 mmol, 42%).

Entry 11, Table 2-2

Trimethylsilyl trifluoromethanesulfonate (23 μL , 0.122 mmol, 0.5 eq.) was added dropwise at -20°C to a stirred solution of donor **1c** (180 mg, 0.366 mmol, 1.5 eq.), methyl 6-(hydroxymethyl)picolinate **2a** (41 mg, 0.244 mmol, 1.0 eq.) and 4Å MS (200 mg – 300 mg) in freshly distilled CH_2Cl_2 (3 mL). The reaction was stirred at -20°C for 40 min. Triethylamine (0.2 mL, 1.4 mmol, 5.7 eq.) was injected at -20°C to quench the reaction. The reaction mixture was filtered and the solid was washed with CH_2Cl_2 . The solvent was evaporated, then, the residue was purified by silica gel column chromatography (PE:EtOAc, 9:1 to 6:4) to afford compound **3a** (~6 mg, 0.012 mmol, 5%). The main product was the silylated acceptor methyl 6-(trimethylsilyloxymethyl)picolinate (**2b**) (30 mg, 0.126 mmol, 51%).

Entry 12, Table 2-2

To a solution of methyl 6-(hydroxymethyl)picolinate (**2a**) (41 mg, 0.244 mmol, 1.0 eq.) in CH₂Cl₂ (2 mL) was added PhBF₂ (60 μL, 0.48 mmol, 2.0 eq.) at room temperature. The mixture was cooled to -78°C. A cooled solution (-78°C) of donor **1c** (240 mg, 0.488 mmol, 2.0 eq.) in CH₂Cl₂ (2 mL) was added into the reaction. The reaction was stirred at -78°C for 3 h then quenched with satd aq. NaHCO₃ solution (25 mL) and extracted with CH₂Cl₂. The organic layers were washed with H₂O and dried (MgSO₄). The solvent was evaporated, the residue was purified by silica gel column chromatography (PE:EtOAc, 9:1 to 1:1) to afford compound **3a** as white foam (19 mg, 0.038 mmol, 16%).

Entry 13, Table 2-2

To a solution of methyl 6-(hydroxymethyl)picolinate (**2a**) (41 mg, 0.244 mmol, 1.0 eq.) in CH₂Cl₂ (2 mL) was added PhBF₂ (60 μL, 0.48 mmol, 2.0 eq.) at room temperature. The mixture was cooled to -78°C. A cooled solution (-78°C) of donor **1c** (240 mg, 0.488 mmol, 2.0 eq.) in CH₂Cl₂ (1.5 mL) was added into the reaction mixture. Then, the reaction was stirred at -20°C for 2 h, quenched with satd aq. NaHCO₃ solution (30 mL) and extracted with CH₂Cl₂ (3×30 mL). The organic layers were washed with H₂O, dried (MgSO₄). The solvent was evaporated and the residue was purified by silica gel column chromatography (PE:EtOAc, 9:1 to 1:1) to afford compound **3a** as white foam (17 mg, 0.034 mmol, 14%).

Entry 14, Table 2-2

Boron trifluoride etherate (11.4 μL, 0.09 mmol, 1.0 eq.) was added dropwise at -20°C under argon to a stirred solution of methyl 6-(hydroxymethyl)picolinate (**2a**) (41 mg, 0.244 mmol, 1.0 eq.) and donor **1d** (190 mg, 0.366 mmol, 1.5 eq.) in freshly distilled CH₂Cl₂ (3 mL). The reaction mixture was stirred at -20°C for 2 h. Triethylamine (0.2 mL, 1.4 mmol, 5.7 eq.) was added into the reaction mixture at -20°C to quench the reaction. The reaction mixture was concentrated and the residue was purified by silica gel column chromatography (PE:EtOAc, 9:1 to 6:4) to afford compound **3a** as white foam (39 mg, 0.078 mmol, 32%).

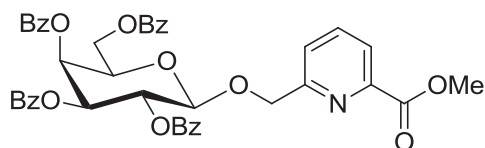
Entry 18, Table 2-3

Trimethylsilyl trifluoromethanesulfonate (9 μL, 0.05 mmol, 0.5 eq.) was added dropwise at -20°C to a stirred solution of donor **1c** (74 mg, 0.15 mmol, 1.5 eq.), methyl 6-(trimethylsilyloxymethyl)picolinate (**2b**) (24 mg, 0.1 mmol, 1.0 eq.) and 4Å MS (200 mg – 300 mg) in freshly distilled CH₂Cl₂ (3 mL). After 80 min., another portion of TMSOTf (9 μL, 0.05 mmol, 0.5 eq.) was added into the reaction. After another 100 min, the starting material **1c** was consumed. Triethylamine (0.2 mL, 1.4 mmol, 14.0 eq.) was injected at -20°C to quench the reaction. The reaction mixture was filtered and the solid was washed with CH₂Cl₂. The solvent was evaporated. The desired glycosylated compound **3a** was obtained in ~ 5% yield as estimated by TLC.

(6-Methoxycarbonylpyrid-2-yl)methyl 2,3,4,6-tetra-*O*-acetyl-β-D-galactopyranoside (**3a**)

R_f = 0.26 (PE:EtOAc = 1:2); [α]_D²⁰ = -14.0 (*c* = 0.5, CH₂Cl₂); ¹H NMR (400 MHz, CDCl₃), δ (ppm): 8.04 (d, *J* = 7.7 Hz, 1H, H_{pyr}), 7.86 (t, *J* = 7.7 Hz, 1H, H_{pyr}), 7.65 (d, *J* = 7.7 Hz, 1H, H_{pyr}), 5.41 (bd, *J* = 3.3 Hz, 1H, H₄), 5.34 (dd, *J* = 10.5, 7.9 Hz, 1H, H₂), 5.15 (d, *J* = 13.8 Hz, 1H, OCH_{2a}), 5.04 (dd, *J* = 10.5, 3.3 Hz, 1H, H₃), 4.86 (d, *J* = 13.8 Hz, 1H, OCH_{2b}), 4.65 (d, *J* = 7.9

Hz, 1H, H₁), 4.16 – 4.12 (m, 2H, H₆), 4.00 (s, 3H, OMe), 3.95 (dd, *J* = 6.4, 6.4 Hz, 1H, H₅), 2.16 (s, 3H, COCH₃), 2.05 (s, 6H, 2×COCH₃), 1.99 (s, 3H, COCH₃); ¹³C NMR (100 MHz, CDCl₃), δ (ppm): 170.6 (C=O), 170.4 (C=O), 170.2 (C=O), 169.7 (C=O), 165.7 (CO₂Me), 158.3 (C_{Pyr}), 147.2 (C_{Pyr}), 138.0 (C_{PyrH}), 124.6 (C_{PyrH}), 124.2 (C_{PyrH}), 101.2 (C₁), 71.8 (OCH₂), 71.1 (C₅), 70.9 (C₃), 69.0 (C₂), 67.2 (C₄), 61.6 (C₆), 53.2 (OMe), 20.9 (COCH₃), 20.8 (COCH₃), 20.8 (COCH₃), 20.7 (COCH₃); HRMS *m/z*: calcd. for C₂₂H₂₈NO₁₂, [M+H]⁺ 498.1606, found 498.1604.



(6-Methoxycarbonylpyrid-2-yl)methyl 2,3,4,6-tetra-O-benzoyl- β -D-galactopyranoside (3b)

Entry 15, Table 2-2

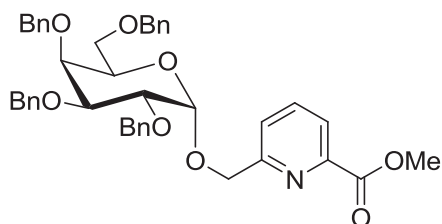
Donor **1e** (87 mg, 0.117 mmol, 1.3 eq.) was dissolved in freshly distilled CH₂Cl₂ (5 mL) under argon in the presence of 4Å MS (200 mg – 300 mg). Then, the mixture was cooled down to -20°C. Trimethylsilyl trifluoromethanesulfonate (3.3 μ L, 0.018 mmol, 0.2 eq.) was added at -20°C, then, methyl 6-(hydroxymethyl)picolinate (**2a**) (15 mg, 0.090 mmol, 1.0 eq.) dissolved in freshly distilled CH₂Cl₂ (1.5 mL) was added. The reaction mixture was stirred at -20°C for 30 min. Three news portions of TMSOTf were successively added (3.3 μ L, 0.018 mmol, 0.2 eq. after 1.5 h then 6.6 μ L, 0.039 mmol, 0.4 eq. after 2.5 h and 16.5 μ L, 0.090 mmol, 1.0 eq. after 4.5 h) and stirring was maintained for 16 h at -20°C. Triethylamine (0.2 mL, 1.4 mmol, 15.5 eq.) was injected at -20°C to quench the reaction. After filtration of the reaction mixture, the solid was washed with CH₂Cl₂. The solvent was evaporated and the residue was purified by silica gel column chromatography (PE:EtOAc, 9:1 to 7:3) to afford compound **3b** as white foam (22 mg, 0.030 mmol, 33%).

Entry 16, Table 2-2

Boron trifluoride etherate (11.4 μ L, 0.09 mmol, 1.0 eq.) was added dropwise at -20°C under argon to a stirred solution of methyl 6-(hydroxymethyl)picolinate (**2a**) (15 mg, 0.09 mmol, 1.0 eq.) and donor **1e** (87 mg, 0.117 mmol, 1.3 eq.) in freshly distilled CH₂Cl₂ (3 mL). The reaction mixture was stirred at -20°C for 1 h. Then, BF₃·Et₂O (11.4 μ L) was added again and after another 2 h, more BF₃·Et₂O (11.4 μ L) was added. After 17 h, Et₃N (0.2 mL, 1.4 mmol, 15.5 eq.) was added at -20°C into the reaction mixture to quench the reaction. The reaction mixture was concentrated and the residue was purified by silica gel column chromatography (PE:EtOAc, 9:1 to 7:3) to afford compound **3b** as white foam (28 mg, 0.038 mmol, 42%).

*R*_f = 0.21 (PE:EtOAc = 2:1); [α]_D²⁰ = +10.0 (*c* = 0.8, CH₂Cl₂); ¹H NMR (400 MHz, CDCl₃), δ (ppm) = 8.17 – 7.19 (m, 23H, H_{Ar}), 6.05 – 5.98 (m, 1H, H₄), 5.92 (dd, *J* = 8.4 Hz, 1H, H₂), 5.68 – 5.59 (m, 1H, H₃), 5.24 (d, *J* = 14.2 Hz, 1H, OCH_{2a}), 5.07 – 4.96 (m, 2H, H₁, OCH_{2b}), 4.64 (dd, *J* = 10.4, 5.9 Hz, 1H, H_{6a}), 4.44 (dd, *J* = 10.4, 4.8 Hz, 1H, H_{6b}), 4.38 (bd, *J* = 5.9 Hz, 1H, H₅), 3.99 (d, *J* = 1.5 Hz, 3H, OMe); ¹³C NMR (100 MHz, CDCl₃), δ (ppm) = 166.2 (C=O), 165.7 (C=O), 165.4 (C=O), 158.3 (C=O), 146.9 (C=O), 138.1, 133.8, 133.6, 133.5 (s, 2C), 130.2 (s, 2C), 129.92 (s, 4C), 129.89 (s, 2C), 128.8 (s, 2C), 128.63 (s, 2C), 128.58 (s, 2C), 128.4 (s, 2C),

125.1, 124.2, 101.6 (C₁), 72.0 (OCH₂), 71.7 (C₅), 71.6 (C₃), 69.9 (C₂), 68.2 (C₄), 62.2 (C₆), 53.2 (OMe); HRMS *m/z*: calcd. for C₄₂H₃₆NO₁₂, [M+H]⁺ 746.2232, found 746.2221.

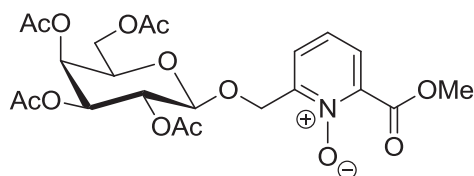


(6-Methoxycarbonylpyrid-2-yl)methyl 2,3,4,6-tetra-*O*-benzoyl- α -D-galactopyranoside (3c)

Entry 17, Table 2-2

In a dried round bottom flask containing donor **1f** (618 mg, 0.896 mmol, 1.0 eq.) and methyl 6-(hydroxymethyl)picolinate (**2a**) (164 mg, 0.896 mmol, 1.0 eq.) in CH₂Cl₂ (1 mL) was added methyl iodide (0.18 mL, 2.68 mmol, 3.0 eq.). Then, the reaction mixture was stirred at 50°C at presence of 4Å MS (200 mg – 300 mg). After 22 h, another portion of methyl iodide (0.09 mL, 1.34 mmol, 1.5 eq.) was added. After another 55 h, the reaction mixture was filtered through celite, washed with CH₂Cl₂ and evaporated to dryness. The residue was purified by silica gel column chromatography (PE:EtOAc, 4:1 to 3:1) to afford compound **3c** as white foam (463 mg, 0.672 mmol, 75%).

*R*_f = 0.24 (PE:EtOAc = 3:1); [α]_D²⁰ = +46.0 (*c* = 0.2, CH₂Cl₂); ¹H NMR (400 MHz, CDCl₃), δ (ppm): 8.01 (d, *J* = 7.4 Hz, 1H, H_{PyR}), 7.79 (d, *J* = 7.7 Hz, 1H, H_{PyR}), 7.71 (t, *J* = 7.7 Hz, 1H, H_{PyR}), 7.44 – 7.27 (m, 20H, H_{Ar}), 4.99 – 4.73 (m, 7H, H₁, OCH₂_{PyR}, 4×CH₂Ph), 4.67 (d, *J* = 11.9 Hz, 1H, CH₂Ph), 4.59 (d, *J* = 11.4 Hz, 1H, CH₂Ph), 4.43 (dd, *J* = 14.0, 11.7 Hz, 2H, 2× CH₂Ph), 4.13 (dd, *J* = 10.3, 3.1 Hz, 1H, H₂), 4.08 – 4.00 (m, 3H, H₃, H₄, H₅), 3.99 (s, 3H, OMe), 3.62 – 3.55 (m, 1H, H_{6a}), 3.48 (dd, *J* = 9.1, 5.5 Hz, 1H, H_{6b}); ¹³C NMR (100 MHz, CDCl₃), δ (ppm): 165.9 (CO₂Me), 159.2, 147.3, 138.84, 138.79, 138.7, 138.0 (C_{PyRH}), 137.8, 128.6 (s, 2C), 128.51 (s, 2C), 128.49 (s, 2C), 128.36 (s, 2C), 128.27 (s, 2C), 128.1 (s, 2C), 128.0 (s, 2C), 127.9, 127.8, 127.69, 127.65, 127.6 (s, 2C), 124.9 (C_{PyRH}), 124.0 (C_{PyRH}), 98.0 (C₁), 79.2 (C₃ or C₄ or C₅), 76.7 (C₂), 75.0 (s, 2C, C₃ or C₄ or C₅, OCH₂), 73.9 (OCH₂), 73.7 (OCH₂), 73.1 (OCH₂), 70.0 (OCH₂), 69.8 (C₃ or C₄ or C₅), 68.7 (C₆), 53.1 (OMe); HRMS *m/z*: calcd. for C₄₂H₄₄NO₈, [M+H]⁺ 690.3061, found 690.3052.



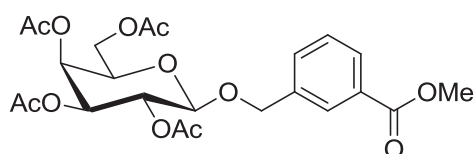
(6-Methoxycarbonylpyrid-2-yl)methyl 2,3,4,6-tetra-*O*-acetyl- β -D-galactopyranoside *N*-oxide (3d)

Entry 19, Table 2-3

Boron trifluoride etherate (24 μL, 0.03 mmol, 0.6 eq.) was added at -20°C to a stirred solution of methyl 6-(hydroxymethyl)picolinate *N*-oxide (**2c**) (56 mg, 0.31 mmol, 1.0 eq.) and donor **1c** (344 mg, 0.70 mmol, 2.25 eq.) in freshly distilled CH₂Cl₂ (3 mL). After 3 h, Et₃N (0.2 mL, 1.4 mmol, 4.5 eq.) was added at -20°C to quench the reaction. The reaction mixture was

concentrated and the residue was purified by silica gel column chromatography (PE:EtOAc, 1:1 to MeOH:EtOAc, 5:95) to afford 19 mg of a mixture containing the deactivated donor:unreacted acceptor **2c**: α anomer of **3d**: β anomer **3d** (1:1:0.46:1) as white foam (7% yield calculated for **3d**).

β anomer: $R_f = 0.23$ (PE:EtOAc = 1:3); $^1\text{H NMR}$ (400 MHz, CDCl_3), δ (ppm): 8.36 (dd, $J = 7.7, 1.1$ Hz, 1H, H_{Pyr}), 8.15 (dd, $J = 7.7, 1.1$ Hz, 1H, H_{Pyr}), 8.06 (t, $J = 7.7$ Hz, 1H, H_{Pyr}), 5.44 – 5.38 (m, 1H, H_4), 5.34 (dd, $J = 10.5, 7.9$ Hz, 1H, H_2), 5.19 – 5.13 (m, 1H, $\text{OCH}_{2\text{aPyr}}$), 5.10 – 5.04 (m, 1H, H_3), 4.87 (d, $J = 16.4$ Hz, 1H, $\text{OCH}_{2\text{bPyr}}$), 4.69 (d, $J = 7.9$ Hz, 1H, H_1), 4.17 – 4.12 (m, 2H, H_6), 4.07 (s, 3H, OMe), 4.02 – 3.93 (m, 1H, H_5), 2.19 – 1.96 (m, 12H, COCH_3); HRMS m/z : calcd. for $\text{C}_{22}\text{H}_{27}\text{NNaO}_{13}$, $[\text{M}+\text{H}]^+$ 536.1375, found 536.1350; MS m/z : $[\text{M}+\text{H}]^+$ 514.2, $[\text{M}+\text{Na}]^+$ 536.1.



(1-Methoxycarbonylbenz-3-yl)methyl 2,3,4,6-tetra-*O*-acetyl- β -D-galactoside (**3e**)

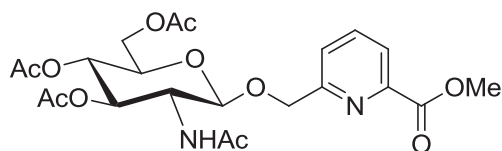
Entry 20, Table 2-3

Boron trifluoride etherate (7 μL , 0.056 mmol, 0.2 eq.) was added dropwise at -20°C under argon to a stirred solution of donor **1c** (209 mg, 0.424 mmol, 1.5 eq.) and methyl 3-hydroxymethylbenzoate (**2d**) (47 mg, 0.283 mmol, 1.0 eq.) in freshly distilled CH_2Cl_2 (3 mL). After 2 h, Et_3N (0.2 mL, 1.4 mmol, 4.9 eq.) was injected into the reaction mixture. Then, the solvent was evaporated, the residue was purified by silica gel column chromatography (PE:EtOAc, 5:1 to 3:1) to afford compound **3e** as a white foam (62 mg, 0.125 mmol, 44%) and acetylated acceptor (22 mg, 0.106 mmol, 37%).

Entry 21, Table 2-3

Boron trifluoride etherate (25 μL , 0.20 mmol, 0.2 eq.) was added dropwise at -20°C under argon to a stirred solution of donor **1c** (500 mg, 1.01 mmol, 1.0 eq.) and methyl 3-hydroxymethylbenzoate (**2d**) (503 mg, 3.03 mmol, 3.0 eq.) in freshly distilled CH_2Cl_2 (8 mL). After 1 h, Et_3N (0.2 mL, 1.4 mmol, 1.4 eq.) was injected into the reaction mixture. Then, the solvent was evaporated, the residue was purified by silica gel column chromatography (PE:EtOAc, 5:1 to 3:1) to afford compound **3e** as white foam (397 mg, 0.800 mmol, 79%).

$R_f = 0.27$ (PE:EtOAc = 2:1); $[\alpha]_{\text{D}}^{20} = -31.8$ ($c = 0.4$, CH_2Cl_2); $^1\text{H NMR}$ (400 MHz, CDCl_3), δ (ppm): 7.98 – 7.90 (m, 2H, 2 H_{Ar}), 7.46 (d, $J = 7.6$ Hz, 1H, H_{Ar}), 7.40 (t, $J = 7.6$ Hz, 1H, H_{Ar}), 5.36 (bd, $J = 3.4$ Hz, 1H, H_4), 5.26 (dd, $J = 10.4, 8.0$ Hz, 1H, H_2), 4.97 (dd, $J = 10.4, 3.4$ Hz, 1H, H_3), 4.91 (d, $J = 12.6$ Hz, 1H, $\text{OCH}_{2\text{aPh}}$), 4.65 (d, $J = 12.6$ Hz, 1H, $\text{OCH}_{2\text{bPh}}$), 4.51 (d, $J = 8.0$ Hz, 1H, H_1), 4.21 – 4.06 (m, 2H, H_6), 3.91 – 3.85 (m, 4H, OMe, H_5), 2.13 (s, 3H, COCH_3), 2.03 (s, 3H, COCH_3), 2.03 (s, 3H, COCH_3), 1.95 (s, 3H, COCH_3); $^{13}\text{C NMR}$ (100 MHz, CDCl_3), δ (ppm): 170.5 (C=O), 170.3 (C=O), 170.2 (C=O), 169.6 (C=O), 166.8 (COOMe), 137.3 (C_{Ar}), 132.2 ($\text{C}_{\text{Ar-H}}$), 130.4 (C_{Ar}), 129.2 ($\text{C}_{\text{Ar-H}}$), 128.70 ($\text{C}_{\text{Ar-H}}$), 128.65 ($\text{C}_{\text{Ar-H}}$), 100.0 (C_1), 70.9 (C_3), 70.8 (C_5), 70.1 (OCH_2), 68.8 (C_2), 67.1 (C_4), 61.3 (C_6), 52.2 (OMe), 20.7 (s, 3C, $3 \times \text{COCH}_3$), 20.6 (COCH_3); HRMS m/z : calcd. for $\text{C}_{23}\text{H}_{28}\text{NaO}_{12}$, $[\text{M}+\text{Na}]^+$ 519.1473, found 519.1466.



(6-Methoxycarbonylpyrid-2-yl)methyl 2-acetamido-3,4,6-tri-*O*-acetyl-2-deoxy-β-D-glucopyranoside (3f)

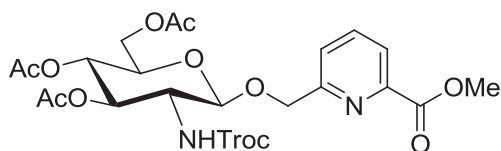
Entry 22, Table II-4

Methyl 6-(hydroxymethyl)picolinate (**2a**) (84 mg, 0.5 mmol, 1.0 eq.) and (1*R*)-(-)-camphorsulfonic acid (23.2 mg, 0.1 mmol, 0.2 eq.) were dissolved in freshly distilled CH₂Cl₂ (3 mL) containing activated 4Å molecular sieves. The mixture was stirred at r.t. for 30 min, after which donor **1g** (186 mg, 0.56 mmol, 1.1 eq.) in CH₂Cl₂ (1 mL) was added dropwise. Then, the reaction was stirred at 60°C in a sealed vessel. After 2 h, additional CSA (116 mg, 0.5 mmol, 1.0 eq.) was added into the reaction. After another 3.5 h, Et₃N (1 mL, 7 mmol, 14.0 eq.) was injected into the reaction mixture to quench the reaction. Then, the solvent was evaporated and the residue was purified by silica gel column chromatography (PE:EtOAc, 1:1 to EtOAc) to afford compound **3f** as white foam (41 mg, 0.083 mmol, 17%).

Entry 23, Table II-4

Donor **1g** (195 mg, 0.59 mmol, 1.5 eq.) and methyl 6-(hydroxymethyl)picolinate (**2a**) (66 mg, 0.39 mmol, 1.0 eq.) were dissolved in freshly distilled CH₂Cl₂ (3 mL) containing activated 4Å molecular sieves. The mixture was stirred at r.t. for 30 min, after which BF₃·Et₂O (50 μL, 0.39 mmol, 1.0 eq.) was added dropwise. After 2 h, additional BF₃·Et₂O (50 μL, 0.39 mmol, 1.0 eq.) was added into the reaction at r.t. After another 4 h, another portion of BF₃·Et₂O (50 μL, 0.39 mmol, 1.0 eq.) was added to the reaction at r.t. After 16 h, Et₃N (0.2 mL, 1.4 mmol, 3.6 eq.) was injected into the reaction mixture to quench the reaction. Then, the solvent was evaporated and the residue was purified by silica gel column chromatography (PE:EtOAc, 9:1 to 1:1) to afford compound **3f** as white foam (39 mg, 0.079 mmol, 20%).

$R_f = 0.18$ (PE:EtOAc = 1:2); $[\alpha]_D^{20} = +10.0$ ($c = 0.3$, CH₂Cl₂); ¹H NMR (400 MHz, CDCl₃), δ (ppm): 8.02 (d, $J = 7.8$ Hz, 1H, H_{pyr}), 7.83 (t, $J = 7.8$ Hz, 1H, H_{pyr}), 7.51 (d, $J = 7.8$ Hz, 1H, H_{pyr}), 6.56 (d, $J = 8.7$ Hz, 1H, NHAc), 5.22 – 4.84 (m, 5H, H₁, H₃, H₄, OCH₂_{pyr}), 4.27 – 4.16 (m, 2H, H₂, H_{6a}), 4.14 – 4.07 (m, 1H, H_{6b}), 3.69 (ddd, $J = 9.3, 4.6, 2.1$ Hz, 1H, H₅), 2.06 (s, 3H, COCH₃), 2.02 (s, 3H, COCH₃), 2.00 (s, 3H, COCH₃), 1.87 (s, 3H, COCH₃); ¹³C NMR (100 MHz, CDCl₃), δ (ppm): 171.1, 170.9, 170.6, 169.5, 165.6, 158.3, 147.0, 138.0 (C_{pyrH}), 124.8 (C_{pyrH}), 124.1 (C_{pyrH}), 101.3 (C₁), 73.2 (C₃ or C₄), 72.2 (C₅), 70.3 (OCH₂), 68.5 (C₃ or C₄), 62.2 (C₆), 54.2 (C₂), 53.1 (OMe), 23.2 (COCH₃), 20.9 (COCH₃), 20.8 (COCH₃), 20.7 (COCH₃); HRMS m/z : calcd. for C₂₂H₂₉N₂O₁₁, $[M+H]^+$ 497.1766, found 497.1756.



(6-Methoxycarbonylpyrid-2-yl)methyl 3,4,6-tri-*O*-acetyl-2-deoxy-2-trichloroethoxy-carbonylamino- β -D-glucopyranoside (3g**)**

Entry 24, Table II-4

Trimethylsilyl trifluoromethanesulfonate (54 μ L, 0.3 mmol, 1.0 eq.) was added dropwise at -20°C under argon to a stirred solution of methyl 6-(hydroxymethyl)picolinate (**2a**) (50 mg, 0.30 mmol, 1.0 eq.) and donor **1h** (172 mg, 0.33 mmol, 1.1 eq.) in freshly distilled CH_2Cl_2 (5 mL). After 1.5 h, additional TMSOTf (54 μ L, 0.3 mmol, 1.0 eq.) was added. After another 1 h, the reaction temperature was increased to 0°C . After another 2.5 h, more TMSOTf (54 μ L, 0.3 mmol, 1.0 eq.) was added into the reaction mixture at -20°C and the reaction mixture was stirred at -20°C for another 17 h. Then, Et_3N (0.2 mL, 1.4 mmol, 4.7 eq.) was injected into the reaction mixture at -20°C . The solvent was evaporated and the residue was purified by silica gel column chromatography (PE:EtOAc, 9:1 to 1:1) to afford compound **3g** as white foam (47 mg, 0.075 mmol, 25%).

Entry 25, Table II-4

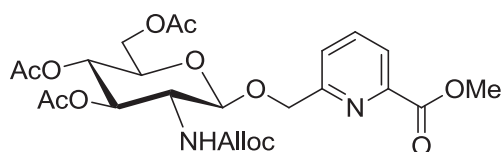
Trimethylsilyl trifluoromethanesulfonate (54 μ L, 0.3 mmol, 1.0 eq.) was added dropwise at -20°C under argon to a stirred solution of methyl 6-(hydroxymethyl)picolinate (**2a**) (50 mg, 0.30 mmol, 1.0 eq.) and donor **1i** (206 mg, 0.33 mmol, 1.1 eq.) in freshly distilled CH_2Cl_2 (3 mL). After 1 h, another fraction of donor **1i** (93 mg, 0.15 mmol, 0.5 eq.) and TMSOTf (54 μ L, 0.3 mmol, 1.0 eq.) were added to the reaction. After another 3.5 h, Et_3N (0.2 mL, 1.4 mmol, 4.7 eq.) was injected into the reaction mixture at -20°C to quench the reaction. Then, the solvent was evaporated, the residue was purified by silica gel column chromatography (PE:EtOAc, 9:1 to 1:1) to afford compound **3g** as white foam (90 mg, 0.143 mmol, 48%).

Entry 26, Table II-4

Boron trifluoride etherate (38 μ L, 0.3 mmol, 1.0 eq.) was added dropwise at -20°C under argon to a stirred solution of methyl 6-(hydroxymethyl)picolinate (**2a**) (50 mg, 0.30 mmol, 1.0 eq.) and donor **1i** (206 mg, 0.33 mmol, 1.1 eq.) in freshly distilled CH_2Cl_2 (3 mL). After 2 h, additional $\text{BF}_3 \cdot \text{Et}_2\text{O}$ (38 μ L, 0.3 mmol, 1.0 eq.) was added to the reaction. After another 1 h, Et_3N (0.2 mL, 1.4 mmol, 4.7 eq.) was injected into the reaction mixture at -20°C to quench the reaction. Then, the solvent was evaporated and the residue was purified by silica gel column chromatography (PE:EtOAc, 9:1 to 1:1) to afford compound **3g** as white foam (124 mg, 0.197 mmol, 66%).

$R_f = 0.32$ (PE:EtOAc = 1:1); $[\alpha]_D^{20} = -10.2$ ($c = 1.2$, CH_2Cl_2); $^1\text{H NMR}$ (400 MHz, CDCl_3), δ (ppm): 8.03 (d, $J = 7.8$ Hz, 1H, H_{pyr}), 7.82 (t, $J = 7.8$ Hz, 1H, H_{pyr}), 7.47 (d, $J = 7.8$ Hz, 1H, H_{pyr}), 6.34 (d, $J = 9.1$ Hz, 1H, NH), 5.25 – 5.19 (m, 1H, H_3), 5.12 (t, $J = 9.6$, 9.6 Hz, 1H, H_4), 5.06 – 5.03 (m, 2H, H_1 , OCH_{2a}), 4.92 (d, $J = 15.0$ Hz, 1H, OCH_{2b}), 4.70 – 4.57 (m, 2H, CH_2CCl_3), 4.26 (dd, $J = 12.3$, 4.9 Hz, 1H, H_{6a}), 4.15 – 4.12 (m, 1H, H_{6b}), 4.02 (s, 3H, OMe), 3.94 (dd, $J = 10.1$, 9.1 Hz, 1H, H_2), 3.72 (ddd, $J = 9.6$, 4.9, 2.2 Hz, 1H, H_5), 2.03 (s, 3H, COCH_3), 2.03 (s, 3H, COCH_3), 2.02 (s, 3H, COCH_3); $^{13}\text{C NMR}$ (100 MHz, CDCl_3), δ (ppm):

170.9 (C=O), 170.8 (C=O), 169.5 (C=O), 165.5 (C_{pyr}), 156.0 (C=O), 154.9 (C=O), 147.2 (C_{pyr}), 137.9 (C_{pyrH}), 124.6 (C_{pyrH}), 124.2 (C_{pyrH}), 101.5 (C₁), 95.6 (CCl₃), 74.5 (CH₂CCl₃), 72.9 (C₃), 72.3 (C₅), 70.3 (OCH₂), 68.5 (C₄), 62.2 (C₆), 56.3 (C₂), 53.2 (OMe), 20.9 (COCH₃), 20.8 (COCH₃), 20.7 (COCH₃); HRMS *m/z*: calcd. for C₂₃H₂₈Cl₃N₂O₁₂, [M+H]⁺ 629.0702, found 629.0697.



(6-Methoxycarbonylpyrid-2-yl)methyl 3,4,6-tri-*O*-acetyl-2-allyloxycarbonylamino-2-deoxy- β -D-glucopyranoside (3h**)**

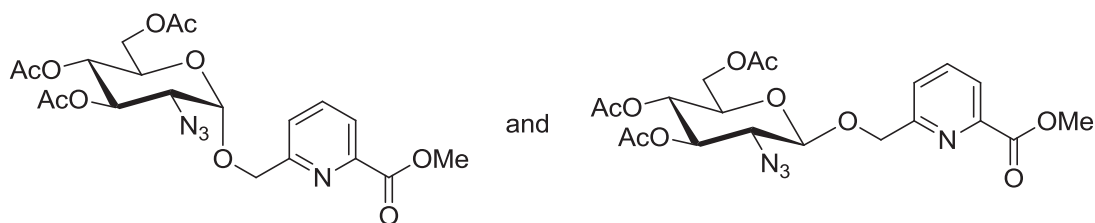
Entry 27, Table II-4

Trimethylsilyl trifluoromethanesulfonate (46 μ L, 0.244 mmol, 1.0 eq.) was added dropwise at -20°C to a stirred solution of methyl 6-(hydroxymethyl)picolinate (**2a**) (41 mg, 0.244 mmol, 1.0 eq.) and 1,3,4,6-tetra-*O*-acetyl-2-allyloxycarbonylamino-2-deoxy- α -D-glucopyranose (**1j**) (158 mg, 0.366 mmol, 1.5 eq.) in freshly distilled CH₂Cl₂ (3 mL). After 1 h, additional TMSOTf (46 μ L, 0.244 mmol, 1.0 eq.) was added to the reaction. After another 1 h, another portion of TMSOTf (46 μ L, 0.244 mmol, 1.0 eq.) was added to the reaction. After 1.5 h, the reaction temperature was increased to r.t. After another 15.5 h, Et₃N (0.2 mL, 1.4 mmol, 5.7 eq.) was injected into the reaction mixture. Then, the solvent was evaporated, the residue was purified by silica gel column chromatography (PE:EtOAc, 9:1 to 1:1) to afford compound **3h** as white foam (36 mg, 0.067 mmol, 27%).

Entry 28, Table II-4

Boron trifluoride etherate (76 μ L, 0.60 mmol, 2.0 eq.) was added dropwise at -20°C to a stirred solution of methyl 6-(hydroxymethyl)picolinate (**2a**) (50 mg, 0.30 mmol, 1.0 eq.) and 3,4,6-tri-*O*-acetyl-2-allyloxycarbonylamino-2-deoxy- α -D-glucopyranosyl trichloroacetimidate (**1k**) (176 mg, 0.33 mmol, 1.1 eq.) in freshly distilled CH₂Cl₂ (3 mL). After 1 h, additional BF₃·Et₂O (38 μ L, 0.30 mmol, 1.0 eq.) was added to the reaction. Then, the reaction mixture was stirred at -20°C. After 16 h, Et₃N (0.2 mL, 1.4 mmol, 4.7 eq.) was injected into the reaction mixture. The solvent was evaporated and the residue was purified by silica gel column chromatography (PE:EtOAc, 9:1 to 1:1) to afford compound **3h** as white foam (77 mg, 0.143 mmol, 48%) contaminated with 0.13 eq. of methyl 6-(hydroxymethyl)picolinate (**2a**).

R_f = 0.14 (PE:EtOAc = 1:1), ¹H NMR (300 MHz, CDCl₃), δ (ppm): 7.97 (d, *J* = 7.8 Hz, 1H, H_{pyr}), 7.78 (t, *J* = 7.8 Hz, 1H, H_{pyr}), 7.54 (d, *J* = 7.8 Hz, 1H, H_{pyr}), 5.87 – 5.71 (m, 1H, CH=CH₂), 5.60 (s, 1H, NH), 5.18 – 4.79 (m, 7H, H₁, H₃, H₄, OCH₂pyr, C=CH₂), 4.46 (s, 2H, COOCH₂), 4.21 (dd, *J* = 12.3, 5.0 Hz, 1H, H_{6a}), 4.06 (dd, *J* = 12.3, 2.0 Hz, 1H, H_{6b}), 3.94 (s, 3H, OMe), 3.88 – 3.75 (m, 1H, H₂), 3.68 (ddd, *J* = 9.7, 5.0, 2.0 Hz, 1H, H₅); HRMS *m/z*: calcd. for C₂₄H₃₁N₂O₁₂, [M+H]⁺ 539.1872, found 539.1862.



(6-Methoxycarbonylpyrid-2-yl)methyl 3,4,6-tri-*O*-acetyl-2-azido-2-deoxy- α -D-glucopyranoside (3i α**)**

(6-Methoxycarbonylpyrid-2-yl)methyl 3,4,6-tri-*O*-acetyl-2-azido-2-deoxy- β -D-glucopyranoside (3i β**)**

Entry 29, Table II-4

Trimethylsilyl trifluoromethanesulfonate (65 μ L, 0.36 mmol, 2.0 eq.) was added dropwise at -20°C under argon to a stirred solution of donor **11** (103 mg, 0.28 mmol, 1.5 eq.) and methyl 6-(hydroxymethyl)picolinate (**2a**) (30 mg, 0.18 mmol, 1.0 eq.) in freshly distilled CH_2Cl_2 (2 mL). After 2.5 h, another portion of TMSOTf (65 μ L, 0.36 mmol, 2.0 eq.) was added to the reaction and the reaction temperature was increased to r.t. After 16 h, Et_3N (0.2 mL, 1.4 mmol, 7.8 eq.) was injected into the reaction mixture. The yield of the desired product was about 5% as estimated by TLC and the major product of the reaction was the acetylated acceptor (53%).

Entry 30, Table II-4

Boron trifluoride etherate (61 μ L, 0.48 mmol, 2.0 eq.) was added dropwise at -20°C under argon to a stirred solution of donor **11** (133 mg, 0.36 mmol, 1.5 eq.) and methyl 6-(hydroxymethyl)picolinate (**2a**) (40 mg, 0.24 mmol, 1.0 eq.) in freshly distilled CH_2Cl_2 (2 mL). After 2.5 h, another portion of $\text{BF}_3 \cdot \text{Et}_2\text{O}$ (61 μ L, 0.48 mmol, 2.0 eq.) was added to the reaction and the reaction temperature was increased to r.t. After 16 h, Et_3N (0.2 mL, 1.4 mmol, 5.8 eq.) was injected into the reaction mixture. Then, the solvent was evaporated. The residue was purified by silica gel column chromatography (PE:EtOAc, 4:1 to 3:1) to afford compound **3i α** as white foam (40 mg, 0.08 mmol, 35%).

Entry 31, Table II-4

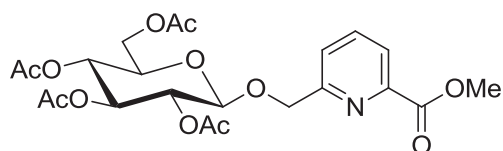
Trimethylsilyl trifluoromethanesulfonate (92 μ L, 0.48 mmol, 2.0 eq.) was added dropwise at -20°C under argon to a stirred solution of donor **1m** (171 mg, 0.36 mmol, 1.5 eq.) and methyl 6-(hydroxymethyl)picolinate (**2a**) (41 mg, 0.24 mmol, 1.0 eq.) in freshly distilled CH_2Cl_2 (2 mL). After 2 h, Et_3N (0.2 mL, 1.4 mmol, 5.8 eq.) was injected into the reaction mixture. Then, the solvent was evaporated. The residue was purified by silica gel column chromatography (PE:EtOAc, 4:1 to 2:1) to afford compound **3i α** as white foam (20 mg, 0.04 mmol, 17%).

Entry 32, Table II-4

Boron trifluoride etherate (62 μ L, 0.48 mmol, 2.0 eq.) was added dropwise at -20°C under argon to a stirred solution of donor **1m** (171 mg, 0.36 mmol, 1.5 eq.) and methyl 6-(hydroxymethyl)picolinate (**2a**) (41 mg, 0.24 mmol, 1.0 eq.) in freshly distilled CH_2Cl_2 (2 mL). After 2 h, another portion of $\text{BF}_3 \cdot \text{Et}_2\text{O}$ (62 μ L, 0.48 mmol, 2.0 eq.) was added to the reaction and the reaction temperature was increased to r.t. After 16 h, Et_3N (0.2 mL, 1.4 mmol, 5.8 eq.) was injected into the reaction mixture. Then, the solvent was evaporated. The residue

was purified by silica gel column chromatography (PE:EtOAc, 4:1 to 2:1) to afford compound **3i** as a α : β 72:28 mixture of anomers (95 mg, 0.20 mmol, 82%).

R_f = 0.38 (PE:EtOAc = 1:1); **α anomer** $[\alpha]_D^{20}$ = +126.9 (c = 1.0, CH₂Cl₂); ¹H NMR (400 MHz, CDCl₃), δ (ppm): 8.06 (d, J = 7.7 Hz, 1H, H_{pyr}), 7.91 (t, J = 7.7 Hz, 1H, H_{pyr}), 7.76 (d, J = 7.7 Hz, 1H, H_{pyr}), 5.53 (dd, J = 10.6, 9.3 Hz, 1H, H₃), 5.13 (d, J = 3.5 Hz, 1H, H₁), 5.10 – 5.03 (m, 1H, H₄), 4.99 (d, J = 13.9 Hz, 1H, OCH_{2aPyr}), 4.82 (d, J = 13.9 Hz, 1H, OCH_{2bPyr}), 4.31 – 4.24 (m, 1H, H_{6a}), 4.08 (ddd, J = 8.3, 4.4, 2.1 Hz, 1H, H₅), 4.02 (dd, J = 12.4, 2.1 Hz, 1H, H_{6b}), 3.47 (dd, J = 10.6, 3.5 Hz, 1H, H₂), 2.08 (s, 3H, COCH₃), 2.07 (s, 3H, COCH₃), 2.01 (s, 3H, COCH₃); ¹³C NMR (100 MHz, CDCl₃), δ (ppm): 170.7 (C=O), 170.2 (C=O), 169.7 (C=O), 165.5 (C_{Pyr}), 157.4 (C=O), 147.4 (C_{Pyr}), 138.3 (C_{PyrH}), 124.8 (C_{PyrH}), 124.4 (C_{PyrH}), 97.7 (C₁), 70.6 (s, 2C, C₃, OCH₂), 68.5 (C₄), 68.1 (C₅), 61.8 (C₆), 61.1 (C₂), 53.1 (OMe), 20.8 (COCH₃), 20.8 (COCH₃), 20.7 (COCH₃); **β anomer** $[\alpha]_D^{20}$ = -29.0 (c = 1.0, CH₂Cl₂); ¹H NMR (400 MHz, CDCl₃), δ (ppm): 8.06 (d, J = 7.8 Hz, 1H, H_{pyr}), 7.89 (t, J = 7.8 Hz, 1H, H_{pyr}), 7.75 (d, J = 7.8 Hz, 1H, H_{pyr}), 5.17 (d, J = 13.9 Hz, 1H, OCH_{2aPyr}), 5.03 – 4.88 (m, 3H, H₃, H₄, OCH_{2bPyr}), 4.55 (d, J = 8.1 Hz, 1H, H₁), 4.25 (dd, J = 12.3, 5.0 Hz, 1H, H_{6a}), 4.08 (dd, J = 12.3, 1.9 Hz, 1H, H_{6b}), 4.00 (s, 3H, OMe), 3.71 – 3.65 (m, 1H, H₅), 3.65 – 3.59 (m, 1H, H₂), 2.08 (s, 3H, COCH₃), 2.06 (s, 3H, COCH₃), 2.01 (s, 3H, COCH₃); ¹³C NMR (100 MHz, CDCl₃), δ (ppm): 170.7 (C=O), 170.1 (C=O), 169.8 (C=O), 165.6 (C_{Pyr}), 157.8 (C=O), 147.3 (C_{Pyr}), 138.1 (C_{PyrH}), 124.9 (C_{PyrH}), 124.4 (C_{PyrH}), 101.5 (C₁), 72.6 (C₃ or C₄), 72.2 (s, 2C, OCH₂, C₅), 68.4 (C₃ or C₄), 64.0 (C₂), 62.0 (C₆), 53.2 (OMe), 20.9 (COCH₃), 20.8 (COCH₃), 20.7 (COCH₃); HRMS m/z : calcd. for C₂₀H₂₄N₄NaO₁₀, $[M+Na]^+$ 503.1385, found 503.1362.



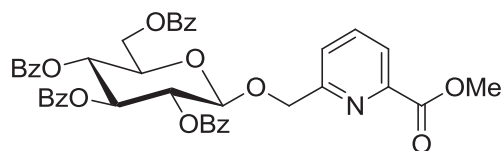
(6-Methoxycarbonylpyrid-2-yl)methyl 2,3,4,6-tetra-*O*-acetyl- β -D-glucopyranoside (**3j**)

Entry 33, Table 2-5

Boron trifluoride etherate (31 μ L, 0.244 mmol, 1.0 eq.) was added dropwise at -20°C under argon to a stirred solution of methyl 6-(hydroxymethyl)picolinate (**2a**) (41 mg, 0.244 mmol, 1.0 eq.) and donor **1n** (180 mg, 0.366 mmol, 1.5 eq.) in freshly distilled CH₂Cl₂ (3 mL). After addition, the reaction mixture was stirred at -20°C. After 1 h, another 1 eq. of BF₃·Et₂O (31 μ L) was added. After another 2 h, another 1.0 eq. of BF₃·Et₂O (31 μ L) was added. After 17 h, Et₃N (0.2 mL, 1.4 mmol, 5.7 eq.) was added at -20°C into the reaction mixture to quench the reaction. The reaction mixture was concentrated and the residue was purified by silica gel column chromatography (PE:EtOAc, 9:1 to 5:5) to afford compound **3j** as white foam (64 mg, 0.129 mmol, 53%).

R_f = 0.26 (PE:EtOAc = 1:1); $[\alpha]_D^{20}$ (c = 0.9, CH₂Cl₂) = -18.9; ¹H NMR (400 MHz, CDCl₃), δ (ppm): 8.01 (d, J = 7.7 Hz, 1H, H_{pyr}), 7.83 (t, J = 7.7 Hz, 1H, H_{pyr}), 7.59 (d, J = 7.7 Hz, 1H, H_{pyr}), 5.19 (dd, J = 9.4, 9.4 Hz, 1H, H₃), 5.14 – 5.03 (m, 3H, H₂, H₄, OCH_{2aPyr}), 4.83 (d, J = 14.0 Hz, 1H, OCH_{2bPyr}), 4.65 (d, J = 7.8 Hz, 1H, H₁), 4.21 (dd, J = 12.3, 4.9 Hz, 1H, H_{6a}), 4.07 (dd, J = 12.3, 1.6 Hz, 1H, H_{6b}), 3.96 (s, 3H, OMe), 3.74 – 3.67 (m, 1H, H₅), 2.03 (s, 3H, COCH₃), 2.00

(s, 3H, COCH₃), 1.99 (s, 3H, COCH₃), 1.98 (s, 3H, COCH₃); ¹³C NMR (100 MHz, CDCl₃), δ (ppm): 170.7 (C=O), 170.3 (C=O), 169.5 (C=O), 169.4 (C=O), 165.6 (C=O), 158.2 (C_{PyR}), 147.2 (C_{PyR}), 137.8 (C_{PyRH}), 124.6 (C_{PyRH}), 124.1 (C_{PyRH}), 100.6 (C₁), 72.7 (C₃), 72.0 (C₅), 71.8 (OCH₂PyR), 71.4 (C₂ or C₄), 68.4 (C₂ or C₄), 62.0 (C₆), 53.1 (OMe), 20.79 (COCH₃), 20.75 (COCH₃), 20.67 (COCH₃), 20.65 (COCH₃); HRMS *m/z*: calcd. for C₂₂H₂₈NO₁₂, [M+H]⁺ 498.1606, found 498.1604.

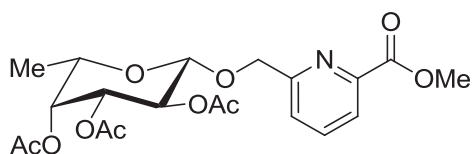


(6-Methoxycarbonylpyrid-2-yl)methyl 2,3,4,6-tetra-*O*-benzoyl- β -D-glucopyranoside (**3k**)

Entry 34, Table 2-5

Donor **1o** (87 mg, 0.117 mmol, 1.3 eq.) was dissolved in freshly distilled CH₂Cl₂ (5 mL) under argon at presence of 4Å MS (200 mg – 300 mg). Then, the mixture was cooled down to -20°C. TMSOTf (3.3 μ L, 0.018 mmol, 0.2 eq.) was added at -20°C, then, methyl 6-(hydroxymethyl)picolinate (**2a**) (15 mg, 0.09 mmol, 1.0 eq.) dissolved in freshly distilled CH₂Cl₂ (1.5 mL) was added. The reaction mixture was stirred at -20°C for 30 min. Another 3.3 μ L of TMSOTf was added. After 1 h, another portion of TMSOTf (3.3 μ L, 0.018 mmol, 0.2 eq.) was added. After 2.5 h, TMSOTf (6.6 μ L, 0.039 mmol, 0.4 eq.) was added. Then, after 2 h, another 1.0 eq. TMSOTf (16.5 μ L) was added and the reaction mixture was stirred at -20°C for another 16 h. Et₃N (0.2 mL, 1.4 mmol, 15.5) was injected at -20°C to quench the reaction. The reaction mixture was filtered and the solid was washed with CH₂Cl₂. The solvent was evaporated, then, the residue was purified by silica gel column chromatography (PE:EtOAc, 9:1 to 7:3) to afford compound **3k** as white foam (41 mg, 0.055 mmol, 61%) contaminated with 0.15 eq. of acceptor **2a**.

R_f = 0.29 (PE:EtOAc = 2:1); ¹H NMR (400 MHz, CDCl₃), δ (ppm): 7.98 – 7.15 (m, 23H, H_{Ar}), 5.85 (t, *J* = 9.7 Hz, 1H, H₃), 5.69 – 5.55 (m, 2H, H₂, H₄), 5.07 (d, *J* = 14.3 Hz, 1H, OCH_{2a}PyR), 4.94 (d, *J* = 7.8 Hz, 1H, H₁), 4.87 (d, *J* = 14.3 Hz, 1H, OCH_{2b}PyR), 4.55 (dd, *J* = 12.2, 2.9 Hz, 1H, H_{6a}), 4.41 (dd, *J* = 12.2, 5.2 Hz, 1H, H_{6b}), 4.16 – 4.08 (m, 1H, H₅), 3.90 (s, 3H, OMe); ¹³C NMR (100 MHz, CDCl₃), δ (ppm): 166.2, 165.9, 165.6, 165.3, 165.2, 158.3, 147.0, 137.7, 133.6, 133.5, 133.4, 133.3, 129.92, 129.91, 129.86, 129.6, 129.2, 128.82, 128.79, 128.53, 128.51, 128.4, 124.9, 124.1, 101.2 (C₁), 72.9, 72.5, 72.2, 72.0, 69.6, 63.1, 53.1; HRMS *m/z*: calcd. for C₄₂H₃₆NO₁₂, [M+H]⁺ 746.2232, found 746.2221.



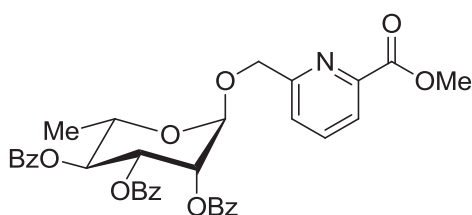
(6-Methoxycarbonylpyrid-2-yl)methyl 2,3,4-tri-*O*-acetyl- β -L-fucopyranoside (**3l**)

Entry 35, Table 2-5

Boron trifluoride etherate (62 μ L, 0.488 mmol, 2.0 eq.) was added dropwise at -20°C under argon into a stirred solution of methyl 6-(hydroxymethyl)picolinate (**2a**) (41 mg, 0.244 mmol, 1.0 eq.) and donor **1p** (159 mg, 0.366 mmol, 1.5 eq.) in freshly distilled CH₂Cl₂ (2 mL). After 2

h, Et₃N (0.2 mL, 1.4 mmol, 5.7 eq.) was injected into the reaction mixture. Then, the solvent was evaporated, the residue was purified by silica gel column chromatography (PE:EtOAc, 9:1 to 1:1) to afford compound **3l** as white foam (43 mg, 0.098 mmol, 39%).

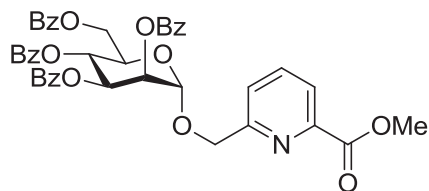
R_f = 0.34 (PE:EtOAc = 1:1); [α]_D²⁰ = +26.0 (*c* = 0.1, CH₂Cl₂); ¹H NMR (500 MHz, CDCl₃), δ (ppm): 8.03 (d, *J* = 7.8 Hz, 1H, H_{PyR}), 7.85 (t, *J* = 7.8 Hz, 1H, H_{PyR}), 7.64 (d, *J* = 7.8 Hz, 1H, H_{PyR}), 5.31 (dd, *J* = 10.4, 7.9 Hz, 1H, H₂), 5.24 (bd, *J* = 3.5 Hz, 1H, H₄), 5.14 (d, *J* = 14.1 Hz, 1H, OCH_{2aPyR}), 5.03 (dd, *J* = 10.4, 3.5 Hz, 1H, H₃), 4.85 (d, *J* = 14.1 Hz, 1H, OCH_{2bPyR}), 4.60 (d, *J* = 7.9 Hz, 1H, H₁), 3.99 (s, 3H, OMe), 3.83 (bd, *J* = 6.3 Hz, 1H, H₅), 2.18 (s, 3H, COCH₃), 2.03 (s, 3H, COCH₃), 1.98 (s, 3H, COCH₃), 1.21 (d, *J* = 6.3 Hz, 3H, H₆); ¹³C NMR (125 MHz, CDCl₃), δ (ppm): 170.9 (C=O), 170.4 (C=O), 169.9 (C=O), 165.8 (C_{PyR}), 158.6 (COOMe), 147.3 (C_{PyR}), 138.0 (C_{PyRH}), 124.7 (C_{PyRH}), 124.2 (C_{PyRH}), 100.9 (C₁), 71.6 (OCH₂), 71.4 (C₃), 70.4 (C₄), 69.6 (C₅), 69.2 (C₂), 53.2 (OMe), 21.1 (COCH₃), 20.93 (COCH₃), 20.86 (COCH₃), 16.2 (C₆); HRMS *m/z*: calcd. for C₂₀H₂₅NNaO₁₀, [M+Na]⁺ 462.1371, found 462.1352.



(6-Methoxycarbonylpyrid-2-yl)methyl 2,3,4-tri-*O*-benzoyl- α -L-rhamnopyranoside (**3m**)

Entry 36, Table 2-5

To a solution of donor **1q** (72 mg, 0.12 mmol, 1.3 eq.) in freshly distilled CH₂Cl₂ (5 mL) under argon at -20 °C was added 4 Å MS (200 mg – 300 mg) and TMSOTf (3.3 μL, 0.02 mmol, 0.2 eq.) and methyl 6-(hydroxymethyl)picolinate (**2a**) (15 mg, 0.09 mmol, 1.0 eq.) dissolved in CH₂Cl₂ (1.5 mL). The mixture was stirred at -20 °C for a total of 4 h and the addition of TMSOTf was according to the following: 3.3 μL (0.2 eq.) after 0.5 h, 3.3 μL (0.2 eq.) after 1.5 h and finally 3.3 μL (0.2 eq.) after 2.5 h. After 1.5 h, the reaction was complete, the reaction mixture was then warmed to room temperature and diluted with 30 mL CH₂Cl₂ and washed with satd aq. NaHCO₃ solution (2×25 mL). The aqueous layer was extracted with CH₂Cl₂ (2×25 mL) and the combined organic layers were washed with brine (25 mL), dried (Na₂SO₄) and concentrated. The crude product was purified by silica gel column chromatography (Hexane:EtOAc, 2:1) to afford compound **3m** as white foam (37 mg, 0.06 mmol, 66%). R_f = 0.31 (Hexane:EtOAc = 2:1); [α]_D²⁰ = +85.4 (*c* = 1.0, CH₂Cl₂); ¹H NMR (600 MHz, CDCl₃), δ (ppm): 8.15 – 7.20 (m, 18H, H_{Ar}), 5.91 (dd, *J* = 10.2, 3.5 Hz, 1H, H₃), 5.82 (dd, *J* = 3.5 Hz, 1.7 Hz, 1H, H₂), 5.73 (dd, *J* = 10.2, 9.8 Hz, 1H, H₄), 5.21 (d, *J* = 1.7 Hz, 1H, H₁), 5.11 (d, *J* = 14.0 Hz, 1H, OCH_{2aPyR}), 4.90 (d, *J* = 14.0 Hz, 1H, OCH_{2bPyR}), 4.26 (dd, *J* = 9.8, 6.2 Hz, 1H, H₅), 4.02 (s, 3 H, OMe), 1.38 (d, *J* = 6.2 Hz, H₆); ¹³C NMR (150 MHz, CDCl₃), δ (ppm): 165.9 (C=O), 165.9 (CO₂Me), 165.7 (C=O), 158.0 (C_{PyR}), 147.5 (C_{PyR}), 138.2 (C_{PyRH}), 133.7, 133.5, 133.3, 130.1, 129.8, 129.4, 129.3, 129.2, 128.7, 128.6, 128.4, 124.6 (C_{PyRH}), 124.3 (C_{PyRH}), 97.6 (C₁), 71.7 (C₄), 70.8 (C₂), 70.2 (OCH_{2PyR}), 70.1 (C₃), 67.3 (C₅), 53.2 (OMe), 17.8 (C₆); HRMS *m/z*: calcd. for C₃₅H₃₁NO₁₀Na, [M+Na]⁺ 648.1846, found 648.1862.



(6-Methoxycarbonylpyrid-2-yl)methyl 2,3,4,6-tetra-*O*-benzoyl- α -D-mannopyranoside (3n**)**

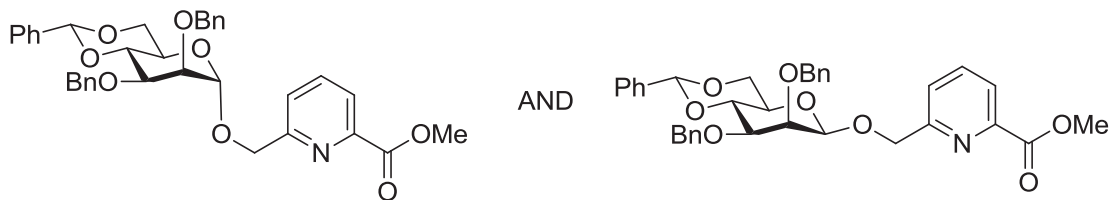
Entry 37, Table 2-5

To a solution of donor **1r** (173 mg, 0.23 mmol, 1.3 eq.) and methyl 6-(hydroxymethyl)picolinate (**2a**) (30 mg, 0.18 mmol, 1.0 eq.) in freshly distilled CH₂Cl₂ (10 mL) at -20°C was added BF₃·OEt₂ (6.5 μ L, 0.036, 0.2 eq.). The reaction was stirred for a total of 22.5 h, and the addition of BF₃·OEt₂ was according to the following: 6.5 μ L (0.2 eq.) after 1 h, 6.5 μ L (0.2 eq.) after 2.5 h, 13 μ L (0.4 eq.) after 4 h, and finally another 32.5 μ L (1.0 eq.) after 6.5 h, for a total of 2 equivalents. After 16 h, the reaction was complete, the reaction mixture was diluted with CH₂Cl₂ (25 mL) and washed with satd aq. NaHCO₃ solution (2×25 mL). The aqueous layer was extracted with CH₂Cl₂ (2×25 mL), after which the combined organic layers were washed with brine (30 mL), dried (Na₂SO₄) and concentrated. The crude product was purified by silica gel column chromatography (PE:EtOAc =2:1) to yield compound **3n** as white foam (64 mg, 0.086 mmol, 48%).

Entry 38, Table 2-5

To a solution of donor **1r** (173 mg, 0.23 mmol, 1.3 eq.) and methyl 6-(hydroxymethyl)picolinate (**2a**) (30 mg, 0.18 mmol, 1.0 eq.) in freshly distilled CH₂Cl₂ (10 mL) at -20°C was added TMSOTf (6.5 μ L, 0.036 mmol, 0.2 eq.). The reaction was stirred for a total of 22.5 h, and the addition of TMSOTf was according to the following: 6.5 μ L (0.2 eq.) after 0.5 h, 19.5 μ L (0.6 eq.) after 2 h, and finally another 33 μ L (1.0 eq.) after 5 h, for a total of 2 equivalents. After 17.5 h the reaction was complete, the reaction mixture was diluted with CH₂Cl₂ (25 mL) and washed with satd aq. NaHCO₃ solution (2×25 mL). The aqueous layer was extracted with CH₂Cl₂ (2×25 mL), after which the combined organic layers were washed with brine (30 mL), dried (Na₂SO₄) and concentrated. The crude product was purified by silica gel column chromatography (PE:EtOAc, 2:1) to yield compound **3n** as white foam (30 mg, 0.04 mmol, 22%).

$R_f = 0.27$ (PE:EtOAc = 2:1); $[\alpha]_D^{20} = -44.5$ ($c = 1.2$, CH₂Cl₂); ¹H NMR (400 MHz, CDCl₃), δ (ppm): 8.25 - 7.00 (m, 23H, H_{Ar}) 6.21 (dd, $J = 10.2, 10.1$ Hz, 1H, H₄), 6.01 (dd, $J = 10.2, 3.3$ Hz, 1H, H₃), 5.86 (dd, $J = 3.3, 1.8$ Hz, 1H, H₂), 5.32 (d, $J = 1.8$ Hz, 1H, H₁), 5.15 (d, $J = 13.7$ Hz, 1H, OCH_{2aPyr}) and 4.95 (d, $J = 13.7$ Hz, 1H, OCH_{2bPyr}), 4.70 (dd, $J = 12.2, 2.5$ Hz, 1H, H_{6a}), 4.51 (dd, $J = 12.2, 3.8$ Hz, 1H, H_{6b}), 4.55 (ddd, $J = 10.1, 3.8, 2.5$ Hz, 1H, H₅), 4.02 (s, 3H, OMe); ¹³C NMR (100 MHz, CDCl₃), δ (ppm): 166.3 (C=O_{Bz}), 165.7 (C=O_{Bz}), 165.6 (CO₂Me), 165.5 (s, 2C, 2×C=O_{Bz}), 157.6 (C_{Pyr}), 147.6 (C_{Pyr}), 138.3 (C_{PyrH}), 133.7, 122.6, 133.4, 133.2, 130.0, 129.9, 129.3, 128.7, 128.6, 128.5, 124.8 (C_{PyrH}), 124.5 (C_{PyrH}), 97.7 (C₁, ¹J_{C-1,H-1} = 172.4 Hz), 70.5 (OCH_{2Pyr}), 70.3 (C₂), 70.1 (C₃), 69.3 (C₅), 66.6 (C₄), 62.6 (C₆), 53.0 (OMe); HRMS m/z : calcd. for C₄₂H₃₆NO₁₂, [M+H]⁺ 746.2232, found 746.2203; C₄₂H₃₅NNaO₁₂, [M+Na]⁺ 768.2051, found 768.2014; C₄₂H₃₅NKO₁₂, [M+K]⁺ 784.1791, found 784.1772.



(6-Methoxycarbonylpyrid-2-yl)methyl 4,6-benzylidene-2,3-di-O-benzyl- α -D-mannopyranoside (3o α)

(6-Methoxycarbonylpyrid-2-yl)methyl 4,6-benzylidene-2,3-di-O-benzyl- β -D-mannopyranoside (3o β)

Entry 39, Table 2-5

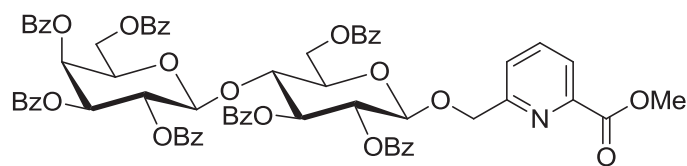
To a solution of donor **1s** (126 mg, 0.23 mmol, 1.3 eq.) and methyl 6-(hydroxymethyl)picolinate (**2a**) (30 mg, 0.18 mmol, 1.0 eq.) in freshly distilled CH_2Cl_2 (10 mL) was added at -40°C NIS (63 mg, 0.28 mmol, 1.56 eq.) and TMSOTf (6.5 μL , 0.036 mmol, 0.2 eq.). The reaction was stirred for a total of 5.5 h, and the addition of TMSOTf was according to the following: 6.5 μL (0.2 eq.) after 1 h, 19.5 μL (0.2 eq.) after 2 h, and finally another 33 μL (1.0 eq.) after 3 h, for a total of 2 equivalents. After 2.5 h the reaction was complete, the reaction was quenched by adding satd aq. NaHCO_3 solution (10 mL). The reaction mixture was diluted with CH_2Cl_2 (50 mL), warmed to room temperature and washed with satd aq. NaHCO_3 solution (2×50 mL). The aqueous layer was extracted with CH_2Cl_2 (2×50 mL), after which the combined organic layers were washed with brine (50 mL), dried (Na_2SO_4) and concentrated. The crude product was purified by silica gel column chromatography (PE:EtOAc, 2:1) to yield compound **3o β** as slightly yellow amorphous solid (73 mg, 0.12 mmol, 68%).

Entry 40, Table 2-5

A solution of donor **1s** (89 mg, 0.16 mmol, 1.0 eq.) in freshly distilled CH_2Cl_2 (5 mL) was cooled down to -60°C and BSP (39.2 mg, 0.19 mmol, 1.2 eq.), TTBP (58.1 mg, 0.24 mmol, 1.5 eq.) and Tf_2O (39 μL , 0.21 mmol, 1.3 eq.) were added. The mixture was stirred at -60°C for 15 min after which 1-octene (56 μL , 0.32 mmol, 2.0 eq.) was added and the reaction mixture was stirred for another 15 min after which the activation was complete (confirmed by TLC). The reaction mixture was cooled down to -78°C after which methyl 6-(hydroxymethyl)picolinate (**2a**) (30 mg, 0.18 mmol, 1.15 eq.) in freshly distilled CH_2Cl_2 (2 mL) was added. The reaction mixture was stirred at -78°C for 3 h and then quenched by adding $\text{P}(\text{OEt})_3$ (0.2 mL, 1.2 mmol, 7.5 eq.). The reaction mixture was diluted with CH_2Cl_2 (25 mL) and washed with satd aq. NaHCO_3 solution (25 mL). The water layer was extracted with CH_2Cl_2 (2×25 mL) and the combined organic layers were washed with brine (25 mL), dried (Na_2SO_4) and concentrated. The crude product was purified by silica gel column chromatography (hexane:EtOAc, 1:1) which yielded both anomers **3o** as slightly yellow amorphous solid in a α : β - 1:4.4 ratio (75 mg, 0.13 mmol, 80%).

α -anomer: $R_f = 0.50$ (Hexane:EtOAc = 1:1); $[\alpha]_D^{20} = +27.4$ ($c = 1.0$, CH_2Cl_2); $^1\text{H NMR}$: (600 MHz, CDCl_3), δ (ppm): 8.05 (dd, $J = 7.8$, 1.0 Hz, 1H, H_{Pyr}), 7.82 (t, $J = 7.8$ Hz, 1H, H_{Pyr}), 7.44 (dd, $J = 7.8$, 1.0 Hz, 1H, H_{Pyr}), 7.55 - 7.47 and 7.40 - 7.25 (m, 15 H, H_{Ar}), 5.66 (s, 4,6-O- CHPh), 4.95 (d, $J = 1.6$ Hz, 1H, H_1), 4.90 (d, $J = 13.7$ Hz, 1H, $\text{OCH}_{2\text{aPyr}}$), 4.87 (d, $J = 12.1$ Hz, 1H, $\text{OCH}_{2\text{Ph}}$), 4.84 (d, $J = 12.3$ Hz, 1H, $\text{OCH}_{2\text{Ph}}$), 4.75 (d, $J = 12.3$ Hz, 1H, $\text{OCH}_{2\text{Ph}}$), 4.69 (d, $J =$

13.7 Hz, 1H, OCH_{2bPyr}), 4.69 (d, $J = 12.1$ Hz, 1H, OCH_{2Ph}), 4.30 (dd, $J = 10.0, 9.4$ Hz, 1H, H₄), 4.22 (dd, $J = 10.3, 4.9$ Hz, 1H, H_{6a}), 4.04 (dd, $J = 10.0, 3.2$ Hz, 1H, H₃), 4.00 (s, 3H, OMe), 3.93 (dd, $J = 3.2, 1.6$ Hz, 1H, H₂), 3.89 (dd, $J = 10.4, 10.3$ Hz, 1H, H_{6b}), 3.84 (ddd, $J = 10.4, 9.4, 4.9$ Hz, 1H, H₅); ¹³C NMR: (150 MHz, CDCl₃), δ (ppm): 165.6 (CO₂Me), 158.0 (C_{Pyr}), 147.5 (C_{Pyr}), 137.8 (C_{PyrH}), 138.6, 138.0, 137.6, 134.6, 134.5, 130.7, 129.6, 129.4, 129.0, 128.8, 128.4, 128.3, 128.2, 128.1, 127.8, 127.6, 127.5, 126.5, 126.2, 126.2 (arom. C), 124.4 (C_{PyrH}) 124.1 (C_{PyrH}), 101.4 (4,6-OCH_{Ph}), 99.1 (C₁, ¹J_{C-1,H-1} = 171.5 Hz), 79.1 (C₄), 76.2 (s, 2C, C₂, C₃), 73.7 (OCH_{2Ph}), 73.3 (OCH_{2Ph}), 69.6 (OCH_{2Pyr}), 68.8 (C₆), 64.6 (C₅), 53.0 (OMe). **β -anomer**: R_f = 0.38 (Hexane:EtOAc = 1:1); [α]_D²⁰ = -111.1 ($c = 1.8$, CH₂Cl₂); ¹H NMR (400 MHz, CDCl₃), δ (ppm): 8.00 (dd, $J = 7.7, 1.0$ Hz, 1H, H_{Pyr}), 7.79 (dd, $J = 7.8, 7.7$ Hz, 1H, H_{Pyr}), 7.56 (dd, $J = 7.8, 1.0$ Hz, 1H, H_{Pyr}), 7.50 - 7.20 (m, 15 H, H_{Ar}), 5.58 (s, 1H, 4,6-OCH_{Ph}), 5.10 (d, $J = 13.9$ Hz, 1H, OCH_{2aPyr}), 4.97 (d, $J = 12.2$ Hz, 1H, OCH_{2Ph}), 4.90 (d, $J = 12.2$ Hz, 1H, OCH_{2Ph}), 4.82 (d, $J = 13.9$ Hz, 1H, OCH_{2bPyr}), 4.70 (d, $J = 12.4$ Hz, 1H, OCH_{2Ph}), 4.59 (d, $J = 12.4$ Hz, 1H, OCH_{2Ph}), 4.58 (bs, 1H, H₁), 4.24 (dd, $J = 10.5, 4.8$ Hz, 1H, H_{6a}), 4.21 (dd, $J = 9.9, 9.3$ Hz, 1H, H₄), 4.00 (bd, $J = 3.0$ Hz, 1H, H₂), 3.95 (s, 3H, OMe), 3.88 (dd, $J = 10.5, 10.1$ Hz, 1H, H_{6b}), 3.60 (dd, $J = 9.9, 3.0$ Hz, 1H, H₃), 3.32 (ddd, $J = 10.1, 9.3, 4.8$ Hz, 1H, H₅); ¹³C NMR (100 MHz, CDCl₃), δ (ppm): 165.6 (CO₂Me), 158.6 (C_{Pyr}), 147.2 (C_{Pyr}), 137.8 (C_{PyrH}), 138.4, 138.3, 137.6, 128.9, 128.7, 127.7, 127.6, 126.1, 124.7 (C_{PyrH}), 124.0 (C_{PyrH}), 101.8 (C₁, ¹J_{C-1,H-1} = 155.5 Hz), 101.5 (4,6-OCH_{Ph}), 78.7 (C₄), 78.0 (C₃), 76.1 (C₂), 75.0 (OCH_{2Ph}), 72.6 (OCH_{2Ph}), 72.0 (OCH_{2Pyr}), 68.2 (C₆), 67.7 (C₅), 53.0 (OMe); HRMS m/z : calcd. for C₃₅H₃₆NO₈, [M+H]⁺ 598.2441, found 598.2432; C₃₅H₃₅NO₈Na, [M+Na]⁺ 620.2260, found 620.2264; C₃₅H₃₅NO₈K, [M+K]⁺ 636.2000, found 636.2042.



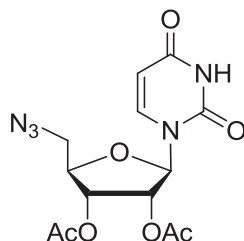
(6-Methoxycarbonylpyrid-2-yl)methyl 2,3,4,6,2',3',6'-hepta-O-benzoyl- β -D-lactopyranoside (3p)

Entry 41, Table 2-5

Boron trifluoride etherate (38 μ L, 0.30 mmol, 2.0 eq.) was added dropwise at -20°C to a stirred solution of methyl 6-(hydroxymethyl)picolinate (**2a**) (25 mg, 0.15 mmol, 1.0 eq.) and donor **1t** (175 mg, 0.15 mmol, 1.0 eq.) in freshly distilled CH₂Cl₂ (2 mL). After 4 h, Et₃N (0.2 mL, 1.4 mmol, 9.3 eq.) was injected into the reaction mixture at -20°C. Then, the solvent was evaporated, the residue was purified by silica gel column chromatography (PE:EtOAc, 7:3 to EtOAc) to afford compound **3p** as white foam (89 mg, 0.073 mmol, 51%).

R_f = 0.19 (PE:EtOAc = 2:1); [α]_D²⁰ = +28.1 ($c = 4.3$, CH₂Cl₂); ¹H NMR (400 MHz, CDCl₃), δ (ppm): 8.15 – 6.89 (m, 38H), 5.74 (t, $J = 9.5$ Hz, 1H), 5.78 – 5.60 (m, 2H), 5.51 (t, $J = 8.9$ Hz, 1H), 5.31 (dd, $J = 10.3, 2.9$ Hz, 1H), 4.97 (d, $J = 14.3$ Hz, 1H, OCH_{2aPyr}), 4.84 – 4.71 (m, 3H, OCH_{2bPyr}, H₁, H_{1'}), 4.52 – 4.36 (m, 2H), 4.21 (t, $J = 9.5, 9.5$ Hz, 1H), 3.85 (s, 3H, OMe), 3.83 – 3.74 (m, 2H), 3.70 – 3.60 (m, 2H); ¹³C NMR (100 MHz, CDCl₃), δ (ppm): 165.9, 165.6, 165.53, 165.45, 165.41, 165.3 (s, 2C), 164.9, 158.2, 146.9, 137.6, 133.6 - 133.3 (m, 7C), 130.0 - 128.3 (m, 32C), 124.7, 124.0, 101.0 (C₁ or C_{1'}), 100.9 (C₁ or C_{1'}), 76.0, 73.2, 72.8, 72.0, 71.8, 71.8,

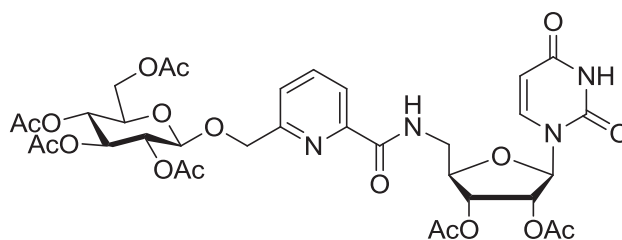
71.4, 69.9, 67.5, 62.3, 61.1, 53.0; HRMS m/z : calcd. for $C_{69}H_{58}NO_{20}$, $[M+H]^+$ 1220.3547, found 1220.3499.



2',3'-Di-*O*-acetyl-5'-azido-5'-deoxy-uridine (**5**)²³²

To a stirred mixture of uridine (5 g, 20.5 mmol, 1.0 eq.), triphenylphosphine (8.056 g, 30.7 mmol, 1.5 eq.), NaN_3 (61.5 mmol, 4.0 g, 3.0 eq.) and tetrabutylammonium iodide (1.515 g, 4.1 mmol, 0.2 eq.) in DMF (50 mL) was added carbon tetrabromide (10.2 g, 30.75 mmol, 1.5 eq.) and the resulting mixture was stirred at r.t. overnight. Then, the reaction mixture was co-evaporated with toluene (15×40 mL) and the residue was purified by silica gel column chromatography (EtOAc to MeOH:EtOAc = 5:95) to afford 5'-azido-5'-deoxy-uridine (5.22 g, 19.4 mmol, 95%). R_f = 0.45 (MeOH: CH_2Cl_2 , 1:9); 1H NMR (300 MHz, D_2O) δ (ppm) = 7.81 (d, J = 8.1 Hz, 1H, H_{6Uri}), 5.93 – 5.85 (m, 2H, H_{5Uri} , H_{1Rib}), 4.43 (t, J = 4.9 Hz, 1H), 4.27 (t, J = 5.6 Hz, 1H), 4.21 (dd, J = 8.6, 5.0 Hz, 1H), 3.81 (dd, J = 13.7, 3.1 Hz, 1H, H_{5aRib}), 3.68 (dd, J = 13.7, 4.9 Hz, 1H, H_{5bRib}).

In a flask containing the crude 5'-azido-5'-deoxy-uridine (232 mg, 0.86 mmol, 1 eq.) in pyridine (7 mL) was added Ac_2O (2 mL). After addition, the reaction mixture was stirred at r.t. overnight under argon. Then, the reaction mixture was poured into satd aq. $NaHCO_3$ solution (100 mL) and extracted by EtOAc (3×100 mL). The organic phase was washed with 1N HCl (2×100 mL) and brine (2×100 mL), dried (Na_2SO_4) and evaporated. The residue was purified by silica gel column chromatography (PE:EtOAc = 1:1) to afford compound **5** as white foam (251mg, 0.71 mmol, 83%). R_f = 0.13 (PE: EtOAc, 1:1); 1H NMR (300 MHz, $CDCl_3$) δ (ppm) = 9.39 (s, 1H, NH_{Uri}), 7.49 (d, J = 8.2 Hz, 1H), 6.08 (dd, J = 3.6, 2.1 Hz, 1H), 5.83 (dd, J = 8.1, 2.1 Hz, 1H), 5.36 – 5.27 (m, 2H), 4.21 (dd, J = 3.0, 3.1 Hz, 1H), 3.79 (dd, J = 13.7, 3.1 Hz, 1H), 3.66 (dd, J = 13.7, 4.9 Hz, 1H), 2.12 (s, 3H, $COCH_3$), 2.09 (s, 3H, $COCH_3$).



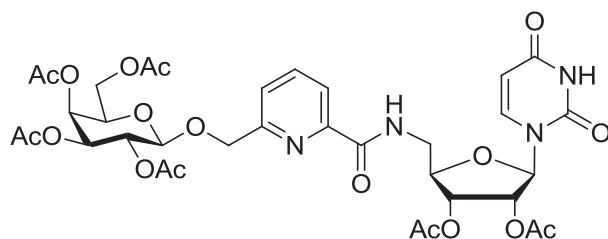
6-(2,3,4,6-Tetra-*O*-acetyl- β -D-glucopyranosyloxymethyl)-*N*-(2',3'-di-*O*-acetyl-uridin-5'-yl)picolinamide (**6-Glc**) (Adapted from Ref.²³³)

(**Pathway A**) A mixture of compound **3j-Glc** (150 mg, 0.3 mmol, 1.0 eq.) and NaI (285 mg, 1.9 mmol, 6.3 eq.) in dry pyridine (5 mL) was stirred at 120°C under an argon atmosphere. After 5 h, the reaction was finished. Pyridine was evaporated and the residue was co-evaporated with toluene (3×15 mL). The residue was solubilized with $CHCl_3$ (10 mL), filtered through celite, washed with $CHCl_3$, dried over Na_2SO_4 . Then, the solvent was evaporated and the residue was purified by silica gel column chromatography (PE:EtOAc = 1:1 to EtOH) to afford compound **4-Glc** (75 mg, 0.155 mmol, 52%).

Then, following the general protocol **A**, compound **6-Glc** was prepared from compound **4-Glc** (60 mg, 0.124 mmol, 1.0 eq.) and compound **5** (66 mg, 0.186 mmol, 1.5 eq.). The crude product was purified by silica gel column chromatography (100% PE to 100% EtOAc) to afford compound **6-Glc** as white foam (60 mg, 0.076 mmol, 61%).

(**Pathway B**) $\text{BF}_3 \cdot \text{Et}_2\text{O}$ (20 μL , 0.164 mmol, 1.0 eq.) was added dropwise to a stirred solution of 6-(hydroxymethyl)-*N*-(2',3'-di-*O*-acetyl-uridin-5'-yl)picolinamide (**10**) (76 mg, 0.164 mmol, 1.0 eq.) and 2,3,4,6-tetra-*O*-acetyl- α -D-glucopyranosyl trichloroacetimidate (**1n-Glc**) (121 mg, 0.246 mmol, 1.5 eq.) in freshly distilled CH_2Cl_2 (3 mL) at -20°C . After 1 h, the reaction temperature was increased to 0°C . After another 1 h, another portion of $\text{BF}_3 \cdot \text{Et}_2\text{O}$ (20 μL , 0.164 mmol, 1.0 eq.) was added into the reaction and 1 mL freshly distilled MeCN and 1 mL freshly distilled THF were added into the reaction for solubility reason. Then, the reaction mixture was stirred at r.t. for 16 h. Et_3N (0.2 mL, 1.44 mmol, 8.8 eq.) was injected to quench the reaction. Then, the reaction mixture was concentrated and the residue was purified by silica gel column chromatography (PE:EtOAc = 9:1 to PE:EtOAc = 1:9) to afford compound **6-Glc** as white foam (43 mg, 0.054 mmol, 33%).

$R_f = 0.45(\text{EtOAc})$; $[\alpha]_{\text{D}}^{20} = +2.7$ ($c = 1.1$, CH_2Cl_2); $^1\text{H NMR}$ (400 MHz, CDCl_3) δ (ppm) = 9.17 (s, 1H, NH_{Uri}), 8.35 (t, $J = 6.0$ Hz, 1H, NHCO), 8.08 (d, $J = 7.7$ Hz, 1H, H_{Pyr}), 7.86 (t, $J = 7.7$ Hz, 1H, H_{Pyr}), 7.53 (d, $J = 7.7$ Hz, 1H, H_{Pyr}), 7.33 (d, $J = 8.1$ Hz, 1H, $\text{H}_{6\text{Uri}}$), 5.79 (d, $J = 4.4$ Hz, 1H, $\text{H}_{1\text{Rib}}$), 5.72 (d, $J = 8.1$ Hz, 1H, $\text{H}_{5\text{Uri}}$), 5.42 (dd, $J = 6.2, 4.4$ Hz, 1H, $\text{H}_{2\text{Rib}}$), 5.33 (bd, $J = 6.2$ Hz, 1H, $\text{H}_{3\text{Rib}}$), 5.25 (t, $J = 9.5$ Hz, 1H, $\text{H}_{3\text{Glc}}$), 5.16 – 5.08 (m, 2H, $\text{H}_{2\text{Glc}}$, $\text{H}_{4\text{Glc}}$), 4.97 (d, $J = 13.6$ Hz, 1H, $\text{OCH}_{2\text{a}}$), 4.80 – 4.70 (m, 2H, $\text{OCH}_{2\text{b}}$, $\text{H}_{1\text{Glc}}$), 4.28 – 4.34 (m, $\text{H}_{4\text{Rib}}$), 4.25 (dd, $J = 12.4, 4.3$ Hz, 1H, $\text{H}_{5\text{aRib}}$), 4.17 (dd, $J = 12.4, 2.2$ Hz, 1H, $\text{H}_{5\text{bRib}}$), 3.91 – 3.75 (m, 3H, $\text{H}_{5\text{Glc}}$, $\text{H}_{6\text{aGlc}}$, $\text{H}_{6\text{bGlc}}$), 2.08 (s, 3H, COCH_3), 2.08 (s, 3H, COCH_3), 2.05 (s, 3H, COCH_3), 2.01 (s, 3H, COCH_3), 2.01 (s, 3H, COCH_3), 2.00 (s, 3H, COCH_3); $^{13}\text{C NMR}$ (100 MHz, CDCl_3) δ (ppm) = 170.8 (COCH_3), 170.4 (COCH_3), 169.8 (COCH_3), 169.8 (COCH_3), 169.6 (COCH_3), 169.5 (COCH_3), 164.8 (NHCO), 162.9 ($\text{C}=\text{O}_{\text{Uri}}$), 156.3 (C_{Pyr}), 150.1 ($\text{C}=\text{O}_{\text{Uri}}$), 148.6 (C_{Pyr}), 141.0 ($\text{C}_{6\text{Uri}}$), 138.4 (C_{PyrH}), 124.4 (C_{PyrH}), 121.5 (C_{PyrH}), 103.3 ($\text{C}_{5\text{Uri}}$), 100.3 ($\text{C}_{1\text{Glc}}$), 90.0 ($\text{C}_{1\text{Rib}}$), 80.2 ($\text{C}_{4\text{Rib}}$), 73.1 ($\text{C}_{2\text{Rib}}$), 72.7 ($\text{C}_{3\text{Glc}}$), 72.0 ($\text{C}_{5\text{Glc}}$), 71.4 ($\text{C}_{2\text{Glc}}$ or $\text{C}_{4\text{Glc}}$), 71.3 (OCH_2), 70.6 ($\text{C}_{3\text{Rib}}$), 68.4 ($\text{C}_{2\text{Glc}}$ or $\text{C}_{4\text{Glc}}$), 61.8 ($\text{C}_{6\text{Glc}}$), 40.3 ($\text{C}_{5\text{Rib}}$), 20.85 (COCH_3), 20.79 (COCH_3), 20.73 (COCH_3), 20.70 (COCH_3), 20.58 (COCH_3), 20.56 (COCH_3); HRMS m/z : calcd. for $\text{C}_{34}\text{H}_{41}\text{N}_4\text{O}_{18}$, $[\text{M}+\text{H}]^+$ 793.2410, found 793.2390.

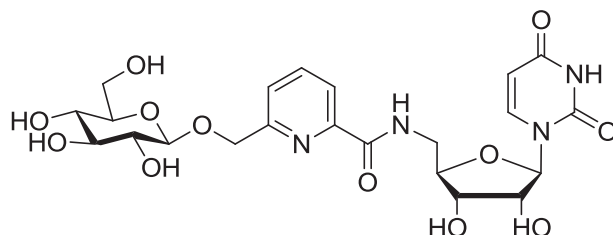


6-(2,3,4,6-Tetra-*O*-acetyl- β -D-galactopyranosyloxymethyl)-*N*-(2',3'-di-*O*-acetyl-uridin-5'-yl)picolinamide (**6-Gal**)

A mixture of methyl 6-(2,3,4,6-tetra-*O*-acetyl- β -D-galactopyranosyloxymethyl)picolinate (**3a-Gal**) (305 mg, 0.61 mmol, 1.0 eq.) and NaI (562 mg, 3.75 mmol, 6.1 eq.) in dry pyridine (9.5 mL) was stirred at 120°C under an argon atmosphere. After 5 h, the reaction was finished. Pyridine was evaporated and the residue was co-evaporated with toluene (3×15 mL). The residue was solubilized with CHCl_3 (10 mL), filtered through celite, washed with CHCl_3 , dried over Na_2SO_4 . Then, the solvent was evaporated and the residue was purified by silica gel

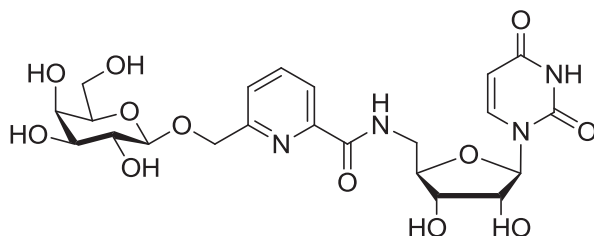
column chromatography (PE:EtOAc = 1:1 to 100% EtOH) to afford compound **4-Gal** (225 mg, 0.466 mmol, 76%).

Then, following the general protocol **A**, compound **6-Gal** was prepared from compound **4-Gal** (225 mg, 0.466 mmol, 1.0 eq.) and compound **5** (247 mg, 0.699 mmol, 1.5 eq.). The crude product was purified by silica gel column chromatography (100% PE to 100% EtOAc) to afford compound **6-Gal** as white foam (116 mg, 0.147 mmol, 31%). $R_f = 0.14$ (PE:EtOAc, 1:4); $[\alpha]_D^{20} = +3.7$ ($c = 0.9$, CH_2Cl_2); $^1\text{H NMR}$ (400 MHz, CDCl_3) δ (ppm) = 9.03 (s, 1H, NH_{Uri}), 8.38 (t, $J = 6.2$ Hz, 1H, NHCO), 8.09 (d, $J = 7.5$ Hz, 1H, H_{Pyr}), 7.86 (t, $J = 7.5$ Hz, 1H, H_{Pyr}), 7.55 (d, $J = 7.5$ Hz, 1H, H_{Pyr}), 7.34 (d, $J = 8.1$ Hz, 1H, $\text{H}_{6\text{Uri}}$), 5.81 (d, $J = 4.4$ Hz, 1H, $\text{H}_{1\text{Rib}}$), 5.73 (dd, $J = 8.1, 2.0$ Hz, 1H, $\text{H}_{5\text{Uri}}$), 5.41 (dd, $J = 6.3, 4.3$ Hz, 2H), 5.36 – 5.30 (m, 2H), 5.09 (dd, $J = 10.5, 3.4$ Hz, 1H), 4.99 (d, $J = 13.6$ Hz, 1H, OCH_{2a}), 4.77 (d, $J = 13.6$ Hz, 1H, OCH_{2b}), 4.73 (d, $J = 8.0$ Hz, 1H, $\text{H}_{1\text{Gal}}$), 4.32 (dd, $J = 10.2, 5.8$ Hz, 1H, $\text{H}_{4\text{Rib}}$), 4.22 – 4.10 (m, 2H, $\text{H}_{6a\text{Gal}}, \text{H}_{6b\text{Gal}}$), 4.98 – 4.02 (m, 1H, $\text{H}_{5\text{Gal}}$), 3.92 – 3.77 (m, 2H, $\text{H}_{5a\text{Rib}}, \text{H}_{5b\text{Rib}}$), 2.16 (s, 3H, COCH_3), 2.09 (s, 3H, COCH_3), 2.08 (s, 3H, COCH_3), 2.03 (s, 3H, COCH_3), 2.02 (s, 3H, COCH_3), 1.99 (s, 3H, COCH_3); $^{13}\text{C NMR}$ (100 MHz, CDCl_3) δ (ppm) = 170.6 (COCH_3), 170.4 (COCH_3), 170.3 (COCH_3), 169.84 (COCH_3), 169.83 (COCH_3), 169.76 (COCH_3), 164.9 (NHCO), 162.8 ($\text{C}=\text{O}_{\text{Uri}}$), 156.4 (C_{Pyr}), 150.1 ($\text{C}=\text{O}_{\text{Uri}}$), 148.6 (C_{Pyr}), 140.9 ($\text{C}_{6\text{Uri}}$), 138.4 (C_{PyrH}), 124.4 (C_{PyrH}), 121.4 (C_{PyrH}), 103.3 ($\text{C}_{5\text{Uri}}$), 100.9 ($\text{C}_{1\text{Gal}}$), 89.8 ($\text{C}_{1\text{Rib}}$), 80.2, 73.0, 71.2 (OCH_2), 70.9, 70.8, 70.6, 69.0, 67.1, 61.3 ($\text{C}_{6\text{Gal}}$), 40.4 ($\text{C}_{5\text{Rib}}$), 20.9 (COCH_3), 20.82 (COCH_3), 20.80 (COCH_3), 20.7 (COCH_3), 20.60 (COCH_3), 20.58 (COCH_3); HR-ESI-MS (positive mode) m/z : calcd. for $\text{C}_{34}\text{H}_{41}\text{N}_4\text{O}_{18}$ $[\text{M}+\text{H}]^+$ 793.2410, found 793.2405.



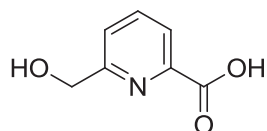
6-(β -D-Glucopyranosyloxymethyl)-N-(uridin-5'-yl)picolinamide (**7-Glc**)

Prepared according to general protocol **E** from compound **6-Glc** (100 mg, 0.13 mmol, 1.0 eq.). The residue was purified by C18 reverse phase column chromatography (100% H_2O to 30% $\text{MeOH}/\text{H}_2\text{O}$) to afford compound **7-Glc** as white foam (44 mg, 0.081 mmol, 63%). $[\alpha]_D^{20} = +12.0$ ($c = 0.1$, H_2O); $^1\text{H NMR}$ (500 MHz, D_2O) δ (ppm) = 8.03 (t, $J = 7.7$ Hz, 1H, H_{Pyr}), 7.97 (d, $J = 7.7$ Hz, 1H, H_{Pyr}), 7.74 (d, $J = 7.7$ Hz, 1H, H_{Pyr}), 7.64 (d, $J = 8.1$ Hz, 1H, $\text{H}_{6\text{Uri}}$), 5.82 (d, $J = 3.7$ Hz, 1H, $\text{H}_{1\text{Rib}}$), 5.70 (d, $J = 8.1$ Hz, 1H, $\text{H}_{5\text{Uri}}$), 5.04 (d, $J = 13.1$ Hz, 1H, OCH_{2a}), 4.91 (d, $J = 13.1$ Hz, 1H, OCH_{2b}), 4.63 (d, $J = 7.9$ Hz, 1H, $\text{H}_{1\text{Glc}}$), 4.40 (bd, $J = 4.2$ Hz, H, $\text{H}_{2\text{Rib}}$), 4.29 – 4.21 (m, 2H, $\text{H}_{3\text{Rib}}, \text{H}_{4\text{Rib}}$), 3.89 (dd, $J = 12.3, 1.8$ Hz, 1H, $\text{H}_{6a\text{Glc}}$), 3.87 – 3.77 (m, 2H, $\text{H}_{5a\text{Rib}}, \text{H}_{5b\text{Rib}}$), 3.72 (dd, $J = 12.3, 5.5$ Hz, 1H, $\text{H}_{6b\text{Glc}}$), 3.53 – 3.47 (m, 1H, $\text{H}_{3\text{Glc}}$), 3.47 – 3.36 (m, 3H, $\text{H}_{2\text{Glc}}, \text{H}_{4\text{Glc}}, \text{H}_{5\text{Glc}}$); $^{13}\text{C NMR}$ (125 MHz, D_2O) δ (ppm) = 167.2 (CONH), 166.0 ($\text{C}=\text{O}_{\text{Uri}}$), 156.2 (C_{Pyr}), 151.4 ($\text{C}=\text{O}_{\text{Uri}}$), 148.3 (C_{Pyr}), 142.0 ($\text{C}_{6\text{Uri}}$), 139.1 (C_{PyrH}), 125.9 (C_{PyrH}), 121.6 (C_{PyrH}), 102.1 ($\text{C}_{5\text{Uri}}$), 102.0 ($\text{C}_{1\text{Glc}}$), 90.5 ($\text{C}_{1\text{Rib}}$), 82.0 ($\text{C}_{4\text{Rib}}$), 76.0 ($\text{C}_{4\text{Glc}}$ or $\text{C}_{5\text{Glc}}$), 75.8 ($\text{C}_{3\text{Glc}}$), 73.13 ($\text{C}_{2\text{Glc}}$ or $\text{C}_{2\text{Rib}}$), 73.10 ($\text{C}_{2\text{Glc}}$ or $\text{C}_{2\text{Rib}}$), 71.4 (OCH_2), 70.5 ($\text{C}_{3\text{Rib}}$), 69.6 ($\text{C}_{4\text{Glc}}$ or $\text{C}_{5\text{Glc}}$), 60.7 ($\text{C}_{6\text{Glc}}$), 40.3 ($\text{C}_{5\text{Rib}}$); HRMS m/z : calcd. for $\text{C}_{22}\text{H}_{28}\text{N}_4\text{NaO}_{12}$, $[\text{M}+\text{Na}]^+$ 563.1596, found 563.1591.



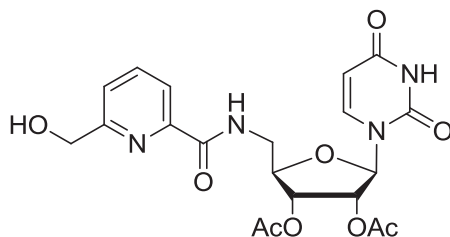
6-(β-D-Galactopyranosyloxymethyl)-N-(uridin-5'-yl)picolinamide (7-Gal)

Prepared according to general protocol E from compound **6-Gal** (116 mg, 0.146 mmol, 1.0 eq.). The residue was purified by C18 reverse phase column chromatography (100% H₂O to 30% MeOH/H₂O) to afford compound **7-Gal** as white foam (79 mg, 0.146 mmol, quant.). $[\alpha]_D^{20} = +24.0$ ($c = 0.1$, H₂O); ¹H NMR (400 MHz, D₂O) δ (ppm) = 7.96 (t, $J = 7.7$ Hz, 1H, H_{Pyr}), 7.88 (d, $J = 7.7$ Hz, 1H, H_{Pyr}), 7.69 (d, $J = 7.7$ Hz, 1H, H_{Pyr}), 7.58 (d, $J = 8.1$ Hz, 1H, H_{6Uri}), 5.73 (d, $J = 3.6$ Hz, 1H, H_{1Rib}), 5.63 (d, $J = 8.1$ Hz, 1H, H_{5Uri}), 4.99 (d, $J = 13.3$ Hz, 1H, OCH_{2a}), 4.84 (d, $J = 13.3$ Hz, 1H, OCH_{2b}), 4.50 (d, $J = 6.7$ Hz, 1H, H_{1Gal}), 4.33 (dd, $J = 3.9, 3.6$ Hz, 1H, H_{2Rib}), 4.18 (t, $J = 4.3$ Hz, 2H), 3.89 (s, 1H), 3.80 – 3.57 (m, 7H); ¹³C NMR (100 MHz, D₂O) δ (ppm) = 166.9 (NHCO), 166.2 (C=O_{Uri}), 156.6 (C_{Pyr}), 151.6 (C=O_{Uri}), 148.1 (C_{Pyr}), 142.4 (C_{6Uri}), 139.9 (C_{PyrH}), 126.2 (C_{PyrH}), 121.9 (C_{PyrH}), 103.0 (C_{5Uri}), 102.9 (C_{1Gal}), 90.9 (C_{1Rib}), 82.3, 75.6, 73.5 (C_{2Rib}), 73.1, 71.3 (OCH₂), 71.1, 70.9, 69.0, 61.3 (C_{6Gal}), 40.8 (C_{5Rib}); HR-ESI-MS (positive mode) m/z : calcd. for C₂₂H₂₉N₄O₁₂ [M+H]⁺ 541.1776, found 541.1752.



6-(Hydroxymethyl)picolinic acid (**8**) (Adapted from Ref.¹⁸⁶)

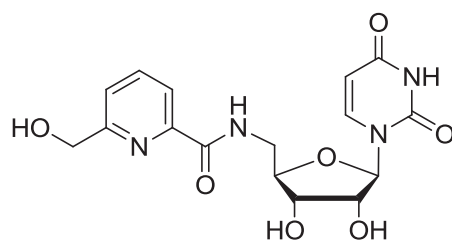
A solution of methyl 6-(hydroxymethyl)picolinate (**2a**) (220 mg, 1.3 mmol, 1.0 eq.) and satd aq. NaOH (0.2 mL) in MeOH (4 mL) was heated for 10 min by microwave irradiation at 100°C. Then, the reaction mixture was neutralized by DOWEX 50W×2 Resin (Fluka, 50-100 mesh, H⁺ form), filtrated and concentrated to afford compound **8** as white solid (205 mg, 1.3 mmol, quant.). ¹H NMR (300 MHz, (CD₃)₂SO) δ (ppm) = 7.85 (s, 2H, 2H_{Pyr}), 7.54 (s, 1H, H_{Pyr}), 4.60 (s, 2H, OCH₂); ESI-MS (positive mode) m/z : [M+H]⁺ 154.0.



6-(Hydroxymethyl)-N-(2',3'-di-O-acetyl-uridin-5'-yl)picolinamide (**9**)

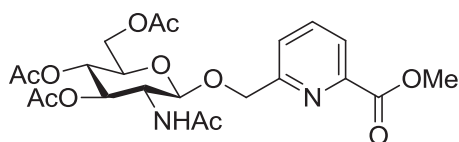
6-(Hydroxymethyl)picolinic acid (**8**) (606 mg, 3.96 mmol, 2.0 eq.) and HOBt (936 mg, 6.93 mmol, 3.5 eq.) were co-evaporated with toluene (3×15 mL) and THF (3×6 mL). The mixture was dried with vacuum for another 1 h. Then, the mixture was dissolved in dry THF (10 mL) under argon and cooled to 0°C. DIC (1.08 mL, 6.93 mmol, 3.5 eq.) was added dropwise at 0°C. After addition, the ice-bath was removed and the reaction was stirred at r.t. for 30 min. At the same time, 2',3'-di-O-acetyl-5'-azido-5'-deoxy-uridine (**5**) (699 mg, 1.98 mmol, 1.0 eq.) was dissolved in dry THF (10 mL) under argon and cooled to 0°C. PMe₃ (3.96 mL, 1 M in THF, 3.96 mmol, 2.0 eq.) was added into the flask at 0°C and the reaction was stirred at 0°C. After 30

min, the solution was transferred into the flask containing the acid. The reaction mixture was stirred with an ice-bath for 1 h, then, the ice-bath was removed, the reaction was stirred at r.t. for 16 h. Then, the reaction mixture was diluted with water (100 mL), extracted with EtOAc (9×100 mL). The combined organic layers were washed with satd Na₂CO₃ (3×100 mL) solution, H₂O (100 mL) and brine (100 mL). The organic phase was dried (Na₂SO₄), concentrated and dried with vacuum. The residue was purified by silica gel column chromatography (EtOAc to EtOAc:MeOH = 95:5) to afford compound **9** as white foam (156 mg, 0.338 mmol, 17%). R_f = 0.51 (CH₂Cl₂:MeOH, 9:1); [α]_D²⁰ = -41.3 (*c* = 0.7, CH₂Cl₂); ¹H NMR (400 MHz, CDCl₃) δ (ppm) = 9.68 (s, 1H, NH_{U_{ri}}), 8.73 (dd, *J* = 6.9, 3.4 Hz, 1H, NHCO), 8.04 (d, *J* = 7.7 Hz, 1H, H_{Py_r}), 7.78 (t, *J* = 7.7 Hz, 1H, H_{Py_r}), 7.32 (d, *J* = 7.7 Hz, 1H, H_{Py_r}), 7.22 (d, *J* = 8.1 Hz, 1H, H_{6U_{ri}}), 5.69 (d, *J* = 8.1 Hz, 1H, H_{5U_{ri}}), 5.52 – 5.45 (m, 2H, H_{2Rib}, H_{3Rib}), 5.43 – 5.35 (m, 1H, H_{1Rib}), 4.78 (s, 2H, OCH_{2a}, OCH_{2b}), 4.35 (dd, *J* = 6.9, 3.5 Hz, 1H, H_{4Rib}), 3.96 (dd, *J* = 14.8, 6.9 Hz, 1H, H_{5aRib}), 3.70 (dd, *J* = 14.8, 3.5 Hz, 1H, H_{5bRib}), 2.06 (s, 3H, COCH₃), 2.04 (s, 3H, COCH₃); ¹³C NMR (100 MHz, CDCl₃) δ (ppm) = 170.2 (COCH₃), 169.8 (COCH₃), 165.2 (NHCO), 162.8 (C=O_{U_{ri}}), 158.3 (C_{Py_r}), 151.0 (C=O_{U_{ri}}), 148.6 (C_{Py_r}), 142.7 (C_{6U_{ri}}), 137.9 (C_{Py_rH}), 123.2 (C_{Py_rH}), 121.2 (C_{Py_rH}), 103.1 (C_{5U_{ri}}), 94.2 (C_{1Rib}), 79.8 (C_{4Rib}), 74.0 (C_{2Rib} or C_{3Rib}), 69.7 (C_{2Rib} or C_{3Rib}), 64.1 (OCH₂), 39.9 (C_{5Rib}), 20.6 (COCH₃), 20.4 (COCH₃); HR-ESI-MS (positive mode) *m/z*: calcd. for C₂₀H₂₃N₄O₉ [M+H]⁺ 463.1460, found 463.1462.



6-Hydroxymethyl-*N*-(uridin-5'-yl)picolinamide (**10**)

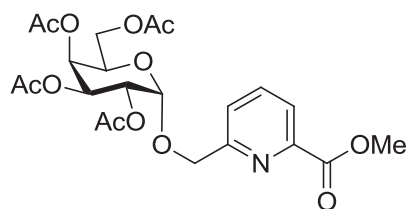
Prepared according to general protocol **E** from compound **9** (33 mg, 0.07 mmol, 1.0 eq.). The residue was purified by C18 reverse phase column chromatography (100% H₂O to 50% MeOH/H₂O) to afford compound **10** as white foam (27 mg, 0.07 mmol, quant.). ¹H NMR (400 MHz, D₂O) δ (ppm) = 7.98 (t, *J* = 7.6 Hz, 1H, H_{Py_r}), 7.91 (d, *J* = 7.6 Hz, 1H, H_{Py_r}), 7.62 (d, *J* = 7.6 Hz, 1H, H_{Py_r}), 7.53 (d, *J* = 7.8 Hz, 1H, H_{6U_{ri}}), 5.82 (d, *J* = 2.7 Hz, 1H, H₁), 5.59 (d, *J* = 7.8 Hz, 1H, H_{5U_{ri}}), 4.75 (s, 2H, CH₂OH), 4.34 (dd, *J* = 4.0, 2.7 Hz, 1H, H₂), 4.26 – 4.17 (m, 2H, H₃, H₄), 3.85 – 3.73 (m, 2H, H_{5a}, H_{5b}); ¹³C NMR (100 MHz, D₂O) δ (ppm) = 181.9, 167.7, 159.4, 148.4, 141.6 (C_{U_{ri}}), 139.4 (C_{Py_r}), 124.8 (C_{Py_r}), 121.5 (C_{Py_r}), 102.7 (C_{U_{ri}}), 90.8 (C₁), 82.2 (C₃ or C₄), 73.6 (C₂), 70.9 (C₃ or C₄), 64.4 (CH₂OH), 40.6 (C₅); HR-ESI-MS (positive mode) *m/z*: calcd. for C₁₆H₁₈N₄O₇ [M+Na]⁺ 401.1068, found 401.1057.



(6-Methoxycarbonylpyrid-2-yl)methyl 3,4,6-tri-*O*-acetyl-2-acetamido-2-deoxy-β-D-glucopyranoside (**11**)

Pd(PPh₃)₄ was added into a solution of (6-methoxycarbonylpyrid-2-yl)methyl 3,4,6-tri-*O*-acetyl-2-allyloxycarbonylamino-2-deoxy-β-D-glucopyranoside (**3h**) (23 mg, 0.043 mmol, 1.0 eq.) and dimethyl malonate (0.05 mL, 0.43 mmol, 10.0 eq.) in dried oxygen-free

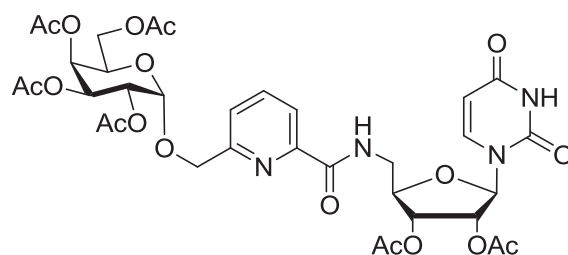
THF (2 mL) under argon. The reaction mixture was stirred under argon for 23 h. Pyridine (2 mL) and acetic anhydride (1 mL) were added into the flask and the reaction was stirred at r.t. overnight. Then, the reaction mixture was concentrated, co-evaporated with toluene (2×5 mL) and ethanol (2×5 mL). The residue was purified by silica gel chromatography (60% EtOAc/PE to 100% EtOAc) to afford compound **11** as white foam (21 mg, quant.). $R_f = 0.18$ (60% EtOAc/PE); $[\alpha]_D^{20} = +10.0$ ($c = 0.3$, CH_2Cl_2); $^1\text{H NMR}$ (400 MHz, CDCl_3) δ (ppm) = 8.02 (d, $J = 7.8$ Hz, 1H, H_{pyr}), 7.83 (t, $J = 7.8$ Hz, 1H, H_{pyr}), 7.51 (d, $J = 7.8$ Hz, 1H, H_{pyr}), 6.60 – 6.53 (m, 1H, NHAc), 5.20 – 5.00 (m, 3H, $\text{H}_{3\text{Gal}}$, $\text{H}_{4\text{Gal}}$, $\text{OCH}_{2\text{a}}$), 4.96 – 4.85 (m, 2H, $\text{H}_{1\text{Gal}}$, $\text{OCH}_{2\text{b}}$), 4.26 – 4.16 (m, 2H, $\text{H}_{2\text{Gal}}$, $\text{H}_{6\text{aGal}}$), 4.12 – 4.06 (m, 1H, $\text{H}_{6\text{bGal}}$), 4.00 (s, 3H, CO_2Me), 3.69 (ddd, $J = 9.3, 4.6, 2.1$ Hz, 1H, $\text{H}_{5\text{Gal}}$), 2.06 (s, 3H, COCH_3), 2.02 (s, 3H, COCH_3), 2.00 (s, 3H, COCH_3), 1.87 (s, 3H, NHCOCH_3); $^{13}\text{C NMR}$ (101 MHz, CDCl_3) δ (ppm) = 171.1, 170.9, 170.6, 169.5, 165.6, 158.3, 147.0, 138.0 (C_{pyrH}), 124.8 (C_{pyrH}), 124.1 (C_{pyrH}), 101.3 ($\text{C}_{1\text{Gal}}$), 73.2 ($\text{C}_{3\text{Gal}}$ or $\text{C}_{4\text{Gal}}$), 72.2 ($\text{C}_{5\text{Gal}}$), 70.3 (OCH_2), 68.5 ($\text{C}_{4\text{Gal}}$ or $\text{C}_{3\text{Gal}}$), 62.2 ($\text{C}_{6\text{Gal}}$), 54.2 ($\text{C}_{2\text{Gal}}$), 53.1 (CO_2CH_3), 23.2 (NHCOCH_3), 20.87 (COCH_3), 20.84 (COCH_3), 20.73 (COCH_3); HR-ESI-MS (positive mode) m/z : calcd for $\text{C}_{22}\text{H}_{29}\text{N}_2\text{O}_{11}$, $[\text{M}+\text{H}]^+$ 497.1766, found 497.1756.



Methyl 6-(2,3,4,6-tetra-*O*-acetyl- α -D-galactopyranosyloxymethyl)picolinate (16**)**
(Adapted from Ref.^{214-215, 234})

Methyl 6-(2,3,4,6-tetra-*O*-benzyl- α -D-galactopyranosyloxymethyl)picolinate (**3c**) (50 mg, 0.072 mmol, 1.0 eq.) was dissolved in EtOAc (2 mL) and then a solution of NaBrO_3 (130 mg, 0.864 mmol, 12.0 eq.) in H_2O (2 mL) was added to the well stirred two phases system. An aqueous solution of $\text{Na}_2\text{S}_2\text{O}_4$ (85% pure, 150 mg, 0.864 mmol, 12.0 eq.) in H_2O (3 mL) was added dropwise over 10 min at 25°C. After addition, the color of the reaction mixture changed from colorless to orange. Then, the reaction was stirred strongly at 25°C for 3 h. $\text{Na}_2\text{S}_2\text{O}_3 \cdot 5\text{H}_2\text{O}$ (214 mg, 0.864 mmol, 12.0 eq.) was added into the reaction and stirred for 10 min; the color was disappeared. Then, the reaction mixture was concentrated. Pyridine (3 mL) and Ac_2O (1 mL) were added and the reaction was stirred at r.t. overnight. The reaction mixture was filtrated and the solid was washed with EtOAc. The filtrate was concentrated and co-evaporated with toluene (2×5 mL) and ethanol (2×5 mL). Then, the residue was purified by silica gel column chromatography (PE:EtOAc = 9:1 to PE:EtOAc = 1:1) to afford compound **16** as white foam (15 mg, 0.03 mmol, 42%). $R_f = 0.43$ (PE:EtOAc = 1:2); $[\alpha]_D^{20} = +54.5$ ($c = 0.4$, CH_2Cl_2); $^1\text{H NMR}$ (500 MHz, CDCl_3) δ (ppm) = 8.07 (d, $J = 7.8$ Hz, 1H, H_{pyr}), 7.89 (t, $J = 7.8$ Hz, 1H, H_{pyr}), 7.67 (d, $J = 7.8$ Hz, 1H, H_{pyr}), 5.48 (dd, $J = 3.4, 1.0$ Hz, 1H, H_4), 5.45 (dd, $J = 10.7, 3.4$ Hz, 1H, H_3), 5.26 (d, $J = 3.6$ Hz, 1H, H_1), 5.22 (dd, $J = 10.7, 3.6$ Hz, 1H, H_2), 4.97 (d, $J = 13.9$ Hz, 1H, $\text{OCH}_{2\text{a}}$), 4.77 (d, $J = 13.9$ Hz, 1H, $\text{OCH}_{2\text{b}}$), 4.30 (dd, $J = 6.8, 1.0$ Hz, 1H, H_5), 4.15 – 4.10 (m, 1H, $\text{H}_{6\text{a}}$), 4.06 (dd, $J = 11.3, 6.8$ Hz, 1H, $\text{H}_{6\text{b}}$), 4.01 (s, 3H, OMe), 2.15 (s, 3H, COCH_3), 2.08 (s, 3H, COCH_3), 2.04 (s, 3H, COCH_3), 2.00 (s, 3H, COCH_3); $^{13}\text{C NMR}$ (125 MHz, CDCl_3) δ (ppm) = 170.6 (COCH_3), 170.38 (COCH_3), 170.37 (COCH_3), 170.26 (COCH_3), 165.7 (CO_2Me), 158.1 (C_{pyr}), 147.6 (C_{pyr}), 138.0 (C_{pyrH}), 124.5 (C_{pyrH}), 124.4 (C_{pyrH}), 96.6 (C_1), 70.7

(OCH₂), 68.2 (C₂), 68.1 (C₄), 67.7 (C₃), 66.9 (C₅), 61.7 (C₆), 53.2 (OMe), 20.93 (COCH₃), 20.86 (COCH₃), 20.83 (COCH₃), 20.80 (COCH₃); HR-ESI-MS (positive mode) *m/z*: calcd. for C₂₂H₂₈NO₁₂ [M+H]⁺ 498.1606, found 498.1601.



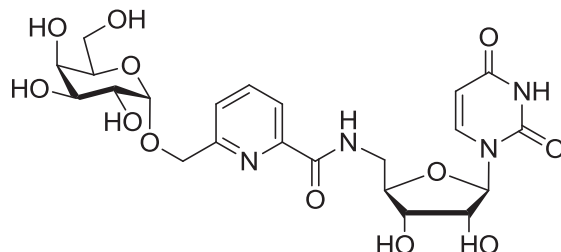
6-(2,3,4,6-Tetra-*O*-acetyl- α -D-galactopyranosyloxymethyl)-*N*-(2,3-di-*O*-acetyl-uridin-5'-yl)picolinamide (18)

A mixture of methyl 6-(2,3,4,6-tetra-*O*-acetyl- α -D-galactopyranosyloxymethyl)picolinate (**16**) (103 mg, 0.21 mmol, 1.0 eq.) and NaI (191 mg, 1.27 mmol, 6.1 eq.) in dry pyridine (3 mL) was stirred at 120°C under an argon atmosphere. After 5 h, the reaction was finished. Pyridine was evaporated and the residue was co-evaporated with toluene (3×10 mL). The residue was solubilized with CHCl₃ (10 mL), filtered through celite, washed with CHCl₃, dried over Na₂SO₄. Then, the solvent was evaporated and the residue was purified by silica gel column chromatography (PE:EtOAc = 1:1 to EtOH) to afford compound **17** as yellow foam (99 mg, 0.21 mmol, quant.).

6-(2,3,4,6-Tetra-*O*-acetyl- α -D-galactopyranosyloxymethyl)picolinic acid (**17**) (123 mg, 0.25 mmol, 1.0 eq.) and HOBT (101 mg, 0.75 mmol, 3.0 eq.) were co-evaporated with toluene (3×10 mL) and THF (3×5 mL). The mixture was dried with vacuum for another 1 h. Then, the mixture was dissolved in dry THF (4 mL) under argon and cooled to 0°C. DIC (0.12 mL, 0.75 mmol, 3.0 eq.) was added dropwise at 0°C. After addition, the ice-bath was removed and the reaction was stirred at r.t. for 30 min. At the same time, 2',3'-di-*O*-acetyl-5'-azido-5'-deoxy-uridine **5** (176 mg, 0.50 mmol, 2.0 eq.) was dissolved in dry THF (4 mL) under argon and cooled to 0°C. PMe₃ (0.75 mL, 1 M in THF, 0.75 mmol, 3.0 eq.) was added into the flask at 0°C and the reaction was stirred at 0°C. After 30 min, the solution was transferred into the flask containing the acid. The reaction mixture was stirred with an ice-bath for 1 h, then, the ice-bath was removed. The reaction was stirred at r.t. for 16 h. Then, the reaction mixture was diluted with water (60 mL), extracted with EtOAc (4×60 mL). The combined organic layers were washed with satd Na₂CO₃ (60 mL), H₂O (60 mL) and brine (60 mL). The organic phase was dried (Na₂SO₄), concentrated and dried with vacuum. The residue was purified by silica gel column chromatography (100% PE to PE:EtOAc = 20:80) to afford compound **18** as white foam (54 mg, 0.068 mmol, 27%).

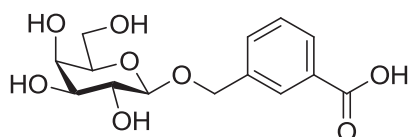
*R*_f = 0.56 (EtOAc); [α]_D²⁰ = +18.1 (*c* = 0.9, CH₂Cl₂); ¹H NMR (500 MHz, CDCl₃) δ (ppm) = 8.45 (s, 1H, NH_{Urid}), 8.40 (t, *J* = 6.1 Hz, 1H, NHCO), 8.16 – 8.13 (m, 1H, H_{Pyrid}), 7.89 (t, *J* = 7.8 Hz, 1H, H_{Pyrid}), 7.56 (dd, *J* = 7.8, 0.7 Hz, 1H, H_{Pyrid}), 7.34 (d, *J* = 8.2 Hz, 1H, H_{6Urid}), 5.75 – 5.70 (m, 2H, H_{5Urid}, H_{1Rib}), 5.48 – 5.38 (m, 5H), 5.16 (dd, *J* = 10.8, 3.7 Hz, 1H), 4.79 (d, *J* = 13.0 Hz, 1H, OCH_{2a}), 4.72 (d, *J* = 13.0 Hz, 1H, OCH_{2b}), 4.36 – 4.29 (m, 2H, H_{4Rib}, H_{5Gal}), 4.10 – 4.06 (m, 1H, H_{6aGal}), 4.00 (dd, *J* = 11.3, 6.6 Hz, 1H, H_{6bGal}), 3.90 – 3.85 (m, 2H, H_{5aRib}, H_{5bRib}), 2.15 (s, 3H, COCH₃), 2.11 (s, 3H, COCH₃), 2.09 (s, 3H, COCH₃), 2.01 (s, 3H, COCH₃), 2.00 (s, 3H, COCH₃), 1.98 (s, 3H, COCH₃); ¹³C NMR (125 MHz, CDCl₃) δ (ppm) = 170.7 (C=O), 170.6 (C=O), 170.4 (C=O), 170.2 (C=O), 169.9 (C=O), 169.7 (C=O), 164.9 (NHCO), 162.5 (C=O_{Urid}),

156.1 (C_{Pyr}), 149.9 (C=O_{Uri}), 149.3 (C_{Pyr}), 141.3 (C_{6Uri}), 138.4 (C_{PyrH}), 125.2 (C_{PyrH}), 121.9 (C_{PyrH}), 103.2 (C_{5Uri}), 96.6 (C_{1Gal}), 90.7 (C_{1Rib}), 80.4, 73.2, 70.8 (OCH₂), 70.4, 68.3, 68.1, 67.5, 66.9, 61.7 (C_{6Gal}), 40.3 (C_{5Rib}), 20.84 (COCH₃), 20.82 (COCH₃), 20.80 (COCH₃), 20.79 (COCH₃), 20.62 (s, 2C, COCH₃); HR-ESI-MS (positive mode) *m/z*: calcd. for C₃₄H₄₁N₄O₁₈ [M+H]⁺ 793.2410, found 793.2404; calcd. for C₃₄H₄₀N₄NaO₁₈ [M+Na]⁺ 815.2230, found 815.2223.



6-(α -D-Galactopyranosyloxymethyl)-N-(uridin-5'-yl)picolinamide (**19**)

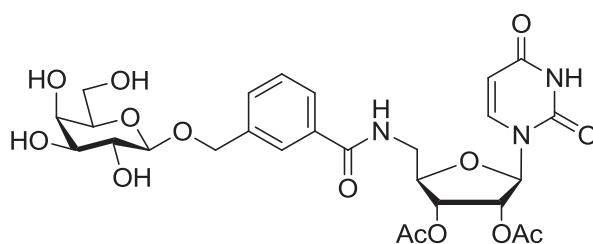
Prepared according to general protocol **E** from compound **18** (30 mg, 0.038 mmol, 1.0 eq.). The residue was purified by C18 reverse phase column chromatography (100% H₂O to 50% MeOH/H₂O) to afford compound **19** as white foam (13 mg, 0.024 mmol, 63%). [α]_D²⁰ = +181 (*c* = 0.1, H₂O); ¹H NMR (500 MHz, D₂O) δ (ppm) = 8.05 (t, *J* = 7.7 Hz, 1H, H_{Pyr}), 7.99 (d, *J* = 7.7 Hz, 1H, H_{Pyr}), 7.77 (d, *J* = 7.7 Hz, 1H, H_{Pyr}), 7.65 (d, *J* = 8.1 Hz, 1H, H_{6Uri}), 5.83 (d, *J* = 3.7 Hz, 1H, H_{1Rib}), 5.69 (d, *J* = 8.1 Hz, 1H, H_{5Uri}), 5.13 (d, *J* = 3.7 Hz, 1H, H_{1Gal}), 4.88 (d, *J* = 13.1 Hz, 1H, OCH_{2a}), 4.82 (d, *J* = 13.1 Hz, 1H, OCH_{2b}), 4.42 (dd, *J* = 4.1, 3.7 Hz, 1H, H_{2Rib}), 4.29 – 4.23 (m, 2H), 4.01 – 3.77 (m, 6H), 3.71 – 3.62 (m, 2H, H_{6aGal}, H_{6bGal}); ¹³C NMR (125 MHz, D₂O) δ (ppm) = 167.3 (NHCO), 166.0 (C=O_{Uri}), 156.6 (C_{Pyr}), 151.4 (C=O_{Uri}), 148.3 (C_{Pyr}), 142.1 (C_{6Uri}), 139.1 (C_{PyrH}), 125.9 (C_{PyrH}), 121.5 (C_{PyrH}), 102.0 (C_{5Uri}), 98.5 (C_{1Gal}), 90.5 (C_{1Rib}), 82.1, 73.1, 71.2, 70.5, 69.8 (OCH₂), 69.4, 69.2, 68.3, 61.0 (C_{6Gal}), 40.2 (C_{5Rib}); HR-ESI-MS (positive mode) *m/z*: calcd. for C₂₂H₂₈N₄NaO₁₂ [M+Na]⁺ 563.1596, found 563.1581.



3- β -D-Galactosyloxymethylbenzoic acid (**20**)

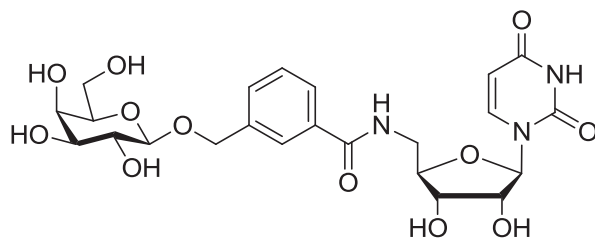
LiOH (134.4 mg, 3.2 mmol, 4.5 eq.) was solubilized in H₂O (2 mL), then, added dropwise into a solution of methyl 3-(2,3,4,6-tetra-*O*-acetyl- β -D-galactosyloxymethyl)benzoate (**3e**) (349 mg, 0.70 mmol, 1.0 eq.) in THF (4 mL). Then, the reaction mixture was stirred at r.t. for 2 days. DOWEX 50W \times 2 Resin (Fluka, 50-100 mesh, H⁺ Form) was added to neutralize the reaction until pH~3. The reaction mixture was filtrated and concentrated to afford compound **20** as white foam (205 mg, 0.653 mmol, 93%). [α]_D = -20.0 (*c* = 0.1, H₂O); ¹H NMR (400 MHz, D₂O) δ (ppm) = 7.89 (s, 1H, H_{Ar}), 7.81 (d, *J* = 7.7 Hz, 1H, H_{Ar}), 7.58 (d, *J* = 7.7 Hz, 1H, H_{Ar}), 7.40 (t, *J* = 7.7 Hz, 1H, H_{Ar}), 4.87 (d, *J* = 12.1 Hz, 1H, OCH_{2a}), 4.68 (d, *J* = 12.1 Hz, 1H, OCH_{2b}), 4.37 (d, *J* = 7.1 Hz, 1H, H₁), 3.86 (bd, *J* = 2.5 Hz, 1H, H₃), 3.78 – 3.66 (m, 2H, H_{6a}, H_{6b}), 3.62 – 3.48 (m, 3H, H₂, H₄, H₅); ¹³C NMR (100 MHz, D₂O) δ (ppm) = 170.6 (CO₂H), 137.6 (C_{Ar}), 133.8 (C_{ArH}), 130.2 (C_{Ar}), 129.7 (s, 2C, 2 C_{ArH}), 129.2 (C_{ArH}), 102.3 (C₁), 75.5 (C₂ or C₄ or C₅), 73.1

(C₂ or C₄ or C₅), 71.1 (C₂ or C₄ or C₅), 71.0 (OCH₂), 68.9 (C₃), 61.2 (C₆); HR-ESI-MS (positive mode) *m/z*: calcd. for C₁₄H₁₈NaO₈ [M+Na]⁺ 337.0894, found 337.0894.



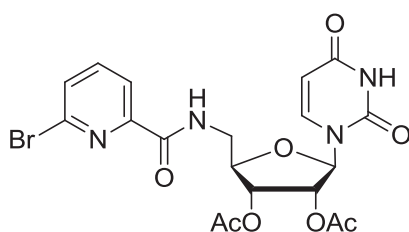
3-(β-D-Galactopyranosyloxymethyl)-N-(2',3'-di-O-acetyl-uridin-5'-yl)benzamide (**21**)

3-β-D-Galactosyloxymethylbenzoic acid (**20**) (33 mg, 0.105 mmol, 1.0 eq.) and HOBT (43 mg, 0.315 mmol, 3.0 eq.) were co-evaporated with toluene (3×5 mL) and THF (3×5 mL). The mixture was dried with vacuum for another 1 h. Then, the mixture was dissolved in dry THF (2 mL) under argon and cooled to 0°C. DIC (0.05 mL, 0.320 mmol, 3.0 eq.) was added dropwise at 0°C. After addition, the ice-bath was removed; the reaction was stirred at r.t. for 30 min. At the same time, 2',3'-di-O-acetyl-5'-azido-5'-deoxy-uridine (**5**) (74 mg, 0.21 mmol, 2.0 eq.) was dissolved in dry THF (2 mL) under argon and cooled to 0°C. PMe₃ (0.3 mL, 1 M in THF, 0.3 mmol, 3.0 eq.) was added into the flask at 0°C and the reaction was stirred at 0°C. After 30 min, the solution was transferred into the flask containing the acid. The reaction mixture was stirred with an ice-bath for 1 h, then, the ice-bath was removed and the reaction was stirred at r.t. for 16 h. The reaction mixture was diluted with water (30 mL); the aqueous phase was washed with CH₂Cl₂ (2×30 mL). Then, the combined organic layer was washed with H₂O (30 mL). The combined aqueous phase was concentrated and dried with vacuum. The residue was purified by C18 reverse phase column chromatography (H₂O to H₂O:MeOH = 7:3) to afford compound **21** as white foam (28 mg, 0.045 mmol, 43%). R_f = 0.55 (MeOH:EtOAc, 4:6); ¹H NMR (500 MHz, D₂O) δ (ppm) = 7.82 (s, 1H, H_{Ar}), 7.74 (d, *J* = 7.7 Hz, 1H, H_{Ar}), 7.66 (d, *J* = 7.7 Hz, 1H, H_{Ar}), 7.63 (d, *J* = 8.1 Hz, 1H, H_{6Uri}), 7.54 (t, *J* = 7.7 Hz, 1H, H_{Ar}), 5.85 (d, *J* = 3.6 Hz, 1H, H_{1Rib}), 5.80 (d, *J* = 8.1 Hz, 1H, H_{5Uri}), 5.59 (dd, *J* = 6.6, 3.6 Hz, 1H, H_{2Rib}), 5.43 (bd, *J* = 6.6 Hz, 1H, H_{3Rib}), 4.99 (d, *J* = 12.1 Hz, 1H, OCH_{2a}), 4.81 (d, *J* = 12.1 Hz, 1H, OCH_{2b}), 4.47 (d, *J* = 7.5 Hz, 1H, H_{1Gal}), 4.46 – 4.41 (m, 1H, H_{4Rib}), 3.93 (bd, *J* = 3.3 Hz, 1H, H_{4Gal}), 3.84 – 3.74 (m, 4H, H_{6aGal}, H_{6bGal}, H_{5aRib}, H_{5bRib}), 3.68 (dd, *J* = 7.8, 4.5 Hz, 1H, H_{5Gal}), 3.63 (dd, *J* = 9.8, 3.3 Hz, 1H, H_{3Gal}), 3.58 (dd, *J* = 9.8, 7.5 Hz, 1H, H_{2Gal}), 2.16 (s, 3H, COCH₃), 2.13 (s, 3H, COCH₃); ¹³C NMR (125 MHz, D₂O) δ (ppm) = 172.61 (COCH₃), 172.59 (COCH₃), 170.7 (CO₂H), 166.0 (C=O_{Uri}), 151.0 (C=O_{Uri}), 143.4 (C_{6Uri}), 137.5 (C_{Ar}), 133.5 (C_{Ar}), 132.2 (C_{ArH}), 129.1 (C_{ArH}), 127.0 (C_{ArH}), 126.9 (C_{ArH}), 102.3 (C_{5Uri}), 102.0 (C_{1Gal}), 90.7 (C_{1Rib}), 79.5 (C_{4Rib}), 75.2 (C_{5Gal}), 73.1 (C_{2Rib}), 72.8 (C_{3Gal}), 70.8 (s, 2C, C_{2Gal}, OCH₂), 70.6 (C_{3Rib}), 68.6 (C_{4Gal}), 61.0 (C_{6Gal}), 39.9 (C_{5Rib}), 19.9 (COCH₃), 19.8 (COCH₃); HR-ESI-MS (positive mode) *m/z*: calcd. for C₂₇H₃₄N₃O₁₄ [M+H]⁺ 624.2035, found 624.2037; calcd. for C₂₇H₃₃N₃NaO₁₄ [M+Na]⁺ 646.1855, found 646.1848.



3-(β-D-Galactopyranosyloxymethyl)-N-(uridin-5'-yl)benzamide (**22**)

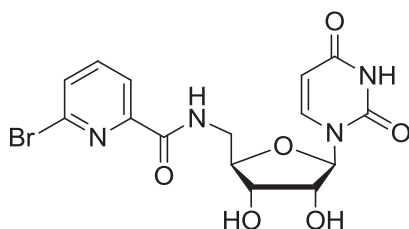
Prepared according to general protocol **E** from compound **21** (27 mg, 0.043 mmol, 1.0 eq.). The residue was purified by C18 reverse phase column chromatography (100% H₂O to 30% MeOH/H₂O) to afford compound **22** as white foam (17 mg, 0.032 mmol, 73%). $[\alpha]_D^{25} = +8.0$ ($c = 0.2$, H₂O); ¹H NMR (500 MHz, D₂O) δ (ppm) = 7.84 (s, 1H, H_{Ar}), 7.78 – 7.74 (m, 1H, H_{Ar}), 7.69 – 7.65 (m, 2H, H_{Ar}, H_{6Uri}), 7.56 (t, $J = 7.7$ Hz, 1H, H_{Ar}), 5.82 (d, $J = 3.7$ Hz, 1H, H_{1Rib}), 5.77 (d, $J = 8.1$ Hz, 1H, H_{5Uri}), 5.01 (d, $J = 12.0$ Hz, 1H, OCH_{2a}), 4.83 (d, $J = 12.1$ Hz, 1H, OCH_{2b}), 4.48 (d, $J = 7.6$ Hz, 1H, H_{1Gal}), 4.43 (dd, $J = 4.7, 3.7$ Hz, 1H, H_{2Rib}), 4.27 – 4.22 (m, 2H, H_{3Rib}, H_{4Rib}), 3.95 – 3.92 (m, 1H, H_{4Gal}), 3.87 – 3.75 (m, 4H, H_{5aRib}, H_{5bRib}, H_{6aGal}, H_{6bGal}), 3.71 – 3.67 (m, 1H, H_{5Gal}), 3.63 (dd, $J = 9.9, 3.3$ Hz, 1H, H_{3Gal}), 3.58 (dd, $J = 9.9, 7.6$ Hz, 1H, H_{2Gal}); ¹³C NMR (125 MHz, D₂O) δ (ppm) = 170.9 (CONH), 166.1 (C=O_{Uri}), 151.4 (C=O_{Uri}), 142.2 (C_{6Uri}), 137.5 (C_{Ar}), 133.6 (C_{Ar}), 132.2 (C_{ArH}), 129.1 (C_{ArH}), 127.0 (C_{ArH}), 126.9 (C_{ArH}), 102.1 (C_{5Uri}), 101.9 (C_{1Gal}), 90.9 (C_{1Rib}), 81.9 (C_{4Rib}), 75.2 (C_{5Gal}), 73.1 (C_{2Rib}), 72.8 (C_{3Gal}), 70.8 (OCH₂ or C_{2Gal}), 70.8 (OCH₂ or C_{2Gal}), 70.5 (C_{3Rib}), 68.6 (C_{4Gal}), 61.0 (C_{6Gal}), 40.6 (C_{5Rib}); HR-ESI-MS (positive mode) m/z : calcd. for C₂₃H₂₉N₃NaO₁₂ [M+Na]⁺ 562.1643, found 562.1648.



6-Bromo-N-(2',3'-di-O-acetyl-uridin-5'-yl)picolinamide (**24**)

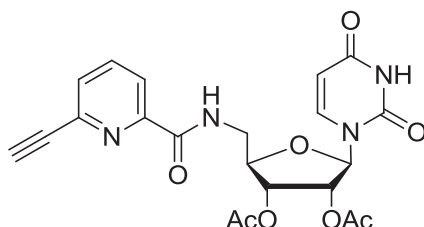
6-Bromopicolinic acid (**23**) (49 mg, 0.24 mmol, 1.2 eq.) and HOBT (48 mg, 0.36 mmol, 1.8 eq.) were co-evaporated with toluene (3×5 mL) and THF (3×8 mL). The mixture was dried with vacuum for another 20 min. Then, the mixture was dissolved in dry THF (2 mL) under argon and cooled to 0°C. DIC (56 μ L, 0.36 mmol, 1.8 eq.) was added dropwise at 0°C. After addition, the ice-bath was removed; the reaction was stirred at r.t. for 30 min. At the same time, 2',3'-di-O-acetyl-5'-azido-5'-deoxy-uridine (**5**) (70 mg, 0.20 mmol, 1.0 eq.) was dissolved in dry THF (2 mL) under argon and cooled to 0°C. PMe₃ (0.36 mL, 1 M in THF, 0.36 mmol, 1.8 eq.) was added into the flask at 0°C and the reaction was stirred at 0°C for 30 min. Then, the solution was transferred into the flask containing the acid. The reaction mixture was stirred with an ice-bath for 1 h, then, the ice-bath was removed and the reaction was stirred at r.t. for 21 h. The reaction mixture was diluted with water (30 mL), extracted with EtOAc (3×40 mL), the combined organic layers were washed with satd Na₂CO₃ solution (3×30 mL), H₂O (30 mL) and brine (30 mL). The organic phase was dried (Na₂SO₄), concentrated and dried with vacuum. The residue was purified by silica gel column chromatography (100% PE to 100% EtOAc) to afford compound **24** as yellow foam (37 mg, 0.073 mmol, 37%). $R_f = 0.24$ (PE:EtOAc, 1:3);

$[\alpha]_D = +27.6$ ($c = 1.6$, CH_2Cl_2); $^1\text{H NMR}$ (400 MHz, CDCl_3) δ (ppm) = 9.25 (s, 1H, NH_{Uri}), 8.20 – 8.10 (m, 2H, CONH, H_{Pyr}), 7.72 (t, $J = 7.7$ Hz, 1H, H_{Pyr}), 7.62 (d, $J = 7.7$ Hz, 1H, H_{Pyr}), 7.35 (d, $J = 8.1$ Hz, 1H, $\text{H}_{6\text{Uri}}$), 5.84 (d, $J = 4.5$ Hz, 1H, $\text{H}_{1\text{Rib}}$), 5.82 (d, $J = 8.1$ Hz, 1H, $\text{H}_{5\text{Uri}}$), 5.42 – 5.34 (m, 1H, $\text{H}_{2\text{Rib}}$), 5.29 (dd, $J = 6.1, 4.7$ Hz, 1H, $\text{H}_{3\text{Rib}}$), 4.32 (dd, $J = 10.0, 4.7$ Hz, 1H, $\text{H}_{4\text{Rib}}$), 4.01 – 3.87 (m, 1H, $\text{H}_{5\text{aRib}}$), 3.77 (ddd, $J = 14.4, 4.7$ Hz, 1H, $\text{H}_{5\text{bRib}}$), 2.10 (s, 3H, COCH_3), 2.07 (s, 3H, COCH_3); $^{13}\text{C NMR}$ (100 MHz, CDCl_3) δ (ppm) = 170.1 (s, 2C, $2 \times \text{COCH}_3$), 163.8 (NHCO), 163.3 ($\text{C}=\text{O}_{\text{Uri}}$), 150.8 (C_{Pyr}), 150.5 ($\text{C}=\text{O}_{\text{Uri}}$), 141.1 (C_{Pyr}), 140.9 ($\text{C}_{6\text{Uri}}$), 140.3 (C_{PyrH}), 131.5 (C_{PyrH}), 122.0 (C_{PyrH}), 104.0 ($\text{C}_{5\text{Uri}}$), 89.8 ($\text{C}_{1\text{Rib}}$), 80.6 ($\text{C}_{4\text{Rib}}$), 73.3 ($\text{C}_{2\text{Rib}}$), 71.0 ($\text{C}_{3\text{Rib}}$), 40.7 ($\text{C}_{5\text{Rib}}$), 20.9 (COCH_3), 20.8 (COCH_3); HR-ESI-MS (positive mode) m/z : calcd. for $\text{C}_{19}\text{H}_{20}\text{BrN}_4\text{O}_8$ $[\text{M}+\text{H}]^+$ 511.0459, found 511.0462.



6-Bromo-*N*-(uridin-5'-yl)picolinamide (**25**)

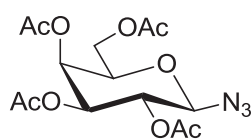
In a flask containing 6-bromo-*N*-(2,3-di-*O*-acetyl-5-deoxy-uridin-5-yl)picolinamide (**24**) (64 mg, 0.125 mmol, 1.0 eq.) were added MeOH (2.5 mL), H_2O (1.25 mL) and Et_3N (1.25 mL) and the reaction mixture was stirred at r.t. After 5 days, the reaction was finished. Then, the reaction mixture was concentrated and co-evaporated with toluene (3×5 mL). The residue was purified by silica gel column chromatography (100% EtOAc to 30% MeOH/EtOAc) to afford compound **25** as white foam (15 mg, 0.035 mmol, 28%). $R_f = 0.59$ (MeOH:EtOAc = 1:4); $[\alpha]_D = +10.2$ ($c = 0.4$, DMSO); $^1\text{H NMR}$ (500 MHz, CD_3OD) δ (ppm) = 8.10 (dd, $J = 7.8, 0.9$ Hz, 1H, H_{Pyr}), 7.88 (t, $J = 7.8$ Hz, 1H, H_{Pyr}), 7.78 (dd, $J = 7.8, 0.9$ Hz, 1H, H_{Pyr}), 7.74 (d, $J = 8.1$ Hz, 1H, $\text{H}_{6\text{Uri}}$), 5.84 (d, $J = 4.7$ Hz, 1H, $\text{H}_{1\text{Rib}}$), 5.73 (d, $J = 8.1$ Hz, 1H, $\text{H}_{5\text{Uri}}$), 4.19 (dd, $J = 5.4, 4.7$ Hz, 1H, $\text{H}_{2\text{Rib}}$), 4.16 – 4.11 (m, 1H, $\text{H}_{4\text{Rib}}$), 4.08 (t, $J = 5.4$ Hz, 1H, $\text{H}_{3\text{Rib}}$), 3.80 (dd, $J = 14.1, 5.9$ Hz, 1H, $\text{H}_{5\text{aRib}}$), 3.71 (dd, $J = 14.1, 4.7$ Hz, 1H, $\text{H}_{5\text{bRib}}$); $^{13}\text{C NMR}$ (125 MHz, CD_3OD) δ (ppm) = 166.1 ($\text{C}=\text{O}_{\text{Uri}}$), 165.6 (NHCO), 152.3 (C_{Pyr}), 152.1 ($\text{C}=\text{O}_{\text{Uri}}$), 142.8 (C_{Pyr}), 142.0 ($\text{C}_{6\text{Uri}}$), 141.6 (C_{PyrH}), 132.5 (C_{PyrH}), 122.6 (C_{PyrH}), 103.1 ($\text{C}_{5\text{Uri}}$), 91.6 (C_1), 83.9 (C_4), 74.9 (C_2), 72.5 (C_3), 42.1 (C_5); HR-ESI-MS (positive mode) m/z : calcd. for $\text{C}_{15}\text{H}_{15}\text{BrN}_4\text{NaO}_6$ $[\text{M}+\text{Na}]^+$ 449.0067, found 449.0046.



6-Ethynyl-*N*-(2',3'-di-*O*-acetyl-uridin-5'-yl)picolinamide (**27**)

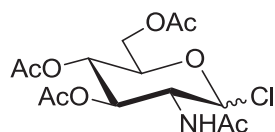
Compound **26** was prepared according to general protocol **D** from compound **24** (436 mg, 0.85 mmol, 1.0 eq.). The crude product was purified by silica gel column chromatography (PE to PE:EtOAc = 1:1) to afford a mixture (496 mg) containing compound **26** and the mixture was used directly for the reaction of next step.

Then, following the general protocol **F**, compound **27** was prepared from compound **26** (a mixture, 496 mg). The crude product was purified by silica gel column chromatography (100% PE to 100% EtOAc) to afford compound **27** as yellow foam (193 mg, 0.42 mmol, two steps 50%). $R_f = 0.17$ (PE: EtOAc, 1:2); $[\alpha]_D = +34.9$ ($c = 1.7$, CH_2Cl_2); $^1\text{H NMR}$ (400 MHz, CDCl_3) δ (ppm) = 9.41 (s, 1H, H_{NHUri}), 8.37 – 8.29 (m, 1H, NHCO), 8.16 (d, $J = 7.8$ Hz, 1H, H_{Pyr}), 7.84 (t, $J = 7.8$ Hz, 1H, H_{Pyr}), 7.61 (d, $J = 7.8$ Hz, 1H, H_{Pyr}), 7.38 (d, $J = 8.1$ Hz, 1H, $\text{H}_{6\text{Uri}}$), 5.86 (d, $J = 4.5$ Hz, 1H, $\text{H}_{1\text{Rib}}$), 5.81 (d, $J = 8.1$ Hz, 1H, $\text{H}_{5\text{Uri}}$), 5.39 – 5.33 (m, 1H, $\text{H}_{2\text{Rib}}$), 5.31 – 5.26 (m, 1H, $\text{H}_{3\text{Rib}}$), 4.31 (dd, $J = 10.0, 5.1$ Hz, 1H, $\text{H}_{4\text{Rib}}$), 4.01 – 3.90 (m, 1H, $\text{H}_{5a\text{Rib}}$), 3.74 (dd, $J = 14.4, 4.6$ Hz, 1H, $\text{H}_{5b\text{Rib}}$), 3.28 (s, 1H, $\text{C}\equiv\text{CH}$), 2.09 (s, 3H, COCH_3), 2.06 (s, 3H, COCH_3); $^{13}\text{C NMR}$ (100 MHz, CDCl_3) δ (ppm) = 169.8, 164.2, 163.1, 150.3, 149.7, 141.0, 140.6 ($\text{C}_{6\text{Uri}}$), 138.0 (C_{PyrH}), 130.4 (C_{PyrH}), 122.4 (C_{PyrH}), 103.7 ($\text{C}_{5\text{Uri}}$), 89.2 ($\text{C}_{1\text{Rib}}$), 82.3 ($\text{C}\equiv\text{CH}$), 80.3 ($\text{C}_{4\text{Rib}}$), 78.5 ($\text{C}\equiv\text{C}$), 73.0 ($\text{C}_{2\text{Rib}}$), 70.6 ($\text{C}_{3\text{Rib}}$), 40.2 ($\text{C}_{5\text{Rib}}$), 20.6 (COCH_3), 20.5 (COCH_3); HR-ESI-MS (positive mode) m/z : calcd. for $\text{C}_{21}\text{H}_{21}\text{N}_4\text{O}_8$ $[\text{M}+\text{H}]^+$ 457.1354, found 457.1363.



2,3,4,6-Tetra-*O*-acetyl- β -D-galactopyranosyl azide (**28-Gal**)²³⁵

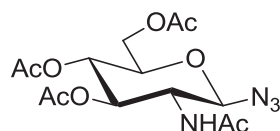
To a solution of 2,3,4,6-tetra-*O*-acetyl- α -D-galactopyranosyl bromide (4.59 g, 11.2 mmol, 1.0 eq.), TBAHS (3.80 g, 11.2 mmol, 1.0 eq.) and NaN_3 (2.91 g, 51.4 mmol, 4.6 eq.) in CH_2Cl_2 (46 mL) was added satd aq. NaHCO_3 (46 mL). The two phase mixture was vigorously stirred at r.t. overnight. Then, EtOAc (300 mL) was added into the reaction. The organic phase was separated and then successively washed with satd aq. NaHCO_3 (100 mL), H_2O (2×100 mL) and brine (100 mL). The combined organic phase was dried over Na_2SO_4 , filtered and evaporated under reduced pressure to afford compound **28-Gal** as white foam (4.166 g, 11.2 mmol, quant.). $R_f = 0.4$ (PE:EtOAc = 2:1); $^1\text{H NMR}$ (300 MHz, CDCl_3) δ = 5.42 (dd, $J = 3.3, 1.0$ Hz, 1H, H_4), 5.17 (dd, $J = 10.4, 8.7$ Hz, 1H, H_2), 5.03 (dd, $J = 10.4, 3.3$ Hz, 1H, H_3), 4.60 (d, $J = 8.7$ Hz, 1H, H_1), 4.19 – 4.14 (m, 2H, $\text{H}_{6a}, \text{H}_{6b}$), 4.02 (ddd, $J = 10.1, 4.0, 1.0$ Hz, 1H, H_5), 2.17 (s, 3H, COCH_3), 2.09 (s, 3H, COCH_3), 2.06 (s, 3H, COCH_3), 1.99 (s, 3H, COCH_3).



2-Acetamido-3,4,6-tri-*O*-acetyl-2-deoxy-D-glucopyranosyl chloride²³⁶

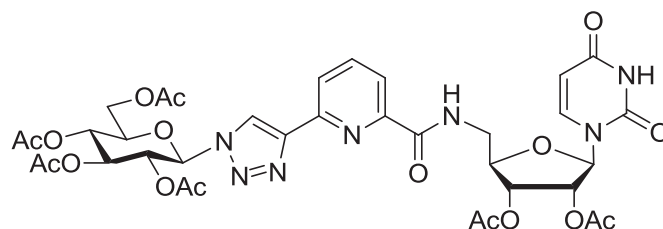
2-Acetamido-2-deoxy-D-glucopyranose (5.00 g, 22.6 mmol, 1.0 eq.) was added to stirred acetyl chloride (10 mL) and the resulting suspension was stirred magnetically at r.t. overnight. Dichloromethane (40 mL) was added into the reaction and the resulting solution was poured into a mixture of ice (40 g) and water (10 mL) with stirring. The organic layer was immediately separated and run into a mixture of saturated aq. NaHCO_3 (40 mL) and ice with stirring, the neutralization being completed in a separating funnel. The organic layer was then separated and dried over MgSO_4 for 10 min. The organic layer was then filtered with suction and the residue was washed with CH_2Cl_2 (15 mL). The resulting deep yellow solution was concentrated to about 10 mL under vacuum. Anhydrous Et_2O (50 mL) was added and the product crystallized 5

min later. The pale yellow solid was then filtered, washed with anhydrous ether (2×15 mL) and allowed to dry with vacuum for 5 min. A mixture of α and β anomers (α : β = 2:1) was afforded (4.627 g, 12.67 mmol, 56%). R_f = 0.71, 0.54 (EtOAc, two spots for α and β anomers, respectively); $^1\text{H NMR}$ (300 MHz, CDCl_3) δ = 6.23 – 6.13 (m, 1H), 5.79 (d, J = 8.6 Hz, 0.65H, $\text{NH}_{\alpha\text{ anomer}}$), 5.55 (d, J = 9.1 Hz, 0.35H, $\text{NH}_{\beta\text{ anomer}}$), 5.37 – 5.16 (m, 2H), 4.52 (m, 1H), 4.33 – 4.20 (m, 2H), 4.10 – 3.93 (m, 1H), 2.21 – 1.91 (m, 12H).



2-Acetamido-3,4,6-tri-*O*-acetyl-2-deoxy- β -D-glucopyranosyl azide (**28-GlcNAc**)²³⁷

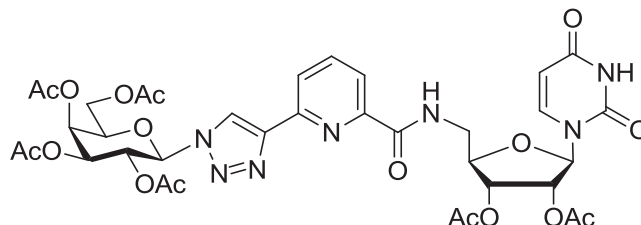
A solution of 2-acetamido-3,4,6-tri-*O*-acetyl-2-deoxy-D-glucopyranosyl chloride (4.093 g, 11.2 mmol, 1.0 eq.) and NaN_3 (1.304 g, 20 mmol, 1.8 eq) in DMF (20 mL) was heated at 80°C for 16 h. Then, the heating was stopped; ice was added into the reaction and the reaction mixture was extracted with EtOAc (3×90 mL). The organic layer was washed with satd NaHCO_3 solution (80 mL), H_2O (2×80 mL) and brine (80 mL). The organic phase was dried over NaSO_4 , filtered and evaporated. The residue was purified by silica gel column chromatography (PE:EtOAc = 1:2) to afford compound **28-GlcNAc** as white foam (1.908 g, 5.1 mmol, 46%). R_f = 0.38 (PE:EtOAc = 1:2); $^1\text{H NMR}$ (300 MHz, CDCl_3) δ (ppm) = 5.51 (d, J = 8.7 Hz, 1H), 5.31 – 5.06 (m, 2H), 4.75 (d, J = 9.3 Hz, 1H), 4.28 (dd, J = 12.5, 4.8 Hz, 1H), 4.20 – 4.13 (m, 1H), 3.78 (ddd, J = 10.0, 4.8, 2.3 Hz, 1H), 2.11 (s, 3H), 2.04 (s, 3H), 2.04 (s, 3H), 1.98 (s, 3H).



6-(2,3,4,6-Tetra-*O*-acetyl- β -D-glucopyranosyl-1*H*-1,2,3-triazol-4-yl)-*N*-(2',3'-di-*O*-acetyl-uridin-5'-yl)picolinamide (**29-Glc**)

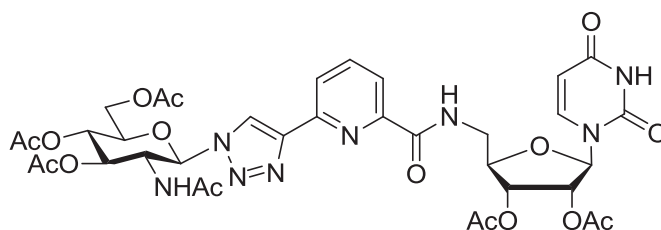
Prepared according to general protocol **C** from compound **28-Glc** (27 mg, 0.072 mmol, 1.0 eq.) and compound **27** (33 mg, 0.072 mmol, 1.0 eq.). The crude product was purified by silica gel column chromatography (100% PE to 100% EtOAc) to afford compound **29-Glc** as white foam (48 mg, 0.058 mmol, 80%). R_f = 0.35 (EtOAc); $[\alpha]_D$ = -44.0 (c = 0.1, CH_2Cl_2); $^1\text{H NMR}$ (400 MHz, CDCl_3) δ (ppm) = 9.05 (s, 1H, NH_{Uri}), 8.56 (s, 1H, $\text{H}_{\text{triazole}}$), 8.50 (t, J = 5.9 Hz, 1H, NHCO), 8.27 (d, J = 7.8 Hz, 1H, H_{Pyr}), 8.17 – 8.11 (m, 1H, H_{Pyr}), 7.94 (t, J = 7.8 Hz, 1H, H_{Pyr}), 7.31 (d, J = 8.1 Hz, 1H, $\text{H}_{6\text{Uri}}$), 5.98 (d, J = 9.2 Hz, 1H, $\text{H}_{1\text{Glc}}$), 5.82 (d, J = 4.3 Hz, 1H, $\text{H}_{1\text{Rib}}$), 5.69 (d, J = 8.1 Hz, 1H, $\text{H}_{5\text{Uri}}$), 5.55 (dd, J = 9.4, 4.3 Hz, 1H, $\text{H}_{2\text{Rib}}$), 5.52 – 5.43 (m, 2H, $\text{H}_{2\text{Glc}}$, $\text{H}_{3\text{Glc}}$), 5.39 (dd, J = 9.4, 6.2 Hz, 1H, $\text{H}_{3\text{Rib}}$), 5.35 – 5.29 (m, 1H, $\text{H}_{4\text{Glc}}$), 4.38 – 4.31 (m, 2H, $\text{H}_{4\text{Rib}}$, $\text{H}_{6a\text{Glc}}$), 4.18 (dd, J = 12.6, 1.9 Hz, 1H, $\text{H}_{6b\text{Glc}}$), 4.09 – 4.01 (m, 1H, $\text{H}_{5\text{Glc}}$), 3.96 – 3.75 (m, 2H, $\text{H}_{5a\text{Rib}}$, $\text{H}_{5b\text{Rib}}$), 2.14 – 1.85 (m, 18H, 6× COCH_3); $^{13}\text{C NMR}$ (100 MHz, CDCl_3) δ (ppm) = 170.7, 170.2, 170.1, 169.8, 169.7, 169.4, 164.7, 162.7, 150.2, 149.3, 148.5, 148.3, 140.8 ($\text{C}_{6\text{Uri}}$),

138.6 (C_{PyrH}), 123.2 (C_{PyrH}), 121.9 (C_{PyrH}), 121.3 (C_{triazole}), 103.5 (C_{5Uri}), 89.9 (C_{1Rib}), 86.0 (C_{1Glc}), 80.1 (C_{4Rib}), 75.4 (C_{5Glc}), 72.9 (C_{2Glc} or C_{3Glc}), 72.8 (C_{2Glc} or C_{3Glc}), 70.70 (C_{2Rib} or C_{3Rib}), 70.69 (C_{2Rib} or C_{3Rib}), 68.0 (C_{4Glc}), 61.9 (C_{6Glc}), 40.5 (C_{5Rib}), 20.8 (COCH₃), 20.69 (COCH₃), 20.64 (COCH₃), 20.61 (COCH₃), 20.56 (COCH₃), 20.3 (COCH₃); HR-ESI-MS (positive mode) *m/z*: calcd. for C₃₅H₄₀N₇O₇ [M+H]⁺ 830.2475, found 830.2462.



6-(2,3,4,6-Tetra-*O*-acetyl-β-D-galactopyranosyl-1*H*-1,2,3-triazol-4-yl)-*N*-(2',3'-di-*O*-acetyl-uridin-5'-yl)picolinamide (29-Gal)

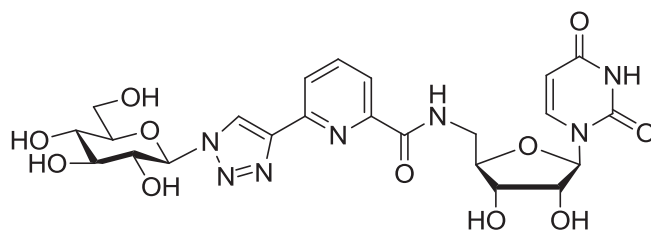
Prepared according to general protocol **B** from compound **27** (50 mg, 0.11 mmol, 1.0 eq.) and **28-Gal** (49 mg, 0.13 mmol, 1.2 eq.). The crude product was purified by silica gel column chromatography (100% PE to 100% EtOAc) to afford compound **29-Gal** as white foam (40 mg, 0.048 mmol, 44%). *R_f* = 0.41 (EtOAc); [α]_D = -17.0 (*c* = 0.2, CH₂Cl₂); ¹H NMR (400 MHz, CDCl₃) δ = 9.30 (d, *J* = 1.4 Hz, 1H, NH_{Uri}), 8.61 (s, 1H, H_{triazole}), 8.47 (t, *J* = 6.3 Hz, 1H, NHCO), 8.26 (d, *J* = 7.8 Hz, 1H, H_{Pyr}), 8.13 (d, *J* = 7.8 Hz, 1H, H_{Pyr}), 7.94 (t, *J* = 7.8 Hz, 1H, H_{Pyr}), 7.33 (d, *J* = 8.1 Hz, 1H, H_{6Uri}), 5.95 (d, *J* = 9.3 Hz, 1H, H_{1Gal}), 5.72 (d, *J* = 3.0 Hz, 1H, H_{1Rib}), 5.70 (dd, *J* = 8.1, 2.2 Hz, 1H, H_{5Uri}), 5.65 (dd, *J* = 10.2, 9.3 Hz, 1H, H_{2Gal}), 5.57 (bd, *J* = 3.4 Hz, 1H, H_{4Gal}), 5.49 – 5.41 (m, 2H, H_{2Rib}, H_{3Rib}), 5.31 (dd, *J* = 10.2, 3.4 Hz, 1H, H_{3Gal}), 4.39 – 4.28 (m, 2H, H_{5Gal}, H_{4Rib}), 4.24 – 4.16 (m, 2H, H_{6aGal}, H_{6bGal}), 3.99 – 3.90 (m, 1H, H_{5aRib}), 4.00 – 3.77 (m, 1H, H_{5bRib}), 2.20 (s, 3H, COCH₃), 2.07 (s, 3H, COCH₃), 2.06 (s, 3H, COCH₃), 2.02 (s, 3H, COCH₃), 2.01 (s, 3H, COCH₃), 1.90 (s, 3H, COCH₃); ¹³C NMR (100 MHz, CDCl₃) δ = 170.5 (C=O), 170.2 (C=O), 170.03 (C=O), 170.01 (C=O), 169.8 (C=O), 169.5 (C=O), 164.9 (NHCO), 162.9 (C=O_{Uri}), 150.2 (C=O_{Uri}), 149.3 (C_{Pyr}), 148.6 (C_{Pyr}), 148.1 (C_{triazole}), 141.3 (C_{6Uri}), 138.5 (C_{PyrH}), 123.4 (C_{PyrH}), 122.0 (C_{PyrH}), 121.3 (C_{triazoleH}), 103.2 (C_{5Uri}), 90.6 (C_{1Rib}), 86.6 (C_{1Gal}), 80.0 (C_{5Gal} or C_{4Rib}), 74.3 (C_{5Gal} or C_{4Rib}), 73.1 (C_{2Rib} or C_{3Rib}), 70.9 (C_{2Rib} or C_{3Rib}), 70.8 (C_{3Gal}), 68.2 (C_{2Gal}), 67.0 (C_{4Gal}), 61.3 (C_{6Gal}), 40.6 (C_{5Rib}), 20.75 (COCH₃), 20.70 (COCH₃), 20.61 (COCH₃), 20.55 (s, 2C, COCH₃), 20.4 (COCH₃); HR-ESI-MS (positive mode) *m/z*: calcd. for C₃₅H₃₉N₇NaO₁₇ [M+Na]⁺ 852.2295, found 852.2287.



6-(2-Acetamido-3,4,6-tri-*O*-acetyl-2-deoxy-1-β-D-glucopyranosyl-1*H*-1,2,3-triazol-4-yl)-*N*-(2',3'-di-*O*-acetyl-uridin-5'-yl)picolinamide (29-GlcNAc)

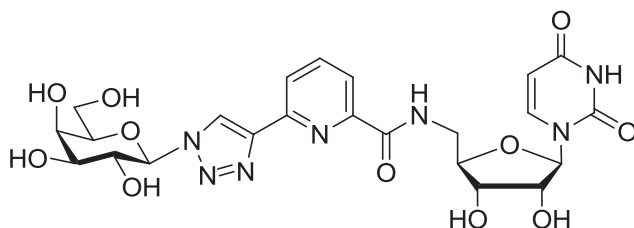
To a solution of 6-ethynyl-*N*-(2',3'-di-*O*-acetyl-uridin-5'-yl)picolinamide (**27-GlcNAc**) (44 mg, 0.10 mmol, 1.0 eq.) and 2-acetamido-3,4,6-tri-*O*-acetyl-2-deoxy-β-D-glucopyranosyl azide

(**28-GlcNAc**) (53 mg, 0.14 mmol, 1.4 eq.) in *t*BuOH/H₂O (4 mL/200 μL) were added CuSO₄ (100 μL, 0.1 M in H₂O, 0.01 mmol, 0.1 eq.), sodium ascorbate (200 μL, 0.1 M in H₂O, 0.02 mmol, 0.2 eq.) and DIPEA (0.1 mL, to adjust pH value around 8). Then, the reaction mixture was stirred at 38°C. After 3 h, the reaction mixture was concentrated and the residue was purified by silica gel column chromatography (60% EtOAc/PE to 10% MeOH/EtOAc) to afford compound **29-GlcNAc** as white foam (41 mg, 0.05 mmol, 50%). *R*_f = 0.10 (EtOAc); [α]_D = -19.3 (*c* = 0.7, CH₂Cl₂); ¹H NMR (400 MHz, CDCl₃) δ (ppm) = 9.90 (s, 1H, H_{3Uri}), 8.63 (t, *J* = 6.0 Hz, 1H, CONH), 8.59 (s, 1H, H_{triazole}), 8.18 (d, *J* = 7.8 Hz, 1H, H_{Pyr}), 8.12 (d, *J* = 7.8 Hz, 1H, H_{Pyr}), 7.91 (t, *J* = 7.8 Hz, 1H, H_{Pyr}), 7.36 (d, *J* = 8.1 Hz, 1H, H_{6Uri}), 7.08 (d, *J* = 8.9 Hz, 1H, NHAc), 6.31 (d, *J* = 9.8 Hz, 1H, H_{1GlcNAc}), 5.74 (d, *J* = 4.7 Hz, 1H, H_{1Rib}), 5.65 – 5.55 (m, 2H, H_{5Uri}, H_{3GlcNAc}), 5.51 (dd, *J* = 5.7, 4.7 Hz, 1H, H_{2Rib}), 5.43 (t, *J* = 5.7 Hz, 1H, H_{3Rib}), 5.27 (t, *J* = 9.6 Hz, 1H, H_{4GlcNAc}), 4.60 (dd, *J* = 10.6, 9.8 Hz, 1H, H_{2GlcNAc}), 4.41 – 4.27 (m, 2H, H_{4Rib}, H_{6aGlcNAc}), 4.19 – 4.11 (m, 2H, H_{5GlcNAc}, H_{6bGlcNAc}), 4.02 (dd, *J* = 14.3, 5.6 Hz, 1H, H_{5aRib}), 3.79 (dd, *J* = 14.3, 4.4 Hz, 1H, H_{5bRib}), 2.13 – 1.99 (m, 15H, 5×COCH₃), 1.76 (s, 3H, NHAc); ¹³C NMR (100 MHz, CDCl₃) δ (ppm) = 171.6 (COCH₃), 170.9 (COCH₃), 170.8 (COCH₃), 170.0 (COCH₃), 169.8 (COCH₃), 169.7 (COCH₃), 165.1, 163.4, 150.4, 149.4, 148.6, 147.7, 141.5 (C_{6Uri}), 138.6 (C_{PyrH}), 123.3 (C_{PyrH}), 122.0 (s, 2C, C_{PyrH}, C_{triazoleH}), 103.2 (C_{5Uri}), 90.5 (C_{1Rib}), 86.0 (C_{1GlcNAc}), 80.4 (C_{4Rib}), 75.0 (C_{5GlcNAc}), 72.7 (C_{2Rib}), 72.3 (C_{3GlcNAc}), 70.6 (C_{3Rib}), 68.3 (C_{4GlcNAc}), 62.1 (C_{6GlcNAc}), 54.1 (C_{2GlcNAc}), 40.2 (C_{5Rib}), 22.85 (COCH₃), 20.82 (COCH₃), 20.75 (COCH₃), 20.74 (COCH₃), 20.60 (COCH₃), 20.55 (COCH₃); HR-ESI-MS (positive mode) *m/z*: calcd. for C₃₅H₄₁N₈O₁₆ [M+H]⁺ 829.2635, found 829.2610.



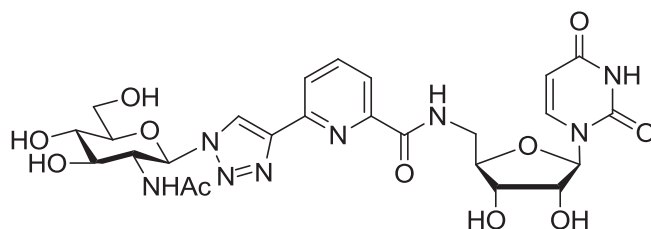
6-(1-β-D-Glucopyranosyl-1H-1,2,3-triazol-4-yl)-N-(uridin-5'-yl)picolinamide (**30-Glc**)

Prepared according to general protocol **E** from compound **29-Glc** (30 mg, 0.036 mmol, 1.0 eq.). The residue was purified by C18 reverse phase column chromatography (100% H₂O to 50% MeOH/H₂O) to afford compound **30-Glc** as white foam (16 mg, 0.028 mmol, 78%). [α]_D = +8.0 (*c* = 0.3, H₂O); ¹H NMR (400 MHz, D₂O) δ (ppm) = 8.62 (s, 1H, H_{triazole}), 7.89 – 7.75 (m, 3H, 3×H_{Pyr}), 7.40 (d, *J* = 7.9 Hz, 1H, H_{6Uri}), 5.77 – 5.72 (m, 2H, H_{1Uri}, H_{1Glc}), 5.35 (d, *J* = 7.9 Hz, 1H), 4.28 (dd, *J* = 4.9, 3.2 Hz, 1H), 4.20 – 4.09 (m, 2H), 4.03 – 3.92 (m, 2H), 3.85 – 3.59 (m, 6H); ¹³C NMR (100 MHz, D₂O) δ (ppm) = 166.5, 161.1, 154.4, 148.3, 147.6, 146.9, 141.7 (C_{6Uri}), 139.5 (C_{PyrH}), 124.0 (C_{triazoleH}), 123.7 (C_{PyrH}), 122.0 (C_{PyrH}), 102.5 (C_{5Uri}), 91.1 (C_{1Rib}), 88.1 (C_{1Glc}), 82.1, 79.4, 76.3, 73.6, 72.8, 70.9, 69.4, 60.9 (C_{6Glc}), 40.3 (C_{5Rib}); HR-ESI-MS (positive mode) *m/z*: calcd. for C₂₃H₂₇N₇NaO₁₁ [M+Na]⁺ 600.1661, found 600.1640.



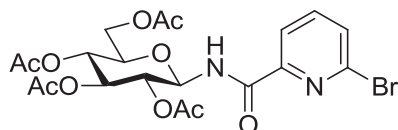
6-(1-β-D-galactopyranosyl-1H-1,2,3-triazol-4-yl)-N-(uridin-5'-yl)picolinamide (30-Gal)

Prepared according to general protocol E from compound **29-Gal** (42 mg, 0.05 mmol, 1.0 eq.). The residue was purified by C18 reverse phase column chromatography (100% H₂O to 50% MeOH/H₂O) to afford compound **30-Gal** as white foam (23 mg, 0.04 mmol, 80%). $[\alpha]_D = +98.5$ ($c = 0.2$, H₂O); ¹H NMR (400 MHz, D₂O) $\delta = 8.59$ (s, 1H, H_{triazole}), 7.81 – 7.65 (m, 3H, H_{Pyr}), 7.34 (d, $J = 7.7$ Hz, 1H, H_{6Uri}), 5.77 (d, $J = 2.5$ Hz, 1H, H_{1Rib}), 5.70 (d, $J = 9.1$ Hz, 1H, H_{1Gal}), 5.31 (d, $J = 7.7$ Hz, 1H, H_{5Uri}), 4.30 – 4.21 (m, 2H), 4.19 – 4.01 (m, 4H), 3.93 – 3.71 (m, 4H), 3.65 – 3.56 (m, 1H, H_{5bUri}); ¹³C NMR (100 MHz, D₂O) $\delta = 172.12$ (C=O_{Uri}), 166.3 (NHCO), 156.1 (C=O_{Uri}), 148.1 (C_{Pyr}), 147.5 (C_{Pyr}), 146.9 (C_{triazole}), 141.2 (C_{6Uri}), 139.4 (C_{PyrH}), 123.7 (C_{triazoleH}), 123.5 (C_{PyrH}), 121.9 (C_{PyrH}), 102.7 (C_{5Uri}), 90.9 (C_{1Rib}), 88.7 (C_{1Gal}), 82.0, 78.8, 73.6, 73.4, 71.0, 70.1, 69.0, 61.4 (C_{6Gal}), 40.3 (C_{5Rib}); HR-ESI-MS (positive mode) m/z : calcd. for C₂₃H₂₇N₇NaO₁₁ [M+Na]⁺ 600.1661, found 600.1658.



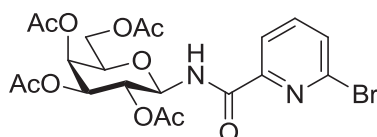
6-(2-Acetamido-2-deoxy-1-β-D-glucopyranosyl-1H-1,2,3-triazol-4-yl)-N-(uridin-5'-yl)picolinamide (30-GlcNAc)

Prepared according to general protocol E from compound **29-GlcNAc** (41 mg, 0.05 mmol, 1.0 eq.). The residue was purified by C18 reverse phase column chromatography (100% H₂O to 70% MeOH/H₂O) to afford compound **30-GlcNAc** as white foam (35 mg, 0.05 mmol, quant.). $[\alpha]_D = +19.1$ ($c = 0.4$, H₂O); ¹H NMR (400 MHz, D₂O) δ (ppm) = 8.68 (s, 1H, H_{triazole}), 7.90 – 7.78 (m, 3H, H_{Pyr}), 7.48 (d, $J = 7.9$ Hz, 1H, H_{6Uri}), 5.86 (d, $J = 9.6$ Hz, 1H, H_{1GlcNAc}), 5.74 (d, $J = 3.0$ Hz, 1H, H_{1Rib}), 5.45 (d, $J = 7.9$ Hz, 1H, H_{5Uri}), 4.33 – 4.28 (m, 1H, H_{2Rib}), 4.27 – 4.11 (m, 3H), 4.02 – 3.95 (m, 1H, H_{6aGlcNAc}), 3.90 – 3.64 (m, 6H), 1.78 (s, 3H, NHAc); ¹³C NMR (100 MHz, D₂O) δ (ppm) = 174.5, 168.4, 166.6, 153.3, 148.5, 147.7, 146.9, 141.9 (C_{6Uri}), 139.6 (C_{PyrH}), 123.8 (C_{PyrH}), 123.4 (C_{triazole}), 122.0 (C_{PyrH}), 102.4 (C_{5Uri}), 91.0 (C_{1Rib}), 86.9 (C_{1GlcNAc}), 82.2, 79.4, 73.8, 73.5 (C_{2Rib}), 71.0, 69.7, 61.0 (C_{6GlcNAc}), 56.0 (C_{2GlcNAc}), 40.5 (C_{5Rib}), 22.0 (NHCOCH₃); HR-ESI-MS (positive mode) m/z : calcd. for C₂₅H₃₀N₈NaO₁₁ [M+Na]⁺ 641.1926, found 641.1920.



6-Bromo-*N*-(2,3,4,6-tetra-*O*-acetyl- β -D-glucopyranosyl)picolinamide (**31-Glc**)

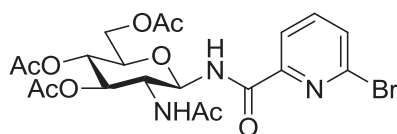
6-Bromopicolinic acid (**23**) (812 mg, 4.02 mmol, 3.0 eq.) and HOBT (633 mg, 4.69 mmol, 3.5 eq.) were co-evaporated with toluene (3×15 mL) and THF (3×6 mL). The mixture was dried with vacuum for another 1 h. Then, the mixture was dissolved in dry THF (8 mL) under argon and cooled to 0°C. DIC (720 μ L, 4.69 mmol, 3.5 eq.) was added dropwise at 0°C. After addition, the ice-bath was removed; the reaction was stirred at r.t. for 30 min. At the same time, 2,3,4,6-tetra-*O*-acetyl- β -D-glucopyranosyl azide (**28-Glc**) (500 mg, 1.34 mmol, 1.0 eq.) was dissolved in dry THF (8 mL) under argon and cooled to 0°C. PMe_3 (2.7 mL, 1 M in THF, 2.68 mmol, 2.0 eq.) was added into the flask at 0°C and the reaction was stirred at 0°C for 30 min. When there was no bubbling (~30 min), the solution was transferred into the flask containing the acid. The reaction mixture was stirred with an ice-bath for 1 h, then, the ice-bath was removed and the reaction was stirred at r.t. for 16 h. The reaction mixture was diluted with water (150 mL), extracted with EtOAc (3×200 mL), the combined organic layers were washed with satd Na_2CO_3 solution (3×100 mL), H_2O (100 mL) and brine (100 mL). The organic phase was dried (Na_2SO_4), concentrated and dried with vacuum. The residue was purified by silica gel column chromatography (PE to PE:EtOAc = 1:1) to afford compound **31-Glc** as yellow foam (552 mg, 1.04 mmol, 78%). $R_f = 0.45$ (PE:EtOAc, 1:1); $[\alpha]_D = -31.1$ ($c = 2.0$, CH_2Cl_2); $^1\text{H NMR}$ (400 MHz, CDCl_3) $\delta = 8.46$ (d, $J = 9.7$ Hz, 1H, NHCO), 8.12 (dd, $J = 7.7, 0.8$ Hz, 1H, H_{Pyr}), 7.71 (t, $J = 7.7$ Hz, 1H, H_{Pyr}), 7.64 (dd, $J = 7.9, 0.8$ Hz, 1H, H_{Pyr}), 5.44 (dd, $J = 9.7, 9.6$ Hz, 1H, $\text{H}_{1\text{Glc}}$), 5.35 (t, $J = 9.5$ Hz, 1H, $\text{H}_{3\text{Glc}}$), 5.19 – 5.09 (m, 2H, $\text{H}_{2\text{Glc}}, \text{H}_{4\text{Glc}}$), 4.30 (dd, $J = 12.5, 4.3$ Hz, 1H, $\text{H}_{6a\text{Glc}}$), 4.14 – 4.04 (m, 1H, $\text{H}_{6b\text{Glc}}$), 3.88 (ddd, $J = 10.1, 4.3, 2.1$ Hz, 1H, $\text{H}_{5\text{Glc}}$), 2.07 (s, 3H, COCH_3), 2.03 (s, 3H, COCH_3), 2.02 (s, 3H, COCH_3), 1.97 (s, 3H, COCH_3); $^{13}\text{C NMR}$ (100 MHz, CDCl_3) δ (ppm) = 170.8, 170.3, 170.2, 169.6, 163.6, 149.6, 141.0, 139.7 (C_{PyrH}), 131.7 (C_{PyrH}), 121.8 (C_{PyrH}), 78.5 ($\text{C}_{1\text{Glc}}$), 73.9 ($\text{C}_{5\text{Glc}}$), 73.1 ($\text{C}_{3\text{Glc}}$), 70.6 ($\text{C}_{2\text{Glc}}$ or $\text{C}_{4\text{Glc}}$), 68.7 ($\text{C}_{2\text{Glc}}$ or $\text{C}_{4\text{Glc}}$), 61.8 ($\text{C}_{6\text{Glc}}$), 20.9 (COCH_3), 20.73 (COCH_3), 20.71 (COCH_3), 20.67 (COCH_3); HR-ESI-MS (positive mode) m/z : calcd. for $\text{C}_{20}\text{H}_{24}\text{BrN}_2\text{O}_{10}$ $[\text{M}+\text{H}]^+$ 531.0609, found 531.0614.



6-Bromo-*N*-(2,3,4,6-tetra-*O*-acetyl- β -D-galactopyranosyl)picolinamide (**31-Gal**)

6-Bromopicolinic acid (**23**) (648 mg, 3.21 mmol, 3.0 eq.) and HOBT (506 mg, 3.70 mmol, 3.5 eq.) were co-evaporated with toluene (3×15 mL) and THF (3×8 mL). The mixture was dried with vacuum for another 1 h. Then, the mixture was dissolved in dry THF (8 mL) under argon and cooled to 0°C. DIC (576 μ L, 3.70 mmol, 3.5 eq.) was added dropwise at 0°C. After addition, the ice-bath was removed; the reaction was stirred at r.t. for 30 min. At the same time, 2,3,4,6-tetra-*O*-acetyl- β -D-galactopyranosyl azide (**28-Gal**) (400 mg, 1.07 mmol, 1.0 eq.) was dissolved in dry THF (8 mL) under argon and cooled to 0°C. PMe_3 (2.1 mL, 1 M in THF, 2.14 mmol, 2.0 eq.) was added into the flask at 0°C and the reaction was stirred at 0°C for 30 min.

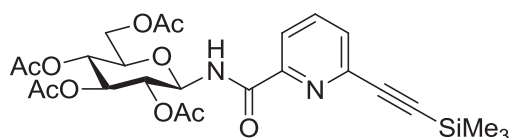
When there was no bubbling (~30 min), the solution was transferred into the flask containing the acid. The reaction was stirred with an ice-bath for 1 h, then, the ice-bath was removed and the reaction was stirred at r.t. for 16 h. The reaction mixture was diluted with water (100 mL), extracted with EtOAc (3×150 mL), the combined organic layers were washed with satd Na₂CO₃ solution (3×100 mL), H₂O (100 mL) and brine (100 mL). The organic phase was dried (Na₂SO₄), concentrated and dried with vacuum. The residue was purified by silica gel column chromatography (PE to PE:EtOAc = 1:1) to afford compound **31-Gal** as yellow foam (579 mg, contaminated with 1,3-Diisopropylurea, according to *Synlett*. **2010**, 8, 1276-1280): ¹H NMR (300 MHz, CDCl₃) δ (ppm) = 1.14 (d, *J* = 6.4 Hz, 12H), 3.87 – 3.80 (m, 2H); ¹³C NMR (75 MHz, CDCl₃) δ (ppm) = 23.5, 42.2, 157.0. R_f = 0.45 (PE:EtOAc = 1:1); ¹H NMR (400 MHz, CDCl₃) δ (ppm) = 8.48 (d, *J* = 9.5 Hz, 1H, NH), 8.13 (d, *J* = 7.7 Hz, 1H, H_{PyR}), 7.71 (t, *J* = 7.7 Hz, 1H, H_{PyR}), 7.64 (d, *J* = 8.7 Hz, 1H, H_{PyR}), 5.46 (bd, *J* = 3.4 Hz, 1H, H₄), 5.41 (d, *J* = 9.4 Hz, 1H, H₁), 5.33 (dd, *J* = 10.1, 9.4 Hz, 1H, H₂), 5.17 (dd, *J* = 10.1, 3.4 Hz, 1H, H₃), 4.16 – 4.05 (m, 3H, H_{6a}, H_{6b}, H₅), 2.18 (s, 3H, COCH₃), 2.02 (s, 3H, COCH₃), 2.00 (s, 3H, COCH₃), 1.97 (s, 3H, COCH₃); ¹³C NMR (100 MHz, CDCl₃) δ (ppm) = 170.52 (C=O), 170.47 (C=O), 170.3 (C=O), 170.1 (C=O), 163.5 (NHCO), 149.7 (C_{PyR}), 141.0 (C_{PyR}), 139.7 (C_{PyRH}), 131.7 (C_{PyRH}), 121.8 (C_{PyRH}), 78.8 (C₁), 72.6 (C₅), 71.2 (C₃), 68.3 (C₂), 67.3 (C₄), 61.4 (C₆), 20.80 (s, 2C, COCH₃), 20.74 (COCH₃), 20.69 (COCH₃); HR-ESI-MS (positive mode) *m/z*: calcd. for C₂₀H₂₄BrN₂O₁₀ [M+H]⁺ 531.0609, found 531.0610.



6-Bromo-*N*-(2-acetamido-3,4,6-tri-*O*-acetyl-2-deoxy-β-*D*-glucopyranosyl)picolinamide (**31-GlcNAc**)

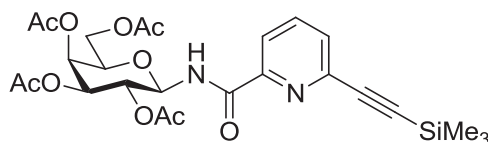
6-Bromopicolinic acid (**23**) (812 mg, 4.02 mmol, 3.0 eq.) and HOBT (633 mg, 4.69 mmol, 3.5 eq.) were co-evaporated with toluene (3×15 mL) and THF (3×6 mL). The mixture was dried under vacuum for another 1 h. Then, the mixture was dissolved in dry THF (8 mL) under argon and cooled to 0°C. DIC (720 μL, 4.69 mmol, 3.5 eq.) was added dropwise at 0°C. After addition, the ice-bath was removed and the reaction was stirred at r.t. for 30 min. At the same time, 2-acetamido-3,4,6-tri-*O*-acetyl-2-deoxy-β-*D*-glucopyranoside azide (**28-GlcNAc**) (500 mg, 1.34 mmol, 1.0 eq.) was dissolved in dry THF (8 mL) under argon and cooled to 0°C. PMe₃ (2.7 mL, 1 M in THF, 2.14 mmol, 2.0 eq.) was added into the flask at 0°C and the reaction was stirred at 0°C for 30 min. When there was no bubbling (~30 min), the solution was transferred into the flask containing the acid. Then, the color of the reaction mixture changed from transparent to orange. The reaction mixture was stirred with an ice-bath for 1 h, then, the ice-bath was removed and the reaction was stirred at r.t. for 16 h. The reaction mixture was diluted with water (150 mL), extracted with EtOAc (3×200 mL), the combined organic layers were washed with satd Na₂CO₃ solution (3×100 mL), H₂O (100 mL) and brine (100 mL). The organic phase was dried (Na₂SO₄), concentrated and dried under vacuum. The residue was purified by silica gel column chromatography (PE to PE:EtOAc = 3:7) to afford compound **31-GlcNAc** as yellow foam [678 mg, 95%, with 0.17 eq. contaminant 1,3-diisopropylurea, according to *Synlett*. **2010**, 8, 1276-1280, data of 1,3-diisopropylurea: ¹H NMR (300 MHz, CDCl₃) δ (ppm) = 1.14 (d, *J* = 6.4 Hz, 12H), 3.87 – 3.80 (m, 2H); ¹³C NMR (75 MHz, CDCl₃) δ

(ppm) = 23.5, 42.2, 157.0). R_f = 0.19 (PE:EtOAc = 1:2)]; $^1\text{H NMR}$ (400 MHz, CDCl_3) δ (ppm) = 8.71 (d, J = 9.3 Hz, 1H, NHCO), 8.11 (dd, J = 7.5, 0.7 Hz, 1H, H_{Pyr}), 7.74 – 7.58 (m, 2H, 2 H_{Pyr}), 6.16 (d, J = 9.1 Hz, 1H, NHAc), 5.36 (dd, J = 9.7, 9.3 Hz, 1H, H_1), 5.22 – 5.13 (m, 2H, H_3 , H_4), 4.39 (dd, J = 9.7, 9.1 Hz, 1H, H_2), 4.28 (dd, J = 12.5, 4.3 Hz, 1H, H_{6a}), 4.10 (dd, J = 12.5, 2.0 Hz, 1H, H_{6b}), 3.91 – 3.59 (m, 1H, H_5), 2.10 – 2.01 (m, 9H, 3 \times COCH₃), 1.85 (s, 3H, COCH₃); $^{13}\text{C NMR}$ (100 MHz, CDCl_3) δ (ppm) = 171.7 (COCH₃), 171.0 (COCH₃), 170.9 (COCH₃), 169.4 (COCH₃), 164.0 (CONH), 149.7 (C_{Pyr}), 141.1 (C_{Pyr}), 139.6 (C_{PyrH}), 131.6 (C_{PyrH}), 121.7 (C_{PyrH}), 78.0 (C_1), 74.0 (C_5), 73.4 (C_3), 68.0 (C_4), 61.9 (C_6), 53.3 (C_2), 23.1 (COCH₃), 20.88 (COCH₃), 20.86 (COCH₃), 20.7 (COCH₃); HR-ESI-MS (positive mode) m/z : calcd. for $\text{C}_{20}\text{H}_{25}\text{BrN}_3\text{O}_9$, $[\text{M}+\text{H}]^+$ 530.0769, found 530.0776.



6-(2-(Trimethylsilyl)ethynyl)-*N*-(2,3,4,6-tetra-*O*-acetyl- β -D-glucopyranosyl)picolinamide (32-Glc)

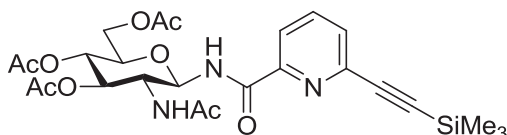
Prepared according to general protocol **D** from compound **31-Glc** (310 mg, 0.58 mmol, 1.0 eq.). The crude product was purified by silica gel column chromatography (100% PE to 30% EtOAc/PE) to afford compound **32-Glc** as yellow foam (288 mg, 0.526 mmol, 90%). R_f = 0.43 (PE:EtOAc, 1:1); $[\alpha]_D$ = -35.4 (c = 2.4, CH_2Cl_2); $^1\text{H NMR}$ (400 MHz, CDCl_3) δ (ppm) = 8.57 (d, J = 9.9 Hz, 1H, NHCO), 8.09 (dd, J = 7.8, 0.8 Hz, 1H, H_{Pyr}), 7.79 (t, J = 7.8 Hz, 1H, H_{Pyr}), 7.58 (dd, J = 7.8, 0.8 Hz, 1H, H_{Pyr}), 5.49 (d, J = 9.6 Hz, 1H, $\text{H}_{1\text{Glc}}$), 5.34 (t, J = 9.5 Hz, 1H, $\text{H}_{3\text{Glc}}$), 5.20 – 5.11 (m, 2H, $\text{H}_{2\text{Glc}}$, $\text{H}_{4\text{Glc}}$), 4.30 (dd, J = 12.5, 4.3 Hz, 1H, $\text{H}_{6a\text{Glc}}$), 4.08 (dd, J = 12.5, 1.9 Hz, 1H, $\text{H}_{6b\text{Glc}}$), 3.87 (ddd, J = 10.1, 4.3, 1.9 Hz, 1H, $\text{H}_{5\text{Glc}}$), 2.07 (s, 3H, COCH₃), 2.03 (s, 3H, COCH₃), 2.01 (s, 3H, COCH₃), 1.96 (s, 3H, COCH₃), 0.30 (s, 9H, SiMe₃); $^{13}\text{C NMR}$ (100 MHz, CDCl_3) δ (ppm) = 170.8, 170.2, 170.1, 169.6, 164.4, 148.8, 142.1, 137.6 (C_{PyrH}), 130.7 (C_{PyrH}), 122.1 (C_{PyrH}), 102.9 (C_{alkyne}), 96.6 (C_{alkyne}), 78.3 ($\text{C}_{1\text{Glc}}$), 73.9 ($\text{C}_{5\text{Glc}}$), 73.4 ($\text{C}_{3\text{Glc}}$), 70.7 ($\text{C}_{2\text{Glc}}$ or $\text{C}_{4\text{Glc}}$), 68.2 ($\text{C}_{2\text{Glc}}$ or $\text{C}_{4\text{Glc}}$), 61.8 ($\text{C}_{6\text{Glc}}$), 20.9 (COCH₃), 20.73 (COCH₃), 20.72 (COCH₃), 20.69 (COCH₃), -0.2 (s, 3C, SiMe₃); HR-ESI-MS (positive mode) m/z : calcd. for $\text{C}_{25}\text{H}_{33}\text{N}_2\text{O}_{10}\text{Si}$ $[\text{M}+\text{H}]^+$ 549.1899, found 549.1898.



6-(2-(Trimethylsilyl)ethynyl)-*N*-(2,3,4,6-tetra-*O*-acetyl- β -D-galactopyranosyl)picolinamide (32-Gal)

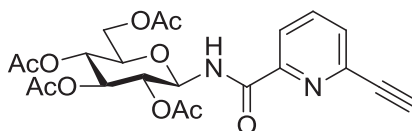
Prepared according to general protocol **D** from compound **31-Gal** (543 mg, 1.0 mmol, 1.0 eq.). The crude product was purified by silica gel column chromatography (100% PE to 30% EtOAc/PE) to afford compound **32-Gal** as yellow foam (512 mg, 0.93 mmol, 93%). R_f = 0.43 (PE:EtOAc = 1:1); $^1\text{H NMR}$ (400 MHz, CDCl_3) δ = 8.59 (d, J = 9.8 Hz, 1H, NHCO), 8.10 (dd, J = 7.8, 0.9 Hz, 1H, H_{pyr}), 7.79 (t, J = 7.8 Hz, 1H, H_{pyr}), 7.59 (dd, J = 7.8, 0.9 Hz, 1H, H_{pyr}), 5.49 – 5.42 (m, 2H, H_1 , H_4), 5.35 (t, J = 9.7 Hz, 1H, H_2), 5.17 (dd, J = 9.7, 3.4 Hz, 1H, H_3), 4.15 –

4.04 (m, 3H, H₅, H_{6a}, H_{6b}), 2.19 (s, 3H, COCH₃), 2.02 (s, 3H, COCH₃), 1.99 (s, 3H, COCH₃), 1.96 (s, 3H, COCH₃), 0.30 (s, 9H, SiMe₃); ¹³C NMR (100 MHz, CDCl₃) δ = 170.5 (COCH₃), 170.32 (COCH₃), 170.31 (COCH₃), 170.1 (COCH₃), 164.4 (CONH), 148.9 (C_{Pyr}), 142.1 (C_{Pyr}), 137.6 (C_{PyrH}), 130.8 (C_{PyrH}), 122.1 (C_{PyrH}), 103.0 (C_{alkyne}), 96.5 (C_{alkyne}), 78.7 (C₁), 72.7 (C₅), 71.5 (C₃), 68.4 (C₂), 67.4 (C₄), 61.5 (C₆), 20.80 (s, 2C, COCH₃), 20.76 (COCH₃), 20.69 (COCH₃), -0.2 (SiMe₃); HR-ESI-MS (positive mode) *m/z*: calcd. for C₂₅H₃₃N₂O₁₀Si [M+H]⁺ 549.1899, found 549.1908.



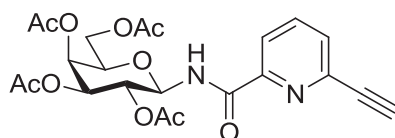
6-(2-Trimethylsilylethynyl)-*N*-(2-acetamido-3,4,6-tri-*O*-acetyl-2-deoxy-β-*D*-glucopyranosyl)picolinamide (**32-GlcNAc**)

Prepared according to general protocol **D** from compound **31-GlcNAc** (543 mg, 1.0 mmol, 1.0 eq.). The crude product was purified by silica gel column chromatography (100% PE to 60% EtOAc/PE) to afford compound **32-GlcNAc** as yellow foam (552 mg, 98%, with a little contaminant at aromatic zone ~7.5). *R*_f = 0.32 (PE:EtOAc = 1:3); ¹H NMR (300 MHz, CDCl₃) δ (ppm) = 8.73 (d, *J* = 9.7 Hz, 1H, NHCO), 8.09 (d, *J* = 7.8 Hz, 1H, H_{Pyr}), 7.78 (t, *J* = 7.8 Hz, 1H, H_{Pyr}), 7.58 (d, *J* = 7.8 Hz, 1H, H_{Pyr}), 6.23 (d, *J* = 9.4 Hz, 1H, NHAc), 5.44 (dd, *J* = 9.7, 9.4 Hz, H₁), 5.26 – 5.10 (m, 2H, H₃, H₄), 4.40 (dd, *J* = 9.7, 9.4 Hz, 1H, H₂), 4.27 (dd, *J* = 12.5, 4.3 Hz, 1H, H_{6a}), 4.09 (dd, *J* = 12.5, 4.6 Hz, 1H, H_{6b}), 3.88 – 3.78 (m, 1H, H₅), 2.08 (s, 3H, COCH₃), 2.05 (s, 3H, COCH₃), 2.03 (s, 3H, COCH₃), 1.83 (s, 3H, COCH₃), 0.29 (s, 9H, SiMe₃); ESI-MS (positive mode) *m/z*: [M+H]⁺ 548.2, [M+Na]⁺ 570.2.



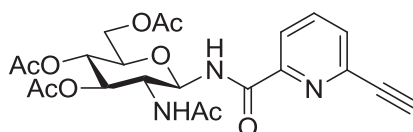
6-Ethynyl-*N*-(2,3,4,6-tetra-*O*-acetyl-β-*D*-glucopyranosyl)picolinamide (**33-Glc**)

Prepared according to general protocol **F** from compound **32-Glc** (236 mg, 0.42 mmol, 1.0 eq.). The crude product was purified by silica gel column chromatography (100% PE to 35% EtOAc/PE) to afford compound **33-Glc** as yellow foam (154 mg, 0.324 mmol, 77%). *R*_f = 0.39 (PE:EtOAc = 1:1); [α]_D²⁰ = -50.0 (*c* = 0.8, CH₂Cl₂); ¹H NMR (400 MHz, CDCl₃) δ (ppm) = 8.59 (d, *J* = 9.9 Hz, 1H, NHCO), 8.14 (dd, *J* = 7.8, 1.1 Hz, 1H, H_{Pyr}), 7.83 (t, *J* = 7.8 Hz, 1H, H_{Pyr}), 7.61 (dd, *J* = 7.8, 1.1 Hz, 1H, H_{Pyr}), 5.47 (d, *J* = 9.6 Hz, 1H, H₁), 5.35 (t, *J* = 9.5 Hz, 1H, H₃), 5.17 – 5.06 (m, 2H, H₂, H₄), 4.29 (dd, *J* = 12.5, 4.3 Hz, 1H, H_{6a}), 4.15 – 4.05 (m, 1H, H_{6b}), 3.88 (ddd, *J* = 10.1, 4.3, 2.1 Hz, 1H, H₅), 3.22 (s, 1H, C≡CH), 2.07 (s, 3H, COCH₃), 2.03 (s, 3H, COCH₃), 2.02 (s, 3H, COCH₃), 1.96 (s, 3H, COCH₃); ¹³C NMR (100 MHz, CDCl₃) δ (ppm) = 170.8 (C=O), 170.18 (C=O), 170.15 (C=O), 169.6 (C=O), 164.2 (CONH), 149.0 (C_{Pyr}), 141.3 (C_{Pyr}), 137.8 (C_{PyrH}), 130.7 (C_{PyrH}), 122.5 (C_{PyrH}), 82.0 (C≡CH), 78.5 (C₁), 78.4 (C≡CH), 73.9 (C₅), 73.3 (C₃), 70.6 (C₂ or C₄), 68.2 (C₂ or C₄), 61.8 (C₆), 20.9 (COCH₃), 20.74 (COCH₃), 20.73 (COCH₃), 20.66 (COCH₃); HR-ESI-MS (positive mode) *m/z*: calcd. for C₂₂H₂₄N₂NaO₁₀ [M+Na]⁺ 499.1323, found 499.1346.



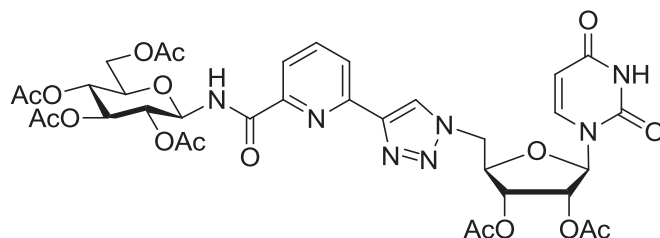
6-Ethynyl-*N*-(2,3,4,6-tetra-*O*-acetyl- β -D-galactopyranosyl)picolinamide (**33-Gal**)

Prepared according to general protocol **F** from compound **32-Gal** (496 mg, 0.55 mmol, 1.0 eq.). The crude product was purified by silica gel column chromatography (100% PE to 35% EtOAc/PE) to afford compound **33-Gal** as yellow foam (207 mg, 0.435 mmol, 79%). $R_f = 0.38$ (PE:EtOAc = 1:1); $[\alpha]_D^{20} = -26.5$ ($c = 2.2$, CH_2Cl_2); $^1\text{H NMR}$ (400 MHz, CDCl_3) δ (ppm) = 8.60 (d, $J = 9.8$ Hz, 1H, NHCO), 8.12 (d, $J = 7.8$ Hz, 1H, H_{Pyr}), 7.81 (t, $J = 7.8$ Hz, 1H, H_{Pyr}), 7.63 – 7.56 (m, 1H, H_{Pyr}), 5.49 – 5.38 (m, 2H, H_4 , H_1), 5.31 (dd, $J = 10.2$, 9.7 Hz, 1H, H_2), 5.15 (dd, $J = 10.2$, 3.4 Hz, 1H, H_3), 4.16 – 4.00 (m, 3H, H_5 , H_6), 3.23 (s, 1H, $\text{C}\equiv\text{CH}$), 2.15 (s, 3H, COCH_3), 1.99 (s, 3H, COCH_3), 1.97 (s, 3H, COCH_3), 1.93 (s, 3H, COCH_3); $^{13}\text{C NMR}$ (100 MHz, CDCl_3) δ (ppm) = 170.5 (C=O), 170.30 (C=O), 170.25 (C=O), 167.0 (C=O), 164.0 (CONH), 149.0 (C_{Pyr}), 141.2 (C_{Pyr}), 137.8 (C_{PyrH}), 130.6 (C_{PyrH}), 122.5 (C_{PyrH}), 82.0 ($\text{C}\equiv\text{CH}$), 78.6 ($\text{C}\equiv\text{CH}$), 78.4 (C_1), 72.5 (C_5), 71.3 (C_3), 68.3 (C_2), 67.3 (C_4), 61.4 (C_6), 20.71 (s, 2C, COCH_3), 20.66 (COCH_3), 20.62 (COCH_3); HR-ESI-MS (positive mode) m/z : calcd. for $\text{C}_{22}\text{H}_{24}\text{N}_2\text{NaO}_{10}$ $[\text{M}+\text{Na}]^+$ 499.1323, found 499.1307.



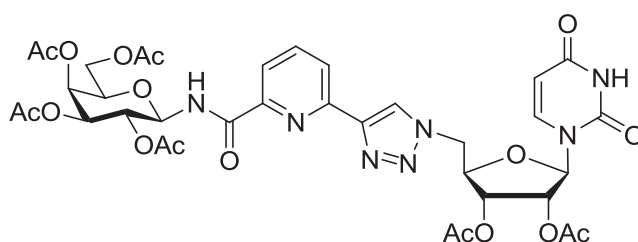
6-Ethynyl-*N*-(2-acetamido-3,4,6-tri-*O*-acetyl-2-deoxy- β -D-glucopyranosyl)picolinamide (**33-GlcNAc**)

Prepared according to general protocol **F** from compound **32-GlcNAc** (250 mg, 0.46 mmol, 1.0 eq.). The crude product was purified by silica gel column chromatography (100% PE to 70% EtOAc/PE) to afford compound **33-GlcNAc** as yellow foam (144 mg, 0.30 mmol, 66%). $R_f = 0.21$ (PE:EtOAc = 1:3); $[\alpha]_D = -56.4$ ($c = 2.2$, CH_2Cl_2); $^1\text{H NMR}$ (400 MHz, CDCl_3) δ (ppm) = 8.80 (d, $J = 9.6$ Hz, 1H, NHCO), 8.13 (d, $J = 7.7$ Hz, 1H, H_{Pyr}), 7.80 (t, $J = 7.7$ Hz, 1H, H_{Pyr}), 7.57 (d, $J = 7.7$ Hz, 1H, H_{Pyr}), 6.45 (d, $J = 9.3$ Hz, 1H, NHAc), 5.45 (dd, $J = 9.7$, 9.6 Hz, 1H, H_1), 5.28 – 5.19 (m, 1H, H_3), 5.26 – 5.09 (m, 1H, H_4), 4.42 (dd, $J = 9.7$, 9.3 Hz, 1H, H_2), 4.25 (dd, $J = 12.5$, 4.3 Hz, 1H, H_{6a}), 4.09 (dd, $J = 12.5$, 2.0 Hz, 1H, H_{6b}), 3.85 (ddd, $J = 9.8$, 4.3, 2.0 Hz, 1H, H_5), 3.20 (s, 1H, $\text{C}\equiv\text{CH}$), 2.05 (d, 6H, 2 \times COCH_3), 2.02 (s, 3H, COCH_3), 1.81 (s, 3H, COCH_3); $^{13}\text{C NMR}$ (100 MHz, CDCl_3) δ (ppm) = 171.5 (COCH_3), 170.9 (s, 2C, 2 \times COCH_3), 169.4 (COCH_3), 164.6 (NHCO), 149.0 (C_{Pyr}), 141.3 (C_{Pyr}), 137.7 (C_{PyrH}), 130.5 (C_{PyrH}), 122.4 (C_{PyrH}), 81.9 ($\text{C}\equiv\text{CH}$), 79.6 (C_1), 78.5 ($\text{C}\equiv\text{CH}$), 73.9 (C_5), 73.5 (C_3), 68.2 (C_4), 62.0 (C_6), 53.2 (C_2), 23.1 (COCH_3), 20.8 (s, 2C, 2 \times COCH_3), 23.7 (COCH_3); HR-ESI-MS (positive mode) m/z : calcd. for $\text{C}_{22}\text{H}_{25}\text{N}_3\text{NaO}_9$ $[\text{M}+\text{Na}]^+$ 498.1483, found 498.1487.



6-[1-(2',3'-Di-*O*-acetyl-uridin-5'-yl)-1*H*-1,2,3-triazol-4-yl]-*N*-(2,3,4,6-tetra-*O*-acetyl-1- β -D-glucopyranosyl)picolinamide (34-Glc)

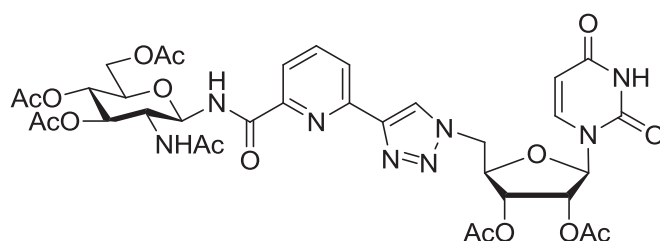
Prepared according to general protocol **B** from compound **33-Glc** (62 mg, 0.13 mmol, 1.0 eq.) and compound **5** (46 mg, 0.13 mmol, 1.0 eq.). The crude product was purified by silica gel column chromatography (100% PE to 80% EtOAc/PE) to afford compound **34-Glc** as white foam (90 mg, 0.109 mmol, 83%). $R_f = 0.17$ (PE:EtOAc = 1:4); $[\alpha]_D = +14.1$ ($c = 0.7$, CH₂Cl₂); ¹H NMR (400 MHz, CDCl₃) δ (ppm) = 9.55 (s, 1H, NH_{Urid}), 8.90 (d, $J = 9.1$ Hz, 1H, NHCO), 8.53 (s, 1H, H_{triazole}), 8.29 (d, $J = 7.7$ Hz, 1H, H_{Pyr}), 8.06 (d, $J = 7.7$ Hz, 1H, H_{Pyr}), 7.94 – 7.87 (m, 1H, H_{Pyr}), 7.13 (d, $J = 8.1$ Hz, 1H, H_{6Urid}), 5.74 – 5.63 (m, 2H, H_{5Urid}, H_{1Rib}), 5.57 – 5.29 (m, 4H, H_{1Glc}, H_{3Glc}, H_{2Rib}, H_{3Rib}), 5.19 – 5.09 (m, 2H, H_{2Glc}, H_{4Glc}), 4.92 (dd, $J = 14.3, 2.8$ Hz, 1H, H_{5aRib}), 4.85 – 4.75 (m, 1H, H_{5bRib}), 4.57 – 4.49 (m, 1H, H_{4Rib}), 4.35 (dd, $J = 12.6, 3.1$ Hz, 1H, H_{6aGlc}), 4.12 – 4.01 (m, 1H, H_{6bGlc}), 3.96 – 3.89 (m, 1H, H_{5Glc}), 2.13 – 1.93 (6s, 18H, 6 \times COCH₃); ¹³C NMR (100 MHz, CDCl₃) δ (ppm) = 171.4 (COCH₃), 170.7 (COCH₃), 170.2 (COCH₃), 169.82 (COCH₃), 169.80 (COCH₃), 169.7 (COCH₃), 164.8 (NHCO), 163.0 (C=O_{Urid}), 150.2 (C=O_{Urid}), 149.0 (C_{Pyr}), 148.1 (C_{Pyr}), 147.8 (C_{triazole}), 141.9 (C_{6Urid}), 138.6 (C_{PyrH}), 124.7 (C_{triazoleH}), 123.2 (C_{PyrH}), 121.7 (C_{PyrH}), 103.2 (C_{5Urid}), 92.2 (C_{1Rib}), 80.6 (C_{4Rib}), 78.9 (C_{1Glc}), 73.8 (C_{5Glc}), 73.1 (C_{3Glc} or C_{2Rib} or C_{3Rib}), 72.6 (C_{3Glc} or C_{2Rib} or C_{3Rib}), 71.1 (C_{3Glc} or C_{2Rib} or C_{3Rib}), 70.4 (C_{2Glc} or C_{4Glc}), 68.5 (C_{2Glc} or C_{4Glc}), 61.8 (C_{6Glc}), 51.7 (C_{5Rib}), 20.80 (COCH₃), 20.74 (s, 2C, COCH₃), 20.69 (COCH₃), 20.52 (COCH₃), 20.47 (COCH₃); HR-ESI-MS (positive mode) m/z : calcd. for C₃₅H₄₀N₇O₁₇ [M+H]⁺ 830.2475, found 830.2458.



6-[1-(2',3'-Di-*O*-acetyl-uridin-5'-yl)-1*H*-1,2,3-triazol-4-yl]-*N*-(2,3,4,6-tetra-*O*-acetyl-1- β -D-galactopyranosyl)picolinamide (34-Gal)

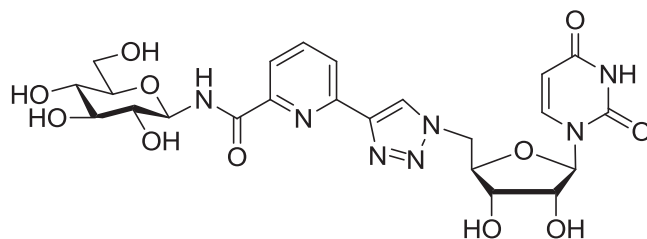
Prepared according to general protocol **B** from compound **33-Gal** (88 mg, 0.185 mmol, 1.0 eq.) and compound **5** (65 mg, 0.185 mmol, 1.0 eq.). The crude product was purified by silica gel column chromatography (100% PE to 50% EtOAc/PE) to afford compound **34-Gal** as white foam (100 mg, 0.121 mmol, 64%). $R_f = 0.17$ (PE:EtOAc = 1:4); $[\alpha]_D = +62.4$ ($c = 0.4$, CH₂Cl₂); ¹H NMR (400 MHz, CDCl₃) δ (ppm) = 9.57 (s, 1H, NH_{Urid}), 8.99 – 8.89 (m, 1H, NHCO), 8.58 (s, 1H, H_{triazole}), 8.29 (d, $J = 7.8$ Hz, 1H, H_{Pyr}), 8.06 (d, $J = 7.8$ Hz, 1H, H_{Pyr}), 7.92 (t, $J = 7.8$ Hz, 1H, H_{Pyr}), 7.14 (d, $J = 8.1$ Hz, 1H, H_{6Urid}), 5.72 (d, $J = 3.7$ Hz, 1H, H_{1Rib}), 5.65 (d, $J = 8.1$ Hz, 1H, H_{5Urid}), 5.51 – 5.42 (m, 3H, H_{2Rib}, H_{3Rib}, H_{4Gal}), 5.38 – 5.30 (m, 2H, H_{1Gal}, H_{2Gal}), 5.23 (dd, $J = 9.4, 4.2$ Hz, 1H, H_{3Gal}), 4.92 (dd, $J = 14.4, 3.6$ Hz, 1H, H_{5aRib}), 4.77 (dd, $J = 14.5, 7.2$ Hz, 1H,

H_{5bRib}), 4.53 (dd, $J = 7.2, 3.6$ Hz, 1H, H_{4Rib}), 4.19 – 4.09 (m, 3H, H_{5Gal}, H_{6aGal}, H_{6bGal}), 2.14 (s, 3H, COCH₃), 2.08 (s, 3H, COCH₃), 2.07 (s, 3H, COCH₃), 2.04 (s, 3H, COCH₃), 2.00 (s, 3H, COCH₃), 1.92 (s, 3H, COCH₃); ¹³C NMR (100 MHz, CDCl₃) δ (ppm) = 171.7 (C=O), 170.5 (C=O), 170.2 (C=O), 167.0 (C=O), 169.8 (C=O), 169.7 (C=O), 164.8 (NHCO), 162.9 (C=O_{Uri}), 150.2 (C=O_{Uri}), 148.9 (C_{Pyr}), 148.2 (C_{Pyr}), 147.8 (C_{triazole}), 141.5 (C_{6Uri}), 138.6 (C_{PyrH}), 124.8 (C_{triazoleH}), 123.2 (C_{PyrH}), 121.7 (C_{PyrH}), 103.1 (C_{5Uri}), 91.4 (C_{1Rib}), 80.2 (C_{4Rib}), 79.2 (C_{1Gal}), 73.0 (C_{2Rib} or C_{3Rib} or C_{4Gal}), 72.5 (C_{5Gal}), 70.86 (C_{3Gal}), 70.84 (C_{2Rib} or C_{3Rib} or C_{4Gal}), 68.2 (C_{2Gal}), 67.4 (C_{2Rib} or C_{3Rib} or C_{4Gal}), 61.2 (C_{6Gal}), 51.6 (C_{5Rib}), 20.8 (COCH₃), 20.73 (COCH₃), 20.67 (COCH₃), 20.66 (COCH₃), 20.5 (COCH₃), 20.4 (COCH₃); HR-ESI-MS (positive mode) m/z : calcd. for C₃₅H₄₀N₇O₁₇ [M+H]⁺ 830.2475, found 830.2469.



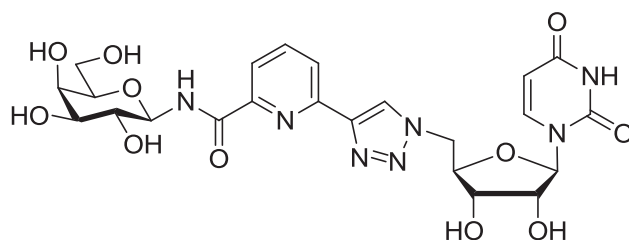
6-[1-(2',3'-Di-O-acetyl-uridin-5'-yl)-1H-1,2,3-triazol-4-yl]-N-(2-acetamido-3,4,6-tri-O-acetyl-2-deoxy- β -D-glucopyranosyl)picolinamide (34-GlcNAc)

Prepared according to general protocol **B** from compound **33-GlcNAc** (89 mg, 0.19 mmol, 1.0 eq.) and compound **5** (66 mg, 0.19 mmol, 1.0 eq.). The crude product was purified by silica gel column chromatography (100% PE to 100% EtOAc) to afford compound **34-GlcNAc** as white foam (105 mg, 0.13 mmol, 68%). $R_f = 0.41$ (EtOAc); $[\alpha]_D = +0.30$ ($c = 0.7$, CH₂Cl₂); ¹H NMR (400 MHz, CDCl₃) δ (ppm) = 9.89 (s, 1H, NHCO_{Uri}), 9.23 (d, $J = 8.3$ Hz, 1H, NHCO), 8.89 (s, 1H, H_{triazole}), 8.25 (d, $J = 7.8$ Hz, 1H, H_{Pyr}), 8.03 (d, $J = 7.8$ Hz, 1H, H_{Pyr}), 7.88 (t, $J = 7.8$ Hz, 1H, H_{Pyr}), 7.05 (d, $J = 8.1$ Hz, 1H, H_{6Uri}), 6.63 (d, $J = 8.9$ Hz, 1H, NHAc), 5.68 (d, $J = 3.0$ Hz, 1H, H_{1Rib}), 5.58 (d, $J = 8.1$ Hz, 1H, H_{5Uri}), 5.56 – 5.48 (m, 2H, H_{2Rib}, H_{3Rib}), 5.32 – 5.12 (m, 3H, H_{1GlcNAc}, H_{3GlcNAc}, H_{4GlcNAc}), 4.90 (dd, $J = 14.3, 3.2$ Hz, 1H, H_{5aRib}), 4.83 (dd, $J = 14.3, 5.9$ Hz, 1H, H_{5bRib}), 4.54 (dd, $J = 9.8, 5.9, 3.2$ Hz, 1H, H_{4Rib}), 4.39 (dd, $J = 9.8, 8.9$ Hz, 1H, H_{2GlcNAc}), 4.30 (dd, $J = 12.5, 4.3$ Hz, 1H, H_{6aGlcNAc}), 4.08 – 4.03 (m, 1H, H_{6bGlcNAc}), 3.94 – 3.85 (m, 1H, H_{5GlcNAc}), 2.09 (s, 3H, COCH₃), 2.08 (s, 3H, COCH₃), 2.08 (s, 3H, COCH₃), 2.03 (s, 3H, COCH₃), 2.01 (s, 3H, COCH₃), 1.78 (s, 3H, COCH₃); ¹³C NMR (100 MHz, CDCl₃) δ (ppm) = 172.1, 171.8, 170.9, 169.8, 169.6, 165.5, 163.1, 150.3, 149.0 (C_{triazole}), 148.3, 147.8, 141.9 (C_{6Uri}), 138.5 (C_{PyrH}), 125.6 (C_{triazoleH}), 122.8 (C_{PyrH}), 121.5 (C_{PyrH}), 103.0 (C_{5Uri}), 92.0 (C_{1Rib}), 80.6 (C_{1GlcNAc}), 80.4 (C_{4Rib}), 73.5 (C_{5GlcNAc}), 73.0 (C_{2Rib} or C_{3Rib}), 72.8 (C_{3GlcNAc} or C_{4GlcNAc}), 71.1 (C_{2Rib} or C_{3Rib}), 68.5 (C_{3GlcNAc} or C_{4GlcNAc}), 62.1 (C_{6GlcNAc}), 52.6 (C_{2GlcNAc}), 51.5 (C_{5Rib}), 23.0 (COCH₃), 20.9 (COCH₃), 20.8 (COCH₃), 20.7 (COCH₃), 20.51 (COCH₃), 20.46 (COCH₃); HR-ESI-MS (positive mode) m/z : calcd. for C₃₅H₄₁N₈O₁₆ [M+H]⁺ 829.2635, found 829.2606.



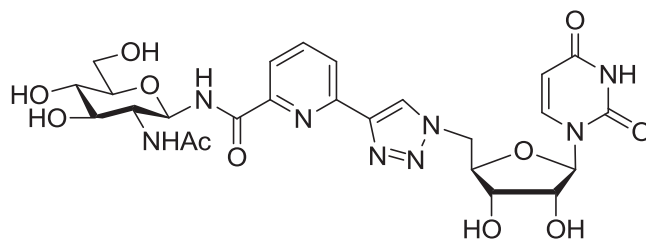
6-[1-(uridin-5'-yl)-1H-1,2,3-triazol-4-yl]-N-(β-D-glucopyranosyl)picolinamide (35-Glc)

Prepared according to general protocol E from compound **34-Glc** (96 mg, 0.12 mmol, 1.0 eq.). The residue was purified by C18 reverse phase column chromatography (100% H₂O to 50% MeOH/H₂O) to afford compound **35-Glc** as white foam (59 mg, 0.102 mmol, 85%). $[\alpha]_D = +27.5$ ($c = 0.08$, DMSO); ¹H NMR (500 MHz, (CD₃)₂SO) δ (ppm) = 8.97 (s, 1H, H_{triazole}), 8.15 (d, $J = 7.8$ Hz, 1H, H_{Py}), 8.01 (t, $J = 7.8$ Hz, 1H, H_{Py}), 7.92 (d, $J = 7.8$ Hz, 1H, H_{Py}), 7.12 (br, 1H, H_{6Uri}), 5.57 (d, $J = 5.4$ Hz, 1H, H_{1Rib}), 5.33 (d, $J = 7.7$ Hz, 1H, H_{5Uri}), 4.91 (d, $J = 9.0$ Hz, 1H, H_{1Glc}), 4.71 (dd, $J = 14.4, 6.1$ Hz, 1H, H_{5aRib}), 4.68 – 4.60 (m, 1H, H_{5bRib}), 4.11 (dd, $J = 9.2, 6.1, 4.3$ Hz, 1H, H_{4Rib}), 3.86 (dd, $J = 9.2, 4.8$ Hz, 1H, H_{3Rib}), 3.78 (s, 1H, H_{2Rib}), 3.59 (bd, $J = 10.8$ Hz, 1H, H_{6aGlc}), 3.31 – 3.23 (m, 2H, H_{2Glc}, H_{6bGlc}), 3.22 – 3.11 (m, 2H, H_{3Glc}, H_{5Glc}), 3.07 (t, $J = 9.1$ Hz, 1H, H_{4Glc}); ¹³C NMR (125 MHz, (CD₃)₂SO) δ (ppm) = 164.0, 149.4, 149.0, 146.6, 140.9 (C_{6Uri}), 139.1 (C_{PyH}), 125.6 (C_{triazoleH}), 122.2 (C_{PyH}), 121.3 (C_{PyH}), 102.3 (C_{5Uri}), 90.0 (C_{1Rib}), 81.3 (C_{4Rib}), 79.8 (C_{1Glc}), 78.9 (C_{5Glc}), 78.0 (C_{3Glc}), 71.9 (C_{2Glc}), 71.4 (C_{2Rib}), 70.3 (C_{3Rib}), 70.1 (C_{4Glc}), 61.1 (C_{6Glc}), 51.6 (C_{5Rib}); HR-ESI-MS (positive mode) m/z : calcd. for C₂₃H₂₇N₇NaO₁₁ [M+Na]⁺ 600.1661, found 600.1684.



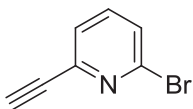
6-[1-(Uridin-5'-yl)-1H-1,2,3-triazol-4-yl]-N-(β-D-galactopyranosyl)picolinamide (35-Gal)

Prepared according to general protocol E from compound **34-Gal** (92.6 mg, 0.11 mmol, 1.0 eq.). The residue was purified by C18 reverse phase column chromatography (100% H₂O to 50% MeOH/H₂O) to afford compound **35-Gal** as white foam (50 mg, 0.087 mmol, 78%). $[\alpha]_D^{20} = +39.8$ ($c = 1.2$, H₂O); ¹H NMR (400 MHz, D₂O) δ (ppm) = 8.29 (s, 1H, H_{triazole}), 7.83 (m, 3H, H_{PyH}), 6.78 (d, $J = 7.8$ Hz, 1H, H_{6Uri}), 5.73 (s, 1H, H_{1Rib}), 5.18 (d, $J = 7.8$ Hz, 1H, H_{5Uri}), 5.13 (d, $J = 9.0$ Hz, 1H, H_{1Gal}), 4.85 – 4.70 (m, 2H, H_{5aRib}, H_{5bRib}), 4.37 – 4.29 (m, 1H), 4.23 – 4.17 (m, 1H), 4.04 – 3.77 (m, 7H); ¹³C NMR (100 MHz, D₂O) δ (ppm) = 172.0 (C=O_{Uri}), 167.2 (NHCO), 156.3 (C=O_{Uri}), 148.0 (C_{PyH}), 147.7 (C_{PyH}), 146.8 (C_{triazole}), 140.6 (C_{6Uri}), 139.6 (C_{PyH}), 126.2 (C_{triazoleH}), 123.7 (C_{PyH}), 122.2 (C_{PyH}), 102.8 (C_{5Uri}), 91.3 (C_{1Rib}), 80.7 (C_{1Gal}), 80.2, 77.2, 73.7, 72.7, 70.2, 69.4, 69.2, 61.5 (C_{6Gal}), 50.6 (C_{5Rib}); HR-ESI-MS (positive mode) m/z : calcd. for C₂₃H₂₇N₇NaO₁₁ [M+Na]⁺ 600.1661, found 600.1640.



6-[(1-Uridin-5'-yl)-1H-1,2,3-triazol-4-yl]-N-(2-acetamido-2-deoxy-β-D-glucopyranosyl)picolinamide (**35-GlcNAc**)

Prepared according to general protocol **E** from compound **34-GlcNAc** (104.7 mg, 0.126 mmol, 1.0 eq.). The residue was purified by C18 reverse phase column chromatography (100% H₂O to 30% MeOH/H₂O) to afford compound **35-GlcNAc** as white foam (66 mg, 0.11 mmol, 85%). R_f = 0.50 (EtOAc:MeOH = 2:3); $[\alpha]_D$ = +19.5 (c = 0.8, MeOH); ¹H NMR (400 MHz, D₂O) δ (ppm) = 8.44 (s, 1H, H_{triazole}), 7.83 – 7.69 (m, 3H, H_{pyr}), 7.00 (d, J = 7.9 Hz, 1H, H_{6Uri}), 5.69 (d, J = 2.2 Hz, 1H, H_{1Rib}), 5.38 (d, J = 7.9 Hz, 1H, H_{5Uri}), 5.11 (d, J = 9.6 Hz, 1H, H_{1GlcNAc}), 4.87 – 4.68 (m, 2H, H_{5Rib}), 4.34 – 4.28 (m, 1H, H_{4Rib}), 4.19 – 4.09 (m, 2H, H_{2Rib}, H_{3Rib}), 4.04 – 3.89 (m, 2H, H_{2GlcNAc}, H_{6aGlcNAc}), 3.79 (dd, J = 12.4, 4.8 Hz, 1H, H_{6bGlcNAc}), 3.75 – 3.65 (m, 1H, H_{3GlcNAc}), 3.65 – 3.50 (m, 2H, H_{4GlcNAc}, H_{5GlcNAc}), 1.85 (s, 3H, NHCOCH₃); ¹³C NMR (100 MHz, D₂O) δ (ppm) = 175.1, 168.5, 166.9, 153.4, 147.9, 147.6, 146.8, 141.8 (C_{6Uri}), 139.4 (C_{pyrH}), 126.1 (C_{triazoleH}), 123.3 (C_{pyrH}), 122.0 (C_{pyrH}), 102.5 (C_{5Uri}), 91.4 (C_{1Rib}), 80.7 (C_{4Rib}), 79.8 (C_{1GlcNAc}), 78.0 (C_{5GlcNAc}), 74.2 (C_{3GlcNAc}), 72.9 (C_{2Rib} or C_{3Rib}), 70.4 (C_{2Rib} or C_{3Rib}), 70.2 (C_{4GlcNAc}), 61.1 (C_{6GlcNAc}), 54.6 (C_{2GlcNAc}), 51.2 (C_{5Rib}), 22.4 (NHCOCH₃); HR-ESI-MS (positive mode) m/z : calcd. for C₂₅H₃₀N₈NaO₁₁ [M+Na]⁺ 641.1926, found 641.1911.

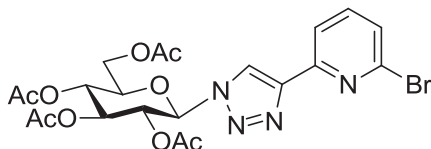


2-Bromo-6-ethynylpyridine (**38**)²¹⁶

In a 50 mL flask containing 2,6-dibromopyridine (**36**) (1 g, 4.2 mmol, 3.0 eq.), CuI (14 mg, 0.07 mmol, 0.05 eq.) and Pd(PPh₃)₄ (81 mg, 0.07 mmol, 0.05 eq.) in toluene (5.6 mL) was bubbled with argon. Then, diisopropylamine (0.56 mL, 4.0 mmol, 2.9 eq.) and trimethylsilylacetylene (0.2 mL, 1.4 mmol, 1.0 eq.) were injected into the reaction. The reaction mixture was stirred overnight. Then, the reaction mixture was filtered, washed with CH₂Cl₂. The filtrate was poured into satd aq. NH₄Cl (50 mL) solution, extracted with CH₂Cl₂ (4×50 mL). The extract was washed with H₂O (40 mL) and brine (40 mL), dried over MgSO₄, concentrated, the residue was purified by silica gel column chromatography (PE:CH₂Cl₂ = 9:1 to PE:CH₂Cl₂ = 9:2) to afford a mixture (851 mg) containing 2,6-dibromopyridine **36** and 2-bromo-6-(trimethylsilyl)ethynylpyridine **37**. The mixture was used directly for the reaction of next step without further purification.

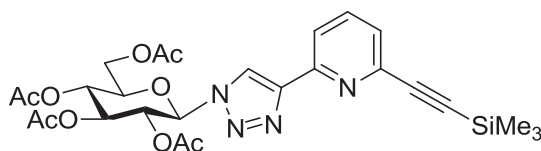
In a 10 mL round-bottom flask containing 2-bromo-6-(trimethylsilyl)ethynylpyridine (**37**) (750 mg, a mixture as mentioned above) was added K₂CO₃ (1.426 mg, 10.6 mmol), THF (5 mL) and MeOH (5 mL). The resulting suspension was stirred at r.t. for 2 h. Then, the reaction mixture was poured into H₂O (50 mL), extracted with EtOAc (4×50 mL). The combined organic layers were washed with brine (50 mL). The organic phase was dried (Na₂SO₄) and concentrated. The residue was purified by silica gel column chromatography (PE:CH₂Cl₂ = 9:1 to PE:CH₂Cl₂ =

7:3) to afford compound **38** as dark grey solid (176 mg, 0.97 mmol, two steps 79%). $R_f = 0.29$ (PE:CH₂Cl₂ = 7:3); ¹H NMR (300 MHz, CDCl₃) δ (ppm) = 7.56 – 7.40 (m, 3H, H_{Pyr}), 3.21 (s, 1H, C≡CH); ¹³C NMR (75 MHz, CDCl₃) δ (ppm) = 142.86 (C_{Pyr}), 141.92 (C_{Pyr}), 138.50 (C_{PyrH}), 128.40 (C_{PyrH}), 126.48 (C_{PyrH}), 81.53 (C≡CH), 78.92 (C≡CH); HR-ESI-MS (positive mode) m/z : calcd. for C₇H₄BrNNa, [M+Na]⁺ 203.9419, found 203.9421.



2-Bromo-6-(2,3,4,6-tetra-*O*-acetyl- β -D-glucopyranosyl-1*H*-1,2,3-triazol-4-yl)pyridine (**39**)

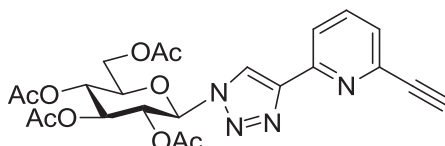
Prepared according to general protocol C from compound **28-Glc** (85 mg, 0.23 mmol, 1.0 eq.) and compound **38** (50 mg, 0.28 mmol, 1.2 eq.). The crude product was purified by silica gel column chromatography (10% EtOAc/PE to 30% EtOAc/PE) to afford compound **39** as yellow foam (119 mg, 0.215 mmol, 93%). $R_f = 0.29$ (PE:EtOAc = 7:3); $[\alpha]_D = -66.0$ ($c = 0.5$, CH₂Cl₂); ¹H NMR (400 MHz, CDCl₃) δ (ppm) = 8.45 (s, 1H, H_{triazole}), 8.09 (d, $J = 7.8$ Hz, 1H, H_{Pyr}), 7.61 (t, $J = 7.8$ Hz, 1H, H_{Pyr}), 7.41 (d, $J = 7.8$ Hz, 1H, H_{Pyr}), 5.91 (d, $J = 8.7$ Hz, 1H, H_{1Glc}), 5.51 – 5.40 (m, 2H, H_{2Glc}, H_{3Glc}), 5.30 – 5.21 (m, 1H, H_{4Glc}), 4.31 (dd, $J = 12.6, 4.8$ Hz, 1H, H_{6aGlc}), 4.15 (dd, $J = 12.6, 1.7$ Hz, 1H, H_{6bGlc}), 4.02 (ddd, $J = 10.1, 4.8, 1.7$ Hz, 1H, H_{5Glc}), 2.09 (s, 3H, COCH₃), 2.06 (s, 3H, COCH₃), 2.03 (s, 3H, COCH₃), 1.88 (s, 3H, COCH₃); ¹³C NMR (100 MHz, CDCl₃) δ (ppm) = 170.7 (COCH₃), 170.1 (COCH₃), 169.4 (COCH₃), 169.0 (COCH₃), 150.7, 147.8, 141.9, 139.3 (C_{PyrH}), 127.5 (C_{PyrH}), 121.5 (C_{triazoleH}), 119.1 (C_{PyrH}), 86.1 (C_{1Glc}), 75.3 (C_{5Glc}), 72.7 (C_{2Glc} or C_{3Glc}), 70.7 (C_{2Glc} or C_{3Glc}), 67.7 (C_{4Glc}), 61.6 (C_{6Glc}), 20.8 (COCH₃), 20.7 (2×COCH₃), 20.3 (COCH₃); HR-ESI-MS (positive mode) m/z : calcd. for C₂₁H₂₄BrN₄O₉, [M+H]⁺ 555.0721, found 555.0722.



2-(2-Trimethylsilylethynyl)-6-(2,3,4,6-tetra-*O*-acetyl- β -D-glucopyranosyl-1*H*-1,2,3-triazol-4-yl)pyridine (**40**)

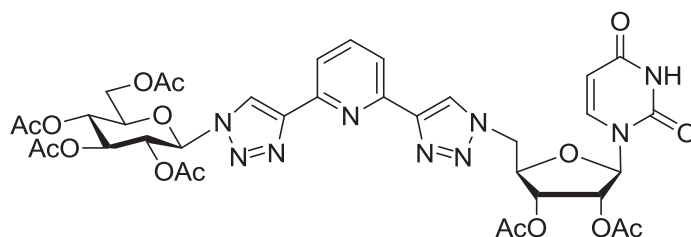
In a 50 mL round-bottom flask containing compound **39** (80 mg, 0.144 mmol, 1.0 eq.), CuI (1.4 mg, 0.007 mmol, 0.05 eq.) and Pd(PPh₃)₄ (8.3 mg, 0.007 mmol, 0.05 eq.) in toluene (1 mL) was bubbled with argon. Then, diisopropylamine (0.02 mL, 0.142 mmol, 1.0 eq.) and trimethylsilylacetylene (0.04 mL, 0.288 mmol, 2.0 eq.) were injected into the reaction. The reaction mixture was stirred at r.t. overnight with protection of light. Then, the reaction mixture was filtered, washed with CH₂Cl₂. The filtrate was poured into satd aq. NH₄Cl (20 mL) solution, extracted with CH₂Cl₂. The extract was washed with H₂O (20 mL) and brine (20 mL), dried over MgSO₄, concentrated. The residue was purified by silica gel column chromatography (PE:EtOAc = 9:1 to PE:EtOAc = 7:3) to afford compound **40** as yellow foam (78 mg, 0.136 mmol, 95%). $R_f = 0.26$ (PE:EtOAc = 7:3); $[\alpha]_D = -58.3$ ($c = 1.0$, CH₂Cl₂); ¹H NMR (400 MHz, CDCl₃) δ (ppm) = 8.50 (s, 1H, H_{triazole}), 8.09 (d, $J = 7.8$ Hz, 1H, H_{Pyr}), 7.72 (t, $J = 7.8$ Hz, 1H, H_{Pyr}), 7.40 (d, $J = 7.8$ Hz, 1H, H_{Pyr}), 5.91 (d, $J = 8.7$ Hz, 1H, H_{1Glc}), 5.51 – 5.39

(m, 2H, H_{2Glc}, H_{3Glc}), 5.30 – 5.21 (m, 1H, H_{4Glc}), 4.30 (dd, *J* = 12.6, 4.8 Hz, 1H, H_{6aGlc}), 4.16 – 4.11 (m, 1H, H_{6bGlc}), 4.04 – 3.98 (ddd, *J* = 10.1, 4.8, 1.8 Hz, 1H, H_{5Glc}), 2.10 (s, 3H, COCH₃), 2.06 (s, 3H, COCH₃), 2.03 (s, 3H, COCH₃), 1.88 (s, 3H, COCH₃), 0.28 (s, 9H, SiMe₃); ¹³C NMR (100 MHz, CDCl₃) δ (ppm) = 170.7 (COCH₃), 170.2 (COCH₃), 169.4 (COCH₃), 169.0 (COCH₃), 150.1, 148.5, 143.0, 137.1 (C_{PyrH}), 127.1 (C_{PyrH}), 121.5 (C_{triazoleH}), 119.9 (C_{PyrH}), 103.7 (C≡C), 95.2 (C≡C), 86.0 (C_{1Glc}), 75.2 (C_{5Glc}), 72.8 (C_{2Glc} or C_{3Glc}), 70.7 (C_{2Glc} or C_{3Glc}), 67.7 (C_{4Glc}), 61.6 (C_{6Glc}), 20.8 (COCH₃), 20.7 (2×COCH₃), 20.3 (COCH₃), -0.1 (s, 3C, SiMe₃); HR-ESI-MS (positive mode) *m/z*: calcd. for C₂₆H₃₃N₄O₉Si, [M+H]⁺ 573.2011, found 573.2006.



2-Ethynyl-6-(2,3,4,6-tetra-*O*-acetyl-β-*D*-glucopyranosyl-1*H*-1,2,3-triazol-4-yl)pyridine (41)

Prepared according to general protocol **F** from compound **40** (116 mg, 0.203 mmol, 1.0 eq.). The crude product was purified by silica gel column chromatography (20% EtOAc/PE to 70% EtOAc/PE) to afford compound **41** as yellow foam (97 mg, 0.194 mmol, 96%). *R*_f = 0.17 (PE:EtOAc = 1:2); [α]_D = -111.0 (*c* = 1.5, CH₂Cl₂); ¹H NMR (400 MHz, CDCl₃) δ (ppm) = 8.50 (s, 1H, H_{triazole}), 8.13 (d, *J* = 7.8 Hz, 1H, H_{Pyr}), 7.74 (t, *J* = 7.8 Hz, 1H, H_{Pyr}), 7.42 (d, *J* = 7.8 Hz, 1H, H_{Pyr}), 5.94 – 5.87 (m, 1H, H_{1Glc}), 5.50 – 5.38 (m, 2H, H_{2Glc}, H_{3Glc}), 5.30 – 5.20 (m, 1H, H_{4Glc}), 4.30 (dd, *J* = 12.6, 4.8 Hz, 1H, H_{6aGlc}), 4.13 (dd, *J* = 12.6, 2.0 Hz, 1H, H_{6bGlc}), 4.02 (ddd, *J* = 10.1, 4.8, 2.0 Hz, 1H, H_{5Glc}), 3.19 (s, 1H, C≡CH), 2.09 (s, 3H, COCH₃), 2.06 (s, 3H, COCH₃), 2.02 (s, 3H, COCH₃), 1.87 (s, 3H, COCH₃); ¹³C NMR (100 MHz, CDCl₃) δ (ppm) = 170.7 (COCH₃), 170.1 (COCH₃), 169.4 (COCH₃), 168.9 (COCH₃), 150.2, 148.4, 142.2, 137.2 (C_{PyrH}), 127.0 (C_{PyrH}), 121.4 (C_{triazoleH}), 120.3 (C_{PyrH}), 86.0 (C_{1Glc}), 82.8 (C≡CH), 77.4 (C≡CH), 75.2 (H_{5Glc}), 72.7 (H_{2Glc}), 70.7 (H_{3Glc}), 67.7 (H_{4Glc}), 61.6 (H_{6Glc}), 20.8 (COCH₃), 20.6 (2×COCH₃), 20.3 (COCH₃); HR-ESI-MS (positive mode) *m/z*: calcd. for C₂₃H₂₅N₄O₉, [M+H]⁺ 501.1616, found 501.1610.



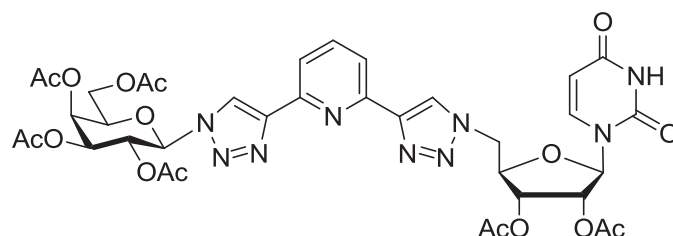
2-(2,3,4,6-Tri-*O*-acetyl-β-*D*-glucopyranosyl-1*H*-1,2,3-triazol-4-yl)-6-[1-(2',3'-di-*O*-acetyl-uridin-5'-yl)-1*H*-1,2,3-triazol-4-yl]pyridine (42-Glc)

(**Pathway A**) DIPEA (0.2 mL, 7.5 eq.) was added into a microwave tube containing 2',3'-di-*O*-acetyl-5'-azido-5'-deoxy-uridine (**5**) (45 mg, 0.13 mmol, 1.0 eq.), compound **41** (70 mg, 0.14 mmol, 1.1 eq.) and CuI (13 mg, 0.065 mmol, 0.5 eq.) in DMF (2 mL). The reaction was heated for 15 min by microwave irradiation at 100°C. Then, the reaction suspension was diluted with ethyl acetate (40 mL), washed with satd aq. Na₂CO₃ solution (2×25 mL) and H₂O (25 mL). The organic phase was dried (Na₂SO₄) and concentrated; the residue was purified by

silica gel column chromatography (PE:EtOAc = 1:2 to PE: EtOAc = 1:4) to afford compound **42** as yellow foam (82 mg, 0.096 mmol, 74%).

(Pathway B) DIPEA (0.1 mL, 30 eq.) was added into a microwave tube containing 2,3,4,6-tetra-*O*-acetyl- β -D-glucopyranosyl azide (**28-Glc**) (8.5 mg, 0.022 mmol, 1.2 eq.), compound **47** (9 mg, 0.019 mmol, 1.0 eq.) and CuI (2 mg, 0.01 mmol, 0.5 eq.) in DMF (2 mL). The reaction was heated for 15 min by microwave irradiation at 100°C. Then, the reaction suspension was diluted with ethyl acetate (40 mL), washed with satd aq. Na₂CO₃ solution (2×25 mL) and H₂O (25 mL). The organic phase was dried (Na₂SO₄) and concentrated, the residue was purified by silica gel column chromatography (PE:EtOAc = 1:2 to PE: EtOAc = 1:4) to afford compound **42-Glc** as yellow foam (14 mg, 0.0164 mmol, 86%).

R_f=0.27 (PE:EtOAc = 1:4); [α]_D = -18.4 (*c* = 1.85, CH₂Cl₂); ¹H NMR (400 MHz, CDCl₃) δ (ppm) = 9.36 (s, 1H, H_{3Uri}), 8.40 (s, 1H, H_{triazole}), 8.32 (s, 1H, H_{triazole}), 8.11 – 8.02 (m, 2H, H_{PyR}), 7.84 (t, *J* = 7.8 Hz, 1H, H_{PyR}), 7.05 (d, *J* = 8.1 Hz, 1H, H_{6Uri}), 5.96 (d, *J* = 9.4 Hz, 1H, H_{1Glc}), 5.74 – 5.59 (m, 3H, H_{1Rib}, H_{5Uri}, H_{2Glc}), 5.52 – 5.38 (m, 3H, H_{2Rib}, H_{3Rib}, H_{3Glc}), 5.31 (t, *J* = 9.8 Hz, 1H, H_{4Glc}), 4.89 – 4.78 (m, 2H, H_{5Rib}), 4.54 (dd, *J* = 10.6, 5.8 Hz, 1H, H_{4Rib}), 4.31 (dd, *J* = 12.6, 5.6 Hz, 1H, H_{6aGlc}), 4.17 (dd, *J* = 12.6, 1.8 Hz, 1H, H_{6bGlc}), 4.09 – 4.03 (m, 1H, H_{5Glc}), 2.10 (s, 3H, COCH₃), 2.09 (s, 3H, COCH₃), 2.07 (s, 3H, COCH₃), 2.03 (s, 3H, COCH₃), 2.03 (s, 3H, COCH₃), 1.89 (s, 3H, COCH₃); ¹³C NMR (100 MHz, CDCl₃) δ (ppm) = 170.8, 170.2, 169.8, 169.8, 169.6, 169.5, 162.7, 150.3, 149.9, 149.4, 149.0, 148.5, 141.5 (C_{6Uri}), 138.0 (C_{PyRH}), 124.2 (C_{triazoleH}), 120.8 (C_{triazoleH}), 119.7 (C_{PyRH}), 119.7 (C_{PyRH}), 103.7 (C_{5Uri}), 91.6 (C_{1Rib}), 85.9 (C_{1Glc}), 80.2 (C_{4Rib}), 75.2 (C_{5Glc}), 72.9 (C_{3Glc} or C_{2Rib} or C_{3Rib}), 72.6 (C_{3Glc} or C_{2Rib} or C_{3Rib}), 70.9 (C_{3Glc} or C_{2Rib} or C_{3Rib}), 70.5 (C_{2Glc}), 68.0 (C_{4Glc}), 62.0 (C_{6Glc}), 51.2 (C_{5Rib}), 20.8 (COCH₃), 20.70 (COCH₃), 20.66 (COCH₃), 20.53 (COCH₃), 20.51 (COCH₃), 20.4 (COCH₃); HR-ESI-MS (positive mode) *m/z*: calcd. for C₃₆H₄₀N₉O₁₆, [M+H]⁺ 854.2588, found 854.2570.



2-(2,3,4,6-Tetra-*O*-acetyl- β -D-galactopyranosyl-1*H*-1,2,3-triazol-4-yl)-6-[1-(2',3'-di-*O*-acetyl-uridin-5'-yl)-1*H*-1,2,3-triazol-4-yl]pyridine (42-Gal**) (Adapted from Ref.²¹⁷)**

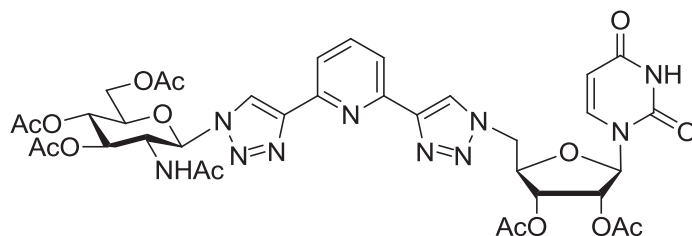
(Pathway A) DIPEA (6 μ L, 0.036 mmol, 0.25 eq.) was added into a flask containing 2',3'-di-*O*-acetyl-5'-azido-5'-deoxy-uridine (**5**) (50 mg, 0.14 mmol, 1.0 eq.), 2-ethynyl-6-(2-trimethylsilylethynyl)pyridine (**48**) (28 mg, 0.14 mmol, 1.0 eq.) and CuI (2.7 mg, 0.01 mmol, 0.1 eq.) in DMF (2 mL). The reaction was stirred at r.t. with protection of light for 17 h. AgBF₄ (55 mg, 0.28 mmol, 2.0 eq.) was added into the reaction and the reaction mixture was stirred at r.t. with protection of light under argon for another 24 h. Then, 2,3,4,6-tetra-*O*-acetyl- β -D-galactopyranoside azido (**28-Gal**) (64 mg, 0.17 mmol, 1.2 eq.), CuI (15 mg, 0.078 mmol, 0.5 eq.) and DIPEA (30 μ L, 0.18 mmol, 1.25 eq.) were added into the reaction and the reaction was stirred at r.t. with protection of light. After 24 h, the reaction mixture was diluted with EtOAc (50 mL), washed with satd aq. Na₂CO₃ solution (2×25 mL) and H₂O (30 mL). The combined aqueous phase was extracted with EtOAc (3×30 mL). The

combined organic phases were dried (Na₂SO₄) and concentrated. The residue was purified by silica gel column chromatography (100% PE to 100% EtOAc) to afford compound **42-Gal** as yellow foam (37 mg, 0.0434 mmol, 31%).

(Pathway B) DIPEA (6 μL, 0.036 mmol, 0.25 eq.) was added into a flask containing 2',3'-di-*O*-acetyl-5'-azido-5'-deoxy-uridine (**5**) (50 mg, 0.14 mmol, 1.0 eq.), 2-ethynyl-6-(2-trimethylsilylethynyl)pyridine (**48**) (28 mg, 0.14 mmol, 1.0 eq.) and CuI (2.7 mg, 0.01 mmol, 0.1 eq.) in DMF (2 mL). The reaction was stirred at r.t. with protection of light for 24 h. CuI (5.4 mg, 0.02 mmol, 0.2 eq.), 2,3,4,6-tetra-*O*-acetyl-β-D-galactopyranoside azido (**28-Gal**) (64 mg, 0.17 mmol, 1.2 eq.) and DIPEA (18 μL, 0.108 mmol, 0.75 eq.) were added into the reaction and the reaction mixture was stirred at 35°C under argon with protection of light for 23 h. The reaction mixture was then diluted with EtOAc (30 mL), washed with satd aq. Na₂CO₃ solution (2×25 mL) and H₂O (30 mL). The combined aqueous phase was extracted with EtOAc (3×30 mL). The combined organic phases were dried (Na₂SO₄) and concentrated. The residue was purified by silica gel column chromatography (100% PE to 100% EtOAc) to afford compound **42-Gal** as yellow foam (49 mg, 0.0574 mmol, 41%).

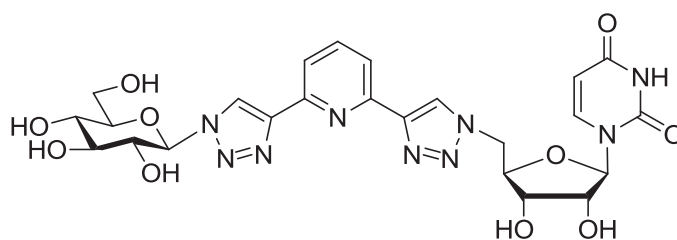
(Pathway C) DIPEA (6 μL, 0.036 mmol, 0.25 eq.) was added into a flask containing 2',3'-di-*O*-acetyl-5'-azido-5'-deoxy-uridine (**5**) (50 mg, 0.14 mmol, 1.0 eq.), 2-ethynyl-6-(2-trimethylsilylethynyl)pyridine (**48**) (28 mg, 0.14 mmol, 1.0 eq.) and CuI (2.7 mg, 0.01 mmol, 0.1 eq.) in DMF (2 mL). The reaction was stirred at r.t. with protection of light for 17 h. AgBF₄ (55 mg, 0.28 mmol, 2.0 eq.) and 2,3,4,6-tetra-*O*-acetyl-β-D-galactopyranoside azido (**28-Gal**) (64 mg, 0.17 mmol, 1.2 eq.) were added into the reaction and the reaction mixture was stirred at 35°C under argon with protection of light for 16 h. Then, the reaction mixture was diluted with EtOAc (30 mL), washed with satd aq. Na₂CO₃ solution (2×25 mL) and H₂O (30 mL). The combined aqueous phase was extracted with EtOAc (3×30 mL). The combined organic phases were dried (Na₂SO₄) and concentrated. The residue was purified by silica gel column chromatography (100% PE to 100% EtOAc) to afford compound **42-Gal** as yellow foam (72 mg, 0.0844 mmol, 60%).

$R_f = 0.34$ (PE:EtOAc = 1:3); $[\alpha]_D^{20} = -13.4$ ($c = 1.1$, CH₂Cl₂); ¹H NMR (400 MHz, CDCl₃) δ (ppm) = 9.07 (s, 1H, NH_{U_{ri}}), 8.48 (s, 1H, H_{triazole}), 8.36 (s, 1H, H_{triazole}), 8.10 (d, $J = 7.8$ Hz, 2H, 2 H_{Pyr}), 7.88 (t, $J = 7.8$ Hz, 1H, H_{Pyr}), 7.04 (d, $J = 8.1$ Hz, 1H, H_{6U_{ri}}), 5.93 (d, $J = 9.3$ Hz, 1H, H_{1Gal}), 5.74 – 5.61 (m, 3H, H_{5U_{ri}}, H_{1Rib}, H_{2Gal}), 5.58 (bd, $J = 3.3$ Hz, 1H, H_{4Gal}), 5.48 – 5.39 (m, 2H, H_{2Rib}, H_{3Rib}), 5.30 (dd, $J = 10.3, 3.3$ Hz, 1H, H_{3Gal}), 4.90 – 4.75 (m, 2H, H_{5aRib}, H_{5bRib}), 4.55 (bd, $J = 4.2$ Hz, 1H, H_{4Rib}), 4.32 – 4.26 (m, 1H, H_{5Gal}), 4.23 – 4.16 (m, 2H, H_{6aGal}, H_{6bGal}), 2.25 (s, 3H, COCH₃), 2.11 (s, 3H, COCH₃), 2.10 (s, 3H, COCH₃), 2.04 (s, 3H, COCH₃), 2.02 (s, 3H, COCH₃), 1.91 (s, 3H, COCH₃); ¹³C NMR (100 MHz, CDCl₃) δ (ppm) = 170.6 (C=O), 170.3 (C=O), 170.0 (C=O), 169.8 (C=O), 169.8 (C=O), 169.5 (C=O), 162.6 (C=O_{U_{ri}}), 150.1 (C=O_{U_{ri}}), 149.8 (C_{Pyr}), 149.6 (C_{Pyr}), 148.6 (C_{triazole}), 148.3 (C_{triazole}), 141.4 (C_{6U_{ri}}), 138.1 (C_{PyrH}), 124.3 (C_{triazoleH}), 121.0 (C_{triazoleH}), 120.0 (C_{PyrH}), 119.9 (C_{PyrH}), 103.6 (C_{5U_{ri}}), 91.6 (C_{1Rib}), 86.5 (C_{1Gal}), 80.2 (C_{4Rib}), 74.3 (C_{5Gal}), 72.9 (C_{3Gal} or C_{2Rib} or C_{3Rib}), 71.0 (C_{3Gal} or C_{2Rib} or C_{3Rib}), 70.9 (C_{3Gal} or C_{2Rib} or C_{3Rib}), 68.1 (C_{2Gal}), 67.0 (C_{4Gal}), 61.4 (C_{6Gal}), 51.4 (C_{5Rib}), 20.9 (COCH₃), 20.8 (COCH₃), 20.6 (COCH₃), 20.54 (COCH₃), 20.51 (COCH₃), 20.47 (COCH₃); HR-ESI-MS (positive mode) m/z : calcd. for C₃₆H₄₀N₉O₁₆ [M+H]⁺ 854.2588, found 854.2569.



2-(2-Acetamido-3,4,6-tri-O-acetyl-2-deoxy-1- β -D-glucopyranosyl-1H-1,2,3-triazol-4-yl)-6-[1-(2',3'-di-O-acetyl-uridin-5'-yl)-1H-1,2,3-triazol-4-yl]pyridine (42-GlcNAc)

Prepared according to general protocol C from compound **28-GlcNAc** (54 mg, 0.15 mmol, 1.0 eq.) and compound **47** (70 mg, 0.15 mmol, 1.0 eq.). The crude product was purified by silica gel column chromatography (100% PE to 100% EtOAc) to afford compound **42-GlcNAc** as yellow foam (50 mg, 0.06 mmol, 40%). $R_f = 0.16$ (EtOAc); $[\alpha]_D = -44.0$ ($c = 0.1$, CH_2Cl_2); $^1\text{H NMR}$ (400 MHz, CDCl_3) δ (ppm) = 9.96 (s, 1H, NH_{Uri}), 8.43 (s, 1H, $\text{H}_{\text{triazole}}$), 8.31 (s, 1H, $\text{H}_{\text{triazole}}$), 8.14 – 7.95 (m, 2H, H_{Pyr}), 7.82 (s, 1H, H_{Pyr}), 7.04 – 6.88 (m, 2H, $\text{H}_{6\text{Uri}}$, NHAc), 6.29 (d, $J = 9.7$ Hz, 1H, $\text{H}_{1\text{GlcNAc}}$), 5.72 (d, $J = 4.2$ Hz, 1H, $\text{H}_{1\text{Rib}}$), 5.64 – 5.51 (m, 3H, $\text{H}_{5\text{Uri}}$, $\text{H}_{2\text{Rib}}$, $\text{H}_{3\text{GlcNAc}}$), 5.43 – 5.27 (m, 2H, $\text{H}_{4\text{GlcNAc}}$, $\text{H}_{3\text{Rib}}$), 5.00 – 4.72 (m, 3H, $\text{H}_{5\text{aRib}}$, $\text{H}_{5\text{bRib}}$, $\text{H}_{2\text{GlcNAc}}$), 4.61 – 4.53 (m, 1H, $\text{H}_{4\text{Rib}}$), 4.31 (dd, $J = 12.5, 5.1$ Hz, 1H, $\text{H}_{6\text{aGlcNAc}}$), 4.20 – 4.09 (m, 2H, $\text{H}_{6\text{bGlcNAc}}$, $\text{H}_{5\text{GlcNAc}}$), 2.15 – 2.01 (m, 15H, COCH_3), 1.78 (s, 3H, NHCOCH_3); $^{13}\text{C NMR}$ (100 MHz, CDCl_3) δ (ppm) = 171.5, 171.0, 170.8, 169.8, 169.7, 169.7, 163.0, 150.5, 149.9, 149.6, 148.7, 148.5, 141.6 ($\text{C}_{6\text{Uri}}$), 137.9 (C_{PyrH}), 124.6 ($\text{C}_{\text{triazoleH}}$), 121.2 ($\text{C}_{\text{triazoleH}}$), 119.7 (C_{PyrH}), 119.5 (C_{PyrH}), 103.6 ($\text{C}_{5\text{Uri}}$), 91.4 ($\text{C}_{1\text{Rib}}$), 85.9 ($\text{C}_{1\text{GlcNAc}}$), 80.1 ($\text{C}_{4\text{Rib}}$), 75.0 ($\text{C}_{5\text{GlcNAc}}$), 72.6 ($\text{C}_{2\text{Rib}}$ or $\text{C}_{3\text{GlcNAc}}$), 72.0 ($\text{C}_{2\text{Rib}}$ or $\text{C}_{3\text{GlcNAc}}$), 70.8 ($\text{C}_{3\text{Rib}}$ or $\text{C}_{4\text{GlcNAc}}$), 68.4 ($\text{C}_{3\text{Rib}}$ or $\text{C}_{4\text{GlcNAc}}$), 62.2 ($\text{C}_{6\text{GlcNAc}}$), 53.6 ($\text{C}_{2\text{GlcNAc}}$), 50.8 ($\text{C}_{5\text{Rib}}$), 23.0 (NHCOCH_3), 20.85 (COCH_3), 20.83 (COCH_3), 20.78 (COCH_3), 20.56 (COCH_3), 20.55 (COCH_3); HR-ESI-MS (positive mode) m/z : calcd. for $\text{C}_{36}\text{H}_{41}\text{N}_{10}\text{O}_{15}$ $[\text{M}+\text{H}]^+$ 853.2747, found 853.2724.



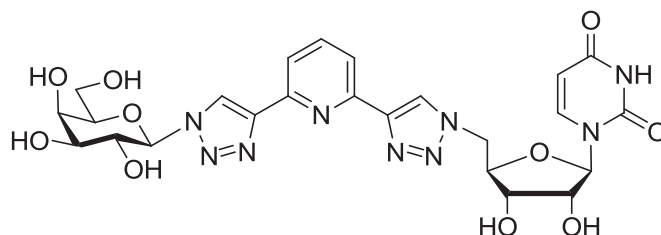
2-(1- β -D-Glucopyranosyl-1H-1,2,3-triazol-4-yl)-6-[1-(uridin-5'-yl)-1H-1,2,3-triazol-4-yl]pyridine (43-Glc)

(Method I) Prepared according to general protocol E from compound **42-Glc** (51 mg, 0.06 mmol, 1.0 eq.). The residue was purified by C18 reverse phase column chromatography (100% H_2O to 50% $\text{MeOH}/\text{H}_2\text{O}$) to afford compound **43-Glc** as white foam (14 mg, 0.023 mmol, 39%).

(Method II) In a flask containing compound **42-Glc** (38 mg, 0.045 mmol, 1.0 eq.) were added MeOH (2.5 mL), H_2O (1.25 mL) and Et_3N (5 mL) and the reaction mixture was stirred at r.t. for 7 days. Then, the reaction mixture was concentrated and co-evaporated with toluene (3×5 mL). The residue was purified by C18 reverse phase column chromatography (100% H_2O to 50% $\text{MeOH}/\text{H}_2\text{O}$) to afford compound **43-Glc** as white foam (22 mg, 0.0366 mmol, 82%).

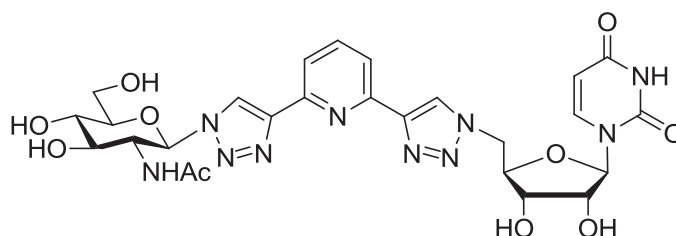
$[\alpha]_D = +70.0$ ($c = 0.1$, MeOH); $^1\text{H NMR}$ (500 MHz, D_2O) δ (ppm) = 8.52 (s, 1H, $\text{H}_{\text{triazole}}$), 8.22 (s, 1H, $\text{H}_{\text{triazole}}$), 7.73 (t, $J = 7.6$ Hz, 1H, H_{Pyr}), 7.60 (d, $J = 7.6$ Hz, 1H, H_{Pyr}), 7.56 (d, $J = 7.6$ Hz,

1H, H_{Pyr}), 7.12 (d, *J* = 8.0 Hz, 1H, H_{6Uri}), 5.71 (d, *J* = 9.1 Hz, 1H, H_{1Glc}), 5.55 (d, *J* = 2.2 Hz, 1H, H_{1Rib}), 5.44 (d, *J* = 8.0 Hz, 1H, H_{5Uri}), 4.73 (bs, 1H, H_{5aRib}), 4.70 (bd, *J* = 5.3 Hz, 1H, H_{5bRib}), 4.28 (bs, 1H, H_{4Rib}), 4.22 (dd, *J* = 5.2, 2.2 Hz, 1H, H_{2Rib}), 4.08 – 4.03 (m, 1H, H_{3Rib}), 3.95 (bd, *J* = 10.8 Hz, 1H, H_{6aGlc}), 3.88 (dd, *J* = 9.2, 9.1 Hz, 1H, H_{2Glc}), 3.80 – 3.70 (m, 3H, H_{3Glc}, H_{4Glc}, H_{6bGlc}), 3.59 (bd, *J* = 9.4 Hz, 1H H_{5Glc}); ¹³C NMR (125 MHz, D₂O) δ (ppm) = 166.1, 151.5, 149.0, 148.8, 147.8, 147.6, 142.6 (C_{6Uri}), 139.4 (C_{PyrH}), 125.7 (C_{triazoleH}), 123.7 (C_{triazoleH}), 120.5 (C_{PyrH}), 120.3 (C_{PyrH}), 102.6 (C_{5Uri}), 92.3 (C_{1Rib}), 88.3 (C_{1Glc}), 81.1 (C_{4Rib}), 79.6 (C_{3Glc} or C_{4Glc}), 76.5 (C_{3Glc} or C_{4Glc}), 73.2 (C_{2Glc}), 73.1 (C_{2Rib}), 70.4 (C_{3Rib}), 69.7 (C_{5Glc}), 61.2 (C_{6Glc}), 51.3 (C_{5Rib}); HR-ESI-MS (positive mode) *m/z*: calcd. for C₂₄H₂₈N₉O₁₀, [M+H]⁺ 602.1954, found 602.1956.



2-(1-β-D-galactopyranosyl-1*H*-1,2,3-triazol-4-yl)-6-[1-(uridin-5'-yl)-1*H*-1,2,3-triazol-4-yl]pyridine (43-Gal)

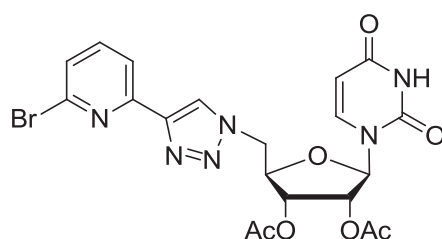
In a flask containing compound **42-Gal** (61 mg, 0.071 mmol, 1.0 eq.) were added MeOH (4 mL), H₂O (2 mL) and Et₃N (10 mL) and the reaction mixture was stirred at r.t. for 11 days. Then, the reaction mixture was concentrated and co-evaporated with toluene (3×5mL) to afford compound **43-Gal** as white foam (42 mg, 0.070 mmol, quant.) [α]_D = +28.5 (*c* = 0.2, DMSO); ¹H NMR (500 MHz, (CD₃)₂SO) δ (ppm) = 11.37 (s, 1H, NH_{Uri}), 8.77 (d, 2H, H_{triazole}), 8.00 (s, 3H, H_{Pyr}), 7.61 (d, *J* = 6.3 Hz, 1H, H_{6Uri}), 5.80 – 5.73 (m, 1H, H_{1Gal}), 5.67 – 5.51 (m, 2H, H_{1Rib}, H_{5Uri}), 5.54 (bs, 1H, OH), 5.43 (bs, 1H, OH), 5.34 (bs, 1H, OH), 5.08 (bs, 1H, OH), 4.87 – 4.67 (m, 4H, H_{5aRib}, H_{5bRib}, OH, OH), 4.28 (bs, 1H, H_{4Rib}), 4.17 – 4.00 (m, 3H, H_{2Rib}, H_{3Rib}, H_{2Gal}), 3.85 – 3.74 (m, 2H, H_{4Gal}, H_{5Gal}), 3.65 – 3.48 (m, 3H, H_{3Gal}, H_{6aGal}, H_{6bGal}); ¹³C NMR (125 MHz, (CD₃)₂SO) δ (ppm) = 162.8, 150.5, 149.8, 149.7, 147.1, 141.0 (C_{6Uri}), 138.2 (C_{Pyr}), 124.1 (C_{triazoleH}), 121.9 (C_{triazoleH}), 118.4 (C_{Pyr}), 101.9 (C_{5Uri}), 89.1 (C_{1Rib}), 88.4 (C_{1Gal}), 81.5 (C_{4Rib}), 78.4 (C_{4Gal} or C_{5Gal}), 73.5 (C_{3Gal}), 72.0 (C_{2Gal}), 70.5 (C_{2Rib} or C_{3Rib}), 69.5 (C_{2Rib} or C_{3Rib}), 68.4 (C_{4Gal} or C_{5Gal}), 60.4 (C_{6Gal}), 51.4 (C_{5Rib}); HR-ESI-MS (positive mode) *m/z*: calcd. for C₂₄H₂₈N₉O₁₀, [M+H]⁺ 602.1954, found 602.1956.



2-(2-Acetamido-2-deoxy-1-β-D-glucopyranosyl-1*H*-1,2,3-triazol-4-yl)-6-[1-(uridine-5'-yl)-1*H*-1,2,3-triazol-4-yl]pyridine (43-GlcNAc)

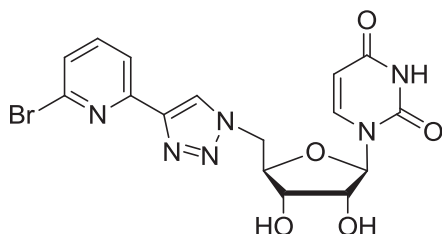
Prepared according to general protocol E from compound **42-GlcNAc** (35 mg, 0.04 mmol, 1.0 eq.). The residue was purified by C18 reverse phase column chromatography (100% H₂O to 80% MeOH/H₂O) to afford compound **43-GlcNAc** as white foam (24 mg, 0.036 mmol, 91%).

$[\alpha]_D = -28.8$ ($c = 0.08$, DMSO); $^1\text{H NMR}$ (400 MHz, $\text{D}_2\text{O}:\text{CD}_3\text{OD} = 2:1$) δ (ppm) = 8.72 (s, 1H, $\text{H}_{\text{triazole}}$), 8.55 (s, 1H, $\text{H}_{\text{triazole}}$), 8.06 – 7.98 (m, 1H, H_{Pyr}), 7.91 – 7.82 (m, 2H, H_{Pyr}), 7.21 (d, $J = 8.0$ Hz, 1H, $\text{H}_{6\text{Uri}}$), 5.94 (d, $J = 9.7$ Hz, 1H, $\text{H}_{1\text{GlcNAc}}$), 5.78 (d, $J = 3.3$ Hz, 1H, $\text{H}_{1\text{Rib}}$), 5.60 (d, $J = 8.0$ Hz, 1H, $\text{H}_{5\text{Uri}}$), 4.94 (dd, $J = 14.8, 3.5$ Hz, 1H, $\text{H}_{5\text{aRib}}$), 4.86 (dd, $J = 14.8, 5.7$ Hz, 1H, $\text{H}_{5\text{bRib}}$), 4.40 (ddd, $J = 9.9, 5.7, 3.5$ Hz, 1H, $\text{H}_{4\text{Rib}}$), 4.34 (t, $J = 9.7$ Hz, 1H, $\text{H}_{2\text{GlcNAc}}$), 4.28 (dd, $J = 5.6, 3.3$ Hz, 1H, $\text{H}_{2\text{Rib}}$), 4.22 – 4.15 (m, 1H, $\text{H}_{3\text{Rib}}$), 3.96 (dd, $J = 12.4, 1.8$ Hz, 1H, $\text{H}_{6\text{aGlcNAc}}$), 3.89 – 3.68 (m, 4H, $\text{H}_{3\text{GlcNAc}}, \text{H}_{4\text{GlcNAc}}, \text{H}_{5\text{GlcNAc}}, \text{H}_{6\text{bGlcNAc}}$), 1.82 (s, 3H, NHCOCH_3); $^{13}\text{C NMR}$ (100 MHz, $\text{D}_2\text{O}:\text{CD}_3\text{OD} = 2:1$) δ (ppm) = 174.7, 150.0, 149.8, 148.3, 141.8 ($\text{C}_{6\text{Uri}}$), 140.1 (C_{PyrH}), 126.4 ($\text{C}_{\text{triazoleH}}$), 123.9 ($\text{C}_{\text{triazoleH}}$), 121.2 (s, 2C, $2\times\text{C}_{\text{PyrH}}$), 103.6 ($\text{C}_{5\text{Uri}}$), 92.5 ($\text{C}_{1\text{Rib}}$), 87.6 ($\text{C}_{1\text{GlcNAc}}$), 81.6 ($\text{C}_{4\text{Rib}}$), 80.2 ($\text{C}_{3\text{GlcNAc}}$ or $\text{C}_{4\text{GlcNAc}}$ or $\text{C}_{5\text{GlcNAc}}$), 74.7 ($\text{C}_{3\text{GlcNAc}}$ or $\text{C}_{4\text{GlcNAc}}$ or $\text{C}_{5\text{GlcNAc}}$), 73.9 ($\text{C}_{3\text{GlcNAc}}$ or $\text{C}_{4\text{GlcNAc}}$ or $\text{C}_{5\text{GlcNAc}}$), 71.4 ($\text{C}_{2\text{Rib}}$), 70.5 ($\text{C}_{3\text{Rib}}$), 61.6 ($\text{C}_{6\text{GlcNAc}}$), 56.6 ($\text{C}_{2\text{GlcNAc}}$), 52.2 ($\text{C}_{5\text{Rib}}$), 22.6 (NHCOCH_3); HR-ESI-MS (positive mode) m/z : calcd. for $\text{C}_{26}\text{H}_{30}\text{N}_{10}\text{NaO}_{10}$ $[\text{M}+\text{Na}]^+$ 665.2039, found 665.2023.



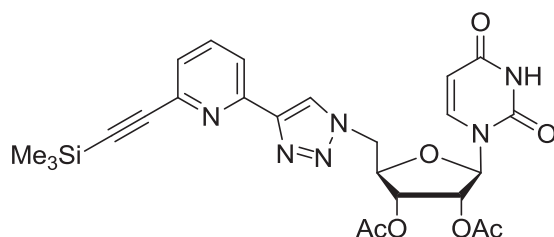
2-Bromo-6-[1-(2',3'-di-*O*-acetyl-uridin-5'-yl)-1*H*-1,2,3-triazol-4-yl]pyridine (**44**)

DIPEA (0.19 mL, 1.065 mmol, 7.5 eq.) was added into a microwave tube containing 2',3'-di-*O*-acetyl-5'-azido-uridine (**5**) (50 mg, 0.142 mmol, 1.0 eq.), 2-bromo-6-ethynylpyridine (**38**) (31 mg, 0.17 mmol, 1.2 eq.) and CuI (14 mg, 0.017 mmol, 0.5 eq.) in DMF (2 mL). The reaction was heated for 15 min by microwave irradiation at 100°C. Then, the reaction suspension was diluted with ethyl acetate (25 mL), washed with satd aq. Na_2CO_3 solution (2×25 mL) and H_2O (30 mL). The organic phase was dried (Na_2SO_4) and concentrated. The residue was purified by silica gel column chromatography (PE:EtOAc = 2:3 to PE:EtOAc = 1:2) to afford compound **44** as white foam (72 mg, 0.135 mmol, 95%). $R_f = 0.16$ (PE:EtOAc = 2:3); $[\alpha]_D = +54.6$ ($c = 0.7$, CH_2Cl_2); $^1\text{H NMR}$ (400 MHz, CDCl_3) $\delta = 9.02$ (s, 1H, NH_{Uri}), 8.28 (s, 1H, $\text{H}_{\text{triazole}}$), 8.12 (d, $J = 7.8$ Hz, 1H, H_{Pyr}), 7.63 (t, $J = 7.8$ Hz, 1H, H_{Pyr}), 7.41 (d, $J = 7.8$ Hz, 1H, H_{Pyr}), 7.06 (d, $J = 8.1$ Hz, 1H, $\text{H}_{6\text{Uri}}$), 5.75 (dd, $J = 8.1, 2.0$ Hz, 1H, $\text{H}_{5\text{Uri}}$), 5.64 (d, $J = 4.0$ Hz, 1H, $\text{H}_{1\text{Rib}}$), 5.44 (dd appears as t, $J = 6.5$ Hz, 1H, $\text{H}_{3\text{Rib}}$), 5.34 (dd, $J = 6.5, 4.0$ Hz, 1H, $\text{H}_{2\text{Rib}}$), 4.85 (dd, $J = 14.5, 3.4$ Hz, $\text{H}_{5\text{aRib}}$), 4.78 (dd, $J = 14.5, 6.5$ Hz, 1H, $\text{H}_{5\text{bRib}}$), 4.50 (ddd appears as td, $J = 6.5, 3.4$ Hz, 1H, $\text{H}_{4\text{Rib}}$), 2.12 (s, 3H, COCH_3), 2.10 (s, 3H, COCH_3); $^{13}\text{C NMR}$ (100 MHz, CDCl_3) $\delta = 169.9$ (COCH_3), 169.8 (COCH_3), 162.7, 151.1, 150.1, 147.4, 141.9, 141.6 ($\text{C}_{6\text{Uri}}$), 139.4 (C_{PyrH}), 127.4 (C_{PyrH}), 124.6 ($\text{C}_{\text{triazoleH}}$), 119.0 (C_{PyrH}), 103.6 ($\text{C}_{5\text{Uri}}$), 91.9 ($\text{C}_{1\text{Rib}}$), 80.4 ($\text{C}_{4\text{Rib}}$), 73.0 ($\text{C}_{2\text{Rib}}$), 70.8 ($\text{C}_{3\text{Rib}}$), 51.6 ($\text{C}_{5\text{Rib}}$), 20.6 (COCH_3), 20.5 (COCH_3); HR-ESI-MS (positive mode) m/z : calcd. for $\text{C}_{20}\text{H}_{20}\text{BrN}_6\text{O}_7$, $[\text{M}+\text{H}]^+$ 535.0571, found 535.0568.



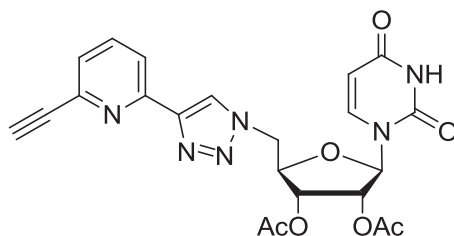
2-Bromo-6-[1-(uridin-5'-yl)-1H-1,2,3-triazol-4-yl]pyridine (**45**)

Prepared according to general protocol **E** from compound **44** (10 mg, 0.019 mmol, 1.0 eq.). The residue was purified by C18 reverse phase column chromatography (100% H₂O to 30% MeOH/H₂O) to afford compound **45** as white foam (7 mg, 0.0156 mmol, 82%). $R_f = 0.18$ (EtOAc); $[\alpha]_D = +51.0$ ($c = 0.3$, MeOH); ¹H NMR (500 MHz, CD₃OD) δ (ppm) = 8.50 (s, 1H, H_{triazole}), 8.03 (d, $J = 7.8$ Hz, 1H, H_{Pyr}), 7.77 (t, $J = 7.8$ Hz, 1H, H_{Pyr}), 7.53 (d, $J = 7.8$ Hz, 1H, H_{Pyr}), 7.40 (d, $J = 8.0$ Hz, 1H, H_{6Uri}), 5.76 (d, $J = 3.6$ Hz, 1H, H_{1Rib}), 5.63 (d, $J = 8.0$ Hz, 1H, H_{5Uri}), 4.89 (dd, $J = 14.5, 3.7$ Hz, 1H, H_{5aRib}), 4.81 (dd, $J = 14.5, 6.6$ Hz, 1H, H_{5bRib}), 4.31 (ddd, $J = 6.6, 6.6, 3.7$ Hz, 1H, H_{4Rib}), 4.18 – 4.13 (m, 2H, H_{2Rib}, H_{3Rib}); ¹³C NMR (125 MHz, CD₃OD) δ (ppm) = 165.96 (C=O_{Uri}), 152.24 (C_{Pyr}), 152.07 (C=O_{Uri}), 147.96 (C_{triazole}), 143.20 (C_{6Uri}), 142.94 (C_{Pyr}), 141.06 (C_{PyrH}), 128.52 (C_{PyrH}), 126.16 (C_{triazoleH}), 119.92 (C_{PyrH}), 103.05 (C_{6Uri}), 93.23 (C_{1Rib}), 82.91 (C_{4Rib}), 74.22 (C_{2Rib} or C_{3Rib}), 71.98 (C_{2Rib} or C_{3Rib}), 52.63 (C_{5Rib}); HR-ESI-MS (positive mode) m/z : calcd. for C₁₆H₁₆BrN₆O₅, [M+H]⁺ 451.0360, found 451.0359.



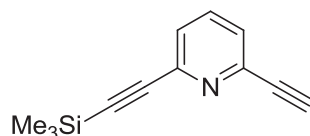
2-(2-Trimethylsilylethynyl)-6-[1-(2',3'-di-O-acetyl-uridin-5'-yl)-1H-1,2,3-triazol-4-yl]pyridine (**46**)

Prepared according to general protocol **D** from compound **44** (30 mg, 0.056 mmol, 1.0 eq.). The crude product was purified by silica gel column chromatography (60% EtOAc/PE to 70% EtOAc/PE) to afford compound **46** as yellow foam (22 mg, 0.04 mmol, 71%). $R_f = 0.42$ (PE:EtOAc = 1:3); ¹H NMR (400 MHz, CDCl₃) δ (ppm) = 8.92 (s, 1H, H_{3Uri}), 8.33 (s, 1H, H_{triazole}), 8.12 (d, $J = 7.7$ Hz, 1H, H_{Pyr}), 7.73 (t, $J = 7.7$ Hz, 1H, H_{Pyr}), 7.41 (d, $J = 7.7$ Hz, 1H, H_{Pyr}), 7.06 (d, $J = 8.1$ Hz, 1H, H_{6Uri}), 5.75 (d, $J = 8.1$ Hz, 1H, H_{5Uri}), 5.65 (d, $J = 4.1$ Hz, 1H, H_{1Rib}), 5.45 (dd appears as t, $J = 6.5$ Hz, 1H, H_{3Rib}), 5.30 (dd, $J = 6.5, 4.1$ Hz, 1H, H_{2Rib}), 4.84 (dd, $J = 14.5, 3.2$ Hz, 1H, H_{5aRib}), 4.76 (dd, $J = 14.5, 6.8$ Hz, 1H, H_{5bRib}), 4.48 (ddd appears as td, $J = 6.8, 6.5, 3.2$ Hz, 1H, H_{4Rib}), 2.12 (s, 3H, COCH₃), 2.09 (s, 3H, COCH₃), 0.27 (s, 9H, SiMe₃); ¹³C NMR (100 MHz, CDCl₃) δ (ppm) = 169.83 (COCH₃), 169.78 (COCH₃), 162.7, 150.4, 150.0, 148.2, 142.9, 141.5 (C_{6Uri}), 137.2 (C_{PyrH}), 127.1 (C_{PyrH}), 124.5 (C_{triazoleH}), 119.9 (C_{PyrH}), 103.7 (C \equiv C), 103.6 (C \equiv C), 95.4 (C_{5Uri}), 91.6 (C_{1Rib}), 80.4 (C_{4Rib}), 73.0 (C_{2Rib}), 70.8 (C_{3Rib}), 51.6 (C_{5Rib}), 20.56 (COCH₃), 20.55 (COCH₃), -0.1 (s, 3C, SiMe₃); HR-ESI-MS (positive mode) m/z : calcd. for C₂₅H₂₉N₆O₇Si, [M+H]⁺ 553.1862, found 553.1850.



2-Ethynyl-6-[1-(2',3'-di-*O*-acetyl-uridin-5'-yl)-1*H*-1,2,3-triazol-4-yl]pyridine (**47**)

Prepared according to general protocol F from compound **46** (20 mg, 0.036 mmol, 1.0 eq.). The crude product was purified by silica gel column chromatography (100% PE to 100% EtOAc) to afford compound **47** as yellow foam (9 mg, 0.0188 mmol, 52%). $R_f = 0.25$ (PE:EtOAc, 1:3); ^1H NMR (400 MHz, CDCl_3) δ (ppm) = 8.70 (s, 1H, NH_{Uri}), 8.34 (s, 1H, $\text{H}_{\text{triazole}}$), 8.17 (d, $J = 7.8$ Hz, 1H, H_{Pyr}), 7.77 (t, $J = 7.8$ Hz, 1H, H_{Pyr}), 7.43 (d, $J = 7.8$ Hz, 1H, H_{Pyr}), 7.04 (d, $J = 8.1$ Hz, 1H, $\text{H}_{6\text{Uri}}$), 5.75 (dd, $J = 8.1, 2.1$ Hz, 1H, $\text{H}_{5\text{Uri}}$), 5.65 (d, $J = 4.1$ Hz, 1H, $\text{H}_{1\text{Rib}}$), 5.42 (t, $J = 6.5$ Hz, 1H, $\text{H}_{3\text{Rib}}$), 5.30 (dd, $J = 6.5, 4.1$ Hz, 1H, $\text{H}_{2\text{Rib}}$), 4.85 (dd, $J = 14.5, 3.3$ Hz, 1H, $\text{H}_{5a\text{Rib}}$), 4.78 (dd, $J = 14.5, 6.5$ Hz, 1H, $\text{H}_{5b\text{Rib}}$), 4.49 (ddd, $J = 6.5, 6.5, 3.3$ Hz, 1H, $\text{H}_{4\text{Rib}}$), 3.20 (s, 1H, $\text{C}\equiv\text{CH}$), 2.13 (s, 3H, COCH_3), 2.09 (s, 3H, COCH_3); ^{13}C NMR (100 MHz, CDCl_3) δ (ppm) = 169.83, 169.76, 150.6, 150.0, 148.1, 142.1, 141.5 ($\text{C}_{6\text{Uri}}$), 137.4 (C_{Pyr}), 127.0 (C_{Pyr}), 124.5 ($\text{C}_{\text{triazoleH}}$), 120.3 (C_{Pyr}), 103.6 ($\text{C}_{5\text{Uri}}$), 91.6 ($\text{C}_{1\text{Rib}}$), 82.8 ($\text{C}\equiv\text{CH}$), 80.4 ($\text{C}_{4\text{Rib}}$), 77.4 ($\text{C}\equiv\text{CH}$), 72.9 ($\text{C}_{2\text{Rib}}$), 70.7 ($\text{C}_{3\text{Rib}}$), 51.5 ($\text{C}_{5\text{Rib}}$), 20.57 (COCH_3), 20.55 (COCH_3); HR-ESI-MS (positive mode) m/z : calcd. for $\text{C}_{22}\text{H}_{21}\text{N}_6\text{O}_7$ [$\text{M}+\text{H}$] $^+$ 481.1466, found 481.1464.

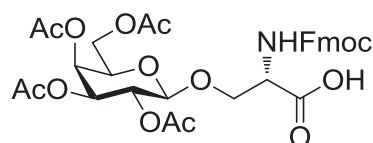


2-Ethynyl-6-(2-(trimethylsilyl)ethynyl)pyridine (**48**)²¹⁸

In a 100 mL round-bottom flask containing 2,6-dibromopyridine (**36**) (5 g, 21.1 mmol, 1.0 eq.), $\text{Pd}(\text{PPh}_3)_4$ (1.22 g, 1 mmol, 0.05 eq.) and CuI (190 mg, 1 mmol, 0.05 eq.) in toluene (100 mL) was degassed with argon. Then, trimethylsilylacetylene (9 mL, 63.3 mmol, 3.0 eq.) and diisopropylamine (8.4 mL, 59.9 mmol, 2.8 eq.) were injected. The reaction was stirred at r.t. with protection of light for 42 h. Then, another portion of $\text{Pd}(\text{PPh}_3)_4$ (294 mg, 0.24 mmol, 0.01 eq.), CuI (50 mg, 0.26 mmol, 0.01 eq.), trimethylsilylacetylene (0.36 mL, 2.53 mmol, 0.12 eq.) and diisopropylamine (0.4 mL, 2.85 mmol, 0.14 eq.) were added into the reaction. After 48 h, the reaction mixture was filtered and the filtrate was poured into satd aq. NH_4Cl solution (250 mL), extracted with CH_2Cl_2 (3×300 mL). The combined organic layers were washed with H_2O (200 mL) and brine (200 mL). The organic phase was dried (MgSO_4) and the solvent was evaporated. The residue was then purified by silica gel column chromatography (5% $\text{CH}_2\text{Cl}_2/\text{PE}$ to 30% $\text{CH}_2\text{Cl}_2/\text{PE}$) to afford 2,6-bis(2-trimethylsilylethynyl)pyridine (5.6 g, 20.68 mmol, 98%). $R_f = 0.73$ (PE:EtOAc, 2:1); ^1H NMR (300 MHz, CDCl_3) δ (ppm) = 7.62 – 7.55 (m, 1H, H_{Pyr}), 7.40 – 7.35 (m, 2H, 2 H_{Pyr}), 0.25 (s, 18H, SiMe_3).

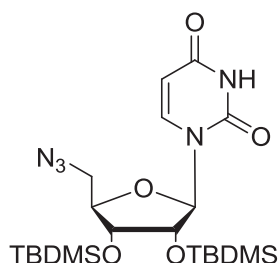
A solution of 2,6-bis(2-trimethylsilylethynyl)pyridine (2.189 g, 8.1 mmol, 1.0 eq.) in MeOH (90 mL) was degassed with argon then 1 M aq. KOH (20 μL) was added. The reaction mixture was stirred at r.t. under argon. After 100 min, the reaction mixture was poured into pentane (300 mL), washed successively with H_2O (3×100 mL) and brine (100 mL). The aqueous layer was

extracted with CH₂Cl₂ (300 mL) and the combined organic layers were dried over MgSO₄, concentrated. The residue was purified by silica gel column chromatography (5% CH₂Cl₂/PE to 30% CH₂Cl₂/PE) to afford compound **48** as brown solid (528 mg, 2.65 mmol, 33%). R_f = 0.42 (PE:EtOAc, 2:1); ¹H NMR (300 MHz, CDCl₃) δ (ppm) = 7.62 (t, *J* = 7.8 Hz, 1H, H_{Pyr}), 7.44 – 7.38 (m, 2H, H_{Pyr}), 3.14 (s, 1H, C≡CH), 0.26 (s, 9H, SiMe₃).



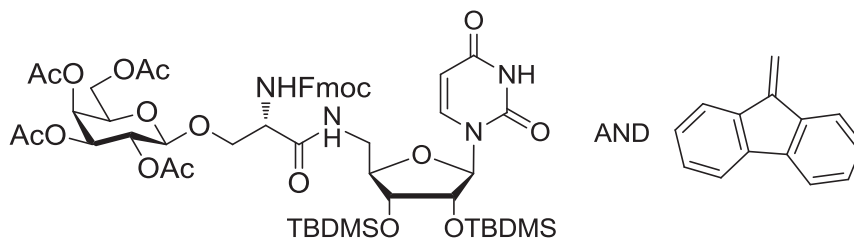
***N*-(9-Fluorenylmethoxycarbonyl)-*O*-(2,3,4,6-tetra-*O*-acetyl-β-*D*-galactopyranosyl)-*L*-serine (**49**)²²³**

To a solution of β-*D*-galactose pentaacetate (4.7 g, 12.04 mmol, 1.0 eq.) and *N*-Fmoc-*L*-ser-OH (5 g, 14.63 mmol, 1.2 eq.) in dry CH₃CN (50 mL) was added BF₃ etherate (5.12 g, 36.10 mmol, 3.0 eq.) at 0°C. The reaction was stirred at room temperature under an argon atmosphere overnight. Then, the reaction mixture was diluted with CH₂Cl₂ (70 mL) and washed successively with 0.5 N aq. NaHSO₄ (200 mL) and H₂O (80 mL). The organic phase was dried over MgSO₄, filtered and concentrated under diminished pressure. The residue was purified by silica gel column chromatography (PE:EtOAc=7:3 to PE:EtOAc=1:1) to afford compound **49** as white foam (3.6 g, 5.47 mmol, 45%) as a white foam. ¹H NMR (300 MHz, CD₃OD) δ (ppm) = 7.85 – 7.77 (m, 2H), 7.73 – 7.62 (m, 2H), 7.46 – 7.29 (m, 4H), 5.49 (s, 1H), 5.39 – 5.34 (m, 1H), 5.15 – 5.02 (m, 2H), 4.65 (d, *J* = 6.5 Hz, 1H), 4.45 – 4.33 (m, 3H), 4.29 – 4.21 (m, 1H), 4.19 – 4.01 (m, 4H), 3.96 – 3.88 (m, 1H), 2.14 – 1.91 (m, 12H).



5'-Azido-5'-deoxy-2',3'-di-*O*-(*tert*-butyldimethylsilyl)uridine (50**)²³⁸**

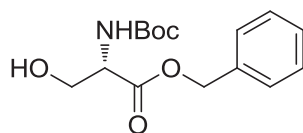
Pyridine (10 mL) was added into a flask containing 5'-azido-5'-deoxyuridine (from synthesis of compound **5**, 1.5 g, 5.57 mmol, 1.0 eq.), imidazole (2.276 g, 33.43 mmol, 6.0 eq.) and TBDMSCl (5.04 g, 33.43 mmol, 6.0 eq.). After addition, the reaction mixture was stirred at r.t. for 64 h. Then, the reaction mixture was concentrated and co-evaporated with toluene (3×15 mL). The residue was purified by silica gel column chromatography (PE:EtOAc, 4:1) to afford compound **50** (2.59 g, 5.2 mmol, 93%) as white foam. R_f = 0.37 (PE:EtOAc, 4:1); NMR (300 MHz, CDCl₃) δ (ppm) = 9.57 (s, 1H, H_{3Uri}), 7.69 (d, *J* = 8.1 Hz, 1H, H_{6Uri}), 5.77 (dd, *J* = 8.1, 2.0 Hz, 1H, H_{5Uri}), 5.65 (d, *J* = 2.9 Hz, 1H, H_{1Rib}), 4.21 (dd, *J* = 4.2, 3.0 Hz, 1H), 4.14 (dd, *J* = 6.5, 3.3 Hz, 1H), 3.96 (dd, *J* = 6.3, 4.3 Hz, 1H), 3.82 (dd, *J* = 13.4, 3.3 Hz, 1H, H_{5aRib}), 3.61 (dd, *J* = 13.4, 3.4 Hz, 1H, H_{5bRib}), 0.90 (s, 9H, CMe₃), 0.89 (s, 9H, CMe₃), 0.12 (s, 3H, SiMe), 0.09 (s, 3H, SiMe), 0.09 (s, 3H, SiMe), 0.08 (s, 3H, SiMe).



N-[2',3'-Di-*O*-(*tert*-butyldimethylsilyl)-5'-deoxy-uridin-5'-yl]-*N'*-(9-fluorenylmethoxycarbonyl)-*O*-(2,3,4,6-tetra-*O*-acetyl- β -D-galactopyranosyl)-serinamide (**51**) AND

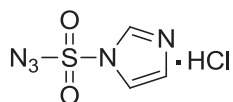
9-Methylene-9*H*-fluorene (**52**)

In a 50 mL round-bottom flask containing compound **49** (631 mg, 0.96 mmol, 1.5 eq), anhydrous DMF (5 mL) was added under argon. The mixture was cooled to -5°C using a NaCl/ice bath, then TBTU (411 mg, 1.28 mmol, 2.0 eq.), EDCI (245 mg, 1.28 mmol, 2.0 eq.) and DIEA (0.22 mL, 1.28 mmol, 2.0 eq.) were added. The reaction mixture was stirred for 40 min at -10°C . Then, a solution of compound **61** (300 mg, 0.64 mmol, 1.0 eq.) in DMF (5 mL) was added dropwise (within 45 min). After addition, the reaction temperature was allowed to be warmed up to r.t. and stirred overnight. Then, the crude mixture was concentrated, diluted with EtOAc (50 mL) and washed with satd NaHCO_3 solution (2×40 mL), water (2×40 mL) and brine (2×40 mL). The organic phase was then concentrated. The residue was purified by silica gel column chromatography (PE:EtOAc = 1:1 to PE:EtOAc = 1:4) to afford compound **51** (90 mg, 0.081 mmol, 13%) as white foam and 9-methylene-9*H*-fluorene **52** (135 mg, 0.76 mmol, 79% respect to the starting material compound **49**) as a byproduct. **51** ESI-MS (positive mode) m/z : c $[\text{M}+\text{H}]^+$ 1111.5, $[2\text{M}+\text{H}]^+$ 2223.9; **52** ^1H NMR (300 MHz, CDCl_3) δ (ppm) = 7.78 – 7.67 (m, 4H), 7.44 – 7.27 (m, 4H), 6.09 (s, 2H).



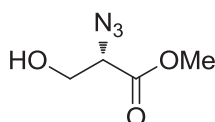
N-Boc-L-serine benzyl ester (**54**)²³⁹

DMSO (20 mL) was added into a 100 mL argon-flushed flask containing *N*-Boc-serine (2.02 g, 9.82 mmol, 1.0 eq.), KHCO_3 (1.48 g, 14.7 mmol, 1.5 eq.) and tetrabutylammonium iodide (363 mg, 0.98 mmol, 0.1 eq.). The resulting white suspension was stirred magnetically at r.t. for 10 min to obtain a homogeneous solution. To this solution was added benzyl bromide (3.6 mL, 29.5 mmol, 3.0 eq.). Then, the reaction mixture was stirred at r.t. overnight. The reaction was quenched by addition of H_2O (100 mL). The DMSO- H_2O layer was extracted with EtOAc (4×100 mL). The combined organic layers were washed with satd aq. NaHCO_3 solution (2×100 mL), satd aq. $\text{Na}_2\text{S}_2\text{O}_3$ (2×100 mL) and brine (100 mL). The organic phase was dried (Na_2SO_4), concentrated and the residue was purified by silica gel column chromatography (PE:EtOAc, 6:1 to PE:EtOAc, 4:1) to afford compound **54** as white foam (1.93 g, 6.54 mmol, 67%). R_f = 0.35 (PE:EtOAc, 2:1); ^1H NMR (300 MHz, CDCl_3) δ (ppm) = 7.36 (s, 5H, Ph), 5.43 (s, 1H, *NHBoc*), 5.22 (d, J = 1.1 Hz, 2H, OCH_2Ph), 4.42 (s, 1H, OH), 4.01 – 3.87 (m, 2H, H_β), 2.12 (s, 1H, H_α), 1.45 (s, 9H, CMe_3).



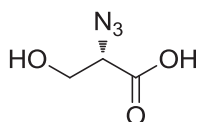
Imidazole-1-sulfonyl azide hydrochloride (**56**)²²⁴

Sulfonyl chloride (16.1 mL, 200 mmol, 1.0 eq.) was added dropwise into an ice-cooled suspension of NaN₃ (13.0 g, 200 mmol, 1.0 eq.) in MeCN (200 mL). After addition, the reaction was stirred at r.t. overnight. Imidazole (25.9 g, 380 mmol, 1.8 eq.) was added portion-wise into the ice-cooled mixture and the resulting slurry was stirred at r.t. for 3 h. Then, the reaction mixture was diluted with EtOAc (400 mL), washed with H₂O (3×200 mL), satd aq. NaHCO₃ (3×200 mL), dried (MgSO₄) and filtered. A solution of HCl in EtOH [obtained by dropwise addition of AcCl (21.3 mL, 300 mmol) to ice-cooled dry ethanol (75 mL)] was added dropwise to the filtrate with stirring. The mixture was cooled to 0°C, filtered and the solid was washed with EtOAc (3×100 mL) to give the imidazole-1-sulfonyl azide hydrochloride salt (**56**) (26.3 g, 125.4 mmol, 63%). ¹H NMR (300 MHz, D₂O) δ (ppm) = 9.37 (t, *J* = 1.4 Hz, 1H), 8.06 – 7.98 (m, 1H), 7.61 (dd, *J* = 2.1, 1.2 Hz, 1H).



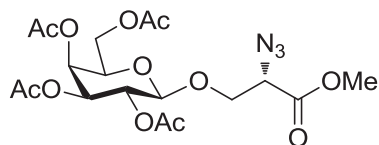
Methyl (*2S*)-2-azido-3-hydroxypropanoate (**57**)²²⁴⁻²²⁵

Imidazole-1-sulfonyl azide hydrochloride (**56**) (250 mg, 1.2 mmol, 1.2 eq.) was added to a solution of L-serine methyl ester hydrochloride salt (156 mg, 1.0 mmol, 1eq.), K₂CO₃ (346 mg, 2.5 mmol, 2.5 eq.) and CuSO₄·5H₂O (2.5 mg, 10 μmol, 0.01 eq.) in MeOH (5 mL). After addition, the reaction was stirred at r.t. for 5 h. Then, the reaction mixture was concentrated, diluted with H₂O (10 mL), extracted with EtOAc (4×10 mL), dried over Na₂SO₄. The organic phase was concentrated and the residue was purified by silica gel column chromatography (10% EtOAc/PE to 20% EtOAc/PE) to afford compound **57** (89 mg, 0.61 mmol, 61%) as colorless oil. R_f = 0.31 (25% EtOAc/PE, revealed as a pink spot with naphthoresorcinol ethanol solution); [α]_D²⁰ = -73.1 (*c* = 1.0, CHCl₃); ¹H NMR (300 MHz, CDCl₃) δ (ppm) = 4.06 (t, *J* = 4.7 Hz, 1H, H_α), 3.91 – 3.87 (m, 2H, H_β), 3.80 (s, 3H, OMe), 2.83 (s, 1H, OH).



(*2S*)-2-Azido-3-hydroxypropanoic acid (**58**)

LiOH (312 mg, 7.74 mmol, 1.2 eq.) was solubilized with H₂O (5 mL) and added dropwise into a solution of methyl (*2S*)-2-azido-3-hydroxypropanoate (**57**) (900 mg, 6.20 mmol, 1.0 eq.) in THF (10 mL). After addition, the reaction mixture was stirred at r.t. for 1 h. DOWEX 50W×2 Resin (Fluka, 50-100 mesh, H⁺ Form) was added until pH~4. Then, the mixture was filtered and concentrated to afford compound **58** (810 mg, 6.18 mmol, quant.) as colorless oil. ¹H NMR (300 MHz, CD₃OD) δ (ppm) = 4.00 (t, *J* = 4.5 Hz, 1H), 3.89 (d, *J* = 4.5 Hz, 2H).

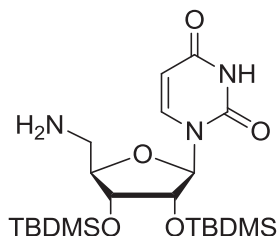


Methyl (2,3,4,6-tetra-*O*-acetyl- β -D-galactopyranosyloxy)-(2*S*)-2-azido-3-propanoate (59**)**

(**Entry 7, Table III-2**) SnCl₄ (1.725 mL, 1 M in CH₂Cl₂, 1.725 mmol, 5.0 eq.) was added dropwise (within 120 min via syringe pump) at 0°C to a stirred solution of β -D-galactopyranosyl pentaacetate **1a** (202 mg, 0.517 mmol, 1.5 eq.), silver trifluoroacetate (190 mg, 0.863 mmol, 2.5 eq.) and methyl (2*S*)-2-azido-3-hydroxypropanoate (**57**) (50 mg, 0.345 mmol, 1.0 eq.) in freshly distilled CH₂Cl₂ (3 mL). The reaction mixture was stirred at 0°C for 17 h with protection of light. Then, satd aq. NaHCO₃ solution (10 mL) was added into the reaction. The resulting mixture was vigorously stirred for 15 min. The suspension was filtered. The solution was extracted with CH₂Cl₂ (3×20 mL). The organic layers were combined, dried (Na₂SO₄) and concentrated. The residue was purified by silica gel column chromatography (PE:EtOAc = 9:1 to PE:EtOAc = 3:1) to afford compound **59** as white foam (90 mg, 0.189 mmol, 55%).

(**Entry 8, Table III-2**) BF₃·Et₂O (6 μ L, 0.042 mmol, 0.2 eq.) was added dropwise into a stirred solution of 2,3,4,6-tetra-*O*-acetyl- α -D-galactopyranosyl trichloroacetimidate (152 mg, 0.31 mmol, 1.5 eq.) and methyl (2*S*)-2-azido-3-hydroxypropanoate (**57**) (30 mg, 0.207 mmol, 1.0 eq.) in freshly distilled CH₂Cl₂ (3 mL) at -20°C. The reaction mixture was stirred at -20°C for 2 h. The reaction mixture was poured into satd aq. Na₂CO₃ (10 mL) solution and extracted with CH₂Cl₂ (4×10 mL). The combined organic layers were dried (Na₂SO₄) and evaporated. The residue was purified by silica gel column chromatography (PE:EtOAc = 9:1 to PE:EtOAc = 3:1) to afford compound **59** as white foam (44 mg, 0.093 mmol, 45%).

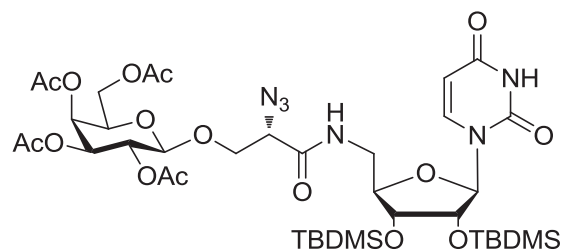
R_f = 0.19 (PE:EtOAc = 3:1); ¹H NMR (400 MHz, CDCl₃) δ (ppm) = 5.35 (bd, *J* = 3.4 Hz, 1H, H₄), 5.14 (dd, *J* = 10.4, 7.9 Hz, 1H, H₂), 4.98 (dd, *J* = 10.4, 3.4 Hz, 1H, H₃), 4.55 (d, *J* = 7.9 Hz, 1H, H₁), 4.21 – 4.04 (m, 3H, H₆, H _{β a}), 4.00 (t, *J* = 4.4 Hz, 1H, H _{α}), 3.92 – 3.82 (m, 2H, H _{β b}, H₅), 3.78 (s, 3H, CO₂Me), 2.11 (s, 3H, COCH₃), 2.03 (s, 3H, COCH₃), 2.01 (s, 3H, COCH₃), 1.94 (s, 3H, COCH₃); ¹³C NMR (100 MHz, CDCl₃) δ (ppm) 170.5 (COCH₃), 170.3 (COCH₃), 170.2 (COCH₃), 169.5 (COCH₃), 168.4 (CO₂Me), 101.2 (C₁), 70.9 (C₅), 70.8 (C₃), 68.8 (C _{β}), 68.4 (C₂), 67.0 (C₄), 61.3 (C _{α}), 61.3 (C₆), 53.0 (CO₂Me), 20.8 (COCH₃), 20.71 (COCH₃), 20.69 (COCH₃), 20.6 (COCH₃); HR-ESI-MS (positive mode) *m/z*: calcd for C₁₈H₂₅N₃NaO₁₁, [M+Na]⁺ 498.1330, found 498.1311.



5'-Amino-2',3'-di-*O*-(*tert*-butyldimethylsilyl)-5'-deoxyuridine (61**)²³⁸**

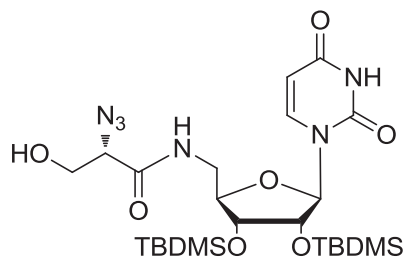
In a flask containing compound **50** (224 mg, 0.45 mmol, 1.0 eq.) and 10% Pd/C (49 mg) was added solvent MeOH (5 mL). The atmosphere was changed first to argon then hydrogen with vacuum. The reaction was stirred at r.t. for 4 h. Then, the reaction mixture was filtered through celite, washed with methanol. The combined methanol solution was dried (Na₂SO₄),

concentrated to afford compound **61** (180 mg, 0.38 mmol, 85%) as white foam. The product was used directly for the reaction of next step without further purification. NMR (300 MHz, CD₃OD) δ (ppm) = 7.71 (d, J = 8.1 Hz, 1H), 5.81 (d, J = 5.8 Hz, 1H), 5.73 (d, J = 8.1 Hz, 1H), 4.38 (dd, J = 5.7, 4.5 Hz, 1H), 4.06 – 3.94 (m, 2H), 2.90 – 2.87 (m, 2H), 0.93 (s, 9H), 0.89 (s, 9H), 0.15 – 0.01 (m, 12H).



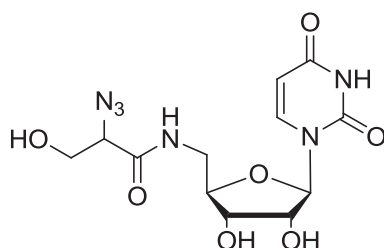
***N*-[2',3'-Di-*O*-(*tert*-butyldimethylsilyl)-uridin-5'-yl]-3-(2,3,4,6-tetra-*O*-acetyl- β -D-galactopyranosyloxy)-(2*S*)-2-azidopropanamide (**62**)**

BF₃·Et₂O (3 μ L, 0.016 mmol, 0.2 eq.) was added dropwise into a stirred solution of 2,3,4,6-tetra-*O*-acetyl- α -D-galactopyranosyl trichloroacetimidate (58 mg, 0.118mmol, 1.5 eq.) and compound **63** (46 mg, 0.079 mmol, 1.0 eq.) in freshly distilled CH₂Cl₂ (3 mL) at -20°C under argon. The reaction mixture was stirred at -20°C for 2 h. Then, the reaction was poured into satd aq. Na₂CO₃ (10 mL) solution and extracted with CH₂Cl₂ (4×10 mL). The combined organic layers were dried (Na₂SO₄) and evaporated. The residue was purified by silica gel column chromatography (PE:EtOAc = 1:1 to PE:EtOAc = 3:1) to afford compound **62** as white foam (44 mg, 0.048 mmol, 61%). R_f = 0.1 (PE:EtOAc, 1:1); ¹H NMR (400 MHz, CDCl₃) δ (ppm) = 9.01 (s, 1H, NH_{Urid}), 7.38 (d, J = 8.1 Hz, 1H, H_{6Urid}), 7.12 (t, J = 5.4 Hz, 1H, NHCO), 5.76 (dd, J = 8.1, 1.7 Hz, 1H, H_{5Urid}), 5.42 (d, J = 5.0 Hz, 1H, H_{1Rib}), 5.38 (bd, J = 3.4 Hz, 1H, H_{4Gal}), 5.23 – 5.15 (m, 1H, H_{2Gal}), 5.02 (dd, J = 10.4, 3.4 Hz, 1H, H_{3Gal}), 4.56 (d, J = 7.9 Hz, 1H, H_{1Gal}), 4.49 (bd, J = 5.0 Hz, 1H, H_{2Rib}), 4.22 – 4.03 (m, 6H, H_{4Rib}, H _{α} , H₆, H _{β}), 3.96 – 3.86 (m, 2H, H_{5Gal}, H_{3Rib}), 3.61 (dd, J = 14.1, 7.1 Hz, 1H, H_{5aRib}), 3.45 (dd, J = 14.1, 4.1 Hz, 1H, H_{5bRib}), 2.15 (s, 3H, COCH₃), 2.06 (s, 3H, COCH₃), 2.04 (s, 3H, COCH₃), 1.98 (s, 3H, COCH₃), 0.90 (s, 9H, CMe₃), 0.87 (s, 9H, CMe₃), 0.08 (2s, 6H, 2×SiMe), 0.06 (s, 3H, SiMe), 0.03 (s, 3H, SiMe); ¹³C NMR (100 MHz, CDCl₃) δ (ppm) = 170.6 (C=O), 170.4 (C=O), 170.2 (C=O), 169.7 (C=O), 167.3 (C=O), 163.1 (C=O), 150.2 (C=O), 142.6 (C_{6Urid}), 102.6 (C_{5Urid}), 101.0 (C_{1Gal}), 94.2 (C_{1Rib}), 83.5 (C_{4Rib}), 73.5 (C_{2Rib}), 73.1 (C_{3Rib}), 71.1 (C_{5Gal}), 70.9 (C_{3Gal}), 69.5 (C _{β}), 68.7 (C_{2Gal}), 67.0 (C_{4Gal}), 63.3 (C _{α}), 61.4 (C_{6Gal}), 41.5 (C_{5Rib}), 25.91 (CMe₃), 25.86 (CMe₃), 21.0 (COCH₃), 20.81 (COCH₃), 20.77 (COCH₃), 20.7 (COCH₃), 18.14 (CMe₃), 18.06 (CMe₃), -4.3 (SiCH₃), -4.58 (SiCH₃), -4.65 (SiCH₃), -4.70 (SiCH₃); HR-ESI-MS (positive mode) m/z : calcd for C₃₈H₆₂N₆NaO₁₆Si₂, [M+Na]⁺ 937.3653, found 937.3629.



***N*-[2',3'-Di-*O*-(*tert*-butyldimethylsilyl)-uridin-5'-yl]-(2*S*)-2-azido-3-hydroxypropanamide (63)**

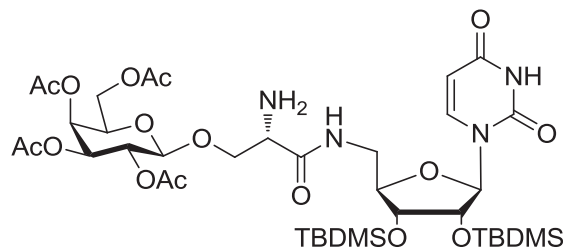
In a flask containing compound **50** (150 mg, 0.30 mmol, 1.0 eq.) and 10% Pd/C (34 mg) was added the solvent MeOH (5 mL). The air inside of the flask was changed with argon, then, filled with H₂. The reaction was stirred at r.t. for 4h. Then, the reaction mixture was filtrated and washed with MeOH. The organic solution was concentrated and the residue was used directly without further purification. compound **58** (27 mg, 0.21 mmol, 1.5 eq.) and HOBt (40 mg, 0.25 mmol, 1.2 eq.) were co-evaporated with toluene (3×5 mL), then, freshly distilled THF (4 mL) was added. The solution was then transferred into a flask containing the amine **61** (150 mg, 0.30 mmol, 1.0 eq.), DCC (52 mg, 0.25 mmol, 1.2 eq.) and DMAP (5 mg, 0.06 mmol, 0.2 eq.). The resulting reaction mixture was stirred at r.t. for 16 h. Then, the reaction mixture was concentrated and the residue was purified by silica gel column chromatography (60% EtOAc/PE) to afford the desired amide **63** as white foam (53 mg, 0.09 mmol, 30%). R_f = 0.1 (PE:EtOAc, 2:3); ¹H NMR (400 MHz, CDCl₃) δ (ppm) = 9.70 (s, 1H, NH_{Urid}), 7.36 – 7.29 (m, 2H, NHCO, H_{Urid}), 5.77 (dd, *J* = 8.0, 2.0 Hz, 1H, H_{Urid}), 5.36 (dd, *J* = 5.5, 2.5 Hz, 1H, H_{1Rib}), 4.54 (bd, *J* = 5.5 Hz, 1H, H_{2Rib}), 4.13 – 4.06 (m, 2H, H_{4Rib}, H_α), 4.04 – 3.91 (m, 3H, H_{3Rib}, H_β), 3.72 – 3.61 (m, 1H, H_{5aRib}), 3.51 – 3.39 (m, 1H, H_{5bRib}), 0.90 (s, 9H, CMe₃), 0.86 (s, 9H, CMe₃), 0.08 (s, 3H, SiCH₃), 0.08 (s, 3H, SiCH₃), 0.05 (s, 3H, SiCH₃), 0.00 (s, 3H, SiCH₃); ¹³C NMR (100 MHz, CDCl₃) δ (ppm) = 169.0 (C=O), 163.7 (C=O), 150.6 (C=O), 143.4 (C_{Urid}), 102.6 (C_{Urid}), 94.9 (C_{1Rib}), 83.8 (C_{4Rib}), 73.1 (C_{2Rib}), 72.9 (C_{3Rib}), 64.6 (CHN₃), 63.1 (CH₂OH), 41.1 (C_{5Rib}), 25.9 (CMe₃), 25.8 (CMe₃), 18.1 (CMe₃), 18.0 (CMe₃), -4.3 (SiCH₃), -4.5 (SiCH₃), -4.66 (SiCH₃), -4.73 (SiCH₃); HR-ESI-MS (positive mode) *m/z*: calcd for C₂₄H₄₄N₆NaO₇Si₂, [M+Na]⁺ 607.2702, found 607.2674.



***N*-(Uridin-5'-yl)-2-azido-3-hydroxypropanamide (64)** (Adapted from Ref²⁴⁰⁻²⁴¹)

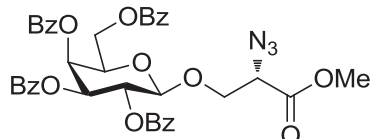
A solution of compound **63** (48 mg, 0.082 mmol, 1.0 eq.) in CH₂Cl₂ (1 mL) was stirred at r.t. Then, 90% TFA (4.4 mL) was added dropwise. After addition, the reaction mixture was stirred at r.t. overnight. MeOH (3 mL) and H₂O (5 mL) were then added into the reaction mixture. The solvent was removed by evaporation and the residue was purified by silica gel column chromatography (EtOAc to 10% MeOH/EtOAc) to afford compound **64** as white foam (L:D = 5:1, 31 mg, 0.087 mmol, quant.). ¹H NMR (400 MHz, CD₃OD) δ = 7.68 (d, *J* = 8.1 Hz, 1H,

H_{6U_{ri}}), 5.77 (d, $J = 4.6$ Hz, 1H, H_{1Rib}), 5.73 (d, $J = 8.1$ Hz, 1H, H_{5U_{ri}}), 4.23 (dd, $J = 5.0, 4.6$ Hz, 1H, H_{2Rib}), 4.06 – 3.99 (m, 3H, H_{3Rib}, H_{4Rib}, H _{α}), 3.94 (dd, $J = 11.4, 4.3$ Hz, 1H, H _{β a}), 3.81 (dd, $J = 11.4, 6.6$ Hz, 1H, H _{β b}), 3.64 – 3.50 (m, 2H, H_{5Rib}); ¹³C NMR (100 MHz, CD₃OD) $\delta = 170.9, 166.1, 152.3, 143.3$ (C_{6U_{ri}}), 102.9 (C_{5U_{ri}}), 92.2 (C_{1Rib}), 83.7 (C _{α}), 74.7 (C_{2Rib}), 72.2 (C_{3Rib} or C_{4Rib}), 66.2 (C_{3Rib} or C_{4Rib}), 63.6 (C _{β}), 41.9 (C_{5Rib}); HR-ESI-MS (positive mode) m/z : calcd for C₁₂H₁₆N₆NaO₇, [M+Na]⁺ 379.0973, found 379.0962.



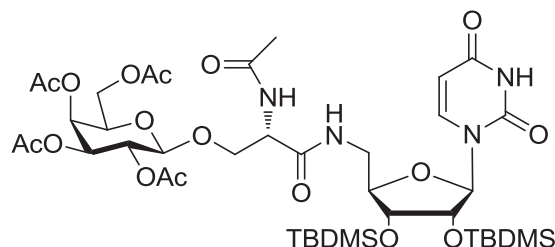
***N*-[2',3'-Di-*O*-(*tert*-butyldimethylsilyl)-uridin-5'-yl]-*O*-(2,3,4,6-tetra-*O*-acetyl- β -D-galactopyranosyl)serinamide (**65**)**

In a flask containing compound **62** (240 mg, 0.026 mmol, 1.0 eq.) and 10% Pd/C (29 mg) was added solvent MeOH (10 mL). The atmosphere in the flask was changed to argon, then, exchanged with hydrogen. The reaction was stirred at r.t. After 5 h, the reaction mixture was filtered through celite, washed with methanol. The combined methanol solution was concentrated to afford a crude product **65** as white foam. The crude product was used directly for the reaction of next step without further purification.



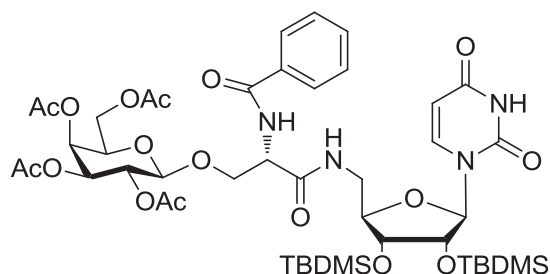
Methyl (2*S*)-2-azido-3-*O*-(2,3,4,6-tetra-*O*-benzoyl- β -D-galactopyranosyloxy)propanoate (66**)**

BF₃·Et₂O (6 μ L, 0.042 mmol, 0.2 eq.) was added dropwise into a stirred solution of 2,3,4,6-tetra-*O*-benzoyl- α -D-galactopyranosyl trichloroacetimidate (225 mg, 0.30 mmol, 1.5 eq.) and methyl (2*S*)-2-azido-3-hydroxypropanoate (**57**) (28 mg, 0.20 mmol, 1.0 eq.) in freshly distilled CH₂Cl₂ (3 mL) at -20°C. After addition the reaction mixture was stirred at -20°C for 2.5 h. Then, the reaction mixture was poured into satd aq. Na₂CO₃ (10 mL) solution and extracted with CH₂Cl₂ (4×10 mL). The combined organic layers were dried (Na₂SO₄) and evaporated. The residue was purified by silica gel column chromatography (PE:EtOAc, 85:15) to afford product **66** (95 mg, 0.131 mmol, 66%) as a mixture of the glycoside and the decomposed sugar donor. Yield was calculated based on the identified glycoside in the mixture from ¹H NMR data.



***N*-[2',3'-Di-*O*-(*tert*-butyldimethylsilyl)-uridin-5'-yl]-*N'*-acetyl-*O*-(2,3,4,6-tetra-*O*-acetyl- β -D-galactopyranosyl)-serinamide (67)**

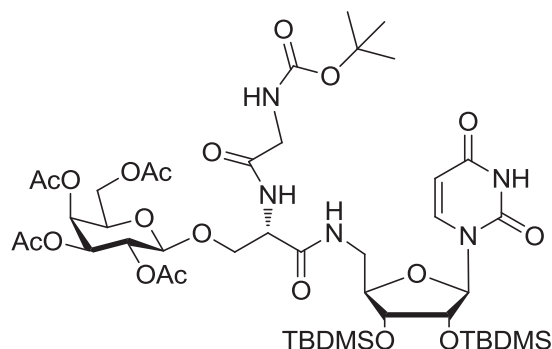
Compound **62** (47 mg, 0.051 mmol, 1.0 eq.) and PPh₃ (41 mg, 0.153 mmol, 3.0 eq.) were solubilized in THF (2 mL), then, H₂O (0.5 mL) was added and the reaction mixture was stirred at r.t. for 17 h. Then, the reaction was concentrated, pyridine (2 mL) and acetic anhydride (1 mL) were added into the flask. The resulting solution was stirred at r.t. for 16 h. MeOH (10 mL) was added and stirring continued for another 15 min. The resulting reaction mixture was co-evaporated with toluene (3×10 mL) and the residue was purified by silica gel column chromatography (50% EtOAc/PE to 100% EtOAc) to afford compound **67** as white foam (10 mg, 0.011 mmol, 21%). *R*_f = 0.1 (PE:EtOAc, 2:3); ¹H NMR (500 MHz, CDCl₃) δ (ppm) = 8.68 (s, 1H, NH_{Urid}), 7.39 (d, *J* = 8.1 Hz, 1H, H_{6Urid}), 7.09 (t, *J* = 5.6 Hz, 1H, NHCO), 6.50 (d, *J* = 7.1 Hz, 1H, NHAc), 5.77 (dd, *J* = 8.1, 1.9 Hz, 1H, H_{5Urid}), 5.42 (d, *J* = 5.6 Hz, 1H, H_{1Rib}), 5.40 – 5.37 (m, 1H, H_{4Gal}), 5.14 (dd, *J* = 10.5, 7.9 Hz, 1H, H_{2Gal}), 5.02 (dd, *J* = 10.5, 3.4 Hz, 1H, H_{3Gal}), 4.65 – 4.60 (m, 1H, H_a), 4.53 (d, *J* = 7.9, 1H, H_{1Gal}), 4.47 (t, *J* = 5.6 Hz, 1H, H_{2Rib}), 4.16 – 4.09 (m, 4H, H_{6Gal}, H_{4Rib}, H _{β a}), 3.97 – 3.92 (m, 2H, H_{3Rib}, H_{5Gal}), 3.77 (dd, *J* = 10.4, 6.8 Hz, 1H, H _{β b}), 3.56 – 3.51 (m, 2H, H_{5Rib}), 2.13 (s, 3H, COCH₃), 2.08 (s, 3H, COCH₃), 2.05 (s, 3H, COCH₃), 2.03 (s, 3H, COCH₃), 1.99 (s, 3H, COCH₃), 0.91 (s, 9H, CMe₃), 0.87 (s, 9H, CMe₃), 0.10 (s, 3H, SiCH₃), 0.09 (s, 3H, SiCH₃), 0.08 (s, 3H, SiCH₃), 0.02 (s, 3H, SiCH₃); ¹³C NMR (125 MHz, CDCl₃) δ (ppm) = 170.7, 170.4, 170.3, 170.2, 170.09, 170.06, 167.9, 162.8, 150.3, 142.9 (C_{6Urid}), 132.6, 131.0, 128.9, 102.6 (C_{5Urid}), 101.8 (C_{1Gal}), 94.3 (C_{1Rib}), 84.1 (C_{4Rib}), 73.3 (C_{2Rib}), 73.0 (C_{3Rib} or C_{5Gal}), 71.2 (C_{3Rib} or C_{5Gal}), 70.7 (C_{3Gal}), 69.4 (C _{β}), 69.0 (C_{2Gal}), 67.0 (C_{4Gal}), 61.3 (C_{6Gal}), 52.9 (C_a), 41.6 (C_{5Rib}), 26.0 (s, 3C, CMe₃), 25.9 (s, 3C, CMe₃), 23.1 (NHCOCH₃), 21.1 (COCH₃), 20.8 (COCH₃), 20.74 (COCH₃), 20.71 (COCH₃), 18.2 (CMe₃), 18.1 (CMe₃), -4.3 (SiCH₃), -4.5 (SiCH₃), -4.6 (SiCH₃), -4.7 (SiCH₃); ESI-MS (positive mode) *m/z*: C₄₀H₆₆N₄NaO₁₇Si₂, [M+Na]⁺ 953.4.



***N*-[2',3'-Di-*O*-(*tert*-butyldimethylsilyl)-uridin-5'-yl]-*N'*-benzoyl-*O*-(2,3,4,6-tetra-*O*-acetyl- β -D-galactopyranosyl)serinamide (68)**

Benzoyl chloride (9 μ L, 0.08 mmol, 1.2 eq.) was added dropwise into a flask containing a solution of the amine **65** (59 mg, 0.067 mmol, 1.0 eq.) and DIPEA (15 μ L, 0.086 mmol, 1.3 eq.) in freshly distilled CH₂Cl₂ (4 mL). The reaction mixture was stirred at r.t. for 16h. Then, the

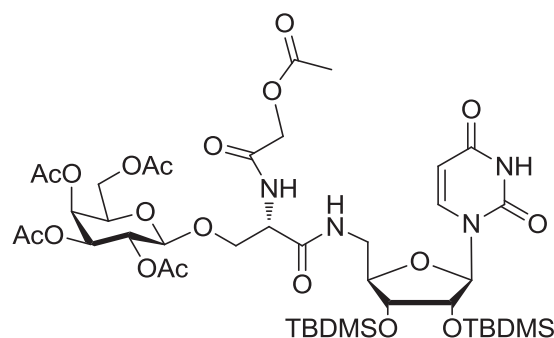
reaction mixture was concentrated and the residue was purified by silica column chromatography (66% EtOAc/PE) to afford the desired amide **68** as white foam (54 mg, 0.054 mmol, two steps 81%). $R_f = 0.19$ (PE:EtOAc, 2:3); $^1\text{H NMR}$ (400 MHz, CDCl_3) δ (ppm) = 8.60 (s, 1H, NH_{Uri}), 7.87 – 7.83 (m, 2H, Ph), 7.57 – 7.50 (m, 1H, Ph), 7.49 – 7.42 (m, 2H, 2 \times Ph), 7.30 (d, $J = 8.1$ Hz, 1H, $\text{H}_{6\text{Uri}}$), 7.22 (d, $J = 7.0$ Hz, 1H, NH_{Bz}), 5.65 (d, $J = 8.1$ Hz, 1H, $\text{H}_{5\text{Uri}}$), 5.39 – 5.35 (m, 2H, $\text{H}_{1\text{Rib}}$, $\text{H}_{4\text{Gal}}$), 5.16 (dd, $J = 10.4, 7.9$ Hz, 1H, $\text{H}_{2\text{Gal}}$), 5.01 (dd, $J = 10.4, 3.4$ Hz, 1H, $\text{H}_{3\text{Gal}}$), 4.90 – 4.84 (m, 1H, H_α), 4.58 (d, $J = 7.9$ Hz, 1H, $\text{H}_{1\text{Gal}}$), 4.47 – 4.42 (m, 1H, $\text{H}_{2\text{Rib}}$), 4.28 (dd, $J = 10.5, 4.7$ Hz, 1H, $\text{H}_{\beta\alpha}$), 4.15 – 4.10 (m, 3H, $\text{H}_{4\text{Rib}}$, $\text{H}_{6\text{Gal}}$), 3.99 – 3.87 (m, 3H, $\text{H}_{\beta\text{b}}$, $\text{H}_{5\text{Gal}}$, $\text{H}_{3\text{Rib}}$), 3.69 – 3.58 (m, 1H, $\text{H}_{5\text{aRib}}$), 3.56 – 3.47 (m, 1H, $\text{H}_{5\text{bRib}}$), 2.11 (s, 3H, COCH_3), 2.03 (s, 3H, COCH_3), 1.98 (s, 3H, COCH_3), 1.97 (s, 3H, COCH_3), 0.90 (s, 9H, CMe_3), 0.84 (s, 9H, CMe_3), 0.10 (s, 3H, SiCH_3), 0.08 (s, 3H, SiCH_3), 0.06 (s, 3H, SiCH_3), 0.03 (s, 3H, SiCH_3); $^{13}\text{C NMR}$ (100 MHz, CDCl_3) δ (ppm) = 170.6, 170.3, 170.2, 170.1, 167.3, 162.8, 150.2, 143.0 ($\text{C}_{6\text{Uri}}$), 133.5, 132.3 (C_{Ph}), 128.8 (s, 2C, 2 \times C_{Ph}), 127.4 (s, 2C, 2 \times C_{Ph}), 102.5 ($\text{C}_{5\text{Uri}}$), 101.6 ($\text{C}_{1\text{Gal}}$), 94.4 ($\text{C}_{1\text{Rib}}$), 84.4 ($\text{C}_{4\text{Rib}}$), 73.0 ($\text{C}_{2\text{Rib}}$), 72.9 ($\text{C}_{5\text{Gal}}$ or $\text{C}_{3\text{Rib}}$), 71.1 ($\text{C}_{5\text{Gal}}$ or $\text{C}_{3\text{Rib}}$), 70.8 ($\text{C}_{3\text{Gal}}$), 69.1 (C_β), 69.0 ($\text{C}_{2\text{Gal}}$), 67.0 ($\text{C}_{4\text{Gal}}$), 61.3 ($\text{C}_{6\text{Gal}}$), 53.3 (C_α), 41.5 ($\text{C}_{5\text{Rib}}$), 25.94 (CMe_3), 25.85 (CMe_3), 20.9 (COCH_3), 20.8 (COCH_3), 20.71 (COCH_3), 20.69 (COCH_3), 18.1 (CMe_3), 18.0 (CMe_3), -4.3 (SiCH_3), -4.5 (SiCH_3), -4.6 (SiCH_3), -4.9 (SiCH_3); HR-ESI-MS (positive mode) m/z : calcd for $\text{C}_{45}\text{H}_{68}\text{N}_4\text{NaO}_{17}\text{Si}_2$, $[\text{M}+\text{Na}]^+$ 1015.4010, found 1015.3982.



***N*-[2',3'-Di-*O*-(*tert*-butyldimethylsilyl)-uridin-5'-yl]-*N'*-[*N''*-(*tert*-butoxycarbonyl)glyciny]-*O*-(2,3,4,6-tetra-*O*-acetyl- β -D-galactopyranosyl)serinamide (**69**)**

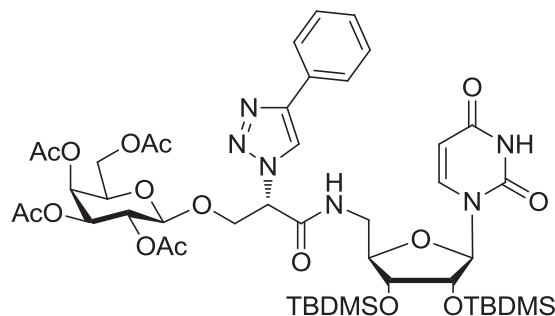
Freshly distilled CH_2Cl_2 (4 mL) was added into a flask containing the amine **65** (57 mg, 0.064 mmol, 1.0 eq.), *N*-Boc-Gly-OSu (21 mg, 0.077 mmol, 1.2 eq.) and DCC (16 mg, 0.077 mmol, 1.2 eq.). The resulting reaction mixture was stirred at r.t. for 16 h. Then, the reaction mixture was concentrated and the residue was purified by silica gel column chromatography (66% EtOAc/PE) to afford the desired amide **69** as white foam (39 mg, 0.037 mmol, two steps 58%). $R_f = 0.22$ (PE:EtOAc, 1:2); $^1\text{H NMR}$ (400 MHz, CDCl_3) δ (ppm) = 9.84 (s, 1H, NH_{Uri}), 7.61 (s, 1H, NHCO), 7.24 (d, $J = 7.9$ Hz, 1H, $\text{H}_{6\text{Uri}}$), 6.64 (d, $J = 7.8$ Hz, 1H, $\text{NHCO}_{\text{CH}_2\text{NHBoc}}$), 5.73 (dd, $J = 7.9, 1.5$ Hz, 1H, $\text{H}_{5\text{Uri}}$), 5.50 (bs, 1H, NH_{Boc}), 5.37 (bd, $J = 2.7$ Hz, 1H, $\text{H}_{4\text{Gal}}$), 5.20 (d, $J = 6.5$ Hz, 1H, $\text{H}_{1\text{Rib}}$), 5.12 (dd, $J = 10.5, 7.8$ Hz, 1H, $\text{H}_{2\text{Gal}}$), 5.00 (dd, $J = 10.5, 2.7$ Hz, 1H, $\text{H}_{3\text{Gal}}$), 4.76 – 4.68 (m, 1H, $\text{H}_{\alpha\text{Ser}}$), 4.56 – 4.46 (m, 2H, $\text{H}_{1\text{Gal}}$, $\text{H}_{2\text{Rib}}$), 4.23 (dd, $J = 10.6, 5.6$ Hz, 1H, $\text{H}_{\beta\alpha\text{Ser}}$), 4.16 – 4.06 (m, 3H, $\text{H}_{6\text{Gal}}$, $\text{H}_{4\text{Rib}}$), 3.98 – 3.82 (m, 6H, $\text{H}_{5\text{Gal}}$, $\text{H}_{5\text{aRib}}$, $\text{H}_{3\text{Rib}}$, $\text{H}_{\alpha\text{Gly}}$, $\text{H}_{\beta\text{bSer}}$), 3.29 – 3.19 (m, 1H, $\text{H}_{5\text{bRib}}$), 2.13 (s, 3H, COCH_3), 2.06 (s, 3H, COCH_3), 2.03 (s, 3H, COCH_3), 1.97 (s, 3H, COCH_3), 1.46 (s, 9H, 3 \times CH_3Boc), 0.89 (s, 9H, SiCMe_3), 0.84 (s, 9H, SiCMe_3), 0.08 (s, 3H, SiCH_3), 0.07 (s, 3H, SiCH_3), 0.05 (s, 3H, SiCH_3), -0.05 (s, 3H, SiCH_3); $^{13}\text{C NMR}$ (100 MHz,

CDCl₃) δ (ppm) = 172.1, 170.6, 170.4, 170.3, 170.2, 170.1, 169.9, 169.2, 163.2, 156.7, 150.7, 144.1 (C_{6Uri}), 102.7 (C_{5Uri}), 101.6 (C_{1Gal}), 95.8 (C_{1Rib}), 85.4 (C_{4Rib}), 72.4 (C_{5Gal} or H_{3Rib}), 72.1 (C_{2Rib}), 71.0 (C_{5Gal} or H_{3Rib}), 70.6 (C_{3Gal}), 69.1 (C _{β Ser}), 69.0 (C_{2Gal}), 67.0 (C_{4Gal}), 61.2 (C_{6Gal}), 52.9 (C _{α Ser}), 44.8 (C _{α Gly}), 41.2 (C_{5Rib}), 28.5 (s, 3C, 3 \times CH₃Boc), 25.9 (s, 3C, SiCMe₃), 25.8 (s, 3C, SiCMe₃), 21.0 (COCH₃), 20.79 (COCH₃), 20.75 (COCH₃), 20.67 (COCH₃), 18.1 (s, 3C, SiCMe₃), 18.0 (s, 3C, SiCMe₃), -4.4 (SiCH₃), -4.6 (SiCH₃), -4.7 (SiCH₃), -5.1 (SiCH₃); HR-ESI-MS (positive mode) m/z : calcd for C₄₅H₇₅N₅NaO₁₉Si₂, [M+Na]⁺ 1068.4487, found 1068.4444.



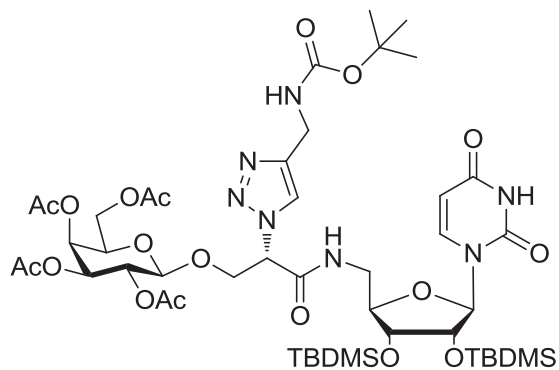
***N*-[2',3'-Di-*O*-(*tert*-butyldimethylsilyl)-uridin-5'-yl]-*N'*-acetoxyacetyl-*O*-(2,3,4,6-tetra-*O*-acetyl- β -D-galactopyranosyl)serinamide (**70**)**

Acetoxyacetyl chloride (9 μ L, 0.088 mmol, 1.2 eq.) was added dropwise into a flask containing a solution of the amine **65** (65 mg, 0.073 mmol, 1.0 eq.) and DIPEA (15 μ L, 0.086 mmol, 1.2 eq.) in freshly distilled CH₂Cl₂ (4 mL). The reaction mixture was stirred at r.t. for 16 h. Then, the reaction mixture was concentrated and the residue was purified by silica gel column chromatography (66% EtOAc/PE) to afford the desired mono-substituted amide **70** (31 mg, 0.031 mmol, two steps 43%) and the di-substituted byproduct (19 mg, 0.017 mmol, two steps 24%). R_f = 0.21 (mono-substituted amide) and 0.29 (di-substituted amide) (PE:EtOAc, 1:2); ¹H NMR (400 MHz, CDCl₃) δ (ppm) = 8.99 (s, 1H, NH_{Uri}), 7.30 (d, J = 8.1 Hz, 1H, H_{6Uri}), 6.98 (d, J = 7.5 Hz, 1H, NHCO_{CH₂OAc}), 5.75 (dd, J = 8.1, 1.5 Hz, 1H, H_{5Uri}), 5.37 (dd, J = 3.4, 1.0 Hz, 1H, H_{4Gal}), 5.28 (d, J = 6.2 Hz, 1H, H_{1Rib}), 5.12 (dd, J = 10.5, 7.8 Hz, 1H, H_{2Gal}), 5.03 (dd, J = 10.5, 3.4 Hz, 1H, H_{3Gal}), 4.76 – 4.71 (m, 1H, CH_{2aOAc}), 4.71 – 4.65 (m, 1H, H _{α}), 4.58 – 4.46 (m, 3H, H_{1Gal}, H_{2Rib}, CH_{2bOAc}), 4.24 (dd, J = 10.9, 4.0 Hz, 1H, H _{β a}), 4.15 – 4.08 (m, 3H, H_{6Gal}, H_{4Rib}), 3.96 – 3.90 (m, 2H, H_{5Gal}, H_{3Rib}), 3.85 (dd, J = 10.9, 6.0 Hz, 1H, H _{β b}), 3.76 – 3.66 (m, 1H, H_{5aRib}), 3.46 – 3.38 (m, 1H, H_{5bRib}), 2.22 (s, 3H, COCH₃), 2.12 (s, 3H, COCH₃), 2.08 (s, 3H, COCH₃), 2.04 (s, 3H, COCH₃), 1.98 (s, 3H, COCH₃), 0.91 (s, 9H, CMe₃), 0.85 (s, 9H, CMe₃), 0.10 (s, 3H, SiCH₃), 0.09 (s, 3H, SiCH₃), 0.08 (s, 3H, SiCH₃), -0.01 (s, 3H, SiCH₃); ¹³C NMR (100 MHz, CDCl₃) δ (ppm) = 170.6, 170.4, 170.22, 170.16, 169.9, 169.4, 167.5, 163.0, 150.4, 143.8 (C_{6Uri}), 102.6 (C_{5Uri}), 101.8 (C_{1Gal}), 95.5 (C_{1Rib}), 84.9 (C_{4Rib}), 72.9 (C_{5Gal} or C_{3Rib}), 72.5 (C_{2Rib}), 71.0 (C_{5Gal} or C_{3Rib}), 70.7 (C_{3Gal}), 69.1 (C _{β}), 68.9 (C_{2Gal}), 67.0 (C_{4Gal}), 63.0 (CH_{2bOAc}), 61.1 (C_{6Gal}), 52.4 (C _{α}), 41.5 (C_{5Rib}), 25.94 (s, 3C, CMe₃), 25.86 (s, 3C, CMe₃), 21.0 (COCH₃), 20.9 (COCH₃), 20.8 (COCH₃), 20.73 (COCH₃), 20.70 (COCH₃), 18.1 (CMe₃), 18.0 (CMe₃), -4.4 (SiCH₃), -4.5 (SiCH₃), -4.7 (SiCH₃), -5.0 (SiCH₃); HR-ESI-MS (positive mode) m/z : calcd for C₄₂H₆₈N₄NaO₁₉Si₂, [M+Na]⁺ 1011.3909, found 1011.3900.



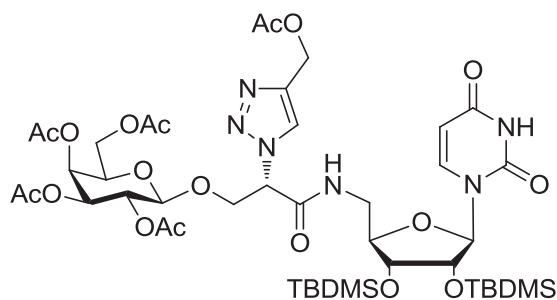
***N*-[2',3'-Di-*O*-(*tert*-butyldimethylsilyl)-uridin-5'-yl]-(2*S*)-2-(4-phenyl-1,2,3-triazol-1-yl)-3-(2,3,4,6-tetra-*O*-acetyl- β -D-galactopyranosyloxy)propanamide (**71**)**

DIPEA (0.07 mL, 0.40 mmol, 8.2 eq.) was added into a microwave tube containing compound **62** (45 mg, 0.049 mmol, 1.0 eq.), phenylacetylene (7.5 mg, 0.074 mmol, 1.5 eq.) and CuI (5 mg, 0.025 mmol, 0.5 eq.) in DMF (2 mL). The reaction was heated for 15 min by microwave irradiation at 100°C. Then, the reaction mixture was co-evaporated with toluene (3×10 mL) and the residue was purified by silica gel column chromatography (75% EtOAc/PE) to afford compound **71** as white foam (50 mg, 0.049 mmol, quanti.). $R_f = 0.15$ (PE:EtOAc, 2:3); ^1H NMR (400 MHz, CDCl_3) δ (ppm) = 9.08 (s, 1H, NH_{Uri}), 8.09 (s, 1H, $\text{H}_{\text{triazole}}$), 7.89 – 7.79 (m, 2H, Ph), 7.45 – 7.38 (m, 2H, Ph), 7.35 – 7.30 (m, 2H, Ph, NHCO), 7.28 (d, $J = 8.1$ Hz, 1H, $\text{H}_{6\text{Uri}}$), 5.71 (dd, $J = 8.1, 1.4$ Hz, 1H, $\text{H}_{5\text{Uri}}$), 5.51 (t, $J = 5.9$ Hz, 1H, H_α), 5.38 – 5.33 (m, 2H, $\text{H}_{4\text{Gal}}, \text{H}_{1\text{Rib}}$), 5.14 (dd, $J = 10.5, 7.9$ Hz, 1H, $\text{H}_{2\text{Gal}}$), 5.00 (dd, $J = 10.5, 3.4$ Hz, 1H, $\text{H}_{3\text{Gal}}$), 4.56 (d, $J = 7.9$ Hz, 1H, $\text{H}_{1\text{Gal}}$), 4.50 – 4.43 (m, 2H, $\text{H}_{2\text{Rib}}, \text{H}_{\beta\text{a}}$), 4.31 (dd, $J = 10.6, 5.7$ Hz, 1H, $\text{H}_{\beta\text{b}}$), 4.17 (dd, $J = 11.3, 6.6$ Hz, 1H, $\text{H}_{6\text{aGal}}$), 4.14 – 4.05 (m, 2H, $\text{H}_{6\text{bGal}}, \text{H}_{4\text{Rib}}$), 3.99 – 3.96 (m, 1H, $\text{H}_{3\text{Rib}}$), 3.94 – 3.89 (m, 1H, $\text{H}_{5\text{Gal}}$), 3.62 – 3.49 (m, 2H, $\text{H}_{5\text{Rib}}$), 2.10 (s, 3H, COCH_3), 2.05 (s, 3H, COCH_3), 1.96 (s, 3H, COCH_3), 1.91 (s, 3H, COCH_3), 0.89 (s, 9H, CMe_3), 0.85 (s, 9H, CMe_3), 0.07 (d, 6H, $2\times\text{SiCH}_3$), 0.05 (s, 3H, SiCH_3), -0.01 (s, 3H, SiCH_3); ^{13}C NMR (100 MHz, CDCl_3) δ (ppm) = 170.7, 170.3, 170.2, 170.0, 166.1, 163.0, 150.4, 148.0, 143.0 ($\text{C}_{6\text{Uri}}$), 130.2, 129.1 (s, 2C, Ph), 128.6 (Ph), 125.8 (s, 2C, Ph), 120.5 ($\text{C}_{\text{triazoleH}}$), 102.7 ($\text{C}_{5\text{Uri}}$), 101.0 ($\text{C}_{1\text{Gal}}$), 94.7 ($\text{C}_{1\text{Rib}}$), 83.5 ($\text{C}_{4\text{Rib}}$), 73.1 (s, $2\times\text{C}$, $\text{C}_{3\text{Rib}}, \text{C}_{2\text{Rib}}$), 71.2 ($\text{C}_{5\text{Gal}}$), 70.6 ($\text{C}_{3\text{Gal}}$), 68.6 ($\text{C}_{2\text{Gal}}$), 68.3 (C_β), 67.0 ($\text{C}_{4\text{Gal}}$), 63.3 (C_α), 61.3 ($\text{C}_{6\text{Gal}}$), 41.7 ($\text{C}_{5\text{Rib}}$), 25.9 (s, 3C, CMe_3), 25.8 (s, 3C, CMe_3), 20.8 (s, 2C, $2\times\text{COCH}_3$), 20.71 (COCH_3), 20.66 (COCH_3), 18.1 (CMe_3), 18.0 (CMe_3), -4.3 (SiCH_3), -4.5 (SiCH_3), -4.66 (SiCH_3), -4.73 (SiCH_3); HR-ESI-MS (positive mode) m/z : calcd for $\text{C}_{46}\text{H}_{69}\text{N}_6\text{NaO}_{16}\text{Si}_2$, $[\text{M}+\text{H}+\text{Na}]^{2+}$ 520.2098, found 520.2090.



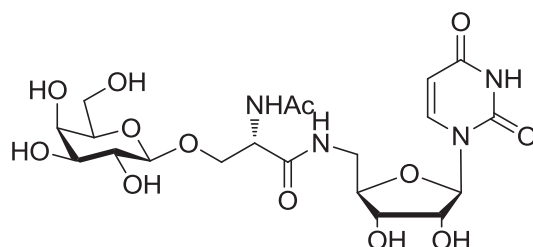
***N*-[2',3'-Di-*O*-(*tert*-butyldimethylsilyl)-uridin-5'-yl]-(2*S*)-2-{4-[*N*-(*tert*-butoxycarbonyl)-aminomethyl]-1,2,3-triazol-1-yl}-3-(2,3,4,6-tetra-*O*-acetyl- β -D-galactopyranosyloxy)propamide (**72**)**

DIPEA (0.08 mL, 0.46 mmol, 7.5eq.) was added into a microwave tube containing compound **62** (56 mg, 0.061 mmol, 1.0 eq.), *N*-Boc-propargylamine (15 mg, 0.092 mmol, 1.5 eq.) and CuI (6 mg, 0.03 mmol, 0.5 eq.) in DMF (2 mL). The reaction was heated for 15 min by microwave irradiation at 100°C. Then, the reaction mixture was co-evaporated with toluene (3×10 mL) and the residue was purified by silica gel column chromatography (75% EtOAc/PE) to afford compound **72** as yellow foam (38 mg, 0.036 mmol, 58%). $R_f = 0.10$ (PE:EtOAc, 2:3); $^1\text{H NMR}$ (400 MHz, CDCl_3) δ (ppm) = 9.62 (s, 1H, NH_{Urid}), 7.79 (s, 1H, $\text{H}_{\text{triazole}}$), 7.31 (s, 1H, CONH), 7.24 (s, 1H, $\text{H}_{6\text{Urid}}$), 5.75 (d, $J = 8.0$ Hz, 1H, $\text{H}_{5\text{Urid}}$), 5.44 – 5.30 (m, 2H, $\text{H}_{4\text{Gal}}$, H_α), 5.25 (d, $J = 5.9$ Hz, 1H, $\text{H}_{1\text{Rib}}$), 5.10 (dd, $J = 10.4, 7.8$ Hz, 1H, $\text{H}_{2\text{Gal}}$), 4.99 (dd, $J = 10.4, 3.4$ Hz, 1H, $\text{H}_{3\text{Gal}}$), 4.60 – 4.50 (m, 2H, $\text{H}_{1\text{Gal}}$, $\text{H}_{2\text{Rib}}$), 4.45 – 4.30 (m, 4H, H_β , NCH_2), 4.15 – 4.02 (m, 3H, $\text{H}_{4\text{Rib}}$, $\text{H}_{6\text{Gal}}$), 3.98 (dd, $J = 4.6, 3.0$ Hz, 1H, $\text{H}_{3\text{Rib}}$), 3.89 (dd, $J = 6.5, 6.5$ Hz, 1H, $\text{H}_{5\text{Gal}}$), 3.68 – 3.56 (m, 1H, $\text{H}_{5\text{aRib}}$), 3.46 – 3.36 (m, 1H, $\text{H}_{5\text{bRib}}$), 2.13 (s, 3H, COCH_3), 2.05 (s, 3H, COCH_3), 2.02 (s, 3H, COCH_3), 1.97 (s, 3H, COCH_3), 1.45 (s, 9H, Boc), 0.89 (s, 9H, SiCMe_3), 0.86 (s, 9H, SiCMe_3), 0.07 (d, 6H, $2 \times \text{SiCH}_3$), 0.06 (s, 3H, SiCH_3), -0.00 (s, 3H, SiCH_3); $^{13}\text{C NMR}$ (100 MHz, CDCl_3) δ (ppm) = 170.8, 169.8, 166.0, 163.1, 156.1, 150.6, 143.7 ($\text{C}_{6\text{Urid}}$), 123.0 ($\text{C}_{\text{triazoleH}}$), 102.9 ($\text{C}_{5\text{Urid}}$), 101.3 ($\text{C}_{1\text{Gal}}$), 95.8 ($\text{C}_{1\text{Rib}}$), 84.0 ($\text{C}_{4\text{Rib}}$), 73.1 ($\text{C}_{3\text{Rib}}$), 72.5 ($\text{C}_{2\text{Rib}}$), 71.1 ($\text{C}_{5\text{Gal}}$), 70.7 ($\text{C}_{3\text{Gal}}$), 68.6 (s, $2 \times \text{C}$, $\text{C}_{2\text{Gal}}$, C_β), 67.0 ($\text{C}_{4\text{Gal}}$), 63.3 (C_α), 61.2 ($\text{C}_{6\text{Gal}}$), 41.6 ($\text{C}_{5\text{Rib}}$), 36.4 (NCH_2), 28.5 (s, 3C, OCMe_3), 25.90 (s, 3C, CMe_3), 25.87 (s, 3C, CMe_3), 20.9 (COCH_3), 20.84 (COCH_3), 20.75 (COCH_3), 20.7 (COCH_3), 18.1 (CMe_3), 18.0 (CMe_3), -4.4 (SiCH_3), -4.5 (SiCH_3), -4.6 (SiCH_3), -4.8 (SiCH_3); HR-ESI-MS (positive mode) m/z : calcd for $\text{C}_{46}\text{H}_{76}\text{N}_7\text{O}_{18}\text{Si}_2$, $[\text{M}+\text{H}]^+$ 1070.4780, found 1070.4757.



***N*-[2',3'-Di-*O*-(*tert*-butyldimethylsilyl)-uridin-5'-yl]-(2*S*)-2-(4-acetoxymethyl-1,2,3-triazol-1-yl)-3-(2,3,4,6-tetra-*O*-acetyl- β -D-galactopyranosyloxy)propanamide (**73**)**

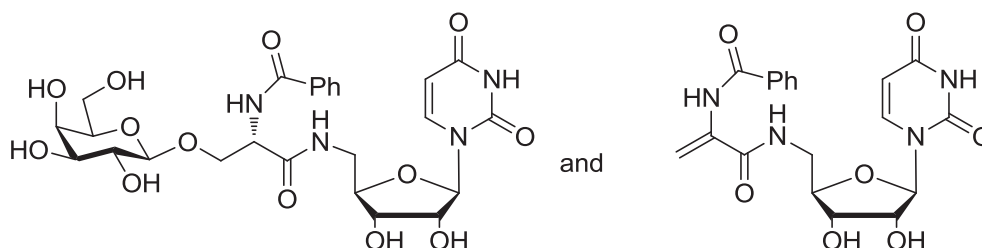
DIPEA (0.07 mL, 0.40 mmol, 7.4 eq.) was added into a microwave tube containing compound **62** (49 mg, 0.054 mmol, 1.0 eq.), propargyl acetate (0.008 mL, 0.08 mmol, 1.5 eq.) and CuI (5 mg, 0.027 mmol, 0.5 eq.) in DMF (2 mL). The reaction was heated for 15 min by microwave irradiation at 100 °C. Then, the reaction mixture was co-evaporated with toluene (3×10 mL) and the residue was purified by silica gel column chromatography (75% EtOAc/PE) to afford compound **73** as white foam (30 mg, 0.030 mmol, 56%). $R_f = 0.13$ (PE:EtOAc, 2:3); $^1\text{H NMR}$ (400 MHz, CDCl_3) δ (ppm) = 9.20 (s, 1H, H_{Uri}), 7.92 (s, 1H, $\text{H}_{\text{triazole}}$), 7.41 – 7.35 (m, 1H, NHCO), 7.29 (d, $J = 8.1$ Hz, 1H, $\text{H}_{6\text{Uri}}$), 5.76 (dd, $J = 8.1, 1.7$ Hz, 1H, $\text{H}_{5\text{Uri}}$), 5.43 (t, $J = 6.1$ Hz, 1H, H_α), 5.39 – 5.35 (m, 1H, $\text{H}_{4\text{Gal}}$), 5.30 (d, $J = 5.8$ Hz, 1H, $\text{H}_{1\text{Rib}}$), 5.22 (s, 2H, CH_2OAc), 5.11 (dd, $J = 10.4, 7.8$ Hz, 1H, $\text{H}_{2\text{Gal}}$), 5.00 (dd, $J = 10.4, 3.4$ Hz, 1H, $\text{H}_{3\text{Gal}}$), 4.58 – 4.51 (m, 2H, $\text{H}_{1\text{Gal}}, \text{H}_{2\text{Rib}}$), 4.37 (dd, $J = 10.6, 6.4$ Hz, 1H, $\text{H}_{\beta\alpha}$), 4.29 (dd, $J = 10.6, 6.1$ Hz, 1H, $\text{OCH}_{\beta\beta}$), 4.19 – 4.04 (m, 3H, $\text{H}_{4\text{Rib}}, \text{H}_{6\text{Gal}}$), 3.99 (dd, $J = 4.7, 3.1$ Hz, 1H, $\text{H}_{3\text{Rib}}$), 3.91 (dd, $J = 6.5, 6.5$ Hz, 1H, $\text{H}_{5\text{Gal}}$), 3.62 (ddd, $J = 14.1, 6.6$ Hz, 1H, $\text{H}_{5\text{aRib}}$), 3.46 (ddd, $J = 14.1, 4.0$ Hz, 1H, $\text{H}_{5\text{bRib}}$), 2.13 (s, 3H, COCH_3), 2.09 (s, 3H, COCH_3), 2.05 (s, 3H, COCH_3), 2.02 (s, 3H, COCH_3), 1.97 (s, 3H, COCH_3), 0.89 (s, 9H, CMe_3), 0.86 (s, 9H, CMe_3), 0.09 – 0.05 (m, 9H, $3\times\text{SiCH}_3$), 0.01 (s, 3H, SiCH_3); $^{13}\text{C NMR}$ (100 MHz, CDCl_3) δ (ppm) = 171.1, 170.7, 170.3, 170.2, 169.8, 165.9, 163.0, 150.5, 143.5 ($\text{C}_{6\text{Uri}}$), 124.6 ($\text{C}_{\text{triazoleH}}$), 102.8 ($\text{C}_{5\text{Uri}}$), 101.2 ($\text{C}_{1\text{Gal}}$), 95.5 ($\text{C}_{1\text{Rib}}$), 83.9 ($\text{C}_{4\text{Rib}}$), 73.1 ($\text{C}_{3\text{Rib}}$), 72.7 ($\text{C}_{2\text{Rib}}$), 71.2 ($\text{C}_{5\text{Gal}}$), 70.6 ($\text{C}_{3\text{Gal}}$), 68.58 (C_β), 68.55 ($\text{C}_{2\text{Gal}}$), 67.0 ($\text{C}_{4\text{Gal}}$), 63.2 (C_α), 61.3 ($\text{C}_{6\text{Gal}}$), 57.8 (CH_2OAc), 41.7 ($\text{C}_{5\text{Rib}}$), 25.90 (s, 3C, CMe_3), 25.86 (s, 3C, CMe_3), 21.0 (COCH_3), 20.91 (COCH_3), 20.85 (COCH_3), 20.75 (COCH_3), 20.67 (COCH_3), 18.1 (CMe_3), 18.0 (CMe_3), -4.3 (SiCH_3), -4.5 (SiCH_3), -4.6 (SiCH_3), -4.7 (SiCH_3); HR-ESI-MS (positive mode) m/z : calcd for $\text{C}_{43}\text{H}_{69}\text{N}_6\text{O}_{18}\text{Si}_2$, $[\text{M}+\text{H}]^+$ 1013.4201, found 1013.4171; for $\text{C}_{43}\text{H}_{68}\text{N}_6\text{NaO}_{18}\text{Si}_2$, $[\text{M}+\text{H}]^+$ 1035.4021, found 1035.3990.



***N*-(Uridin-5'-yl)-*N'*-acetyl-*O*- β -D-galactopyranosylserinamide (**74**)**

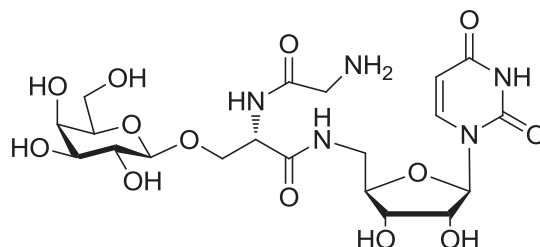
Prepared according to general protocol **G** from compound **67** (10 mg, 0.01 mmol, 1.0 eq.). The crude product was purified by C18 reverse phase column chromatography (100% H_2O to 100% MeOH) to afford compound **74** as white foam (3 mg, 0.0056 mmol, 56% over 2 steps). $[\alpha]_D =$

-8.0 (c = 0.1, H₂O); ¹H NMR (500 MHz, D₂O) δ (ppm) = 7.61 (d, *J* = 7.9 Hz, 1H, H_{6Urid}), 5.91 – 5.87 (m, 1H, H_{5Urid}), 5.85 (d, *J* = 5.2 Hz, 1H, H_{1Rib}), 4.59 (t, *J* = 4.6 Hz, 1H, H_α), 4.42 (d, *J* = 7.8 Hz, 1H, H_{1Gal}), 4.36 (bd, *J* = 5.2 Hz, 1H, H_{2Rib}), 4.27 (dd, *J* = 10.6, 5.2 Hz, 1H, H_{βa}), 4.16 – 4.12 (m, 2H, H_{3Rib}, H_{4Rib}), 3.94 – 3.89 (m, 2H, H_{4Gal}, H_{βb}), 3.80 – 3.60 (m, 6H, H_{5Rib}, H_{6Gal}, H_{3Gal}, H_{5Gal}), 3.54 (dd, *J* = 9.9, 7.8 Hz, 1H, H_{2Gal}), 2.09 (s, 3H, COCH₃); ¹³C NMR (125 MHz, D₂O) δ (ppm) = 174.5, 172.1, 141.5 (C_{6Urid}), 102.7 (s, 2C, C_{5Urid}, C_{1Gal}), 89.8 (C_{1Rib}), 82.1 (C_{3Rib} or C_{4Rib}), 75.2 (C_{5Gal}), 72.9 (C_{2Rib}), 72.6 (C_{3Gal}), 70.7 (C_{2Gal}), 70.4 (C_{3Rib} or C_{4Rib}), 68.7 (C_β), 68.6 (C_{4Gal}), 60.9 (C_{6Gal}), 54.0 (C_α), 40.7 (C_{5Rib}), 21.8 (COCH₃); HR-ESI-MS (positive mode) *m/z*: calcd for C₂₀H₃₀N₄NaO₁₃, [M+Na]⁺ 557.1702, found 557.1694.



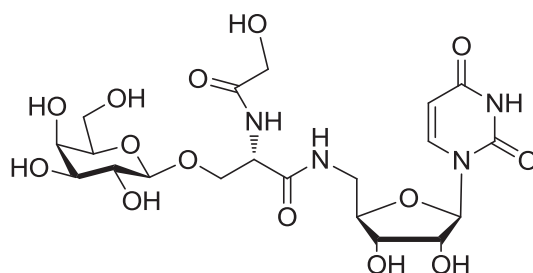
***N*-(Uridin-5'-yl)-*N'*-benzoyl-*O*-β-D-galactopyranosylserinamide (**75**) AND
5'-[(2-Benzamido)-acrylamido]uridine (**76**)**

Prepared according to general protocol **G** from compound **68** (54 mg, 0.054 mmol, 1.0 eq.). The crude product was purified by C18 reverse phase column chromatography (100% H₂O to 100% MeOH) to afford compound **75** (20 mg, 0.033 mmol, 61% over 2 steps) and compound **76** (8 mg, 0.019 mmol, 35%) as a byproduct. **75** [α]_D = +8.0 (c = 0.1, H₂O); ¹H NMR (500 MHz, D₂O) δ (ppm) = 7.81 (d, 2H, Ph), 7.59 (t, *J* = 7.5 Hz, 1H, Ph), 7.49 (t, 2H, Ph), 7.35 (d, *J* = 7.6 Hz, 1H, H_{6Urid}), 5.76 (d, *J* = 5.5 Hz, 1H, H_{1Rib}), 5.55 (d, *J* = 7.6 Hz, 1H, H_{5Urid}), 4.76 – 4.73 (m, 1H, H_α), 4.37 (d, *J* = 7.7 Hz, 1H, H_{1Gal}), 4.30 (dd, *J* = 10.7, 5.6 Hz, 1H, H_{βa}), 4.20 (bd, *J* = 5.5 Hz, 1H, H_{2Rib}), 4.07 – 4.04 (m, 2H, H_{3Rib}, H_{4Rib}), 3.98 (dd, *J* = 10.7, 4.3 Hz, 1H, H_{βb}), 3.85 (bd, *J* = 3.1 Hz, 1H, H_{4Gal}), 3.73 – 3.48 (m, 7H, H_{5Rib}, H_{2Gal}, H_{3Gal}, H_{5Gal}, H_{6Gal}); ¹³C NMR (125 MHz, D₂O) δ (ppm) = 176.3, 171.8, 170.4, 159.2, 140.2 (C_{5Urid}), 132.5 (Ph), 128.7 (s, 2C, Ph), 127.3 (s, 2C, Ph), 103.0 (C_{1Gal}), 102.8 (C_{5Urid}), 89.8 (C_{1Rib}), 81.8 (C_{4Rib}), 75.2 (C_{5Gal}), 72.9 (C_{2Rib}), 72.7 (C_{3Gal}), 70.7 (C_{2Gal}), 70.3 (C_{3Rib}), 68.7 (C_β), 68.6 (C_{4Gal}), 60.8 (C_{6Gal}), 54.6 (C_α), 40.6 (C_{5Rib}); HR-ESI-MS (positive mode) *m/z*: calcd for C₂₅H₃₂N₄NaO₁₃, [M+Na]⁺ 619.1858, found 619.1866; **76** ¹H NMR (300 MHz, CD₃OD) δ (ppm) = 7.92 – 7.86 (m, 2H), 7.65 (d, *J* = 8.0 Hz, 1H), 7.60 – 7.55 (m, 1H), 7.55 – 7.47 (m, 2H), 5.99 (d, *J* = 1.0 Hz, 1H), 5.76 (d, *J* = 4.4 Hz, 1H), 5.63 (dd, *J* = 4.4, 3.5 Hz, 2H), 4.27 (dd, *J* = 5.6, 4.5 Hz, 1H), 4.13 (dd, *J* = 5.6 Hz, 1H), 4.06 (dd, *J* = 10.0, 5.4 Hz, 1H), 3.70 (dd, *J* = 14.2, 5.6 Hz, 1H), 3.60 (dd, *J* = 14.2, 4.4 Hz, 1H); ESI-MS (positive mode) *m/z*: [M+Na]⁺ 439.2.



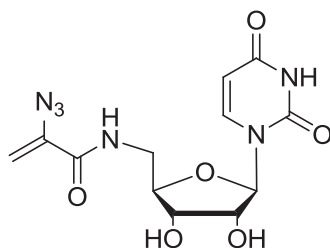
***N*-(Uridin-5'-yl)-*N'*-glycinylo- β -D-galactopyranosylserinamide (77)**

Prepared according to general protocol **G** from compound **69** (39 mg, 0.037 mmol, 1.0 eq.). The crude product was purified by C18 reverse phase column chromatography (100% H₂O to 100% MeOH) to afford compound **77** as white foam (7 mg, 0.013 mmol, 34% over 2 steps). $[\alpha]_D = -3.5$ ($c = 0.2$, H₂O); ¹H NMR (500 MHz, D₂O) δ (ppm) = 7.60 (d, $J = 7.8$ Hz, 1H, H_{6Uri}), 5.87 (d, $J = 7.8$ Hz, 1H, H_{5Uri}), 5.81 (d, $J = 4.9$ Hz, 1H, H_{1Rib}), 4.62 (t, $J = 4.2$ Hz, 1H, H _{α}), 4.40 (d, $J = 7.8$ Hz, 1H, H_{1Gal}), 4.36 (dd, $J = 4.9$ Hz, 1H, H_{2Rib}), 4.26 (dd, $J = 10.6, 5.1$ Hz, 1H, H _{β a}), 4.15 – 4.09 (m, 2H, H_{3Rib}, H_{4Rib}), 3.95 – 3.88 (m, 2H, H _{β b}, H_{4Gal}), 3.79 – 3.58 (m, 6H, H_{5Rib}, H_{3Gal}, H_{5Gal}, H_{6Gal}), 3.54 – 3.49 (m, 1H, H_{2Gal}), 3.45 (bs, 2H, H _{α Gly}); ¹³C NMR (125 MHz, D₂O) δ (ppm) = 175.2, 171.9, 154.6, 141.7 (C_{6Uri}), 102.7 (C_{1Gal}), 102.5 (C_{5Uri}), 90.0 (C_{1Rib}), 82.0 (C_{4Rib}), 75.2 (C_{3Gal} or C_{5Gal}), 72.9 (C_{2Rib}), 72.5 (C_{5Gal} or C_{3Gal}), 70.7 (C_{2Gal}), 70.4 (C_{3Rib}), 68.7 (C _{β}), 68.5 (C_{4Gal}), 60.9 (C_{6Gal}), 53.7 (C _{α}), 43.3 (C _{α Gly}), 40.7 (C_{5Rib}); HR-ESI-MS (positive mode) m/z : calcd for C₂₀H₃₂N₅O₁₃, [M+H]⁺ 550.1991, found 550.1983.



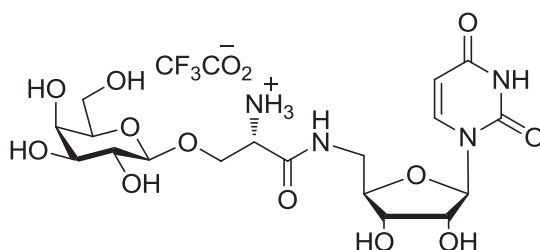
***N*-(Uridin-5'-yl)-*N'*-hydroxyacetylo- β -D-galactopyranosylserinamide (78)**

Prepared according to general protocol **G** from compound **70** (26 mg, 0.026 mmol, 1.0 eq.). The crude product was purified by C18 reverse phase column chromatography (100% H₂O to 100% MeOH) to afford compound **78** as white foam (8 mg, 0.015 mmol, 56% over 2 steps). $[\alpha]_D = -4.0$ ($c = 0.1$, H₂O); ¹H NMR (500 MHz, D₂O) δ (ppm) = 7.63 (d, $J = 8.0$ Hz, 1H, H_{6Uri}), 5.90 (d, $J = 8.0$ Hz, 1H, H_{5Uri}), 5.82 (d, $J = 5.0$ Hz, 1H, H_{1Rib}), 4.68 (t, $J = 4.8$ Hz, 1H, H _{α}), 4.43 (d, $J = 7.9$ Hz, 1H, H_{1Gal}), 4.39 (bd, $J = 5.0$ Hz, 1H, H_{2Rib}), 4.29 (dd, $J = 10.8, 5.4$ Hz, 1H, H _{β a}), 4.19 (s, 2H, COCH₂OH), 4.18 – 4.12 (m, 2H, H_{3Rib}, H_{4Rib}), 3.99 (dd, $J = 10.8, 4.4$ Hz, 1H, H _{β b}), 3.94 (bd, $J = 3.3$ Hz, 1H, H_{4Gal}), 3.81 – 3.59 (m, 6H, H_{5Rib}, H_{3Gal}, H_{5Gal}, H_{6Gal}), 3.54 (dd, $J = 9.9, 7.9$ Hz, 1H, H_{2Gal}); ¹³C NMR (125 MHz, D₂O) δ (ppm) = 175.2, 171.7, 141.9 (C_{6Uri}), 102.9 (C_{1Gal}), 102.5 (C_{5Uri}), 90.2 (C_{1Rib}), 82.0 (C_{4Rib}), 75.2 (C_{5Gal}), 72.9 (C_{2Rib}), 72.6 (C_{3Gal}), 70.6 (C_{2Gal}), 70.3 (C_{3Rib}), 68.8 (C _{β}), 68.6 (C_{4Gal}), 60.9 (s, 2C, CH₂OH, C_{6Gal}), 53.4 (C _{α}), 40.7 (C_{5Rib}); HR-ESI-MS (positive mode) m/z : calcd for C₂₀H₃₀N₄NaO₁₄, [M+Na]⁺ 537.1651, found 537.1656.



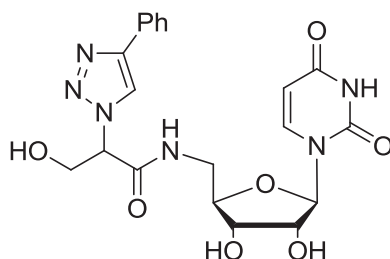
5'-[(2-Azido)-acrylamido]uridine (**79**)

Prepared according to general protocol **G** from compound **62** (44 mg, 0.048 mmol, 1.0 eq.). The crude product was purified by C18 reverse phase column chromatography (100% H₂O to 100% MeOH) to afford compound **79** as white foam (16 mg, 0.047 mmol, quant.). $[\alpha]_D = +17.5$ ($c = 0.2$, H₂O); ¹H NMR (300 MHz, CD₃OD) δ (ppm) = 7.62 (d, $J = 7.9$ Hz, 1H, H_{6Uri}), 5.93 (d, $J = 2.2$ Hz, 1H, H_{aalkene}), 5.78 (d, $J = 4.3$ Hz, 1H, H_{1Rib}), 5.71 (d, $J = 7.9$ Hz, 1H, H_{5Uri}), 5.29 (d, $J = 2.2$ Hz, 1H, H_{balkene}), 4.26 – 4.19 (m, 1H), 4.09 – 3.98 (m, 2H), 3.66 – 3.55 (m, 2H); ESI-MS (positive mode) m/z : $[M+Na]^+$ 361.1.



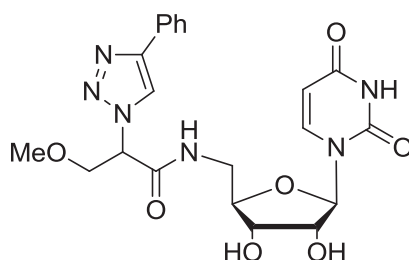
N-(Uridin-5'-yl)-O- β -D-galactopyranosyl-serinamide trifluoroacetate salt (**80**)

Prepared according to general protocol **G** from compound **65** (60 mg, 0.069 mmol, 1.0 eq.). The crude product was purified by C18 reverse phase column chromatography (100% H₂O to 100% MeOH) to afford compound **80** as white foam (42 mg, 0.069 mmol, quant.). $[\alpha]_D = +1.4$ ($c = 0.5$, H₂O); ¹H NMR (500 MHz, D₂O) δ (ppm) = 7.64 (d, $J = 7.9$ Hz, 1H, H_{6Uri}), 5.88 (d, $J = 7.9$ Hz, 1H, H_{5Uri}), 5.82 (d, $J = 5.0$ Hz, 1H, H_{1Rib}), 4.40 – 4.32 (m, 2H, H_{2Rib}, H_{1Gal}), 4.16 – 4.10 (m, 2H, H_{3Rib}, H_{4Rib}), 4.08 (dd, $J = 10.4, 5.0$ Hz, 1H, H _{β a}), 3.90 (bd, $J = 3.3$ Hz, 1H, H_{4Gal}), 3.80 (dd, $J = 10.4, 4.9$ Hz, 1H, H _{β b}), 3.75 – 3.54 (m, 7H, H_{5Rib}, H_{3Gal}, H_{5Gal}, H_{6Gal}, H _{α}), 3.50 (dd, $J = 9.9, 7.8$ Hz, 1H, H_{2Gal}); ¹³C NMR (125 MHz, D₂O) δ (ppm) = 181.5, 175.3, 163.0 (q, $J = 35.4$ Hz, CO₂⁻), 153.9, 141.8 (C_{6Uri}), 116.3 (q, $J = 291.6$ Hz, CF₃), 103.1 (C_{1Gal}), 102.5 (C_{5Uri}), 90.0 (C_{1Rib}), 82.0 (C_{4Rib}), 75.1 (C_{3Gal} or C_{5Gal}), 72.9 (C_{2Rib}), 72.5 (C_{5Gal} or C_{3Gal}), 71.6 (C _{β}), 70.7 (C_{2Gal}), 70.4 (C_{3Rib}), 68.6 (C_{4Gal}), 60.9 (C_{6Gal}), 54.4 (C _{α}), 40.7 (C_{5Rib}); HR-ESI-MS (positive mode) m/z : calcd for C₁₈H₂₉N₄O₁₂, $[M+H]^+$ 493.1776, found 493.1771.



N-(Uridin-5'-yl)-2-(4-phenyl-1,2,3-triazol-1-yl)-3-hydroxy-propanamide (**81**)

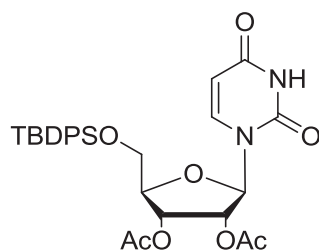
Prepared according to general protocol **G** from compound **71** (17 mg, 0.017 mmol, 1.0 eq.). The crude product was purified by C18 reverse phase column chromatography (100% H₂O to 100% MeOH) to afford compound **81** (8 mg, 0.017 mmol, quant.) as mixture of two diastereomers. ¹H NMR (500 MHz, CD₃OD) δ (ppm) = 8.49 (d, 1H, H_{triazole}), 7.86 – 7.82 (m, 2H, Ph), 7.60 (t, *J* = 8.0 Hz, 1H, H_{6Uri}), 7.46 – 7.41 (m, 2H, Ph), 7.37 – 7.32 (m, 1H, Ph), 5.74 – 5.68 (m, 2H, H_{5Uri}, H_{1Rib}), 4.29 – 4.17 (m, 3H, H_{2Rib}, H _{β}), 4.09 – 3.98 (m, 2H, H_{3Rib}, H_{4Rib}), 3.68 – 3.61 (m, 1H, H_{5aRib}), 3.59 – 3.53 (m, 1H, H_{5bRib}). (**H _{α}** does NOT show up); ¹³C NMR (125 MHz, CD₃OD) δ (ppm) = 169.05, 169.00 (2s, 2C), 148.7, 143.43, 143.39 (2s, 2C, C_{6Uri}), 131.72, 131.71 (2s, 2C, C_{PhH}), 130.0 (s, 2 \times C_{PhH}), 129.4 (s, C_{PhH}), 126.7 (s, 2 \times C_{PhH}), 122.34, 122.29 (2s, 2C, C_{triazole}), 103.15, 103.09 (2s, 2C, C_{5Uri}), 93.11, 93.02 (2s, 2C, C_{1Rib}), 83.65, 83.58 (2s, 2C, C_{4Rib}), 74.66, 74.55 (2s, 2C, C_{2Rib}), 72.13, 72.10 (2s, 2C, C_{3Rib}), 62.99, 62.88 (2s, 2C, CH₂OH), 42.13, 42.10 (2s, 2C, C_{5Rib}). (**C _{α}** does NOT show up); HR-ESI-MS (positive mode) *m/z*: calcd for C₂₀H₂₂N₆NaO₇, [M+Na]⁺ 481.1442, found 481.1427.



N-(Uridin-5'-yl)-(2*S*)-2-(4-phenyl-1,2,3-triazol-1-yl)-3-methoxy-propanamide (**82**)

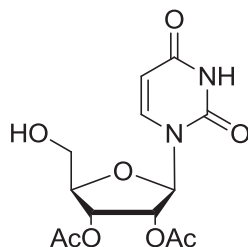
Compound **71** (20 mg, 0.020 mmol, 1.0 eq.) was solubilized with CH₂Cl₂ (0.5 mL). Then, 90% TFA (2.2 mL) was added dropwise. After addition, the reaction mixture was stirred at r.t. overnight. MeOH (3 mL) and H₂O (5 mL) were then added into the reaction mixture. The solvent was removed by evaporation and the residue was used directly for the reaction of next step. Aq. Et₃N (1 mL) was added dropwise into a solution of the residue solubilized in MeOH/H₂O (2 mL/1 mL) at r.t. After addition, the reaction mixture was stirred at r.t. for 24 h. Then, the reaction mixture was concentrated and the residue was purified by C18 reverse phase column chromatography (100% H₂O to 100% MeOH) to afford compound **82** (7 mg, 0.015 mmol, 75%) as mixture of two diastereomers. ¹H NMR (500 MHz, CD₃OD) δ (ppm) = 8.46 (d, 1H, H_{triazole}), 7.87 – 7.80 (m, 2H, Ph), 7.64 – 7.59 (m, 1H, H_{6Uri}), 7.47 – 7.41 (m, 2H, Ph), 7.37 – 7.32 (m, 1H, Ph), 5.76 – 5.69 (m, 2H, H_{5Uri}, H_{1Rib}), 5.65 – 5.59 (m, 0.36H, H _{α}), 4.27 – 4.18 (m, 1H, H_{2Rib}), 4.15 – 4.09 (m, 1H, H _{β a}), 4.07 – 3.97 (m, 3H, CH _{β b}, H_{3Rib}, H_{4Rib}), 3.67 – 3.59 (m, 1H, H_{5aRib}), 3.60 – 3.52 (m, 1H, H_{5bRib}), 3.42 – 3.37 (s, 3H, OCH₃); ¹³C NMR (125 MHz, CD₃OD) δ (ppm) = 168.67, 168.63 (2s, 2C), 166.12, 166.10 (2s, 2C), 152.4, 148.8, 143.48, 143.43 (2s, 2C, C_{6Uri}), 131.63, 131.61, 130.0 (s, 2 \times C_{Ph}), 129.4 (C_{Ph}), 126.7 (s, 2 \times C_{Ph}), 122.28, 122.21 (2s,

2C, C_α), 103.07, 103.02 (2s, 2C, C_{5Uri}), 92.64, 92.48 (2s, 2C, C_{1Rib}), 83.7 (C_{4Rib}), 74.5 (C_{2Rib}), 72.59, 72.49 (2s, 2C, C_β), 72.17, 72.14 (2s, 2C, C_{3Rib}), 64.6 (C_α), 59.5 (OCH₃), 42.25, 42.17 (2s, 2C, C_{5Rib}); HR-ESI-MS (positive mode) *m/z*: calcd for C₂₁H₂₄N₆NaO₇, [M+Na]⁺ 495.1599, found 495.1587.



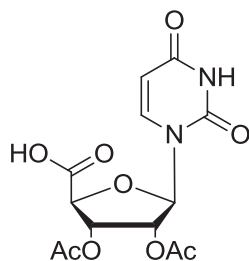
5'-*O*-*tert*-Butyldiphenylsilyl-2',3'-di-*O*-acetyl-uridine (**89**)

TBDPSCl (1.3 mL, 4.9 mmol, 1.2 eq.) was added dropwise into a solution of uridine (1 g, 4.1 mmol, 1.0 eq.) and imidazole (422 mg, 6.2 mmol, 1.5 eq.) in pyridine (20 mL). After addition, the solution was stirred at r.t. for 3 h. Then, Ac₂O (10 mL) was added into the reaction mixture at 0°C. The reaction was stirred at r.t. overnight. Then, the reaction mixture was concentrated and co-evaporated with toluene (3×10 mL). The residue was purified by silica gel column chromatography (PE:EtOAc, 1:1) to afford compound **89** as white foam (2.047 g, 3.6 mmol, 88% over two steps). R_f = 0.2 (PE:EtOAc, 1:1); ¹H NMR (300 MHz, CDCl₃) δ (ppm) = 7.72 (d, *J* = 8.2 Hz, 1H), 7.69 – 7.60 (m, 4H), 7.48 – 7.26 (m, 6H), 6.30 (d, *J* = 6.5 Hz, 1H), 5.55 – 5.39 (m, 3H), 4.20 – 4.14 (m, 1H), 4.04 – 3.97 (m, 1H), 3.84 (dd, *J* = 11.8, 1.8 Hz, 1H), 2.10 (s, 3H), 2.08 (s, 3H), 1.11 (s, 9H).



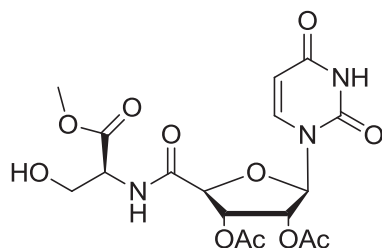
2',3'-(Di-*O*-acetyl)-uridine (**90**)²⁵⁶

TBAF (4 mL, 1 M in THF, 4 mmol, 1.1 eq) was added dropwise into a solution of 5'-*O*-(*tert*-butyldiphenylsilyl)-2',3'-(di-*O*-acetyl)-uridine (**89**) (2.00 g, 3.63 mmol, 1.0 eq.) in THF (10 mL). After addition, the reaction was stirred at r.t. for 4 h. Then, the reaction mixture was concentrated and the residue was purified by silica gel column chromatography (50% EtOAc/PE to 100% EtOAc) to afford compound **90** as white foam (839 mg, 2.56 mmol, 70%). R_f = 0.15 (PE:EtOAc, 1:2); ¹H NMR (300 MHz, CDCl₃) δ (ppm) = 8.72 (s, 1H), 7.72 (d, *J* = 8.2 Hz, 1H), 6.10 – 6.02 (m, 1H), 5.78 (dd, *J* = 8.1, 2.1 Hz, 1H), 5.53 – 5.40 (m, 2H), 4.24 – 4.19 (m, 1H), 3.96 (dd, *J* = 12.0, 2.2 Hz, 1H), 3.87 (dd, *J* = 12.0, 2.2 Hz, 1H), 2.14 (s, 3H), 2.09 (s, 3H).



2',3'-Di-O-acetyl-uridine-5'-carboxylic acid (91)²²⁷

BAIB (709 mg, 2.2 mmol, 2.2 eq.), TEMPO (32 mg, 0.2 mmol, 0.2 eq.) and compound **90** (328 mg, 1.0 mmol, 1.0 eq.) were added into a flask and a mixture of solvent CH₃CN:H₂O (1:1) was added at -5°C. After addition, the reaction was stirred at -5°C with protection of light. After 6 h, another fraction of BAIB (355 mg, 1.1 mmol, 1.1 eq.) and TEMPO (64 mg, 0.6 mmol, 0.6 eq.) were added into the reaction and the reaction was stirred at -5°C with protection of light for another 16 h. Then, the reaction mixture was concentrated and the resulting yellow gum was triturated with diethyl ether, filtrated and washed with Et₂O (5×5 mL). The highly hygroscopic yellow solid was then purified by reverse phase column (10% MeOH/H₂O to 100% MeOH) to afford the product **91** as white foam (277 mg, 0.81 mmol, 81%). R_f = 0.5 (EtOAc); ¹H NMR (400 MHz, D₂O) δ (ppm) = 7.99 (d, *J* = 8.0 Hz, 1H, H_{6U_{ri}}), 6.11 (d, *J* = 5.2 Hz, 1H, H_{1R_{ib}}), 5.88 (d, *J* = 8.0 Hz, 1H, H_{5U_{ri}}), 5.73 – 5.65 (m, 1H, H_{3R_{ib}}), 5.51 (bd, *J* = 5.2 Hz, 1H, H_{2R_{ib}}), 4.79 (bs, 1H, H_{4R_{ib}}), 2.17 (s, 3H, COCH₃), 2.12 (s, 3H, COCH₃); ¹³C NMR (100 MHz, D₂O) δ (ppm) = 172.7 (s, 2C, COCH₃), 172.4 (CO₂H), 166.3 (C=O), 151.8 (C=O), 143.1 (C_{U_{ri}}), 103.0 (C_{U_{ri}}), 89.5 (C_{1R_{ib}}), 80.4 (C_{4R_{ib}}), 73.4 (C_{2R_{ib}}), 73.0 (C_{3R_{ib}}), 20.3 (COCH₃), 20.1 (COCH₃); HR-ESI-MS (positive mode) *m/z*: calcd for C₁₃H₁₄N₂NaO₉, [M+Na]⁺ 365.0592, found 365.0589.



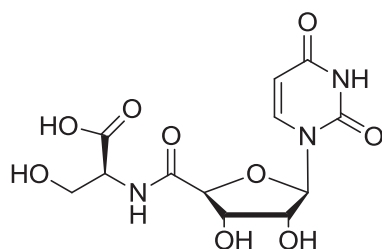
N-[(2S)-1-Hydroxy-4-oxa-3-oxo-pent-2-yl]-1-uracyl-2,3-di-O-acetyl-β-D-ribofuranurona mide (92)

(Method I) Compound **91** (122 mg, 0.35 mmol, 1.0 eq.) and HOBt (67 mg, 0.43 mmol, 1.2 eq.) were co-evaporated with toluene (3×8 mL). Then, to a stirred solution of compound **91** (122 mg, 0.35 mmol, 1.0 eq.), HOBt (67 mg, 0.43 mmol, 1.2 eq.), L-serine methyl ester hydrogen chloride (83 mg, 0.54 mmol, 1.5 eq.) and DCC (88 mg, 0.43 mmol, 1.2 eq.) in freshly distilled MeCN (5 mL) was added triethylamine (44 mg, 0.073 mL, 0.54 mmol, 1.5 eq.) dropwise at -5°C. After addition, the reaction temperature was slowly increased to r.t. and the reaction was stirred at r.t. for 24 h. Then, the reaction mixture was filtrated, washed with CH₂Cl₂ and concentrated. The resulting mixture was purified by silica gel column chromatography (80% EtOAc/PE to 100% EtOAc) to afford the desired amide **92** (57 mg, 0.129 mmol, 36%) and a methyl ester of **91** as a byproduct (30 mg, 0.084 mmol, 24%).

(Method II) Compound **91** (85 mg, 0.25 mmol, 1.0 eq.), DCC (78 mg, 0.375 mmol, 1.5 eq.) and HOBt (59 mg, 0.375 mmol, 1.5 eq.) were co-evaporated with toluene (3×8 mL). Then, the mixture was solubilized with MeCN (3 mL). The solution was transformed to a stirred solution of L-serine methyl ester hydrogen chloride (98 mg, 0.625 mmol, 2.5 eq.) and triethylamine

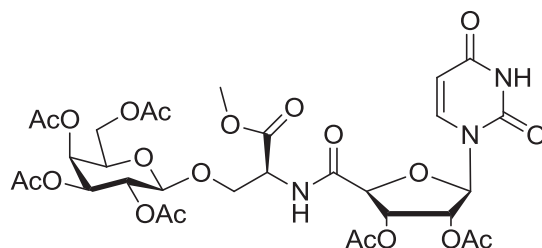
(0.087 mL, 0.625 mmol, 2.5 eq.) in freshly distilled MeCN (3 mL) at -5°C. After addition, the reaction temperature was slowly increased to r.t. and the reaction was stirred at r.t. for 16 h. Then, the reaction mixture was filtrated, washed with CH₂Cl₂ and concentrated. The resulting mixture was purified by silica gel column chromatography (80% EtOAc/PE to 100% EtOAc) to afford the desired amide **92** as white foam (100 mg, 0.226 mmol, 90%).

$R_f = 0.18$ (EtOAc); ¹H NMR (400 MHz, CDCl₃) δ (ppm) = 7.75 – 7.65 (m, 2H, H_{6Uri}, NHCO), 5.84 (d, $J = 5.5$ Hz, 1H, H_{1Rib}), 5.77 (d, $J = 8.0$ Hz, 1H, H_{5Uri}), 5.67 – 5.57 (m, 2H, H_{2Rib}, H_{3Rib}), 4.69 – 4.59 (m, 2H, H_{4Rib}, H _{α}), 4.03 – 3.88 (m, 2H, H _{β}), 3.73 (s, 3H, CO₂Me), 2.12 (s, 3H, COCH₃), 2.04 (s, 3H, COCH₃); ¹³C NMR (100 MHz, CDCl₃) δ (ppm) = 170.9, 170.2, 170.2, 168.8, 164.0, 151.3, 143.0 (C_{6Uri}), 103.9 (C_{5Uri}), 91.5 (C_{1Rib}), 82.0 (C_{4Rib}), 73.4 (C_{2Rib} or C_{3Rib}), 72.3 (C_{2Rib} or C_{3Rib}), 62.6 (C _{β}), 54.9 (C _{α}), 53.2 (CO₂Me), 21.0 (COCH₃), 20.8 (COCH₃); HR-ESI-MS (positive mode) m/z : calcd for C₁₇H₂₁N₃NaO₁₁, [M+Na]⁺ 466.1068, found 466.1052.



(2S)-3-Hydroxy-2-(1-uracyl- β -D-ribofuranuronamido)propanoic acid (93)

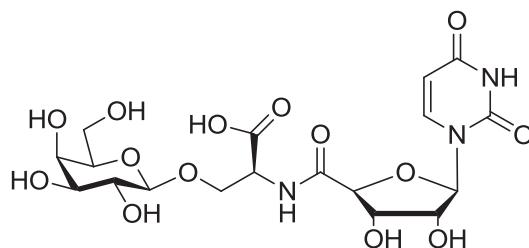
Aq. LiOH solution (24 mg in 1 mL of H₂O) was added dropwise into a solution of compound **92** (63 mg, 0.142 mmol, 1.0 eq.) in THF (2 mL) at r.t. After addition, the reaction mixture was stirred at r.t. for 2 h. 10 drops of AcOH (glacial) was then added into the reaction mixture (until pH~3). Then, the reaction was concentrated and the residue was purified by C18 reverse phase column chromatography (100% H₂O) to afford compound **93** as white foam (35 mg, 0.101 mmol, 71%). $[\alpha]_D = +7.7$ (c = 0.3, H₂O); ¹H NMR (400 MHz, D₂O) δ (ppm) = 7.96 (d, $J = 8.1$ Hz, 1H, H_{6Uri}), 5.92 (d, $J = 5.5$ Hz, 1H, H_{1Rib}), 5.88 (d, $J = 8.1$ Hz, 1H, H_{5Uri}), 4.55 (d, $J = 4.0$ Hz, 1H, H_{4Rib}), 4.50 (bd, $J = 5.5$ Hz, 1H, H_{2Rib}), 4.45 (dd, $J = 5.5, 4.0$ Hz, 1H, H_{3Rib}), 4.33 (bd, $J = 4.7$ Hz, 1H, H _{α}), 3.92 – 3.82 (m, 2H, H _{β}); ¹³C NMR (100 MHz, D₂O) δ (ppm) = 170.9, 166.1, 151.7, 142.9 (C_{6Uri}), 102.5 (C_{5Uri}), 90.7 (C_{1Rib}), 82.8 (C_{4Rib}), 72.4 (C_{2Rib} or C_{3Rib}), 72.3 (C_{2Rib} or C_{3Rib}), 61.8 (C _{β}), 57.1 (C _{α}); HR-ESI-MS (positive mode) m/z : calcd for C₁₂H₁₅N₃NaO₉, [M+Na]⁺ 368.0701, found 368.0706.



***N*-[(2S)-1-(2,3,4,6-Tetra-*O*-acetyl- β -D-galactopyranosyloxy)-4-oxa-3-oxo-pent-2-yl]-1-uracil-2,3-di-*O*-acetyl- β -D-ribofuranuronamide (94)**

BF₃·Et₂O (2 μ L, 0.009 mmol, 0.2 eq.) was added dropwise into a stirred solution of 2,3,4,6-tetra-*O*-acetyl- α -D-galactopyranosyl trichloroacetimidate (45 mg, 0.09 mmol, 2.0 eq.) and compound **92** (20 mg, 0.045 mmol, 1.0 eq.) in freshly distilled CH₂Cl₂ (3 mL) at -20°C. The

reaction mixture was stirred at -20°C for 2 h. The reaction mixture was then poured into satd aq. Na_2CO_3 (10 mL) solution and extracted with CHCl_3 (4×15 mL). The combined organic layers were dried (Na_2SO_4) and evaporated. The residue was purified by silica gel column chromatography (30% EtOAc to 100% EtOAc) to afford compound **94** as white foam (14 mg, 0.018 mmol, 40%). $R_f = 0.42$ (EtOAc); ^1H NMR (400 MHz, CDCl_3) δ (ppm) = 9.16 (s, 1H, NH_{Uri}), 7.52 (d, $J = 8.1$ Hz, 1H, $\text{H}_{6\text{Uri}}$), 7.24 (d, $J = 7.4$ Hz, 1H, NHCO), 5.83 (dd, $J = 8.1, 7.4$ Hz, 1H, $\text{H}_{5\text{Uri}}$), 5.79 (bd, $J = 5.8$ Hz, 1H, $\text{H}_{3\text{Rib}}$), 5.68 (d, $J = 4.3$ Hz, 1H, $\text{H}_{1\text{Rib}}$), 5.65 – 5.61 (m, 1H, $\text{H}_{2\text{Rib}}$), 5.37 (bd, $J = 3.5$ Hz, 1H, $\text{H}_{4\text{Gal}}$), 5.33 (dd, $J = 10.1, 3.5$ Hz, 1H, $\text{H}_{3\text{Gal}}$), 5.09 (dd, $J = 10.1, 7.9$ Hz, 1H, $\text{H}_{2\text{Gal}}$), 4.74 – 4.70 (m, 1H, H_α), 4.68 (d, $J = 7.9$ Hz, 1H, $\text{H}_{1\text{Gal}}$), 4.50 (bd, $J = 5.8$ Hz, 1H, $\text{H}_{4\text{Rib}}$), 4.20 – 4.14 (m, 3H, $\text{H}_{6\text{Gal}}, \text{H}_{\beta\alpha}$), 4.06 (dd, $J = 11.7, 2.5$ Hz, 1H, $\text{H}_{\beta\text{b}}$), 3.97 (dd, $J = 6.8, 6.8$ Hz, 1H, $\text{H}_{5\text{Gal}}$), 3.76 (s, 3H, CO_2Me), 2.14 (s, 6H, $2 \times \text{COCH}_3$), 2.12 (s, 3H, COCH_3), 2.06 – 2.01 (m, 9H, $3 \times \text{COCH}_3$); ^{13}C NMR (100 MHz, CDCl_3) δ (ppm) = 171.1, 170.5, 170.4, 170.1, 169.9, 169.6, 169.5, 167.9, 162.6, 150.3, 142.5 ($\text{C}_{6\text{Uri}}$), 103.7 ($\text{C}_{5\text{Uri}}$), 101.2 ($\text{C}_{1\text{Gal}}$), 92.7 ($\text{C}_{1\text{Rib}}$), 80.2 ($\text{C}_{4\text{Rib}}$), 72.9 ($\text{C}_{2\text{Rib}}$), 71.8 ($\text{C}_{3\text{Rib}}$), 71.0 ($\text{C}_{5\text{Gal}}$), 70.6 ($\text{C}_{3\text{Gal}}$), 69.6 ($\text{C}_{2\text{Gal}}$), 68.1 (C_β), 67.3 ($\text{C}_{4\text{Gal}}$), 61.1 ($\text{C}_{6\text{Gal}}$), 53.4 (C_α), 53.1 (CO_2Me), 20.9 (s, 2C, COCH_3), 20.82 (s, COCH_3), 20.78 (s, COCH_3), 20.68 (s, COCH_3), 20.64 (s, COCH_3); HRMS m/z : calcd. for $\text{C}_{31}\text{H}_{40}\text{N}_3\text{O}_{20}$, $[\text{M}+\text{H}]^+$ 774.2200, found 774.2161; $\text{C}_{31}\text{H}_{39}\text{N}_3\text{NaO}_{20}$, $[\text{M}+\text{Na}]^+$ 796.2019, found 796.2005.



***N*-[(2*S*)-1-(β -*D*-Galactopyranosyloxy)-3-oxo-pent-2-yl]-1-uracyl- β -*D*-ribofuranuronamide (**95**)**

Aq. LiOH solution (64 mg in 2 mL of H_2O) was added dropwise into a solution of compound **94** (148 mg, 0.19 mmol, 1.0 eq.) in THF (4 mL) at r.t. After addition, the reaction mixture was stirred at r.t. for 2 h. DOWEX 50W \times 2 Resin (Fluka, 50-100 mesh, H^+ Form) was added into the reaction mixture until pH \sim 3. Then, the reaction was filtered, concentrated and the residue was purified by C18 reverse phase column chromatography (100% H_2O) to afford compound **95** as white foam (48 mg, 0.095 mmol, 50%). $[\alpha]_{\text{D}} = +8.0$ ($c = 0.4, \text{H}_2\text{O}$); ^1H NMR (400 MHz, D_2O) δ (ppm) = 7.97 (d, $J = 8.1$ Hz, 1H, $\text{H}_{6\text{Uri}}$), 5.93 – 5.87 (m, 2H, $\text{H}_{5\text{Uri}}, \text{H}_{1\text{Rib}}$), 4.69 (t, $J = 4.0$ Hz, 1H, H_α), 4.57 (bd, $J = 4.1$ Hz, 1H, $\text{H}_{4\text{Rib}}$), 4.52 (dd, $J = 5.2, 5.2$ Hz, 1H, $\text{H}_{2\text{Rib}}$), 4.47 (dd, $J = 5.2, 4.1$ Hz, 1H, $\text{H}_{3\text{Rib}}$), 4.43 – 4.32 (m, 2H, $\text{H}_{1\text{Gal}}, \text{H}_{\beta\alpha}$), 3.96 (dd, $J = 10.8, 3.6$ Hz, 1H, $\text{H}_{\beta\text{b}}$), 3.89 (bd, $J = 3.4$ Hz, 1H, $\text{H}_{4\text{Gal}}$), 3.81 – 3.68 (m, 2H, $\text{H}_{6\text{Gal}}$), 3.65 (dd, $J = 7.9, 4.2$ Hz, 1H, $\text{H}_{5\text{Gal}}$), 3.58 (dd, $J = 9.9, 3.4$ Hz, 1H, $\text{H}_{3\text{Gal}}$), 3.49 (dd, $J = 9.9, 7.8$ Hz, 1H, $\text{H}_{2\text{Gal}}$); ^{13}C NMR (100 MHz, D_2O) δ (ppm) = 173.1, 171.5, 166.2, 151.7, 143.2 ($\text{C}_{6\text{Uri}}$), 103.2 ($\text{C}_{1\text{Gal}}$), 102.5 ($\text{C}_{5\text{Uri}}$), 91.3 ($\text{C}_{1\text{Rib}}$), 82.7 ($\text{C}_{4\text{Rib}}$), 75.1 ($\text{C}_{5\text{Gal}}$), 72.6 ($\text{C}_{3\text{Gal}}$), 72.5 ($\text{C}_{3\text{Rib}}$), 72.4 ($\text{C}_{2\text{Rib}}$), 70.5 ($\text{C}_{2\text{Gal}}$), 68.9 (C_β), 68.5 ($\text{C}_{4\text{Gal}}$), 60.9 ($\text{C}_{6\text{Gal}}$), 53.3 (C_α); HR-ESI-MS (positive mode) m/z : calcd for $\text{C}_{18}\text{H}_{24}\text{N}_3\text{O}_{14}$, $[\text{M}-\text{H}]^-$ 506.1264, found 506.1269.

V.3 Cloning, expression and purification of GTs

The mutant enzyme was cloned and expressed in *E. coli* using standard mutagenesis techniques^{27, 242-243}. All other GalT were expressed and purified as previously described²⁴³⁻²⁴⁵ apart from β -1,4-GalT, which was obtained commercially (Sigma-Aldrich). Both GTB and AAGlyB were purified by ionexchange and affinity chromatography²⁴⁶ and yielded ~10-15 mg pure protein per liter cell culture. At the end of purification, excess UDP was removed from the eluted protein solution by dialysis in buffer (50 mM MOPS pH 7, 0.1 M NaCl, 1 mM DTT, 5 mM MnCl₂) before concentrating the protein to 15-17 mg/mL. Protein stock containing 5 mM MnCl₂, 50 mM MOPS pH 7, 100 mM NaCl and 1 mM DTT were stripped of metal using buffer with 50 mM EDTA and solvent exchanged into 50 mM MOPS pH7, 100 mM NaCl and 1 mM DTT by serie dilutions and concentrations using an Amicon Ultra centrifugal concentrator (Millipore, 10 kDa cutoff). Final concentration of the protein stock was approximately 12 mg/mL. The recombinant protein OGT was purified by HisTrap (Amersham) column with gradient imidazole elution. Pure protein was pooled, concentrated and subsequently digested with recombinant enterokinase to cleave the GSTs (glutathione *S*-transferase) tag which was subsequently removed using column chromatography on glutathione-agarose resin.

V.4 Enzymatic assays

GalT: Radiochemical assay: Radiochemical enzyme assays were performed in a final volume of 15 μ L, containing the corresponding enzyme, radioactive labeled UDP-[³H]Gal, the requisite acceptor α -L-Fucp-(1 \rightarrow 2)- β -D-Galp-O-C₈H₁₇, β -D-GlcNAc-O-(CH₂)₈-CO₂Me or β -D-Lac-O-(CH₂)₈-CO₂Me as acceptor substrates and inhibitor (0 to 3 mM). The reaction mixture was incubated in MOPS (50 mM), MnCl₂ (20 mM), pH 7.0, bovine serum albumin (1 mg.mL⁻¹) for a certain time at 37°C (a time for which linear rates are obtained using these assay conditions) and the reaction was quenched with cold water (400 μ L). The enzymatic product was isolated by purification with Sep-Pak RC C¹⁸ cartridges (Waters). Radioactivity was measured by using a Beckman CoulterTM LS 6500 multi-purpose scintillation counter. The K_m values for UDP-Gal and the requisite acceptor α -L-Fucp-(1 \rightarrow 2)- β -D-Galp-O-C₈H₁₇, β -D-GlcNAc-O-(CH₂)₈-CO₂Me or β -D-Lac-O-(CH₂)₈-CO₂Me with different GT were determined previously by a standard radiochemical Sep-Pak assay.^{28, 81, 247} The inhibition assays at 1 mM and the IC₅₀ values with β -1,4-GalT, GTB, α -1,4-GalT, α -1,3-GalT and AAGlyB were determined in analogous fashion using the requisite acceptor. The inhibition assays at 1 mM inhibitor and various GT were carried out at concentration of donor at K_m value and concentration of acceptor at K_m value or higher. The IC₅₀ values were determined by constructing a dose-response curve and examining the effect of 10 different concentrations of each inhibitor ranging from 0 μ M to 3000 μ M at concentration of donor at near 1/5th K_m value and concentration of acceptor at K_m value or higher. The lowest calculated R² value from the fitted lines of each experiment was 0.95. 500 μ M acceptor for α -1,3-GalT, 2 mM acceptor for α -1,4-GalT, 500 μ M acceptor for β -1,4-GalT, 500 μ M acceptor for GTB and 20 μ M acceptor for AAGlyB were used. For all the assays, inhibitors were dissolved in MilliQ H₂O, except compounds 24, 34-Gal, 44 and 49, for which a maximum of 3% final concentration of

DMSO/H₂O were used due to poor solubility with a corresponding 3% F.C. of DMSO/H₂O no inhibitor assays as control.

OGT: The ability of small molecule to inhibit OGT activity was assessed using radiolabelled [³H]-UDP-GlcNAc (American Radiolabel) as the donor and recombinant nup62 as the acceptor. For IC₅₀ assays, 8 μM nup62, 1 μM UDP-GlcNAc (about 1/5th of *K_m* value of donor, constant specific activity of 0.14 Ci/mmol of [³H]-UDP-GlcNAc), 200 nM hOGT and various concentrations of small molecule inhibitors were used. For *K_i* evaluation, 10 μM nup62, 1 μM UDP-GlcNAc (constant specific activity of 0.8 Ci/mmol of [³H]-UDP-GlcNAc) or 50 μM UDP-GlcNAc (constant specific activity of 0.35 Ci/mmol of [³H]-UDP-GlcNAc), 100 nM hOGT, and various concentrations of small molecule, 1000, 500, 250, 125, 62.5 and 31.25 μM, were used for the assays. Reactions were initiated by the addition of enzyme by pipette and incubated at 37 °C for 1 h (a time for which linear rates are obtained using these assay conditions). Reactions were placed on ice after 1 hr of incubation, then immediately applied to a 1.5 by 3 cm piece of nitrocellulose membrane (BioRad) and allowed to air dry. The quantity of protein loaded onto each piece of nitrocellulose was at least ten times less than the binding capacity of the membrane (as detailed in the manufacturer's protocol). The membranes were washed with four consecutive large volumes (100 mL) of PBS and air dried. The pieces of membrane were loaded into scintillation vials, 4 mL of scintillation fluid (Amersham) was added, and the levels of tritium were quantified using a liquid scintillation counter (Beckman LS6000). All assays were done in triplicate (2 minute for sample counting). The *K_i* value is calculated from an equation generated based on the establishment of Dixon plot of each inhibitors and where it intersects with the 1/*V*_{max}.

V.5 Crystallization and structure refinement

The metal free protein was crystallized at 20 °C by the sitting drop method with drops containing 1.6 μL of protein stock and 1.6 μL of reservoir solution containing 13% or 15% PEG 3350, 50 mM or 150 mM ammonium sulfate and 50 mM MOPS pH7. Seeding was performed with a horse hair from previous similar drops, and the drops were allowed to equilibrate over 500 μL of reservoir solution. Crystals of the apo form of the protein grew to a final size of approx 200 μm in one week. Drop wells containing the best crystals were opened, 2.4 μL of 50 mM MOPS pH 7, 50 mM MnCl₂ and 100 mM inhibitor was added followed by 0.8 μL of 200 mM α-L-Fucp-(1→2)-β-D-Galp-O-(CH₂)₇-CH₃ solution. The drops were mixed, resealed, allowed to equilibrate for 45 minutes, then, opened again and 3 μL of reservoir solution mixed 1:1 with glycerol added as cryoprotectant. After one minute the crystals were mounted in Mitegen loops and flash frozen in liquid nitrogen.

Diffraction data for crystals with each of inhibitors **7-Gal**, **7-Glc** and **19** were collected in Beamline ID23-2 at ESRF at a wavelength of 0.873 Å with a crystal to detector of 167.5 mm with 1° oscillations, 180 images per crystals and exposure times of 0.1 to 0.5 seconds per image. Diffraction data was integrated and scaled with XDS²⁴⁸. The structures were refined using PDB_ID:3IOI⁸¹ as the starting model followed by rigid body refinement in lieu of molecular replacement. Geometry descriptions for the inhibitors were made with Sketcher from the CCP4i suite²⁴⁹. Refinement was carried on with Refmac5²⁵⁰, model building with Coot²⁵¹ and figures were rendered with Pymol. A full atom anisotropic model was used for **19** and **7-Glc**, while TLS + isotropic atoms were used for **7-Gal**. Data collection and refinement

statistics are listed in **Table V-1**. The atomic coordinates and structure factors have been deposited at the Protein Data Bank with the following accession codes: 4KC2, 4KC4 and 4KC1.

Table V-1. Data collection for crystallography and refinement statistics.

| Inhibitor | 7-Gal | 19 | 7-Glc |
|--|--|--|--|
| Space group | C222 ₁ | C222 ₁ | C222 ₁ |
| Unit cell parameters | a=55.88 Å, b=149.90 Å, c=80.03 Å, α=β=γ=90° | a=55.93 Å, b=149.87 Å, c=80.10 Å, α=β=γ=90° | a=55.85 Å, b=149.87 Å, c=80.00 Å, α=β=γ=90° |
| Resolution | 1.7 Å (1.9 Å) | 1.6 Å (1.8 Å) | 1.5 Å (1.7 Å) |
| Unique reflections | 35437 | 42400 | 51220 |
| Completeness | 100.0% (100.0%) | 99.9% (100.0%) | 99.9% (100.0%) |
| Redundancy | 7.3 | 5.7 | 5.7 |
| Rmerge | 14.3% (66.4%) | 9.3% (64.3%) | 8.5% (58.7%) |
| I/σI | 11.44 (3.02) | 11.92 (2.87) | 14.47 (2.99) |
| R _{work} | 17.6% | 14.6% | 14.1% |
| R _{free} | 20.5% | 19.2% | 18.1% |
| Av. B factor | 13.9 Å ² | 20.0 Å ² | 16.2 Å ² |
| R.M.S.D. bonds | 0.006 Å | 0.007 Å | 0.006 Å |
| R.M.S.D. angles | 1.06° | 1.16° | 1.12° |
| Ramachandran plot (% in favored / allowed regions) | 97.2% / 99.6% | 97.9% / 100.0% | 97.6% / 100% |
| PDB_ID | 4KC2 | 4KC4 | 4KC1 |

*As assessed by Molprobit²⁵². Numbers in brackets are for the high resolution shell.

#Rmerge = $\sum_{hkl} \sum_i |I_i(hkl) - \langle I(hkl) \rangle| / \sum_{hkl} \sum_i I_i(hkl)$.

+Rwork = $\sum_{hkl} ||F_{obs}| - |F_{calc}|| / \sum_{hkl} |F_{obs}|$.

§Rfree = $\sum_{hkl} ||F_{obs}| - |F_{calc}|| / \sum_{hkl} |F_{obs}|$ calculated using a random set containing 3% of the reflections that were not included throughout structure refinement.

V.6 Non-Linear Dixon plots and Michaelis-Menten plots

Figure V.6.1. Non-Linear Dixon Plots of 7-Gal Inhibition of β -1,4-GalT

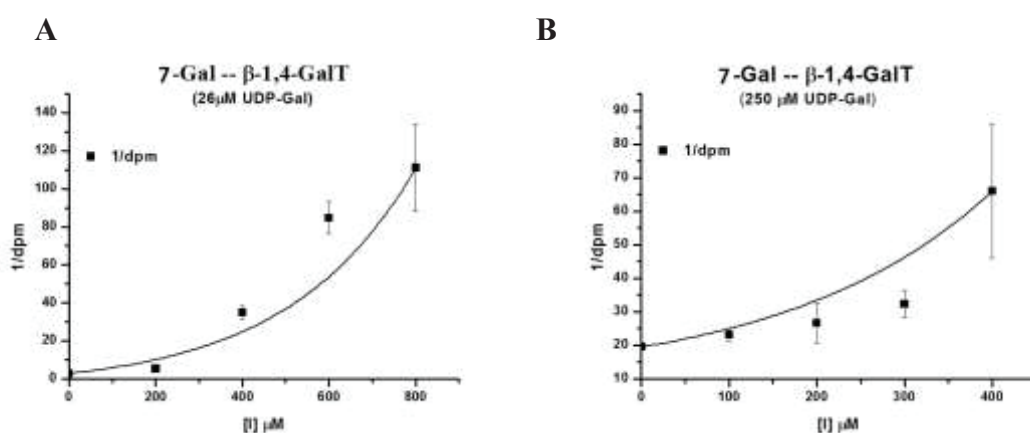


Figure V.6.1. Dixon plots of 7-Gal inhibition of β -1,4-GalT carried out at saturating acceptor concentrations. **A.** The concentration of UDP-Gal was 26 μ M, approx. the K_m for donor, the concentration of β -D-GlcNAc-O-(CH₂)₈-CO₂Me acceptor was 500 μ M with 4 concentrations of 7-Gal, from 200-800 μ M. Assays were carried out in duplicate showing non-linear dependence on inhibitor concentration ($r^2 = 0.6110$ was obtained from linear regression analysis of the data points). **B.** The concentration of UDP-Gal was 250 μ M, the concentration of acceptor was 500 μ M with 4 concentrations of 7-Gal, from 100-400 μ M. Assays were carried out in duplicate with non-linear dependence of inhibitor concentration ($r^2 = 0.6291$ was obtained for linear regression of the data).

Figure V.6.2. Michaelis-Menten Plots of 7-Gal Inhibition of β -1,4-GalT

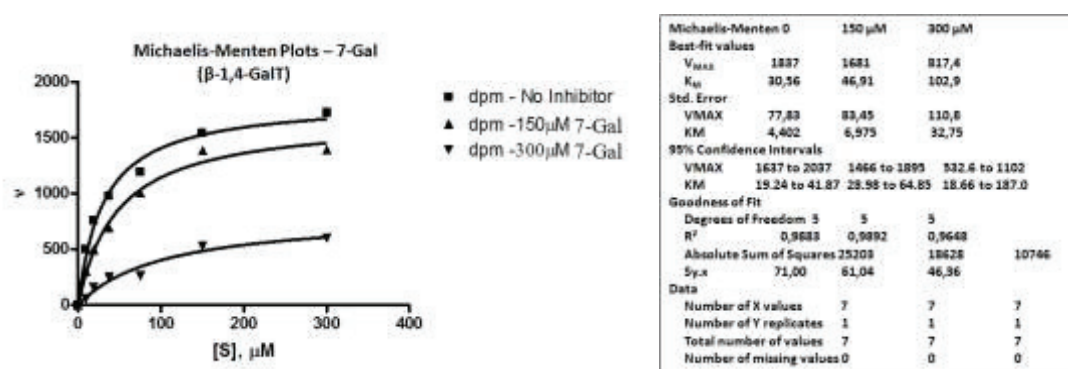


Figure V.6.2. Michaelis Menten plots for different concentrations of 7-Gal as an inhibitor of β -1,4-GalT. The kinetics assays were carried out at concentration of donor of 0, 9.375 μ M, 18.75 μ M, 37.5 μ M, 75 μ M, 150 μ M and 300 μ M, the concentration of acceptor was 500 μ M with 2 concentrations of 7-Gal, 150 μ M, 300 μ M. Non-linear regression analysis with GraphPad Prism was used to obtain K_m and V_{max} values and standard errors.

Figure V.6.3. Non-Linear Dixon Plots of 19 Inhibition of β -1,4-GalT

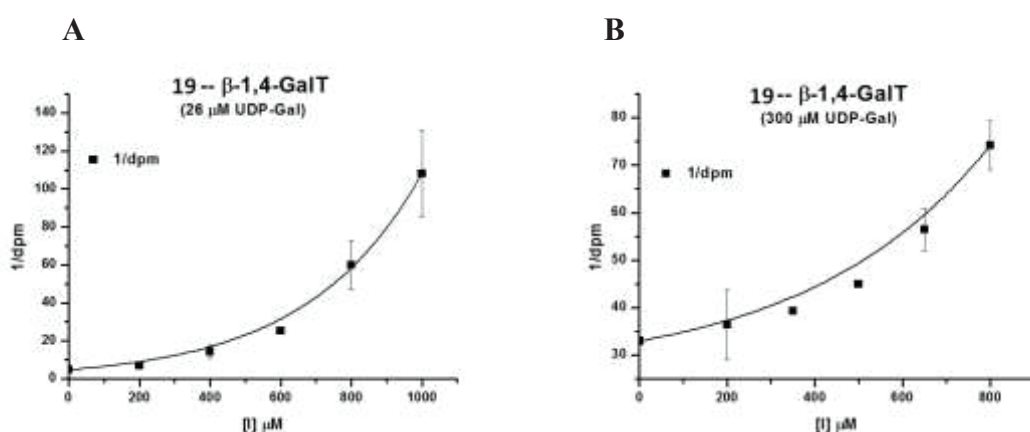


Figure V.6.3. Dixon plots of 19 inhibition of β -1,4-GalT carried out at saturating acceptor concentrations. **A.** The concentration of UDP-Gal was 26 μ M, approx. the K_m for donor, the concentration of β -D-GlcNAc-O-(CH₂)₈-CO₂Me acceptor was 500 μ M with 5 concentrations of 19, from 200-1000 μ M. Assays were carried out in duplicate showing non-linear dependence on

inhibitor concentration ($r^2 = 0.5792$ was obtained from linear regression analysis of the data points). **B.** The concentration of UDP-Gal was $300 \mu\text{M}$, the concentration of acceptor was $500 \mu\text{M}$ with 5 concentrations of **19**, from $200\text{--}800 \mu\text{M}$. Assays were carried out in duplicate with non-linear dependence of inhibitor concentration ($r^2 = 0.8222$ was obtained for linear regression of the data).

Figure V.6.4. Michaelis-Menten Plots of 19 Inhibition of β -1,4-GalT

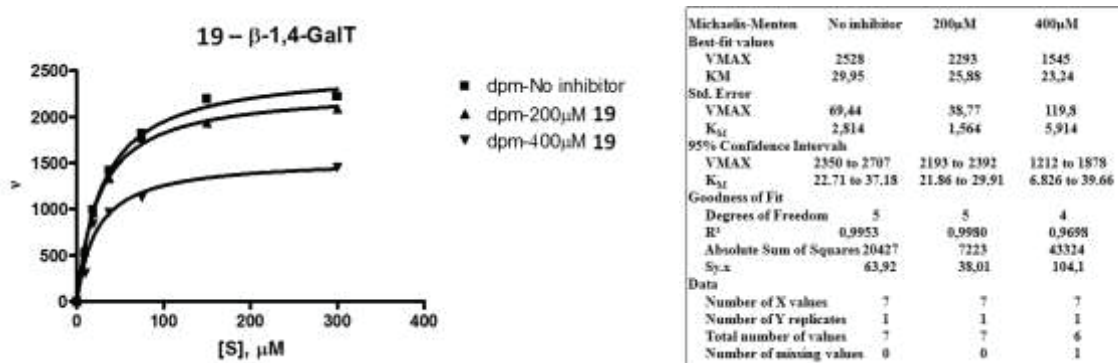


Figure V.6.4. Michaelis Menten plots for different concentrations of **19** as an inhibitor of β -1,4-GalT. The kinetics assays were carried out at concentration of donor of 0, 9.375 μM , 18.75 μM , 37.5 μM , 75 μM , 150 μM and 300 μM , the concentration of acceptor was 500 μM with 2 concentrations of **19**, 200 μM , 400 μM . Non-linear regression analysis with GraphPad Prism was used to obtain K_m and V_{max} values and standard errors.

Figure V.6.5. Non-Linear Dixon Plots of 7-Gal and 19 Inhibition of AAGlyB

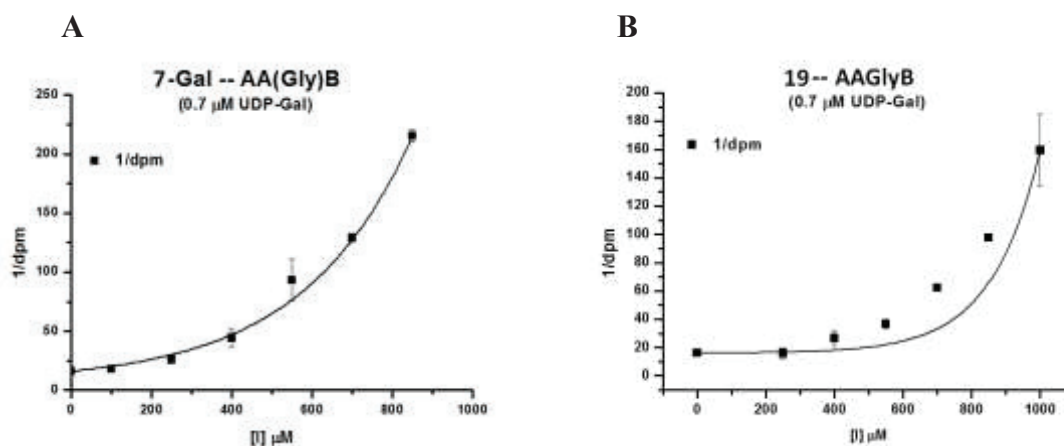


Figure V.6.5. Dixon plots of **7-Gal** and **19** inhibition of AAGlyB carried out at saturating acceptor concentrations. **A.** The concentration of UDP-Gal was $0.7 \mu\text{M}$, approx. the K_m for donor, the concentration of α -L-Fucp-(1 \rightarrow 2)- β -D-Galp-O-C₈H₁₅ acceptor was $20 \mu\text{M}$ with 6 concentrations of **7-Gal**, from $100\text{--}850 \mu\text{M}$. Assays were carried out in duplicate showing non-linear dependence on inhibitor concentration ($r^2 = 0.8684$ was obtained from linear regression analysis of the data points). **B.** The concentration of UDP-Gal was $0.7 \mu\text{M}$, approx. the K_m for donor, the concentration of α -L-Fucp-(1 \rightarrow 2)- β -D-Galp-O-C₈H₁₅ acceptor was $20 \mu\text{M}$ with 6 concentrations of **19**, from $250\text{--}1000 \mu\text{M}$. Assays were carried out in duplicate showing non-linear dependence on inhibitor concentration ($r^2 = 0.7770$ was obtained from linear regression analysis of the data points).

Figure V.6.6. Michaelis-Menten Plots of 7-Gal Inhibition of AAGlyB

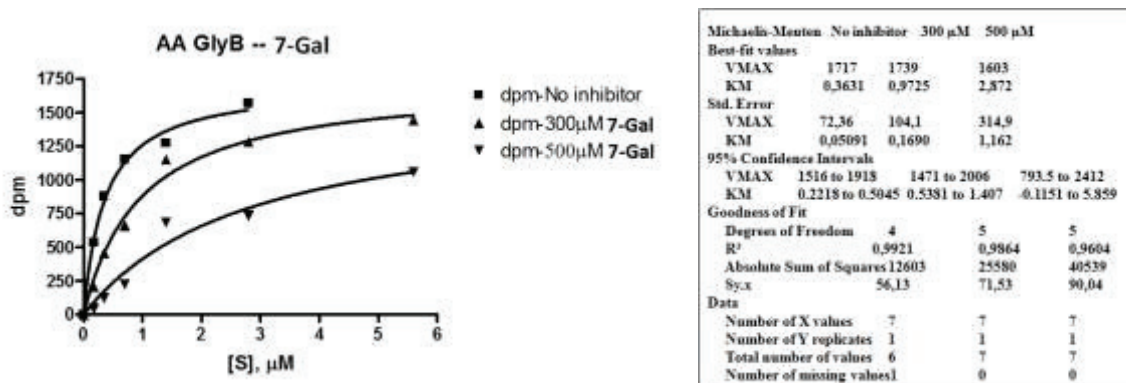


Figure V.6.6. Michaelis Menten plots for different concentrations of 7-Gal as an inhibitor of AAGlyB. The kinetics assays were carried out at concentration of donor of 0, 0.175 μM , 0.35 μM , 0.7 μM , 1.4 μM , 2.8 μM and 5.6 μM , the concentration of acceptor was 20 μM with 2 concentrations of 7-Gal, 300 μM , 500 μM . Non-linear regression analysis with GraphPad Prism was used to obtain K_m and V_{max} values and standard errors.

Figure V.6.7. Michaelis-Menten Plots of 19 Inhibition of AAGlyB

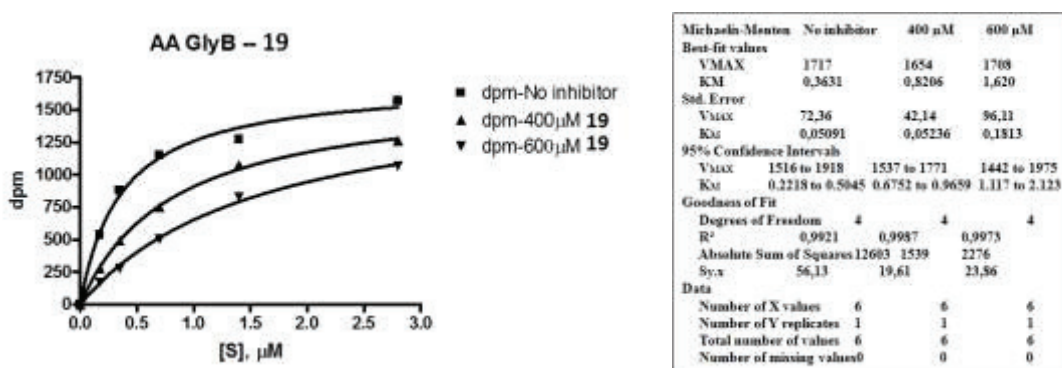


Figure V.6.7. Michaelis Menten plots for different concentrations of 19 as an inhibitor of AAGlyB. The kinetics assays were carried out at concentration of donor of 0, 0.175 μM , 0.35 μM , 0.7 μM , 1.4 μM and 2.8 μM , the concentration of acceptor was 20 μM with 2 concentrations of 19, 400 μM , 600 μM . Non-linear regression analysis with GraphPad Prism was used to obtain K_m and V_{max} values and standard errors.

Figure V.6.8. Michaelis-Menten Plots of 7-Gal Inhibition of α -1,4-GalT

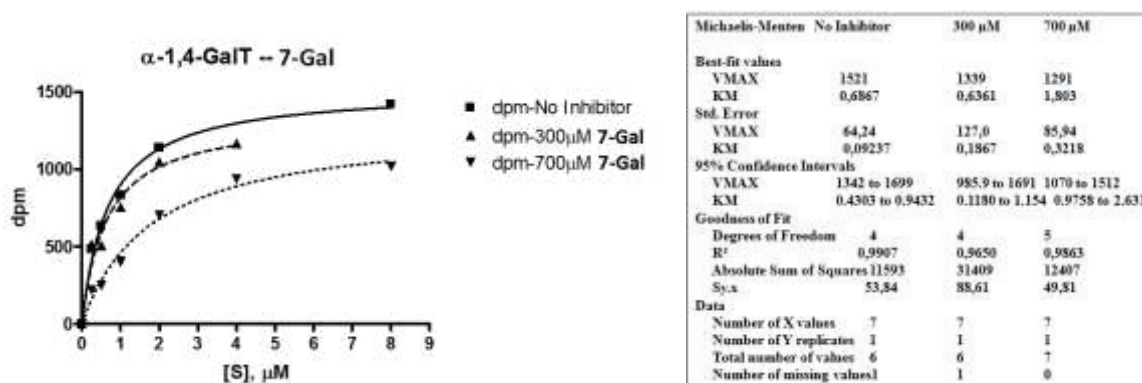


Figure V.6.8. Michaelis Menten plots for different concentrations of 7-Gal as an inhibitor of α -1,4-GalT. The kinetics assays were carried out at concentration of donor of 0, 0.25 μM , 0.50 μM , 1.00 μM , 2.00 μM , 4.00 μM and 8.00 μM , the concentration of acceptor was 20 μM with 2 concentrations of 7-Gal, 300 μM , 700 μM . Non-linear regression analysis with GraphPad Prism was used to obtain K_m and V_{max} values and standard errors.

Figure V.6.9. Michaelis-Menten Plots of 19 Inhibition of α -1,4-GalT

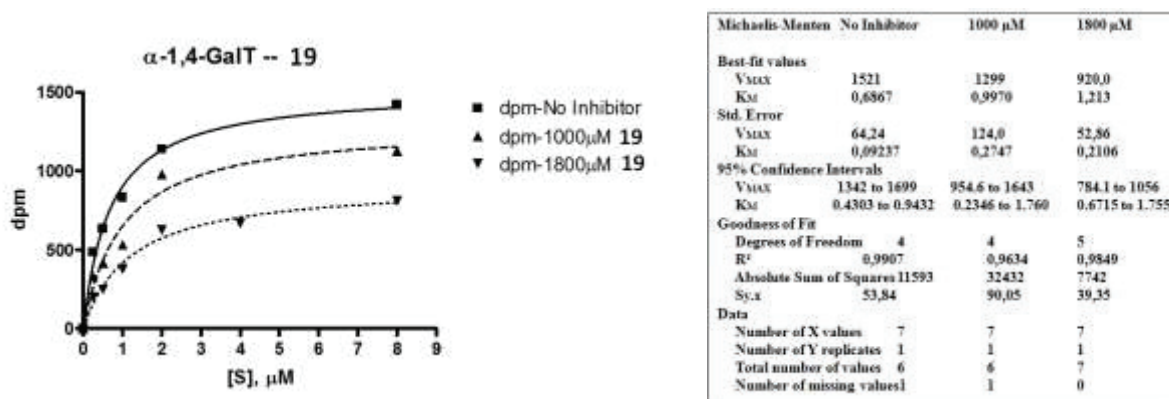


Figure V.6.9. Michaelis Menten Plots for different concentrations of 19 as an inhibitor of α -1,4-GalT. The kinetics assays were carried out at concentration of donor of 0, 0.25 μ M, 0.50 μ M, 1.00 μ M, 2.00 μ M, 4.00 μ M and 8.00 μ M, the concentration of acceptor was 20 μ M with 2 concentrations of 19, 1000 μ M, 1800 μ M. Non-linear regression analysis with GraphPad Prism was used to obtain K_m and V_{max} values and standard errors.

Figure V.6.10. Michaelis-Menten Plots of 7-Gal Inhibition of α -1,3-GalT

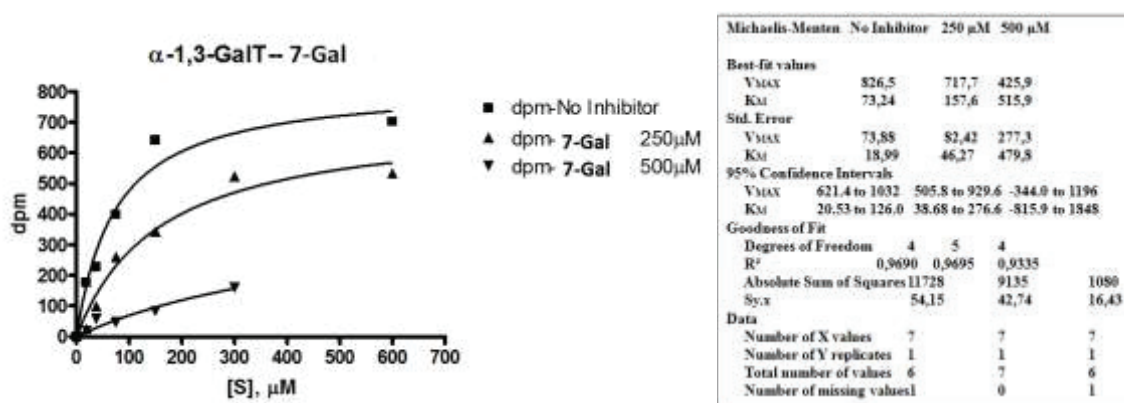


Figure V.6.10. Michaelis Menten Plots for different concentrations of 7-Gal as an inhibitor of α -1,3-GalT. The kinetics assays were carried out at concentration of donor of 0, 18.75 μ M, 37.50 μ M, 75.00 μ M, 150.00 μ M, 300.00 μ M and 600.00 μ M, the concentration of acceptor was 500 μ M with 2 concentrations of 7-Gal, 250 μ M, 500 μ M. Non-linear regression analysis with GraphPad Prism was used to obtain K_m and V_{max} values and standard errors.

Figure V.6.11. Michaelis-Menten Plots of 19 Inhibition of α -1,3-GalT

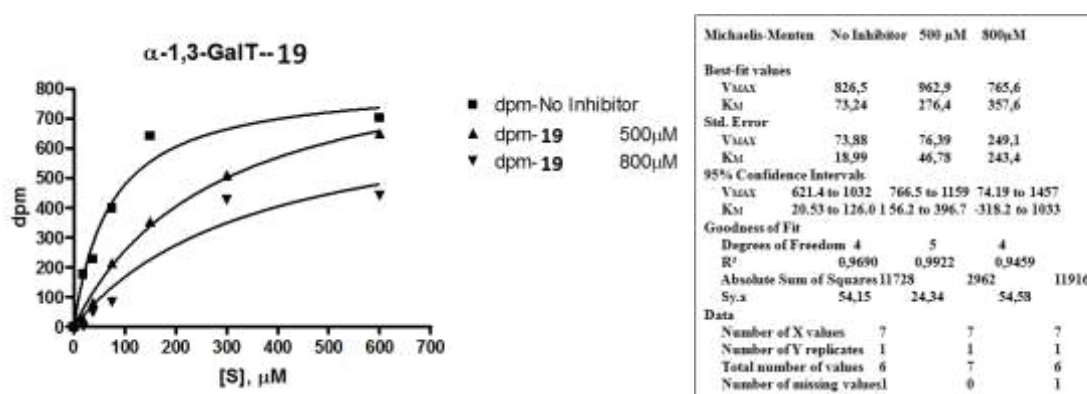


Figure V.6.11. Michaelis Menten plots for different concentrations of 19 as an inhibitor of α -1,3-GalT. The kinetics assays were carried out at concentration of donor of 0, 18.75 μ M, 37.50 μ M, 75.00 μ M, 150.00 μ M, 300.00 μ M and 600.00 μ M, the concentration of acceptor was 500 μ M with 2 concentrations of 19, 500 μ M, 800 μ M. Non-linear regression analysis with GraphPad Prism was used to obtain K_m and V_{max} values and standard errors.

Figure V.6.12. Michaelis-Menten Plots of 7-Gal Inhibition of GTB

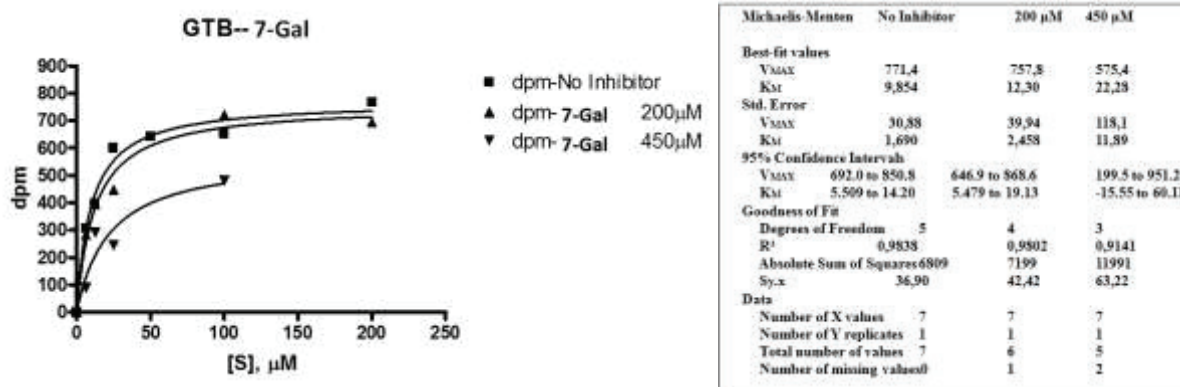


Figure V.6.12. Michaelis Menten plots for different concentrations of 7-Gal as an inhibitor of GTB. The kinetics assays were carried out at concentration of donor of 0, 6.25 μM, 12.50 μM, 25.00 μM, 50.00 μM, 100.00 μM and 200.00 μM, the concentration of acceptor was 500 μM with 2 concentrations of 7-Gal, 200 μM, 450 μM. Non-linear regression analysis with GraphPad Prism was used to obtain K_m and V_{max} values and standard errors.

Figure V.6.13. Michaelis-Menten Plots of 19 Inhibition of GTB

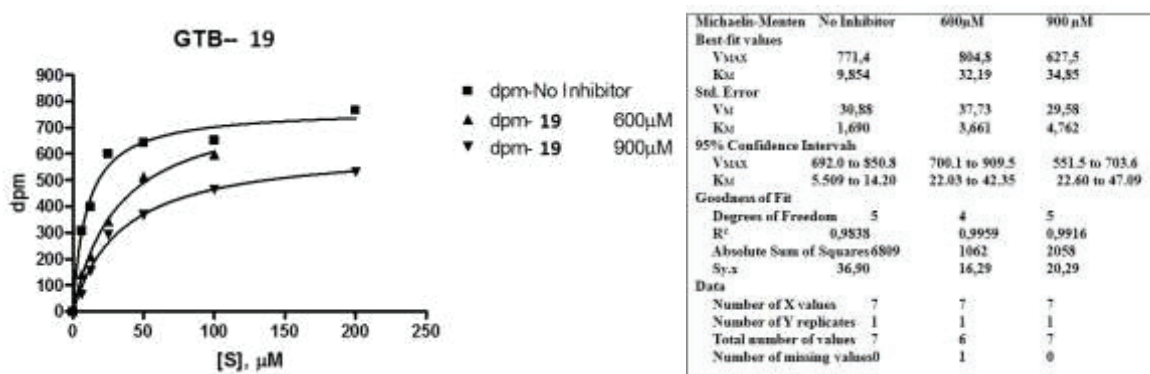


Figure V.6.13. Michaelis Menten plots for different concentrations of 19 as an inhibitor of GTB. The kinetics assays were carried out at concentration of donor of 0, 6.25 μM, 12.50 μM, 25.00 μM, 50.00 μM, 100.00 μM and 200.00 μM, the concentration of acceptor was 500 μM with 2 concentrations of 19, 600 μM, 900 μM. Non-linear regression analysis with GraphPad Prism was used to obtain K_m and V_{max} values and standard errors.

Figure V.6.14. Michaelis-Menten Plots of 81 Inhibition of AAGlyB

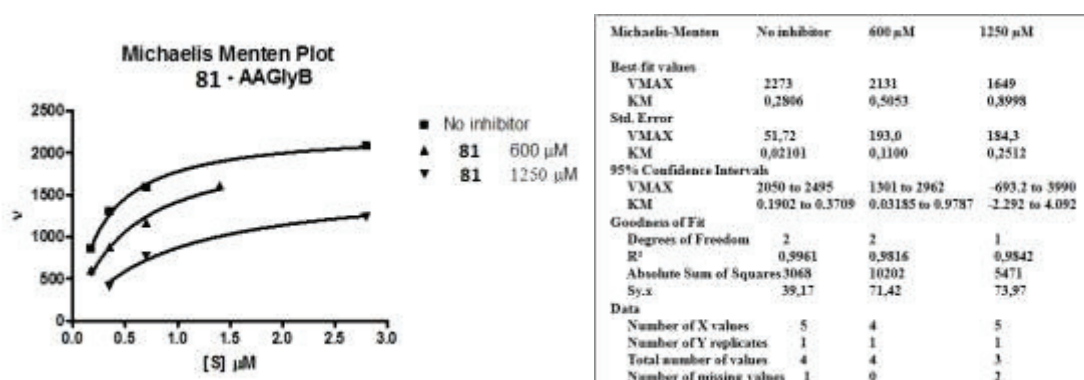


Figure V.6.14. Michaelis Menten plots for different concentrations of 81 as an inhibitor of AAGlyB. The kinetics assays were carried out at concentration of donor of 0, 0.175 μM, 0.35 μM, 0.7 μM, 1.4 μM and 2.8 μM, the concentration of acceptor was 20 μM with 2 concentrations of 81, 600 μM, 1250 μM. Non-linear regression analysis with GraphPad Prism was used to obtain K_m and V_{max} values and standard errors.

Figure V.6.15. Michaelis-Menten Plots of 81 Inhibition of GTB

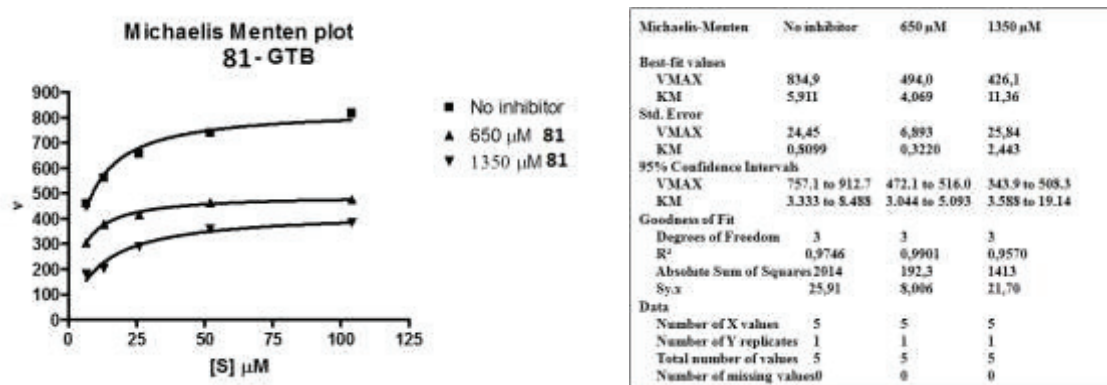


Figure V.6.15. Michaelis Menten plots for different concentrations of **81** as an inhibitor of **GTB**. The kinetics assays were carried out at concentration of donor of 0, 6.5 μM, 13 μM, 26 μM, 52 μM and 104 μM, the concentration of acceptor was 500 μM with 2 concentrations of **81**, 650 μM, 1350 μM. Non-linear regression analysis with GraphPad Prism was used to obtain K_m and V_{max} values and standard errors.

Figure V.6.16. Michaelis-Menten Plots of 90 Inhibition of α-1,3-GalT

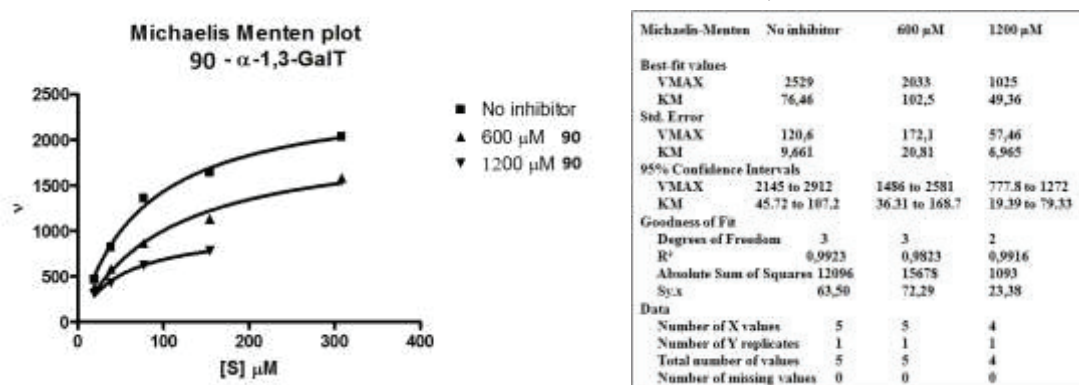


Figure V.6.16. Michaelis Menten plots for different concentrations of **90** as an inhibitor of **α-1,3-GalT**. The kinetics assays were carried out at concentration of donor of 0, 19.25 μM, 38.5 μM, 77 μM, 154 μM and 308 μM, the concentration of acceptor was 500 μM with 2 concentrations of **90**, 600 μM, 1200 μM. Non-linear regression analysis with GraphPad Prism was used to obtain K_m and V_{max} values and standard errors.

Figure V.6.17. Radioactive OGT assay for K_i determination of 35-Glc

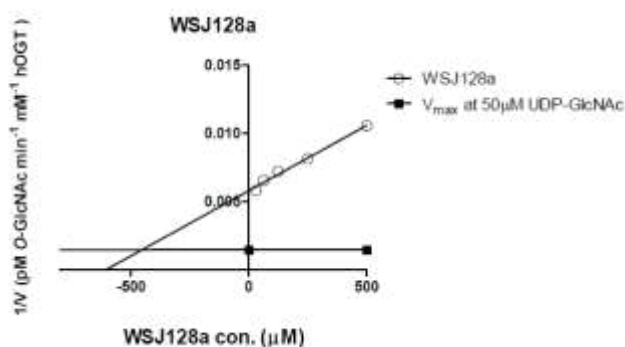


Figure V.6.17. Radioactive OGT assay for K_i determination of **35-Glc**. Assays contained 10 μM nup62, 1 μM UDP-GlcNAc for the assay (constant specific activity of 0.8 Ci/mmol of [³H]-UDP-GlcNAc) or 50 μM UDP-GlcNAc (constant specific activity of 0.35 Ci/mmol of [³H]-UDP-GlcNAc), 100 nM hOGT, and various concentrations of small molecule (1000, 500, 250, 125, 62.5 and 31.25 μM). The K_i value is calculated from an equation generated based on the establishment of Dixon plot of the inhibitor and where it is intersect with the $1/V_{max}$. WSJ128a = **35-Glc**.

V.7 Cell assays

V.7.1 Cell culture

Human breast cancer epithelial MCF7 cells and human embryonic kidney HEK293 cells were grown in Dulbecco's Modified Eagle's Medium (DMEM) (Lonza, Basel, Switzerland) supplemented with 10% (v/v) fetal calf serum (FCS) (Lonza), 200 mM L-glutamine, 10 U/mL penicillin and 10 µg/mL streptomycin (Life Technologies, Invitrogen, St Aubin, France). Human *mammary epithelial MCF10A* cells were grown in the Mammary Epithelial cell Growth Medium (MEGM) composed of Mammary Epithelial Basal Medium (MEBM) supplemented with 13 mg/mL bovine pituitary extract (BPE), 10 µg/mL human epidermal growth factor (hEGF), 0.5 mg/mL hydrocortisone, and 5 mg/mL insulin (Lonza). Cells were grown at 37 °C in a humidified atmosphere enriched with 5% CO₂.

To test the various compounds, cells were grown in a 24-wells plate in complete medium. When cells reached 70% confluence, medium was changed and the compound was added at the indicated concentrations (from 50 µM to 500 µM) for 24 h or 48 h. The OGT potent inhibitor Ac-5SGlcNAc (2-acetamido-1,3,4,6-tetra-O-acetyl-2-deoxy-5-thio- α -D-glycopyranose) was used as a positive control (50 µM, 100 µM) (gift of Pr. David Vocadlo).

V.7.2 Cell lysis and Western blotting

After treatment, cells were lysed on ice for 10 min in 100 µL lysis buffer (50 mM Tris-HCl pH 7.5, 150 mM NaCl, 0.1% (w/v) SDS, 1% (v/v) Triton-X100) containing the complete protease inhibitors cocktail (Roche Diagnostics, Meylan, France), 50 mM sodium fluoride (Sigma-Aldrich) and 100 µM orthovanadate (Sigma-Aldrich). Cell lysate was centrifuged at 20,000 ×g for 10 min and supernatant was collected. Protein concentration was measured using the microBCA protein assay kit (Pierce, Fisher Scientific, Illkirch, France). Proteins (20 µg) were separated by SDS-PAGE and transferred onto nitrocellulose membrane (Hybond™-C EXTRA, GE Healthcare, Orsay, France). Membranes were blocked in 5% (w/v) nonfat dry milk in Tris-Buffered Saline with 0.05% (v/v) Tween 20 (TBS-T) and probed with primary antibodies directed against O-GlcNAc (RL2, 1:4000) (Ozyme, Montigny le Bretonneux, France), and GAPDH (1:5000) (Abcam, Cambridge, UK) overnight at 4 °C. After 3 washes in TBS-T, membranes were incubated with the appropriate horseradish peroxidase-conjugated secondary antibody (anti-rabbit IgG-HRP linked, 1:30,000, GE Healthcare) for 1 h at room temperature. After several washes, blots were developed using enhanced chemiluminescence (ECL Prime Reagent, Hyperfilm™ MP; GE Healthcare, Velizy-Villacoublay, France).

V.8 Permeation assays

1-Palmitoyl-2-oleoyl-*sn*-glycero-3-phosphocholine (POPC) solution (stock solution, 25 mg/mL in chloroform, Avanti Polar Lipids) was dried in a round bottom flask, and dispersed with buffer (PBS buffer containing inhibitors (0.01 M) or PBS buffer). The suspension was vortexed for 5-10 min until an emulsion was formed. Then, the emulsion was submitted to 5 freeze/thaw cycles (5 min in liquid N₂ / 10 min in water bath at 37°C / 1 min vortex) to yield unilamellar structures, followed by extrusion to the desired size of ca. 200 nm. To check inhibitor penetration across lipid membrane, liposomes were incubated overnight at 37°C for 24 h in a shaking incubator. Separation of liposomes from free inhibitors was performed using gel filtration chromatography (G-25 column - GE Healthcare). Liposomes (200 nm in diameter)

are eluted in the 4 mL void volume of the column. Small size molecules penetrated inside column gel, and were eluted later with more than 6 mL. After 30 mL of elution, UV absorption at 260 nm and UV spectra of 230 – 400 nm regions were measured for each fraction using Tecan Infinite M200 reader.

Test on 7-Gal: Method I. Prepared liposomes (size 200 nm, final concentration of 5 mg/mL in PBS) were incubated with **7-Gal** (final concentration of 1×10^{-2} M in PBS) in a final volume of 1 mL at 37°C for 24 h in a shaking incubator. Then, liposome complex were separated from free **7-Gal** by G-25 column. After 30 mL elution, UV absorption at 260 nm and UV spectra of the ultraviolet region (230 – 400 nm) were measured for each fraction by Tecan Infinite M200 reader. Further incubation was performed on **liposome-7-Gal** complex fraction (tube 4). After separation, UV absorption at 260 nm was measured for each fraction. **Method II.** Liposomes were prepared (size 200 nm, final concentration of 5 mg/mL in PBS) with **7-Gal**/PBS solution (final concentration of 1×10^{-2} M in PBS) to a final volume of 1 mL. Then, liposome complex were separated from free **7-Gal** by G-25 column immediately. UV absorption at 260 nm and UV spectra of the ultraviolet region (230 – 400 nm) was measured for each fraction by Tecan Infinite M200 reader. The liposome complex fraction (tube 4) was incubated at 37°C in a shaking incubator. After 24 h, the mixture was encounter to another separation. UV absorption at 260 nm was measured for each fraction.

Test on 35-Glc: Method I. Prepared POPC liposomes (size 200 nm, final concentration of 5 mg/mL in PBS) were incubated with **35-Glc** (final concentration of 1×10^{-2} M in PBS) in a final volume of 500 μ L at 37°C for 24 h in a shaking incubator. Then, liposome complex were separated from free **35-Glc** by G-25 column. After 30 mL elution, UV absorption at 253 nm, 300 nm and UV spectra of 230 – 450 nm regions were measured for each fraction by Tecan Infinite M200 reader. Further incubation was performed on complex fraction (tube 3). After separation, UV absorption at 253 nm, 300 nm and UV spectra of 230 – 450 nm regions were measured for each fraction. **Method II.** Liposomes were prepared (size 200 nm, final concentration of 5 mg/mL in PBS) with **35-Glc**/PBS solution (final concentration of 1×10^{-2} M in PBS) to a final volume of 1 mL. Then, liposome complex were separated from free **35-Glc** by G-25 column immediately. UV absorption at 253 nm, 300nm and UV spectra of the ultraviolet region (230 – 400 nm) was measured for each fraction by Tecan Infinite M200 reader. The liposome complex fraction (tube 3) was incubated at 37°C in a shaking incubator. After 24 h, the mixture was encounter to another separation. UV absorption at 253, 300 nm was measured for each fraction.

V.9 Docking studies

The *O*-GlcNAc transferase (OGT) crystal structure (PDB: 4GZ5) was protonated by Molprobit²⁵², and chain B was extracted after the removal of water, ions, and substrate to serve as the model macromolecule in the docking study. All four OGT inhibitors were built with the ribose and GlcNAc (Glc) ring conformations identical to those of the natural substrate in the crystal structure.²⁵³ The macromolecule and four inhibitors were then processed by AutoDockTools to remove non-polar hydrogens.²⁵⁴ A grid box centered on the position of the natural substrate was constructed using 24 \times 24 \times 24 points and a spacing of 1 Å. Subsequently, each inhibitor was docked into OGT by AutoDock Vina,²⁵⁵ which automatically calculates the grid maps and clusters the results, with the value of the exhaustiveness parameter being 32.

Bibliography

Bibliography

1. Bertozzi, C. R. and Kiessling, L. L. "Chemical glycobiology" *Science*, **2001**, *291*, 2357-2364.
2. Dwek, R. A. "Glycobiology: Toward understanding the function of sugars" *Chem. Rev.*, **1996**, *96*, 683-720.
3. Varki, A. "Biological roles of oligosaccharides - all of the theories are correct" *Glycobiology*, **1993**, *3*, 97-130.
4. Bernardi, A.; Jimenez-Barbero, J.; Casnati, A.; De, C. C.; Darbre, T.; Fieschi, F.; Finne, J.; Funken, H.; Jaeger, K.-E.; Lahmann, M.; Lindhorst, T. K.; Marradi, M.; Messner, P.; Molinaro, A.; Murphy, P. V.; Nativi, C.; Oscarson, S.; Penades, S.; Peri, F.; Pieters, R. J.; Renaudet, O.; Reymond, J.-L.; Richichi, B.; Rojo, J.; Sansone, F.; Schaffer, C.; Turnbull, W. B.; Velasco-Torrijos, T.; Vidal, S.; Vincent, S.; Wennekes, T.; Zuilhof, H. and Imberty, A. "Multivalent glycoconjugates as anti-pathogenic agents" *Chem. Soc. Rev.*, **2013**, *42*, 4709-4727.
5. Galili, U. "The alpha-gal epitope and the anti-Gal antibody in xenotransplantation and in cancer immunotherapy" *Immunol. Cell Biol.*, **2005**, *83*, 674-686.
6. Werz, D. B.; Ranzinger, R.; Herget, S.; Adibekian, A.; von der Lieth, C.-W. and Seeberger, P. H. "Exploring the structural diversity of mammalian carbohydrates ("Glycospace") by statistical databank analysis" *ACS Chem. Biol.*, **2007**, *2*, 685-691.
7. Laine, R. A. "A calculation of all possible oligosaccharide isomers both branched and linear yields 1.05×10^{12} structures for a reducing hexasaccharide - the isomer-barrier to development of single-method saccharide sequencing or synthesis systems" *Glycobiology*, **1994**, *4*, 759-767.
8. Hart, G. W. and Copeland, R. J. "Glycomics hits the big time" *Cell*, **2010**, *143*, 672-676.
9. Coutinho, P. M.; Deleury, E.; Davies, G. J. and Henrissat, B. "An evolving hierarchical family classification for glycosyltransferases" *J. Mol. Biol.*, **2003**, *328*, 307-317.
10. Unligil, U. M. and Rini, J. M. "Glycosyltransferase structure and mechanism" *Curr. Opin. Struct. Biol.*, **2000**, *10*, 510-517.
11. Lairson, L. L.; Henrissat, B.; Davies, G. J. and Withers, S. G. "Glycosyltransferases: structures, functions, and mechanisms" *Annu. Rev. Biochem.*, **2008**, *77*, 521-555.
12. Campbell, J. A.; Davies, G. J.; Bulone, V. and Henrissat, B. "A classification of nucleotide-diphospho-sugar glycosyltransferases based on amino acid sequence similarities" *Biochem. J.*, **1997**, *326*, 929-939.
13. Cantarel, B. L.; Coutinho, P. M.; Rancurel, C.; Bernard, T.; Lombard, V. and Henrissat, B. "The Carbohydrate-Active EnZymes database (CAZy): an expert resource for Glycogenomics" *Nucleic Acids Res.*, **2009**, *37*, D233-D238.
14. Charnock, S. J. and Davies, G. J. "Structure of the nucleotide-diphospho-sugar transferase, SpsA from *Bacillus subtilis*, in native and nucleotide-complexed forms" *Biochemistry*, **1999**, *38*, 6380-6385.
15. Vrielink, A.; Ruger, W.; Driessen, H. P. C. and Freemont, P. S. "Crystal-structure of the dna modifying enzyme beta-glucosyltransferase in the presence and absence of the substrate uridine diphosphoglucose" *EMBO J.*, **1994**, *13*, 3413-3422.
16. Igura, M.; Maita, N.; Kamishikiryo, J.; Yamada, M.; Obita, T.; Maenaka, K. and Kohda, D. "Structure-guided identification of a new catalytic motif of oligosaccharyltransferase" *EMBO J.*, **2008**, *27*, 234-243.
17. Roychoudhury, R. and Pohl, N. L. B. "New structures, chemical functions, and inhibitors for glycosyltransferases" *Curr. Opin. Chem. Biol.*, **2010**, *14*, 168-173.
18. Breton, C.; Fournel-Gigleux, S. and Palcic, M. M. "Recent structures, evolution and mechanisms of glycosyltransferases" *Curr. Opin. Struct. Biol.*, **2012**, *22*, 540-549.
19. Chan, P. H. W.; Weissbach, S.; Okon, M.; Withers, S. G. and McIntosh, L. P. "Nuclear magnetic resonance spectral assignments of alpha-1,4-galactosyltransferase IgtC from *Neisseria meningitidis*: Substrate binding and multiple conformational states" *Biochemistry*, **2012**, *51*, 8278-8292.
20. Errey, J. C.; Lee, S. S.; Gibson, R. P.; Martinez, F. C.; Barry, C. S.; Jung, P. M. J.; O'Sullivan, A. C.; Davis, B. G. and Davies, G. J. "Mechanistic insight into enzymatic glycosyl transfer with retention of configuration through analysis of glycomimetic inhibitors" *Angew. Chem., Int. Ed.*, **2010**, *49*, 1234-1237.
21. Baisch, G.; Ohrlein, R. and Ernst, B. "Enzymatic galactosylation of non-natural glucosamide-acceptors" *Bioorg. Med. Chem. Lett.*, **1996**, *6*, 749-754.
22. Koeller, K. M. and Wong, C. H. "Synthesis of complex carbohydrates and glycoconjugates: Enzyme-based and programmable one-pot strategies" *Chem. Rev.*, **2000**, *100*, 4465-4493.

23. Erwin, A. L.; Allen, S.; Ho, D. K.; Bonthius, P. J.; Jarisch, J.; Nelson, K. L.; Tsao, D. L.; Unrath, W. C. T.; Watson, M. E., Jr.; Gibson, B. W.; Apicella, M. A. and Smith, A. L. "Role of IgtC in resistance of nontypeable *Haemophilus influenzae* strain R2866 to human serum" *Infect. Immun.*, **2006**, *74*, 6226-6235.
24. Tzeng, Y. L. and Stephens, D. S. "Epidemiology and pathogenesis of *Neisseria meningitidis*" *Microb. Infect.*, **2000**, *2*, 687-700.
25. Gotschlich, E. C. "Genetic locus for the biosynthesis of the variable portion of *Neisseria gonorrhoeae* lipooligosaccharide." *J. Exp. Med.*, **1994**, *180*, 2181-2190.
26. Letts, J. A.; Rose, N. L.; Fang, Y. R.; Barry, C. H.; Borisova, S. N.; Seto, N. O. L.; Palcic, M. M. and Evans, S. V. "Differential recognition of the type I and IIIH antigen acceptors by the human ABO(H) blood group A and B glycosyltransferases" *J. Biol. Chem.*, **2006**, *281*, 3625-3632.
27. Seto, N. O. L.; Palcic, M. M.; Compston, C. A.; Li, H.; Bundle, D. R. and Narang, S. A. "Sequential interchange of four amino acids from blood group B to blood group A glycosyltransferase boosts catalytic activity and progressively modifies substrate recognition in human recombinant enzymes" *J. Biol. Chem.*, **1997**, *272*, 14133-14138.
28. Jorgensen, R.; Grimm, L. L.; Sindhuwinata, N.; Peters, T. and Palcic, M. M. "A glycosyltransferase inhibitor from a molecular fragment library simultaneously interferes with metal ion and substrate binding" *Angew. Chem., Int. Ed.*, **2012**, *51*, 4171-4175.
29. Hart, G. W.; Slawson, C.; Ramirez-Correa, G. and Lagerlof, O. "Cross talk between *O*-GlcNAcylation and phosphorylation: roles in signaling, transcription, and chronic disease" *Annu. Rev. Biochem.*, **2011**, *80*, 825-858.
30. Wang, Z.; Gucek, M. and Hart, G. W. "Cross-talk between GlcNAcylation and phosphorylation: site-specific phosphorylation dynamics in response to globally elevated *O*-GlcNAc" *Proc. Natl. Acad. Sci. U.S.A.*, **2008**, *105*, 13793-13798.
31. Comer, F. I. and Hart, G. W. "*O*-glycosylation of nuclear and cytosolic proteins: dynamic interplay between *O*-GlcNAc and *O*-phosphate" *J. Biol. Chem.*, **2000**, *275*, 29179-29182.
32. Wells, L.; Vosseller, K. and Hart, G. W. "Glycosylation of nucleocytoplasmic proteins: Signal transduction and *O*-GlcNAc" *Science*, **2001**, *291*, 2376-2378.
33. Lazarus, M. B.; Nam, Y.-S.; Jiang, J.-Y.; Sliz, P. and Walker, S. "Structure of human *O*-GlcNAc transferase and its complex with a peptide substrate" *Nature*, **2011**, *469*, 564-567.
34. Lynch, T. P.; Ferrer, C. M.; Jackson, S. R.; Shahriari, K. S.; Vosseller, K. and Reginato, M. J. "Critical role of *O*-linked beta-*N*-acetylglucosamine transferase in prostate cancer invasion, angiogenesis and metastasis" *J. Biol. Chem.*, **2012**, *287*, 11070-11081.
35. Slawson, C. and Hart, G. W. "*O*-GlcNAc signalling: implications for cancer cell biology" *Nat. Rev. Cancer*, **2011**, *11*, 678-684.
36. Yuzwa, S. A.; Shan, X.; Macauley, M. S.; Clark, T.; Skorobogatko, Y.; Vosseller, K. and Vocadlo, D. J. "Increasing *O*-GlcNAc slows neurodegeneration and stabilizes tau against aggregation" *Nat. Chem. Biol.*, **2012**, *8*, 393-399.
37. Dias, W. B. and Hart, G. W. "*O*-GlcNAc modification in diabetes and Alzheimer's disease" *Mol. BioSyst.*, **2007**, *3*, 766-772.
38. Lefebvre, T.; Guinez, C.; Dehennaut, V.; Beseme-Dekeyser, O.; Morelle, W. and Michalski, J.-C. "Does *O*-GlcNAc play a role in neurodegenerative diseases?" *Exp. Rev. Proteomics*, **2005**, *2*, 265-275.
39. Zachara, N. E. and Hart, G. W. "The emerging significance of *O*-GlcNAc in cellular regulation" *Chem. Rev.*, **2002**, *102*, 431-438.
40. Majumdar, G.; Wright, J.; Markowitz, P.; Martinez-Hernandez, A.; Raghov, R. and Solomon, S. S. "Insulin stimulates and diabetes inhibits *O*-linked *N*-acetylglucosamine transferase and *O*-glycosylation of Sp1" *Diabetes*, **2004**, *53*, 3184-3192.
41. Robertson, J. G. "Mechanistic basis of enzyme-targeted drugs" *Biochemistry*, **2005**, *44*, 5561-5571.
42. Wagner, G. K. and Pesnot, T. "Glycosyltransferases and their assays" *ChemBioChem*, **2010**, *11*, 1939-1949.
43. Breton, C.; Snajdrova, L.; Jeanneau, C.; Koca, J. and Imberty, A. "Structures and mechanisms of glycosyltransferases" *Glycobiology*, **2006**, *16*, 29R-37R.
44. Gloster, T. M. and Vocadlo, D. J. "Developing inhibitors of glycan processing enzymes as tools for enabling glycobiology" *Nat. Chem. Biol.*, **2012**, *8*, 683-694.
45. Gloster, T. M. and Vocadlo, D. J. "Mechanism, structure, and inhibition of *O*-GlcNAc processing enzymes" *Curr. Signal Transduction Ther.*, **2010**, *5*, 74-91.
46. Jung, K.-H. and Schmidt, R. R. "Glycosyltransferase inhibitors" In *Carbohydrate-Based Drug Discovery*, Wong, C. H. Ed.; Wiley-VCH Verlag GmbH & Co. KGaA: Weinheim, **2003**, Chap. 23, pp. 609-659.

47. Qian, X. and Palcic, M. M. "Glycosyltransferase inhibitors" In *Carbohydrates in Chemistry and Biology*, Ernst, B.; Hart, G. W. and Sinay, P. Eds.; Wiley-VCH Verlag GmbH: Weinheim, **2000**, Chap. 56, pp. 293-312.
48. Kajimoto, T. and Node, M. "Synthesis of glycosyltransferase inhibitors" *Synthesis*, **2009**, 3179-3210.
49. Izumi, M.; Yuasa, H. and Hashimoto, H. "Bisubstrate analogues as glycosyltransferase inhibitors" *Curr. Top. Med. Chem.*, **2009**, *9*, 87-105.
50. Zou, W. "C-glycosides and Aza-C-glycosides as potential glycosidase and glycosyltransferase inhibitors" *Curr. Top. Med. Chem.*, **2005**, *5*, 1363-1391.
51. Compain, P. and Martin, O. R. "Carbohydrate mimetics-based glycosyltransferase inhibitors" *Bioorg. Med. Chem.*, **2001**, *9*, 3077-3092.
52. Whalen, L. J.; Greenberg, W. A.; Mitchell, M. L. and Wong, C.-H. "Iminosugar-based glycosyltransferase inhibitors" In *Synthesis to Therapeutic Applications*, Compain, P. and Martin, O. Eds.; John Wiley & Sons Ltd.: Chichester, **2007**, Chap. 7, pp. 153-176.
53. Cipolla, L.; La, F. B. and Gregori, M. "Combinatorial approaches to iminosugars as glycosidase and glycosyltransferase inhibitors" *Comb. Chem. High Throughput Screening*, **2006**, *9*, 571-582.
54. Compain, P. and Martin, O. R. "Design, synthesis and biological evaluation of iminosugar-based glycosyltransferase inhibitors" *Curr. Top. Med. Chem.*, **2003**, *3*, 541-560.
55. Vaghefi, M. M.; Bernacki, R. J.; Dalley, N. K.; Wilson, B. E. and Robins, R. K. "Synthesis of glycopyranosylphosphonate analogs of certain natural nucleoside diphosphate sugars as potential inhibitors of glycosyltransferases" *J. Med. Chem.*, **1987**, *30*, 1383-1391.
56. Vaghefi, M. M.; Bernacki, R. J.; Hennen, W. J. and Robins, R. K. "Synthesis of certain nucleoside methylenediphosphonate sugars as potential inhibitors of glycosyltransferases" *J. Med. Chem.*, **1987**, *30*, 1391-1399.
57. Saotome, C.; Kanie, Y.; Kanie, O. and Wong, C. H. "Synthesis and enzymatic evaluation of five-membered iminocyclitols and a pseudodisaccharide" *Bioorg. Med. Chem.*, **2000**, *8*, 2249-2261.
58. Takayama, S.; Chung, S. J.; Igarashi, Y.; Ichikawa, Y.; Sepp, A.; Lechler, R. I.; Wu, J.; Hayashi, T.; Siuzdak, G. and Wong, C.-H. "Selective inhibition of β -1,4- and α -1,3-galactosyltransferases: donor sugar-nucleotide based approach" *Bioorg. Med. Chem.*, **1999**, *7*, 401-409.
59. Yuasa, H.; Palcic, M. M. and Hindsgaul, O. "Synthesis of the carbocyclic analog of uridine 5'-(α -D-galactopyranosyl diphosphate) (UDP-Gal) as an inhibitor of beta(1->4)-galactosyltransferase" *Can. J. Chem.*, **1995**, *73*, 2190-2195.
60. Endo, T.; Kajihara, Y.; Kodama, H. and Hashimoto, H. "Novel aspects of interaction between UDP-Gal and GlcNAc β -1,4-galactosyltransferase: transferability and remarkable inhibitory activity of UDP-(mono-*O*-methylated Gal), UDP-Fuc and UDP-Man" *Bioorg. Med. Chem.*, **1996**, *4*, 1939-1948.
61. Caravano, A.; Dohi, H.; Sinay, P. and Vincent, S. P. "A new methodology for the synthesis of fluorinated exo-glycals and their time-dependent inhibition of UDP-galactopyranose mutase" *Chem. Eur. J.*, **2006**, *12*, 3114-3123.
62. Grizot, S.; Salem, M.; Vongsouthi, V.; Durand, L.; Moreau, F.; Dohi, H.; Vincent, S.; Escaich, S. and Ducruix, A. "Structure of the *Escherichia coli* heptosyltransferase WaaC: Binary complexes with ADP and ADP-2-deoxy-2-fluoro heptose" *J. Mol. Biol.*, **2006**, *363*, 383-394.
63. Eppe, G.; Peltier, P.; Daniellou, R.; Nugier-Chauvin, C.; Ferrieres, V. and Vincent, S. P. "Probing UDP-galactopyranose mutase binding pocket: A dramatic effect on substitution of the 6-position of UDP-galactofuranose" *Bioorg. Med. Chem. Lett.*, **2009**, *19*, 814-816.
64. Dohi, H.; Perion, R.; Durka, M.; Bosco, M.; Roue, Y.; Moreau, F.; Grizot, S.; Ducruix, A.; Escaich, S. and Vincent, S. P. "Stereoselective glycal fluorophosphorylation: Synthesis of ADP-2-fluoroheptose, an inhibitor of the LPS biosynthesis" *Chem. Eur. J.*, **2008**, *14*, 9530-9539.
65. Hayashi, T.; Murray, B. W.; Wang, R. and Wong, C.-H. "A chemoenzymic synthesis of UDP-(2-deoxy-2-fluoro)galactose and evaluation of its interaction with galactosyltransferase" *Bioorg. Med. Chem.*, **1997**, *5*, 497-500.
66. Takayama, S.; Martin, R.; Wu, J.; Laslo, K.; Siuzdak, G. and Wong, C.-H. "Chemoenzymic preparation of novel cyclic imine sugars and rapid biological activity evaluation using electrospray mass spectrometry and kinetic Analysis" *J. Am. Chem. Soc.*, **1997**, *119*, 8146-8151.
67. Schengrund, C. L. and Kovac, P. "UDP-6-deoxy-6-fluoro- α -D-galactose binds to two different galactosyltransferases, but neither can effectively catalyze transfer of the modified galactose to the appropriate acceptor" *Carbohydr. Res.*, **1999**, *319*, 24-28.
68. Takaya, K.; Nagahori, N.; Kurogochi, M.; Furuike, T.; Miura, N.; Monde, K.; Lee, Y. C. and Nishimura, S.-I. "Rational design, synthesis and characterization of novel inhibitors for human β 1,4-galactosyltransferase" *J. Med. Chem.*, **2005**, *48*, 6054-6065.

69. Saotome, C.; Wong, C. H. and Kanie, O. "Combinatorial library of five-membered iminocyclitol and the inhibitory activities against glyco-enzymes" *Chem. Biol.*, **2001**, *8*, 1061-1070.
70. Kim, Y. J.; Ichikawa, M. and Ichikawa, Y. "A rationally designed inhibitor of α -1,3-galactosyltransferase" *J. Am. Chem. Soc.*, **1999**, *121*, 5829-5830.
71. Zhang, Y.; Ren, S.; Sun, D. and Tao, J. "Synthesis and evaluation of the analogues for galactosyl donors as inhibitors of β -1,4-galactosyltransferase" *Synth. Commun.*, **2010**, *40*, 328-336.
72. Schaefer, A. and Thiem, J. "Synthesis of novel donor mimetics of UDP-Gal, UDP-GlcNAc, and UDP-GalNAc as potential transferase inhibitors" *J. Org. Chem.*, **2000**, *65*, 24-29.
73. Vidal, S.; Bruyere, I.; Malleron, A.; Auge, C. and Praly, J.-P. "Non-isosteric C-glycosyl analogues of natural nucleotide diphosphate sugars as glycosyltransferase inhibitors" *Bioorg. Med. Chem.*, **2006**, *14*, 7293-7301.
74. Kolb, V.; Amann, F.; Schmidt, R. R. and Duszenko, M. "Specific inhibition of an alpha-galactosyltransferase from *Trypanosoma brucei* by synthetic substrate analogues" *Glycoconj. J.*, **1999**, *16*, 537-544.
75. Wang, R.; Steensma, D. H.; Takaoka, Y.; Yun, J. W.; Kajimoto, T. and Wong, C.-H. "A search for pyrophosphate mimics for the development of substrates and inhibitors of glycosyltransferases" *Bioorg. Med. Chem.*, **1997**, *5*, 661-672.
76. Yeoh, K. K.; Butters, T. D.; Wilkinson, B. L. and Fairbanks, A. J. "Probing replacement of pyrophosphate via click chemistry; synthesis of UDP-sugar analogues as potential glycosyl transferase inhibitors" *Carbohydr. Res.*, **2009**, *344*, 586-591.
77. Vembaiyan, K.; Pearcey, J. A.; Bhasin, M.; Lowary, T. L. and Zou, W. "Synthesis of sugar-amino acid-nucleosides as potential glycosyltransferase inhibitors" *Bioorg. Med. Chem.*, **2011**, *19*, 58-66.
78. Trunkfield, A. E.; Gurcha, S. S.; Besra, G. S. and Bugg, T. D. H. "Inhibition of *Escherichia coli* glycosyltransferase MurG and Mycobacterium tuberculosis Gal transferase by uridine-linked transition state mimics" *Bioorg. Med. Chem.*, **2010**, *18*, 2651-2663.
79. Gastinel, L. N.; Cambillau, C. and Bourne, Y. "Crystal structures of the bovine β 4galactosyltransferase catalytic domain and its complex with uridine diphosphogalactose" *EMBO J.*, **1999**, *18*, 3546-3557.
80. Alfaro, J. A.; Zheng, R. B.; Persson, M.; Letts, J. A.; Polakowski, R.; Bai, Y.; Borisova, S. N.; Seto, N. O. L.; Lowary, T. L.; Palcic, M. M. and Evans, S. V. "ABO(H) blood group A and B glycosyltransferases recognize substrate via specific conformational changes" *J. Biol. Chem.*, **2008**, *283*, 10097-10108.
81. Pesnot, T.; Jorgensen, R.; Palcic, M. M. and Wagner, G. K. "Structural and mechanistic basis for a new mode of glycosyltransferase inhibition" *Nat. Chem. Biol.*, **2010**, *6*, 321-323.
82. Descroix, K. and Wagner, G. K. "The first C-glycosidic analog of a novel galactosyltransferase inhibitor" *Org. Biomol. Chem.*, **2011**, *9*, 1855-1863.
83. Evitt, A.; Tedaldi, L. M. and Wagner, G. K. "One-step synthesis of novel glycosyltransferase inhibitors" *Chem. Commun.*, **2012**, *48*, 11856-11858.
84. Wandzik, I.; Bieg, T. and Czaplicka, M. "Synthesis of 2-deoxy-hexopyranosyl derivatives of uridine as donor substrate analogs for glycosyltransferases" *Bioorg. Chem.*, **2009**, *37*, 211-216.
85. Ballell, L.; Young, R. J. and Field, R. A. "Synthesis and evaluation of mimetics of UDP and UDP- α -D-galactose, dTDP and dTDP- α -D-glucose with monosaccharides replacing the key pyrophosphate unit" *Org. Biomol. Chem.*, **2005**, *3*, 1109-1115.
86. Chabre, Y. M. and Roy, R. "Design and creativity in synthesis of multivalent neoglycoconjugates" *Adv. Carbohydr. Chem. Biochem.*, **2010**, *63*, 165-393.
87. Hatanaka, K.; Takeshige, H.; Kanno, K.-I.; Maruyama, A.; Oishi, J.; Kajihara, Y. and Hashimoto, H. "New polymeric inhibitor of galactosyl transferase" *J. Carbohydr. Chem.*, **1997**, *16*, 667-672.
88. Schaefer, K.; Albers, J.; Sindhuwinata, N.; Peters, T. and Meyer, B. "A new concept for glycosyltransferase inhibitors: nonionic mimics of the nucleotide donor of the human blood group B galactosyltransferase" *ChemBioChem*, **2012**, *13*, 443-450.
89. Schaefer, K.; Sindhuwinata, N.; Hackl, T.; Koetzler, M. P.; Niemeyer, F. C.; Palcic, M. M.; Peters, T. and Meyer, B. "A nonionic inhibitor with high specificity for the UDP-Gal donor binding site of human blood group B galactosyltransferase: Design, synthesis, and characterization" *J. Med. Chem.*, **2013**, *56*, 2150-2154.
90. Hindsgaul, O.; Kaur, K. J.; Srivastava, G.; Blaszczykthurin, M.; Crawley, S. C.; Heerze, L. D. and Palcic, M. M. "Evaluation of deoxygenated oligosaccharide acceptor analogs as specific inhibitors of glycosyltransferases" *J. Biol. Chem.*, **1991**, *266*, 17858-17862.

91. Lowary, T. L. and Hindsgaul, O. "Recognition of synthetic deoxy and deoxyfluoro analogs of the acceptor α -L-Fucp-(1 \rightarrow 2)- β -D-Galp-OR by the blood-group A and B gene-specified glycosyltransferases" *Carbohydr. Res.*, **1993**, 249, 163-195.
92. Persson, K.; Ly, H. D.; Dieckelmann, M.; Wakarchuk, W. W.; Withers, S. G. and Strynadka, N. C. J. "Crystal structure of the retaining galactosyltransferase LgtC from *Neisseria meningitidis* in complex with donor and acceptor sugar analogs" *Nat. Struct. Biol.*, **2001**, 8, 166-175.
93. Helland, A.-C.; Hindsgaul, O.; Palcic, M. M.; Stults, C. L. M. and Macher, B. A. "Methyl 3-amino-3-deoxy- β -D-galactopyranosyl-(1 \rightarrow 4)-2-acetamido-2-deoxy- β -D-glucopyranoside: an inhibitor of UDP-D-galactose: β -D-galactopyranosyl-(1 \rightarrow 4)-2-acetamido-2-deoxy-D-glucose (1 \rightarrow 3)- α -D-galactopyranosyltransferase" *Carbohydr. Res.*, **1995**, 276, 91-98.
94. Brown, J. R.; Yang, F.; Sinha, A.; Ramakrishnan, B.; Tor, Y.; Qasba, P. K. and Esko, J. D. "Deoxygenated disaccharide analogs as specific inhibitors of β 1-4-galactosyltransferase 1 and selectin-mediated tumor metastasis" *J. Biol. Chem.*, **2009**, 284, 4952-4959.
95. Chung, S. J.; Takayama, S. and Wong, C.-H. "Acceptor substrate-based selective inhibition of galactosyltransferases" *Bioorg. Med. Chem. Lett.*, **1998**, 8, 3359-3364.
96. Hashimoto, H.; Endo, T. and Kajihara, Y. "Synthesis of the first tricomponent bisubstrate analog that exhibits potent inhibition against GlcNAc: β -1,4-galactosyltransferase" *J. Org. Chem.*, **1997**, 62, 1914-1915.
97. Waldscheck, B.; Streiff, M.; Notz, W.; Kinzy, W. and Schmidt, R. R. " α (1-3)-Galactosyltransferase inhibition based on a new type of disubstrate analogue" *Angew. Chem., Int. Ed.*, **2001**, 40, 4007-4011.
98. Gao, Y.; Lazar, C.; Szarek, W. A. and Brockhausen, I. "Specificity of β 1,4-galactosyltransferase inhibition by 2-naphthyl 2-butanamido-2-deoxy-1-thio- β -D-glucopyranoside" *Glycoconj. J.*, **2010**, 27, 673-684.
99. Hanover, J. A.; Krause, M. W. and Love, D. C. "The hexosamine signaling pathway: O-GlcNAc cycling in feast or famine" *Biochim. Biophys. Acta: Gen. Subj.*, **2010**, 1800, 80-95.
100. Banerjee, P. S.; Hart, G. W. and Cho, J. W. "Chemical approaches to study O-GlcNAcylation" *Chem. Soc. Rev.*, **2013**,
101. Gross, B. J.; Kraybill, B. C. and Walker, S. "Discovery of O-GlcNAc transferase inhibitors" *J. Am. Chem. Soc.*, **2005**, 127, 14588-14589.
102. D'Alessandris, C.; Andreozzi, F.; Federici, M.; Cardellini, M.; Brunetti, A.; Ranalli, M.; Del, G. S.; Lauro, D.; Del, P. S.; Marchetti, P.; Lauro, R. and Sesti, G. "Increased O-glycosylation of insulin signaling proteins results in their impaired activation and enhanced susceptibility to apoptosis in pancreatic beta-cells" *FASEB J.*, **2004**, 18, 959-961.
103. Konrad, R. J.; Zhang, F.; Hale, J. E.; Knierman, M. D.; Becker, G. W. and Kudlow, J. E. "Alloxan is an inhibitor of the enzyme O-linked N-acetylglucosamine transferase" *Biochem. Biophys. Res. Commun.*, **2002**, 293, 207-212.
104. Dorfmueller, H. C.; Borodkin, V. S.; Blair, D. E.; Pathak, S.; Navratilova, I. and Aalten, D. M. F. "Substrate and product analogues as human O-GlcNAc transferase inhibitors" *Amino Acids*, **2011**, 40, 781-792.
105. Hajduch, J.; Nam, G.; Kim, E. J.; Froehlich, R.; Hanover, J. A. and Kirk, K. L. "A convenient synthesis of the C-1-phosphonate analog of UDP-GlcNAc and its evaluation as an inhibitor of O-linked GlcNAc transferase (OGT)" *Carbohydr. Res.*, **2008**, 343, 189-195.
106. Jiang, J.; Lazarus, M. B.; Pasquina, L.; Sliz, P. and Walker, S. "A neutral diphosphate mimic crosslinks the active site of human O-GlcNAc transferase" *Nat. Chem. Biol.*, **2012**, 8, 72-77.
107. Gross, B. J.; Swoboda, J. G. and Walker, S. "A strategy to discover inhibitors of O-linked glycosylation" *J. Am. Chem. Soc.*, **2008**, 130, 440-441.
108. Varki, A.; Cummings, R. D.; Esko, J. D.; Freeze, H. H.; Stanley, P.; Bertozzi, C. R.; Hart, G. W. and Etzler, M. E. "Essentials of glycobiology; Second Edition"; Cold Spring Harbor Laboratory Press: New York, **2009**, pp. 1-784.
109. Lee, J.-H.; Jeong, A. R.; Jung, J.-H.; Park, C.-M. and Hong, J.-I. "A highly selective and sensitive fluorescence sensing system for distinction between diphosphate and nucleoside triphosphates" *J. Org. Chem.*, **2011**, 76, 417-423.
110. Tanaka, H.; Yoshimura, Y.; Jorgensen, M. R.; Cuesta-Seijo, J. A. and Hindsgaul, O. "A simple synthesis of sugar nucleoside diphosphates by chemical coupling in water" *Angew. Chem., Int. Ed.*, **2012**, 51, 11531-11534.
111. Arlt, M. and Hindsgaul, O. "Rapid chemical synthesis of sugar nucleotides in a form suitable for enzymic oligosaccharide synthesis" *J. Org. Chem.*, **1995**, 60, 14-15.

112. Huang, M.; Garrett, G. E.; Birlirakis, N.; Bohe, L.; Pratt, D. A. and Crich, D. "Dissecting the mechanisms of a class of chemical glycosylation using primary C-13 kinetic isotope effects" *Nat. Chem.*, **2012**, *4*, 663-667.
113. Galonic, D. P. and Gin, D. Y. "Chemical glycosylation in the synthesis of glycoconjugate antitumor vaccines" *Nature*, **2007**, *446*, 1000-1007.
114. Demchenko, A. V. "Stereoselective chemical 1,2-cis *O*-glycosylation: from "sugar ray" to modern techniques of the 21st century" *Synlett*, **2003**, 1225-1240.
115. Juaristi, E. and Cuevas, G. "Recent studies of the anomeric effect" *Tetrahedron*, **1992**, *48*, 5019-5087.
116. Ferrieres, V.; Bertho, J.-N. and Plusquellec, D. "A new synthesis of *O*-glycosides from totally *O*-unprotected glycosyl donors" *Tetrahedron Lett.*, **1995**, *36*, 2749-2752.
117. Hanessian, S. and Banoub, J. "Preparative and exploratory carbohydrate chemistry. Chemistry of the glycosidic linkage. *O*-Glycosylations catalyzed by stannic chloride, in the D-ribofuranose and D-glucopyranose series" *Carbohydr. Res.*, **1977**, *59*, 261-267.
118. Magnusson, G.; Noori, G.; Dahmen, J.; Frejd, T. and Lave, T. "Boron trifluoride-etherate induced formation of 2,2,2-trichloroethyl glycopyranosides. Selective visualization of carbohydrate derivatives on TLC plates" *Acta Chem. Scand., Ser. B*, **1981**, *B35*, 213-216.
119. Mukaiyama, T.; Takashima, T.; Katsurada, M. and Aizawa, H. "A highly stereoselective synthesis of α -glucosides from 1-*O*-acetyl glucose by use of tin(IV) chloride-silver perchlorate catalyst system" *Chem. Lett.*, **1991**, 533-536.
120. Cecioni, S.; Goyard, D.; Praly, J.-P. and Vidal, S. "Synthesis of azido-functionalized carbohydrates for the design of glycoconjugates" *Meth. Mol. Biol.*, **2012**, *808*, 57-68.
121. Xue, J. L.; Cecioni, S.; He, L.; Vidal, S. and Praly, J.-P. "Variations on the SnCl₄ and CF₃CO₂Ag-promoted glycosidation of sugar acetates: a direct, versatile and apparently simple method with either alpha or beta stereocontrol" *Carbohydr. Res.*, **2009**, *344*, 1646-1653.
122. Koenigs, W. and Knorr, E. "Ueber einige derivate des traubenzuckers und der galactose" *Ber. Dtsch. Chem. Ges.*, **1901**, *34*, 957-981.
123. Igarashi, K. "The Koenigs-Knorr reaction" *Adv. Carbohydr. Chem. Biochem.*, **1977**, *34*, 243-283.
124. Helferich, B. and Wedemeyer, K. F. "Preparation of glucosides from acetobromoglucose" *Liebigs Ann. Chem.*, **1949**, *563*, 139-145.
125. Hanessian, S. and Banoub, J. "Chemistry of the glycosidic linkage. An efficient synthesis of 1,2-trans-disaccharides" *Carbohydr. Res.*, **1977**, *53*, C13-C16.
126. Lemieux, R. U.; Hendriks, K. B.; Stick, R. V. and James, K. "Halide ion catalyzed glycosidation reactions. Syntheses of α -linked disaccharides" *J. Am. Chem. Soc.*, **1975**, *97*, 4056-4062.
127. Schmidt, R. R. and Michel, J. "Facile synthesis of α - and β -*O*-glycosyl imidates; Preparation of glycosides and disaccharides" *Angew. Chem. Int. Ed.*, **1980**, *19*, 731-732.
128. Schmidt, R. R. and Grundler, G. " α -Linked disaccharides from *O*-(β -D-glycopyranosyl) trichloroacetimidates using trimethylsilyl trifluoromethanesulfonate as catalyst" *Angew. Chem. Int. Ed.*, **1982**, *21*, 781-782.
129. Yu, B. and Tao, H. "Glycosyl trifluoroacetimidates. Part 1: Preparation and application as new glycosyl donors" *Tetrahedron Lett.*, **2001**, *42*, 2405-2407.
130. Crich, D. and Smith, M. "1-Benzenesulfinyl piperidine/trifluoromethanesulfonic anhydride: A potent combination of shelf-stable reagents for the low-temperature conversion of thioglycosides to glycosyl triflates and for the formation of diverse glycosidic linkages" *J. Am. Chem. Soc.*, **2001**, *123*, 9015-9020.
131. Mereyala, H. B. and Reddy, G. V. "Stereoselective synthesis of α -linked saccharides by use of per-*O*-benzylated 2-pyridyl 1-thiohexopyranosides as glycosyl donors and methyl iodide as an activator" *Tetrahedron*, **1991**, *47*, 6435-6448.
132. Konradsson, P.; Mootoo, D. R.; McDevitt, R. E. and Fraser-Reid, B. "Iodonium ion generated in situ from *N*-iodosuccinimide and trifluoromethanesulfonic acid promotes direct linkage of disarmed pent-4-enyl glycosides" *Chem. Commun.*, **1990**, 270-272.
133. Kim, K. S. and Jeon, H. B. "Lactonization-mediated glycosylations and their application to oligosaccharide synthesis" *Chem. Rec.* **2008**, *8*, 46.
134. Halcomb, R. L. and Danishefsky, S. J. "On the direct epoxidation of glycals: application of a reiterative strategy for the synthesis of β -linked oligosaccharides" *J. Am. Chem. Soc.*, **1989**, *111*, 6661-6666.
135. Ogawa, T.; Beppu, K. and Nakabayashi, S. "Trimethylsilyl trifluoromethanesulfonate as an effective catalyst for glycoside synthesis" *Carbohydr. Res.*, **1981**, *93*, C6-C9.
136. Fraser-Reid, B.; Konradsson, P.; Mootoo, D. R. and Udodong, U. "Direct elaboration of pent-4-enyl glycosides into disaccharides" *Chem. Commun.*, **1988**, 823-825.

137. Ghose, A. K.; Viswanadhan, V. N. and Wendoloski, J. J. "A knowledge-based approach in designing combinatorial or medicinal chemistry libraries for drug discovery. 1. A qualitative and quantitative characterization of known drug databases" *J. Comb. Chem.*, **1999**, *1*, 55-68.
138. Montalbetti, C. A. G. N. and Falque, V. "Amide bond formation and peptide coupling" *Tetrahedron*, **2005**, *61*, 10827-10852.
139. Beckwith, A. L. J. "Synthesis of amides" Zabicky, J. Ed.; Interscience: Chichester, **1970**, Chap. 2, pp. 73-185.
140. Gololobov, Y. G.; Zhmurova, I. N. and Kasukhin, L. F. "Sixty years of Staudinger reaction" *Tetrahedron*, **1981**, *37*, 437-472.
141. Bosch, I.; Romea, P.; Urpi, F. and Vilarrasa, J. "Alternative procedures for the macrolactamization of ω -azido acids" *Tetrahedron Lett.*, **1993**, *34*, 4671-4674.
142. Bosch, I.; Gonzalez, A.; Urpi, F. and Vilarrasa, J. "On the reaction of acyl chlorides and carboxylic anhydrides with phosphazenes" *J. Org. Chem.*, **1996**, *61*, 5638-5643.
143. Ariza, X.; Urpi, F. and Vilarrasa, J. "A practical procedure for the preparation of carbamates from azides" *Tetrahedron Lett.*, **1999**, *40*, 7515-7517.
144. Bachi, M. D. and Vaya, J. "Phosphinimines as useful intermediates in the synthesis of 3-(acylamino)- β -lactams" *J. Org. Chem.*, **1979**, *44*, 4393-4396.
145. Soellner, M. B.; Nilsson, B. L. and Raines, R. T. "Staudinger ligation of α -azido acids retains stereochemistry" *J. Org. Chem.*, **2002**, *67*, 4993-4996.
146. Kleineweischede, R. and Hackenberger, C. P. R. "Chemoselective peptide cyclization by traceless Staudinger ligation" *Angew. Chem. Int. Ed.*, **2008**, *47*, 5984-5988.
147. Kurosawa, W.; Kan, T. and Fukuyama, T. "Stereocontrolled total synthesis of (-)-Ephedradine A (Orantine)" *J. Am. Chem. Soc.*, **2003**, *125*, 8112-8113.
148. Chapuis, H. and Strazewski, P. "Shorter puromycin analog synthesis by means of an efficient Staudinger-Vilarrasa coupling" *Tetrahedron*, **2006**, *62*, 12108-12115.
149. Charafeddine, A.; Dayoub, W.; Chapuis, H. and Strazewski, P. "First synthesis of 2'-deoxyfluoropuromycin analogues: experimental insight into the mechanism of the Staudinger reaction" *Chem. Eur. J.*, **2007**, *13*, 5566-5584.
150. Charafeddine, A.; Chapuis, H. and Strazewski, P. "Facile and rapid access to inosine puromycin analogues through the use of adenylate deaminase" *Org. Lett.*, **2007**, *9*, 2787-2790.
151. Chapuis, H.; Bui, L.; Bestel, I. and Barthelemy, P. "2'-Lipid-modified oligonucleotides via a Staudinger-Vilarrasa' reaction" *Tetrahedron Lett.*, **2008**, *49*, 6838-6840.
152. Kolb, H. C.; Finn, M. G. and Sharpless, K. B. "Click chemistry: diverse chemical function from a few good reactions" *Angew. Chem. Int. Ed.*, **2001**, *40*, 2004-2021.
153. Spiteri, C. and Moses, J. E. "Copper-catalyzed azide-alkyne cycloaddition: regioselective synthesis of 1,4,5-trisubstituted 1,2,3-triazoles" *Angew. Chem. Int. Ed.*, **2010**, *49*, 31-33.
154. Hoyle, C. E. and Bowman, C. N. "Thiol-ene Click chemistry" *Angew. Chem. Int. Ed.*, **2010**, *49*, 1540-1573.
155. Stoeckmann, H.; Neves, A. A.; Stairs, S.; Brindle, K. M. and Leeper, F. J. "Exploring isonitrile-based click chemistry for ligation with biomolecules" *Org. Biomol. Chem.*, **2011**, *9*, 7303-7305.
156. Himo, F.; Lovell, T.; Hilgraf, R.; Rostovtsev, V. V.; Noodleman, L.; Sharpless, K. B. and Fokin, V. V. "Copper(I)-catalyzed synthesis of azoles. DFT study predicts unprecedented reactivity and intermediates" *J. Am. Chem. Soc.*, **2005**, *127*, 210-216.
157. Rodionov, V. O.; Fokin, V. V. and Finn, M. G. "Mechanism of the ligand-free CuI-catalyzed azide-alkyne cycloaddition reaction" *Angew. Chem. Int. Ed.*, **2005**, *44*, 2210-2215.
158. Worrell, B. T.; Malik, J. A. and Fokin, V. V. "Direct evidence of a dinuclear copper intermediate in Cu(I)-catalyzed azide-alkyne cycloadditions" *Science*, **2013**, *340*, 457-460.
159. Weignerova, L.; Suzuki, Y.; Hunkova, Z.; Sedmera, P.; Havlicek, V.; Marek, R. and Kren, V. "Pyridoxine as a substrate for screening synthetic potential of glycosidases" *Collect. Czech. Chem. Commun.*, **1999**, *64*, 1325-1334.
160. Kurashima, K.; Fujii, M.; Ida, Y. and Akita, H. "Simple synthesis of β -D-glycopyranosides using β -glycosidase from almonds" *Chem. Pharm. Bull.*, **2004**, *52*, 270-275.
161. Tramice, A.; Giordano, A.; Andreotti, G.; Mollo, E. and Trincone, A. "High-yielding enzymatic α -glucosylation of pyridoxine by marine α -glucosidase from *Aplysia fasciata*" *Mar. Biotechnol.*, **2006**, *8*, 448-452.
162. Asano, Y. and Wada, K. "Regioselective glucosylation of pyridoxine by microorganisms" *Biosci., Biotechnol., Biochem.*, **2003**, *67*, 499-507.

163. Wada, K. and Asano, Y. "Use of borate to control the 5'-position-selective microbial glucosylation of pyridoxine" *Appl. Environ. Microbiol.*, **2003**, *69*, 7058-7062.
164. Schultz, M. and Zoerkler, G. "Synthesis of a metabolite of ciamexon conjugated with D-glucuronic acid" *Liebigs Ann. Chem.*, **1989**, 393-395.
165. Watts, A. G.; Kantner, T. and MacKenzie, A. B. "Vinylpyridines as functionalizing reagents for polypeptides" WO2010070300A2, **2010**, 50 pp.
166. Muller, C.; Diehl, V. and Lichtenthaler, F. W. "Building blocks from sugars. Part 23. Hydrophilic 3-pyridinols from fructose and isomaltulose" *Tetrahedron*, **1998**, *54*, 10703-10712.
167. Wang, S.; Lafont, D.; Rahkila, J.; Picod, B.; Leino, R. and Vidal, S. "Glycosylation of 'basic' alcohols: methyl 6-(hydroxymethyl)picolinate as a case study" *Carbohydr. Res.*, **2013**, *372C*, 35-46.
168. Xue, J. L.; Cecioni, S.; He, L.; Vidal, S. and Praly, J.-P. "Variations on the SnCl₄ and CF₃CO₂Ag-promoted glycosidation of sugar acetates: a direct, versatile and apparently simple method with either α or β stereocontrol" *Carbohydr. Res.*, **2009**, *344*, 1646-1653.
169. Helferich, B. and Zirner, J. "Synthesis of tetra-O-acetylhexoses with a free 2-hydroxyl group. Synthesis of disaccharides" *Chem. Ber.*, **1962**, *95*, 2604-2611.
170. Schmidt, R. R. and Michel, J. "Facile synthesis of α - and β -O-glycosyl imidates; Preparation of glycosides and disaccharides" *Angew. Chem., Int. Ed.*, **1980**, *19*, 731-732.
171. Milat, M. L.; Zollo, P. A. and Sinay, P. "Application of the imidate procedure to α -D-galactosylation" *Carbohydr. Res.*, **1982**, *100*, 263-271.
172. Kumar, A.; Kumar, V.; Dere, R. T. and Schmidt, R. R. "Glycoside bond formation via acid-base catalysis" *Org. Lett.*, **2011**, *13*, 3612-3615.
173. Kumar, A. and Schmidt, R. R. "Reversal of anomeric selectivity with O-glycosyl trichloroacetimidates as glycosyl donors and thiols as acceptors under acid/base catalysis" *Eur. J. Org. Chem.*, **2012**, *2012*, 2715-2719.
174. Thomas, M.; Gesson, J.-P. and Papot, S. "First O-glycosylation of hydroxamic acids" *J. Org. Chem.*, **2007**, *72*, 4262-4264.
175. Rio, S.; Beau, J. M. and Jacquinet, J. C. "Synthesis of glycopeptides from the carbohydrate-protein linkage region of proteoglycans" *Carbohydr. Res.*, **1991**, *219*, 71-90.
176. Du, Y.; Zhang, M.; Yang, F. and Gu, G. "A simple access to 3,6-branched oligosaccharides: Synthesis of a glycopeptide derivative that relates to *Lycium barbarum* L" *J. Chem. Soc., Perkin Trans. 1*, **2001**, 3122-3127.
177. Wu, C.-Y. and Wong, C.-H. "Programmable one-pot glycosylation" In *Reactivity Tuning in Oligosaccharide Assembly*, FraserReid, B. and Lopez, J. C. Eds.; Springer Berlin Heidelberg: Berlin, **2011**, pp. 223-252.
178. Premathilake, H. D. and Demchenko, A. V. "Superarmed and superdisarmed building blocks in expeditious oligosaccharide synthesis" In *Reactivity Tuning in Oligosaccharide Assembly*, FraserReid, B. and Lopez, J. C. Eds.; Springer Berlin Heidelberg: Berlin, **2011**, pp. 189-221.
179. Gomez, A. M. "A survey of Ley's reactivity tuning in oligosaccharide synthesis" In *Reactivity Tuning in Oligosaccharide Assembly*, FraserReid, B. and Lopez, J. C. Eds.; Springer Berlin Heidelberg: Berlin, **2011**, pp. 31-68.
180. Fraser-Reid, B. and Cristobal Lopez, J. "Armed-disarmed effects in carbohydrate chemistry: history, synthetic and mechanistic studies" In *Reactivity Tuning in Oligosaccharide Assembly*, FraserReid, B. and Lopez, J. C. Eds.; Springer Berlin Heidelberg: Berlin, **2011**, pp. 1-29.
181. Premathilake, H. D. and Demchenko, A. V. "Superarmed and superdisarmed building blocks in expeditious oligosaccharide synthesis" *Top. Curr. Chem.*, **2011**, *301*, 189-221.
182. Kunz, H. and Sager, W. "Stereoselective glycosylation of alcohols and silyl ethers using glycosyl fluorides and boron trifluoride etherate" *Helv. Chim. Acta*, **1985**, *68*, 283-287.
183. Kreuzer, M. and Thiem, J. "Synthesis of oligosaccharides with glycosyl fluorides under Lewis acid catalysis" *Carbohydr. Res.*, **1986**, *149*, 347-361.
184. Ziegler, T. "The glycosylation of silylated alcohols" *J. Prakt. Chem.*, **1998**, *340*, 204-213.
185. Keizers, P. H. J.; Saragliadis, A.; Hiruma, Y.; Overhand, M. and Ubbink, M. "Design, synthesis and evaluation of a lanthanide chelating protein probe: CLaNP-5 yields predictable paramagnetic effects independent of environment" *J. Am. Chem. Soc.*, **2008**, *130*, 14802-14812.
186. Breschi, M. C.; Calderone, V.; Digiaco, M.; Macchia, M.; Martelli, A.; Martinotti, E.; Minutolo, F.; Rapposelli, S.; Rossello, A.; Testai, L. and Balsamo, A. "New NO-releasing pharmacodynamic hybrids of losartan and its active metabolite: design, synthesis, and biopharmacological properties" *J. Med. Chem.*, **2006**, *49*, 2628-2639.

187. Matta, K. L. and Bahi, O. P. "Synthesis of enzyme substrates. I. Synthesis of 6-*O*-(2-acetamido-2-deoxy- β -D-glucopyranosyl)-D-mannose" *Carbohydr. Res.*, **1972**, *21*, 460-464.
188. Paulsen, H. and Krogmann, C. "Building units of oligosaccharides. XCIV. Synthesis of KDO-containing tri- and tetrasaccharide sequences of the inner core and lipid a region of lipopolysaccharides" *Liebigs Ann. Chem.*, **1989**, 1203-1213.
189. Boullanger, P.; Jouineau, M.; Bouammali, B.; Lafont, D. and Descotes, G. "The use of *N*-alkoxycarbonyl derivatives of 2-amino-2-deoxy-D-glucose as donors in glycosylation reactions" *Carbohydr. Res.*, **1990**, *202*, 151-164.
190. Paulsen, H. and Helpap, B. "Components of oligosaccharides. 96. Synthesis of partial structures of *N*-glycoproteins of the complex type" *Carbohydr. Res.*, **1991**, *216*, 289-313.
191. Schworer, R. and Schmidt, R. R. "Efficient sialyltransferase inhibitors based on glycosides of *N*-acetylglucosamine" *J. Am. Chem. Soc.*, **2002**, *124*, 1632-1637.
192. Boullanger, P.; Banoub, J. and Descotes, G. "*N*-Allyloxycarbonyl derivatives of D-glucosamine as promoters of 1,2-trans-glycosylation in Koenigs-Knorr reactions and in Lewis acid-catalyzed condensations" *Can. J. Chem.*, **1987**, *65*, 1343-1348.
193. Vargas-Berenguel, A.; Meldal, M.; Paulsen, H. and Bock, K. "Convenient synthesis of *O*-(2-acetamido-2-deoxy- β -D-glucopyranosyl)-serine and -threonine building blocks for solid-phase glycopeptide assembly" *J. Chem. Soc., Perkin Trans. 1*, **1994**, 2615-2619.
194. Lafont, D. and Boullanger, P. "Syntheses of L-glucosamine donors for 1,2-trans-glycosylation reactions" *Tetrahedron: Asymmetry*, **2007**, *17*, 3368-3379.
195. Vasella, A.; Witzig, C.; Chiara, J. L. and Martin-Lomas, M. "Convenient synthesis of 2-azido-2-deoxy-aldoses by diazo transfer" *Helv. Chim. Acta*, **1991**, *74*, 2073-2077.
196. Orgueira, H. A.; Bartolozzi, A.; Schell, P.; Litjens, R. E. J. N.; Palmacci, E. R. and Seeberger, P. H. "Modular synthesis of heparin oligosaccharides" *Chem. Eur. J.*, **2003**, *9*, 140-169.
197. Arungundram, S.; Al-Mafraji, K.; Asong, J.; Leach, F. E., III; Amster, I. J.; Venot, A.; Turnbull, J. E. and Boons, G.-J. "Modular synthesis of heparan sulfate oligosaccharides for structure-activity relationship studies" *J. Am. Chem. Soc.*, **2009**, *131*, 17394-17405.
198. Schmidt, R. R.; Michel, J. and Roos, M. "Glycosyl imidates, 12. Direct synthesis of *O*- α - and *O*- β -glycosyl imidates" *Liebigs Ann. Chem.*, **1984**, 1343-1357.
199. Ivanova, I. A.; Ross, A. J.; Ferguson, M. A. J. and Nikolaev, A. V. "Parasite glycoconjugates. Part 9. Synthesis of dec-9-enyl- β -D-galactopyranosyl-(1-4)- α -D-mannopyranosyl phosphate and its epimers at the D-galactose moiety, substrate analogs for the elongating α -D-mannopyranosylphosphate transferase in the Leishmania" *J. Chem. Soc., Perkin Trans. 1*, **1999**, 1743-1754.
200. Becker, D. J. and Lowe, J. B. "Fucose: biosynthesis and biological function in mammals" *Glycobiology*, **2003**, *13*, 41R-53R.
201. Schmidt, R. R.; Wegmann, B. and Jung, K. H. "Glycosyl imidates. 47. Stereospecific synthesis of α - and β -L-fucopyranosyl phosphates and of GDP-fucose via trichloroacetimidate" *Liebigs Ann. Chem.*, **1991**, 121-124.
202. Ziegler, T.; Bien, F. and Jurisch, C. "Chemoenzymic synthesis of enantiomerically pure alkene 1,2-diols and glycosides thereof" *Tetrahedron: Asymmetry*, **1998**, *9*, 765-780.
203. Heng, L.; Ning, J. and Kong, F. "Synthesis of a mannotetraose - the repeating unit of the cell-wall mannans of *Microsporium gypseum* and related species of Trychophyton" *J. Carbohydr. Chem.*, **2001**, *20*, 285-296.
204. Crich, D. and Sun, S. "Direct chemical synthesis of β -mannopyranosides and other glycosides via glycosyl triflates" *Tetrahedron*, **1998**, *54*, 8321-8348.
205. Bock, K. and Pedersen, C. "Carbon-13-hydrogen coupling constants in hexopyranoses" *J. Chem. Soc., Perkin Trans. 2*, **1974**, 293-297.
206. Barrientos, A. G.; de, I. F. J. M.; Rojas, T. C.; Fernandez, A. and Penades, S. "Gold glyconanoparticles: Synthetic polyvalent ligands mimicking glycocalyx-like surfaces as tools for glycobiological studies" *Chem. Eur. J.*, **2003**, *9*, 1909-1921.
207. Sajiki, H.; Kuno, H. and Hirota, K. "Chemoselective inhibition of the hydrogenolysis of the MPM protective group for phenolic hydroxy functions using a Pd/C-pyridine catalyst" *Tetrahedron Lett.*, **1997**, *38*, 399-402.
208. Sajiki, H. "Selective inhibition of benzyl ether hydrogenolysis with Pd/C due to the presence of ammonia, pyridine or ammonium acetate" *Tetrahedron Lett.*, **1995**, *36*, 3465-3468.
209. Ikemoto, N. and Schreiber, S. L. "Total synthesis of (-)-hikizimycin employing the strategy of two-directional chain synthesis" *J. Am. Chem. Soc.*, **1992**, *114*, 2524-2536.

210. Rahim, M. A.; Matsumura, S. and Toshima, K. "Deprotection of benzyl ethers using 2,3-dichloro-5,6-dicyano-p-benzoquinone (DDQ) under photoirradiation" *Tetrahedron Lett.*, **2005**, *46*, 7307-7309.
211. Hoye, T. R.; Caruso, A. J.; Dellaria, J. F., Jr. and Kurth, M. J. "Two syntheses of dl-aplysin" *J. Am. Chem. Soc.*, **1982**, *104*, 6704-6709.
212. Mayhoub, A. S.; Talukdar, A. and Cushman, M. "An oxidation of benzyl methyl ethers with NBS that selectively affords either aromatic aldehydes or aromatic methyl esters" *J. Org. Chem.*, **2010**, *75*, 3507-3510.
213. Chen, F.-E.; Peng, Z.-Z.; Fu, H.; Meng, G.; Cheng, Y. and Lu, Y.-X. "A novel and efficient method for the oxidative removal of *O*-benzyl protective groups of carbohydrates by tetrabutylammonium peroxydisulfate" *Synlett*, **2000**, 627-628.
214. Adinolfi, M.; Barone, G.; Guariniello, L. and Iadonisi, A. "Facile cleavage of carbohydrate benzyl ethers and benzylidene acetals using the NaBrO₃/Na₂S₂O₄ reagent under two-phase conditions" *Tetrahedron Lett.*, **1999**, *40*, 8439-8441.
215. Niemietz, M.; Perkams, L.; Hoffman, J.; Eller, S. and Unverzagt, C. "Selective oxidative debenzoylation of mono- and oligosaccharides in the presence of azides" *Chem. Commun.*, **2011**, *47*, 10485-10487.
216. Orita, A.; Nakano, T.; An, D. L.; Tanikawa, K.; Wakamatsu, K. and Otera, J. "Metal-assisted assembly of pyridine-containing arylene ethynylene strands to enantiopure double helicates" *J. Am. Chem. Soc.*, **2004**, *126*, 10389-10396.
217. Aucagne, V. and Leigh, D. A. "Chemoselective formation of successive triazole linkages in one pot: "Click-Click" chemistry" *Org. Lett.*, **2006**, *8*, 4505-4507.
218. Li, Y.; Pink, M.; Karty, J. A. and Flood, A. H. "Dipole-promoted and size-dependent cooperativity between pyridyl-containing triazolophanes and halides leads to persistent sandwich complexes with iodide" *J. Am. Chem. Soc.*, **2008**, *130*, 17293-17295.
219. Mann, M. and Jensen, O. N. "Proteomic analysis of post-translational modifications" *Nat. Biotechnol.*, **2003**, *21*, 255-261.
220. Lin, H.; Thayer, D. A.; Wong, C.-H. and Walsh, C. T. "Macrolactamization of glycosylated peptide thioesters by the thioesterase domain of tyrocidine synthetase" *Chem. Biol.*, **2004**, *11*, 1635-1642.
221. Jensen, K. J.; Meldal, M. and Bock, K. "Glycosylation of phenols: preparation of 1,2-cis and 1,2-trans glycosylated tyrosine derivatives to be used in solid-phase glycopeptide synthesis" *J. Chem. Soc., Perkin Trans. 1*, **1993**, 2119-2129.
222. Fahmi, N. E.; Dedkova, L.; Wang, B.; Golovine, S. and Hecht, S. M. "Site-specific incorporation of glycosylated serine and tyrosine derivatives into proteins" *J. Am. Chem. Soc.*, **2007**, *129*, 3586-3597.
223. Fahmi, N. E.; Golovine, S.; Wang, B. and Hecht, S. M. "Studies toward the site specific incorporation of sugars into proteins: Synthesis of glycosylated aminoacyl-tRNAs" *Carbohydr. Res.*, **2001**, *330*, 149-164.
224. Goddard-Borger, E. D. and Stick, R. V. "An efficient, inexpensive, and shelf-stable diazotransfer reagent: imidazole-1-sulfonyl azide hydrochloride" *Org. Lett.*, **2007**, *9*, 3797-3800.
225. Manabe, S.; Sakamoto, K.; Nakahara, Y.; Sisido, M.; Hohsaka, T. and Ito, Y. "Preparation of glycosylated amino acid derivatives for glycoprotein synthesis by *in vitro* translation system" *Bioorg. Med. Chem.*, **2002**, *10*, 573-581.
226. Sharma, B. K. "Instrumental methods of chemical analysis" Sharma, B. K. Ed.; Goel Pub. Hse.: Meerut, **1976**, pp. S783-S784.
227. Epp, J. B. and Widlanski, T. S. "Facile preparation of nucleoside-5'-carboxylic acids" *J. Org. Chem.*, **1999**, *64*, 293-295.
228. Gloster, T. M.; Zandberg, W. F.; Heinonen, J. E.; Shen, D. L.; Deng, L.-H. and Vocadlo, D. J. "Hijacking a biosynthetic pathway yields a glycosyltransferase inhibitor within cells" *Nat. Chem. Biol.*, **2011**, *7*, 174-181.
229. Alfaro, J. A.; Zheng, R. B.; Persson, M.; Letts, J. A.; Polakowski, R.; Bai, Y.; Borisova, S. N.; Seto, N. O. L.; Lowary, T. L.; Palcic, M. M. and Evans, S. V. "ABO(H) blood group A and B glycosyltransferases recognize substrate via specific conformational changes" *J. Biol. Chem.*, **2008**, *283*, 10097-10108.
230. Zeng, X.; Coquiere, D.; Alenda, A.; Garrier, E.; Prange, T.; Li, Y.; Reinaud, O. and Jabin, I. "Efficient synthesis of calix 6 tmpa: A new calix 6 azacryptand with unique conformational and host-guest properties" *Chem. Eur. J.*, **2006**, *12*, 6393-6402.
231. Chen, M. H.; Davidson, J. G.; Freisler, J. T.; Iakovleva, E. and Magano, J. "An efficient and scalable synthesis of methyl 3-hydroxymethylbenzoate" *Org. Prep. Proced. Int.*, **2000**, *32*, 381-384.

232. Yamamoto, I.; Sekine, M. and Hata, T. "One-step synthesis of 5'-azido nucleosides" *J. Chem. Soc., Perkin Trans. 1*, **1980**, 306-310.
233. Schierholt, A.; Shaikh, H. A.; Schmidt-Lassen, J. and Lindhorst, T. K. "Utilizing Staudinger ligation for the synthesis of glycoamino acid building blocks and other glycomimetics" *Eur. J. Org. Chem.*, **2009**, 3783-3789.
234. Kikuchi, D.; Sakaguchi, S. and Ishii, Y. "An alternative method for the selective bromination of alkylbenzenes using NaBrO₃/NaHSO₃ reagent" *J. Org. Chem.*, **1998**, *63*, 6023-6026.
235. Tropper, F. D.; Andersson, F. O.; Braun, S. and Roy, R. "Phase transfer catalysis as a general and stereoselective entry into glycosyl azides from glycosyl halides" *Synthesis*, **1992**, 618-620.
236. Macmillan, D.; Daines, A. M.; Bayrhuber, M. and Flitsch, S. L. "Solid-phase synthesis of thioether-linked glycopeptide mimics for application to glycoprotein semisynthesis" *Org. Lett.*, **2002**, *4*, 1467-1470.
237. Cunha, A. C.; Pereira, L. O. R.; de Souza, R. O. P.; de Souza, M. and Ferreira, V. F. "Synthesis of 4-acyl-1*H*-1,2,3-triazolic nucleosides" *Nucleos. Nucleot. Nucl.*, **2001**, *20*, 1555-1569.
238. Peterson, M. A.; Nilsson, B. L.; Sarker, S.; Doboszewski, B.; Zhang, W. and Robins, M. J. "Amide-linked ribonucleoside dimers derived from 5'-amino-5'-deoxy- and 3'-(carboxymethyl)-3'-deoxynucleoside precursors" *J. Org. Chem.*, **1999**, *64*, 8183-8192.
239. Tummatorn, J.; Albinak, P. A. and Dudley, G. B. "Synthesis of benzyl esters using 2-benzyloxy-1-methylpyridinium triflate" *J. Org. Chem.*, **2007**, *72*, 8962-8964.
240. Spork, A. P.; Wiegmann, D.; Granitzka, M.; Stalke, D. and Ducho, C. "Stereoselective synthesis of uridine-derived nucleosyl amino acids" *J. Org. Chem.*, **2011**, *76*, 10083-10098.
241. Behr, J.-B.; Goullain, T.; Helimi, A. and Guillerme, G. "Design, synthesis and biological evaluation of hetaryl-nucleoside derivatives as inhibitors of chitin synthase" *Bioorg. Med. Chem. Lett.*, **2003**, *13*, 1713-1716.
242. Seto, N. O. L.; Palcic, M. M.; Hindsgaul, O.; Bundle, D. R. and Narang, S. A. "Expression of a recombinant human glycosyltransferase from a synthetic gene and its utilization for synthesis of the human blood group B trisaccharide" *Eur. J. Biochem.*, **1995**, *234*, 323-328.
243. Martinez-Fleites, C.; Macauley, M. S.; He, Y.; Shen, D. L.; Vocadlo, D. J. and Davies, G. J. "Structure of an *O*-GlcNAc transferase homolog provides insight into intracellular glycosylation" *Nat. Struct. Mol. Biol.*, **2008**, *15*, 764-765.
244. Rich, J. R.; Szpacenko, A.; Palcic, M. M. and Bundle, D. R. "Glycosyltransferase-catalyzed synthesis of thiooligosaccharides" *Angew. Chem. Int. Ed.*, **2004**, *43*, 613-615.
245. Sujino, K.; Uchiyama, T.; Hindsgaul, O.; Seto, N. O. L.; Wakarchuk, W. W. and Palcic, M. M. "Enzymatic synthesis of oligosaccharide analogues: Evaluation of UDP-Gal analogues as donors for three retaining α -galactosyltransferases" *J. Am. Chem. Soc.*, **2000**, *122*, 1261-1269.
246. Seto, N. O. L.; Compston, C. A.; Szpacenko, A. and Palcic, M. M. "Enzymatic synthesis of blood group A and B trisaccharide analogues" *Carbohydr. Res.*, **2000**, *324*, 161-169.
247. Marcus, S. L.; Polakowski, R.; Seto, N. O. L.; Leinala, E.; Borisova, S.; Blancher, A.; Roubinet, F.; Evans, S. V. and Palcic, M. M. "A single point mutation reverses the donor specificity of Human Blood Group B - synthesizing galactosyltransferase" *J. Biol. Chem.*, **2003**, *278*, 12403-12405.
248. Kabsch, W. "Software XDS for image rotation, recognition and crystal symmetry assignment" *Acta Crystallogr., Sect. D: Biol. Crystallogr.*, **2010**, *D66*, 125-132.
249. Bailey, S. "The CCP4 suite: programs for protein crystallography" *Acta Crystallogr., Sect. D: Biol. Crystallogr.*, **1994**, *D50*, 760-763.
250. Murshudov, G. N.; Vagin, A. A. and Dodson, E. J. "Refinement of macromolecular structures by the maximum-likelihood method" *Acta Crystallogr., Sect. D: Biol. Crystallogr.*, **1997**, *D53*, 240-255.
251. Emsley, P.; Lohkamp, B.; Scott, W. G. and Cowtan, K. "Features and development of Coot" *Acta Crystallogr., Sect. D: Biol. Crystallogr.*, **2010**, *D66*, 486-501.
252. Chen, V. B.; Arendall, W. B., III; Headd, J. J.; Keedy, D. A.; Immormino, R. M.; Kapral, G. J.; Murray, L. W.; Richardson, J. S. and Richardson, D. C. "MolProbity: all-atom structure validation for macromolecular crystallography" *Acta Crystallogr., Sect. D: Biol. Crystallogr.*, **2010**, *66*, 12-21.
253. Lazarus, M. B.; Jiang, J.; Gloster, T. M.; Zandberg, W. F.; Whitworth, G. E.; Vocadlo, D. J. and Walker, S. "Structural snapshots of the reaction coordinate for *O*-GlcNAc transferase" *Nat. Chem. Biol.*, **2012**, *8*, 966-968.
254. Morris, G. M.; Huey, R.; Lindstrom, W.; Sanner, M. F.; Belew, R. K.; Goodsell, D. S. and Olson, A. J. "AutoDock4 and AutoDockTools4: Automated Docking with selective receptor flexibility" *J. Comput. Chem.*, **2009**, *30*, 2785-2791.

255. Trott, O. and Olson, A. J. "Software news and update AutoDock vina: Improving the speed and accuracy of docking with a new scoring function, efficient optimization, and multithreading" *J. Comput. Chem.*, **2010**, *31*, 455-461.
256. Bavaro, T.; Rocchietti, S.; Ubiali, D.; Filice, M.; Terreni, M. and Pregnotato, M. "A versatile synthesis of 5'-functionalized nucleosides through regioselective enzymatic hydrolysis of their peracetylated precursors" *Eur. J. Org. Chem.*, **2009**, 1967.
257. Fügedi P. "Glycosylation methods" In *The Organic Chemistry of Sugars*, Levy D. E., Fügedi P. Eds.; CRC Press: Boca Raton, **2006**, Chap. 4, pp. 89-179.
258. Kamp, F.; Kizilbash, N.; Corkey, B. E.; Berggren, P. O.; Hamilton, J. A. "Sulfonylureas rapidly cross phospholipid bilayer membranes by a free-diffusion mechanism" *Diabetes*, **2003**, *52*, 2526-2531.
259. Nyffeler, P. T.; Liang, C. H.; Koeller, K. M.; Wong, C. H. "The chemistry of amine-azide interconversion: Catalytic diazotransfer and regioselective azide reduction" *J. Am. Chem. Soc.* **2002**, *124*, 10773-10778.

TITRE :

Synthèse et évaluation biologique d'inhibiteurs neutres de glycosyltransférases

RESUME

Les glycosyltransférases sont responsables de la biosynthèse d'oligosaccharides, de polysaccharides et de glycoconjugués. Etant donné le nombre croissant de processus biologiques reliés aux saccharides, il existe un grand intérêt pour la compréhension des rôles biologiques des ces saccharides et étudier leurs applications thérapeutiques potentielles. Ce projet concerne la conception, la synthèse, l'évaluation biologique et l'analyse structurale de deux nouveaux types d'inhibiteurs de glycosyltransférases analogues du substrat donneur naturel. L'analogie repose sur l'incorporation d'une unité pyridine ou amino-acide neutre comme mime du motif pyrophosphate afin de fournir des substrats capables de pénétrer les cellules pour des applications potentielles *in cellulo* ou *in vivo*. Les synthèses d'inhibiteurs neutres de GTs ont été réalisées en utilisant une combinaison de réactions de conjugaison créant une liaison *O*-glycosidique, amide ou triazole. Au total, 26 inhibiteurs neutres de GTs ont ainsi été synthétisés. L'évaluation de l'inhibition pour cinq galactosyltransférases et une GlcNAc-transférase (OGT) a révélé des inhibitions modestes de l'ordre du micromolaire. La co-cristallisation des meilleurs inhibiteurs avec l'une de ces galactosyltransférases a démontré que le motif pyridine neutre chélate le cation manganèse impliqué dans le site catalytique de l'enzyme. Cependant, le motif galactose est orienté vers l'extérieur du site catalytique et loin de la position initiale du substrat naturel (UDP-Gal) et indique donc un nouveau mode de liaison. Le concept d'inhibiteur neutre a aussi été examiné sur un système modèle de membrane pour leur perméation membranaire.

MOTS-CLES : glycosylation, carbohydrate, inhibiteur, glycosyltransférase, chimie médicinale

TITLE :

Synthesis and biological evaluation of neutral glycosyltransferase inhibitors

ABSTRACT

Glycosyltransferase is an important class of enzyme in living organisms responsible for the biosynthesis of oligosaccharides, polysaccharides and glycoconjugates. As more and more carbohydrate related biological processes are elucidated, there is great interest to define the biological roles of a given carbohydrate and examine its potential therapeutic applications. The present study reports the design, synthesis, biological evaluation and structural analysis of two novel types of glycosyltransferase donor substrate analogues. The design rationale is to make analogues of sugar nucleotide diphosphate substrates, but incorporating a 'neutral' pyridine or amino-acid moiety as the pyrophosphate surrogate in order to provide cell permeable substrates for potential *in cellulo* or *in vivo* applications. The syntheses of "neutral" GTs inhibitors were performed using a combination of conjugations through *O*-glycoside bond, amide bond or triazole functionalities. A total number of 26 "neutral" GT inhibitors were prepared. The evaluation of inhibition towards five galactosyltransferases and one GlcNAc-transferase (OGT) revealed moderate inhibitions in the micromolar range. More interestingly, co-crystallization could be achieved for the most potent compounds in complex with a glycosyltransferase. The designed 'neutral' pyridine linker could chelate the manganese cation involved in the enzyme catalytic site. Whereas the sugar head-group was oriented away from the position found in the related complex with natural substrate (UDP-Gal) indicating a new binding mode. The concept of 'neutral' inhibitor was examined by an artificial cell membrane penetration test.

KEYWORDS : glycosylation, carbohydrate, inhibitor, glycosyltransferase, medicinal chemistry

DISCIPLINE : Chimie Organique

UMR-CNRS 5246, ICBMS, Laboratoire de Chimie Organique 2, Batiment Curien – CPE, 43 boulevard du 11 novembre 1918, F-69622 Villeurbanne CEDEX.